Corrosion of reinforcement : field and laboratory studies for modelling and service life : proceedings of the Nordic seminar in Lund, February 1-2, 1995

Tuutti, Kyösti

1995

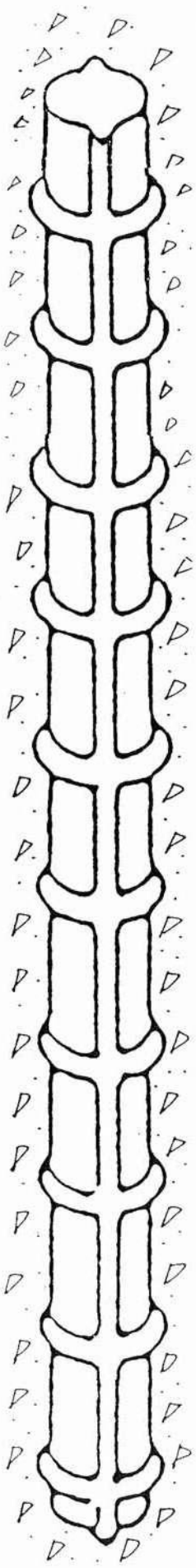

Proceedings of the Nordic Seminar in Lund

Kyösti Tuutti, Editor

February 1-2, 1995

CORROSION OF REINFORCEMENT

Field and Laboratory Studies for Modelling and Service Life

UNIVERSITY OF LUND
LUND INSTITUTE OF TECHNOLOGY
Division of Building Materials

Report TVBM-3064

ISRN: LUTVDG/TVBM--95/3064--SE(1-418)

ISSN: 0348-7911 TVBM

Lund Institute of Technology
Division of Building Materials
Box 118
S-221 00 Lund, Sweden

Telephone: 46-46-222 7415
Telefax: 46-46-222 4427

Foreword

The durability of building materials, especially the corrosion of reinforcement in concrete structures, has been a main research area in Scandinavia during the last decades. Results from many laboratories in the Scandinavian countries, and outside of Scandinavia, indicate that there are certain relationships between the service life and different concrete parameters, such as the water/binder ratio, the type of binder, the concrete cover, etc. It is quite clear, however, that there is, in many cases, lacking agreement between observations in the laboratory and observations in the field. Such discrepancies are especially frequent in connection with chloride penetration and chloride induced corrosion. Therefore, future research in this area ought to be more concentrated towards finding correlations between the laboratory and the field, and to find the reasons behind the discrepancies.

This Nordic seminar was organized in order to summarize the state-of-the-art within the field of chloride induced corrosion. Field studies were highlighted at the seminar. All participants were invited personally, and almost everyone made presentations at the seminar. This volume contains all the papers that were presented. Only a minor editing has been made of the original papers.

Lund, June 6, 1995

Göran Fagerlund Kyösti Tuutti

CONTENTS

Theme 1

CHLORIDE PROFILES IN THE FIELD

Tema 6

FUTURE DEMANDS AND POSSIBILITIES

Chloride profiles in the field

Chloride Profiles

Determination, Interpretation and Practice

State-of-the-art report – An Introduction to Session 1

Nordic Mini Seminar 1st and 2nd February 1995, Sweden

Lund Institute of Technology, Division of Building Materials

Ervin Poulsen. AEClaboratory, 20 Staktoften. DK-2850 Vedbæk, Denmark

ABSTRACT

In Session No. 1 of this Nordic Mini Seminar 1995 on inspection records for the modelling of service lifetime – corrosion of reinforcement, 10 papers are presented. This State-of-the-Art Report deals with the progress in the Nordic countries of the determination, interpretation and practice of chloride profiles as a measure of the concrete's reaction to chloride contaminated environments.

Keywords. Grinding and drilling equipment, chloride ingress, chloride distribution, chloride profile, chloride diffusivity, field exposure.

INTRODUCTION

It has always been a problem to obtain a long service lifetime for concrete and reinforced concrete when exposed to a marine environment, i.e. the seawater's constituents chloride, magnesium and sulphate. Efforts have been made to make the concrete watertight and without cracks, but these did not prevent corrosion of the rebars, e.g. as described by *Fulton* [1957] and *Halstead* et al [1955]. Since *Collepardi,* [1970] and [1972], applied the diffusion theory by *Fick* and showed the way to describe the chloride ingress into concrete by the chloride profile there has been a growing interest in the chloride profiles of concrete exposed to a marine environment, cf. e.g. *Browne* [1980].

Definition

A chloride profile of concrete is the chloride concentration of the concrete versus its distance from the chloride exposed concrete surface. Chloride in concrete is not well defined. It exists as free chloride in the pore liquid as well as bound chloride, chemically and physically. There are several types of chloride profiles. Furthermore, the chloride concentration at a certain point of the concrete could be referred to as mass of concrete, mass of binder and even mass of pore liquid. The distribution of the binder is not even throughout the concrete, as it has a higher intensity at the surface, free or cast in a mould. Therefore, when speaking of chloride profiles one ought to make a distinction between the various types of chloride profiles.

The development in the Nordic countries

Since the first Nordic mini seminar on chloride penetration into concrete took place in 1993 in Gothenburg there has been a significant progress of all aspects of the term »chloride profiles«.

Internationally, there are two schools with different aims and means. One school declares for *Collepardi,* [1970] and [1972], i.e. consider the chloride profile as the response to the chloride exposure from the environment and claims that it should be possible to estimate the service life-time from the chloride diffusivity of the concrete and the degree of chloride exposure from the environment. The second school declares for *Whiting,* [1981] and [1984], i.e. consider the test method of *AASHTO* [1980] to be relevant for the inspection of the concrete's chloride diffusivity.

In the Nordic countries the determination of chloride profiles was introduced by *Sørensen* [1979] and *Frederiksen* [1984]

The requirement for the resistance of chloride ingress into concrete used for the tunnel at the Great Belt Link was a diffusion coefficient of less than 600×10^{-15} m^2/s, corresponding to appx. 20 mm^2/year tested at a maturity age of 28 days by a bulk diffusion test method.

A similar requirement was put forward in the General Technical Specifications for the concrete of AF Troll Olje Plattform. The requirement was a chloride diffusion coefficient less than 30 mm^2/year found by the test method APM 302.

The test method of AASHTO

By determination of a chloride profile it is possible to calculate the parameters of the chloride diffusivity of the concrete exposed to the environment in question, i.e. the chloride diffusion coefficient D, the surface ordinate of the chloride concentration C_s and the initial chloride concentration of the concrete C_i. By these parameters it is possible to estimate the future ingress of chloride into the concrete and the surface lifetime on condition that the changes of the diffusivity of the concrete and the chloride exposure are known or estimated.

By the test method of *AASHTO* the amount of electrical current passed through a 51 mm thick slice of concrete, 95 mm in diameter. The cast end of the core is immersed in a solution of 3.0 per cent NaCl and the sawn end of the cylinder is immersed in a solution oh 0.3 N NaOH. A potential difference of 60 vdc. is maintained across the core for six hours. The total charge passed (in coulombs) is related to chloride permeability. The current versus time is plotted and the area under the curve is used to obtain the coulombs (ampere-seconds) of charge passed during the six hour test period.

Typical values quoted in the test method of *AASHTO* are:

- High chloride permeability: more than 4,000 coulombs
- Average chloride permeability: 2,000 to 4000 coulombs
- Low chloride permeability: less than 2,000 coulombs

The requirement of the chloride permeability of the concrete for the Øresund Link is less than 1,200 coulombs.

The test method of *AASHTO* has now given rise to an excited discussion in the USA. At the 1994 Fall Convention of ACI on »special applications and specialty uses of concrete«, *Donald W. Pfeifer,* Principal and Vice President of Wiss, Janney, Elstner Associates presented a very critical paper titled: »The Coulomb Test: Chloride Penetration or What?« He is quoted as demanding that the test method of *AASHTO* be withdrawn and as claiming that a concrete structure accepted by the test method of *AASHTO* did not necessarily have a sufficient service lifetime. He also criticized that all the documentation concerning the test method of *AASHTO* was carried out by one person only, namely *Whiting*. There were no objections to his presentation.

The papers from the Nordic Mini Seminars in Gothenburg in 1993 and in Lund 1995 demonstrate that the school of *Collepardi* dominates at the expense of the school of *Whiting*. However, the test method of *AASHTO* is applied to important structures like the Øresund Link, but there is no paper dealing with the test method of *AASHTO* at this Nordic Mini Seminar in Lund 1995, nor was there at the Nordic Mini Seminar in Gothenburg 1993.

Other test methods

The rapid way of getting a result by the electro-chemically based test methods is very attractive. Thus, several electro-chemical test methods have been developed where an external electric field is applied across the specimen. Steady state methods as well as non-steady state methods have been developed. However, they do not belong to the family of »chloride profiles«.

Some of the electro-chemical methods are able to determine a chloride diffusion coefficient, but since they are rapid methods they do not determine a reliable value of the surface chloride

concentration. A non-steady state electro-chemical test method, the rapid CTH-method has been compared to the bulk diffusion test method APM 302 by *Tang* and *Nilsson* [1993]. No significant difference was found when testing concrete with Portland cement as a binder. However, when the concrete contained flyash a slight difference was found.

REVIEW OF PAPERS AT SESSION 1 ON CHLORIDE PROFILES

Generally speaking there are two main types of chloride profiles:

- *Achieved chloride profiles* found in the near-to-surface layer of a concrete structure exposed to an marine environment (or any other chloride contaminated environment).
- *Potential chloride profiles* of concrete exposed to a standard chloride solution under laboratory conditions.

The potential chloride diffusivity determined by a potential chloride profile determines the intrinsic diffusivity of the concrete. The achieved chloride diffusivity determined by an achieved chloride profile determines characteristics of the concrete as well as of the exposure.

Determination of chloride profiles

The equipment for the determination of chloride profiles of the near-to-surface layer of concrete which has been exposed to chloride have been further developed. Commercial grinding equipment by *Claus Germann Petersen* [1995] and drilling equipment by *Jan Erik Carlsen* [1995], both of them for in-situ determination, are now available for quick and accurate determination of chloride profiles. The equipment for in-lab determination of chloride profiles has not been been further developed since the Nordic Mini Seminar in Gothenburg 1993, and seems to have found its final version.

A chloride profile is a graph which describes the chloride concentration (by mass concrete or mass binder) versus the distance from the chloride exposed concrete surface. A step-wise determination of a chloride profile now allows small steps of appx. 1 mm, and even down to 0.5 mm. This gives very detailed information of a chloride profile.

Significant sources of uncertainties are caused by the sampling of concrete for determination of chloride profiles. *Frederiksen* [1994] recommends a procedure which for each of the local environments include at least one sample. When drilling a core the test methods *DS 423.28* [1984] or *NT Build 208* [1984] require a diameter of at least three times the maximum size of the aggregates of the concrete. *Germann Petersen* [1995] applies a diameter of 73 mm which allows a chloride profile of a concrete having aggregates of a maximum size of appx. 25 mm to be determined when using one sample of one specimen. However, the Profile Grinder PF 1100, Mark II, is so quick a method (appx. 5-10 minutes for a normal profile) that a sample of two or three specimens could easily be used if necessary.

Carlsen [1995] has further developed the method of drilling into a structure from the surface and in this way collected dust samples for the chloride analysis. The test methods *DS 423.28* [1984] and *NT Build* [1984] require that the drill steel should be at least 18 mm whereas *Carlsen* applies a 24 mm drill steel. *Farstad et al* [1993] have shown that more than five specimens (drill holes) are needed, but the drill method developed by *Carlsen* is claimed to be rapid, time saving and convenient to apply. However, it is not clear how the influence of dust from the sides of the hole is avoided.

We now have three excellent methods of determining a chloride profile of concrete structures exposed to chloride contaminated environment. It would be of interest to have a round robin test of the three test methods: the Profile Grinder Mark II, the Carlsen-method and the APM 207. A lot of chloride profiles will be determined during the years to come.

Interpretation of observations

The observation of the chloride concentration versus the distance from the chloride exposed concrete surface is generally modelled by Fick's second law of diffusion. However, deviations from this established mathematical model become visual by the very detailed chloride profiles which it is possible to obtain by the techniques of profile grinding and dust drilling of today. This fact has inspired *Tang Luping* and *Lars-Olof Nilsson* [1995] to discuss the influence of determining parameters on the chloride distribution in concrete. Their conclusion is that Fick's second law of diffusion has to be modified before applying it to the prediction of chloride ingress into concrete. They suggest that a non-linear binding should be considered in this modification.

Ervin Poulsen [1995] raises the question of the influences of defects and particularly the influences of the alteration of the cement matrix in the near-to-surface concrete layer due to the exposure. It is pointed out that there is a need for a Standard of the interpretation of the observations concerning chloride profiles, especially of what should be the criteria for the rejection of single observations when determining a chloride profile and its parameters.

Several papers deal with the calculation of the parameters of concrete's chloride diffusivity applying simple methods, particularly for in-situ testing and quick estimates. *Henrik Sørensen* [1995] introduces a semi-graphic method applying a special preprinted diagram paper suitable for an excellent overview. *Ervin Poulsen* [1995] presents several simple methods for a rapid determination of the approximative parameters of chloride diffusivity determined by an observed chloride profile.

Field exposure of concrete specimens

It is a dilemma that the relation between chloride exposed concrete specimens in the laboratory and concrete structures exposed to chloride contaminated environment is not unambiguous. This fact has inspired to several field exposure tests in the Nordic countries, e.g. the field test in the harbour of Träslövsläge and the field test at the beach of Nyborg Strand by the Great Belt Link. Observations from these important field tests are not reported at the Nordic Mini Seminar 1995 at Lund.

One of the oldest field exposure tests in the Nordic countries is reported by *Justesen*. He describes the long-term durability tests established in 1983, cf. *Nepper-Christensen et al* [1994], presented at the Third International Conference 1994 in Nice on Durability of Concrete. These field tests include large size panels installed in the Hirtshals Harbour, and a ten-year observation of the chloride ingress into these is now available. The various types of concrete tested contain binders of cement, flyash and silica fume.

Chloride ingress into concrete bridges in marine environment

Østmoen and *Steen* [1995] report on inspection and detailed examination of concrete bridges along the coast of Norway. The chloride penetration is found to vary with the local environment and the difference between these is found to be significantly higher in concentration and penetration at the leeward side compared with the windward side, all other conditions being equal.

An interesting finding is the influence of the maturity of the concrete on the penetration of chloride. *Østmoen* and *Steen* [1995] find *no* big difference in chloride content if the bridges are younger or older than 15 years. Several explanations could be given to explain this phenomenon. It would be of great interest to know the reasons, and the best way would be to examine old concrete structures in marine environment. Even if field exposure tests could be planned to include several parameters in a systematic way they are long-term tests, and the oldest field exposure test in the Nordic countries is only about 10 years old.

Stoltzner [1995] reports on a measuring programme by the Danish Road Directorate in order to determine the chloride penetration in Danish bridges. With the object of developing a reliable lifetime model the chloride penetration into the concrete of three motorway bridges and columns of the Farø Bridges have been examined at time intervals of three years. The motorway bridges are exposed to de-icing salt during wintertime and the Farø Bridges are exposed to a marine environment.

The programme started in 1989 and it is among the first systematic investigations carried out in Denmark into the penetration of chloride into concrete bridges in chloride contaminated environments. Great interest is attached to the collecting of such data from the achieved chloride diffusivity of concrete in structures.

Fluge and *Blankvoll* [1995] report on more than 4500 chloride analyses carried out in 1992 at the Gimsøystaumen Bridge in Norway by the in-situ method RCT. Additional chloride measurements by laboratory test methods were performed in connection with trial repairs in 1993 and 1994. This is doubtlessly the most extensive investigation carried out so far.

The average achieved chloride diffusion coefficient was found to be 35 mm^2/year with a standard deviation of 7.5 mm^2/year. The height above the sea level and the exposure of the leeward side versus the windward side were found to be of major importance for the chloride ingress and the chloride content of the near-to-surface layer of the exposed concrete surfaces.

FUTURE RESEARCH AND DEVELOPMENT

Twenty-five years have passed since *Collepardi* [1970] published his paper demonstrating that Fick's laws on diffusion could form a mathematical model of chloride ingress into concrete. Today the term »chloride profile« is everyday lamguage among concrete technologists dealing with concrete's durability. The Nordic Mini Seminar 1995 in Lund has proven that achieved chloride profiles play an important role when describing the concrete's response to chloride contaminated environments. However, the Nordic Mini Seminar 1995 has also proven that there is still a long way to go before we fully understand all aspects of a chloride profile and how it responds to various environments, defects and types of binders.

A chloride profile is a »tool« which is nothing in itself. Only by combining the chloride profile with the knowledge about its development in time and the critical concentration of chloride in concrete it becomes possible to estimate the service lifetime of reinforced concrete structures exposed to a marine environment.

The examination of concrete structures in marine environment is not the final stage, but it might give new ideas of how to carry out concrete a mixture design that would survive a required service lifetime when exposed to a specified marine environment. There may be a long way to go, but it should be remembered that even if it is a long time ago since *Zielinszki* [1909] showed that the *w/c*-ratio was a fundamental parameter of concrete, it took many years before *Bolomey* [1925] showed how a concrete could be proportioned in such a way as to achieve a required strength.

Influences of environment

As shown by *Østmoen* and *Steen* [1995] marine exposure is not a simple »chloride load«. We have to find ways of precise description. A »chloride load« is as complicated as a traffic load on a bridge, but it is not more complicated than it can be solved. However, marine exposure can be described in several ways. Thus, standardisation and cooperation between Road Directorates of the Nordic countries is a »must«.

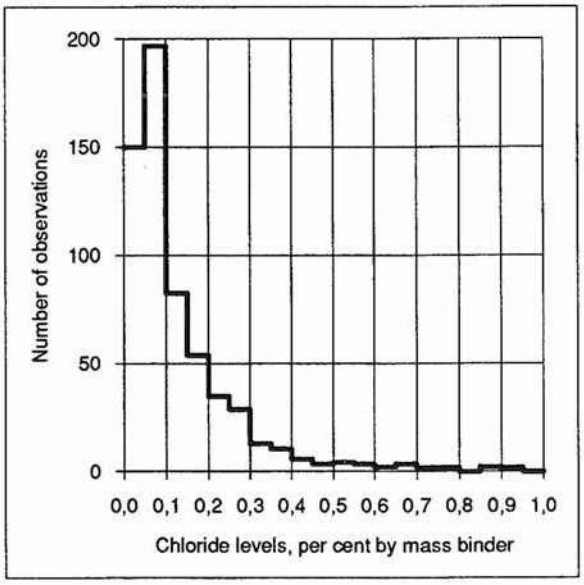

Figure 1. Histogram for the chloride levels in the concrete of piers of 52 bridges in England. The unit of the chloride content is »per cent total chloride by mass cement (binder)«. The chloride level is defined as the average chloride content of a 50 mm deep near-to-surface layer of the exposed concrete. This examination covers 600 observations. Chloride levels greater than 1.0 per cent by mass cement were found in the cases of five observations. It is noticed that the distribution is not symmetrical. The mean value is 0.13 per cent by mass cement and the standard deviation is 0.16 per cent by mass cement. Source: Wallbank [1989].

Influences of defects

As pointed out by *Tang* and *Nilsson* [1995] and *Poulsen* [1995] the mathematical model of a quasi homogeneous material as concrete will sometimes deviate significantly from the observed chloride profile. It may be due to the fact that a mathematical model simplifies the mechanism of chloride ingress. Concrete has often defects like cracks, delamination and internal honeycombing which influence the chloride ingress. Furthermore, the humidity is not uniformly distributed in the concrete, and often the environment changes the surface layer of the exposed concrete by e.g. freezing, carbonation and leaching.

Tang and *Nilsson* [1995] point out that a better approach to the modelling of chloride ingress by complicated transport mechanisms into defect concrete might be to apply the methods of numerical analysis. There are several programmes, but in the future they should be developed to take complicated transport mechanisms and defects into account.

Chloride ingress into partially saturated concrete

Until now the research on chloride ingress into concrete has mainly been carried out on saturated concrete. However, chloride also penetrates partially saturated concrete, e.g. into concrete in marine atmosphere (airborne chloride) and parking decks (de-icing salt).

It is not considered economic to predict chloride ingress into partially saturated concrete assuming the model of saturated concrete. Thus, in the near future the research on chloride ingress into concrete has to deal with partially saturated concrete – in fact the future has already begun.

Criterion of corrosion of rebars in concrete

Chloride profile is a measure or a tool by which it should be possible to estimate the service lifetime of a reinforced concrete structure exposed to chloride contaminated environment, e.g. seawater, marine atmosphere and de-icing salt. In order to decide where the area of future research ought to be, it is of interest to study the criteria of corrosion of rebars embedded in concrete.

The criterion of non-corrosion could be written as:

$$C_x \leq C_{cr} \mid x \geq c \Rightarrow \text{non-corrosion} \qquad \text{eq. (1)}$$

i.e. as long as the chloride concentration C_x of the concrete at a distance x from the chloride exposed concrete surface is smaller than the critical value C_{cr} on condition that x is greater

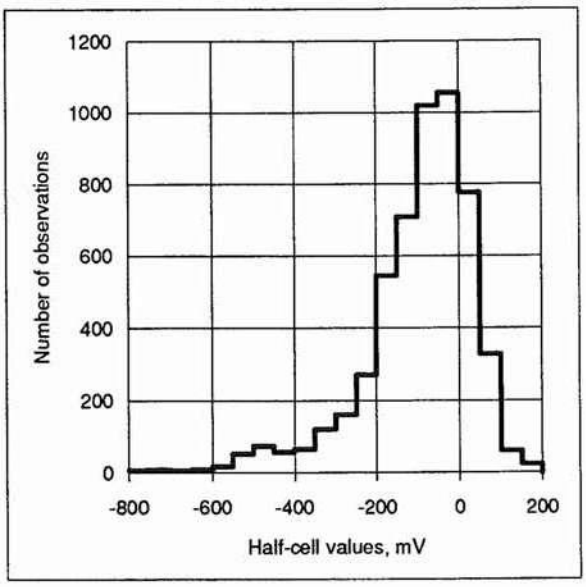

Figure 2. *Histogram for the half-cell potential in concrete piers of 105 bridges in England. The unit of the half-cell value is mV and the test method of ASTM C 876-80 is used applying a saturated copper-copper sulphate half-cell. This examination covers 5418 observations. It is noticed that the distribution is not symmetrical. The mean value is – 48.2 mV and the standard deviation is 134.5 mV. Source: Wallbank [1989].*

or equal to the concrete cover c of the rebar no corrosion will take place. Here C_x, C_{cr} and c are stochastic variables, cf. Figures 1-3. Thus a probabilistic approach should be used in stead of a deterministic approach. It is well-known that C_{cr} is a stochastic variable with a high deviation, even bigger than that of C_x.

The probability of corrosion of rebars is:

$$P\{\text{corrosion}\} = 1 - P\{C_x \leq C_{cr} \mid x \geq c\} \qquad \text{eq. (2)}$$

Until now the research in the Nordic countries on chloride penetration into concrete has concentrated on the determination of the distribution of C_x and has begun the determination of the distribution of C_{cr}. However, we must not forget that the distribution of the cover c of rebars is just as important a parameter.

Inspection of concrete structures has shown that c also varies very much. *Wallbank* [1989] reports on the performance of concrete in bridges. On the basis of a survey of 200 highway bridges he reports not only about the distribution of minimum cover of all elements of bridges built from 1980 onwards, cf. Figure 3, but he also reports on chloride levels in various structural elements of highway bridges exposed to de-icing salts, cf. Figure 1. He concludes:

»The concentration of chloride in a bridge is dependent upon many variables: exposure to spray, to salt water run-off, or to rain, amount of traffic, amount of salt used, geographical location of the bridge, position of the concrete in the bridge, concrete quality, age, past or present leaks, and the history of maintetance«.

The inspection carried out also included examination of reinforcement corrosion by half-cell analysis, cf. Figure 2. From the observations obtained he concludes:

»Chloride contamination was also shown to be related to the incidence of reinforcement corrosion, but there does not appear to be a simple threshold value which trigges corrosion. Circumstances vary from bridge to bridge, and probably also vary with time: a slight change of conditions may be sufficient to start corrosion«.

As it is understood from these results the application of equation (1) is not simple. Besides research on chloride profiles it is important to gain more basic knowledge about the threshold or critical value of chloride in concrete, especially its statistical distribution.

Figure 3. Histogram of minimum cover of rebars of all elements of 152 bridges built from 1960 onwards in England. The unit of the cover is mm. This examination covers 8623 observations. It is noticed that the distribution is not symmetrical. The mean value is 43.6 mm and the standard deviation is 17.5 mm. Source: Wallbank [1989].

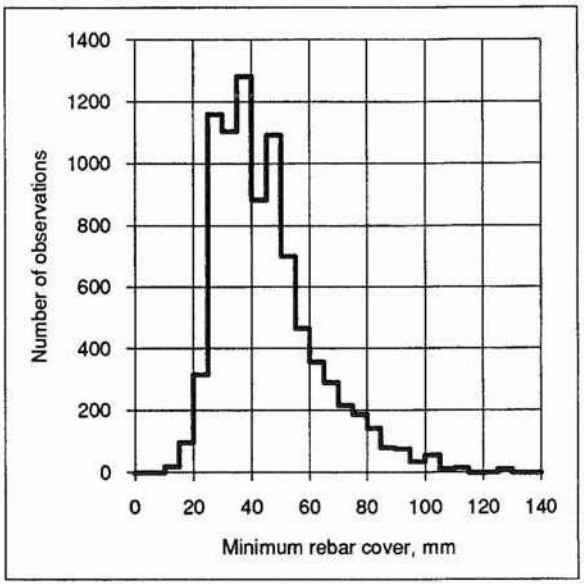

LIST OF LITTERATURE

1909 *Zielinszki, C.* »Die Entwicklung der Erhärtung der Roman- und Portlandzemente im Brei, im Mörtel und im Beton«. IATM Kongres Copenhagen.

1955 *Halstead, S., Woodworth, L. A.* »Deterioration of reinforced concrete structures under coastal conditions«. Transactions South African Institute of Civil Engineers Vol. 5 No. 4.

1957 *Fulton, F. S.* »Concrete Technology, a South African Handbook« The Concrete Association, Johannesburg.

1970 *Collepardi, M., Marcialis, A., Turriziani, R.* »The kinetics of penetration of chloride ions into the concrete«. Il Cemento Vol 4.

1972 *Collepardi, M. et al.* »Penetration of chloride ions into cement pastes and concrete«. American Ceranic Society Vol. 55.

1979 *Sørensen, Birgit.* »Dæklagsundersøgelse i Storebæltsområdet, chloridindtrængning i beton«. Instituttet for Metallære, DTU.

1980 *AASHTO Designation T 259-80.* »Standard Method of Test for Resistance of Concrete to Chloride Ion Penetration«. American Association of State Highway and Transportation Officials. Washington.

1980 *Browne, Roger D.* »Mechanisms of corrosion of steel in concrete in relation to design, inspection, and repair of offshore and coatal structures«. ACI Publication SP-65. American Concrete Institute.

1981 *Whiting, D.* »Rapid Determination of Chloride Permability of Concrete«. Report No. FHWA/RD-81/119 Federal Fighway Administration. Washington D.C.

1984 *DS 423.28.* »Betonprøvning. Hærdnet beton. Chloridindhold«. Dansk Standard, Hellerup.

1984 *NT Build 208.* »Concrete, hardened: Chloride content« Edition 2, Nordtest Methods. Esbo, Finland.

1984 *Whiting, D.* »In Situ Measurement of the Permeability of Concrete to Chloride Ions«. International Conference on In Situ / Nondestructive Testing of Concrete. CANMET ACI, Publication SP-82.

1985 *Frederiksen, J. M. et al.* »Chloridindtrængning i beton«. Eksamensprojekt, Danmarks Ingeniørakademi, Bygningsafdelingen København.

1989 *Wallbank, E. J.* »The Performance of Concrete in Bridges. A Survey of 200 Highway Bridges«. Department of Transport, London.

1993 *Farstad, T., Gran, H. C., Reknes, K.* »Measurements of chlorides in concrete. An evaluation of two different sampling techniques«. Nordtest Project No. 978-91. Oslo.

1993 *Tang, L., Nilsson, L-O.* »A rapid method for measuring chloride diffusivity by using an electrical field«. Nordic Mini Seminar 1993, Gothenborg.

1994 *Frederiksen, J. M.* »Beskyttelse af beton mod salt, malingsystemer, metoder, modeller«. Vejdirektoratet. Broafdelingen, København.

1994 *Nepper-Christensen, P., Kristensen, B. W., Rasmussen, T. H.* »Long-Term Durability of Special High Strength Concretes«. Durability of Concrete, 3th International Conference, Nice, France 1994, ACI Publication SP-145.

1995 *Carlsen, J. E.* »Chloride profile based on sampling of dust by hand drill with vacuum attachment«. Nordic Mini Seminar 1995, Lund.

1995 *Fluge, Finn., Blankvoll, Aage.* »Chloride exposure on Gimsøystraumen Bridge – results from extended condition survey«. Nordic Mini Seminar 1995, Lund.

1995 *Germann Petersen, C.* »The Profile Grinder PF-1100, Mark II«. Nordic Mini Seminar 1995, Lund.

1995 *Pedersen, Vebjørn.* »Long-term field and laboratory exposure tests on chloride penetration. Uncertainties in determination and interpretation of chloride profiles«. Nordic Mini Seminar 1995, Lund.

1995 *Poulsen, E.* »Chloride profiles, analysis and interpretation of observations«. Nordic Mini Seminar 1995, Lund.

1995 *Steen, P. E.* »Chloride penetration in marine environment. Part 2: Results from field tests on coastal bridges in Norway«. Nordic Mini Seminar 1995, Lund.

1995 *Stoltzner, E.* »Chloride penetration in Danish bridges«. Nordic Mini Seminar 1995, Lund.

1995 Sørensen, H. E. »Simple estimation of chloride penetration parameters«. Nordic Mini Seminar 1995, Lund.

1995 *Tang, Luping. Nilsson, L-O.* »Evaluation and interpretation of chloride distributions in concrete – questions and possible solutions«. Nordic Mini Seminar 1995, Lund.

1995 *Østmoen, T., Steen, P. E.* »Chloride penetration in marine environment. Part 1: Computer program calculating average chloride content«. Nordic Mini Seminar 1995, Lund.

CHLORIDE PROFILE BASED ON SAMPLING OF DUST BY HAND DRILL WITH VACUUM ATTACHMENT.

Jan Erik Carlsen, Selmer A.S, P.O.Box 1175 Sentrum, 0107 Oslo, Norway.

ABSTRACT

This paper presents a method used by Selmer A.S for sampling of dust for determination of chloride profiles in concrete. The method is based on using a pneumatic operated hand drill, with an incorporated vacuum evacuator. It is suitable for both in situ and laboratory analysis, and for drilling in all directions. The diameter of the drill is 24 mm. The drilling is executed in several steps in the same hole without removing the drill. From each step, the dust is gathered in separate paper filter bags for analysis. The depth of the hole is measured just once, after the drilling is completed. A computer program is developed to calculate the chloride profile, based on the chloride content of the dust samples, the weight of the samples, and the total depth of the hole.
The paper discusses the accuracy of the method.

Keywords: Chloride penetration, Chloride profile, Drilling machine.

1. WHY THE METHOD WAS DEVELOPED

During the last 3 years Selmer A.S has been doing a number of tests in laboratory on 140 mm concrete cubes of different mixes. The specimens have got different curing conditions, and different chloride exposure. The cubes were tested for chloride penetration after different termini, and then laid back to their chloride environment. For two reasons we where looking for a method that would be simple to perform, and with an acceptable degree of accuracy :

- We had a very large number of profiles to be taken.
- Each cube should be tested several (5-7) times.

2. DESCRIPTION OF THE METHOD

There is to be drilled in several steps in the same hole without removing the drill. The dust from each step is gathered in separate paper filter bags for analysis. Each bag is marked with number, and weighted. The total depth of the hole is measured. It is then easy to calculate which depths the different bags represent.
The total profile should consist of 6-8 steps or bags, minimum 3 bags. One should differ on the total depth for a young and dense concrete (10-40mm), and an old and porous concrete (50-100mm), which means that a dense concrete should have shorter steps into the concrete.

Figure 3 shows a sketch of the method / drilling machine.

3. QUESTION OF ACCURACY

This is the main issue of this paper.
It is obvious that this method could never compete with the accuracy of profiles made from cores of diameter 80-100 mm with steps of 2.5 mm or similar, according to APM 207.

The degree of accuracy will depend on:

- The diameter of the hole versus the Dmax of the aggregate.
- The number of steps in the profile. By our method 5-8 steps versus x times more steps by the APM 207.
- The number of profiles to obtain a representative report on the condition of the structure. This method can more easily produce a higher number of profiles.

To enlighten these questions, two series of results will be presented:

3.1 Laboratory testing on 140 mm cubes. Two and two holes in distance of about 20 mm

These tests indicate if the method is able to produce the same result on the same object, and the influence of remaining dust in the hole, and in the hand drill and tubes.
The question of Dmax is of less importance in this case, since Dmax is much less than 24 mm.

The method is based on not removing the small amount of dust remaining in the hole and in the drill/tubes between each step. However, to verify the method, there are done some parallel profiles where this dust is removed by blowing it away between each step.

The cubes are made of lightweight aggregate concrete (1500-1900kg/m^3), w/b=0.38, age 0.5-1 year. Dmax = 12-16 mm.

Fig. 4-15 shows the chloride profiles with D (chloride diffusion coeff. acc. to Fick's 2. law), and Cs (%Cl of concrete at surface) from cubes tested in Selmer's laboratory. The hand drill and cube are fixed in a bench, and two holes are drilled with a distance of 10 to 30 mm. The profiles from these two holes are drawn on the same figure, to show the "within test variation".

Three types of comparison of profiles from two holes in distance about 20 mm are shown:

- No dust was blown from any hole. Conf. fig. 4, 5, 10, 11 and 13, and table 1.

- One hole where no dust was blown away, and one hole where dust was blown away from both the hole and the drill/tubes. Conf. fig. 6, 7, 8, 9, and table 2.

- One hole where no dust was blown away, and one hole where dust was blown away from the hole (not from the drill/tubes). Conf. fig. 12, 14, 15, and table 3.

The idea of blowing dust away, is to prevent dust from the previous/outer part of the hole to be mixed with dust from the actual step, and thereby increase the chloride content of the sample incorrectly.

3.2 In situ construction / Comparison of profiles from cores versus this method.

Figure 1 and 2 shows "Shore Approach", a culvert for pipelines on the west coast of Norway. Dmax = 22 mm. w/b = 0.36. Age = 12 years.

In 1994 Selmer drilled some cores and holes on this construction. Fig. 1 shows where the cores were taken, and were the holes were made, all from the tidal zone.
All profiles named SINTEF are performed by SINTEF on 90 mm cores, in steps of about 3.5 mm, according to APM 207.

All profiles named Selmer are derived by our alternative method, those with a number+'K' are drilled from the middle of a core, those with just a number are taken 100 mm aside of the companion SINTEF tested cores.

Three types of comparison of profiles are shown:

- Results from core and hole. Conf. fig. 16, 17, 20, 21, 24, 25, and table 6.
- Results from core and core. Conf. fig. 18, 22, and table 4.
- Results from hole and hole. Conf. fig. 19, 23, and table 5.

Figure 26 - 27 shows results from bulk diffusion tests done by SINTEF and Selmer. The profiles differ very much, but since the cores were prepared and put in tanks at different places, the reason could have several explanations.

4 CONCLUSION

Figures 4-15 do not show much difference between profiles were a hole is blown for dust or not. Blowing of dust seems unnecessary.

Figures 18 and 22 shows comparison of profiles for two cores with distance 150 mm.
Even the profiles on these figures shows a small difference on the same figure.

Figures 19 and 23 shows comparison of profiles for to holes with distance 150 mm.
These shows a small difference when looking at the points in the profile. However, these differences in the outer and inner parts of the profiles are very critical when interpreting the results and calculating the diffusion parameters. These profiles would have gained in getting one or two more points along the profile.

Comparison of profiles from cores versus profiles from holes (table 6) shows a higher variation between the latter.

Altogether the results from the holes are in the same range as the results from cores.
A significance test taken on the differences D2-D1 in table 6 concludes that the two methods do not differ significantly at a 5 % level.
Having in mind the general accuracy on these types of tests and the uncertainty in making the regression analysis to calculate the coefficient D, we regard this as a rather promising result.

The major advantage is however the cost-effectiveness of this simplified method. By the same efforts, a considerable higher numbers of profiles might be produced, which again improves the representativeness of the reported condition of the structure.

However, there is still room for improvements, and we are working to achieve additional refinements.

Tables of results from Lightweight aggregate concrete cubes exposed in laboratory.
Age: approx. 1 year . All results obtained by the Selmer method.

no1 no2	D1	D2	Δ D%	Cs1	Cs2	Δ Cs%
1 2	50	47	6%	0.77	0.73	5%
3 4	55	67	20%	0.60	0.52	14%
7 9	31	32	3%	1.58	1.38	14%
10 12	71	71	0%	0.53	0.48	10%
15 16	84	89	6%	0.92	0.85	8%
17 18	77	89	15%	0.79	0.69	14%
21 22	51	59	11%	0.67	0.59	13%
26 28	46	43	7%	0.88	0.63	33%
MEAN:			9%			14%
Sdev:			7%			8%

Table 1

Two holes without blowing dust away between steps of drilling.

no1 no2	D1	D2	Δ D%	Cs1	Cs2	Δ Cs%
6 5	38	35	8%	0.55	0.59	7%
7 8	31	35	12%	1.58	1.55	2%
9 8	32	35	9%	1.38	1.55	12%
10 11	71	53	29%	0.53	0.49	8%
14 13	89	87	2%	1.12	1.22	9%
MEAN:			12%			8%
Sdev:			10%			4%

Table 2

One hole without dust-blowing (no1), and one with dust-blowing from drill and hole (no2).

no1 no2	D1	D2	Δ D%	Cs1	Cs2	Δ Cs%
20 19	31	36	15%	1.11	1.15	4%
24 23	63	67	6%	0.16	0.16	0%
26 25	46	51	11%	0.76	0.91	22%
28 27	43	39	10%	0.63	0.81	25%
MEAN:			10%			13%
Sdev:			4%			13%

Table 3

One hole without dust-blowing (no1), and one with dust-blowing from hole only (no2).

Tables of results from "Shore Approach". Age: approx. 12 years.
Comparison results from SINTEF (on cores), and the "Selmer method".

no1 no2	D1	D2	Δ D%	Cs1	Cs2	Δ Cs%
33 35	11	10	10%	0.72	0.72	0%
37 39	12	12	0%	0.38	0.33	14%

Table 4

SINTEF-results. Two and two cores with distance approx. 150mm.

no1 no2	D1	D2	Δ D%	Cs1	Cs2	Δ Cs%
34 36	18	12	40%	0.60	0.70	15%
38 40	12	15	20%	0.37	0.31	17%

Table 5

Selmer-results. Two and two holes with distance approx. 150mm.

		D1	D2	Cs1	Cs2
From Fig. 1	no1 no2	SINTEF	Selmer	SINTEF	Selmer
1K 1	32 31	8	11	0.57	0.87
3K 3	33 34	11	18	0.72	0.60
4K 4K	35 36	10	12	0.72	0.70
5K 5K	37 38	12	12	0.38	0.37
6K 6	39 40	12	15	0.33	0.31
7K 7	42 41	12	12	0.51	0.60
Mean:		10.8	13.3	0.54	0.57
Sdev:		1.6	2.7	0.17	0.21

Table 6

Comparison SINTEF-results on cores (no1) and Selmer-results on holes (no2).
The distance between a core and a hole on the same line in the table is 0-150mm.

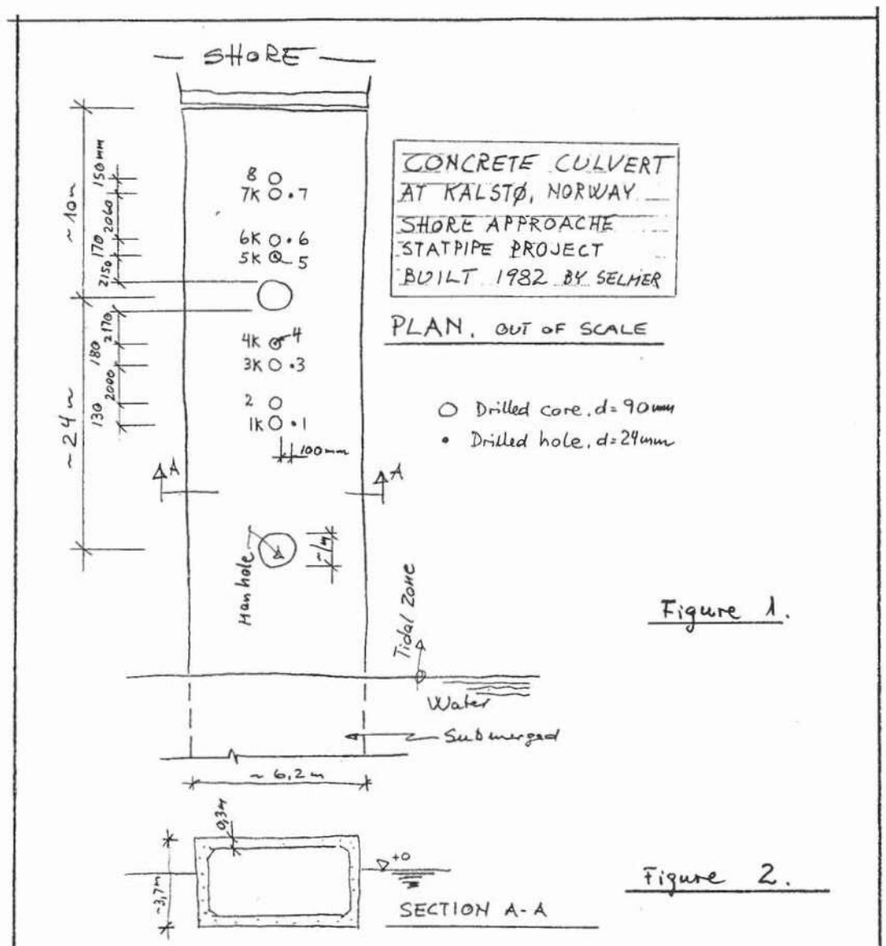

Figure 1.

Figure 2.

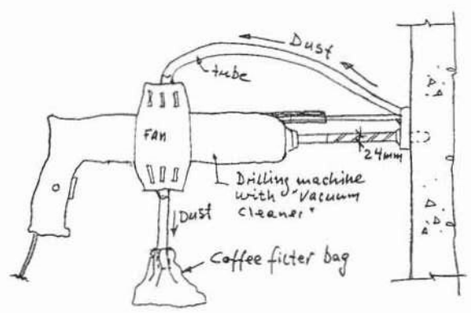

Figure 3.

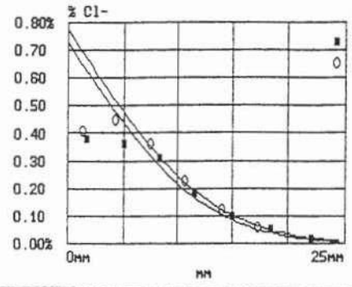

Cs	Set of data	no	D (mm^2/year)
0.77	A1.1df-360d	/1	50
0.73	A1.1df-360d	/2	47

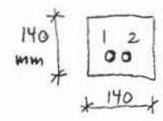

cube

Fig. 4.

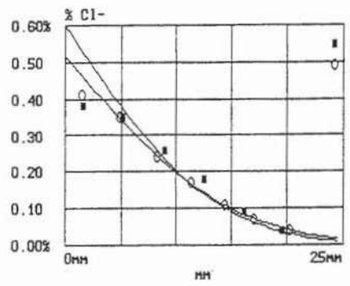

Cs	Set of data	no	D (mm^2/year)
0.60	A1.7df-360d	/3	55
0.52	A1.7df-360d	/4	67

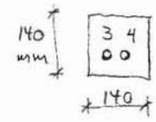

cube

Fig. 5.

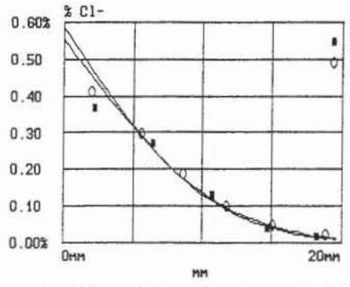

Cs	Set of data	no	D (mm^2/year)
0.59	A1.28df-360d	/5	35
0.55	A1.28df-360d	/6	38

Dust blown both from hole and drilling machine each time

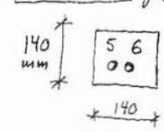

cube

Fig. 6.

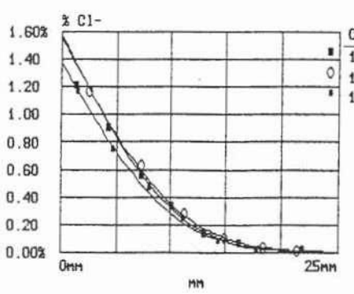

Cs	Set of data	no	D (mm^2/year)
1.58	A5.28df-360d	/7	31
1.55	A5.28df-360d	/8	35
1.38	A5.28df-360d	/9	32

Dust blown both from hole and drilling machine each time

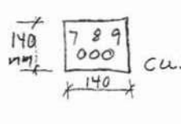

cube

Fig. 7.

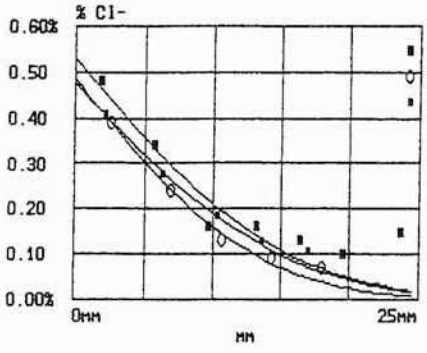

Cs	Set of data	no	D (mm²/year)
0.53	B1.28df-360d	/10	71
0.49	B1.28df-360d	/11	53
0.48	B1.28df-360d	/12	71

/11 Dust blown both from hole and drilling machine each time

/12 : Dust blown from drilling machine

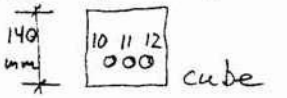

Fig. 8.

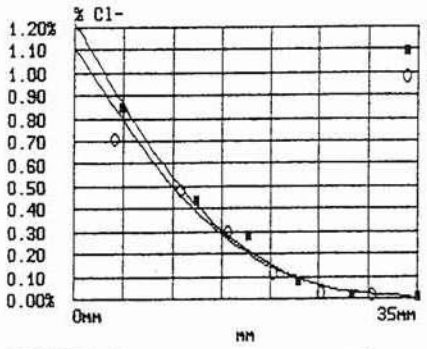

Cs	Set of data	no	D(mm²/year)
1.22	C1.1df-355d	/13	87
1.12	C1.1df-355d	/14	89

Dust blown both from hole and drilling machine each time

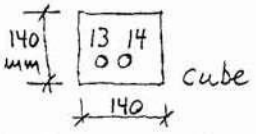

Fig. 9.

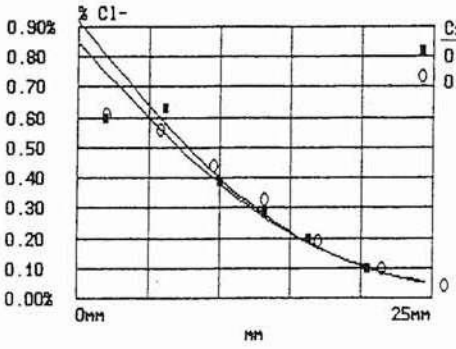

Cs	Set of data	no	D (mm²/year)
0.92	E1.1df-355d	/15	84
0.85	E1.1df-355d	/16	89

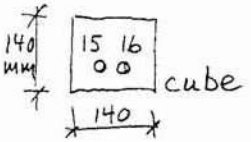

Fig. 10.

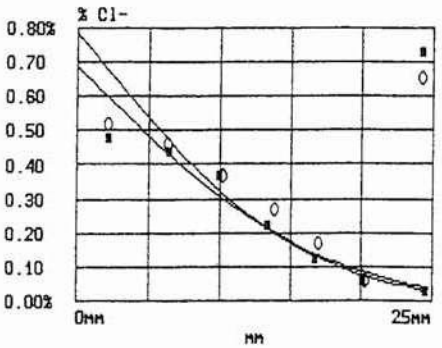

Cs	Set of data	no	D (mm²/year)
0.79	E1.7df-350d	/17	77
0.69	E1.7df-350d	/18	89

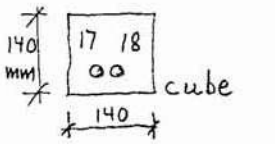

Fig. 11.

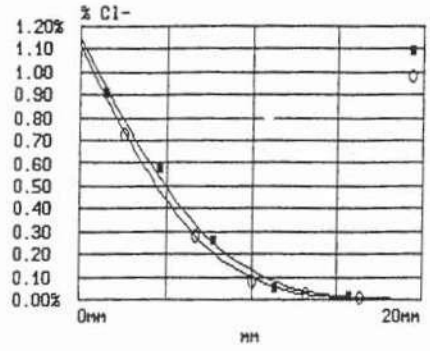

Cs	Set of data	no	D (mm²/year)
1.15	G5.28df-200d	/19	36
1.11	G5.28df-200d	/20	31

Dust blown from hole each time (= each sample)

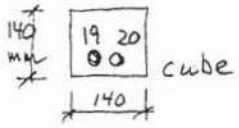

Fig. 12.

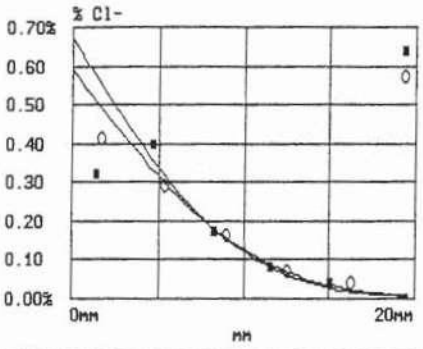

Cs	Set of data	no	D (mm²/year)
0.67	G6.28df-200d	/21	51
0.59	G6.28df-200d	/22	59

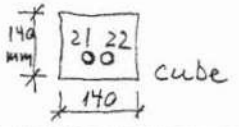

Fig. 13.

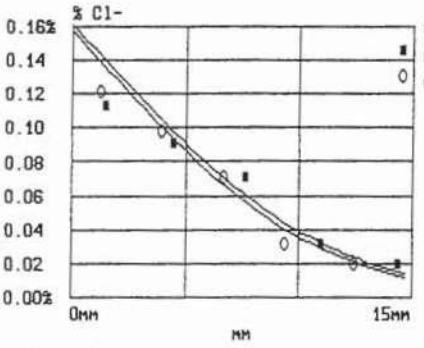

Cs	Set of data	no	D (mm²/year)
0.16	G7.28df-200d	/23	67
0.16	G7.28df-200d	/24	63

Dust blown from hole each time (= each sample)

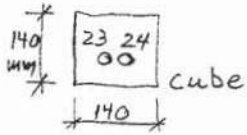

Fig. 14

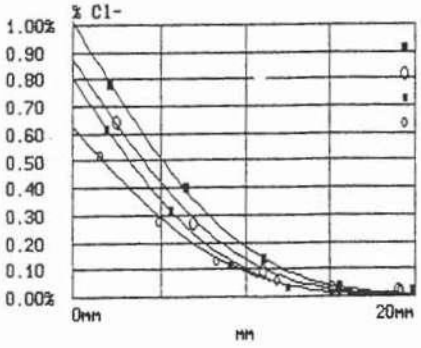

Cs	Set of data	no	D (mm²/year)
1.02	G9.28df-200d	/25	51
0.88	G9.28df-200d	/26	46
0.81	G9.28df-200d	/27	39
0.63	G9.28df-200d	/28	43

Dust blown from hole each time

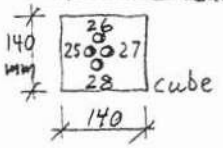

Fig. 15

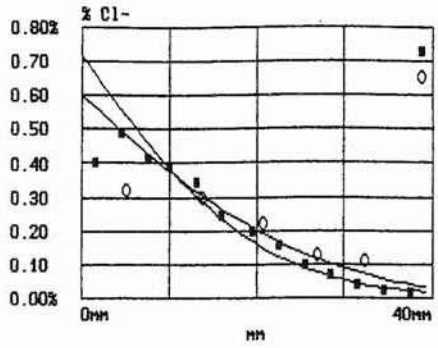

Cs	Set of data	no	D (mm²/year)
0.72	SINTEF 3K	/ 33	11
0.60	Selmer 3	/ 34	18

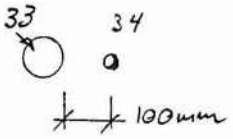

Fig. 16.

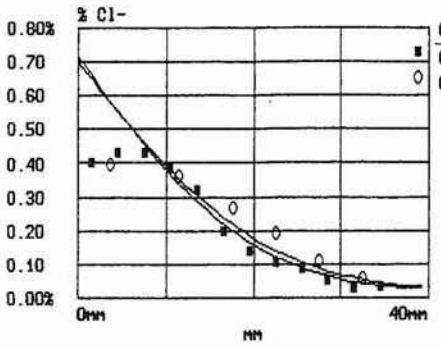

Cs	Set of data	no	D (mm²/year)
0.72	SINTEF 4K	/ 35	10
0.70	Selmer 4K	/ 36	12

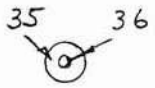

Fig. 17.

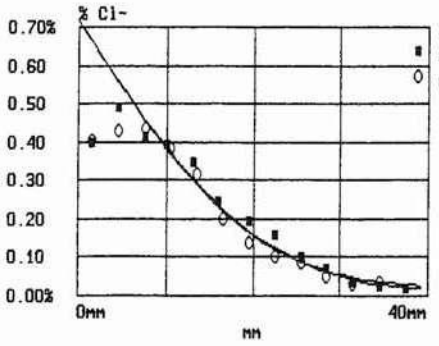

Cs	Set of data	no	D (mm²/year)
0.72	SINTEF 3K	/ 33	11
0.72	SINTEF 4K	/ 35	10

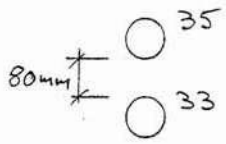

Fig. 18

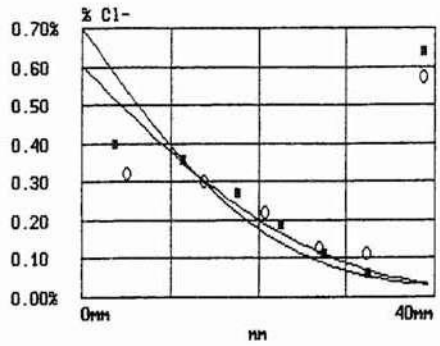

Cs	Set of data.	no	D (mm²/year)
0.70	Selmer 4K	/ 36	12
0.60	Selmer 3	/ 34	18

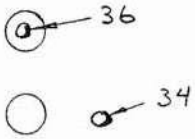

Fig. 19.

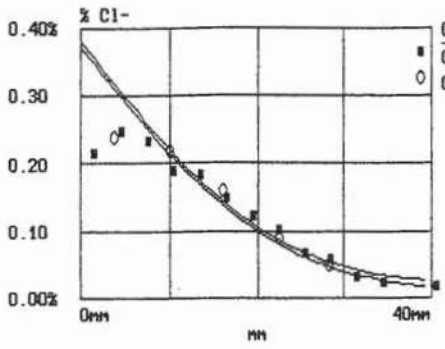

Cs	Set of data	no	D (mm²/year)
0.38	SINTEF 5K	/ 37	12
0.37	Selmer 5K	/ 38	12

Fig. 20.

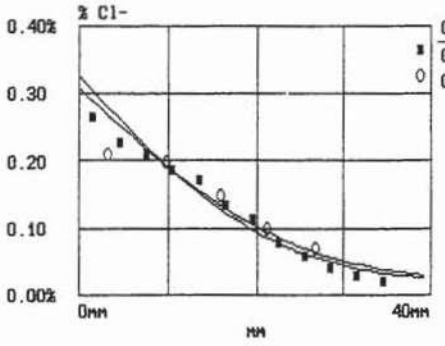

Cs	Set of data	no	D (mm²/year)
0.33	SINTEF 6K	/ 39	12
0.31	Selmer 6	/ 40	15

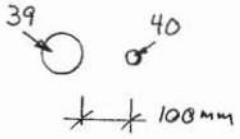

Fig. 21.

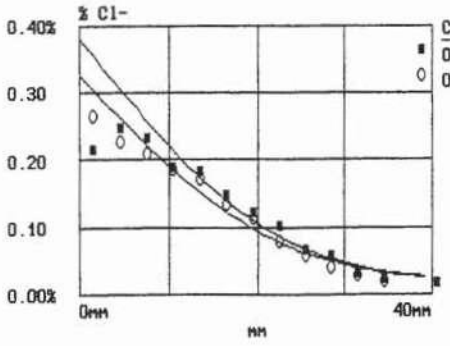

Cs	Set of data	no	D (mm²/year)
0.38	SINTEF 5K	/ 37	12
0.33	SINTEF 6K	/ 39	12

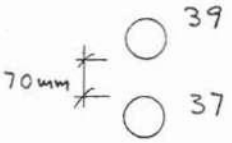

Fig. 22.

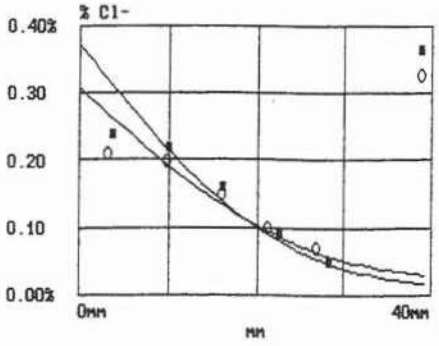

Cs	Set of data	no	D (mm²/year)
0.37	Selmer 5K	/ 38	12
0.31	Selmer 6'	/ 40	15

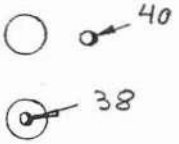

Fig. 23.

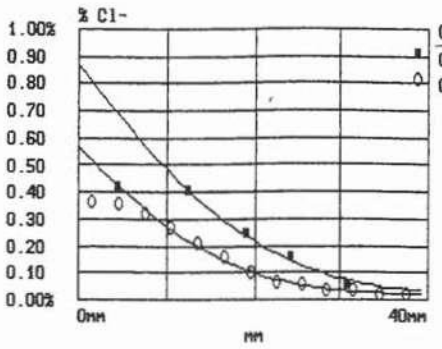

Cs	Set of data	no	D (mm²/year)
0.87	Selmer 1	/ 31	11
0.57	SINTEF 1K	/ 32	8

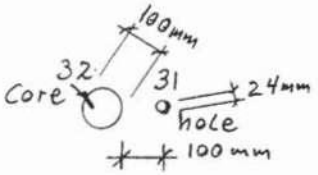

Fig. 24.

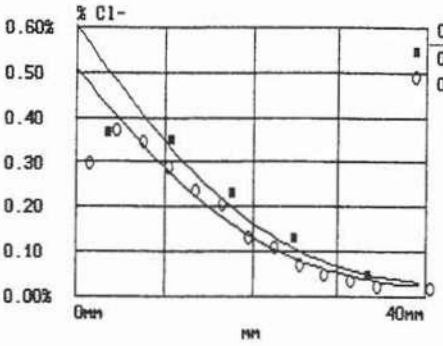

Cs	Set of data	no	D (mm²/year)
0.60	Selmer 7	/ 41	12
0.51	SINTEF 7K	/ 42	12

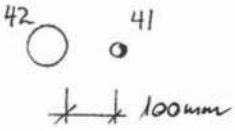

Fig. 25.

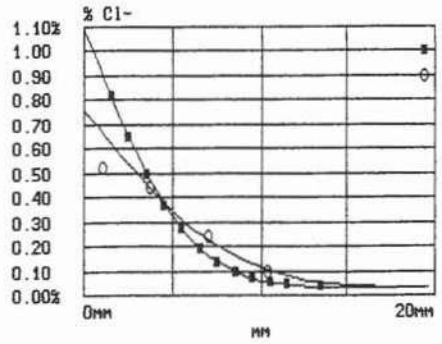

Cs	Set of data	no	D (mm²/year)
1.09	SIN-302 1K	/ 43	111
0.76	Sel-302 2K	/ 44	209

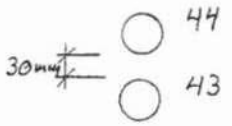

Bulk diff.
APM 302

Fig. 26

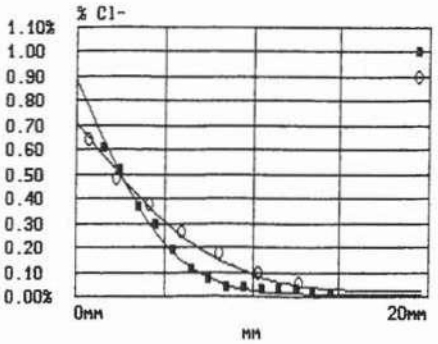

Cs	Set of data	no	D (mm²/year)
0.89	SIN-302 7K	/ 45	94
0.71	Sel-302 8K	/ 46	196

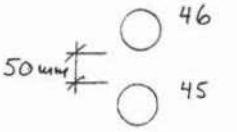

Bulk diff.
APM 302

Fig. 27.

The Profile Grinder PF-1100, Mark II

Claus Germann Petersen, Germann Instruments A/S, 102 Emdrupvej, DK-2400 Copenhagen

Abstract:

The newly developed Profile Grinder PF-1100, Mark II, is presented. The dimensions chosen of the grinding area and the maximum grinding depth is substantiated and the operation of the grinder outlined. Applications are illustrated on horisontal and vertical surfaces, in-situ, as well as on specimens in the laboratory. Finally, a short summary of the experience with the grinder is given.

Sampling of dust may be obtained accurately at depth increments between 0.25 mm and 2.00 mm chosen by the operator, for chemical analysis of the dust to be performed to establish accurate profiles of relevant concrete properties, e.g. of chlorides or pH.

The PF-1100 Profile Grinder Mark II offers the following advantages over conventional dust collection techniques:

1. The dust is obtained only from a thin slice with a well-defined thickness at the bottom of the 73 mm dia. cavity, not from the side.
2. The dust has a fineness and a homogeneousness equivalent to that of pulverizing concrete of sliced cores in the laboratory using a planetary ball mill.
3. The sampling may be performed entirely on-site eliminating costly and time consuming coring, slicing of the core and pulverizing of the slices in the laboratory.
4. A complete set of samples, e.g. consisting of 20 samples, may be performed within one hour.

Keywords: Profile grinding, Chloride profile, In-situ testing

The Profile Grinder PF-1100, Mark II

1. The need of profile grinding

Profile grinding for establishment of e.g. a chloride profile is traditionally performed by drilling out of dust using percussion drill equipment and dust collection devices with or without vacuum attachments. Such drilling may produce dust with variable particle sizes depending on the force applied to the drill machine, and the dust is not necessasrily drilled out from the bottom of the hole. Also, it is not possible to drill out dust at small depth increments if needed, when the chloride profile is steep in the vicinity of the surface. Dust collection in this manner may, furthermore, require drilling at several locations to make sure the maximum aggregate size is not influencing the representativitines of the sample. However, the sampling is quick and inexpensive to perform.

Otherwise, the most common practice is to drilled out a core with a sufficient diameter, slice it in the laboratory by saw-cutting and pulverize the slices in a ball mill to a required fineness. Alternatively, the core may be attached in a turning lathe and dust produced by means of a diamond bit mounted at the lathe center. Such procedures allow dust at distinct and small depth increments to be produced and collected. The disadvantages are high costs and time consumption, and that rather large holes are left in the structure from the coring often requiring the reinforcement to be cut.

In the following paper the Profile Grinder PF-1100, Mark II, developed by Germann Instruments A/S, is described. The grinder may be used entirely on-site combining quick and inexpensive sampling with laboratory accuracy in terms of how representative the sample is, the fineness of the dust and sampling at small and exact depth increments, if so desired. The standard equipment grinds out dust from an area of 73 mm in diameter. Sampling may, however, also be performed in other patterns with special designed attachment plates, e.g. in between reinforcement in tension without disrupting it.

2. Dimensions of the grinding area and the max. depth of grinding

The grinding area is 73 mm in diameter and the maximum depth is 50 mm.

At each depth increment of 1.0 mm approximately 9.0 gram of dust is available for analysis. For a maximum aggregate size of 15-20 mm this amount of dust is sufficient for the dust sample not to be affected by the presence of aggregates. For a maximum aggregate size between 25-35 mm, 18 gram of dust is needed, corresponding to a depth increment of 2.0 mm.

3. Operation of the grinder

To start out with, the diamond bit tip has to rest against the concrete surface when the grinder is held against the plate felt, see figure 1. This may be done by adjusting the position of the grinding machine in the grinder housing.

The pitch of the thread between the housing and the handle cover is 2.00 mm, consequently e.g. 45 degrees turning of the housing relative to the cover will adjust the diamond bit 0.25 mm downwards downwards if turned clockwise. Each 45 degrees are marked on the housing.

The housing and the handle cover is kept in a locked position prior to grinding by means of a counter nut threaded on the grinder housing. To adjusting the depth for further grinding the counter nut has to be released.

The grinder unit flange is made to rest against the felt and the unit is moved sidewards for the flange to be fully caught between the felt and the plastic cover.

The machine is turned on. The speed of the machine may be selected between 3100 and 7000 r.p.m. In general, the harder the aggregates are, the higher speed is needed. For normal concrete a speed around 4000 r.p.m. is recommended, maximizing the diamond bit life.

The counter nut is released, and the grinding machine with housing is turned clockwise relative to the handle cover, e.g. 90 degrees if 1.00 mm depth increment is needed.

The counter nut is tightened and grinding may commence.

Grinding takes place with both hands on the handles. The grinder is moved in a circle so the flange is following the inner recess of the plate. After one full rotation, the grinder is moved 15-18 mm towards the center of the plate and another rotation is completed for the total 73 mm diameter surface to be worked over with the bit. The grinder is centered in the plate, the machine turned off and the unit removed.

On horisontal surfaces (fig. 1 and 3), the dust is collected with a Dustbuster and poured into a plastic bag. On vertical faces the dust is collected during grinding in a plastic bag attached to the plate (fig.2).

4. Applications

The following figures illustrates the typical applications, grinding in-situ on horisontal and on vertical surfaces and grinding of specimens in the laboratory.

4.1 Grinding in-situ on horisontal surfaces.

The reinforcement is located with a covermeter and the grinding location chosen. Two anchor holes are drilled, supplied with anchors and attached to the clamping pliers. The plate is secured firmly to the surface by means of the pliers at the chosen location.

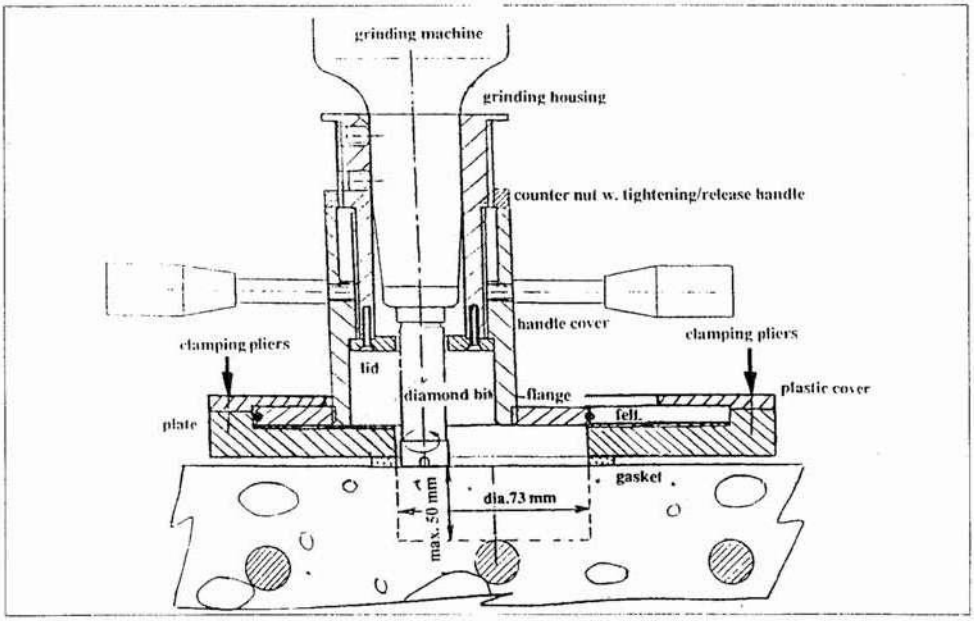

Figure 1. The PF-1100 Profile Grinder, Mark II, used in-situ for grinding out of dust on a horisontal surface.

Grinding takes place as illustrated in section 3. Dust is collected with the Dustbuster and poured into a plastic bag marked with the test location and the depth sampled at, ready for chemical analysis. The Dustbuster has a re-usable filter.

Repeated sampling takes place at the required depth increments until the needed full depth has been reached.

4.2 Grinding in-situ on vertical surfaces

The location of the grinding and the clamping of the plate to the surface is made as previously described. On circular columns the anchors are placed in the direction of the centerline of the column.

Make sure the dust channel of the plate turns downwards. Open the channel by sliding its half-ring sidewards. Attach a plastic bag to the plate as illustrated in figure 2.

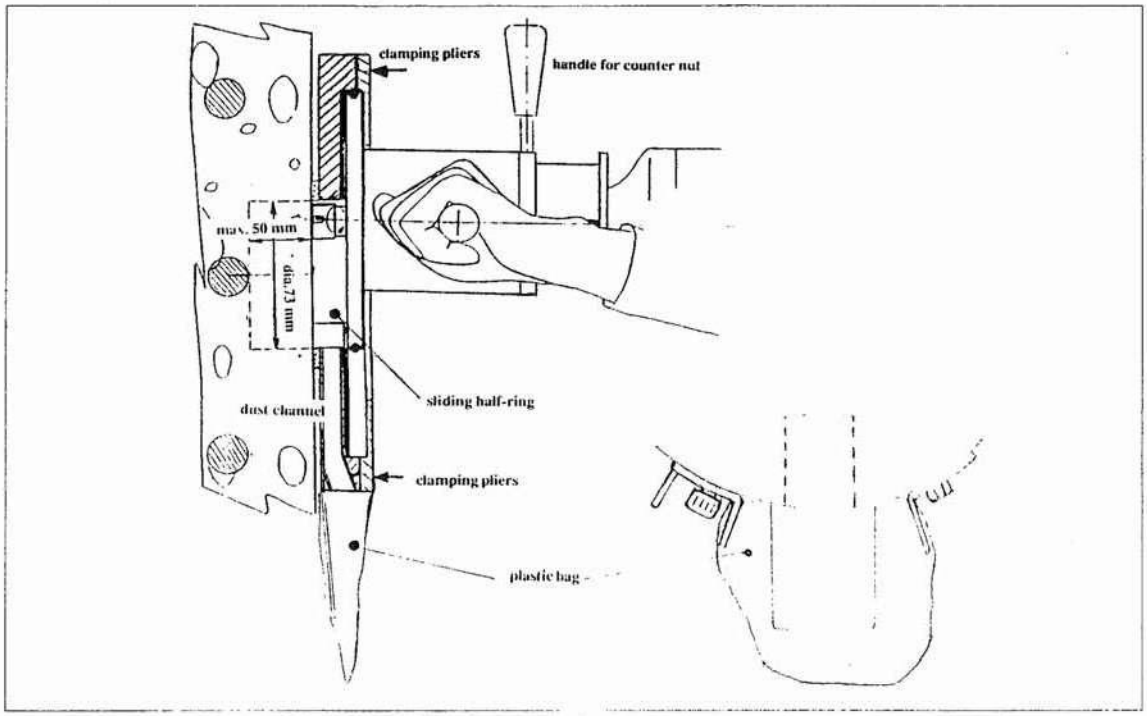

Figure 2. The PF-1100 Profile Grinder, Mark II, used in-situ for grinding out of dust on a vertical surface.

Grinding takes place as outlined in section 3.

After each grinding sequence has been completed the grinding machine is turned off and removed. Remaining dust in the cavity is released with a brush and brushed into the channel of the plate leading to the plastic bag, which is removed and labelled with the test location and the depth sampled at.

Sampling is repeated until the required depth has been reached.

4.3 Grinding in the laboratory on specimens

The PF-1100 Profile Grinder, Mark II, is designed for drilling out of dust of specimens in the laboratory as well, the specimens having a diameter between 95 mm and 105 mm and a height between 60 mm and 70 mm.

Grinding may take place horisontally (shown in figure 3), or vertically by the use of an angle iron attached to the bench plate and secured to the table.

The ring is attached to the plate by means of two bolts, see figure 3, and clamped to the bench plate with the specimen in between. The bench plate is secured to a table with a screw clamp.

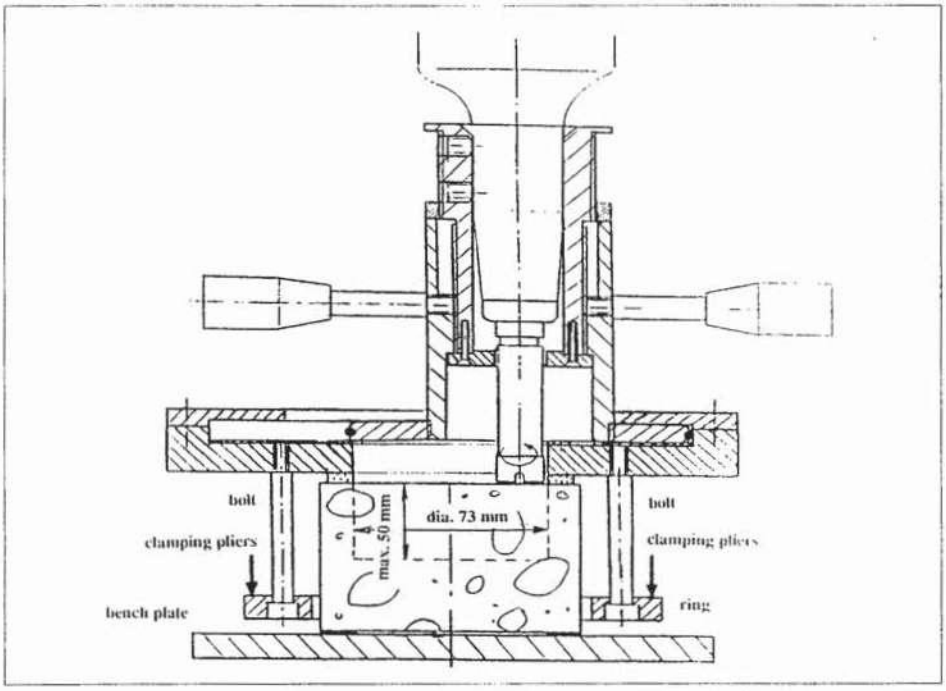

Figure 3. The PF-1100 Profile Grinder, Mark II, used in the laboratory for grinding out of dust of a specimem, the horisontal option being shown.

Grinding takes place as described in section 3.

In case the specimen is placed horisontally as illustrated in figure 3, the dust is collected with the Dustbuster and poured into a plastic bag. For a vertical positioning of the specimen the dust channel of the plate is opened and a plastic bag is secured to the plate at the outlet location so the dust is automatically collected in the bag during grinding.

5. Experience with the PF-1100 Profile Grinder, Mark II

In average, the grinding of each depth increment of e.g. 1 mm, last 30 seconds, and the dust collection about one minut for a trained operator. This is if sampling takes place on a vertical surface. A full profile grinding involving 15-25 samples may be completed within one hour.

On horisontal surfaces where the Dustbuster has to be used for dust collection, the total time elapsed will be 1.5 to 2 hours for a similar number of samples.

The drill bit is worn out after about 200 samples have been taken when grinding on normal concrete. If the concrete contains very hard aggregates or is of a high strength type, the maximum number of samples are about the half before the diamond bit has to be replaced.

The operation of the grinder illustrated and its maintenance has proven to be fairly simple and straight-forwarded for testing technicians.

EVALUATION AND INTERPRETATION OF CHLORIDE DISTRIBUTIONS IN CONCRETE
—Questions and possible solutions

Tang Luping and Lars-Olof Nilsson,
Department of Building Materials, Chalmers University of Technology,
S-412 96 GÖTEBORG, Sweden.

ABSTRACT

In this paper, the methods for the determination of chloride profiles in concrete are briefly reviewed and the evaluation of chloride distributions with respect to the different parameters of concrete is critically discussed. Some questions involved in the interpretation of chloride distributions, such as the validity of Fick's law, effect of binding, influence of moisture distributions and so on, are discussed and the possible solutions are suggested.
Keywords: chloride, concrete, diffusion.

1. INTRODUCTION

Chloride penetration into concrete is a rather complicated transport process /1/ which involves combined mechanisms, including diffusion, capillary suction, convection with flowing water, and sometimes electromigration, accompanied by chemical and physical binding. One of the hot topics in this aspect is how to predict chloride penetration in the real structures by measuring proper parameters in the laboratory, with the help of the field information. It is important to investigate and evaluate sufficient field data for checking various prediction models. There are many reports on the field studies in the literature, but the reported data often cause confusion due to unclear clarification or definition and oversimplification in the evaluation of experimental results. Nilsson /2/ has made a theoretical attempt to clarify some of the confusing sources. In this paper the current methods for the determination, evaluation and interpretation of chloride penetration profiles in concrete will be discussed.

2. DETERMINATION OF CHLORIDE PROFILES

2.1 Sampling

In order to determine the chloride penetration profiles in concrete, the samples must be taken from different depths of a concrete structure. The usual way is to drill cores at certain positions from the structure and grind the core in the laboratory to obtain powdered samples from different depths. In some laboratories the core is cut into thin slices and the slice is then ground into powder. In this way the interval of depth is very large, usually over 10 mm. At the AEC Consulting Engineers in Denmark, a lathe with a diamond driller is employed to grind the core successively from one end of the core. With this method the accuracy of depth is greatly increased and the interval of depth can be as small as 0.5 mm /3/. In our laboratory, this method is modified by replacing the driller with a dry diamond saw. In this case there is almost no limit to the interval of depth, because with a certain angle the saw can grind the core successively like a driller, as well as can dry cut the core at any deeper position to get the powder. Recently a Profile Grinding Kit for both on-site and laboratory has become commercially available /4/.

2.2 Total chloride content

According to many standards /5-7/, the total chloride content should be determined using the methods of acid extraction and titration. Dhir et al /8/ pointed out that the chlorides may not be completely extracted from powdered concrete samples if the strength and contact time of the acid is not sufficient in the acid extraction regime, therefore they classified the chlorides from the acid extraction procedure as acid soluble chlorides, which might be less than total chloride content. Tang /9/ suggested that a small sample size could make the extraction of chlorides easier, and found that the total chlorides could be extracted from concrete by using sufficient amount of acid and choosing suitable sample size. Hans /10/ found that the accuracy of chloride analysis by titration depends on the experience of a laboratory. Another common used method for determining chloride content is ion selective electrode (ISE) /8, 10/. It should be noticed, however, that the calibration must be carried out before testing, because the temperature, pH value and other coexisting ions will influence the reading from the electrode. Other methods for determining chloride content in concrete include X-ray fluorescence spectrometry, atomic absorption and ion chromatography. These techniques require expensive equipment as well as careful calibration. A rapid method called RCT (Rapid Chloride Test) has been developed /4/ for determining chloride content on-site, but it also requires careful calibration.

2.3 Free chloride content

Free chlorides is essentially important regarding to the corrosion of reinforcement in concrete. It is difficult, however, to disassociate the "free" part from the total chlorides, because the "bound" part, especially the physically adsorbed part, is susceptible to "freedom". In practice, free chlorides are often represented by water soluble chlorides. Arya and Newman /11/ investigated different methods for determining free chloride content, including pore-fluid squeeze and analysis, leaching techniques, and quantitative X-ray diffraction analysis.

The method of pore-fluid squeeze and analysis requires special equipment and a large sample size. Besides, there are some uncertainties involved in the pore-fluid squeeze, the most questionable being the phenomenon of higher chloride concentration in the squeezed pore-fluid than in the surrounding solution, which has been observed by many researchers /12-14/. One possible reason might be that the chloride ions in the very fine pores have a lower ion activity /12/, probably due to the effect of diffuse double layer, see Fig. 1. The diffuse double layer is stripped under a high pressure and the pore-fluid bringing these high concentrated chloride ions flows out, resulting in a higher chloride content in the squeezed liquid. Another reason might be the piezo-effect, that is, the high pressure in the squeezing process changes the surface character of the pores, releasing the physically bound chlorides into the pore-fluid.

The leaching techniques are sensitive to the leaching procedures. Different procedures likely produce different results /9, 11, 15/, except that Dhir et al /8/ reported a contrary finding, i.e. different leaching procedure brought similar results.

The method of quantitative X-ray diffraction analysis involves detecting Friedel's salt as bound chloride and then subtracting it from the total chlorides to gain the free chloride content. As Arya /11/ concluded, this method overestimates the free chloride content by underestimating the bound part, because the bound part includes not only Friedel's salt but also other chemically bound and physically bound chlorides.

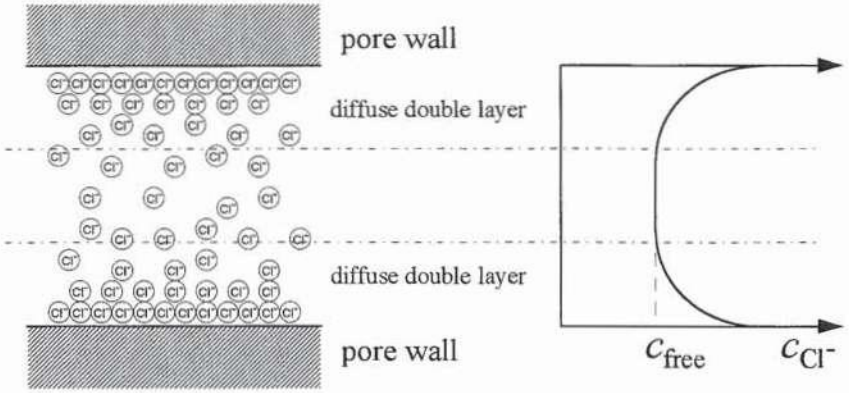

Fig. 1 Diffuse double layer in pore-fluid.

It seems that none of the methods is suitable for the determination of free chloride content associated with the chloride penetration profiles, due to the difficulties in the disassociation of the free part. A solution might be to calculate the free chloride profile from the total chloride profile by using suitable chloride binding isotherms, as suggested by Sandberg and Larsson /16/.

3. EVALUATION OF CHLORIDE DISTRIBUTIONS

It is not difficult to obtain the distribution of chlorides in concrete if the chloride content has been determined. The important thing is to express the unit clearly and correctly, because the unit tremendously influences the shape of a distribution curve, which in turn influences the evaluation of chloride penetration, as will be discussed below. The binder may not homogeneously distribute in concrete, see Fig. 2. Therefore, the binder distribution should be taken into account when using a unit of chloride content by weight of binder, as shown in Fig. 3. It can be seen that the curves in % by weight of sample are steeper than those % by weight of binder, and as a consequence the former will result in an underestimation of chloride diffusivity.

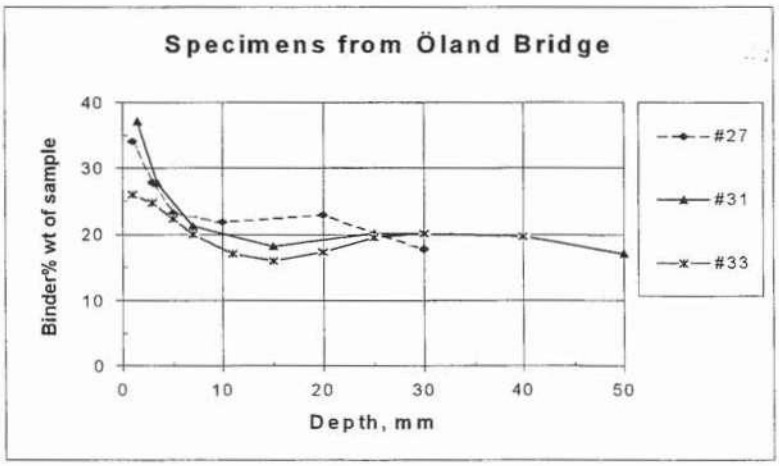

Fig. 2 Distribution of binder in concrete.

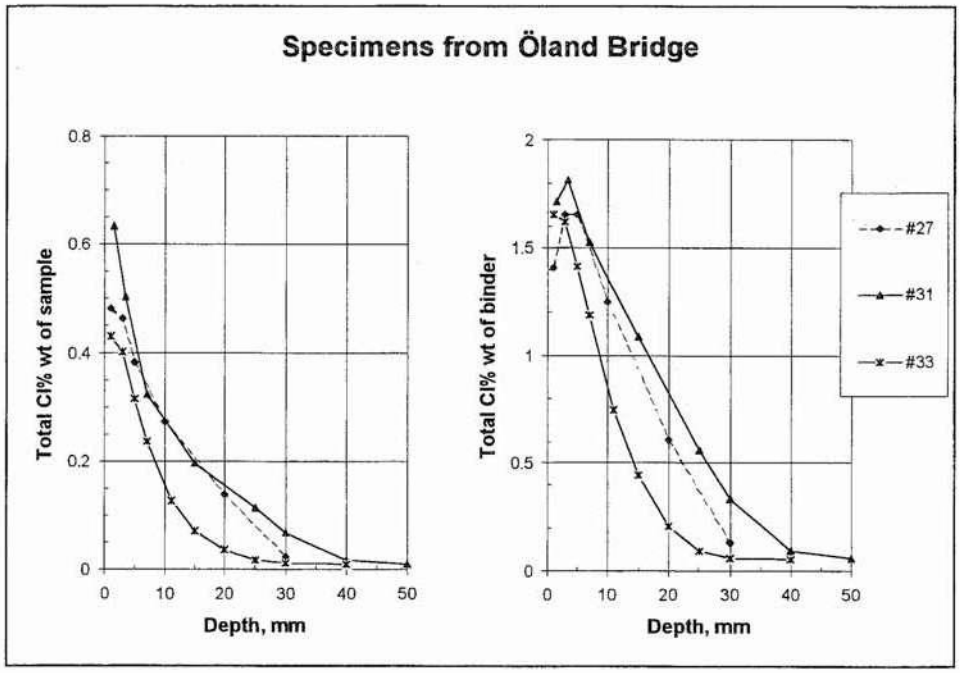

Fig. 3 Chloride distributions in different units.

Fig. 4 shows another example of great difference in chloride penetration curves when using different units.

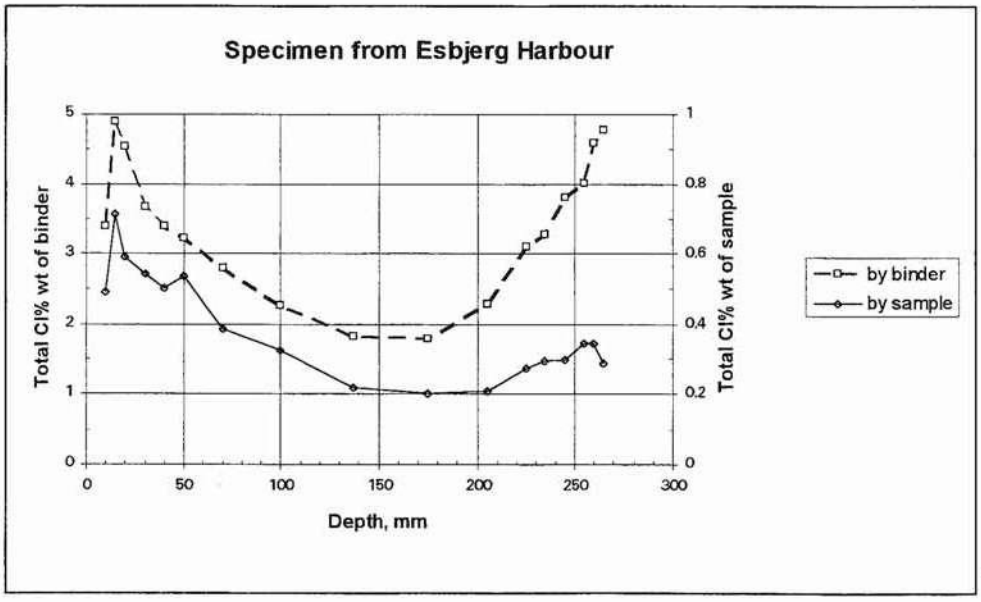

Fig. 4 Great difference in chloride distributions due to different units.

4. INTERPRETATION OF CHLORIDE DISTRIBUTIONS

4.1 Fick's law

Fick's law is usually applied to describe the diffusion process. For non-steady state process, Fick's law can be expressed by the following equation (Fick' second law):

$$\frac{\partial c}{\partial t} = D\frac{\partial^2 c}{\partial x^2} \tag{4.1}$$

where in principle, c is the concentration, t is the time, D is the diffusion coefficient, and x is the distance. It should be kept in mind that the units of c and D require very clear clarification /2/, otherwise the confusion will be caused. Under the assumption of pure diffusion, a chloride distribution curve is usually used to determine the chloride diffusion coefficient by curve fitting to the analytical solution to Fick's law (semi-infinite condition):

$$c = c_s\left[1 - \mathrm{erf}\left(\frac{x}{2\sqrt{D \cdot t}}\right)\right] \tag{4.2}$$

where c_s is the concentration at the surface, and erf denotes the error function. In curve fitting, two parameters, D and c_s, will be optimised according to the principle of least square. It is obvious that c_s changes with many parameters, such as the free chloride concentration in the surrounding solution, chloride binding capacity, binder content, porosity, etc. The parameter D determined in this way is just a coefficient under the restricted condition and, therefore, can hardly be used to interpret the chloride distributions from other conditions. An example is shown in Fig. 5, where completely different values of D are drawn by curve fitting from the concrete with the same quality but under different exposure conditions.

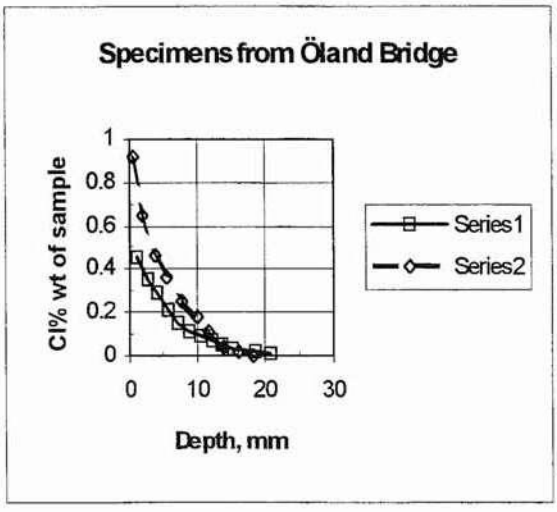

Series 1
Immersed in the seawater with a chloride concentration of 3~5.2 g/l, for a period of 3.8 years.
D by curve fitting: 0.24×10^{-12} m^2/s.

Series 2
Immersed in a solution with a chloride concentration of 164.7 g/l, for a period of 40.8 days.
D by curve fitting: 8.12×10^{-12} m^2/s.

Fig. 5 Rather different values of D due to different exposure conditions. (Data from AEC Consulting Engineers).

4.2 Effect of chloride binding

Theoretically speaking, chloride binding will definitely decrease the chloride transport process. Under the assumption of diffusion accompanied by a linear binding, i.e. $c_b = A \cdot c$, where c_b is the bound chloride content and A is the constant, a modified Fick's law can be derived:

$$\frac{\partial c}{\partial t} = \frac{D}{1+A} \cdot \frac{\partial^2 c}{\partial x^2} = D_{\text{eff}} \frac{\partial^2 c}{\partial x^2} \tag{4.3}$$

where D_{eff} is the effective diffusion coefficient. It can be seen by comparing with Eq. (4.1) that chloride binding decreases the diffusion process just simply by a factor of A. Unfortunately, in the most cases the chloride binding does not follow a linear relationship, but the binding capacity usually decreases with the concentration /16, 17, 18/. Nilsson /2/ theoretically analysed the effect of non-linear binding on chloride transport in concrete and derived a mathematical expression for the process of diffusion accompanied by a non-linear binding:

$$\frac{\partial c_f}{\partial t} = \frac{D}{1+\dfrac{\partial c_b}{\partial c_f}} \cdot \frac{\partial^2 c_f}{\partial x^2} = D_{\text{eff}} \frac{\partial^2 c_f}{\partial x^2} \tag{4.4}$$

where c_b and c_f are the bound and free chloride concentrations, individually, and $\dfrac{\partial c_b}{\partial c_f}$ is defined as binding capacity. In our previous study /17/, the relationship c_b and c_f has been found as

$$c_b = A \cdot c_f^B \tag{4.5}$$

where A and B are constants. Therefore, the binding capacity is

$$\frac{\partial c_b}{\partial c_f} = A \cdot B \cdot c_f^{B\text{-}1} \tag{4.6}$$

It is obvious that in this case the effective diffusion coefficient becomes a function of free chloride concentration, and it decreases greatly at a low concentration since $\dfrac{\partial c_b}{\partial c_f}$ greatly increases with the decrease in free chloride concentration, as shown in Fig. 6. Owing to the dependence of binding capacity on free chloride concentration, Eq. (4.4) can only be solved by numerical methods. An example is given in Fig. 7. If the points in Fig. 7 are used for curve fitting by applying Eq. (4.2), it will results in a value of $D = 1.6 \times 10^{-12}$ m^2/s, much smaller than that measured in the laboratory (7.24×10^{-12} m^2/s), implying an uncertainty of the curve fitting method.

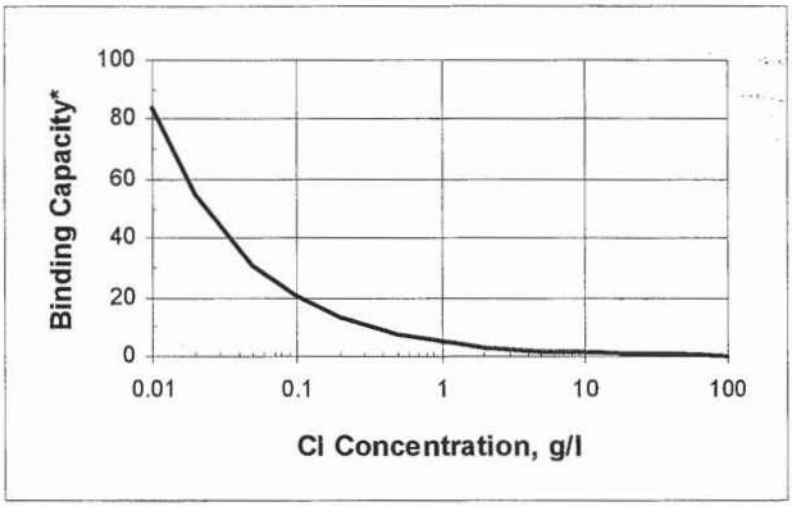

* see Eq. (4.6), where $A = 10^{1.14}/35.45B/\varepsilon_{gel}$, $B = 0.38$, and porosity $\varepsilon_{gel} = 0.28$ (ref. /17/).

Fig. 6 Relationship between chloride binding capacity and concentration.

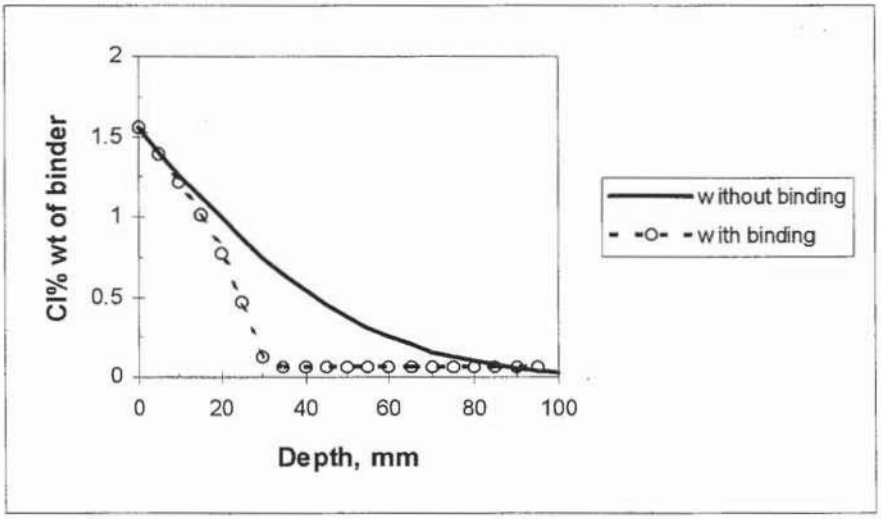

Öland Bridge Concrete, $D_0 = 7.24\times10^{-12}$ m^2/s, $t = 4$ years, $c_{f0} = 4.1$ g/l.

Fig. 7 Comparison with and without chloride binding.

4.3 Influence of moisture distributions

Since chloride ions can diffuse into concrete only through the water filled paths, the moisture distribution in concrete has strong influence on the distribution of total chlorides. For example, if the moisture content in the surface zone is higher than inside the structure, a steeper distribution of chlorides will be found, resulting in an underestimated value of D when curve fitting method is used. It has been found that the moisture content inside concrete is indeed lower than the surface zone, even after 37 years' immersion under seawater /19/, as shown in Fig. 8.

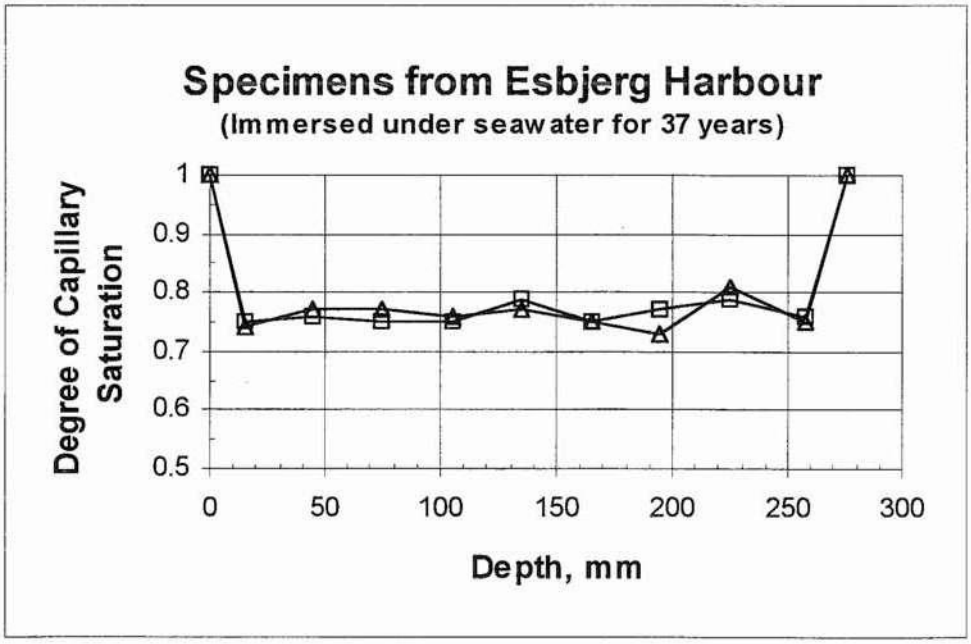

Fig. 8 Moisture distribution in concrete after 37 years' immersion under seawater.

4.4 Influences of environmental parameters

In the field the environmental parameters, such as temperature and chloride concentration in the seawater, may vary very much in the exposure duration. According to Arrhenius' law, the diffusivity changes with temperature, implying a variable diffusion coefficient. The changes in concentration results in a variable boundary condition. All of these make it impossible to reach an analytical solution to Fick's law. Therefore, numerical methods for the modelling of chloride penetration /20/ perhaps is a better approach. An example model is shown in Fig. 9. In this model two main procedures has been considered: 1) chloride penetration through pore solution and 2) distribution of total chloride content in concrete. The changes in surface concentration and temperature, degree of hydration, pore content, binder content in concrete, etc., have also been taken into consideration in the example model.

5. CONCLUDING REMARKS

There are many methods for the determination of total chloride profiles, but at the present no suitable method available for the determination of free chloride profiles, due to the difficulties in disassociating the free chloride ions from the total chlorides.

It is important to express the unit clearly and correctly in the presentation of chloride distributions, otherwise the confusion or misinterpretation in chloride penetration may be caused. It is recommended that an evaluation of binder distribution should be made in regard to the chloride distribution.

Fick's law must be modified before being applied to the prediction of chloride penetration into concrete. It is suggested that non-linear binding should be considered in the modification. In practice, environmental parameters should also be taken into account in the modelling of

chloride penetration. Considering the complication in transport mechanisms, a better approach to the modelling of chloride penetration may be the numerical methods.

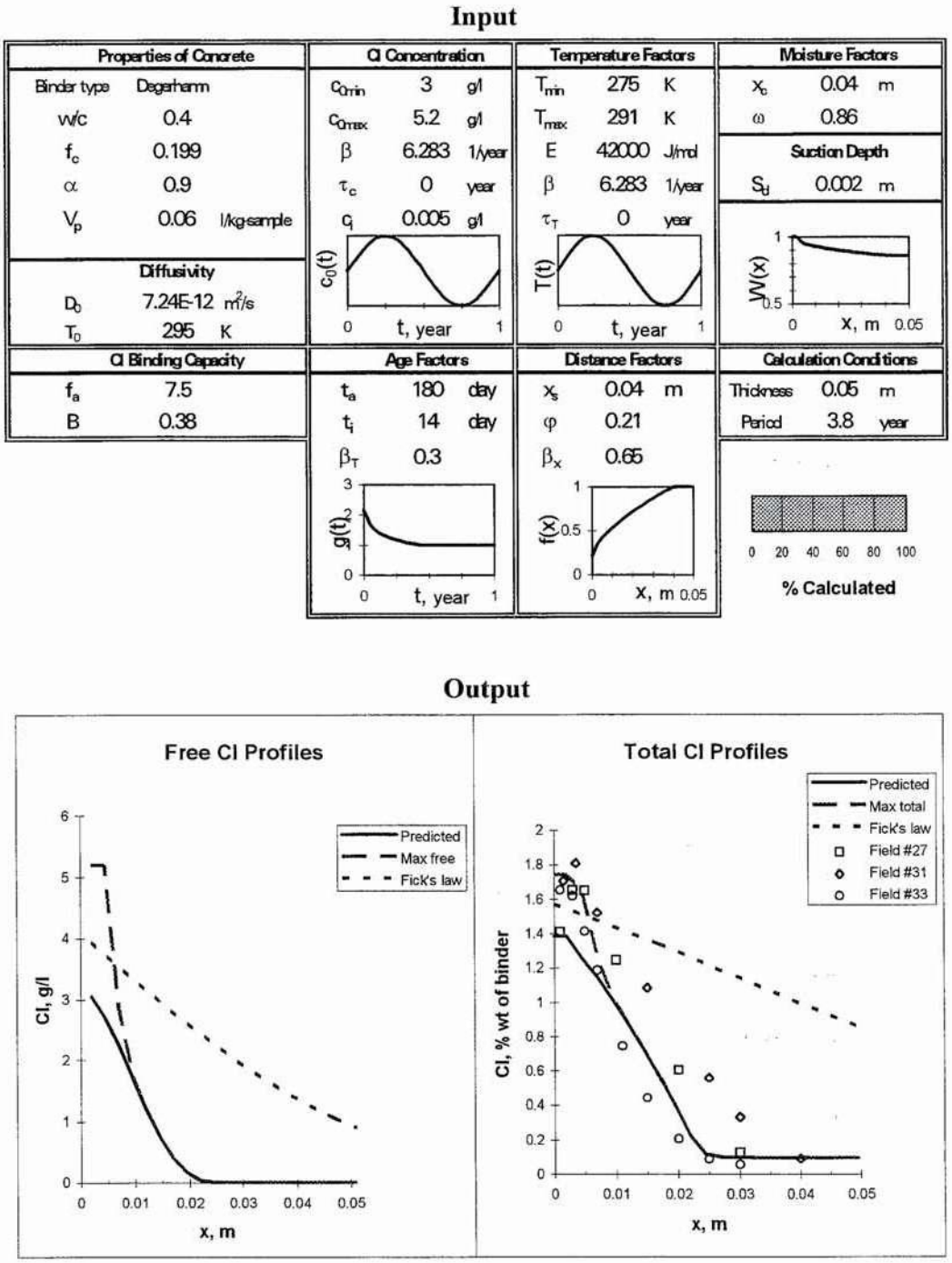

Fig. 9 Example of the predicted chloride penetration profiles.
Concrete: #27, #31 and 33 from Öland bridge /20/.

6. REFERENCES

/1/ Nilsson, L.-O. and Tang, L., "Transport mechanisms in porous materials—An introduction to their basic laws and correlations", presented at the NATO/RILEM Workshop, July 1994, St. Rémy-lès-Chevreuse, and to be published in *The Modelling of Microstructure and its Potential for Studying Transport Properties and Durability*, ed. H. Jennings et al.

/2/ Nilsson, L.-O., "A theoretical study on the effects of non-linear chloride binding on chloride diffusion measurements in concrete", Publ. P-92:13, Dept. of Building Materials, Chalmers University of Technology, Göteborg, 1992.

/3/ Sørensen, H. and Frederiksen, J.M., "Testing and modelling of chloride penetration into concrete", Proceedings of Nordic Concrete Research Meeting, pp. 354-356, Trondheim, 1990.

/4/ Petersen, C.G., "RCT profile grinding kit for in-situ evaluation of the chloride diffusion coefficient and the remaining service life of a reinforced concrete structure", in *Chloride Penetration into Concrete Structures—Nordic Miniseminar*, ed. L.-O. Nilsson, pp.182-192, Publ. P-93:1, Dept. of Building Materials, Chalmers University of Technology, Göteborg, 1993.

/5/ AASHTO, "Standard Method of Sampling and Testing for Total Chloride Ion in Concrete and Concrete Raw Materials", American Association of State Highway and Transportation Officials, Designation: T 260-84, Washington D.C., 1984.

/6/ British Standards Institution, "Methods for analysis of hardened concrete", BS 1881:part 124, London, 1988.

/7/ ASTM, "Standard test Methods for chemical analysis of hydraulic cement", Designation: C 114-88, Philadelphia, 1988.

/8/ Dhir, R.K., Jones, M.R. and Ahmed, H.E.H., "Determination of total and soluble chlorides in concrete", Cement and Concrete Research, Vol. 20, No. 4, pp. 579-590, 1990.

/9/ Tang, L., "A simple method for preparing reference concrete containing chlorides", in *Chloride Penetration into Concrete Structures - Nordic Miniseminar*, ed. by L.-O. Nilsson, Division of Building Materials, Chalmers University of Technology, Göteborg, pp. 81-89 Publication P-93:1, Jan. 1993.

/10/ Gran, H.C., "Measurement of chlorides in concrete—An evaluation of three different analysis techniques", Nordtest Technical Report 188, Norweigian Building Research Institute, Oslo, 1992.

/11/ Arya, C. and Newman, J.B., "An assessment of four methods of determining the free chloride content of concrete", Materials and Structures, Vol. 23, pp. 319-330, 1990.

/12/ Tritthart, J., "Chloride binding in cement: I. Investigations to determine the composition of porewater in hardened cement", Cem. Concr. Res., vol. 19, No. 4, pp. 586-594 , 1989.

/13/ Nagataki, S., Otsuki, N., Wee, T.-H. & Nakashita, K., "Condensation of chloride ion in hardened cement matrix materials and on embedded steel bars", ACI Materials Journal, Vol.90, No. 4, pp. 323-332, 1993.

/14/ Sandberg, P., "Chloride binding capacity in concretes exposed in the field", unpublished paper, Cementa AB/Lund Institute of Technology, Lund, 1993.

/15/ Buenfield, N., Conc. Rep. Maint., No.2, p. 7 (1986).

/16/ Sandberg, P. and Larsson, J., "Chloride binding in cement pastes in equilibrium with synthetic pore solutions", in *Chloride Penetration into Concrete Structures - Nordic Miniseminar*, ed. by L.-O. Nilsson, Division of Building Materials, Chalmers University of Technology, Göteborg, pp. 98-107, Publication P-93:1, Jan. 1993.

/17/ Tang, L. and Nilsson, L-O., "Chloride binding capacity and binding isotherms of OPC pastes and mortars", Cement and Concrete Research, Vol. 23, No. 2, pp. 347-353, 1993.

/18/ Byfors K., "Chloride-initiated reinforcement corrosion—Chloride binding", CBI Report 1:90, Swedish Cement and Concrete Research Institute, Stockholm, 1990.

/19/ Mats, R. and Nilsson, L.-O., "Moisture profiles from a marine concrete structure in Esbjerg Harbour", internal report, , Dept. of Building Materials, Chalmers University of Technology, Göteborg, 1994.

/20/ Tang, L. and Nilsson, L-O., "A numerical method for prediction of chloride penetration into concrete structures", presented at the NATO/RILEM Workshop, July 10-13, 1994, St. Rémy-lès-Chevreuse, and to be published in *The Modelling of Microstructure and its Potential for Studying Transport Properties and Durability*, ed. H. Jennings et al.

Matematisk modellering af

tidens indflydelse på chloridindtrængning i beton

vurderet ud fra feltmålinger

Ervin Poulsen, AEClaboratoriet. Vedbæk 1995-01-15

Baggrund

Beton er et materiale, som i løbet af sin funktionstid ændrer sig meget med hensyn til egenskaber og karakteristika.

Chloridindtrængning i frisk beton

Beton har væskeegenskaber ved udstøbningen $t = 0$. Ved chloridpåvirkning af frisk beton vil chloridindtrængningen være at sammenligne med chloriddiffusion i en væske , dvs. frisk cementpasta.

Chloridindtrængning i ung beton

Blot få timer efter udstøbningen har beton undergået en faseændring og fået en begyndende struktur, der er porøs og gennemtrængelig. Der er udført enkelte laboratorieforsøg med chloridindtrængning i ung beton, jf. [Carlsen 1993] og [Luping 1992]. I denne tilstand yder den unge beton ikke særlig stor modstand mod chloridindtrængning. Det er fx kendt fra en tidligere danske betonnorm, jf. [DIF 1926], hvor der står følgende:

»Hærdningstiden, regnet til betonens udsættelse for havvandet, skal for beton af portlandcement mindst være 6 uger. Såfremt betonen overtjæres eller beskyttes på anden særlig måde, er alene styrkehensynet bestemmende«.

Et uheld

At nyudstøbt beton ikke yder særlig stor modstand mod chloridindtrængning, fremgår fx af et registreret, men ikke offentliggjort eksempel. Et armeret fundament til udvidelse af en bygning blev udstøbt en fredag. I løbet af weekenden kom der et brud på det kloakrør, der udledte chloridholdigt spildevand fra bygningen. Om mandagen blev der målt en chloridindtrængning (0,05 %BE) på ca. $a = 10$ mm.

Sættes eksponeringsperioden til t = ca. 2 dg; det svarer til ca. 0,005 år. Derved bliver chloriddiffusionskoefficienten stort regnet til:

$$D = \frac{a^2}{\pi \cdot t} \cong \frac{10^2}{\pi \cdot 0,005} = 6400 \text{ mm}^2/\text{år}$$

Tidens indflydelse på chloridindtrængning

Betons struktur ændrer sig med modenheden. Hærdning, der foregår i vandmættet tilstand, medfører en tættere struktur end hærdning, der sker i tørrere tilstand eller uden væsentlig fugttilførsel.

Potentiel chloriddiffusivitet i laboratoriet

Den gunstigste lagring under hydratiseringen forekommer ved lagring af beton i vandbad i laboratoriet. Måling af betons potentielle chloriddiffusivitet under denne form for gunstig lagring har da også vist, jf. [Luping 1991], at betons potentielle chloriddiffusionskoefficient aftager med betonens modenhed efter følgende model:

$$D_p(t) = D_{pex}\left(\frac{t_{ex}}{t}\right)^{\beta}$$

Heri er t_{ex} tidspunktet for chlorideksponeringens start og t er betonens alder, alt regnet som modenhed eller klokketid ved konstant temperatur. Størrelsen D_{pex} er betons chloridkoefficient til tiden $t = t_{ex}$ og den afhænger af parametre som *v/b*-forholdet, bindemiddeltype og kompakteringen. Eksponenten β afhænger af blandt andet bindemidlets indhold af mikrosilica.

Potentiel chloriddiffusivitet i felten

Lagringsbetingelser er ikke altid så gode som i laboratoriets vandlagringskar. Betonen i marine konstruktioner *under* vandlinien har gode betingelser, når først den påvirkes af vand. Der er imidlertid gået en tid forud, hvor betonen, efter afformningen, ikke havde gode hærdningsbetingelser.

Betonen i marine konstruktioner *over* vandoverfladen hærdner kun med det fugttilskud, som kommer fra kapillarsugning, slagregn og bølgesprøjt. Samtidig medfører blæst en udtørrende effekt, som kan opveje fugttilførslen – i det mindste i betonens overfladelag, som danner armeringens dæklag.

Undersøgelser af betonemner, som er udsat i havnen i Träslövsläge, har vist, at måling af den eksponerede betons potentielle chloriddiffusivitet ved APM 302 på udborede betonkerner i uforstyrret beton, ikke altid følger den lov, som findes for potentiel chloriddiffusivitet i laboratoriet. Man har således nok fundet, at neddykket betons potentielle chloriddiffusionskoefficient aftager med tiden, men for den beton, som befinder sig over vandoverfladen kan man også finde, at den potentielle chloriddiffusionskoefficient vokser med tiden.

Årsagen hertil kan naturligvis være den ufuldstændige hydrationsproces, som finder sted med underskud af vand. Det kan imidlertid også være et udtryk for, at betonen ikke er vandmættet i konstruktionen (som i laboratoriets vandbad) og at det forsøg, som gøres i APM 302 på at vandmætte beton inden chlorideksponering ikke er tilstrækkeligt. Dét må nok undersøges nærmere.

Opnået chloriddiffusivitet i felten

Chloridpåvirkning i felten er mindre intensiv end i laboratoriets prøvningsmetode APM 302, som bruger eksponering af beton med en opløsning af 10 procent chlorid ved en temperatur på $T = 23$ °C.

Beton i marine konstruktioner *over* vandlinien får tilført luftbåren chlorid ved blæst. Derfor har læ og luv en markant indflydelse på chloridindtrængningen, jf. [Sand 1993].

Det er umiddelbart acceptabelt, at beton over vandlinien med sporadisk chloridindtrængning, ikke har den hastige chloridindtrængning som konstateres ved APM 302. Det kan imidlertid undre, at beton i marine konstruktioner *under* vandlinien også har en markant mindre chloridindtrængningshastighed end man ser i APM 302.

For beton i marine konstruktioner, såvel over som under vandoverfladen og i selve splashzonen, kan man efter målinger i felten, både i Träslövsläge havn og andre steder,

jf. [Takewaka 1988] og [Mangat 1994], modellere betons opnåede chloriddiffusionskoefficient, bestemt ved APM 207 eller tilsvarende prøvningsmetode, med følgende relation:

$$D_a(t) = D_{aex}\left(\frac{t_{ex}}{t}\right)^{\alpha}$$

Heri er t_{ex} tidspunktet for chlorideksponeringens start og t er betonens alder, alt regnet som modenhed eller klokketid ved konstant temperatur. Størrelsen D_{aex} er betonens opnåede chloridkoefficient til tiden $t = t_{ex}$ og den afhænger af parametre som chlorideksponeringens intensitet, *v/b*-forholdet, bindemiddeltype og kompakteringen. Eksponenten α kan afhænge af betonens placering i konstruktionen (læ, luv og afstand over vandoverfladen) samt naturligvis bindemidlets indhold af mikrosilica mv.

Opnået chloridprofils randværdi C_s

Af de andre af chloridprofilets parametre C_i og C_s er C_i konstant ifølge sin betydning som betons initiale indhold af chlorid, tilført af delmaterialerne (tilsætningsstoffer og sømaterialer) i blandingstidspunktet.

Beregnet værdi af C_s

De første års målinger af opnåede chloridprofiler i beton i Träslövsläge viser, at chloridprofilers randværdi, dvs. den beregnede værdi C_s ved ikke-lineær regressionsanalyse af observerede chloridkoncentrationer i beton versus afstand fra den chlorideksponerede betonoverflade, ikke er konstant, som normalt antaget, men vokser med eksponeringstiden de første par år. Derefter synes C_s at blive konstant.

Aktuel værdi af C_s i betonoverfladen

Mange ydre forhold synes at påvirke det aktuelle indhold af chlorid i en betonoverflade, fx udludning og carbonatisering af betonoverfladen, jf. [Tuutti 1982].

Dette forhold påvirker betonens opnåede chloridprofil nær betonoverfladen. Det er imidlertid opfattelsen, at denne virkning kan negligeres nær armeringens placering, blot man ser bort fra et passende antal observationer i betonens overflade, jf. [Poulsen 1995], – og helst dokumenteret ved tyndslibsanalyse.

Forhold mellem opnået og potentiel diffusionskoefficient

Chloridindtrængningshastigheden i beton i en konstruktion kan ydtrykkes ved den opnåede chloriddiffusionskoefficient. Chloridindtrængningshastigheden kan imidlertid være stor af flere grunde:

- Fordi chloridbelastingen på betonen er stor.
- Fordi betonens modstandsevne mod chloridindtrængning er lille af materialebetingede grunde.

For at »rense« målet for chloridindtrængningshastighed for de materialebetingede grunde, jf. [Maage 1993] kan man derfor anvende forholdet mellem opnået diffusionskoefficient $D_a(t)$ og potentiel diffusionskoefficient $D_p(t)$ til samme tid:

$$\delta(t) = \frac{D_a(t)}{D_p(t)}$$

Da $D_a(t)$ og $D_p(t)$ begge afhænger af tiden, vil $\delta(t)$ også kunne afhænge af tiden t. Det viser sig imidlertid, at $\delta(t)$ kan skrives på følgende form, jf. [Maage 1993]:

$$\delta(t) = \left(\frac{t_{ex}}{t}\right)^{\gamma}$$

Heri er t_{ex} tidspunktet for chlorideksponeringens start og t er betonens alder, alt regnet som modenhed eller klokketid ved konstant temperatur. Eksponenten γ synes efter vurdering af de første målinger at være uafhængig af tiden, men γ afhænger væsentligt af af betonens placering i konstruktionen (læ, luv og afstand over vandoverfladen), jf. [Maage 1993] og [Mangat 1994].

Eksponenten γ er derfor egnet til at beskrive en marin betonkonstruktions chloridpåvirkning i dens typiske zoner i et givet miljø (over og under vandlinien samt i splashzonen).

Det ses umiddelbart, at $\alpha = \beta + \gamma$, således at kun to af disse tre parametre er nødvendige. Det er dog bekvemt at anvende alle tre parametre til at beskrive tidsafhængigheden af betons chloriddiffusivitet.

Modelverifikation ved feltmålinger

Der er en del usikkerheder ved bestemmelse af såvel betons potentielle som opnåede chloridprofil, jf. [Poulsen 1995]. Denne er imidlertid ikke større end, at chloriddiffusivitetens afhængighed af tiden kan bestemmes ved feltforsøg som fx Cementas i Träslövsläge og A/S Storebæltsforbindelsens på Nyborg strand, blot der er målt med passende tidsintervaller og over en tilstrækkelig lang periode.

Mange feltforsøg, som i tidens løb er blevet gennemført i et stort omfang, har ikke altid som grundlag haft en generel hypotese. Derfor har det ofte været vanskeligt at konkludere andet om chloridindtrængningen end gældende for den chlorideksponering, som de pågældende prøveemner har været udsat for under det pågældende feltforsøg. Det gælder fx de ellers udmærkede feltforsøg i UK, jf. [Mangat 1994].

Ved estimering af de bestemmende parametre α, β og γ, kan man gå to forskellige veje:

- *Stepvis regression.* Først fastlægges D_p og D_a ud fra chloridprofilernes observerede chloridkoncentrationer versus afstanden x fra chlorideksponeret betonoverflade ved ikke-lineær regressionsanalyse. Derefter kan man bestemme α, β og γ ved lineær regressionsanalyse.
- *Samlet regression.* Bestemmelse af α, β og γ sker direkte ved ikke-lineær regression af samtlige observationer.

Den første metode er den ingeniørmæssigt mest overskuelige. Den svarer til den fremgangsmetode, man vil anvende ved estimering af levetiden for marine betonkonstruktioner på basis af planlagt inspektion med prøvning.

Estimering af α

Under forudsætning af, at der i den valgte forsøgsperiode er et passende antal bestemmelser af opnåede chloridprofiler, og at de er bestemt over en tilstrækkelig lang periode, kan variationen af α findes i afhængighed af eksponeringstiden.

I et dobbelt logaritmisk koordinatsystem vil D_a plottet i relation af t tilnærmelsvis afbilde en ret linie. Heraf kan α bestemmes ved ikke-lineær regressionsanalyse af de fundne data. Problemet er, at feltforsøg ofte er gennemført ved observationer med konstante tidsintervaller. I stedet burde tidsintervallerne være logaritmisk fordelt, således at den første bestemmelse af et opnået chloridprofil blev foretaget til det tidspunkt, der alene var bestemt af hvornår det er måleteknisk muligt at foretage en passende nøjagtig bestemmelse, dvs. på det tidspunkt, hvor chloridindtrængningen er så stor, at der kan opnås fx 5 observationer på chloridprofilet.

Feltundersøgelsen bør strækkes over en passende lang tid, således at det kan opnås tilstrækkelig mange værdier for α versus tiden til, at:

- α kan bestemmes med den ønskede nøjagtighed.
- det kan fastslås, at det er rimeligt at regne α konstant.

Estimering af β og γ

Tilsvarende forhold gælder for β og γ, som er beskrevet under estimering af α.

Normmæssig fastsættelse af α, β og γ

Det endelige mål er indflydelse på normer for projektering og udførelse af marine betonkonstruktioner. Her kan man næppe anvende α, β og γ. I stedet vil tabeller i normen over *armerings dæklag* i afhængighed af følgende parametre være acceptabelt (det svarer til forholdene i dag, hvor man kun har én tabel for aggressiv miljøklasse):

- Levetid, fx 50 og 100 års funktionstid (før korrosionsstart).
- Armeringens placering i konstruktioner, fx under og over vandlinien (læ og luv) samt i splashzonen.
- Betonens sammensætning, fx på tre forskellige niveauer, dvs. efter chloriddiffusivitet bestemt ved *v/b*-forhold og pulversammensætning.

Der er naturligvis andre måder at præsentere resultatet, fx ved et regneprogram (på diskette) eller ved diagrammer til bestemmelse af det nødvendige dæklag for armeringen i de forskellige situationer.

En afgørende parameter for bestemmelsen af armerings nødvendige dæklag er den kritiske chloridkoncentration og sikkerhedsniveauet. Dette medtages ikke i dette notat.

Litteratur

Carlsen, Jan Erik. »Chloride penetration in green high performance concrete – some results«. Nordic Miniseminar, CTH. Göteborg 1993.

DIF. »Foreløbige regler for beregning og udførelse af jernbetonkonstruktioner i vandbygning«. Dansk Ingeniørforening. København 1926.

Luping, Tang og Nilsson, Lars-Olof. »Chloride diffusivity in high strength concrete at different ages«. Nordic Concrete Research, publication no. 11. Oslo 1992.

Maage, M., Helland, S., og Carlsen, J. E. »Chloride penetration in high performance concrete exposed to marine environment«. Symposium on Utilization og High Strength Concrete. Lillehammer, 1993.

Mangat, P. S., og Molloy, B. T. »Prediction of long term chloride concentration in concrete«. Materials and Structures, 1994, Vol. 27, No. 170.

Poulsen, Ervin. »Chloride profiles, analysis and interpretation of observations. Nordic Miniseminar, LTH. Lund 1995.

Sand, Berit Tora. »The effect of the environmental load on chloride penetration«. Nordic Miniseminar, CTH. Göteborg 1993.

Takewaka, K., og Mastumoto, S. »Quality and cover thickness of concrete based on the estimation of chloride penetration in marine environments«. Concrete in Marine Environment, Proceedings, Second International Conference St. Andrews by-the-Sea, Canada 1988, ACI SP-109.

Tuutti, Kyösti. »Corrosion of steel in concrete«. CBI research fo 4-82. Cement- och betonginstitutet. Stockholm 1982.

CHLORIDE PROFILES

Analysis and Interpretation of Observations

Ervin Poulsen. AEClaboratory, 20 Staktoften. DK-2850 Vedbæk, Denmark.

ABSTRACT

When unprotected concrete is exposed to aggressive substances containing chloride, the chloride will penetrate the concrete. The natural content of chloride in the pore liquid and the binder of the near-to-surface layer of concrete will rise. It is possible to describe the chloride exposure and the ingress by the content and distribution of chloride in the near-to-surface layer of concrete. The distribution of chloride of the near-to-surface layer of concrete is named the chloride profile of the concrete.

The paper describes how a chloride profile can be determined, i.e. the grinding techniques of producing the powder samples, the analyses of their chloride contents and the interpretation of these observations. Furthermore, it is described how the chloride profile can be reduced to three parameters when the chloride ingress is caused by chloride diffusion. Finally, it is discussed how these parameters are estimated from a given chloride profile.

Keywords. Chloride profile, grinding techniques, chloride analysis, diffusion, curve-fitting.

INTRODUCTION

When concrete is exposed to chloride it has become normal practice to describe the concrete's response to the chloride exposure by its chloride profile, i.e. the distribution of the chloride content of the concrete in its near-to-surface layer or the concentration-distance curve. The techniques of how to determine a chloride profile have developed through the years, but a standard technique for the procedure has not yet been established. There are various grinding and drilling techniques, but there are neither standard requirements to the grinding and drilling techniques nor recommendations as to interpretation of the observations found using these techniques.

Sources of chlorides

There are several sources of chlorides. Traditionally, the origins of chlorides in concrete are divided into

- *Chlorides incorporated* in the concrete when it was mixed, e.g. from salty aggregates, salty mixing water and admixtures containing chloride.
- *Chlorides penetrating* into the concrete from the environment, e.g. from seawater, salty pool-water, salty groundwater, sea spray, de-icing salts, from processing or storage of halites, and from other industries like the food-industries (slaughterhouses, osterias etc.).

Only a decade ago it was believed that the chlorides incorporated in the concrete when it was mixed were bound (insoluble) chlorides and should therefore not be risky as long as the content of chloride was kept at a maximum of 2 per cent by mass binder. Now several cases have shown that bound chlorides will be released by carbonation and leaching leading to corrosion.

Types of chloride ingress

Chloride can penetrate into the hardened concrete from its environment applying various mechanisms of transport

- *Absorption* of salty water by capillary suction, i.e. the water moves towards the driest part.
- *Permeation* of salty water caused by hydrostatic pressure, i.e. the water moves towards part of the concrete with less pressure.
- *Diffusion* of chlorides caused by differences in chloride concentration, i.e. the chloride moves towards part of the concrete with less chloride concentration.

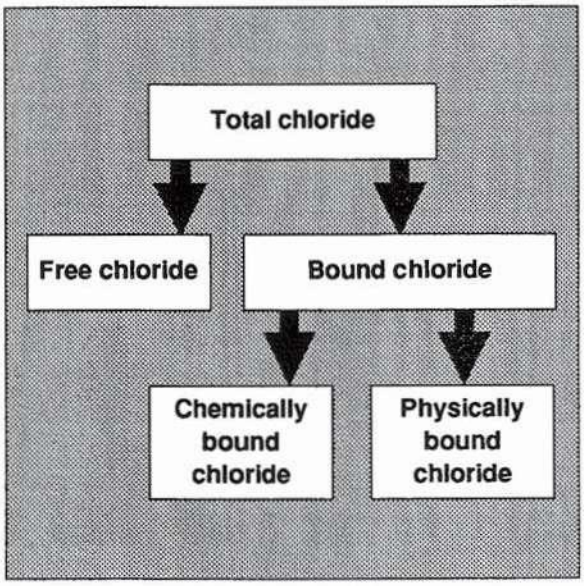

Figure 1. *The chlorides of concrete are bound to the cementing matrix in various degrees. Some chlorides are free and found in the pore liquid as a solution. Some chlorides are bound to the cement gel, i.e. the C-S-H particles of the binder. Physical binding (adsorption) as well as chemical binding exist.*

The relationship between the free and the bound chlorides will vary with the type of binder and has to be determined experimentally.

- *Electro-migration* of chlorides caused by differences in electrical potential, i.e. the chloride moves towards part of the concrete with higher electrical potential.

In general chloride ingress into concrete is a combination of several transport mechanisms but with one mechanism as the predominant. A special case is »wetting and drying« of concrete in the splash-zone where the cycling effect will increase the absorption of chloride.

The dominant transport mechanism of uncracked high performance concrete is diffusion, while permeation is the dominant transport mechanism of any cracked concrete.

Types of chloride profiles

Concrete contains »free« chloride in its pore liquid and chloride »bound« to its cementing matrix. The bound chlorides are chemically as well as physically bound (adsorption). The »total« chloride is defined as the content of free and bound chloride. The various types of chlorides in concrete call for four different chloride profiles.

The gradation of the coarse aggregates changes with the distance from the concrete surface, cf. [Suenson, 1942, p.228] and [Frederiksen 1993, p.90]. The content of cement matrix is higher in the near-to-surface layer. For concrete cast in a mould this layer will be of the order of half the maximum grain size of the aggregates. At horizontal concrete surfaces where separation of the coarse aggregates has taken place the layer of concrete being rich in cement matrix will often be significantly thicker.

The chlorides of concrete are present in the cement matrix, either as free chlorides in the pore liquid or bound to the binder, e.g. the cement and flyash. Thus, when relating the chloride to the binder of the concrete the concrete's »binder profile« must be known. When the aggregate does not contain calcite the distribution of binder through the near-to-surface layer of the concrete is determined by means of the calcium profile of the concrete.

Measurements of chlorides

The various types of chlorides in concrete are determined by measurements in different ways. The total amount of chloride is found as acid-soluble chloride while the free chloride is found as water-soluble chloride. Thus the bound chloride is the difference between the total and the free chloride.

It is the free chlorides that are able to cause corrosion of embedded reinforcement and inserts of corrosive metals. Therefore, it is of interest to measure the free chlorides of concrete, especially, since the ratio bound to free chlorides varies with the types of binders. E.g. concrete

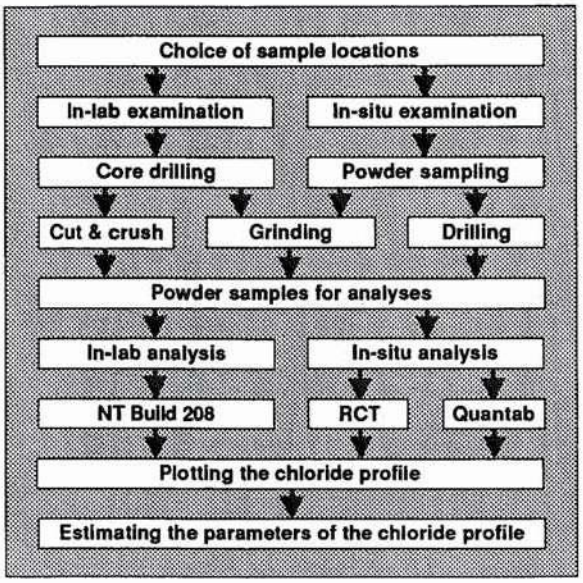

Figure 2. *Flow-diagram of the possible ways for the determination of a chloride profile. It can either be determined in-situ by grinding or drilling techniques and obtain enough (7-10 nos.) powder samples to determine a chloride profile, cf. Figure 4, by the test method RCT or by Quantab in order to determine the chloride content of each powder sample.*

In can also be done by drilling a core from the concrete structure and produce enough powder samples in the laboratory by cutting or grinding techniques, cf. Figure 3, so that the chloride profile can be determined by the test method NT Build 208 in order to determine the chloride content of each powder sample.

Each of the operations of this flow-diagram will add uncertainties to the determination of the chloride profile. This has to be studied in detail before the application of the chloride profile, e.g. for the determination of the structure's service lifetime.

made with flyash and slag as part of the binder has a high binding capacity. Even concretes made with the various types of cement have different binding capacities. Concrete made with sulphate resisting cement for example has a lower binding capacity than concrete made with other Portland cements, other parameters made equal.

When in the USA the chloride content of concrete became an important parameter to control ACI required in 1977 that the free (water soluble) chloride of the concrete was kept at a low level. Later this was changed to a requirement to the total (acid soluble) chloride content of concrete, determined by the test method ASTM C 114, due to lack of reproduciability of the content of the free chlorides.

Sources of uncertainties

There are several sources of uncertainties and even mistakes can take place as shown by several round robin tests. There are four main sources of uncertainties

- *Exposure conditions,* in field as well as in laboratory.
- *Preparing samples for analyses,* in-situ as well as in laboratory.
- *Analysis of chloride content,* the test methods chosen in-situ as well as in the laboratory.
- *Interpretation of observations,* when rejecting or accepting observations for curve-fitting.

A few comments on these main sources are given as follows.

Exposure conditions in field

The local environment plays an important role for the chloride ingress, cf. [Sand 1993, p.113]. A predominant direction for strong winds leads to difference in chloride ingress at windward and leeward parts of a structure exposed to airborne chloride, e.g. in coastal regions. Generally speaking the concrete at the leeward part of the structure will contain more chloride than the concrete at the windward side, other parameters being equal. The concrete at the leeward side is often sheltered from the heavy rains which at the windward side tend to wash down most of the chlorides deposited at the concrete surface by sea spray, salty fogs etc.

Besides the influence from this shelter effect the concentration of the airborne chloride is not constant but varies with the level above sea-level and the distance from the beach.

When sampling concrete in order to determine its chloride content one has to take the above mentioned influences into account. No guidance, recommendation or standard exist for the sampling of concrete for this purpose.

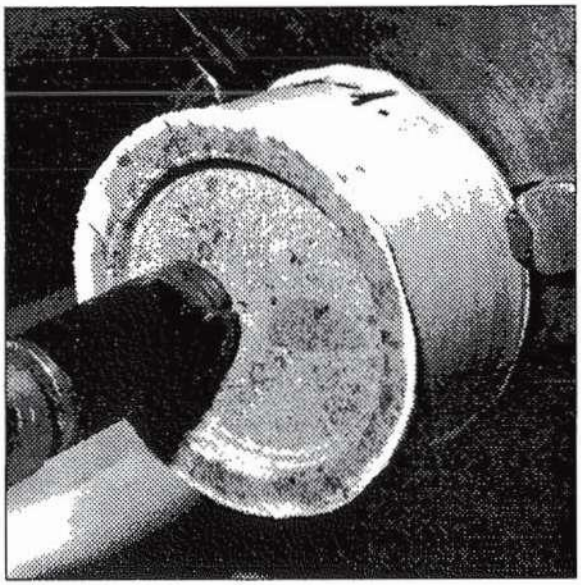

Figure 3. Equipment for the grinding and collecting of concrete powder from thin layers, each from 0.7 mm to 2 mm. The photograph shows a technique used for the grinding process when applying a turning lathe. The concrete core is fixed into the lathe and rotates simultaniously while very thin layers of concrete powder are milled away by a rotating diamand tool which moves horizontally.

The concrete powder is collected and analysed by a chemical test method, e.g. NT Build 208, in order to determine the chloride content of the powder.

The diameter of the core and the thickness of the layers milled away should be chosen such that the cement content of a powder sample for an analysis fulfil the requirement given by NT Build 208 or similar test method used for the analysis of the chloride content.

Laboratory exposure conditions

In order to characterise the intrinsic chloride diffusivity of concrete, samples of concrete are exposed to a standard solution of chloride as for the test method APM 302, cf. [AEC 1991] and [Frederiksen 1992], or a similar test method. By keeping important parameters like temperature, chloride concentration and exposure period constant and by cutting off a 10 mm thick slice of the concrete from the exposed surface, the deviation of the observation is kept at a minimum.

However, the deviations found by round robin test are not negligible and the sources of the uncertainties may be found in minor differences in test conditions, the microstructure of the concrete (degree of compaction and intensity of defects), and the processing of the powder samples for analyses more than the application of titration procedures.

Preparation of powder samples for analyses

As explained later several techniques are used in order to prepare samples of the exposed concrete. The various sampling methods involve different types of deviation and it is important for the application of the found chloride profiles that this is taken into account. Furthermore, the choice of the numbers of observations to determine one chloride profile is also important, cf. [Pedersen 1993, p.81].

There is a need for several techniques for the preparation of the powder samples for analyses. However, one should realize the difference in the accuracy when applying a chloride profile determined by analyses of three powder sampels prepared by hammer drilling compared with a chloride profile determined by a dozen observations found by powder grinding. Both test methods are needed but the accuracy should be taken into account when applying the profiles.

Analysis of chloride content

Several test methods exist suitable for measurements in-situ as well as for laboratory purposes, cf. [Gran 1992], [Gran 1993, p.71] and [Reknes 1994]. Applied test methods in the Nordic countries are

- *RCT-method,* the Rapid Chloride Test method.
- *Quantab-method.*
- *Volhard-titration,* e.g. NT Build 208, cf. [NT Build 208 1984].
- *Potentiometric titration.*

The conclusion from the round robin test reported by [Reknes 1994] is that sufficient accuracy is obtained if

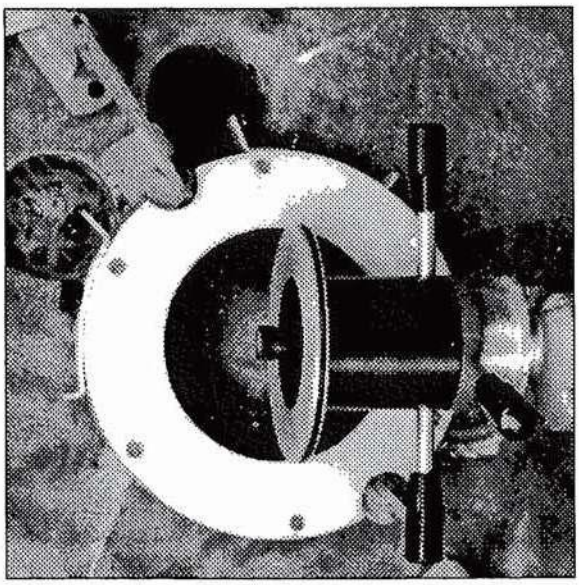

Figure 4. In-situ equipment for the grinding and collecting of concrete powder from thin layers, each by depth increment of 0.5 mm and upwords.

The Profile Grinding Kit is fixed to a concrete surface and the principle of milling correspond to that of Figure 3. On horizontal surfaces the powder is collected with a dustbuster with re-usable filter. On a vertical surface the collection of powder is made automatically in a plastic bag attached to the grinding plate.

The grinding area is circular with a diameter of 73 mm. The maximum depth of grinding is 50 mm. One powder sample from a 2 mm thick layer of concrete may be collected in appx. 5 minutes.

When a chloride profile has to be determined e.g. in the tensile zone of a beam it is not possible to use grinding of the concrete from a circular area with a diameter of 73 mm. Thus an oblong grinding area is used in order to avoid harming the rebars.

- □ Skilled personal should have fixed routines for the test method applied.
- □ The test equipment should be calibrated and well-kept.
- □ In-situ methods should not be applied in laboratory testing.
- □ Blind test samples should be incorporated to reveal any mistakes during the analysis.

Interpretation of observations

Based upon the theory of the assumed transport mechanism the observations are fitted to an analytic equation. This is discussed in details in the following section of the present paper.

PARAMETERS OF THE CHLORIDE PROFILE

Chloride ingress into the surface of a concrete structure can be determined and described by the achieved chloride profile. The total information about the environment, the exposure time and the achieved chloride profile will give a clear but also an inconvenient picture of the chloride exposure and the response of the concrete.

The information given by the exposure time and the achieved chloride profile of the concrete may be simplified by a few parameters, sufficient to determine the shape of the chloride profile from a mathematical point of view. The values of these parameters, their stocastic distributions and their development with time will give a convenient way of handling the chloride ingress into concrete.

As previously said the transport mechanism may vary with the composition, the compaction and the intensity and widths of the cracks of the concrete. Here, it is assumed that *diffusion is the predominant mechanism* of the chloride ingress and that the concrete is a quasi homogeneous material. These assumptions have proved to be valid for test specimens of uncracked high performance concrete having water/binder-ratios from 0.35 to 0.7 and tested by field exposure at Träslövsläge Harbour in Sweden. Similar agreement is found by the Great Belt Link Ltd. for a test specimen placed at the beach of Nyborg in Denmark.

Chloride profiles for diffusion

It is convenient to speak about two different chloride profiles, the *achieved chloride profile* and the *potential chloride profile*. These chloride profiles may determine bound chlorides as well as free chlorides according to the purpose of testing.

The achieved chloride profile is found in a concrete structure or a concrete specimen when

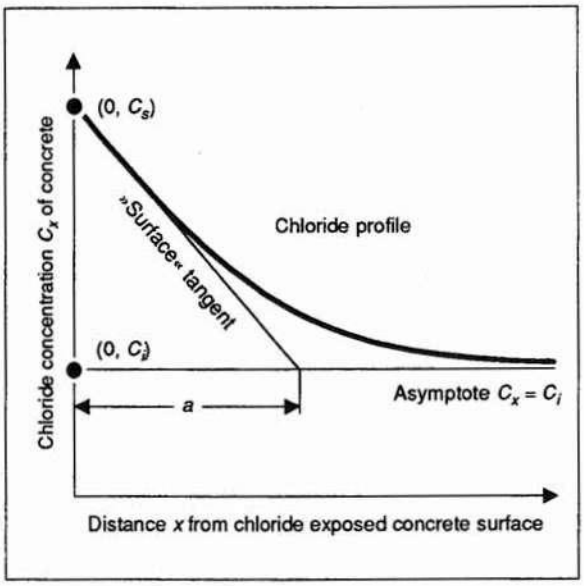

Figure 5. The definition of the line segment a as the distance along the asymptote $C = C_i$ from the ordinate axis to the intersection between the asymptote and the »surface« tangent.

field exposed to chloride. It could be said that the achieved chloride profile is the concrete's response to the chloride exposure from a given environment.

The potential chloride profile is found in a concrete specimen when exposed to a standard solution of chloride at a standard temperature and during a standard length of time. It could be said that the potential chloride profile is the concrete's intrinsic parameter, i.e. a materials constant.

For comparison it could be said that the achieved parameters and potential parameters are to be compared with the mechanical stresses in a loaded concrete structural member and the strength parameters of the concrete respectively – measured in a standard manner.

Achieved chloride profile

According to the assumptions given above the achieved chloride profile for chloride diffusion will be unambiguously determined by the following three parameters

- The initial chloride content C_{ia} of the concrete.
- The ordinate C_{sa} of the chloride profile at the surface of the concrete.
- The chloride diffusion coefficient D_a of the concrete.

As said these three parameters are not materials constants but they refer to the exposure load, including the exposure time and the age of the concrete. The achieved chloride profiles are determined by the test method APM 207, cf. [AEC 1989], or a similar test method.

Potential chloride profile

According to the assumptions given above the potential chloride profile for chloride diffusion will be unambiguously determined by the following three parameters

- The initial chloride content C_{ip} of the concrete.
- The ordinate C_{sp} of the chloride profile at the surface of the concrete.
- The chloride diffusion coefficient D_p of the concrete.

These three parameters are materials constants, but they refer to the test method. Potential chloride profiles are determined by the test method APM 302, cf. [AEC 1991], or any similar test method.

Equation of a chloride profile

The equation of a chloride profile created by chloride diffusion in concrete, the achieved as well as the potential chloride profile, is found by solving Fick's second law of diffusion for a semi-infinite medium, cf. [Crank 1973] and [Poulsen 1993]. When the chloride exposure

Figure 6. *Observations for a potential chloride profile found by means of the test method APM 302, cf. [AEC 1991]. The chloride profile is determined by the chloride contents C_x of 11 nos. of powder samples, each given by its distance x from the chloride exposed concrete surface.*

These observations are the basis for the examples covered by this paper. Various methods of estimation of the parameters of the chloride profile of the concrete are illustrated by the examples given, cf. examples 1-5.

Observation no.	Distance x mm	Chloride C_x % by mass concrete
1	0.40	0.440
2	1.30	0.306
3	2.25	0.227
4	3.00	0.145
5	3.80	0.094
6	4.80	0.051
7	6.15	0.025
8	7.90	0.011
9	9.35	0.005
10	48.25	0.001
11	53.20	0.001

remains constant the analytical expression of the chloride profile may be written as

$$C_x = C_i + (C_s - C_i)\,\mathrm{erfc}\left(\frac{x}{\sqrt{4\,t\,D}}\right)$$

Here and in the following the index a and p for achieved and potential properties respectively are left out. How to estimate the three parameters D, C_s and C_i from a given set of observations is dealt with later.

Deviations from the ideal shape

It is common knowledge that sometimes the above given mathematical equation will deviate from the shape of a determined chloride profile. Several possible reasons for such deviations could be mentioned. However, in each case the concrete should be investigated (e.g. by microstructural examination) before jumping to conclusions.

Two main deviations are observed, namely at the exposed concrete surface and at a small distance from the surface. The observed types of deviations are not the same for achieved and potential chloride profiles. Some reasons are listed below.

- A carbonated surface layer of chloride exposed concrete will have a much smaller binding effect than the non-carbonated concrete. This means that the concrete cannot be considered as a quasi homogeneous material but rather as two layers of different materials. This will not be relevant to the potential chloride profile since the concrete is not exposed to carbonation, cf. [AEC 1991].
- A leached surface layer of chloride exposed concrete will have a much smaller binding effect than the non-leached concrete. This means that the concrete cannot be considered as a quasi homogeneous material but rather as two layers of different materials. This will not be relevant to the potential chloride profile since the concrete normally is only exposed for a short period (35 days) to a chloride solution and care is taken to minimize any leaching effect, cf. [AEC 1991].
- A significant part of the penetrating chloride is bound to the C-S-H particles in the cement matrix of the concrete. Since the cement matrix is not uniformly distributed through the concrete (highest content at surface) the concrete is not a quasi homogeneous material. This phenomenon could be taken into account by another mathematical solution than given above. However, it is also a possible way to neglect the observations of chloride content in the outermost layer corresponding to appx. half the size of the coarse aggregate, i.e. appx. 10 mm. When determining a concrete's potential chloride profile this is done physically by cutting away the outermost layer of a thickness of 10 mm, cf. [AEC 1991].
- The exposure of concrete specimens to a concentrated solution of chlorides, as applied by

Figure 7. The observations (x, C_x) given in the Table of figure 6 plotted and the best estimate of the »surface« tangent drawn, i.e. tha tangent of the chloride profile at $x = 0$, cf. example 1.

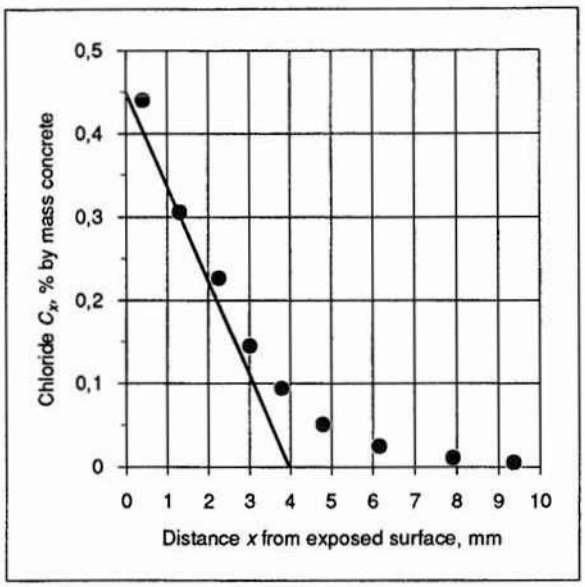

the test method APM 302 or similar methods, often results in a higher chloride concentration at the concrete surface ($x = 0$) than appears from the mathematical solution given above, cf. [Frederiksen 1993]. It is generally believed that chloride concentrates in cavities and voids of the exposed surface and this phenomenon has nothing to do with the diffusion mechanism.

Approximative methods of graphical estimations

It is a typical engineering method to plot the chloride profile and to estimate the parameters from the shape of the graph.

There are several such engineering methods the use of which mainly is for a first estimate of the parameters of chloride profiles, e.g. for a more accurate estimation by one of the iterative methods.

Method of »surface tangent«

From the graph of a chloride profile it is possible to give fairly accurate estimates of C_i and C_s while the estimate of D is not possible without a geometrical estimate of the position of the tangent of the chloride profile at the exposed concrete surface.

The slope of the chloride profile at the point (x, C_x) is the partial derivative of the function modeling the chloride profile

$$\frac{\partial C_x}{\partial x} = - \frac{C_s - C_i}{\sqrt{\pi t D}} \exp\left(- \frac{x^2}{4 t D}\right)$$

Thus the tangent of the chloride profile at the point $(0, C_s)$ determines a line segment a of the asymptote from the ordinate axis to the intersection between the tangent and the asymptote. The length of a is

$$a = \sqrt{\pi t D}$$

From this equation it is seen that the chloride diffusion coefficient D could be expressed as

$$D = \frac{a^2}{\pi t}$$

Figure 8. Observations for a potential chloride profile found by means of the test method APM 302, cf. [AEC 1991]. The chloride profile is determined by the chloride content C_x of 11 nos. of powder samples, each given by its distance x from the chloride exposed concrete surface.

For the purpose of approximative determination of the diffusion coefficient D by linear curve-fitting a new ordinate y is calculated, where

$$y = \text{erfc}^{-1}\left(\frac{C_x - C_i}{C_s - C_i}\right)$$

Observation no.	Distance x, mm	Chlorid C_x,% by mass concr.	Transformed y no unit
1	0.40	0.440	—
2	1.30	0.306	0.292
3	2.25	0.227	0.473
4	3.00	0.145	0.702
5	3.80	0.094	0.892
6	4.80	0.051	1.127
7	6.15	0.025	1.369
8	7.90	0.011	1.620
9	9.35	0.005	1.798
10	48.25	0.001	—
11	53.20	0.001	—

This equation leads to a simple rule: from the graph of the chloride profile the asymptote C_i is estimated. The line segment $b = C_s - C_i$ of the ordinate axis cut off by the chloride profile and the asymptote is estimated and the parameter yields $C_s = b + C_i$. Finally the line segment a of the asymptote from the ordinate axis to the intersection between the tangent and the asymptote is estimated and the chloride diffusion coefficient is calculated from the above found formula where t is the exposure time.

Example 1. A chloride profile has been determined by measuring the simultaneous values of x and C_x as shown in the table of Figure 6. The observations were obtained by means of the test method APM 302, cf. [AEC 1991], and the exposure period was $t = 0.18$ year.

The initial chloride content of the concrete C_i was measured on samples of virgin concrete at a distance of appx. 50 mm from the exposed concrete surface, cf. samples nos. 10 and 11 in the Table of Figure 6. This yields the initial chloride content as

$$C_i = 0.001 \text{ per cent by mass concrete}$$

The chloride profile is drawn, cf. Figure 7. From this graph it yields that the ordinate of the chloride profile at the surface of the concrete is

$$C_s = 0.45 \text{ per cent by mass concrete}$$

The tangent of the chloride profile at the point $(0, C_s)$ is drawn and the the segment line a is estimated to be $a = 4$ mm, cf. Figure 7. Thus the chloride diffusion coefficient yields

$$D = \frac{a^2}{\pi t} = \frac{4^2}{\pi \times 0.18} = 28 \text{ mm}^2/\text{year}$$

Estimation by means of three sets of observation

Estimation of the parameters of a chloride profile by the above mentioned method requires that the chloride profile is undisturbed at the surface. However, an achieved chloride profile will often be influenced by side effects as described above. This means that it may be difficult to estimate the position of the tangent of the chloride profile at the concrete surface.

From the shape of a given chloride profile it is possible to estimate C_i and C_s with a suitable accuracy even if the chloride profile is disturbed at the surface ($x = 0$). In order to estimate the diffusion coefficient D a suitable point (x_m, C_m) of the chloride profile can be estimated. The parameter D is then determined in such a way that the chloride profile

- Starts at $(x, C_x) = (0, C_s)$.
- Passes through $(x, C_x) = (x_m, C_m)$.
- For $x \to \infty$ yields the asymptote $C_x = C_i$.

Figure 9. The transformed ordinate y plotted versus the distance x from the chloride exposed concrete surface. Two lines found by curve-fitting are shown – one taking samples nos. 2-9 into account and one taking samples nos. 2-7 into account, cf. example 3.

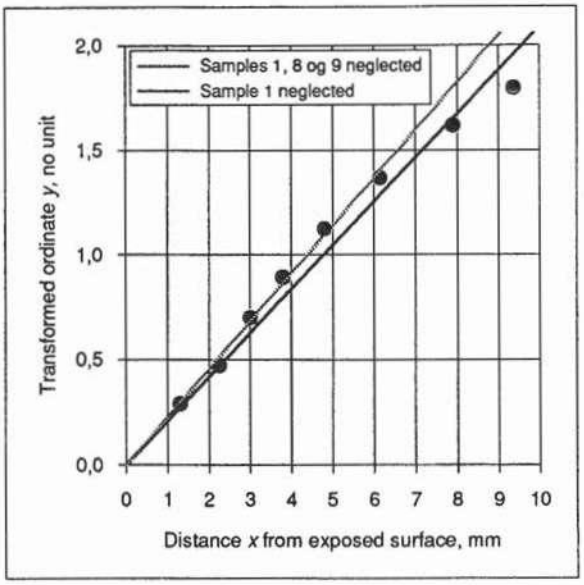

These conditions will give a convenient determination of D. However, the result depends on the choice of the point (x_m, C_m) and the determination of D is not unambiguous.

Thus, it is required that (x_m, C_m) is a point of the chloride profile

$$C_x = C_i + (C_s - C_i)\,\mathrm{erfc}\left(\frac{x}{\sqrt{4\,t\,D}}\right)$$

This means that D can be determined by the following equation

$$C_m = C_i + (C_s - C_i)\,\mathrm{erfc}\left(\frac{x_m}{\sqrt{4\,t\,D}}\right)$$

By introducing a new parameter y_m defined by the expression

$$y_m = \mathrm{erfc}^{-1}\left(\frac{C_m - C_i}{C_s - C_i}\right)$$

the diffusion coefficient is found by the following solution

$$D = \left(\frac{x_m}{y_m\sqrt{4\,t}}\right)^2$$

Values of the functions erfc and erfc^{-1} are tabled in suitable handbooks of mathematics, cf. [Spiegel 1968], and in textbooks on diffusion theory, cf. [Crank 1973].

Example 2. For the same chloride profile as dealt with in Example 1 it is estimated that it should pass through a point with abscisse $x_m = 3.0$ mm and ordinate $C_m = 0.145$ per cent by mass concrete, corresponding to the observation no. 4 in the Table of Figure 6.

As in Example 1 the values of the parameters $C_i = 0.001$ per cent by mass cement and $C_s = 0.45$ per cent by mass cement are estimated. Thus the parameter y_m is

$$y_m = \mathrm{erfc}^{-1}\left(\frac{0.145 - 0.001}{0.15 - 0.001}\right) = \mathrm{erfc}^{-1}(0.321) = 0.702$$

By applying $x_m = 3.0$ mm, $y_m = 0.702$ and taking that the chloride exposure period was $t = 0.18$ year the

Figure 10. *Observations for a potential chloride profile found by means of the test method APM 302, cf. [AEC 1991]. The chloride profile is determined by the chloride contents C_x of 11 nos. of powder samples, each given by its distance x from the chloride exposed concrete surface.*

For the purpose of approximative determination of D and C_s by linear curve-fitting a new ordinate y is calculated, cf. example 4, where

$$y = \sqrt{C_x - C_i}$$

Observation no.	Distance x, mm	Chloride C_x,% by mass concrete	$\sqrt{C_x - C_i}$
1	0.40	0.440	0.663
2	1.30	0.306	0.552
3	2.25	0.227	0.475
4	3.00	0.145	0.379
5	3.80	0.094	0.305
6	4.80	0.051	0.224
7	6.15	0.025	0.155
8	7.90	0.011	—
9	9.35	0.005	—
10	48.25	0.001	—
11	53.20	0.001	—

chloride diffusion coefficient D is determined by the formula given above and yields

$$D = \left(\frac{3.0}{0.702 \times \sqrt{4 \times 0.18}} \right)^2 = 25 \text{ mm}^2/\text{year}$$

Approximative methods of linear curve-fitting

The semi-grafical methods as explained above are just suitable for rough estimates of the parameters of a chloride profile. There is a certain need for approximative methods of estimation which apply to all observations. This can be done at two levels as described in the following.

Estimation of D by linear curve-fitting

It is possible to rewrite the mathematical equation of the chloride profile

$$C_x = C_i + (C_s - C_i) \operatorname{erfc}\left(\frac{x}{\sqrt{4\,t\,D}} \right)$$

into a simpler form

$$y = \frac{x}{\sqrt{4\,t\,D}}$$

Here y is defined as

$$y = \operatorname{erfc}^{-1}\left(\frac{C_x - C_i}{C_s - C_i} \right)$$

By plotting the observations as x and y in a cartesian coordinate system the observations will be represented by a straight line plot. By a linear curve-fitting the straight line best fitting the observations and also passing through origo is determined. From the slope of this straight line the chloride diffusion coefficient D is determined when the exposure period t is known.

Example 3. The chloride diffusion coefficient D should be estimated from all observations in the Table of figure 6, assuming that C_i = 0.001 per cent by mass concrete and C_s = 0.45 per cent by mass concrete. The necessary and sufficient calculations are shown in the Table of Figure 8.

By a linear curve-fitting of the transformed observations (x, y) the following straight line is found

$$y = 0.209\,x$$

Figure 11. The transformed ordinate y plotted versus the distance x from the chloride exposed concrete surface. Two lines are shown found by means of curve-fitting – one taking samples nos. 1-7 into account and one taking samples nos. 2-6 into account, cf. example 4 and the Table of Figure 10.

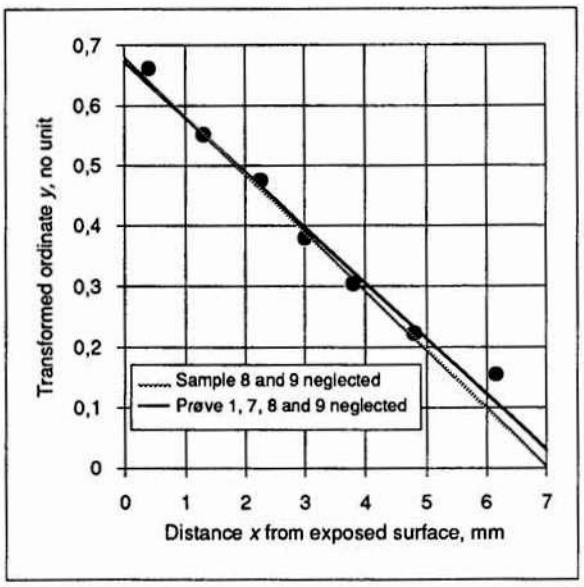

where $R^2 = 0.994$. The plot of the transformed observations are shown in the Diagram of Figure 9. Thus the chloride diffusion coefficient is determined by solving the following equation

$$\frac{1}{\sqrt{4\,t\,D}} = 0.209$$

Since the exposure time is $t = 0.18$ year the chloride diffusion coefficient yields

$$D = \frac{0.25}{0.18 \times 0.209^2} = 32 \text{ mm}^2/\text{year}$$

By neglecting the observations nos. 8 and 9, cf. the Table in Figur 8, the following straight line $y = 0.228\,x$ is found with $R^2 = 0.999$. Thus the following value of D is obtained

$$D = \frac{0.25}{0.18 \times 0.228^2} = 27 \text{ mm}^2/\text{year}$$

This difference may be caused by a non-homogeneous microstructure of the concrete. However it may also be caused by inaccuracy in the analyses if the samples nos. 8 and 9. Only further examination of the concrete can tell about the reason for the deviation found.

Estimating C_s and D by linear curve-fitting

It is possible to estimate not only D but also C_s by linear curve-fitting. An approximation is introduced for the error function complement

$$\text{erfc}(z) \approx \left(1 - \frac{z}{\sqrt{3}}\right)^2$$

This approximation is valid in practice in the interval $0 \le z < \sqrt{3}$. By using this approximation the mathematical expression of the chloride profile yields

$$C_x = C_i + (C_s - C_i)\left(1 - \frac{x}{\sqrt{12\,t\,D}}\right)^2$$

This approximation is not, as said above, valid for all values of x. However, by following the rule of thumb, cf. [Pedersen 1993], that the major part of the observations made for the determination of a chloride profile should fulfil the requirement $x < 5 \times \sqrt{t\,D}$, the following

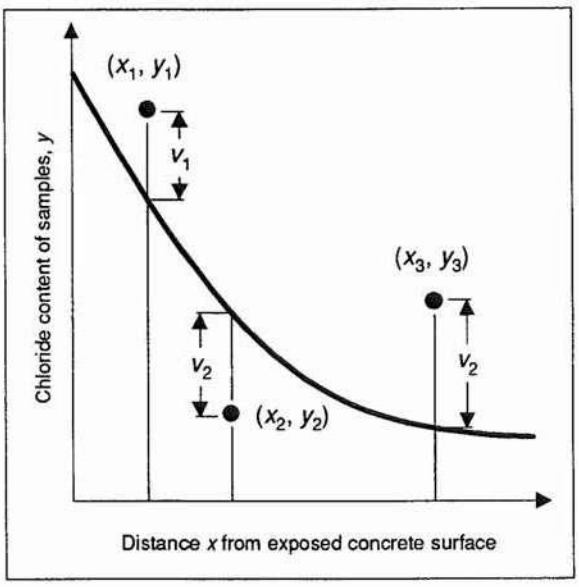

Figure 12. *Under the conditions that the graph shown should pass the observations (x_1, y_1), (x_2, y_2) and (x_3, y_3) the parameters of the graph should be determined in such a way that the sum of the squares of the deviations $v_1^2 + v_2^2 + v_3^2$ will obtain a minimum. This is the principle of curve-fitting by the method of least squares.*

limit of the approximation will often leave a sufficient number of observations for the analysis

$$0 \leq x < \sqrt{12\,t\,D}$$

Thus, the limit is generally not a hindrance. By rewriting the mathematical expression of the chloride profile in the following way

$$\sqrt{C_x - C_i} = \sqrt{C_s - C_i} - x\sqrt{\frac{C_s - C_i}{12\,t\,D}}$$

it is seen that it obeys the well-known expression of a straight line $y = \alpha\,x + q$, if the following substitutions are introduced

$$y = \sqrt{C_x - C_i}$$

$$q = \sqrt{C_s - C_i}$$

$$\alpha = -\sqrt{\frac{C_s - C_i}{12\,t\,D}} = -\frac{q}{\sqrt{12\,t\,D}}$$

When α and q are found by linear curve-fitting the parameters of the chloride profile yield

$$C_s = q^2 + C_i$$

$$D = \frac{(q/\alpha)^2}{12\,t}$$

The initial chloride content C_i of the concrete is determined by analysis of virgin concrete.

Example 4. The chloride difusion coefficient D and the ordinate C_s of the chloride profile at surface ($x = 0$) should be estimated by linear curve-fitting applying the above given approximation and the observations in the Table of Figure 6.

In the Table of Figure 10 the observations (x, C_x) are repeated and the transformation y shown. The initial chloride content is found by the observations nos. 10 and 11, i.e. $C_i = 0.001$ per cent by mass concrete. From a linear curve-fitting of the observations nos. 1 to 7 (see later about x_{max}) the following straight line is found

$$y = 0.673 - 0.0902\,x$$

with $R^2 = 0.982$. By applying $\alpha = -0.0902$ and $q = 0.673$ the parameters of the chloride profile yield

Figure 13. Chloride content in powder samples versus their distance from the chloride exposed concrete surface. The parameters of the chloride profile are determined by non-linear curve-fitting taking all observations into account (second column) and only a part of the observations (third column), cf. example 5.

Distance x, mm	Chloride C_x % by mass concrete	Chloride C_x % by mass concrete
0.40	0.440	—
1.30	0.306	0.306
2.25	0.227	0.227
3.00	0.145	0.145
3.80	0.094	0.094
4.80	0.051	0.051
6.15	0.025	0.025
7.90	0.011	—
9.35	0.005	—
C_s	0.486 % mass concrete	0.466 % mass concrete
D	23.9 mm^2/year	25.4 mm^2/year
C_i	0.001 % mass concrete	0.001 % mass concrete

$$C_s = 0.673^2 + 0.001 = 0.454 \text{ per cent by mass concrete}$$

$$D = \frac{(0.673 / 0.0902)^2}{12 \times 0.18} = 26 \text{ mm}^2/\text{year}$$

cf. the diagram of Figure 11. The limit of x for the application of the approximation is

$$x_{max} = \sqrt{12 \times 0.18 \times 26} = 7.5 \text{ mm}$$

Methods of non-linear curve-fitting

For any final estimation of the parameters of a chloride profile a non-linear curve-fitting should be applied. Here it is the choice if the parameter C_i should be estimated by the curve-fitting (i.e. three parameters to estimate) or the observations should be planned in such way that the observations are divided into two groups – one for the estimation of D and C_s and another for the estimation of C_i. It has become general practice to use the last choice and only this is described in detail in the following.

Assumptions

It is supposed that a chloride profile has been determined by the following observations

$$(x_1, C_1),\ (x_2, C_2),\ (x_3, C_3), \ldots,\ (x_n, C_n)$$

From these observations C_s and D in the the following equation should be determined

$$C = C_i + (C_s - C_i)\ \text{erfc}\left(\frac{x}{\sqrt{4\,t\,D}}\right)$$

assuming that the values of C_i and t are known. This will give n equations and two unknowns. Thus, the determination of C_s and D is not unambiguous unless further assumptions are made. If the observations are plotted into a Cartesian coordinate system it is unlikely that a chloride profile described by the equation given above for any chosen values of C_s and D will pass through all the observations.

However, if it is required that a measure of the deviations between the chloride profile and the observations is at the minimum the determination of C_s and D will become unambiguous. The accuracy by which x is determined when using a grinding technique is far better than the accuracy of C. However, this is not the case when a hammer-drill technique is applied but

Figure 14. Observations of the chloride content of concrete versus the distance from the chloride exposed concrete surface. In the same diagram is also shown the chloride profile found by the non-linear curve-fitting, cf. example 5. The deviations between the observed and the estimated chloride profile are shown in Figure15.

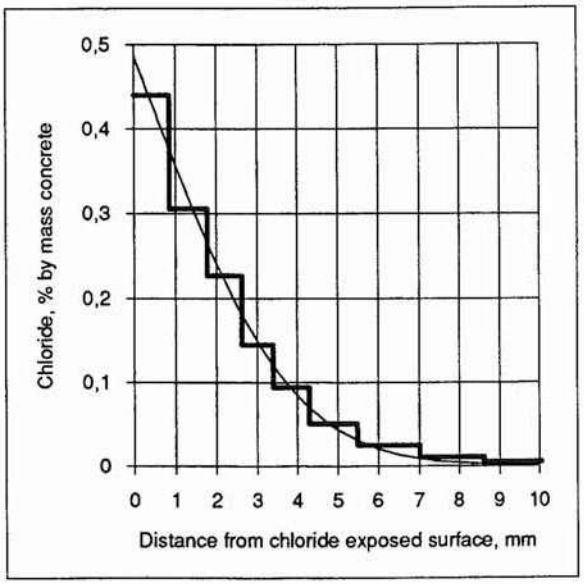

documentation has not been reported. Here the use of the grinding technique is assumed.

Assuming that the inaccuracy of C plays the predominant role and x should be considered deterministic the method of least squares will lead to an unambiguous determination of C_s and D, i.e. it is required that

$$v_1^2 + v_2^2 + v_3^2 + \ldots + v_n^2 = \text{minimum}$$

cf. Figure 12. Here v_1 is the deviation between the observation C_1 and the ordinates for x_1 of the equation in question, i.e.

$$v_1 = C_i + (C_s - C_i)\,\text{erfc}\left(\frac{x_1}{\sqrt{4\,t\,D}}\right) - C_1$$

and so on for the deviations $v_2, v_3, v_4, \ldots, v_n$.

Example 5. The observations given in the Table of Figure 6 are finaly used in order to determine C_s and D by application of a non-linear curve-fitting. Observations nos. 10 and 11 determine $C_i = 0.001$ per cent by mass concrete. The found values of the parameters are shown in Figure 13. In Figure 14 the determined values of the mathematical chloride profile are shown together with the observed. The Table of Figure 15 illustrates these findings.

Deviations between mathematical and observed chloride profiles

No curve fitting, linear or non-linear, is able to determine the mathematical model of a chloride profile. Only the knowledge of the transport mechanism and the influences from the concrete and its environment will be able to determine the mathematical model of a chloride profile.

In this paper the mathematical model of diffusion into a quasi homogeneous semi-infinite medium is supposed. However, the medium may not be quasi homogeneous. It is well-known that D is a function of the distance from the exposed concrete surface, and open cracks will disturb the flow of chloride in concrete, while a time dependent medium does not change the shape of the chloride profile, cf. [Poulsen 1993].

By plotting the determined and observed chloride profiles into one Cartesian coordinate system it can be seen if the observations have a systematic deviation from the determined chloride profile. If so, it is advisable that the reason for this deviation is examined depending on the future application of the determined chloride profile.

Figure 15. Table of the observed chloride content, obs{C_x}, in the powder samples and the estimated chloride content, est{C_x}, found by means of the non-linear curve-fitting applied in example 5, which determined the parameters equal to C_s = 0.486 per cent by mass concrete and D = 23.9 mm^2/year. The initial chloride content of the concrete was estimated to C_i = 0.001 per cent by mass concrete from samples nos. 10 and 11 (not shown here). The deviations v(x) are also shown versus the distance x from the chloride exposed concrete surface.

Distance x, mm	obs{C_x},% by mass concrete	est{C_x},% by mass concrete	$v(x)$,% by mass concrete
0.40	0.440	0.431	– 0.009
1.30	0.306	0.322	+ 0.016
2.25	0.227	0.217	– 0.010
3.00	0.145	0.151	+ 0.006
3.80	0.094	0.095	+ 0.001
4.80	0.051	0.050	– 0.001
6.15	0.025	0.019	– 0.006
7.90	0.011	0.004	– 0.007
9.35	0,005	0.002	– 0.003

As mentioned before carbonation or leaching of the outermost concrete surface will change the chloride binding effect of the cement matrix. Since it is the change of the chloride profile around the rebars in concrete which is important for the service lifetime of the reinforced concrete, the observations (x, C_x) in the carbonated or leached surface layer could be omitted instead of trying to formulate a mathematical model for this special case.

However, neither recommendations nor standards deal with this problem. Thus, the determination of parameters C_s and D of a chloride profile from observations are in fact not unambiguous – *but it ought to be!*

LIST OF REFERENCES

- **AEC**. Chloride ingress into concrete, test method APM 302, Edition 2. AEClaboratory, AEC Consulting Engineers Ltd., Vedbæk Denmark, **1991**.
- **AEC**. Chloride profile (micro), test method APM 207. AEClaboratory, AEC Consulting Engineers Ltd., Vedbæk Denmark, **1989**.
- **Crank, John**. The mathematics of diffusion. 2. edition, Clarendon Press. Oxford UK, **1986**.
- **Frederiksen, Jens M**. APM 302 – Danish test method for the chloride ingress into concrete. Dansk Beton no. 2:92. Copenhagen Denmark, **1992**.
- **Frederiksen, Jens M**. Chloride binding in concrete surfaces. Nordic Miniseminar. Chalmers University of Technology, Göteborg Sweden, **1993**.
- **Gran, Hans Christian**. Measurement of chlorides in concrete. An evaluation of three different analysis techniques. NBI-report no. 110. Oslo Norway, **1992**.
- **Gran, Hans Christian**. Measurements of chlorides in concrete – an evaluation of three different analysis techniques. Nordic Miniseminar. Chalmers University of Technology, Göteborg Sweden, **1993**.
- **Nilsson, Lars-Olof**. The effect of non-linear chloride binding on chloride diffusivities and chloride penetration – a theoretical approach. Nordic Miniseminar. Chalmers University of Technology, Göteborg Sweden, **1993**.
- **NT Build 208**. Concrete hardened: Chloride content. Edition 2, approved 1984-5. Esbo Finland, 1984.
- **Pedersen, Thomas Fich, and Klinghoffer, Oskar**. Factors influencing the uncertainty in the determination of diffusion coefficients by non-linear curve-fitting. Nordic Miniseminar. Chalmers University of Technology, Göteborg Sweden, **1993**.
- **Poulsen, Ervin**. Chloride and 100 years service lifetime. Dansk Betonforening, punlication no. 36. Copenhagen Denmark, **1990**. (In Danish).
- **Poulsen, Ervin**. On a model of chloride ingress into concrete having timedependent diffusion coefficient. Nordic Miniseminar. Chalmers University of Technology, Göteborg Sweden, **1993**.
- **Poulsen, Ervin**. The chloride diffusion characteristics of concrete. Approximative determination by linear regression analysis. Nordic Concrete Research, no. 9. Oslo Norway, **1982**.
- **Reknes, Kåre**. Round robin test. In-situ and laboratory test methods for the measurements of chlorides in concrete. BRI-report, project O 6563. Oslo Norway, **1994**. (In Norwegian).
- **Sand, Berit Tora**. The effect of the environmental load on chloride penetration. Nordic Miniseminar. Chalmers University of Technology, Göteborg Sweden, **1993**.
- **Sørensen, Birgit, and Maahn, Ernst**. Penetration rate of chloride in marine concrete structures. Nordic Concrete Research, no. 1. Oslo Norway, **1982**.
- **Spiegel, Murray R**. Mathematical Handbook of formulas and tables. Schaum's outline series in mathematics. McGraw-Hill Book Company. New York USA, **1968**.
- **Suenson, E**. Building materials – Rocks and aggregates. Jul. Gjellerups Forlag. Copenhagen Denmark, **1942**. (In Danish).

LIST OF NOTATIONS

α	Slope of a straight line in Cartesian coordinates.
a	The line segment of the asymptote from the ordinate axis to the intersection between the »surface tangent« of the chloride profile and the asymptote.
b	$= C_s - C_i$.
C	General notation for chloride content (contration) of concrete.
$C_1, C_2, C_3, \ldots$	Chloride content of concrete at the distances $x_1, x_2, x_3, \ldots, x_n$ from the chloride exposed concrete surface.
C_i	Initial chloride content of concrete
C_{ia}	Initial chloride content of concrete referring to achieved chloride diffusivity.
C_{ip}	Initial chloride content of concrete referring to potential chloride diffusivity.
C_m	Chloride content of concrete at the distance x_m from the chloride exposed surface.
C_s	Ordinate of a concrete's chloride profile at the chloride exposed concrete surface, i.e. at $x = 0$.
C_{sa}	Ordinate of a concrete's achieved chloride profile at the chloride exposed concrete surface, i.e. at $x = 0$.
C_{sp}	Ordinate of a concrete's potential chloride profile at the chloride exposed concrete surface, i.e. at $x = 0$.
C_x	Chloride content of concrete at the distance x from the exposed surface.
C-S-H	Calcium silicate hydrate gel formed by the hydration of silicates in Portland cement.
D	General notation for the chloride diffusion coefficient of concrete.
D_a	Chloride diffusion coefficient referring to achieved chloride diffusivity.
D_p	Chloride diffusion coefficient referring to achieved potential diffusivity.
erfc	The error-function complement.
erfc^{-1}	The inverse error-function complement.
est$\{C_x\}$	Estimated chloride content of concrete at the distance x from the chloride exposed concrete surface.
obs$\{C_x\}$	Observed chloride content of concrete at the distance x from the chloride exposed concrete surface.
q	The line segment of the ordinate axis between the origin and the intersection of a straight line.
R^2	Squared sample correlation coefficient.
t	Time period of chloride exposure.
$v(x)$	Deviation versus x of an observation from the corresponding ordinate of the fitted curve.
$v_1, v_2, v_3, \ldots$	Deviations of observations from the corresponding ordinates of a fitted curve at the points 1, 2, 3, . . , n.
x	Distance from a chloride exposed concrete surface.
x_m	Distance from a chloride exposed concrete surface to a point near the centre of the samples determining the chloride profile.
$x_1, x_2, x_3, \ldots$	Distances from a chloride exposed concrete surface to the points 1, 2, 3, . . , n.
y	General notation of an ordinate which is transformed by a function of chloride content of the concrete.
y_m	Ordinate with sepcial reference to x_m transformed by a function of chloride content of the concrete.
$y_1, y_2, y_3, \ldots$	Ordinates of the points 1, 2, 3, . . , n.
z	General notation of an independent variable.

SIMPLE ESTIMATION OF CHLORIDE PENETRATION PARAMETERS

Henrik Erndahl Sørensen, AEClaboratory, AEC Consulting Engineers (LtD) A/S, Staktoften 20, DK-2950 Vedbæk, Denmark, Phone (int+45) 45 66 12 66.

ABSTRACT

So far, calculations of chloride penetration parameters from measured chloride profiles requires either a PC-based programme or time-consuming look up in tables. This paper introduces a new simple and rapid method to produce a reliable estimation in the field. It is possible to calculate the chloride penetration parameters C_s, D_{app} and K_{cr} from a plot of two lines in a special diagram using a ruler and a pocket calculator. Furthermore the plot gives a good visual evaluation of the quality of the curve-fit.

Keywords: Concrete, chlorides, diffusion, permeability, mathematical models.

1. INTRODUCTION

The ability of concrete to resist chloride penetration has become a subject of great interest during the last decade as maintenance costs due to repair of chloride-initiated corroding reinforcement in concrete structures has increased dramatically.

A wide range of test methods to evaluate the resistivity of concrete to chloride penetration has been developed – some more thoroughly considered than others!

The use of the error function solution (eq1) of Fick's second law for a semi-infinite medium to model chloride penetration into concrete is very common today. Even though observations indicate, that this model has its limitations, it seems to be the most applicable method so far. One of the disadvantages of the model is, that it involves a complex mathematical function - the Gauss' error function. The values of this function have to be calculated from an infinite series or looked up in a table. Without a personal computer this is a time-consuming process.

Several approximations of the error function have been developed, but unfortunately it is nescessary to use many constants to secure sufficient accuracy. In these cases, the use of spreadsheet calculations or other PC-based programmes is convenient.

This paper introduces a diagram, which facilitates calculation by hand and pocket calculator of the most commonly used chloride penetration parameters (i.e the apparent chloride diffusion coefficient D_{app}, the surface concentration C_s and the penetration parameter K_{cr}) from chloride profiles, e.g. measured according to APM 207 [AEC, 1992].

2. THEORY

The commonly used solution of Fick's second law when concrete is considered as a semi-infinite medium with a constant boundary condition [Crank, 1975] is:

(eq1) $$C(x,t) = C_i - (C_s - C_i)\ \mathrm{erfc}\left(\frac{x}{\sqrt{4\ t\ D_{app}}}\right)$$

where $C(x,t)$ is the chloride content at the depth x at the exposure time t.
C_s is the boundary condition at the exposed surface (calculated surface concentration)
C_i is the initial chloride content
x is the depth below the exposed surface (to the middle of a layer)
t is the time period of chloride exposure
D_{app} is the apparent chloride diffusion coefficient
and erfc is the Gauss' error function complement defined by:

(eq2) $$\mathrm{erfc}\ u = 1 - \frac{2}{\sqrt{\pi}}\int_0^u \exp(-\eta^2)\,d\eta$$

The solution can be rearranged to:

(eq3) $$\frac{C(x,t) - C_i}{C_s - C_i} = \mathrm{erfc}\left(\frac{x}{\sqrt{4\ t\ D_{app}}}\right)$$

By applying the inverse Gauss' error function complement (inv erfc) the solution can be written as:

(eq4) $$\mathrm{inverfc}\left(\frac{C(x,t) - C_i}{C_s - C_i}\right) = \left(\frac{1}{\sqrt{4\ t\ D_{app}}}\right) x$$

When the left hand side of this equation is plotted against x a straight line is obtained, where the apparent chloride diffusion coefficient can be calculated from the slope.

The inverse Gauss' error function complement is a complex function, where the function values are not easy to calculate. However, if this function is build into the diagram, where the measurements are plotted, extensive calculations of function values can be avoided.

3. ESTIMATION OF PARAMETERS

The chloride penetration parameters can be estimated from a measured chloride profile using a diagram, where the abscissa has a linear scale and the ordinate has a scale according to the inverse Gauss' error function complement - see figure 1.

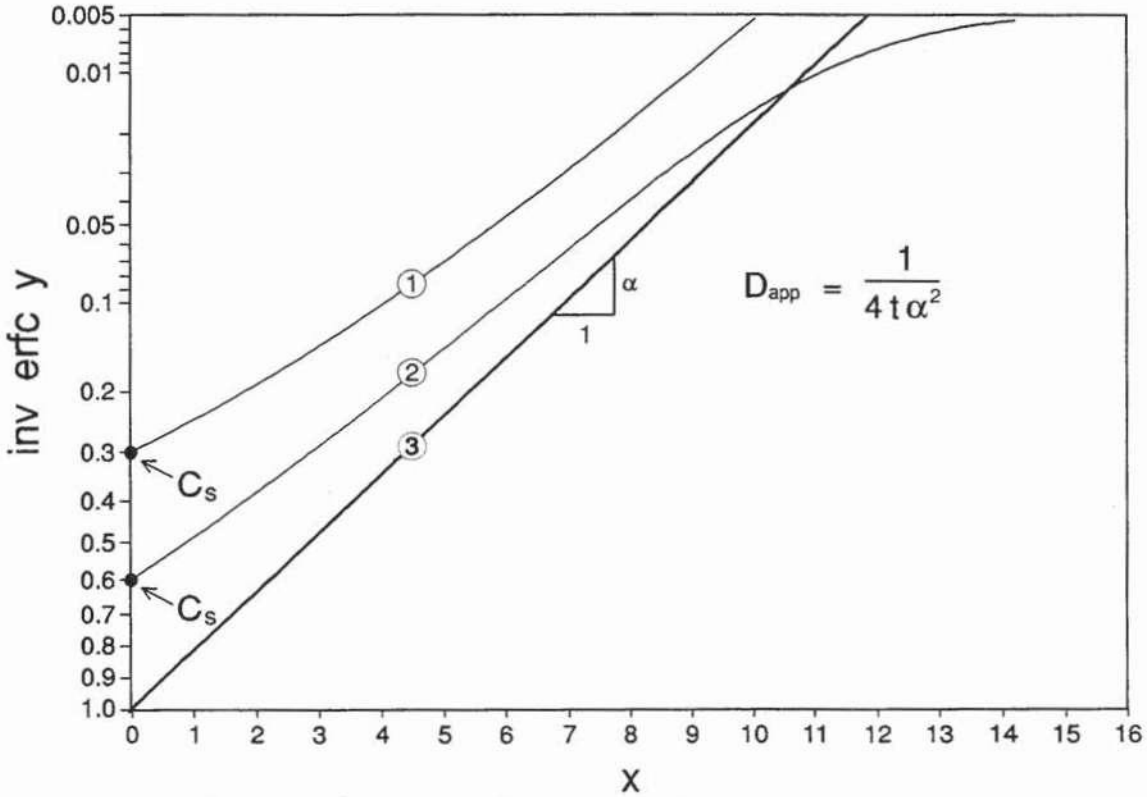

Figure 1: Single inverse Gauss' error function complement diagram.

The curve marked "1" is a plot of C(x,t) versus x. The C(x,t)-values are calculated from the model with the following parameters: D_{app} = 100 mm^2/year, C_s = 0.3 %, C_i = 0 % and t = 0.1 years. (All % stated are given as per cent by mass of dry concrete).

The curve marked "2" is a similar plot calculated with following parameters:
D_{app} = 100 mm^2/year, C_s = 0.6 %, C_i = 0.05 % and t = 0.1 years.

The curve marked "3" is a normalized plot of the two curves "1" and "2". The two curves are normalized by use of the expression inside the parenthesis on the left-hand side of equation (eq4). The slope of the linear normalized plot is used to calculate D_{app}.

The sheet given i figure 2 is designed to be used for estimation of chloride penetration parameters from plots by hand of chloride profiles, e.g. at inspection in field. How to use this sheet is described in the following.

3.1 Estimation of C_s

The curves in figure 1 representing plots of the C(x,t)-values versus x is close to linear near the ordinate. For this reason, the intersection between the ordinate and the regression line of the outmost 3 to 5 points (C(x,t),x) of the chloride profile will give a good estimation of C_s.

Note that the first point below the surface is not taken into consideration when drawing the regression line because it is very close to the exposed surface and do not fit the model.

3.2 Estimation of D_{app}

To estimate D_{app} it is nescessary to draw a normalized plot of the chloride profile on the diagram. The normalized values are calculated from:

(eq5)
$$\frac{C(x,t) - C_i}{C_s - C_i} \approx \frac{C(x,t)}{C_s} \quad \forall\ C(x,t) >> C_i$$

In most cases it is sufficient to calculate the ratio $C(x,t)/C_i$.

The normalized values are plotted versus x on the graph paper and the regression line is drawn with intercept at 1.0 on the ordinate. D_{app} is calculated from the slope (α) of the regression line using:

(eq6)
$$D_{app} = \frac{1}{4t\alpha^2}$$

Note that the linear scale on the left-hand ordinate on the sheet is scaled 10 times with respect to the abscissa. If the slope of the regression line on the sheet is calculated using this scale the equation given on the sheet must be used. This corresponds to multiply the result from equation (eq6) by a factor of 100.

3.3 Estimation of K_{cr}

It is often useful to calculate the penetration parameter (K_{cr}). It combines C_i, C_s and D_{app} to a value that gives the first year penetration of a predefined reference chloride concentration (C_r) into the concrete assuming that the actual conditions and parameters remains constant. K_{cr} will also represent a measure for the amount of chlorides penetrated into the concrete. The penetration parameter is defined by:

(eq7)
$$K_{cr} = \sqrt{4D_{app}}\ \text{inverfc}\left(\frac{C_r - C_i}{C_s - C_i}\right) = \frac{x_{cr}}{\sqrt{t}}$$

According to equation (eq7) the penetration parameter is calculated as $K_{cr} = x_{cr}/\sqrt{t}$. The value of x_{cr} is estimated from the normalized plot by finding the corresponding x-value to the normalized reference concentration C_r/C_s. The C_r-value of 0.05 % is often used referring to the nominal chloride threshold value for corrosion.

3.4 Scaling of axes

When the C_s-value is greater than 1.0 mas% it is nescessary to reduce the C(x,t)-values by a factor of 2 or 4 before they are plotted in the sheet.

Similar, the x-values can be scaled if nescessary. In this case it is important to remember to adjust the calculated slope of the regression line according to the scaling factor.

3.5 Quality of estimation

The curve-fit of the normalized plot gives a good visual evaluation of the estimation of the chloride penetration parameters. The degree of linearity of the plotted points is describing how well the model fits the chloride profile. The plot will also show if any points should be omitted in the regression analysis.

4. EXAMPLE

Three concrete samples of identical concrete composition have been exposed according to APM 302 [AEC, 1991]. The samples were exposed to three different exposure times. The chloride penetration parameters are calculated by use of the standard non-linear regression analysis and the sheet given in figure 2, respectively. The results are presented in table 1 and the plot presented in figure 2 corresponds to the data from sample no 1.

	Exposure	Standard non-linear analysis			Sheet (figure 2)		
Sample no	Time [days]	C_s [%]	D_{app} [mm^2/yr]	$K_{0,05}$ [mm/√yr]	C_s [%]	D_{app} [mm^2/yr]	$K_{0,05}$ [mm/√yr]
1	36	0.600	94	24	0.615	93	24
2	70	0.341	110	22	0.342	108	21
3	140	0.362	77	19	0.350	89	20

Table 1: Estimated chloride penetration parameters for three chloride profiles. The initial chloride concentration was C_i = 0.001 %.

Estimation of chloride penetration parameters

AEC

C_r = 0.050 mas%	C_s = 0.615 mas%	C_r/C_s = 0.05/0.615 = 0.081							SAMPLE # 1	
t = 0.0986 years	$K_{cr} = x_{cr}/\sqrt{t}$ = 7.50/$\sqrt{0.0986}$ = 24 mm/$\sqrt{year}$									
C_i = 0.001 mas%	$D_{app} = 25/(t\alpha^2)$ = 25/(0.0986 × 1.65²) = 93 mm²/year									
x [mm]	0.50	1.55	2.55	3.50	4.75	6.25	8.00	9.85		
C(x,t)	0.593	0.433	0.334	0.251	0.149	0.102	0.042	0.012		
$C(x,t)/C_s$	0.964	0.704	0.543	0.408	0.242	0.166	0.068	0.020		

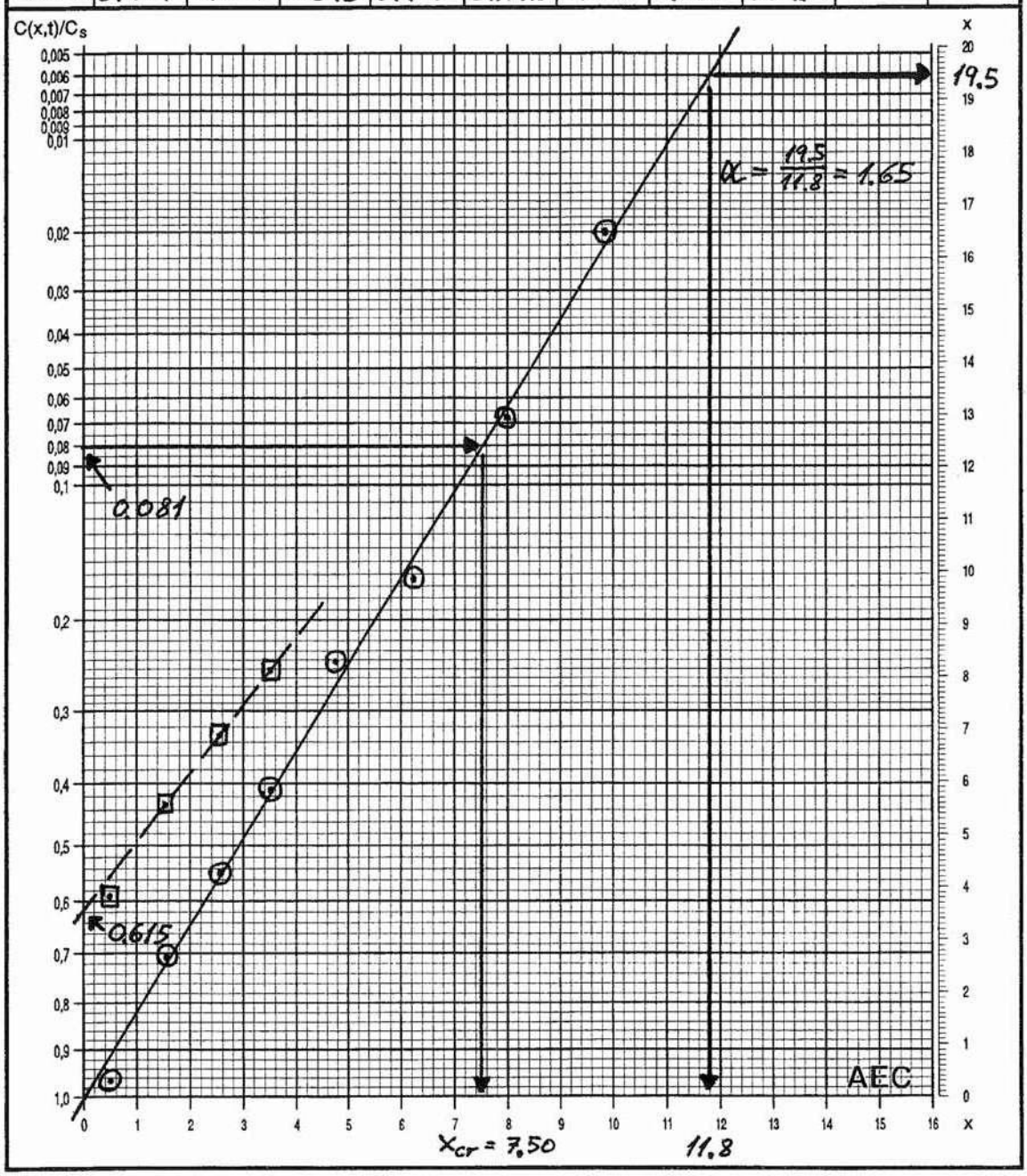

5. CONCLUSION

A simple method to produce a rapid and reliable estimation of chloride penetration parameters without use of a personal computer has been presented. The parameters are estimated from a plot of a measured chloride profile on a diagram involving the inverse Gauss' error function complement. The plot gives a good visual evaluation of the quality of the curve-fit.

6. REFERENCES

AEC. APM 207. Concrete testing. Hardened concrete. Micro chloride profile. AEClaboratory, Staktoften 20, DK-2950 Vedbæk, 1992.

AEC. APM 302. Concrete testing. Hardened concrete. Chloride penetration. 2nd edition. AEClaboratory, Staktoften 20, DK-2950 Vedbæk, 1991.

Crank, J. The Mathematics of Diffusion. 2nd edition, Clarendon Press, Oxford UK, 1975.

7. NOTATIONS

α	Slope of a straight line.
C_i	Initial chloride content of concrete.
C_s	Boundary conditon of chloride profile at the exposed surface (calculated surface concentration).
C_r	A predefined reference chloride concentration.
C(x,t)	Chloride content of concrete at the distance x from the exposed surface to the exposure time t.
D_{app}	Apparent (measured) chloride diffusion coefficient.
erfc	Gauss' error function complement.
exp	Exponential function.
η	General mathematical variable.
inv erfc	Inverse Gauss' error function complement.
K_{cr}	Penetration parameter referring to the reference chloride concentration C_r.
t	Time period of chloride exposure.
u	General mathematical variable.
x	Depth in concrete below chloride exposed surface.
x_{cr}	Depth in concrete below chloride exposed surface of the reference chloride concentration C_r.

Reprint from : Durability of Concrete. Third International Conference
Nice, France 1994

SP 145-9

Long-Term Durability of Special High Strength Concretes

by P. Nepper-Christensen, B.W. Kristensen, and T.H. Rasmussen

Synopsis: The long-term durability of a number of special types of concretes has been tested by exposing various large-scale concrete specimens to different outdoor conditions. The concretes tested include concretes made with different types of cement and incorporating various quantities of fly ash and silica fume (microsilica) as well as mixtures thereof.

In one test series full-scale precast concrete units were installed as functional members of a fish-ladder. The units, comprising concrete with up to 50 percent of silica fume (related to the cement content), are subject to the action of lake water and freezing and thawing. They have been in service for nearly 15 years, and the results demonstrate the excellent durability of concrete with silica fume.

In another test series concrete panels and slabs are exposed to Danish outdoor climate (freezing and thawing during winters) in connection with frequent use of de-icing salts. This test series also comprises large-size panels, installed in a harbour at the west coast of Denmark. For this test series, 10 year results are now available.

Keywords: Cements; compressive strength; concretes; deicers; durability; exposure; fly ash; freeze thaw durability; high strength concretes; seawater; silica fume

Palle Nepper-Christensen (M.Sc., Civil Engineer) has been involved in cement and concrete research and in technical advisory services for more than 30 years in the Danish cement industry (Aalborg Portland A/S, P.O.Box 165, DK-9100 Aalborg). Now manager of Aalborg Portland's R&D and Cement and Concrete Laboratory. He is a fellow of the American Concrete Institute.

Bent W. Kristensen (B.Sc., Civil Engineer) has been working in Aalborg Portland's research laboratories for more than 30 years. A specialist in mechanical testing of concrete and in noise regulation.

Thorkild H. Rasmussen (M.Sc., Civil Engineer) has been active in concrete research and in technical advisory services for about 15 years. Until recently working for Aalborg Portland A/S. Now associated with the promotion of chemical admixtures for concrete in Nordisk Bygge Kemi A/S (Hallandsvej 1, DK-6230 Rødekro).

INTRODUCTION

When, 15 years ago, fly ash and silica fume (microsilica) were introduced in Denmark and shortly after became generally accepted for use in plain and reinforced concrete for all exposure classes, this happened without thorough knowledge about the long-term properties of such concretes. By correlation with concretes incorporating other types of pozzolana, such as for instance various types of natural pozzolana, it was, however, considered most likely that the use of fly ash and silica fume would not present great surprises in the long term either.

Aalborg Portland, promoting the use of fly ash and silica fume, however, found that the opportunity of initiating experiments and tests which during the future years might help in understanding the long-term behavior of these new materials, should be acknowledged.

Therefore, in cooperation with a group of companies from the Danish concrete industry, they started two series of experiments in which various types of concretes, incorporating various types of cements, various quantities of fly ash and silica fume and mixtures thereof, were exposed to Danish outdoor climatic conditions.

The first test series consisted of manufacturing a number of full-scale, reinforced components using different types of concrete and then installing these components as integral parts of a fish-ladder for a local lake. Fourteen year results are now available and are presented for the first time in this paper.

In the second test series, a large number of slabs and plates, manufactured with a variety of different concrete mixtures, have been placed at two different exposure fields, subject to the actions of inland climate (including de-icing salts) and sea-water, respectively. Ten year results are now available and are presented in this paper.

FULL-SCALE TESTS

Precast concrete components, specially designed for use as steps in a fish ladder, were manufactured during the spring of 1979 and installed during the fall of the same year. The components, illustrated in Fig. 1, measured 2.9 m in length, 0.9 m in width, and 1.15 m in height, the wall thickness varied from 120 mm at the top to 150 mm at the bottom. They were installed so as to form a stair where each step consisted of a water-filled box, allowing the fish to jump from one box to the next. A total of 10 components were used to form the ladder.

This configuration of the structure implied that most parts of the concrete in the components were subjected to one-sided pressure of non-freezing water, while only the upper parts, approximately 0.1 m of the walls of the box components, were exposed to splash water and freezing and thawing during winters.

Materials

Nine (9) different concrete mixtures were used for the ten components, only the two upstream components (numbered 1 and 2) of the ladder being identical.

Three types of cement (a normal portland cement, a high sulphate resisting portland cement and a blended cement, consisting of finely ground portland cement and 30 percent of fly ash), one type of fly ash, and one type of silica fume, were used. The characteristics of these materials are set out in Table 1.

Admixtures (a plasticizer, a superplasticizer, and an air-entraining agent) were used in some of the concretes. The super-plasticizer was of the naphthalene-type. A conventional type of pit sand was used as the fine aggregate, while two fractions, 8-12 mm and 12-16 mm, of sea-dredged gravel constituted the coarse aggregate.

Concrete Types

The reference type of concrete used in this investigation was designed according to Danish rules and experiences to be durable when exposed to the conditions described above. The other concrete types were designed accordingly with the reservation, however, that long-term experiences with the use of relatively high quantities of fly ash and silica fume were not available.

Concrete mixture No. 1 was used in component (step) No. 1 (upstream), mixture No. 2 for component No. 2, and so forth. Results from mixture No. 1 (identical to mixture No. 2) are not reported here since casting of component No. 1 was not successful.

Mix proportions and fresh concrete properties are summarized in Table 2.

Manufacturing

The concrete components were cast by a precast concrete manu facturer (Spaencom A/S of Aalborg). From each mixture a number of test cylinders (100 mm by 200 mm) were cast for compressive strength testing at 1, 7, 28 and 90 days and at later ages. Measurements of the ultrasonic velocity were taken on the components, before and after installation as well as at later ages. Some of the reinforcing bars were provided with equipment for measurement of electric potentials.

Installation of the fish-ladder components at the lake site took place a couple of months after manufacture, i.e. during the fall of 1979.

Results

Results achieved in this investigation are as a general rule expressed as means of at least three measurements. They comprise:

1) **Compressive strengths** were measured on companion 100 mm by 200 mm cylinders, stored in water at 20^0C, up to 2,280 days (6.25 years). At an age of approximately 5,000 days (13.75 years), compressive strengths were measured on cores (95 mm by 140 mm) drilled out of the bottoms of the fish ladder box components. Thus the cores were taken from those parts of the components which have been under water and at an average temperature of approximately 8^0C throughout their lifetime. All the strength results are summarized in Table 2.

   For comparison purposes the core strengths have been multiplied by a conversion factor of 1.25 which is considered to

be a conservative value for such small diameter cores. When comparing with the 2,280 days strengths, the difference in storage temperature should also be considered. In addition, the cores contained pieces of steel bars from the reinforcement which most likely have influenced the strength values negatively.

From Table 2 it can be seen that all the concrete mixtures exhibit strength increase up to an age of 6 years. During the following 8 years it seems that the weakest mixtures have had some strength growth whereas the stronger mixtures - probably because of their higher imperviousness - have maintained their high strength level. In particular, it should be noted that the very high strength mixtures, containing moderate to high quantities of silica fume, under the present storage conditions show relative strength growths from 28 days till 6 years at nearly the same level as the weaker mixtures, with or without additions.

2) **Ultrasonic velocities** were measured on the box components at the time of demoulding and then at intervals up to an age of 18 months. The individual results will not be reported here, but the following general trends were observed: After hardening at the plant, just before shipment to the construction site, the ultrasonic velocities varied from 3,500 to 4,100 m/sec in accordance with the strength level. Measurements at an age of one year indicated decreasing velocities (of the order of 800 m/sec), attributed to the result of water saturation of the concretes. After a further 6 months period all the concretes had nearly regained the loss observed at the one year age.

3) Efforts on trying to follow the **rate of corrosion**, if any, were not successful, since the equipment installed did not function satisfactorily.

4) **Durability** was evaluated, partly through examination of thin-sections made from cores taken from the bottom plates of the boxes after approximately 6 years' of service and partly through visual inspections.

The observations from the thin-section examinations are summarized in Table 3. It seems to be a general tendency that the depth of carbonation decreases and the frequency of paste microcracks increases with increasing compressive strength of the concrete.

The visual inspections have up until the spring of 1993, i.e. after nearly 14 years' service, revealed no sign whatsoever of deterioration of any of the types of concretes used in this investigation.

Conclusions of Full Scale Tests

From this investigation it seems justified to conclude that the high numbers of microcracks often observed in very high strength concrete, made with or without silica fume, have no negative effect on the long-term durability of such concrete when exposed to freezing and thawing and brackish splash water at the same time.

EXPOSURE FIELD INVESTIGATIONS

The objective of these investigations was to study the long-term performance of a number of different concrete specimens which in contrast to most laboratory experiments were produced in large scale, and which in contrast to most practical experiences have been very well documented.

The investigations were initiated in 1983 and it is the intention to observe the condition of the specimens for the following 25 years, i.e. until year 2008.

Materials

Relevant combinations of cements and mineral additions were tested at three levels of concrete quality resulting in a total of 16 different concrete mixtures.

Three Danish types of cement were used, a rapid hardening portland cement (RPC), a blended cement with approximately 20 percent of fly ash (BC) and a high sulphate resistant portland cement with low alkali content (HSRC). The mineral additions used were a fly ash (FA) from Danish power stations and a silica fume (SF) from Norway. Chemical and physical data are presented in Table 4.

Originally, it was the intention to use absolutely sound aggregates to avoid aggregate related durability problems. It appeared, however, at a too late stage that the sand (0 to 4 mm) used did contain alkali-reactive substances in the form of porous, opaline flint. The coarse aggregate consisted of rounded granite particles with a maximum size of 16 mm.

An air-entraining agent of the vinsol resin type and a plasticizer based on lignosulphonate were used in all concrete mixtures.

Concrete Mixtures

Concrete mixtures with three levels of cement content, viz. 260, 340 and 390 kg/m^3, were used in the tests. For all the various concrete mixtures the water requirement was approximately 140 kg/m^3 corresponding to w/c ratios ranging from approximately 0.35 to approximately 0.55. When mineral additions were used, a reduction in the cement content was made corresponding to a cementing efficiency factor of 0.3 for fly ash and 3.0 for silica fume. The dosages of fly ash and silica fume were 20 percent and 10 percent by weight, respectively.

All mixtures were air-entrained with an air content of 5-6 percent as measured on site prior to concreting. The specified slump was 60-80 mm. These properties were achieved by the use of an air-entraining agent and a plasticizer as described above.

The various mixtures, their initial properties, and their strength characteristics as determined on 100 by 200 mm cylinders - cast at the same time as manufactering the large specimens, and stored under water at 20^{0}C - are presented in Table 5.

Manufacturing

The concrete was supplied by a ready-mixed concrete manufacturer and delivered to the site. Three slabs, each 1.0 by 1.0 by 0.2 m, two panels each 1.2 by 1.0 by 0.2 m, and a third panel, 2.0 by 1.0 by 0.2 m, were cast from each concrete mixture.

The slabs were cast horizontally and compacted with a screed vibrator, then trowelled by hand and finally broomed with a fibre-broom to achieve a uniform, grooved surface. Immediately after finishing, a curing membrane was sprayed onto the surface to prevent loss of water. The panels were cast vertically and vibrated with a poker vibrator. Immediately after removal of the plywood formwork, which took place after 7 maturity-days, a curing membrane was supplied to the surface.

Exposure Fields

As mentioned the test specimens consisted of three slabs and three panels for each of the sixteen different concrete mixtures.

One of the panels (the largest) from each mixture was installed in the harbour of Hirtshals situated at the North Sea. Here the panels were placed in the splash zone, their upper halves being subjected to the combined actions of chlorides, sulphates,

freezing/thawing and splash water. The panels are placed in a steel frame from which they can be lifted out to the quay for inspection, testing and core taking.

The slabs and the other panels were installed in a specially designed exposure field situated inland, see Figure 2, where they are being subjected to normal Danish outdoor climate which is characterised by average temperatures of approximately -1^0C (February) and approximately 16^0C (July) during summer and winter, respectively. Winters are humid with a high number of freezing and thawing cycles.

Test Programme

Slabs A - are intended for studies of frost resistance in a moderately aggressive environment and of reinforcement corrosion. For the latter purpose they are provided with three reinforcement arrangements placed with 10, 20 and 30 mm concrete covers, respectively. These are used for electrochemical measurements of the potential of the reinforcement. A saturated calomel electrode is being used as the reference.

Slabs B - are identical to Slabs A apart from the reinforcement. They are being used for taking cores (100 by 200 mm cylinders) for various laboratory tests, including tests for compressive strength, modulus of elasticity, density, depth of carbonation and petrographic examination by microscope.

Slabs E - are identical to Slabs A and are used for studies of frost resistance in a more aggressive environment, i.e. combined action of freezing/thawing and de-icing chemicals applied during wintertime.

Panels C - are used for the same purpose as Slabs B, i.e. for core taking and testing. The possible effect from the difference in exposure, due to the difference in orientation, will be studied.

Panels D - are used for the same experimental purposes as Slabs A, and the results from testing these specimens are also considered to reflect differences due to their orientation during casting and exposure.

Besides the large specimens a total of 40 small-size specimens were cast from each of the 16 concrete mixtures. Three specimens were used for each of the following tests:

- Cylinders (100 by 200 mm) for determination of compressive strength, modulus of elasticity, pulse velocity and density.

- Beams (100 by 100 by 500 mm) for determination of modulus of rupture in a three-point bending test.

- Prisms (100 by 100 by 400 mm) for measurement of drying shrinkage at 60-65 percent RH and 20^0C.

- Slabs (200 by 200 by 50 mm) for determination of resistance to freezing and thawing with de-icing chemicals.

Results

All the results from compressive strength testing of the cores taken from the exposure field specimens are given in Table 6 as averages of three single test results. Also the results from visual inspection of the durability of the specimens at the age of 10 years are reported in Table 6.

Due to lack of space, however, test results for corrosion, carbonation depth, modulus of elasticity, density, pulse velocity, drying shrinkage, and frost resistance (in the laboratory) have been omitted in this paper. However, the information obtained from these tests does not provide much help in explaining the results reported in this paper. This may not be valid for the carbonation depth measurements, the results of which are not yet available.

From the results shown in Table 6 it can be seen that Mixtures 4 and 11 have very low strengths and have disintegrated extensively at the age of 10 years, in particular the specimens that have been subjected to de-icing chemicals (sodium chloride) or seawater. Closer examination of cores from these specimens has revealed that alkali-silica reactions have contributed to this deterioration and may be the main cause. These two mixtures are the only one showing serious signs of deterioration and are the only one in which normal, rapid hardening portland cement (containing 0.6 percent alkalies) without any pozzolanic additions has been used; thus it seems as if either the use of low-alkali cement (with 0.3 percent alkalies), blended cement (with 20 percent fly ash) or addition of 10 percent silica fume or 20 percent fly ash to the concrete, under the present exposure conditions are sufficient preventive measures to avoid deleterious alkali-aggregate reactions for at least ten years, even when alkalies are supplied from the surroundings.

Therefore, in analysing the compressive strength results in Tables 5 and 6, Mixtures 4 and 11 are not considered. An analysis of the effects of specimen orientation, type of exposure, and age (without regard to mixture type) reveals the following trends:

- The orientation (vertical or horizontal) of the specimens at the inland exposure field has only an effect at 28 days, those cast vertically having higher strengths than the horizontal. At later ages the difference is insignificant. Orientation

does, however, influence durability, as none of the vertically placed specimens, contrary to some of the horizontal, have deteriorated during the first ten years of their life.

- The seawater specimens (cores taken from the underwater parts) have higher strength than the specimens stored inland, but are at the same strength level as the laboratory specimens cured under water, at the age of 10 years. At earlier ages there is no such effect.

- Taken as a whole, the strength increase from 28 days to 1 year is of the order of 30-40 percent, and the strength remains at the 1 year level for the following nine years.

From an analysis of the effect of the type of mixture on compressive strength and durability the following trends can be observed:

- The observation made above that the strength remains at nearly the same level from 1 year and onwards does also apply for mixtures with silica fume as well as mixtures without silica fume. Considering the laboratory specimens alone a tendency to decreasing strength level from 5 years to 10 years may be observed, both for mixtures with and without silica fume.

- Apart from Mixtures 4 and 11, only Slabs E (subjected to deicing chemicals) from Mixtures 1, 2, 5, 6, and 7 show any sign of insufficient frost resistance in the form of some cracking and scaling. These mixtures have the highest w/c and are besides characterized by having significantly less entrained air than intended (2-3 percent as determined on cores from the hardened concrete). Some of the vertical panels exhibit some surface crazing after 10 years, but this was observed already at the time of demoulding and has not grown worse during the years.

- From comparisons of Mixture 1 with Mixture 5, 2 with 4, 6 with 9, 7 with 11, 8 with 10, 12 with 16, and 14 with 15 in Tables 5 and 6, it is evident that substitution of some cement with either fly ash (substitution ratio 0.3) or silica fume (substitution ratio 3) has no negative effects on either the strength or the durability. On the contrary. Compressive strengths are slightly higher and resistance to frost attacks and alkali-silica reactions is improved when such additions are used in concrete. This applies irrespective of the type of cement used.

Conclusions of Exposure Field Investigations

The most important conclusions that may be drawn from this investigation seem to be the following:

1. Pozzolanic additions, such as fly ash and silica fume, improve the long-term resistance of concrete towards attacks from frost in combination with de-icing chemicals, seawater, and alkali-silica reactions.

2. The use of cement with an alkali content as low as 0.6 percent does not seem to prevent development of deleterious alkali-silica reactions, in particular when extra alkalies may be supplied from the environment. This, on the other hand, seems to be the case when cement with very low alkali content (0.3 percent) is used.

3. Under the exposure conditions dealt with in this investigation the compressive strength gain from 1 to 10 years is insignificant.

GENERAL CONCLUSIONS

The use of pozzolanic additions, such as fly ash, whether incorporated in the cement or added directly to the concrete, and silica fume (microsilica), are efficient means to secure the long-term durability of concrete exposed to aggressive environments.

Speculations on a possible negative, long-term effect from silica fume on the strength of concrete - and consequently on its durability - can not be supported by this investigation. Even concretes with very high quantities of silica fume (up to 50 percent by volume) seem to maintain their high strength level for at least 14 years.

TABLE 1 — CHEMICAL AND PHYSICAL DATA OF CEMENTS, FLY ASH, AND SILICA FUME

Cement/Fly Ash/ Silica Fume	Normal Portland Cement	High Sulphate Resistant Cement	Blended* Cement	Fly Ash	Silica Fume
Used in Concrete Mixture No	2,5,6,7, 8,9,10	3	4	5	8,9,10
Chemical Analysis					
SiO_2, %	21.38	25.75	29.74	50.58	>90
Al_2O_3, %	4.93	1.46	12.06	28.71	
Fe_2O_3, %	2.97	1.72	3.70	4.69	
CaO, %	64.51	67.20	47.76	6.05	
MgO, %	1.24	0.56	1.36	1.35	
SO_3, %	2.37	1.82	2.00	0.68	
Loss on ignition, %	0.90	1.19	3.18	7.83	
K_2O, %	0.63	0.04	0.59	0.73	
Na_2O, %	0.32	0.17	0.29	0.23	
Eq. Na_2O, %	0.74	0.20	0.68	0.71	
C_3A (calc.), %	8.0	1.0	-	-	-
Physical Tests					
Fineness					
- passing 45μm, %	83.5	96.8	96.1	82.9	100
- Blaine, m^2/kg	363	299	436	367	20,000
Specific Density, kg/m^3	3,150	3,170	2,890	2,230	2,200
Compressive Strength					
(ISO), MPa: 1 day	11.7	8.8	8.9	-	-
2 days	21.5	17.6	20.9	-	-
7 days	40.5	30.3	35.5	-	-
28 days	53.6	49.9	49.0	-	-
56 days	59.1	61.7	60.8	-	-
90 days	60.8	66.1	65.9	-	-

* Consists of 70% (by mass) of finely ground portland cement (Blaine: 388 m^2/kg) and 30% of ground Fly Ash (Blaine: 515 m^2/kg)

TABLE 2 — PHYSICAL PROPERTIES OF CONCRETES USED

Concrete Type	2	3	4	5	6	7	8	9	10
Cement Type	PC	HSRC	BC	PC	PC	PC	PC	PC	PC
Casting date - 1979	14/6	15/5	22/5	18/5	29/5	1/6	8/6	12/6	14/8
Concrete Mix, kg/m^3									
Cement (C)	330	330	310	290	400	330	530	415	294
Fly Ash (FA)				125					
Silica Fume (SF)							42*)	125*)	209*)
Water	160	160	150	160	115	102	120	113	105
Sand	710	800	722	664	772	772	698	705	714
Gravel, 8-12 mm	535	533	541	498	579	579	524	530	536
Gravel, 12-16 mm	535	445	541	498	579	579	523	530	536
Admixture - Type	AE	AE	AE	P+AE	SP	AE+SP	SP	SP	SP
-dosage, percent of cement	0.049	0.045	0.329	1.0/0.15	1.2	0.038/1.2	1.2	1.2	3.0
W/(C+FA+SF)	0.48	0.48	0.48	0.39	0.29	0.31	0.21	0.21	0.21
Concrete data									
Temperature at casting, ^{0}C	20	21	18	17	19	23	23	22	21
Slump, mm	25	0	20	15	25	0	145	70	115
VEBE, sec.	2.2	4.7	3.3	3.2	5.2	8-10	1.0	3.5	4.9
Density, kg/m^3	2,280	2,330	2,300	2,280	2,450	2,420	2,470	2,420	2,440
Air content, %	4.9	3.8	3.8	4.0	2.0	3.6	1.5	2.2	1.9
Compressive Strength									
MPa 1 day	12	14	10	11	30	31	51	50	36
7 days	30	35	30	28	58	55	75	85	82
28 days	38	44	40	45	72	66	95	115	114
90 days	42	50	52	56	82	78	115	135	133
1,000 days	48	60	59	65	94	83	116	137	147
2,280 days	52	65	60	71	102	94	125	143	158
5,000 days**)	46	62	52	51	76	80	100	118	117
	(58)	(78)	(65)	(64)	(99)	(100)	(125)	(148)	(146)

Notations: PC = Normal Portland Cement; HSRC = High Sulphate Resistant Portland Cement; BC = Blended Cement; AE = Air Entraining Agent; P = Plastisizer; SP = Superplastisizer;

*) The Silica Fume contents correspond to 10%, 20%, and 50% by volume of the total content of cement + silica fume, respectively.

**) Results obtained at 100 mm dia cores. Figures in brackets are the core strengths multiplied by a conservative cast-cylinder/core correction factor of 1.25.

TABLE 3 — MICROSTRUCTURE AT SIX YEARS

Concrete Type	Air entrainement	Substances in voids	Paste microcraks	Carbonation depth (mm)
2	Nonhomogenous distribution	Some ettringite	Some	0.4 - 1.0
3	Homogeneous distribution	Ettringite, $Ca(OH_2)$, calcite	Some	0.1 - 0.7
4	Homogeneous distribution	A little ettringite and Calcite	A few	0.1 - 0.7
5	Homogeneous distribution	Little ettringite	A few	0.1 - 0.7
6	None	Calcite and $Ca(OH_2)$	Some	0.1 - 0.7
7	Homogeneous distribution	A little ettringite	Many	0.4 - 1.0
8	None	None	Many	0.1 - 0.4
9	None	None	Many	0.1 - 0.3
10	None	A little calcite	Many	Max 0.1

TABLE 4 — DATA FOR CEMENTS AND MINERAL ADDITIONS USED IN EXPOSURE FIELD STUDIES

	BC	RPC	HSRC	Fly Ash	Silica Fume
Chemistry					
SiO_2, %	27	21	24	53	92
Al_2O_3, %	10.3	5.2	2.5	31	2.2
Fe_2O_3, %	3.6	3.0	3.1	7.4	0.3
CaO, %	52	63	66	4.9	0.4
MgO, %	1.1	1.0	0.7	1.4	1.0
SO_3, %	2.5	2.9	1.8	0.7	0.7
Loss on ignition, %	2.3	1.5	0.9	2.4	3.0
Eq. Na_2O, %	0.8	0.6	0.3	1.8	2.6
Insoluble residue %	15	1.6	0.4	-	-
Fly ash content %	20	3	-	-	-
C_3S, %	-	-	55	-	-
C_2S, %	-	-	28	-	-
C_3A, %	-	-	1.5	-	-
C_4AF, %	-	-	9.4	-	-
$CaSO_4$, %	-	-	2.4	-	-
Physics					
Time of set initial, h:min	2:10	1:30	2:30	-	-
final, h:min	2:45	2:00	3:00	-	-
Fineness - Blaine, m^2/kg	450	430	310	-	-
Residue on sieve 200 µm, %	0.3	0.2	0.1	-	-
90 µm, %	1.5	0.9	0.4	-	-
Compressive Strength (ISO), MPa: 1 day	17	19	11	-	-
7 days	40	46	38	-	-
14 days	44	50	44	-	-
28 days	51	54	50	-	-
56 days	58	60	59	-	-

Notations: BC = Blended Cement; RPC = Rapid Hardening Portland Cement;
HSRC = High Sulphate Resistant Portland Cement.

TABLE 5 — PHYSICAL PROPERTIES OF CONCRETE MIXTURES USED IN EXPOSURE FIELD TESTS

Concrete Type	1	2	3	4	5	6	7	8	9	10	11	12	13	14	15	16
Cement Type	BC	RPC	HSRC	RPC	BC	BC	RPC	HSRC	BC	HSRC	RPC	BC	RPC	HSRC	HSRC	BC
Concrete Mix, kg/m³																
Cement (C)	261	200	264	261	199	333	256	340	260	327	334	397	300	390	300	300
Fly Ash (FA)										65						
Silica Fume (SF)		20			21		26		26				30		30	32
Water	141	125	138	140	143	146	141	142	140	141	144	165	140	142	136	143
W/(C+0.3FA+3SF)	0.54	0.48	0.52	0.54	0.55	0.44	0.44	0.42	0.41	0.41	0.43	0.42	0.36	0.36	0.35	0.36
Concrete data																
Air content, %	5.8	5.6	5.7	5.8	5.5	5.6	5.5	6.0	5.9	5.8	5.8	5.4	5.8	5.4	5.6	5.5
Slump, mm	60	50	45	50	40	55	60	60	55	65	50	50	70	60	50	40
Compressive Strength																
MPa 7 days	20	21	17	21	16	24	30	31	21	33	30	28	30	38	39	29
28 days	27	36	25	28	27	32	51	40	34	44	38	38	49	48	62	46
1 year	44	49	35	36	40	50	64	57	47	70	47	54	57	67	69	57
5 years	44	46	38	31	46	49	65	63	54	75	48	58	64	73	73	60
10 years	43	44	37	30	44	47	59	63	50	72	47	59	62	77	74	62
Modulus of Rupture																
MPa 28 days	4.1	4.8	4.3	4.0	4.4	4.6	5.7	5.1	5.0	5.4	4.6	4.8	5.2	6.1	6.4	5.7
1 years	5.1	5.5	4.8	4.2	6.0	5.8	6.8	5.9	5.4	6.9	5.2	6.3	5.6	6.6	7.3	6.5
10 years	5.8	5.8	4.6	3.8	6.5	6.6	7.3	6.6	6.3	7.5	5.4	7.3	5.9	6.7	8.0	6.8

Notations: BC = Blended Cement; RPC = Rapid Hardening Portland Cement;
HSRC = High Sulphate Resistant Portland Cement.

TABLE 6 — RESULTS OF TESTS ON EXPOSURE FIELD SPECIMENS

Concrete Type	1	2	3	4	5	6	7	8	9	10	11	12	13	14	15	16
Air content, %	2.8	2.8	4.7	4.5	2.6	1.9	1.6	5.6	4.7	4.0	4.3	4.7	5.6	3.5	4.7	2.8
Spacing factor, mm	0.13	0.16	0.18	0.10	0.20	0.13	0.23	0.16	0.14	0.15	0.17	0.15	0.16	0.16	0.17	0.15
Compressive strength, MPa																
SE, 28 days	-	-	-	-	-	-	-	-	-	-	-	-	-	-	-	-
IE-Slabs B, 28 days	26	38	19	20	29	28	48	33	38	40	35	26	44	52	61	46
IE-Panels C,28 days	32	28	28	24	28	33	50	38	36	43	40	40	50	51	67	52
SE, 1 year	39	39	43	28	42	44	50	48	44	65	43	53	54	58	65	50
IE-Slabs B, 1 year	39	49	36	28	38	44	69	47	43	52	46	43	57	65	69	52
IE-Panels C, 1 year	42	41	36	36	36	46	62	48	47	62	52	51	57	64	68	55
SE, 10 years	47	43	48	12	50	48	56	58	44	70	35	59	56	71	67	57
IE-Slabs B, 10 years	36	44	35	18	37	44	60	47	42	55	*	43	46	65	59	50
IE-Panels C,10 years	44	37	32	31	38	47	61	46	51	60	41	55	56	59	61	61
Durability (10 years)																
SE,	n	n	n	ccc	n	n	n	n	n	n	ccc	n	n	n	n	n
IE-Slabs A	n	n	n	ccc	n	n	n	n	n	n	n	n	n	n	n	n
IE-Slabs B	n	n	n	n	n	n	n	n	n	n	cc	n	n	n	n	n
IE-Slabs E	c+s	c	n	ccc	s	cc	cc	n	n	n	ccc	n	n	n	n	n
IE-Panels C	n	n	n	h	h	h	h	h	h	n	n	n	n	n	n	n
IE-Panels D	n	n	n	n	n	h	n	h	n	n	n	n	n	n	n	n

Notations: SE = Seawater Exposure; IE = Inland Exposure
n = no deterioration; c = a few craks; cc = some craks;
ccc = extensive cracking (map cracking, gel exudations,
rust deposits); s = some scaling; h = hairline cracks/surface crazing)
Mixture types 1-16: See Table 5.

*) The cores were completely disintegrated and could not be tested.

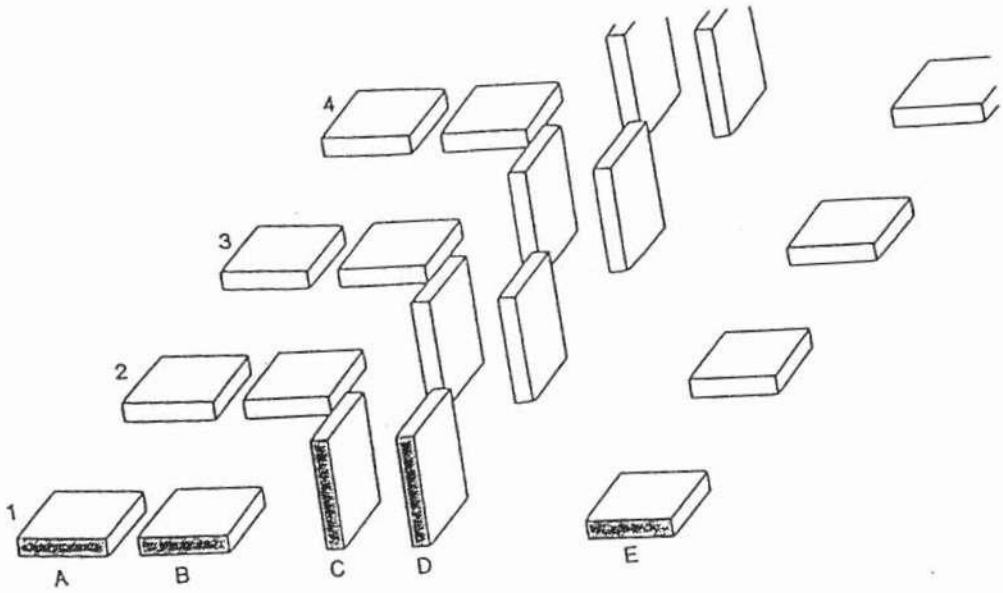

Fig. 1—Isometric illustration of precast box unit for fish ladder

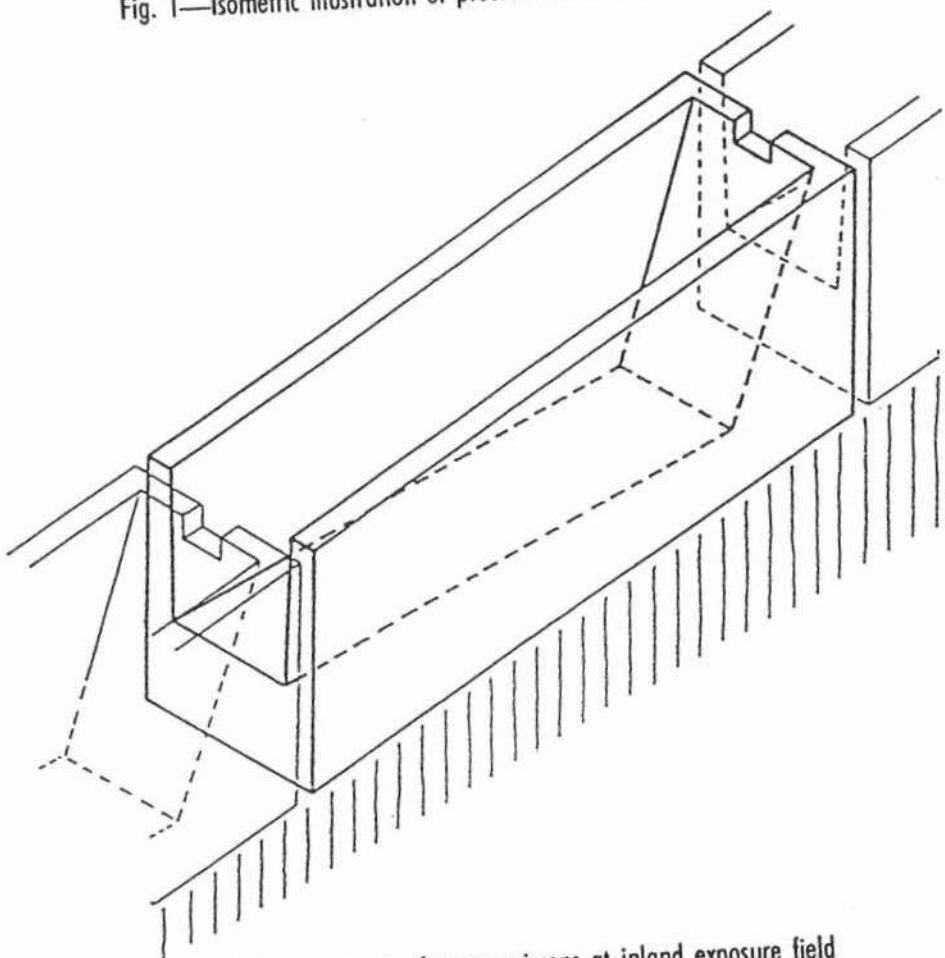

Fig. 2—Arrangement of test specimens at inland exposure field

FIELD MEASUREMENTS AND EXPERIENCE OF CHLORIDE INDUCED CORROSION OF REINFORCEMENT IN SUBMERGED STRUCTURES

Peter Shaw, Materialröntgen AB and Tomas Kutti, AB Färdig Betong, Göteborg, Sweden

ABSTRACT

A summary of measured chloride levels, concrete cover and observed corrosion of reinforcement in concrete structures submerged in sea water is presented. The relationships between these are discussed. The significance of construction details and practice, as well as quality of workmanship on the type and extent of damage is emphasised.

Key words: chloride content, corrosion, concrete cover, construction details

1. INTRODUCTION

In the summer 1992 some evidence of corrosion was observed in the inlet culverts of the cooling water channels to Barsebäck nuclear power plant reactor no 2 (B2). This initiated a major investigation of all accessible concrete surfaces of the cooling water systems to the two reactors B1 and B2 during the year 1993. The object of these investigations was to asses the condition of the structures, with less emphasis being placed on investigating the damage mechanisms. At the time of inspection the cooling water channels had been in service for approximately 20 years.

2. STRUCTURAL DESIGN OF THE COOLING SYSTEMS

There are two identical cooling water systems which feed water from Öresund to the condensors of reactors 1 and 2. The structures consist of filtration tanks, small inlet culverts, a large outlet culvert plus a number of pump chambers, distribution channels and auxiliary culverts.

The rate of flow is 23,3 m^3/s resulting in a flow velocity of approximately 2,6 m/s. The increase in water temperature from inlet to outlet is 10°C. The greater part of the concrete surfaces are permanently submerged. There is a free water surface and splash zone 2-3 m in height (depending on the sea water level at the time) in the tanks, pump chambers and distribution channels. The system is emptied at most every two years for routine inspections and maintenance.

The culverts are designed as statically indeterminate frames with the main loading from the overlying fill material. The roof-slabs are 500-600 mm thick in section and heavily reinforced. The culverts are also designed to withstand internal surging pressures.

All structures are of ordinary reinforced concrete. The specified concrete quality is K40, water impermeable concrete and with an air content of 4,5%. Fixed steel shutters have been used for the culverts, while most of the chambers have been cast with slip-form. The concrete surfaces are untreated with the exception of the filtration tanks, pump chambers and auxiliary inlet culvert which are coated with anti-fouling paint.

3. TESTING AND INSPECTION PROCEDURES

The inspections were of a general nature and included a large number of chloride measurements. The tests were made by ion selective electrode in accordance with the RCT method. Hence, the given results in this work are expressed as the total acid soluble chloride content as a percentage of concrete weight.

It was obvious that chloride levels around the main reinforcement were very high in places. Patterns of reinforcement corrosion were identified and this prompted a detailed structural analysis. The observed reinforcement corrosion was very local in nature, unlike that so often found in atmospherically exposed concrete. A project team was formed which included structural analysts and concrete specialists to re-evaluate the structures on the basis of observed corrosion damage. Cathodic protection was proposed to stem further corrosion and a passive system using magnesium anodes was installed in the summer of 1994. A survey was simultaneously made to quantify the percentage reduction in reinforcement in each part of each structure.

4. CHLORIDE LEVELS AND DAMAGE PATTERNS

Probably the most confounding aspect of the condition of the structures is the enormous variation in chloride levels within one and the same structure. In TABLE 1 calculated values of surface chloride content at different locations in the structures of the cooling water systems are given. Chloride levels around reinforcement may vary by as much as five-fold. The average concentrations around the main reinforcement in the roof slabs of the inlet culverts at 15-30 mm depth under the surface is 0,25%, but may be as much as 0.5%.

TABLE 1. Calculated chloride contents and diffusion coefficients. (Initial chloride content 0,005% of concrete weight).

Sample	**Structure**	**Chloride content on the surface, % of concrete weight**	**Diffusion coefficient, mm^2/year**
B1-1	Inlet culv., wall	0,72	105,4
B1-2	Inlet culv., roof-slab	0,75	82,2
B1-3	Outlet culv., wall	0,14	103,8
B1-4	Outlet culv., wall	0,17	185,4
B1-5	Outlet culv., wall	0,09	201,8
B1-6	Outlet culv., roof-slab	0,68	218,7
B2-1	Aux. inlet culv., wall	0,22	68,1
B2-2	Aux. inlet culv., wall	0,17	45,1
B2-3	Aux. inlet culv., wall	0,15	221,7
B2-4	Pump-chamber, wall, splash zone		
B2-5	Pump-chamber, wall below water level	0.09	19,4
B2-6	Outlet culv., roof-slab	0,62	146,0

There are also recognizable trends of higher chloride levels in roof-slabs compared to walls. In TABLE 2 some selected chloride levels in the outlet culvert of Barsebäck 1 are shown.

TABLE 2. Chloride content, % of concrete weight. (30-45 mm under concrete surface). Outlet culvert, Barsebäck 1.

Structure	Point 1	Point 2	Point 3	Point 4
Roof-slab	0,16	0,33	0,26	0,15
Wall	0,19	0,11	0,14	0,08

In TABLE 3 the chloride levels in different sections of the outlet culvert to Barsebäck 2 are given. These measurements were made in order to locate areas of high corrosion risk, prior to exposing and inspecting the reinforcement. For comparision, the reinforcement on three 1,5m² areas was exposed using high pressure water-jetting. At position +93 m there was evidence of corrosion in the roof-slab in the form of brown rust spots on the concrete surface. Careful inspection of the exposed reinforcement showed an average total reduction in x-section of 15%, with as much as 30% on individual bars. Maximum corrosion (80%) had occcurred on a distribution bar with 25 mm cover.

TABLE 3. Chloride content, visible damage and reduction in reinforcement. Outlet culvert, Barsebäck 2.

Position	Chloride content 25-35 mm under surface, % of concrete weight	Concrete cover, mm Average (Min)	Visible damage on surface, Yes/No	Actual average reduction in reinforcement, %
-10 m, wall	0,11	22 (9)	Yes 1)	100
-10 m, roof	0,10	27 (25)	No	-
+6 m, wall	0,09	44 (43)	No	-
+6 m, roof*	0,07	28 (27)	Yes 2)	10
+25 m, wall	0,29	34 (31)	No	-
+25 m, roof	0,11	29 (28)	No	-
+44 m, wall	0,16	40 (39)	No	-
+44 m, roof*	0,07	46 (44)	Yes	0
+69 m, roof	0,26	36 (35)	-	-
+93 m, wall	0,19	40 (36)	No	-
+93 m, roof*	0,44	31 (30)	Yes 3)	15

*approximately 1,5 m² of reinforcement exposed by water-jetting
1) construction joints
2) rust on 1 of 8 bars
3) rust on 9 of 11 bars. Reduction due to corrosion on distribution bar 80%

Many of the structures are fitted with active cathodic protection in the form of magnetite anodes. These have served to protect the pumps, valves etc. They have been in position since the plants were first brought into service. The investigations show that the protecting current from the anodes has even spread to the reinforcement. As can be seen in TABLE 4 the average chloride levels in the cathodically protected submerged structures are significantly lower than the unprotected structures. The measured electro-chemical potential of the reinforcement of the structures was between -900 and -1000 mV (copper-sulphate-electrode).

TABLE 4. Average chloride content, concrete cover and observed corrosion in different structures.

Structure	Chloride content 15-30 mm under concrete surface, % of concrete weight	Chloride content 30-45 mm under concrete surface, % of concrete weight	Average concrete cover, mm	Min concrete cover, mm	Observed corrosion, Yes/No	Comments
Pump chambers[1], B1	0,04	0,03	34	20	No	Anti-fouling paint, Cathodic protection
Filtration tanks[2], B1	0,15	0,14	32	27	No	Anti-fouling paint
Inlet culverts B1	0,25	0,21	18	15	Yes	
Inlet culverts B2	0,24	0,17	33	15	Yes	

[1] 20 structures [2] 6 structures

An estimation was made of reinforcement reductions due to corrosion by visual survey of concrete surfaces. The results from one of these surveys are given in TABLE 5, which describe the average estimated reduction in roof-slab reinforcement of the inlet culverts to Barsebäck 1. Four areas, approximately 1,5m² were water-jetted to expose reinforcement., and the degree of corrosion was measured, see TABLE 6. Generally the correlation between estimated and actual damage was good. An overestimation of ~10% was normal.

TABLE 5. Estimated reduction in inner surface reinforcement to the roof-slabs in four different inlet culverts of Barsebäck 1. Estimations based on frequency of rust spots on concrete surface.

Culvert No	Point 1	Point 2	Point 3	Point 4	Point 5	Point 6	Point 7
2	70	50	25	10	80	30	50
3	5	80	15	10	30	40	70
4	70	80	50	40	90	80	80
5	50	90	30	30	60	80	90

TABLE 6. Observed corrosion damage after water-jetting. Inlet culverts, Barsebäck 1.

Culvert No/ Position	Chloride content 20-25 mm under surface, % of concrete weight	Concrete cover, mm Average (Min)	Visible damage on surface, Yes/No	Estimated reduction in reinforcement, %	Actual reduction in reinforcement, % (inner surface)
2/21 m	0,5	21 (15)	Yes	80	60 (70)*
5/15 m	-	- (10)	Yes	80	80 (100)*
5/21 m	-	- (23)	Yes	80	70 (90)*
5/35 m	-	- (20)	Yes	90	60 (100)*

( )*Reduction in x-section. Individual bars.

5. COVER TO REINFORCEMENT

From the investigations it was seen that reinforcement corrosion did not occur if the cover is of good quality concrete, homogeneous and at least 40 mm, regardless of chloride content. Cover to reinforcement varies significantly as can be seen in TABLE 4. The average cover thicknesses on the undersides of roof-slabs in the inlet culverts to B1 and B2 is 18 mm and 33 mm respectively. The corresponding reduction in reinforcement due to corrosion is on average 70% and <5%. Typically, the cover in roof-slabs undersides is less than the average cover to walls, see TABLE 7. Cover on the upper sides of slabs is normally very good, i.e min. 50 mm.

TABLE 7. Average cover thicknesses in mm.

Structure	Underside roof-slab	Wall
Auxiliary inlet culvert, B1	25	33
Inlet culvert, B1	18	30
Outlet culvert, B2	33	36

Poor cover to reinforcement can usually be attributed to awkward geometries, small sections, miss-alignment of starter bars, congested reinforcement and sagging. Cover thicknesses of 10 mm are not unusual in the lower parts of walls, where vertical bars have been spliced on to starter bars from floor-slabs. A similar pattern may at times be seen along the upper parts of walls.

Reinforcement corrosion is common where cover thickness is less than ~20 mm, see Figure 2.

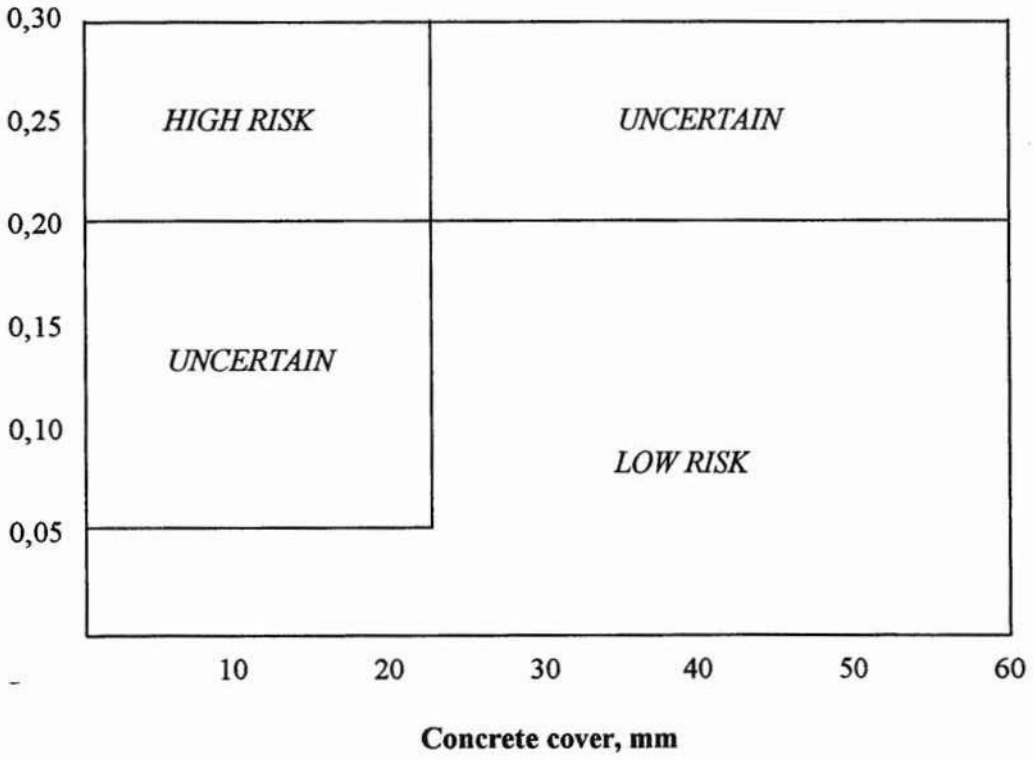

Figure 2. Estimation of corrosion risk in submerged structures based on measured chloride content and concrete cover.

6. DAMAGE TO REINFORCEMENT RELATED TO CONSTRUCTION DETAILS

6.1. Construction/casting joints

Floor-slabs and walls are cast as separate units. The construction joint between these being provided with a water bar to prevent seepage through this break in continuity. Vertical reinforcement through this joint prevents lifting due to internal water pressure, in particular those pressures caused by surging.

Construction joints are one of the most common areas of reinforcement corrosion in culverts. The main causes are poor compaction of concrete and entrapped air. The joint itself is a weak zone which may have further deteriorated due to shrinkage and leaching. The joint surfaces are often sandy, with much of the cement paste leached out. This combined with poor reinforcement cover at the joint, as described above, results in very localised corrosion to vertical bars, sometimes along sections of culvert up to 25 m in length.

The chloride profile through joints is often flat, with no measurable decrease in chloride content with depth from the surface. Bars are typically cut off by corrosion over a length of 25-50 mm coinciding with the joint, the remainder of the bar being quite unaffected.

A similar type of damage is found in casting joints in walls. There is evidence in the standby inlet culvert that the walls have been cast in stages, resulting in two or three horisontal joints with a depth of around 600 mm. Poor compaction in these joints results in localised corrosion to vertical bars as described above. This type of damage pattern is not found in the outlet culverts, presumably these having been cast to their full height in a continuous pour.

6.2. Concrete spacers

Concrete spacers are probably the single most common cause of serious damage to reinforcement in roof-slabs. They are used under distribution bars in the larger outlet culverts while in the inlet culverts they are placed at regular intervals of 1 m under the main reinforcement. They are small, precast blocks with a diameter of 50 mm and depth 30 mm, sometimes less. They consist of mortar only and are of a more porous nature than the surrounding concrete. Test made on spacers drilled from the roof-slab of the outlet culverts show that all of the surfaces are carbonated. This means that the supported bar is in contact locally with a carbonated surface and may therefore not benefit from the protective alkalinity of the concrete at this point.

The spacers cause local and very severe corrosion to reinforcement, while adjacent steel surfaces are unaffected. In some parts of the inlet culverts there is evidence of corrosion at each spacer, resulting in a reduction in reinforcement of 25%. The spacers are placed in lines along the slabs with the result that damage is concentrated to fixed points in the section, which is undesirable from a structural viewpoint.

6.3. Form-ties

Form-ties used in walls may be fixed to vertical bars causing local corrosion attack. The ties themselves tend to corrode leaving small and deep holes into the concrete allowing water and chloride ingress. It is however rare that form-ties are fixed to reinforcement and this is therefore not regarded as a serious problem in generally. They do cause rust spots on the

concrete surfaces of walls, and care should be taken not to confuse these with evidence of relevant corrosion damage.

6.4. Joints between shutters

Joints between shutters allow separation of water and cement paste during casting leaving porous channels in the covering concrete. Although not a common cause of reinforcement corrosion, the problem does exist both in walls and roof-slabs.

A common feature of the mentioned above construction details is that they are not random but form lines along the culverts and thereby significant reinforcement reductions at sections. Random placing of concrete spacers would allow for distribution of stresses from one point to adjacent bars. This is usually not possible where corrosion follows paths created by detailing features.

7. OTHER FACTORS RELEVANT TO CORROSION RISK AND DAMAGE PATTERNS

7.1. Loading

The roof-slab of the standby inlet culvert to B1 is undamaged with the exception of a 15 m long section, where the reduction in reinforcement on the inner surface is 80%. This section lies directly under a water tank which causes extreme bending stresses in the roof-slab underside. The concrete surface is painted with a thick layer of anti-fouling paint which could conceal cracking in the concrete. No closer studies of the condition of the concrete have been made, but it seems probable that the corrosion damage is related to the extreme loading conditions.

7.2. Environment

There are two main categories of structure with respect to flow conditions. The large tanks and pump chambers contain water which is relatively still, particularily at the wall surfaces, while the culverts contain flowing water with varying degrees of turbulence.

It is interesting to note that no corrosion damage occurs anywhere in the submerged surfaces of tanks, despite the fact that construction methods are largely similar. The measured chloride levels are on average one half compared with the culverts, which may possibly be attributed to the anti-fouling paint.

There are indications of a higher frequency of corrosion damage in sections of culvert where water-flow is turbulent, e.g at the mouth of the inlet culverts and outlet culvert where water comes down from the condensor and collides with roof-beams placed across the culvert.

There exists a relationship between flow conditions and risk/rate of corrosion [1], and it may be explained in part by the fact that oxygen-transport to the concrete surface and ultimately to the reinforcement is helped by eddy-currents in turbulent zones.

In laminar flow conditions the transport of oxygen occurs by diffusion, the rate of diffusion increasing with flow-rate as the thickness of the laminar layer decreases. As shown in Figure 1,

a transition from laminar to turbulent flow (at critical Reynolds number) is associated with a sharp increase in corrosion rate.

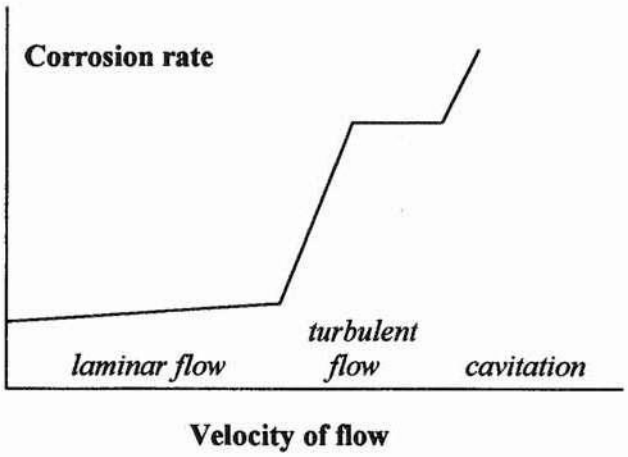

Figure 1. Corrosion rate versus velocity of flow [1].

It has been suggested that cathodically protected reinforcement will not affect concentrations of chlorides in surrounding concrete. As can be seen in TABLE 4 the measured chloride levels in structures (inadvertently) affected by existing cathodic protection are one quarter of those found in similar but unprotected structures. The measurements are consistent with each other and are based on surveys of more than 25 different structures.

7.3. Patterns of reinforcement corrosion - reinforcement spacing

In Figure 3 the distribution of corrosion damage along the main reinforcement of a section of outlet culvert roof-slab is shown. The main reinforcement on the slab underside is placed across the section at c/c-spacing 125 mm, with secondary reinforcement placed on top of these at 200 mm centres (typically). At the point shown the measured chloride levels are 0,45% of concrete weight and cover to main reinforcement is 30 mm. The corrosion damage is in the form of pitting, with reductions of as much as 30% on individual bars. The corrosion is spread up to about 300 mm along sections of the reinforcement and is confined to the surface nearest the exposed surface. The secondary bars are unaffected.

Damage patterns to main reinforcement in the inlet culvert are typically quite different. In the roof-slab, points of attack occur wherever concrete spacers are attached to the main reinforcement. Also a characteristic of the roof-slab reinforcement is severe point corrosion at the exact intersection between the main reinforcement and overlying secondary reinforcement. The degree of corrosion is 50-100% over lengths of approximately 50 mm. The adjacent steel surfaces are free from any indications of corrosion. Corrosion is confined to the main bars, with initiation on the surface nearest the exposed surface. The main bars are normally placed at 200 mm centres with overlying secondary reinforcement at 350-400 mm. The regularity of the points of attack is undesirable from a structural viewpoint.

Given that the conditions in the inlet and outlet culverts are very similar, it would appear that reinforcement spacing influences the nature of corrosion attack.

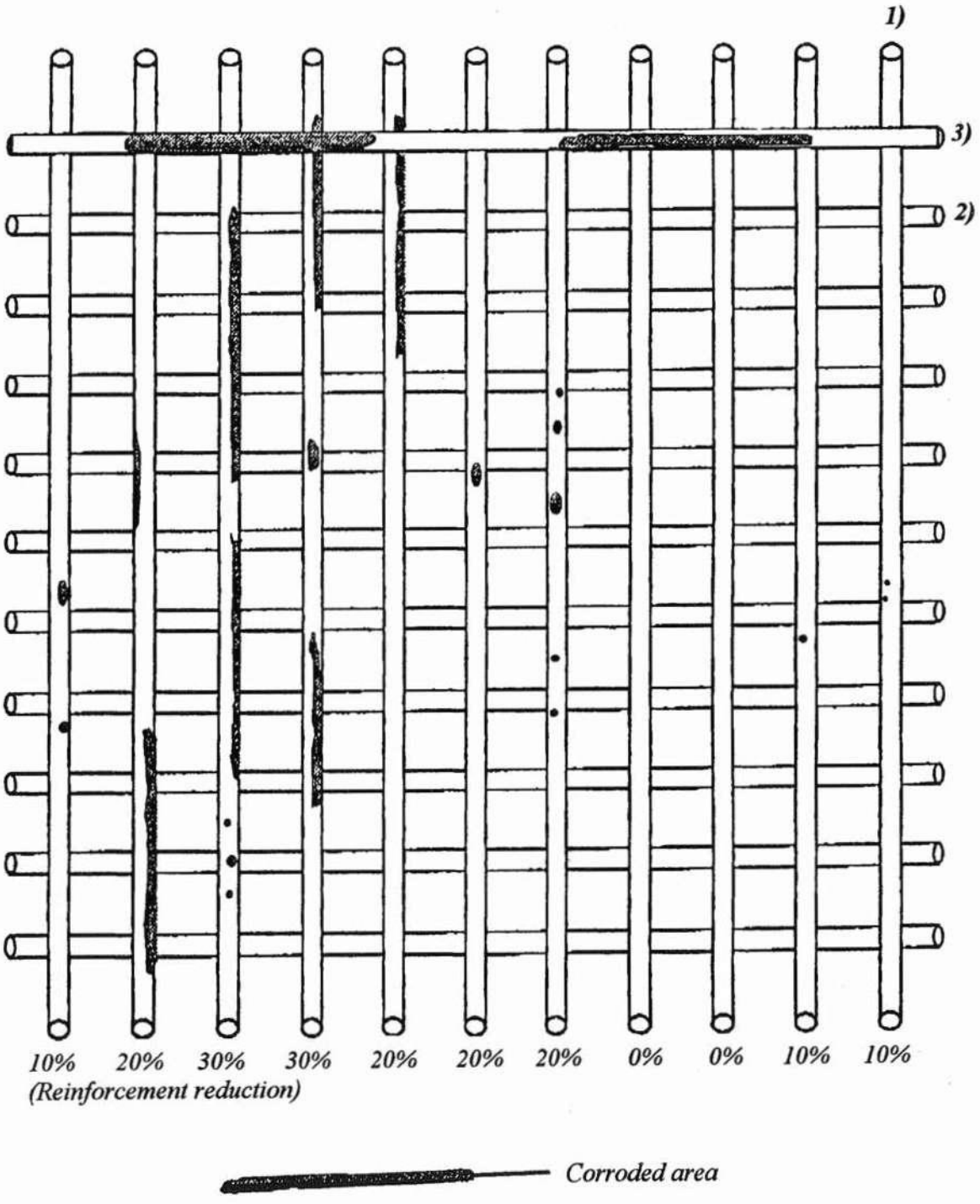

1) Main reinforcement

2) Secondary reinforcement

3) Spreader bar

Figure 3. Corrosion to roof-slab reinforcement. Outlet culvert, Barsebäck 2. Position +93 m. Seen from below. From [2].

8. CONCLUDING REMARKS

The existence or non-existence of serious corrosion damage to reinforcement in submerged structures such as those described can be determined by visual inspection alone. The extent of corrosion can be measured quite accurately by the number of rust spots on the concrete surface and by relating these to the layout of the reinforcement. A 15% reduction in x-section caused by corrosion has been seen to be accompanied by cracking and deposits of corrosion products on the concrete surface.

Non-destructive testing techniques to determine corrosion at an early stage cannot be effectively used without first locating areas of high corrosion risk. Concrete sampling can be carried out quickly and accurately on site to locate such areas. Since the corrosion is very local then testing methods based on the Stern-Geary polarisation theory cannot be used.

In concrete structures built before 1980 the quality of workmanship varies to such an extent, that if conditions are such that there is a risk of reinforcement corrosion, there will be visible evidence in the form of isolated rust spots long before reductions in reinforcement become a serious problem from a structural viewpoint.

The observed patterns of corrosion indicate that initiation of corrosion is caused by variations in concrete environment around one and the same bar or between two bars in contact with each other. Typically corrosion occurs on bars which extend through cracks/construction joints or which are in contact with concrete spacers. A common form of corrosion occurs at the intersection of primary and secondary reinforcement, presumably a result of galvanic action between bars caused by the chloride concentration gradient from the concrete surface.

Corrosion under water is accompanied by cracking of the concrete cover. The cracks are very fine and do not cause spalling of the cover. Since no new points of corrosion initiation , i.e. points which are not accompanied by rust spots on the concrete surface, have been observed on the exposed bars , it seems that corrosion develops along the bar from the orginal point of attack. It is not uncommon for 80% of the bar section to be consumed at these points. This is quite different from the case of concrete exposed to air, as the original point of corrosion attack usually extend along the bar, accompanied by spalling of cover, long before reductions in bar section exceed 50%. It would seem therefore that in submerged structures the corrosion products do not hinder further attack at the initiating point.

Probably the most significant factor governing corrosion at an early stage is thickness of cover to reinforcement.

Cathodic protection to reinforcement will result in significantly lower chloride concentrations in the surrounding concrete.

There is evidence that the rate of corrosion is higher if water flow is turbulent. No corrosion has been obseved in structures containing relatively stagnant water.

REFERENCES

[1] Wranglén, G., Metallers korrosion och ytskydd, Almqvist&Wiksell, 1967. (In Swedish).

[2] Shaw, P.&Larsson, E., MRQ-rapport B1 och B2, 1994. (In Swedish).

CHLORIDE PENETRATION IN MARINE ENVIRONMENT

Part 1: Computer program calculating average chloride content

Trond Østmoen & Per Egil Steen, Public Roads Administration, Bridge Department, Oslo, Norway.

ABSTRACT

There are about 277 concrete bridges with total length 30 m or more along the coast of Norway. Approximately 80 % of these bridges are situated along the coastline, from Hordaland in the south to Finnmark up north, hence being exposed to rather rough weather conditions. Investigations based on 149 of the bridges mentioned above, in some cases show a distinct relationship between the predominant winddirection (regarded as an important parameter) and chloride penetration on the structures being considered. Measurements show the lowest chloride content on that side of columns facing wind and rain. A computer program has been designed to get knowledge about the relationship between maximum and average chloride content, and the penetration depth as a function of height above seawater level.

1. INTRODUCTION

1.1 *Bridges in Norway*

Concrete has been the most commonly used construction material for bridges in Norway and the public has invested a lot of money in these bridge constructions. The bridges have been designed for a service life of 100 years with reasonable level of maintenance. In Norway there are 21300 road bridges distributed on 3 classes of roads.

Table 1. Number of road bridges in Norway

Road class	Number of bridges	Bridge deck area
National roads	8800 bridges	1.5 mill. m^2
County roads	8500 bridges	1.1 mill. m^2
Municipal roads	4000 bridges	0.5 mill. m^2
Total	21300 bridges	3.1 mill. m^2

70 % of the bridges are concrete bridges
60 % of the bridges are built after 1965

Norway has a very long coastline with many fjords and islands. During the last 25 years many bridges have been built in these coastal areas. Many of these coastal bridges have been built as cantilever box girder bridges in posttensioned concrete, and some as prefabricated prestressed beam bridges. During the last years, when these bridges had reached an age of 10-25 years, deterioration caused by chloride induced rebar corrosion has been discovered. Because of this serious and increasing problem the Public Roads Administration has started a strategic program for how to solve the problem.

The first two steps in the strategic program are as follows:

1. Define the deterioration mechanisms.
2. Find the extent of the deterioration problems.

2. DETERIORATION MECHANISMS / EXTENT OF DETERIORATION

2.1 *Discovering the corrosion problems*

The first bridges that were reported with rebar corrosion problems were discovered in connection with the principal inspection of the bridges. This is an inspection that takes place every 5. year on all bridges in Norway. After concrete spalling and rebar corrosion was found, we started to make concrete samplings to measure the chloride penetration.

When reports of bridges with damages continued to increase we understood that we had to make a strategic program for how to get a comprehensive survey over the problem.

1. Geographical location of the bridges
2. How to do special bridge inspections.

2.2 *Geographical location of the bridges*

To get a survey over the bridges with corrosion damages we had to pinpoint the bridges that were located in a marine environment. The bridges that were chosen followed a special criteria:

1. Geographical location along the coast
2. Bridge with span over 30 meters.

The geographical locations of the bridges along the coast are divided into two environmental classes:

1. EME: Extreme Marine Environment

Bridges located along the coastal line and exposed for a huge amount of seawater splashing.

2. MME: Moderate Marine Environment

Bridges located in the fjords and exposed for a moderate amount of seawater splashing.

Table 2. Number of bridges in the coastal area with span over 30 meter.

	Number of bridges Environmental class	
County	EME	MME
Finnmark	3	3
Troms	9	1
Nordland	24	25
Nord-Trøndelag	21	5
Sør-Trøndelag	10	6
Møre og Romsdal	17	38
Sogn og Fjordane	8	6
Hordaland	24	31
Rogaland	13	4
Vest-Agder	11	7
Aust-Agder	0	3
Telemark	0	2
Akershus	0	3
Østfold	0	3
Total (277)	140	137

Of these 277 bridges, 226 were built before 1988, and 51 in the period 1988 to 1993. The distribution of the superstructures are 20 % in steel and 80 % in concrete.

2.3 *Special inspection and investigation*

The next step in the strategic program was to carry out inspections and investigations on the coastal bridges. We had to do this in a systematically way and for this reason we had to develop new procedures for this type of work. The report we prepared with these new procedures has the title *Inspection and investigation of coastal bridges in concrete.*

The inspections routines are split in the following way:

Step 1 inspections: Principal bridge inspection with a small number of concrete sampling (chloride profiles). The purpose of this step inspection is to map the damage dimensions and to give the basis for a more detailed inspection complete with concrete measurements.

Step 2 inspections: Detailed measurements that will give detailed information of the deterioration mechanisms and the dimensions of the damages.

Types of measurements:

1. Mapping of concrete lamination
2. Mapping of concrete cover over the rebars
3. Chloride penetration depths
4. Carbonation depths
5. Half-cell potential mapping
6. Compressive strength
7. tensile strength
8. Water absorption

9. Thin-section petrography of the concrete

2.3 *Observations and findings*

In the period 1990 to 1993 we received 149 inspection reports that had followed the procedures. The results due to visual condition and chloride penetration are presented in table 3. The 149 inspected bridges represent 54 % of the coastal bridges with span over 30 meter. All the inspected bridges are built before 1988.

Table 3. Condition of the 149 inspected bridges built before 1988.

	Number of bridges / Environmental classes	
Type of deterioration	EME	MME
Low chloride penetration, god condition	21 (23%)	28 (50%)
High chloride content, small number of concrete spalling	29 (31%)	8 (14%)
High chloride content, rebar corrosion and concrete spalling	23 (25%)	13 (23%)
Damages are repaired	19 (20%)	6 (11%)
New rebar corrosion in areas repaired earlier	1 (1%)	1 (2%)
Total (149)	93 (100%)	56 (100%)

Other findings from the inspections reports are as followed:

1. Concrete bridges with an age of 10-15 years have more severe damages than older bridges.
2. We have measured dangerous chloride penetration up to 10 meters above sea water level.
3. Chloride levels have been measured to 5% by weight of cement on the concrete surface and to 3% at the rebar level as maximum values.
4. Concrete surfaces that can be washed by rain water have less chloride ingress than surfaces that are not washed with rain water.
5. On concrete beam bridges the underside of the beams often has quite severe corrosion damage.
6. A lot of the damages are caused by insufficient concrete cover and a bad concrete quality.
7. A few of the bridges have damages caused by use of aggregate from marine sediments and also use of sea water as concrete mixwater.

2.4 *Climate load*

One of the findings from the chloride penetration measurement on large columns, is that the chloride content vary from side to side around the column. One example is the Hadsel bridge. The chloride penetration for axis 14 is shown in fig. 1. As we can see the chloride content is 4 to 5 times higher on the north side than on the south.

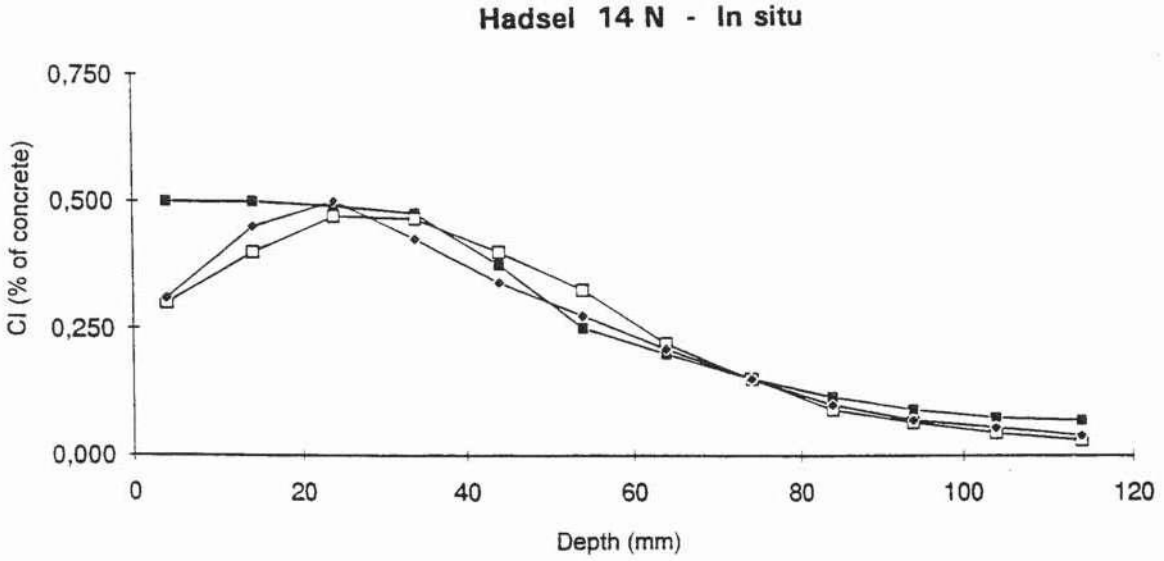

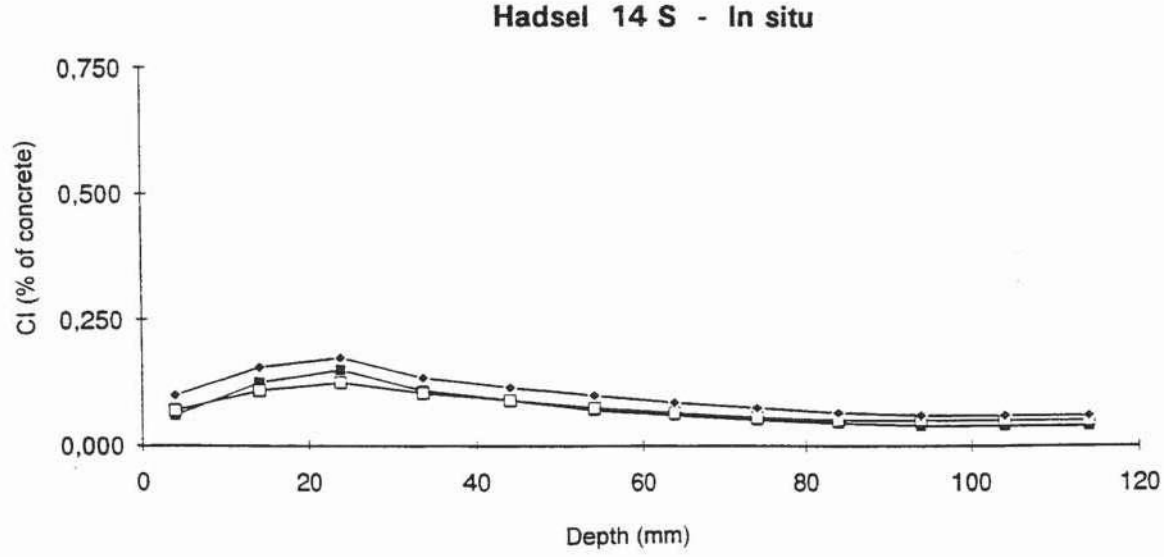

Fig. 1. Chloride penetration on the north- and south side on the column in axis 14 on Hadsel bridge.

In outer coastal areas there are often a predominant direction for strong winds together with rain. Winds from south and west are quite dominant. Bridges in these areas will therefore be exposed to unilateral climate load. The windward side will be exposed to wind, rain and splashing

from the sea. The leeward side is however almost protected from this exposure.

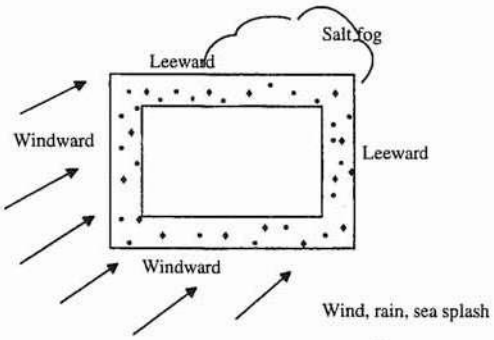

Fig. 2. Climate load on windward side and leeward side.

The topography along the coast with mountains, fjords or open sea will influence the climate load on the bridge site. A bridge may be sheltered for heavy wind and rain due to surrounding mountains, whilst on the other hand the crossing structure can be exposed to the predominantly acting wind and rain along the fjord. The strait crossings are usually situated on the most narrow part of straits and fjords - the area of which one can expect to obtain highest wind velocities.

For the Hadsel bridge the windward side is to the south. Because the rainwater is exposed on this side some of the chlorides will be washed off and the chloride content will be less than on the leeward side (north).

3. COMPUTER PROGRAM

To get a systematic evaluation of all the chloride penetration measurements that have been sampled in connection with the special inspections, it was decided to design a computer program.

This program contains chloride profiles on piers on bridges located in marine environment. It is divided into 3 separate systemes depending on whether profiles are sampled in 15, 20 or 25 mm steps. At the end of 1994 the program contained chloride measurements from 50 bridges.

The following data are registered for each bridge:

- Bridge-name and number
- Concrete quality
- Year built
- Age when inspected
- Environmental class EME/MME
- Chloride content in steps by 2/4 meters above seawater level

The program calculates average and maximum chloride content as a function og height above seawater level, and the data mentioned above. For example, chloride content as a function of age when inspected, or chloride content as a function of environmental class.

3.1 *Results*

As an example the results from the 25 mm step measurements are presented. Table 4 shows the total number of bridge inspections (21) and table 5 the total number of chloride measurements for these bridge inspections. In fig. 3 and 4 the average and maximum chloride content are shown for the 21 bridges. In fig. 5 and 6 the results are divided into bridges older (8 in number) and younger (13 in number) than 15 years.

As can be seen, and as expected, the chloride content decrease with the hight above seawater level and with the depth beneath the concrete surface. The increased chloride content for the level 18-22 meters is caused by the leward effect from the superstructure.

If 50 mm concete cover is used, the critical chloride zone (0,1 % Cl of concrete weigth) will be from 0 to 10 meters above seawater level.

The maximum chloride content (fig. 4) shows the penetration depths and climate load on the leeward side. It is these values wich have to be used when the concrete cover for new bridges is designed.

Fig. 5 and 6 show that it is no big difference in chloride content if the bridges are younger or older than 15 years. This observation may depend of the effect that chloride penetration are faster when the concrete is "young" and then decreases with time.

REFERENCES

T. Østmoen & B. Sand Public Roads Administration, Bridge Department, Oslo, Norway
"Durability of concrete bridges in marine environment in Norway"
Strait Crossings 1994

Bridge name	Number	Concrete quality	Year built	Age when inspected	Environmental class
Havøysund bru	20-1264	C40	1986	6	EME
Hestøy bru	17-1114	C30	1979	14	EME
Kvalsund bru	20-1144	C30	1977	16	EME
Nordsund bru	15-1837	C30	1980	12	MME
Omsund bru	15-1906	C30	1981	11	MME
Salvøy bru	11-0048	C30	1954	38	EME
Sandnessund bru	19-0820	C30	1973	20	EME
Sandnessund bru	19-0820	C30	1973	19	EME
Smines bru	17-1144	C30	1978	15	EME
Solheimsund bru	15-1729	C30	1978	14	MME
Sommarøy bru	19-1004	C30	1978	14	EME
Sommarøy bru	19-1004	C30	1978	13	EME
Sortland bru	18-1633	C30	1975	15	EME
Stamnes bru	17-0847	C30	1970	22	EME
Sørstraumen bru	19-1102	C35	1979	13	EME
Tjeldsund bru	19-0670	C35	1967	26	EME
Torsetsund bru	15-2488	C35	1976	16	MME
Torsetsund bru	15-2488	C35	1976	17	MME
Tromsø bru	19-0511	B35	1960	31	EME
Ullasund bru	15-0929	B35	1970	23	EME
Nordstrømmen bru	17-0631	C35	1964	28	EME

Table 4. Number of bridge inspections (25 mm measuement step)

	0-25 mm	25-50 mm	50-75 mm	75-100 mm
0-2 m	112	104	94	38
2-4 m	211	194	163	11
4-6 m	117	108	63	4
6-8 m	48	43	25	4
8-10 m	74	62	37	14
10-14 m	67	48	23	0
14-18 m	51	42	26	0
18-22 m	20	18	26	0
22-26 m	24	18	8	0

Table 5. Number of measurements for the bridge inspections in table 4

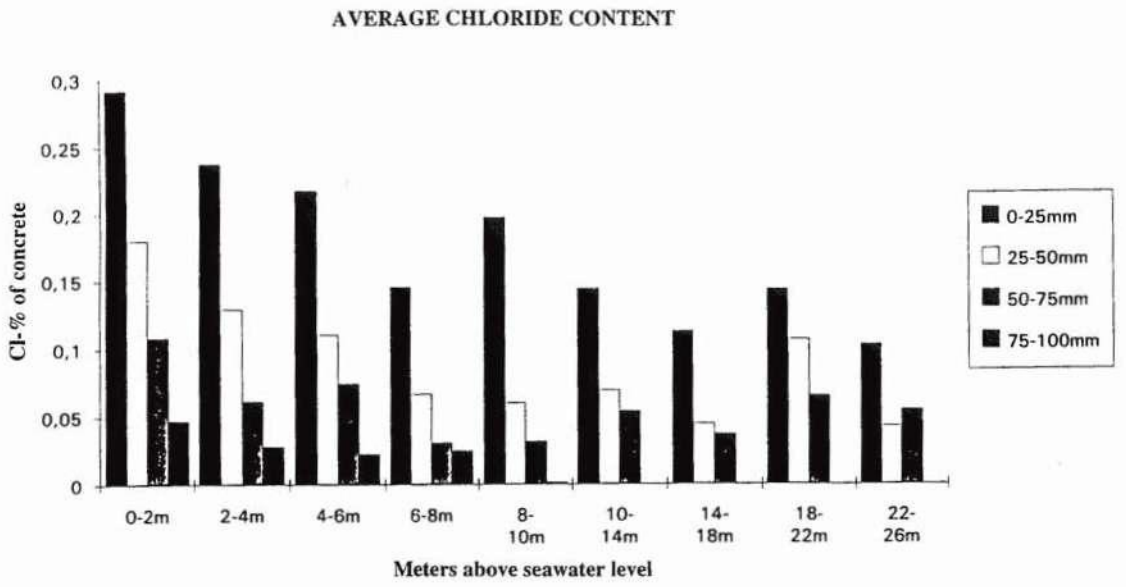

Fig. 3. Average chloride content for 21 bridge inspections
Age when inspected: 6-38 years

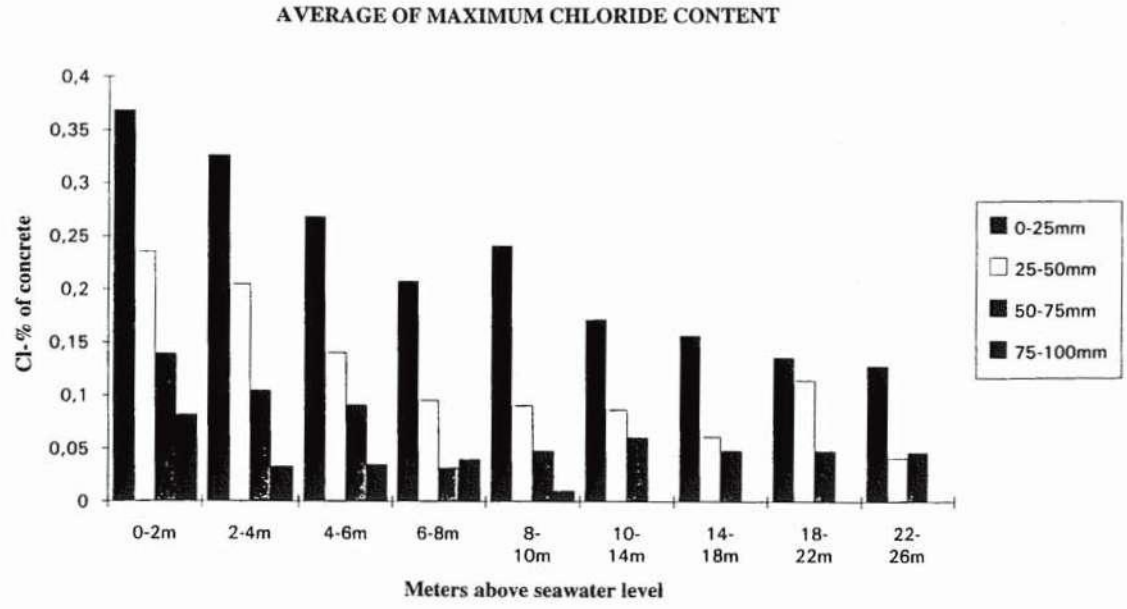

Fig. 4. Maximum chloride content for the bridges in fig. 3

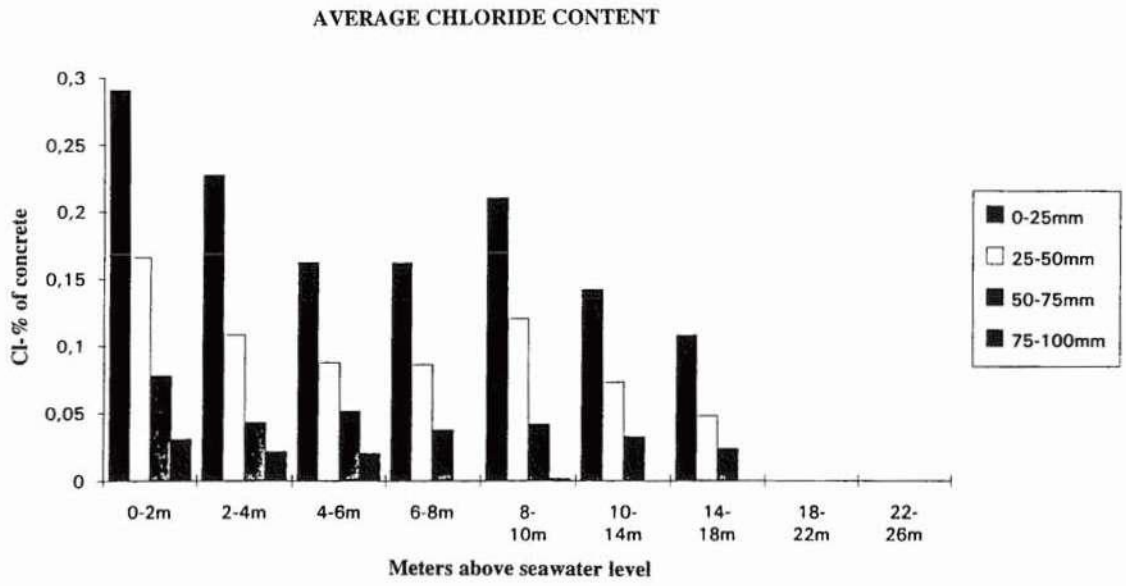

Fig. 5. Average chloride content for the 8 bridge inspections younger than 15 years in fig. 3

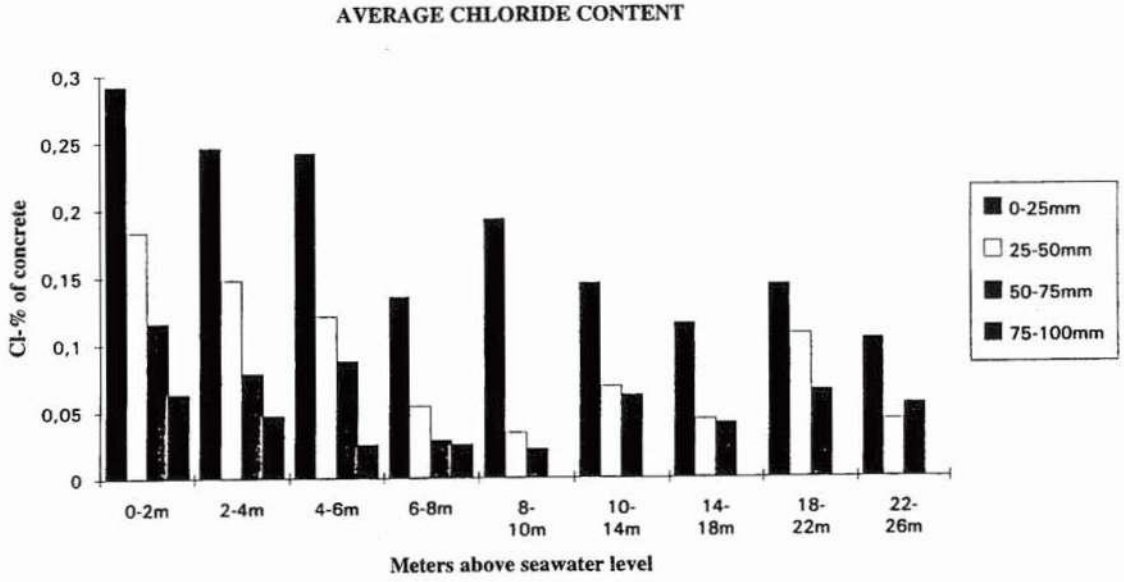

Fig. 6. Average chloride content for the 13 bridge inspections older than 15 years in fig. 3

CHLORIDE PENETRATION IN MARINE ENVIRONMENT

Part 2: Results from field tests on coastal bridges in Norway

by Per Egil Steen, Public Roads Administration - Bridge Department, Oslo

Abstract: At Gimsøystraumen and Giske bridges a total of 32 concrete slabs are instaled . The slabs are locaeted at different levels above seawater on the north, south, east and west side of the pillars and superstructure. After 46 weeks of exposure chloride contents at increasing depths and in-situ diffusion coeffisients have been calculated.

The mean value of the achieved in-situ coeffisients is 5.17 x 10^{-12} m^2/s. Comparable laboratory results, based on concrete cubes with sawed surface exposed for 3 and 6 weeks in salt spray chamber and bulk diffusion tests, show values is about four times higher.

The in-situ chloride profiles clearly show variations in chloride penetration depending on the location. Highest amounts are typically found on the northern side closest to sea water. This variation shows that the environmental effect has to be accounted for when estimating future chloride penetration.

Keywords: Concrete, chloride penetration, environmental effect

1. INTRODUCTION

Reinforcement corrosion in marine environment is induced primarily by ingress of chlorides into the concrete from seawater or by airborne chlorides. Much work has been done during the past years to map the extent of this problem, and it has been demonstrated by several researchers that the main transport mechanism is diffusion. However, while the diffusion model fits quite well for concrete tested in the laboratory this is not necessary the case for concrete exposed in a natural environment. The Bridge departments examination of several coastal bridges in 1991/92 showed clearly that laboratory results gave very conservative values with respect to diffusion coeffisients. The report conluded that diffusion coeffisients based on laboratory results alone was not valid for prediction of in-situ chloride penetration.

This paper present results from a field investigation in Nordland and Møre og Romsdal counties. The field test is conducted as a part of the authers project which focus on chloride penetration and the effect of variations in environmental exposure.

Further, the field test is part of a program where the aim is to evaluate the use of laboratory results, with respect to in-situ chloride penetration. Laboratory studies are performed at the Road Laboratory in Oslo, where salt spray chamber and bulk diffusion methods are used. The main goal in the project is to develop a "prediction model" for chloride penetration that takes into account the environmental effect.

2. EXPERIMENTAL

2.1 Material and specimen preparation

For laboratory and field investigations concrete cubes (100x100x100 mm) and slabs (50x300x500 mm) were cast . Reference concrete group 1 with w/c ratio 0.6, according to Norwegian Standard 3099, was used for specimens in the field. In addition a typical concrete used by the road authorities, with w/c ratio 0.4 and 5 % silica fume was used for supplementary laboratory tests. The mix designs are shown in table 1.

Table 1. Mix designs

		w/c ratio 0.6	w/c ratio 0.4
Cement OPC	(kg/m^3)	350	390
Water	(kg/m^3)	210	167
Fine Aggregate 0-8 mm	(kg/m^3)	980	940
Coarse Aggregate 8-16 mm	(kg/m^3)	230	870
Coarse Agg. crushed 8-16 mm	(kg/m^3)	535	-
Silicafume	(%)		5
Plasticizer	(L/m^3)	-	3
Superplasticizer	(L/m^3)	-	3.5
AEA	(L/m^3)	-	0,15
Mean strength	(MPa)	43.9	69.5

Both slabs and cubes were cast and water cured for more than 90 days in the laboratory before testing and instalation. The slabs are fastened to the bridgestructure with expansion bolts. Between the slabs and original structure a thin layer (10-15 mm) of mortar was used to separate old and new concrete. To prevent any leakage the transition sone was sealed with silicon and coated with epoxy after instalation.

2.2 Exposure

At Gimsøystraumen bridge in the northern part of Norway, 16 slabs were instaled in october 1993. On the superstructure (north, south and lower edge) 6 slabs, 3 slabs on pillar no. 2 at a level 1.25 meter above the foundation (north, south and west) and 7 slabs on pillar no. 3 at a level 1.25 m and 2.75 m (north, south and east). The foundation top is 2.5 m above mean sea water level. In addition to the slabs mounted on the bridge, 3 slabs were submerged at the bottom of the sea close to the bridge. After 46 weeks of exposure a 160 mm sections were cut from the upper part of the slabs. The sections were prepared and grinded in the laboratory.

The same principle was followed at Giske bridge at the western coast of Norway. The sections cut out from these slabs have been prepared and grinded, but the final result from the chloride analyses has not yet been prepared.

3. RESULTS AND DISCUSSION

In this chapter preliminary results from the field test is presented. As allready mentioned only results from Gimsøystraumen are completely analysed, but some results from Giske show the same trend and indicate the same relationship with respect to environmental effect.

All specimens has been grinded in millimeter levels parallell to the exposed surface. For each level the amount of total chloride concentration has been analysed. The spectrofotometric technique has been used. Based on measured penetration depth effective in-situ diffusion coeffisients has been calculated according to the following solution of Ficks's 2. law:

$$C(x,t)= C_s-(C_s-C_i)\text{erf}(x/2(D_{eff}\, t)^{-1/2})$$

$C(x,t)$ = Amount of chlorides in depth x after time t

C_s = Calculated chloride consentration at the surface

C_i = Initial chloride consentration in the concrete

D_{eff} = Effective diffusion coeffisient

x = Distance from exposed surface

t = Time of exposure

erf = Error function $\text{erf}(x) = 1-(1+a_1x+a_2x^2+a_3x^3+a_4x^4)^{-4}$

$a_1 = 0{,}278393$

$a_2 = 0{,}230389$

$a_3 = 0{,}000972$

$a_4 = 0{,}078108$

The values D_{eff} and C_s are found by nonlinear regression analyses (least square principle) and curve fitting of Fick's 2. law. No points has been left out from the chloride profiles in these calculations, which is performed in Excel.

In table 2 data on calculated effictive in-situ diffusion coeffisients, D_{eff}, and surface concentration of chlorides, C_s, are given for the slabs exposed at Gimsøystraumen bridge. In the calculations adjustments are made for measured Cl-values lower than approximatly 0.016 % mass of concrete, due to limitations in the methode used. However, this is only done when it is obvious that the measured value represents limitations in the metode, but it implicates limitations for some of the calculations due to low chloride contents. Especially for the values representing the slabs instaled on the superstructure this seems to be the case.

Table 2. Calculated values for D_{eff} and C_s based on in-situ chloride profiles.

Location	In-situ D_{eff} (10^{-12} m^2/s)	C_s (% mass of concrete)	Penetration g/m^2
Pillar 2 north level 1.25	4,47	0,237	37,99
Pillar 2 south level 1.25	8,37	0,137	25,21
Pillar 2 west level 1.25	12,0	0,195	35,24
Pillar 3 north level 1.25	6,55	0,179	31,27
Pillar 3 west level 1.25	4,15	0,127	21,27
Pillar 3 east level 1.25	4,37	0,095	16,19
Pillar 3 north level 2.75	7,16	0,167	29,64
Pillar 3 south level 2.75	1,3	0,074	11,54
Pillar 3 east level 2.75	4,3	0,066	11,12
Box girder north R1	4,36	0,084	14,2
Box girder south R1	4,99	0,066	11,57
Box girder lower edge R1	(0,55)	0,057	9,26
Box girder north R4	3,92	0,055	9,2
Box girder south R4	-	-	0
Box girder lower edge R4	(0,04)	0,064	9,48
Submerged A	(6,81)	0,32	52,36
Submerged B	(15,2)	0,36	64,79

The values marked ( ) are not part of the calculated mean value

Figure 1 shows the measured chloridprofiles and illustrates even better the differences in exposure conditions.

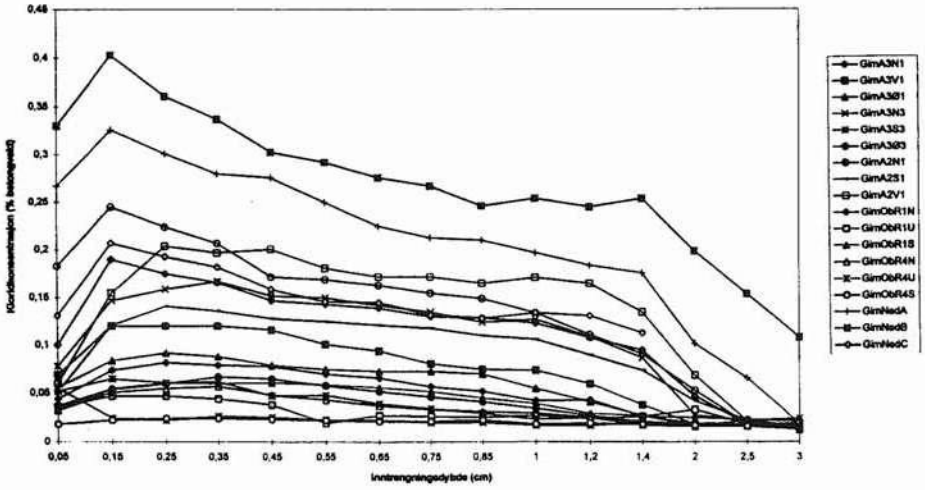

Figure 1. Measured in-situ chloride profiles, % mass of concrete vs. depth (cm)

In table 3 calculated laboratory diffusion coeffisients, D_{lab}, and surface concentration of chlorides, $C_{s\text{-}lab}$, are shown. The test specimens are concrete cubes with sawed exposure surface. All results shown in table 3 are based on 0.6-concrete, and the cubes were cast together with the slabs exposed in the field.

Table 3. Calculated values for D_{lab} and $C_{s\text{-}lab}$ based on measured chloridprofiles.

Methode	D_{lab} (10^{-12} m^2/s)	$C_{s\text{-}lab}$ (% mass of concrete)	Penetration g/m^2
Bulk 16.5 % NaCl-solution (42 days exposure)	14,9	1,173	138,69
	18,4	1,044	111,19
Bulk 16.5 % NaCl-solution (21 days exposure)	17,5	0,943	109,04
	16,0	1,044	115,83
Bulk 3.0 % NaCl-solution (21 days exposure)	28,9	0,411	51,84
	24,3	0,42	53,84
Salt spray chamber 3.0 % (42 days exposure)	25,4	0,516	68,5
	30,9	0,441	62,05
Salt spray chamber 3.0 % (21 days exposure)[1)]	26,5	0,365	48,13
	22,2	0,403	50,22

1) 1 hour spraying and 7 hours drying

The mean value of the achieved in-situ coeffisients is 5.17 x 10^{-12} m^2/s. Compared with laboratory results the value is about four times higher after relatively short time. This illustrates to some extent the effect of laboratory results versus in-situ results.

4. CONCLUDING REMARKS

Table 2 shows a distinct variation in amount of chlorides penetrated through the concrete surface. This variation due to the environment has to be accounted for in a prediction model. An approach might be to use the amount of penetrated chlorides at each location, and combine this with potensial diffusivity and penetration of the same concrete based on laboratory results. A key factor in the model will be the value C_s. The value should be determined as the maximum potential level for the concrete investigated, based on a metode that represent a realistic exposure condition at the construction. This will represent a system that accounts for different chloride contents depending on the severity of the exposure.

The approach will be examined further within this project, but so far no work has been done in this respect. Which laboratory methode to use for evaluation of chloride penetration is to some extent studied in the project. Tests are performed with salt spray chamber and bulk diffusion methods (3 % and 16.5 % NaCl-solutions). Migration tests (12 V) will, depending on resources, be conducted.

KLORIDBESTANDIGHET AV KYSTBROER I BETONG

Forfattere:

TROND ØSTMOEN
Vegdirektoratets broavdeling
GUNNAR LIESTØL
Vegdirektoratets broavdeling
KNUT A. GREFSTAD
Vegdirektoratets broavdeling
BERIT T. SAND
Vegdirektoratets broavdeling
TOM FARSTAD
Norges byggforskningsinstitutt

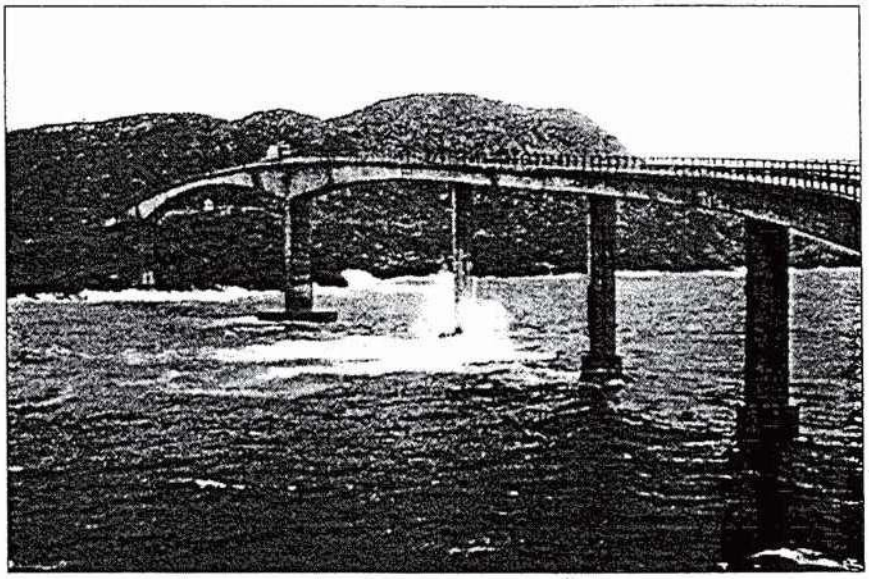

Runde bru i Møre og Romsdal er blant de undersøkte broene i prosjektet.

1. INNLEDNING

Med bakgrunn i de senere års registrerte armeringskorrosjonsskader på kystbroer i betong, ble det i 1991 startet opp forskningsprosjektet "Kloridbestandighet av kystbroer i betong". Prosjektet har vært et samarbeidsprosjekt mellom Statens vegvesen Vegdirektoratet, broavdelingen og veikontorene.

Utarbeidelse av sluttrapport, samt bearbeiding og tolking av måledata er utført i samarbeid mellom Norges byggforskningsinstitutt og Vegdirektoratets Broavdeling.

Målsettingen med prosjektet har vært å finne ut hvilke parametere som styrer kloridinntrengningen i betong samt å vurdere ulike prøvemetoders evne til å klassifisere betongens motstand mot kloridinntrengning.

Prosjektet startet ved veikontorene med å registrere de broene som var beliggende i værharde strøk og dermed utsatt for sjøsprøyt. På dette grunnlaget ble det valgt ut åtte broer for nærmere undersøkelser.

Historisk grunnlagsmateriale for broene er gjennomgått for å finne materialsammensetninger og opplysninger om utførelsen av betongarbeidene. Hovedvekten av arbeidet har bestått i å ta ut og analysere samt å vurdere betongborkjerner fra de 8 broene.

Den styrende parameteren for betongens motstand mot kloridinntrengning er pasta-andelens porestruktur og "tetthet".

Man ønsket derfor å kartlegge en del av de faktorene som påvirker betongens bestandighet:

- v/c-forholdet
- Pastaandel
- Sementmengde
- Sementtype
- Tilsetningsstoffer
- Tilslagstype
- Siktekurve/finhetsmodul
- Utstøpningsforhold/byggemetode
- Herdetemperatur
- Forskalingstype
- Avforskalingstidspunkt
- Etterbehandling/herdetiltak
- Årstid for bygging

2. UTVALG AV BROER OG PRØVEMETODER

Flere av broene med skader var relativt "unge", dvs. en alder på ca. 10-20 år. Broenes aldersammensetning ble valgt fra 1940-tallet og frem til 1991.

Med hensyn til å vurdere bl.a. miljøbelastningen (grad av saltpåsprøyting) er 6 av broene beliggende i ytre kyststrøk og 2 i indre kyststrøk. Broene er av forskjellige konstruksjonstyper, med hovedvekt på fritt-frambyggbroer.

De fylkene som pr. 1991 hadde rapportert om flest skader var Nordland og Møre og Romsdal. Broene i forskningsprogrammet ble derfor valgt ut fra disse 2 fylkene.

Ved uttak av borkjernene ble disse lokalisert til konstruksjonsdelene som var mest utsatt for sjøsprøyt, i hovedsak søylene fra 2 til 6 meter over sjøvannsnivået. Det ble tatt ut ca. 30-40 kjerner pr. bro, fordelt på fasader som vender mot forskjellige himmelretninger. Totalt ble det tatt ut 260 betongkjerner med diametere fra 70 til 100 mm og lengder på ca. 300 mm.

Ved valg av prøvemetoder ble disse gruppert i metoder som vurderte betongens tilstand, materialsammensetning og tetthetsegenskaper. Prøvemetoden ble benyttet slik at betongens dybdeegenskaper og overflateegenskaper kunne bedømmes.

Fylke	Bro nr.	Navn	Bygge-år	Lab. analyser utført av
Møre og Romsdal	299	Steinvågsund	1952	FCB
	625	Vestnes	1955 [1]	FCB
	997	Nerlandsøy	1966-67	FCB
	1364	Runde	1979-81	FCB
Nordland	1732	Hadsel	1976-78	G.M.Idorn
	1837	Gimsøy	1979-81	NBI
	1888	Henningsvær	1980-82	NBI
	2222	Helgelandbrua	1989-91	Cowi

[1] Betongbjelker beregnet brukt i tyske ubåtbunkere, støpt i løpet av 2. verdenskrig (dvs. ca. 50 år gammel betong).

Tabell 1: Broene i forskningsprosjektet

	Analyser utført på	
	overflatebetong	inne i konstruksjon
Betongens tilstand		
- Visuell bedømmelse	X	X
- Trykkfasthet/densitet		X
- Karbonatisering	X	
- Kloridprofil	X	
Materialsammensetning		
- Strukturanalyse - planslip	X	X
- Strukturanalyse - tynnslip	X	X
- Kjemisk analyse		X
- Porevannspressing		X
Tetthetsegenskaper		
- Kloriddiffusjon		X
- Kloridpermeabilitet		X
- Kloridpåsprøyting		X
- Kapillærabsorbasjon / PF	X	X
- Vanninntrengning	X	X
- Elektrisk motstand		X

Tabell 2: Prøvemetoder i prosjektet

Totalt består forskningmaterialet av 960 forskjellige prøveresultat. Analyseringen av betongkjernene er utført av følgende laboratorier:

- Cowi Consult A/S (Danmark)
- Forskningsinstituttet for Cement og Betong (FCB)
- G.M. Idorn Consult A/S (Danmark)
- Norges byggforskningsinstitutt (NBI)

3. RESULTATER

Pga. at broene ikke er fulgt spesielt opp i byggetiden med hensyn til innsamling av bygge- og betongdata, er det begrenset med opplysninger fra det "historiske" materialet som kan benyttes i resultatvurderingen. Parametere som form på siktekurve/finhets-modul, herdetemp., avforskalingstidspunkt, etterbehandling/herdetiltak og ev. bruk av tilsetningsstoffer har vært vanskelig å identifisere entydig. I resultatvurderingen er derfor data om materialsammensetningen i hovedsak hentet fra analysen fra betongkjernene, dvs. planslip/tynnslip (v/c-forhold, pastahomogenitet, tilslagstype) samt kjemisk analyse og porøsitetsmålinger.

3.1 Miljøeffekter

Den metoden som oftest er benyttet for å finne en betongs motstand mot kloridinntrengning er å måle inntrengningsprofiler av klorider ute på konstruksjonen. Dette prosjektet har imidlertid vist at man ikke kan bruke inntrengningsprofiler for å sammenligne betongkvaliteten fra en bro til en annen. Årsaken er at de lokale miljøforholdene spiller en meget vesentlig rolle for kloridbelastningen på konstruksjonen. Av betydning kan nevnes: Topografien rundt broen, vindhastigheter, fremherskende vindretning med regn. Som et eksempel kan nevnes Hadsel bru, der kloridinnholdet på en av søylene er mye høyere på le-siden enn på lo-siden. En av forklaringene til dette er trolig at regnvannet vasker kloridene av på lo-siden. Denne effekten er registrert på flere av broene og spesielt på søyler med store kvadratiske dimensjoner.

3.2 Overflate-/dybdeegenskaper

Et av målene ved oppsett av prøveprogrammet var å se om det var noen forskjeller i prøveresultatene på prøvelegemer som ble eksponert mot sin naturlige overflate (forskalingsflate) sammenlignet med prøvelegemer som var saget ut lengre inn på betongkjernene (dypere inn i betongen). Den metoden som entydig viste en forskjell i resultatene fra

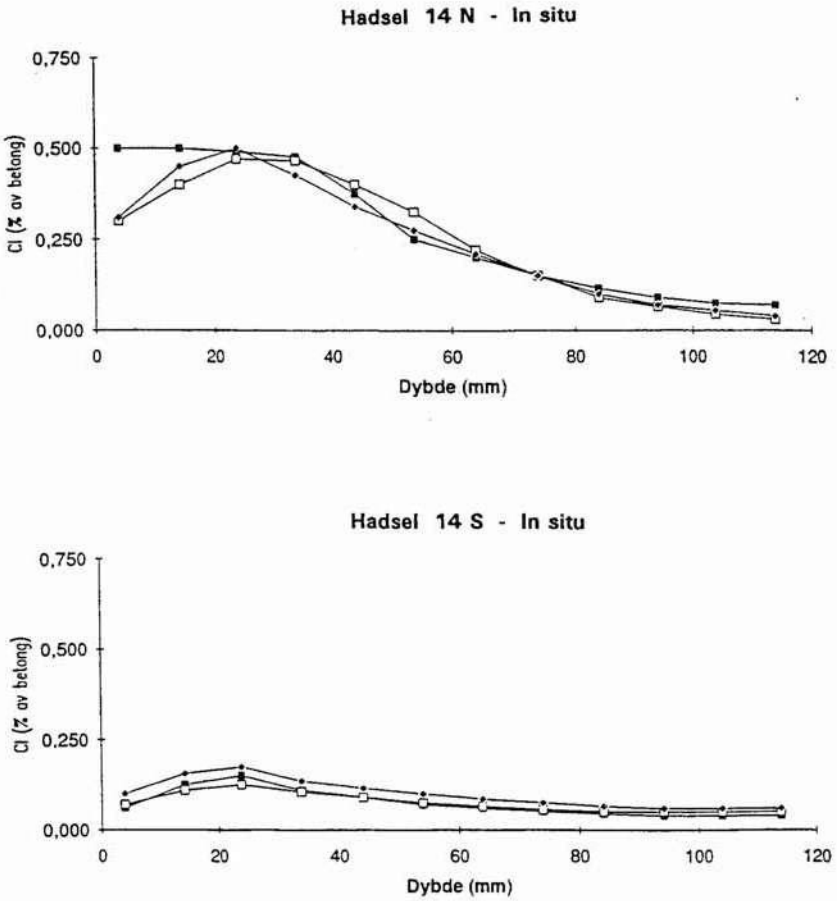

Fig. 1: Kloridinntrengning på nord- og sydsiden på søyle akse 14, Hadsel bru

overflate- og dybdeegenskaper var registrering av motstandstall målt ved kapillær absorpsjon. Prøver med "overflatehud" hadde et høyere motstandstall enn prøver med sagflate. Årsaken til den mer "tette" overflaten kan være flere, en effekt kan være utfelling og porefylling med karbonatiseringsprodukter, begroing og ev. fordi betongen ikke er gjennomskåret og åpnet for en raskere fuktransport i heftsonen tilslag/pasta. Registreringen av v/c-tall med tynnslip i dybder 0-50 mm og 50-100 mm fra overflaten har ikke vist noen forskjell i v/c-tall for overflaten og lengre inn i betongen.

3.3 Akselererte kloridbelastninger i laboratorier

I tillegg til in-situ kloridprofil er motstand mot kloridinntrengning målt med akselererte metoder i laboratoriene:

- Bulk diffusion, kloridbelastning ved neddykking i 10 % natriumkloridløsning.
- Kloridpåsprøyting, kloridbelastning med påsprøyting av 3 % natriumkloridløsning.
- Kloridpermeabilitet, kloridmigrasjon som følge av 12 volt påtrykt spenning.

Målet med prøvemetodene bulk diffudion og kloridpåsprøyting er at de beregnede diffusjonskoeffisientene kan benyttes til å beregne inntrengningshastigheter, som igjen kan benyttes i levetidsbetraktninger.

I dette prosjektet er diffusjonskoeffisientene for de akselererte metodene mye høyere enn det som er registrert in-situ. Korrigert for temperaturforskjellene i laboratoriet og utendørs, er forskjellen i diffusjonskoeffisienten 3-35 ganger større for lab.forsøkene. Dette vanskeliggjør bruken av lab. koeffisientene for levetidsberegninger, da de beregnede inntrengningshastighetene vil bli altfor høye, og man dermed vil få en for kort levetid.

Årsaken til at kloridinntrengningen går saktere ute på konstruksjonene enn simulert i laboratoriet kan være:

- Lab-prøvene ble eksponert på sagflater, noe som trolig gir raskere inntrengning enn in-situ prøvene som har en tettere overflatehud.
- Lab-prøvene har et høyere fuktinnhold enn in-situ prøvene. Kloridene transporteres i fuktfasen, og et høyt fuktinnhold vil derfor trolig gi raskere kloridinntrengning. I tillegg vil fuktinnholdet i in-situ betongen variere avhengig av årstiden.
- Betongen in-situ blir i perioder utsatt for regnvannsvasking. Dette vil senke kloridkonsentrasjonen i betongoverflaten, noe som igjen reduserer inntrengningshastigheten.

3.4 Spredning / inhomogenitet i prøvematerialet samt prøvesystematikk

Sammenhengen mellom trykkfasthet og v/c forhold er trolig den mest aksepterte sammenheng innen betongteknologien. Likevel har man fått resultater som ved første øyekast har stor spredning.

Som eksempel kan nevnes Vestnes bro med en fasthet på 72 MPa og v/c på 0,49 samt Hadsel bru med en fasthet på 37 MPa og v/c på 0,4.

Ved å se nærmere på dette forholdet, kan det på en konstruktiv måte bidra til forståelse av:

- Hvilken sikkerhet man kan forvente i vurdering av enkeltresultater.
- Hvilken systematikk man må ha i planlegging av prøveprogrammet.

Man har to hovedgrupper av feilkilder for slike målinger:

1. Metode- eller systemfeilene:

1.1 Metodetoleranser fasthetsmåling, f.eks. toleranse trykkpresse, inhomogenitetstoleranse, plansliping av prøver etc. En antar at metodetoleransen vil være i størrelsesordenen 5-10 % (Tf = 7 %).

1.2 Metodetoleranse vurdering av v/c fra tynnslip. En vet at laboratorium kan skille mellom forskjell i v/c-forhold med en minste variasjon på 0,05. Omregnet til toleranse i fasthetsvurdering, vil dette tilsvare 10-15 % (Tt = 12 %).

1.3 Forskjellige laboratorier har forskjellige referanseskalaer for vurdering av v/c-forhold fra tynnslip basert på erfaringsmateriale fra lokale resepter og sementer.
Avvikene kan selvsagt også skyldes avvik i fasthetsmåling. Feilkildene for laboratorieavvikstoleranse kan overstige 20 % i trykkfasthetsmåling (=T1).

TM = 24 %

Den annen hovedgruppe av feilkilder er:

2. Praktiske variasjoner

2.1 Utstøpingsvariasjon
En vet fra internasjonal litteratur at man har målt normale avvik i trykkfasthet i høye vegger på 40 % (20 %).
Vi ser ikke bort fra at tilsvarende av-

vik kan forventes i de undersøkte broene. Avvikene kan f.eks. skyldes:
- Separasjon
- Varierende komprimering
- Varierende dispergering av sement
- Reseptjevnhet

2.2 Endring i materialpraksis over tid. Sammenhengen mellom fasthet og v/c forhold baserer seg på lik materialpraksis. Enkelte broer er gamle og trolig er funksjonen fasthet-v/c endret med endring i sementteknologi.

Ovenstående kan i korthet sammenfattes i følgende tre punkter:
1. Streng koordinering må gjennomføres hvis resultater skal sammenliknes fra forskjellige laboratorier.
2. Bestandighetsvurdering basert på vurdering av vikarierende parametere må foretas med meget vide toleransegrenser.
3. Vurdering fra enkeltresultater ut fra målinger må gjøres med stor varsomhet.

4. KONKLUSJONER

- Det lokale miljøet som broen står i har stor betydning for kloridinntrengningen. For store kvadratiske søyler er kloridinnholdet mye større på le-siden enn på lo-siden.

For de betongkvaliteter som her er undersøkt ser det ut som om miljøbelastningen er den dominerende parameteren for kloridinntrengningen.

- Betongprøver med overflatehud virker å være tettere enn betongprøver med sagflate. Dette kan trolig skyldes "tetting" med utfellingsprodukter, ev. begroing.
- Kloridinntrengningen går mye saktere ute på broene enn de inntrengningshastighetene som er beregnet fra de akselererte metodene.
- Relativt store forskjeller i kvalitet fra kjerne til kjerne innenfor samme bro (stor spredning) har gjort det vanskelig å trekke entydige sammenhenger som f.eks. forholdet mellom fasthet og v/c.

Sluttrapporten med bilag for prosjektet "Kloridbestandighet av kystbroer i betong" kan bestilles fra:

Statens Vegvesen, Vegdirektoratet
Broavdelingen
Postboks 8142 Dep.
0033 OSLO
Pris for rapporten med bilag er kr. 200,-

CHLORIDE PENETRATION IN DANISH BRIDGES

Erik Stoltzner, Vejdirektoratet, Vejteknisk Division, Broafdelingen, Niels Juels Gade 13, Postbox 1569, DK-1020 København K, Tlf. +45 33 41 34 36, Fax +45 33 93 20 70

1. ABSTRACT

The Road Directorate has found an increasing number of cases involving chloride corrosion of reinforcement, primarily on concrete columns. The mentioned cases are found both on ordinary road bridges and on bridges in marine environment.

The development of reliable lifetime models, is, therefore, of considerable importance to the Road Directorate. The models should be able to predict the future chloride penetration based on knowledge of the chloride penetration already identified. The models should help with the evaluation of initiatives meant to reduce further chloride penetration, so that future corrosion of reinforcement can be prevented or the risk of corrosion reduced considerably.

One of the conditions for developing such lifetime models is knowledge of the chloride penetration as a function of time for the concretes used in our structures.

This article describes two investigations begun by the Road Directorate to gain knowledge of the development over time of chloride penetration.

2. CHLORIDE PENETRATION IN CONCRETE COLUMNS ON ROAD BRIDGES

2.1 Objective

Chloride penetration in concrete columns on road bridges is caused by NaCl used as de-icing salt in the winter.

The Road Directorate has started a measuring programme on 3 bridges on the Sydmotorvej, Rønnede-Udby to follow the development over time of chloride penetration. The bridges were built in 1989. De-icing salt was used on this stretch of road for the first time during the winter 1990/91.

2.2 Measuring Programme

The following measurements are carried out on one column for each of the three bridges:

- chloride measurement
- resistance measurement
- potential measurement

The measurements were carried out in 1990, 1991 and 1994. The Road Directorate will repeat the measurements every three years.

2.3 Concrete Composition

The concrete used for the columns is described below.

-	concrete, resistant to sulphate with low alkali content	approximately	300 kg/m^3
-	flyash	approximately	20 kg/m^3
-	water	approximately	140 kg/m^3

The columns are designed with a cover layer of 40 mm.

2.4 Chloride Penetration

The below tables give the measured chloride penetration as a function of depth from surface and height above ground.

Height above ground	Depth (mm)	Date		
		1990-12-10	1991-10-24	1994-12-06
0 m	0-10		0.00	0.036
	10-20	0.01	0.00	0.015
	20-30		0.00	0.011
	30-60	0.01	0.00	0.008
	60-90	0.01	0.00	0.008
0.5 m	0-30	0.01	0.00	0.023
	30-60	0.01	0.00	0.010
	60-90	0.01	0.00	0.010
1.0 m	0-30	0.01	0.00	0.026
	30-60	0.01	0.00	0.009
	60-90	0.01	0.00	0.010
2.0 m	0-30	0.01	0.00	0.014
	30-60	0.01	0.00	0.011
	60-90	0.01	0.00	0.009

Table 1. Bridge 30-0035
Chloride measurement in % of dry concrete weight

Height above ground	Depth (mm)	Date		
		1990-12-10	1991-10-24	1994-12-06
0 m	0-10		0.01	0.044
	10-20	0.01	0.00	0.010
	20-30		0.00	0.011
	30-60	0.01	0.00	0.008
	60-90	0.01	0.00	0.007
0.5 m	0-30	0.01	0.00	0.017
	30-60	0.01	0.00	0.009
	60-90	0.01	0.00	0.009
1.0 m	0-30	0.01	0.00	0.020
	30-60	0.01	0.00	0.007
	60-90	0.01	0.00	0.007
2.0 m	0-30	0.01	0.00	0.016
	30-60	0.01	0.00	0.008
	60-90	0.01	0.00	

Table 2. Bridge 30-0043, column 1.2
Chloride measurement in % of dry concrete weight

Height above ground	Depth (mm)	Date		
		1990-12-10	1991-10-24	1994-12-06
0 m	0-10		0.02	0.070
	10-20	0.02	0.01	0.028
	20-30		0.00	0.010
	30-60	0.01	0.00	0.009
	60-90	0.01	0.00	
0.5 m	0-30	0.01	0.00	0.017
	30-60	0.01	0.00	0.008
	60-90	0.01	0.00	0.009
1.0 m	0-30	0.01	0.01	0.020
	30-60	0.01	0.00	0.009
	60-90	0.01	0.00	0.009
2.0 m	0-30	0.01	0.01	0.020
	30-60	0.01	0.01	0.015
	60-90	0.01	0.00	

Table 3. Bridge 30-0044, column 1.1
Chloride measurement in % of dry concrete weight

Measurements carried out in 1990 and 1991 are to be viewed as initial measurements. The measurements were carried out immediately before and after the first winter of de-icing with salt under the bridges.

The Chloride content in the columns was measured as 0.00% and 0.01% of dry concrete weight in the two measurements.

The corresponding measurement in 1994 showed a chloride content in the outer 10 mm of the concrete at ground level of between 0.04% and 0.07% of dry concrete weight.

The chloride content in the outer 10 mm has increased from a factor 4 to a factor 7 after 4 years of de-icing with salt.

One explanation could be that alternate dampening and drying up of the outer part of the concrete causes the chloride content of that part to increase at a relatively fast rate.

There was hardly any change in the chloride content at a depth larger than 30 mm.

A preliminary conclusion, drawn from the measurements of the chloride penetration in concrete columns caused by de-icing salt, is that there is a relatively fast chloride penetration in the outer part of the concrete.

3. CHLORIDE PENETRATION IN CONCRETE COLUMNS IN MARINE ENVIRONMENT

3.1 Objective

In connection with the continuous monitoring of the Farø Bridges, a large number of chloride measurements have been carried out for the columns of the Farø Bridges.

The objective of the investigation was to evaluate whether there is a short-term risk of corrosion to the reinforcement of the Farø Bridges, particularly in the splash zone.

3.2 Measuring Programme

In 1989, 1991 and 1994 cores were bored from column SF06 at level 0.35.

The chloride profiles were determined based on grinding of the cores. 10 - 15 layers of 2-3 mm were ground off the exposed surface (profile grinding) and the grinding dust was then analyzed for chloride in accordance with DS 423.28.

The measured profiles were recorded. On the basis of the measuring points a calculation has been made, by means of Fick's 2nd law, of the actual diffusion coefficient and the actual surface concentration.

3.3 Concrete Composition

The concrete used for the Farø Bridges is described below.

-	concrete, resistant to sulphate with low alkali content	330 kg/m^3
-	flyash	40 kg/m^3
-	water	140 kg/m^3
-	sea sand	622 kg/m^3
-	granite 2/8 mm	285 kg/m^3
-	granite 2/18 mm + 18/25 mm	920 kg/m^3

The columns are designed with a cover layer of 50 mm.

3.4 Chloride Penetration

In Table 4 the results of the chloride measurements of 1989, 1991 and 1994 are given.

Core/year	Diffusion coefficient D x 10^{13} m^2/S	Surface Concentration, C_s, % Cl of Concrete Weight	Depth in mm at C_x = 0.10% of Concrete Weight
1/1994	5	1.22	34.6
2/1994	4	1.38	30.6
3/1994	6	1.11	35.5
Mean 1994	5	1.24	33.6
1.1/1991	6	1.02	31.1
1.2/1991	7	1.06	33.5
2/1991	7	0.96	32.4
3/1991	5	1.38	32.3
Mean 1991	6	1.11	32.3
1989	7	0.88	28.6

Table 4 Chloride content in SF06

If the calculated diffusion coefficients of 1989, 1991 and 1994 are compared, there is a tendency that the diffusion coefficient decreases as a function of time, this is shown in Figure 1. Furthermore, there is a tendency that C_s increases over time.

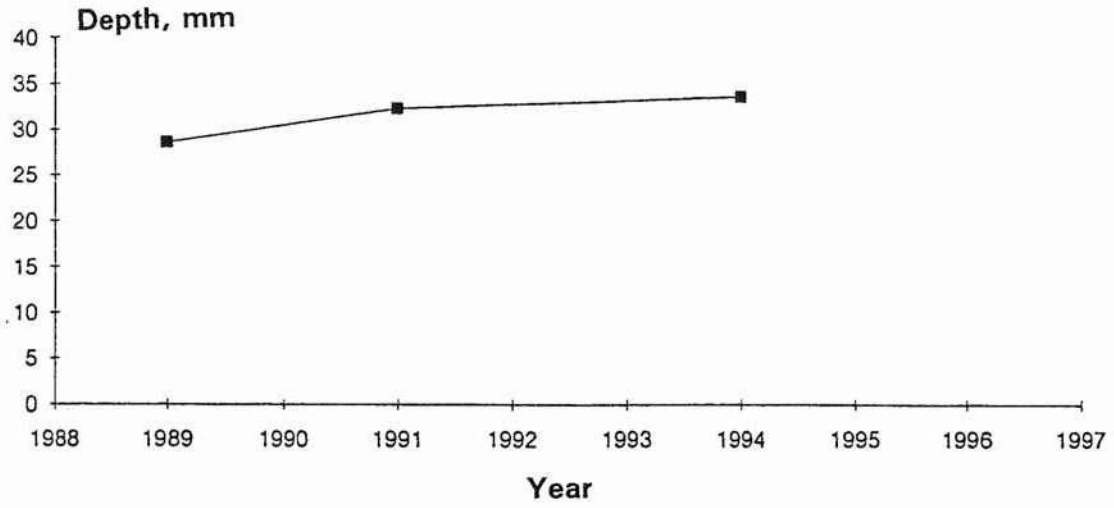

Figure 1 Development of the diffusion coefficient during 1989-1994

To sum up the effect of D and C_s, the penetration depth for C = 0.10% chloride is calculated. It appears from Figure 2 that this penetration depth increases with time. The calculations of the penetration depth are calculated on the basis of the calculated chloride profiles. But here there also seems to be a tendency for the chloride penetration to take place at a decreasing rate.

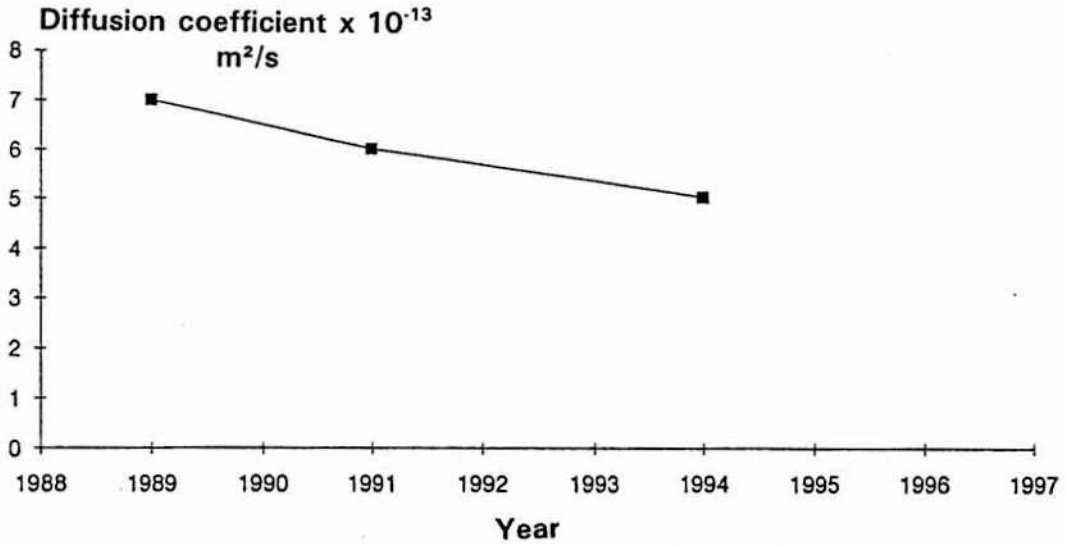

Figure 2 Development of the penetration depth from 1989 to 1994 for a chloride content of 0.10% of dry concrete weight.

The measurements of the chloride profiles of column SF06 indicate that the chloride penetration probably continued during the period 1991-1994, but that the penetration at present takes place with a much lower diffusion coefficient than the mean diffusion coefficient for the period from the construction of the bridge until 1991. The increase of chloride content measured during the period 1991 -1994 is so small that it may only be due to statistic spread in the results.

4. CONCLUDING REMARKS

The above figures are an attempt to illustrate chloride penetration over time for two different types of structures of different ages and subject to different chloride actions.

On the columns of the road bridges the chloride penetration in the outer part of the concrete seems to take place relatively fast. On the column of the Farø Bridges the chloride penetration rate seems to decrease with time.

The Road Directorate hopes the continuous measurements of chloride penetration can contribute to a definition of which parameters control the actual chloride penetration for the concretes used today.

The main objective must be to develop practical models which can predict with a high degree of certainty the effect of a given chloride action on a specified type of concrete.

Do the physics, which form the basis of Fick's 2nd law, actually correspond to what happens in the concrete? Does the crack development in concrete have a considerable effect on the way in which the chloride penetrates the concrete? If this is the case, it is not practical to assume that chloride penetration takes place by way of diffusion.

Another factor of importance for continued chloride penetration is the binding capacity of the concrete and there seem to be indications that this might be larger than assumed so far. If it actually is larger than assumed previously, this would naturally mean that the risk of corrosion of the reinforcement would be smaller than assumed, as only the free chloride penetrates the concrete.

It is therefore a matter of urgency to develop models which can include penetration of chloride by capillary suction, diffusion and through microcracks. The model must also include the possibility of large parts of the chloride becoming bound.

Before discarding Fick's 2nd law completely, it should be noted that Fick's 2nd law has shown itself useful in practice for the prediction of corrosion of the reinforcement on some of the bridges of the Road Directorate.

CHLORIDE EXPOSURE ON GIMSØYSTRAUMEN BRIDGE - RESULTS FROM EXTENDED CONDITION SURVEY

Finn Fluge, Norwegian Road Research Laboratory, PB 8142 Dep, N-0033 Oslo.
Aage Blankvoll, Nordland County Roads Office, Nordstrandv. 41, N-8002 Bodø.

ABSTRACT

An extended condition survey was performed at Gimsøystraumen bridge in 1992. Included in the extended condition survey was more than 4500 chloride analyses. Additional chloride measurements were performed in connection with trial repairs in 1993 and 1994. In the extended condition survey chlorides were analysed using the Rapid Chloride Test (RCT) as a "field-method", while chlorides were analysed by the use of more sophisticated laboratory methods in 1993 and 1994. The results from the RCT measurements were consistent with the results from the laboratory analyses.

A limited part of the results from these investigations, have been used for calculation of diffusion coefficients (D) and chloride exposure coefficients (C_s). The calculated diffusion coefficient (D) varies from 22 - 48 mm^2/year. The average is 35 mm^2/year with a standard deviation of 7,5 mm^2/year. This indicates relatively uniform concrete quality in the structure. The height above the sea level is of major importance for the environmental "chloride load" exposed to the superstructure. The "chloride load" is a lot heavier on the lee side than on the windward side. This effect is of most importance for the parts of the superstructure closest to the sea level. The recorded "chloride load" is consistent with the damage recorded at the superstructure of the bridge.

The accuracy of the RCT-method is considered as good enough for chloride analyses in condition surveys. The use of 10 mm steps for powder sampling does not detect high concentrations of chlorides in thin layers of the concrete. The analysed chloride value closest to the surface must be treated with care in assessments after condition surveys. In calculations of D and C_s the value closest to the surface should be left out.

Keywords: Concrete Bridge, Marine Environment, Chlorides

1. INTRODUCTION

Durability of concrete bridges has been focused in all of the Nordic countries the last decade. To solve problems related to durability and repair of concrete bridges, Norway has used a practical approach. This means, that several condition surveys including visual inspection, chloride measurements, potential mapping and laboratory analyses have been performed. The same way, a lot of different techniques for maintenance and repair have been tried out since 1988. The other Nordic countries have chosen another approach and attached importance to theoretical studies and laboratory analyses rather than gaining experience from field studies.

In the very beginning of the OFU Bridge Repair Project, an extended condition survey

was performed. The extent of this condition survey, is maybe the largest performed ever on one bridge. More than 4500 chloride analyses were performed. In addition, the condition survey consisted of visual inspection, potential mapping, measurements of concrete cover and rebar inspection.

The work presented in this report is a part of investigations in progress.

2. GIMSØYSTRAUMEN BRIDGE

Gimsøystraumen bridge is located 30 km west of Svolvær on the E 10 road in the Nordland County. The bridge was constructed between 1979 - 1981. The bridge is a link between two of the Lofoten Islands, Austvågøy and Gimsøy. The longitudinal bridge axis is roughly east-west. The climate is severe with strong winds and salt spray from the sea. The bridge length is 840 m divided into 9 sections, see fig. 1. The environmental effects vary greatly along the bridge as the bridge deck level varies from 4 m to 36 m above sea level.

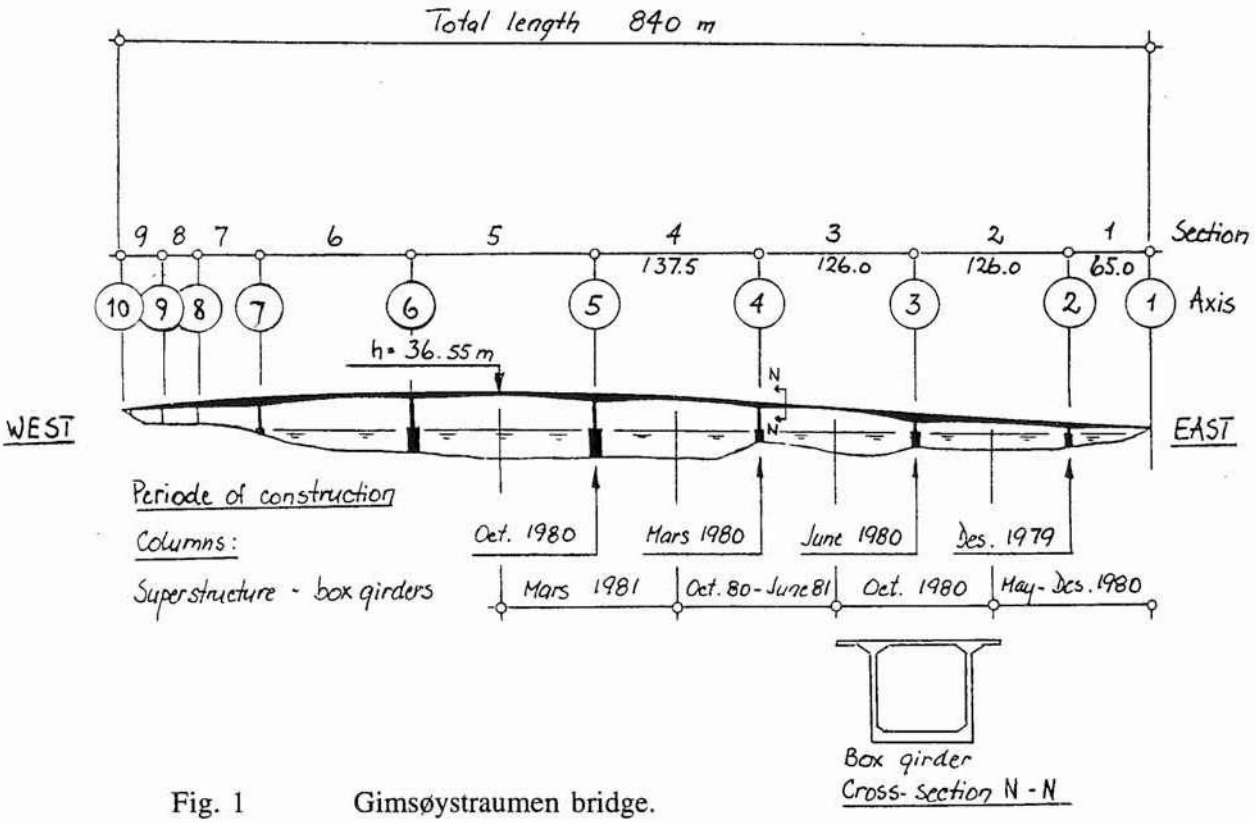

Fig. 1 Gimsøystraumen bridge.

The bridge is a post-tensioned, free cantilevered, box construction. The box height varies from 2,2 m to 7,4 m. The designed concrete strength for substructures was C 35 with 50 mm cover of rebars. For the bridge deck the corresponding values were C 40 and 30 mm. Fixing bars were allowed in the cover zone in horizontal construction elements. The designed quality of reinforcement bars was Ks 50 and Ks 40 for stirrups.

3. EXPERIMENTAL METHODS

The extended condition survey was performed during the autumn of 1992 by Ringtek (ref. 1). From the superstructure of the bridge 11 chloride profiles were measured for every six meters in longitudinal direction of section 1, 2, 3 and 4. This is illustrated in fig. 2. Section 1, 2, 3 and 4 are all together 454,5 m. A total of 752 chloride profiles was analysed from this area of the bridge.

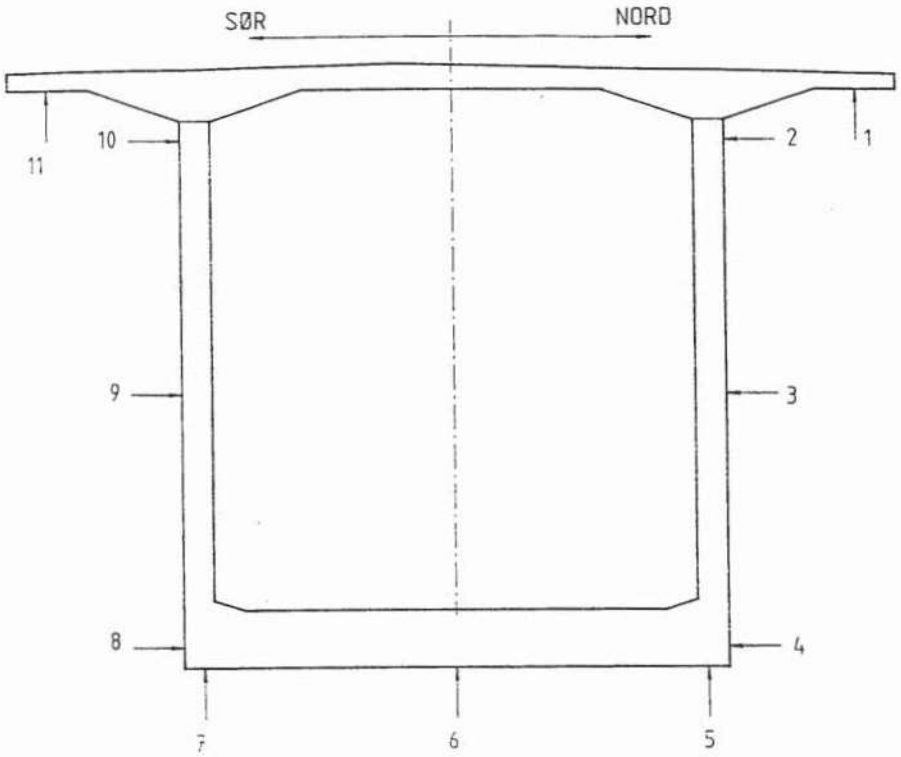

Fig. 2 Measuring points at the box girder in the Ringtek survey.

From the columns in the same area, this means the columns in axis 2, 3, 4 and 5, ten chloride profiles were measured for every four meters. A total of 160 chloride profiles was measured for the columns. The results from the columns are not included in this report.

For the superstructure, concrete powder was drilled out with a 18 mm bit for the depths 0 - 10 mm, 10 - 20 mm, 20 - 30 mm, 30 - 50 mm and 50 - 75 mm. For each location 4 holes were drilled out for powder sampling. Hence, one sample is the average of powder from 4 holes. Chlorides were analysed using the RCT-method. The chloride content is presented as % by weight of cement. In the calculation from % by weight of concrete a factor of 6,4 is used. This means that 375 kg of cement was specified in the concrete mix.

Within the "OFU Bridge Repair Project" additional investigations including chloride measurements are performed during 1993 and 1994. This is reported in ref. 2, 3 and 4.

Rescon performed in 1993 a total of 40 control measurements analysing exactly the same powder Ringtek had analysed in 1992 (ref. 2). The powder had been kept in plastic bags (not PVC) for 10 months. For the control measurements chlorides were analysed using titration after NS 3671.

As a part of investigations before the trial repair in 1993, chloride profiles were determined from three concrete cores drilled out (ref. 3). In connection with the trial repair in 1994, two additional cores were drilled out in section no. 2 (ref. 4). In these investigations concrete powder was grained off the cores in short steps and chlorides were analysed with the potentiometric titration method. Both in 1993 and in 1994 the chloride analyses were performed by Norut Technology.

4. RESULTS AND DISCUSSION

The results from the Ringtek survey in 1992 show very high content of chlorides in some areas of the superstructure. The most exposed areas of the superstructure are close to the sea level on the north side of the box girder. In the discussion, we have chosen the results from 3 cross sections (A, B and C), see fig. 3. The cross sections (A and B) in section no. 2 (between the axis 2 and 3) are inside the testing areas investigated as a part of the Trial Repair in 1993.

The carbonation of concrete might influence the chloride profiles. Carbonation depth of 2 mm is measured by the use of phenolphthalein (ref. 2). Carbonation depth of 1,5 - 6 mm is measured after analyses of thin sections. These analyses were performed by Byggforsk and also reported in ref. 2. The possible influence of carbonation on chloride profiles is not discussed in this report.

4.1 Results from the Ringtek survey in 1992

The highest content of chlorides measured at cross section no. A is 2,43 % by weight of cement. This value is measured on the lowest part of the box girder on the northern side, rcorded at the depth 10 - 20 mm. The highest value on the southern side of the box girder is 0,45 % at the depth 0 - 10 mm. The bridge deck level at cross section no. A is 11,9 m above sea level.

For cross section no. B, the highest value is 1,54 %. This value is recorded both on the north side of the box girder (0 - 10 mm) and on the underside of the box girder (10 - 20 mm). On the south side the highest value is 0,69 % (0 - 10 mm). The bridge deck level for cross section no. B is at 17,6 m.

Cross section no. C is 33,4 m above sea level. The highest chloride content is 0,77 % (0 - 10 mm) on the north side and 0,33 % (0 - 10 mm) on the south side of the box girder.

Detailed results are presented in appendix no. 1.

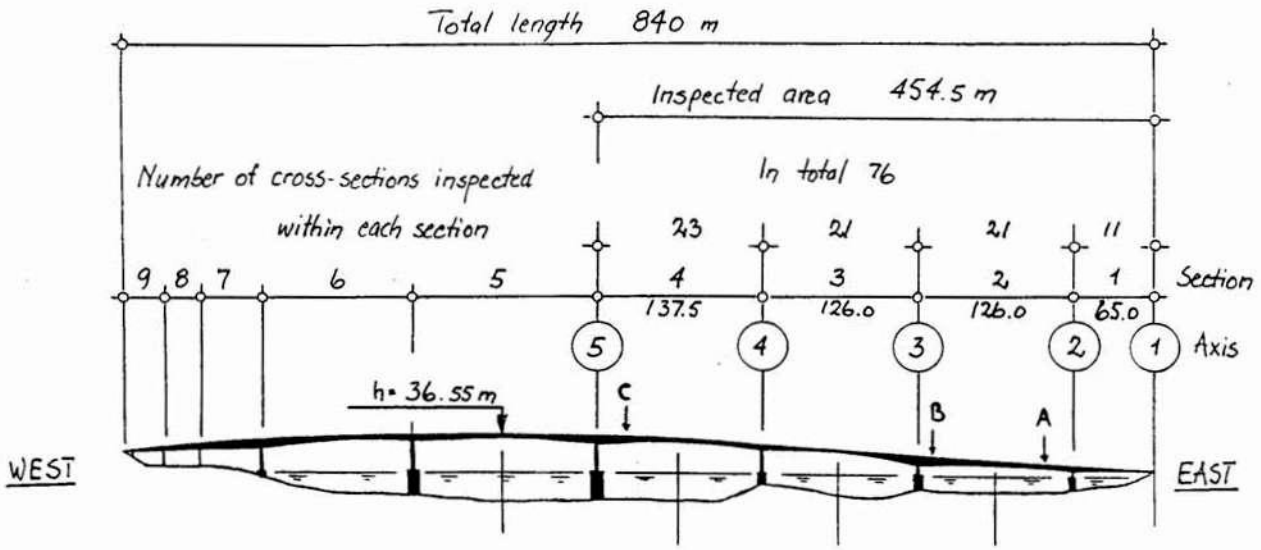

Fig. 3 Location of the cross sections A, B and C.

4.2 Results from Norut analyses in 1993 and 1994

The chloride content is analysed in shorter steps in the Norut analyses than in the Ringtek survey. The average chloride content is calculated for the same steps used by Ringtek. This means 0 - 10 mm, 10 - 20 mm, 20 - 30 mm, 30 - 50 mm and 50 - 75 mm.

Using these steps, the highest chloride content at cross section no. A is recorded at the depth 10 - 20 mm. The recorded value at the analyses in 1993 was 2, 91 % by weight of cement and 2, 34 % at the analyses in 1994. Both chloride profiles were taken from the north side of the box girder. These values are corresponding with the values from the Ringtek survey. The closest chloride profile from the Ringtek survey recorded 2,30 % at this depth. However, it should be noticed that one of the values in the Norut analyses at the depth 8 - 10 mm, showed a chloride content of 3,45 % by weight of cement.

At cross section no. B, chloride profiles from both the north and the south side of the box girder were analysed in 1993, while one profile from the north side was analysed in 1994. Using the steps from the Ringtek survey again, the highest value on the north side is 1,66 % at the depth 0 - 10 mm. Using the finer steps in the Norut analyses in 1994, the highest value is 2, 60 % at the depth 2 - 4 mm. The highest value on the south side is 0,72 % (0 - 10 mm). Using the finer steps in the Norut analyses in 1993, the highest value is 0,98 % at the depth 0 - 5 mm. Also these values are corresponding with the values from the Ringtek survey.

Detailed results from the analyses in 1993 are presented in appendix no. 2, while the detailed results from Norut in 1994 are listed in appendix no.3.

4.3 Calculation of D and C_s

The results from cross sections A, B and C are used for calculation of diffusion coefficients (D) and chloride exposure coefficients (C_s). The calculations are performed using a computer program developed by Selmer.

The calculations of D and C_s are based upon Ficks second law of diffusion. The calculations have taken into account that different parts of the superstructure are build in different time periods and that test material sampling is performed at different points of time. The background chloride concentration used is 0,01 % by weight of cement. Another assumption made, is that the value closest to the surface is left out in the calculations of D and Cs, see fig. 4. Results from the calculations are presented in table 1.

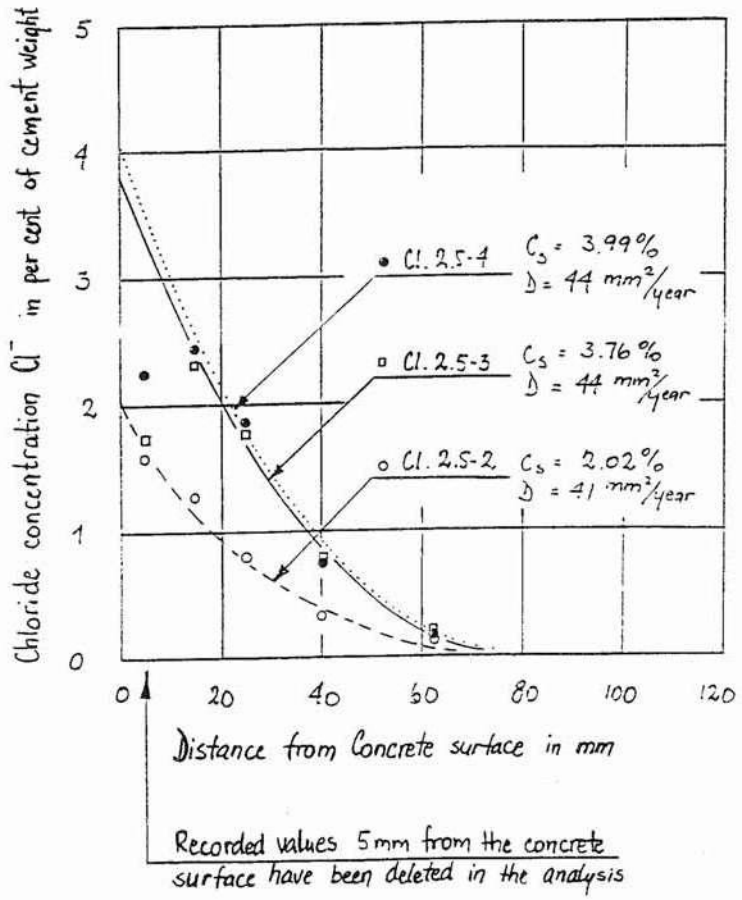

Fig. 4 Chloride profile and calculation of D and C_s.

The calculated diffusion coefficient (D) varies from 22 - 48 mm^2/year. The average is 35 mm^2/year with a standard deviation of 7,5 mm^2/year. This indicates relatively uniform concrete quality in the structure.

The calculated chloride exposure coefficients (C_s) give quantitative numbers to the chloride exposure on the superstructure in the cross sections A, B and C.

Table 1 Diffusion coefficients (D) and chloride exposure coefficients (C_s).

Location	Measuring point (fig.2)	Ringtek 1992		Norut 1993	Norut 1994
		C_s (%)	D (mm^2/year)	C_s / D	C_s / D
Cross section A (2.5) 24 m west of axis no. 2	2.5 - 2	2,02	41		
	2.5 - 3	3,76	44	3,83 / 37	3,55 / 48
	2.5 - 4	3,99	44		
	2.5 - 5	2,61	46		
	2.5 - 6	2,61	37		
	2.5 - 7	2,34	26		
	2.5 - 8	0,53	40		
	2.5 - 9	0,36	45		
	2.5 - 10	0,51	45		
Cross section B (2.20) 114 m west of axis no. 2	2.20 - 2	2,18	38		
	2.20 - 3	2,38	37	2,18 / 25	1,75 / 35
	2.20 - 4	1,96	28		
	2.20 - 5	2,50	28		
	2.20 - 6	2,00	25		
	2.20 - 7	0,30	26		
	2.20 - 8	0,68	27		
	2.20 - 9	0,78	31	0,91 / 22	
	2.20 - 10	0,60	42		
Cross section C (4.20) 114 m west of axis no. 4	4.20 - 2	0,89	40		
	4.20 - 3	0,62	29		
	4.20 - 4	0,61	28		
	4.20 - 5	0,64	26		
	4.20 - 6	0,61	34		
	4.20 - 7	0.31	32		
	4.20 - 8	0,30	40		
	4.20 - 9	0,35	33		
	4.20 - 10	0,26	39		

4.4 Discussion about chloride exposure on the superstructure

The chloride exposure coefficients (C_s) are assumed to represent the "chloride load" on the superstructure. This is presented graphically for the cross sections A, B and C in fig. 5, 6 and 7.

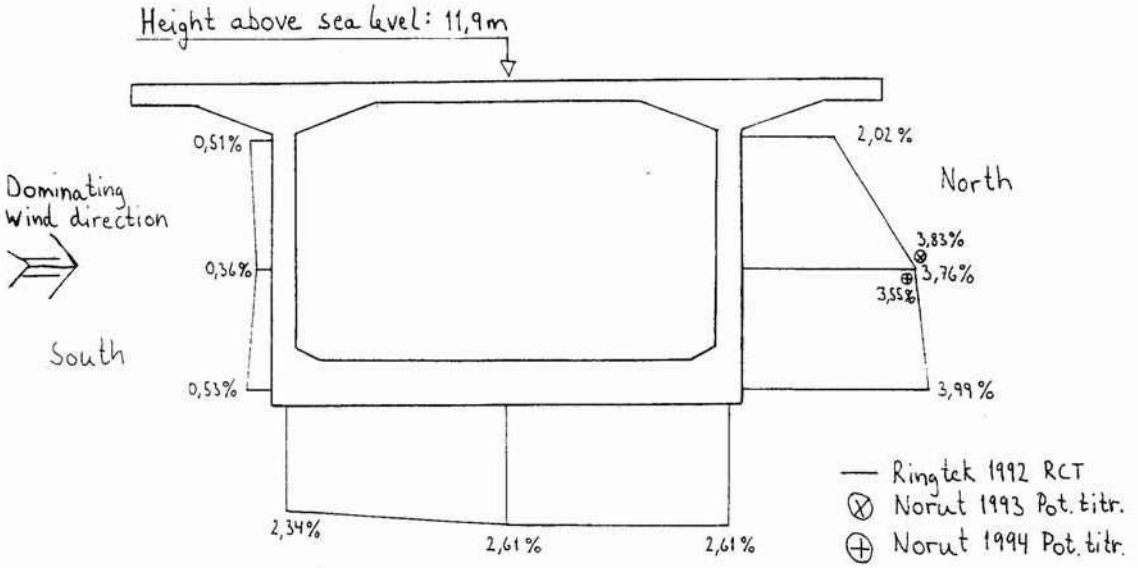

Fig. 5 Chloride load (C_s) on the superstructure at cross section A, 24 m west of axis no. 2. Recorded values in % by weight of cement.

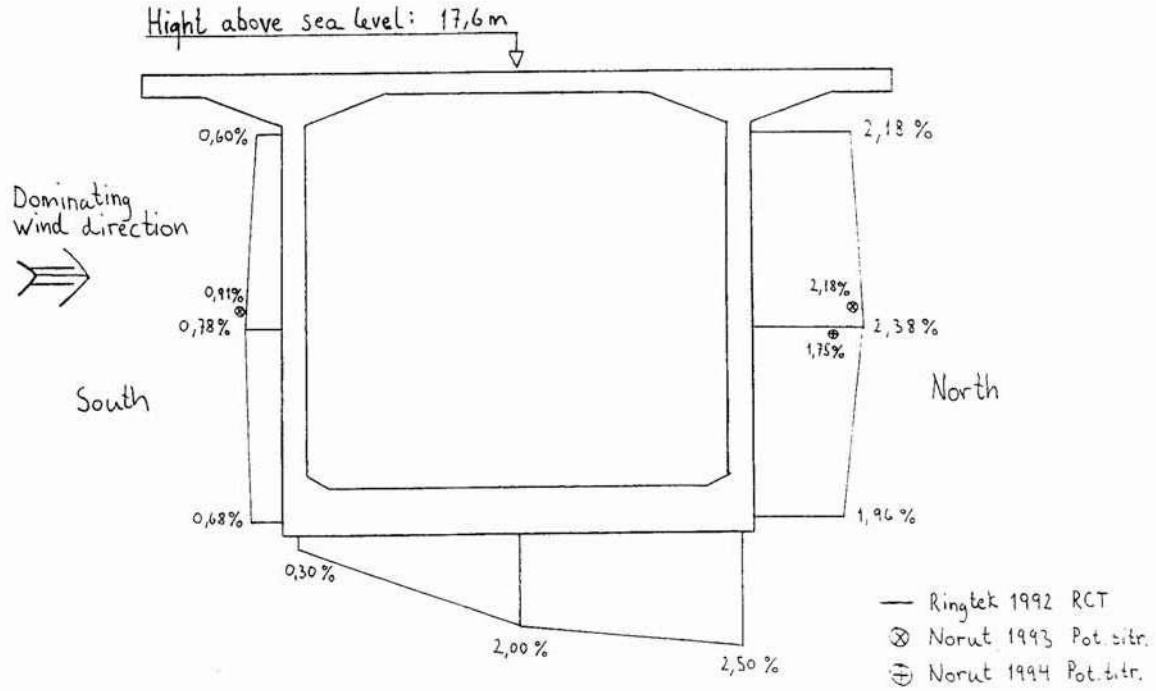

Fig. 6 Chloride load (C_s) on the superstructure at cross section B, 114 m west of axis no. 2. Recorded values in % by weight of cement.

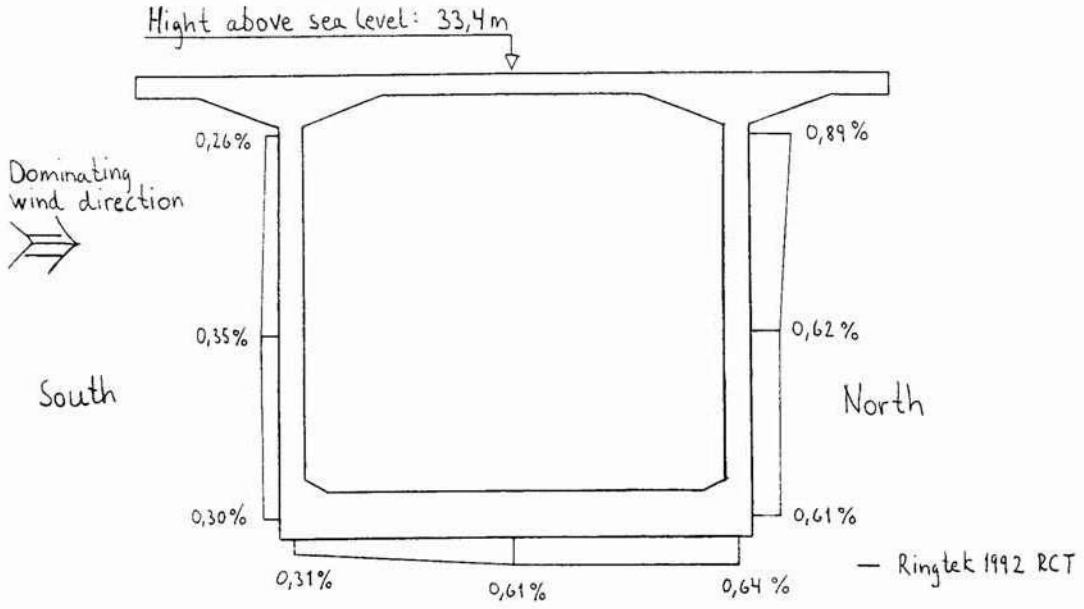

Fig. 7 Chloride load (C_s) on the superstructure at cross section C, 114 m west of axis no. 4. Recorded values in % by weight of cement.

The figures presented show very clearly how the chloride load, which is acting on the structure, is effected by factors as lee / windward side and the height of the structure above the sea level. The exact magnitude of the chloride load might be questionable, but if we use the quantitative numbers in fig. 5 - 7 we might have an idea about the size of these factors.

We can make a comparison between the chloride load on the box girder at different levels above the sea. The chloride load values on the lowest part of the box girder on the north side at cross section no. A and C are compared. The value at cross section no. A at this point is 3,99 %, while the value at cross section no. C is 0,61 %. From this, we can state that the chloride load is up to 6,5 times lower when the superstructure rises from 8 m to 28 m above the sea level.

We can also make a comparison of the chloride load on the lee side and on the windward side at cross section no. A. The chloride load values on the lowest part of the box girder on the north side and on the south side are compered. The value on the north side is 3,99 %, while the value on the south side is 0,53 %. We can record, that at the height of 8 m above the sea level, the chloride load is up to 8 times higher on the lee side than on the windward side. For all locations the environmental chloride load is a lot heavier on the lee side than on the windward side, but the effect is of most importance for the parts of the superstructure closest to the sea level.

Measurements of concrete cover have been performed both in the Ringtek survey (ref. 1) and in connection with the trial repair in 1993 (ref. 3). The recorded concrete cover at

the superstructure varies from 22 mm - 35 mm. Especially, the use of fixing bars within the cover zone has lead to the development of deterioration. The most serious areas of deterioration are on the north side of the box girder close to the sea level. Hence, the damage recorded at the superstructure of the bridge is consistent with the recorded chloride load.

4.5 Reliability of the results from the extended condition survey

The results from the 40 control measurements performed by Rescon (ref. 2) using exactly the same concrete powder drilled out in 1992, were consistent with the results from Ringtek (ref. 1). The results showed an average deviation between the measurements performed by Ringtek (RCT-method) and Rescon (titration NS 3671) of ± 15 %.

The results from the Norut analyses in 1993 and 1994, using the potentiometric titration method, does also show very good correspondence with the results from the extended condition survey using the RCT method. Based on these results, the accuracy of the RCT-method is considered as good enough for chloride analyses in condition surveys.

5. CONCLUSIONS

After the discussion, the following conclusions can be drawn:

i. The height above the sea level is of major importance for the environmental chloride load exposed to the superstructure. The chloride load is up to 6,5 times lower when the superstructure rises from 8 m to 28 m above the sea level.

ii. The chloride load is a lot heavier on the lee side than on the windward side. The effect is of most importance for the parts of the superstructure closest to the sea level. At the height of 8 m above the sea level the chloride load is up to 8 times higher on the lee side than on the windward side.

iii. The recorded chloride load is consistent with the damage recorded at the superstructure of the bridge.

iv. The calculated diffusion coefficient (D) varies from 22 - 48 mm^2/year. The average is 35 mm^2/year with a standard deviation of 7,5 mm^2/year. This indicates uniform concrete quality in the structure.

v. The accuracy of the RCT-method is considered as good enough for chloride analyses in condition surveys.

vi. The use of 10 mm steps for powder sampling does not detect high concentrations of chlorides in thin layers of the concrete.

vii. The analysed chloride value closest to the surface must be treated with care in

assessments after condition surveys. In calculations of D and C_s the value closest to the surface should be left out.

6. ACKNOWLEDGEMENT

The present report is part of "OFU Bridge Repair Project", financed by the Norwegian Public Roads Administration (NPRA), Rescon AS and the Norwegian Industrial and Regional Development Fund (SND). The project is managed by NPRA.

The authors are thankful to Selmer AS for the use of the computer program to calculate diffusion coefficients and chloride exposure coefficients.

7. REFERENCES

All of the references are written in Norwegian.

1. Østvik J.M. og Normann D: "Gimsøystraumen bru, Prøvetaking 1992", Rapport, Ringtek 21.01.93.

2. Norderup Michelson E og Tjugum G: "Sjekking av tidligere Cl-prøver", Notat, OFU Gimsøystraumen bru, Rescon 15.09.93.

3. Larsen C.K.: "Resultater fra forhåndskartleggingen, feltundersøkelser og laboratorieanalyser, Prøvereparasjon I, 1993", Rapport nr. A-94-015, OFU Gimsøystraumen bru 27.05.94.

4. Hognestad S., Kristiansen B. og Myrdal R.: "Sluttrapport Prøvereparasjon II, 1994", Rapport nr. A-94-017, OFU Gimsøystraumen bru 01.12.94.

GIMSØYSTRAUMEN BRU

KLORIDMÅLINGER I FELT 2 REKKE 5:

Lengde m	Pröve	Dybde mm	Cl-innh i vekt-% av sem.innh.	Faktor	CL-innh i vekt% bet	mV	Beliggenhet
24	Cl.2.05.01	0-10	0,41	6,4	0,0640	48	Nordre side, utkraging
		10-20	0,58	6,4	0,0900	40	
		20-30	0,38	6,4	0,0600	50	
		30-50	0,22	6,4	0,0340	63	
		50-75	0,19	6,4	0,0290	67	
24	Cl.2.05.02	0-10	1,60	6,4	0,2500	15	Nordre side, øverst
		10-20	1,28	6,4	0,2000	21	
		20-30	0,80	6,4	0,1250	32	
		30-50	0,32	6,4	0,0500	54	
		50-75	0,12	6,4	0,0185	77	
24	Cl.2.05.03	0-10	1,66	6,4	0,2600	14	Nordre side, midten
		10-20	2,30	6,4	0,3600	6	
		20-30	1,76	6,4	0,2750	12	
		30-50	0,77	6,4	0,1200	33	
		50-75	0,23	6,4	0,0360	62	
24	Cl.2.05.04	0-10	2,24	6,4	0,3500	7	Nordre side, nederst
		10-20	2,43	6,4	0,3800	5	
		20-30	1,86	6,4	0,2900	11	
		30-50	0,74	6,4	0,1150	34	
		50-75	0,17	6,4	0,0270	69	
24	Cl.2.05.05	0-10	1,54	6,4	0,2400	16	Underside mot nord
		10-20	1,54	6,4	0,2400	16	
		20-30	1,38	6,4	0,2150	19	
		30-50	0,47	6,4	0,0740	45	
		50-75	0,14	6,4	0,0215	74	
24	Cl.2.05.06	0-10	1,28	6,4	0,2000	21	Underside på midten
		10-20	1,60	6,4	0,2500	15	
		20-30	0,96	6,4	0,1500	27	
		30-50	0,33	6,4	0,0520	53	
		50-75	0,16	6,4	0,0255	70	
24	Cl.2.05.07	0-10	1,02	6,4	0,1600	26	Underside mot sør
		10-20	1,06	6,4	0,1650	25	
		20-30	0,49	6,4	0,0760	44	
		30-50	0,11	6,4	0,0175	78	
		50-75	0,16	6,4	0,0245	71	
24	Cl.2.05.08	0-10	0,45	6,4	0,0700	46	Søndre side, nederst
		10-20	0,36	6,4	0,0570	51	
		20-30	0,31	6,4	0,0480	55	
		30-50	0,19	6,4	0,0290	67	
		50-75	0,13	6,4	0,0208	75	
24	Cl.2.05.09	0-10	0,31	6,4	0,0480	55	Søndre side, midten
		10-20	0,25	6,4	0,0390	60	
		20-30	0,27	6,4	0,0420	58	
		30-50	0,15	6,4	0,0230	72	
		50-75	0,14	6,4	0,0220	73	

GIMSØYSTRAUMEN BRU

Lengde m	Pröve	Dybde mm	Cl-innh i vekt-% av sem.innh.	Faktor	CL-innh i vekt% bet	mV	Beliggenhet
24	Cl.2.05.10	0-10	0,44	6,4	0,0680	47	Søndre side, øverst
		10-20	0,32	6,4	0,0500	54	
		20-30	0,25	6,4	0,0390	60	
		30-50	0,15	6,4	0,0230	72	
		50-75	0,10	6,4	0,0160	80	
24	Cl.2.05.11	0-10	0,60	6,4	0,0940	39	Søndre side, utkraging
		10-20	0,33	6,4	0,0520	53	
		20-30	0,22	6,4	0,0340	63	
		30-50	0,14	6,4	0,0220	73	
		50-75	0,14	6,4	0,0215	74	

GIMSØYSTRAUMEN BRU

KLORIDMÅLINGER I FELT 2 REKKE 20:

Lengde m	Prøve	Dybde mm	Cl-innh i vekt-% av sem.innh.	Faktor	CL-innh i vekt% bet	mV	Beliggenhet
114	Cl.2.20.01	0-10	0,90	6,4	0,1400	29	Nordre side, utkraging
		10-20	0,88	6,4	0,1380	30	
		20-30	0,40	6,4	0,0620	49	
		30-50	0,14	6,4	0,0215	74	
		50-75	0,10	6,4	0,0150	81	
114	Cl.2.20.02	0-10	1,28	6,4	0,2000	21	Nordre side, øverst
		10-20	1,41	6,4	0,2200	18	
		20-30	0,70	6,4	0,1100	35	
		30-50	0,38	6,4	0,0600	50	
		50-75	0,18	6,4	0,0280	68	
114	Cl.2.20.03	0-10	1,54	6,4	0,2400	16	Nordre side, midten
		10-20	1,47	6,4	0,2300	17	
		20-30	0,88	6,4	0,1380	30	
		30-50	0,33	6,4	0,0520	53	
		50-75	0,18	6,4	0,0280	68	
114	Cl.2.20.04	0-10	1,34	6,4	0,2100	20	Nordre side, nederst
		10-20	1,15	6,4	0,1800	23	
		20-30	0,65	6,4	0,1020	37	
		30-50	0,27	6,4	0,0420	58	
		50-75	0,12	6,4	0,0185	77	
114	Cl.2.20.05	0-10	1,41	6,4	0,2200	18	Underside mot nord
		10-20	1,54	6,4	0,2400	16	
		20-30	0,45	6,4	0,0700	46	
		30-50	0,25	6,4	0,0390	60	
		50-75	0,11	6,4	0,0175	78	
114	Cl.2.20.06	0-10	1,47	6,4	0,2300	17	Underside på midten
		10-20	1,15	6,4	0,1800	23	
		20-30	0,32	6,4	0,0500	54	
		30-50	0,07	6,4	0,0105	87	
		50-75	0,07	6,4	0,0105	87	
114	Cl.2.20.07	0-10	0,29	6,4	0,0460	56	Underside mot sør
		10-20	0,11	6,4	0,0168	79	
		20-30	0,06	6,4	0,0098	88	
		30-50	0,05	6,4	0,0078	92	
		50-75	0,05	6,4	0,0072	93	
114	Cl.2.20.08	0-10	0,55	6,4	0,0860	41	Søndre side, nederst
		10-20	0,24	6,4	0,0370	61	
		20-30	0,16	6,4	0,0255	70	
		30-50	0,03	6,4	0,0054	98	
		50-75	0,06	6,4	0,0092	89	
114	Cl.2.20.09	0-10	0,69	6,4	0,1080	36	Søndre side, midten
		10-20	0,45	6,4	0,0700	46	
		20-30	0,19	6,4	0,0290	67	
		30-50	0,14	6,4	0,0220	73	
		50-75	0,14	6,4	0,0220	73	

GIMSØYSTRAUMEN BRU

Lengde m	Prøve	Dybde mm	Cl-innh i vekt-% av sem.innh.	Faktor	CL-innh i vekt% bet	mV	Beliggenhet
114	Cl.2.20.10	0-10	0,58	6,4	0,0900	40	Søndre side, øverst
		10-20	0,32	6,4	0,0500	54	
		20-30	0,21	6,4	0,0330	64	
		30-50	0,19	6,4	0,0300	66	
		50-75	0,10	6,4	0,0160	80	
114	Cl.2.20.11	0-10	0,47	6,4	0,0740	45	Søndre side, utkraging
		10-20	0,21	6,4	0,0330	64	
		20-30	0,11	6,4	0,0175	78	
		30-50	0,07	6,4	0,0105	87	
		50-75	0,04	6,4	0,0068	94	

GIMSØYSTRAUMEN BRU

KLORIDMÅLINGER I FELT 4 REKKE 20:

Lengde m	Prøve	Dybde mm	Cl-innh i vekt-% av sem.innh.	Faktor	CL-innh i vekt% bet	mV	Beliggenhet
114	Cl.4.20.01	0-10	0,54	6,4	0,0840	42	Nordre side, utkraging
		10-20	0,54	6,4	0,0840	42	
		20-30	0,38	6,4	0,0600	50	
		30-50	0,14	6,4	0,0220	73	
		50-75	0,11	6,4	0,0175	78	
114	Cl.4.20.02	0-10	0,77	6,4	0,1200	33	Nordre side, øverst
		10-20	0,54	6,4	0,0840	42	
		20-30	0,36	6,4	0,0570	51	
		30-50	0,25	6,4	0,0390	60	
		50-75	0,15	6,4	0,0230	72	
114	Cl.4.20.03	0-10	0,55	6,4	0,0860	41	Nordre side, midten
		10-20	0,35	6,4	0,0540	52	
		20-30	0,21	6,4	0,0330	64	
		30-50	0,19	6,4	0,0300	66	
		50-75	0,16	6,4	0,0245	71	
114	Cl.4.20.04	0-10	0,58	6,4	0,0900	40	Nordre side, nederst
		10-20	0,26	6,4	0,0405	59	
		20-30	0,14	6,4	0,0220	73	
		30-50	0,12	6,4	0,0185	77	
		50-75	0,11	6,4	0,0168	79	
114	Cl.4.20.05	0-10	0,55	6,4	0,0860	41	Underside mot nord
		10-20	0,38	6,4	0,0600	50	
		20-30	0,19	6,4	0,0300	66	
		30-50	0,14	6,4	0,0215	74	
		50-75	0,13	6,4	0,0200	76	
114	Cl.4.20.06	0-10	0,54	6,4	0,0840	42	Underside på midten
		10-20	0,35	6,4	0,0540	52	
		20-30	0,17	6,4	0,0270	69	
		30-50	0,13	6,4	0,0208	75	
		50-75	0,14	6,4	0,0215	74	
114	Cl.4.20.07	0-10	0,31	6,4	0,0480	55	Underside mot sør
		10-20	0,14	6,4	0,0220	73	
		20-30	0,10	6,4	0,0160	80	
		30-50	0,15	6,4	0,0230	72	
		50-75	0,09	6,4	0,0140	82	
114	Cl.4.20.08	0-10	0,22	6,4	0,0340	63	Søndre side, nederst
		10-20	0,21	6,4	0,0330	64	
		20-30	0,17	6,4	0,0270	69	
		30-50	0,16	6,4	0,0245	71	
		50-75	0,16	6,4	0,0245	71	
114	Cl.4.20.09	0-10	0,33	6,4	0,0520	53	Søndre side, midten
		10-20	0,19	6,4	0,0290	67	
		20-30	0,16	6,4	0,0245	71	
		30-50	0,17	6,4	0,0270	69	
		50-75	0,16	6,4	0,0255	70	

GIMSØYSTRAUMEN BRU

Lengde m	Prøve	Dybde mm	Cl-innh i vekt-% av sem.innh.	Faktor	CL-innh i vekt% bet	mV	Beliggenhet
114	Cl.4.20.10	0-10	0,23	6,4	0,0360	62	Søndre side, øverst
		10-20	0,17	6,4	0,0270	69	
		20-30	0,14	6,4	0,0220	73	
		30-50	0,18	6,4	0,0280	68	
		50-75	0,12	6,4	0,0185	77	
114	Cl.4.20.11	0-10	0,26	6,4	0,0405	59	Søndre side, utkraging
		10-20	0,14	6,4	0,0220	73	
		20-30	0,13	6,4	0,0200	76	
		30-50	0,12	6,4	0,0185	77	
		50-75	0,14	6,4	0,0215	74	

KLORIDINNHOLD I VEKTPROSENT AV SEMENTMENGDE

Merking og innveiing			Sementmengde			Kloridinnhold	Kloridinnhold
Prøve nr	Sjikt mm	Innveid pr g	CaO pr prøve mg/prøve	CaO i sement %CaO	Sementmengde mg/prøve	Klorider i big pr % Cl-	i vekt% av sementmengden
R1N (24.45, 1,41)	0-5	1,18	176,28	64	275,43	0,2234	0,9571
	5-10	1,19	170,70	64	266,72	0,5675	2,5320
	10-15	1,20	92,91	64	145,17	0,3556	2,9395
	15-20	1,18	60,15	64	93,99	0,2297	2,8839
	20-30	1,17	103,75	64	162,11	0,2532	1,8275
	30-40	1,16	136,51	64	213,30	0,1965	1,0686
	40-50	1,16	159,66	64	249,47	0,1349	0,6273

Merking og innveiing			Sementmengde			Kloridinnhold	Kloridinnhold
Prøve nr	Sjikt mm	Innveid pr g	CaO pr prøve mg/prøve	CaO i sement %CaO	Sementmengde mg/prøve	Klorider i big pr % Cl-	i vekt% av sementmengden
R4N (113,30.1,71)	0-5	1,16	201,92	64	315,49	0,3021	1,1108
	5-10	1,15	112,79	64	176,23	0,2263	1,4768
	10-15	1,18	83,39	64	130,30	0,1643	1,4879
	15-20	1,17	88,08	64	137,63	0,1477	1,2556
	20-30	1,17	141,70	64	221,40	0,1333	0,7044
	30-40	1,17	168,04	64	262,57	0,1014	0,4518
	40-50	1,17	131,79	64	205,92	0,0442	0,2511

Merking og innveiing			Sementmengde			Kloridinnhold	Kloridinnhold
Prøve nr	Sjikt mm	Innveid pr g	CaO pr prøve mg/prøve	CaO i sement %CaO	Sementmengde mg/prøve	Klorider i big pr % Cl-	i vekt% av sementmengden
R4S (112,70.1,72)	0-5	1,15	71,08	64	111,06	0,0944	0,9775
	5-10	1,16	185,35	64	289,60	0,1156	0,4630
	10-15	1,16	132,61	64	207,21	0,0935	0,5234
	15-20	1,18	98,74	64	-154,29	0,0669	0,5117
	20-30	1,15	106,34	64	166,16	0,0362	0,2505
	30-40	1,15	139,08	64	217,31	0,0282	0,1492
	40-50	1,18	142,25	64	222,27	0,0301	0,1598

KLORIDINNHOLD I VEKTPROSENT AV SEMENTMENGDE

Prøve: Brukasse ved R - 1 N

Z= 2,25m x= 25,66 Sementinnhold: 375 kg/m³

Merking og innveiing			Sementmengde			Kloridinnhold	Kloridinnhold
Prøve nr	Sjikt mm	Innveid pr g	CaO pr prøve mg/prøve	CaO i sement %CaO	Sementmengde mg/prøve	Klorider i btg pr % Cl-	i vekt% av sementmengden
Kontroll pr.							0.990
8.1	0-2	1.18			184.38	0.2399	1.535
8.2	2-4	1.23			192.19	0.2576	1.649
8.3	4-6	1.17			182.81	0.2307	1.476
8.4	6-8	1.29			201.56	0.4447	2.846
8.5	8-10	1.20			187.50	0.5395	3.453
8.6	10-15	1.27			198.44	0.4361	2.791
8.7	15-20	1.28			200.00	0.2964	1.897
8.8	20-25	1.23			192.19	0.2840	1.818
8.9	25-30	1.31			204.69	0.2830	1.811
8.10	30-40	1.28			200.00	0.2348	1.503
8.11	40-50	1.24			193.75	0.1249	0.799
8.12	50-60	1.18			184.38	0.0472	0.302
8.13	110-130	1.21			189.06	0.0466	0.298

Prøve: Brukasse ved R-4 N

Z= 2,25m x= 109,53 Sementinnhold: 375 kg/m³

Merking og innveiing			Sementmengde			Kloridinnhold	Kloridinnhold
Prøve nr	Sjikt mm	Innveid pr g	CaO pr prøve mg/prøve	CaO i sement %CaO	Sementmengde mg/prøve	Klorider i btg pr % Cl-	i vekt% av sementmengden
Kontroll pr.							1.012
9.1	0-2	1.18			184.38	0.1873	1.199
9.2	2-4	1.35			210.94	0.4069	2.604
9.3	4-6	1.21			189.06	0.2699	1.727
9.4	6-8	1.21			189.06	0.2232	1.428
9.5	8-10	1.21			189.06	0.2062	1.320
9.6	10-15	1.16			181.25	0.1517	0.971
9.7	15-20	1.36			212.50	0.1295	0.829
9.8	20-25	1.25			195.31	0.0585	0.374
9.9	25-30	1.18			184.38	0.0282	0.180
9.10	30-40	1.19			185.94	0.0163	0.104
9.11	40-50	1.20			187.50	0.0152	0.097
9.12	50-60	1.20			187.50	0.0440	0.282
9.13	140-142	1.19			185.94	0.0296	0.189

A MICROSTRUCTURAL STUDY OF SURFACE RELATED TRANSFORMATIONS IN CONCRETE SHEET PILINGS, ESBJERG HARBOUR

Torben Seir Hansen
AEClaboratory, AEC Consulting Engineers (Ltd.) A/S
DK-2950 Vedbæk, Denmark

ABSTRACT

Samples from a 37 years old concrete sheet piling situated in a marine tidewater environment were analyzed by thin section and polished section techniques. Microstructural defects and transformations were analyzed for the supratidal, intertidal and subtidal zone on the sheet piles situated at different levels in relation to the high and low-water marks. The actual composition of the concrete were estimated by point-counting technique on thin and polished sections.

Keywords: Concrete, marine tidal environment, microstructure, surface related transformation, thin section technique.

1. INTRODUCTION

In order to study the durability of »old« concrete in marine environment several investigations have been carried out on a total of 105 samples (drilled cores) from two of the 37 year old concrete sheet piles in Esbjerg Harbour in august 1993. The investigations forms a part of the project »Durability of Marine Concrete Structures« [1].

The AEClaboratory has participated in the investigations by macrostructural analysis of the concrete. These investigations has formerly been reported in [2].

1.1. Esbjerg harbour

Esbjerg harbour is situated at the west coast of Jutland in Denmark. The harbour is located in a marine tidal area with semidiurnal tidewater variations of ±1-2 m.

1.2. Concrete sheet piling of pier 61, basin 5

Pier 61 of basin 5 situated in the northern part of Esbjerg Harbour was constructed in 1957 as a pile-supported pier with a sheet piling made of reinforced concrete piles, that were driven 2-3 m into the sea bottom cf. sketches in appendix.

The target composition of the concrete is known from the project material and is reproduced in an extracted form in table 1.

Component	Type	Content by mass [kg/m^3]	Content by volume [l/m^3]
Cement	Rapid Hardening Portland Cement	301	96
Coarse aggregate	Grerup Strand (sea-dredged gravel from beach)	1140	438
Fine aggregate	Alslev (natural sand from inland pit)	754	290
Water	-	166	166
Air	-	-	10
Water/cement-ratio	0.55	-	-

Table 1: Target composition of the concrete. Extract from the original project material.

The effect of tidal environment on the concrete is assumed to vary, depending on the vertical position on the sheet piles. In relation to these variations, three different tidal zones can be established according to visibly signs caused by the different water levels on the sheet piles. These zones are the supratidal zone situated above the high-water mark, the intertidal zone situated between the high-water and low-water mark, and the subtidal zone situated below the low-water mark (cf. sketches of piles in appendix). Furthermore the sheet piles had one surface facing the harbour basin, and one surface facing the pier. Both surfaces were in direct contact with the sea-water, but affected by different environmental actions (e.g. direct sunshine).

1.3. Samples

A total of 8 concrete samples from the 2 sheet piles were analyzed. The samples were cylinder shaped cores of the dimensions Ø94x280 mm. The cores were drilled from the surface originally facing the basin. The sheet pile have been pierced in all samples. The samples were labelled according to table 2.

Sheet piling no	Sample labelled	Location on sheet pilings cf. appendix
1	A12	Supratidal zone
	T12	Intertidal zone
	K12	Subtidal zone
2	A24	Supratidal zone
	T24	Intertidal zone
	K24	Subtidal zone

Table 2: Identification examined samples. See appendix for further information concerning the exact location on the sheet pilings.

1.4. Sample preparation

A total of 6 thin sections have been prepared with the object to investigate surface related transformations on both the outward and the inward surface of the pile #1.

With the purpose of estimating the actual mix proportions of the concrete (the concrete composition in table 1 is the projected target composition), one thin section and one polished section was prepared from the central part of each sheet pile.

The thin sections have the dimensions 30x45 mm and are impregnated with fluorescent dye (epoxy). The polished sections have been prepared by cutting the cores parallel with the axis and represents accordingly a presumably representative cross section through the sheet pile. Each polished section has the dimensions 94x285 mm.

1.5. Test procedure

Thin sections and polished sections were tested according to APM 201 - microstructural analysis, and APM 202 - macrostructural analysis, respectively. The test methods includes petrographic analyses of concrete in the thin sections and polished sections, using a petrographic (polarization) microscope for the microstructural analyses and a stereographic microscope for the macrostructural analyses.

2. SURFACE RELATED TRANSFORMATIONS AND DEFECTS

Both exposed surfaces of the pile #1 have been investigated by analyses of thin sections located at different positions in relation to the tidal water levels; i.e. the supratidal zone, the intertidal zone and the subtidal zone (cf. appendix). Both the outward surface and the inward surface have been investigated in each zone.

In the following a brief description is given, of the different defects and surface related transformations. Furthermore, the observations described are summarized in table 3, 4 and 5.

Cement paste: The capillary porosity of the cement paste near the exposed surfaces was evaluated by comparison with concrete standards of known water-cement ratio. A general tendency to a denser paste, with a very low capillary porosity, was observed in the outermost parts of the paste. The capillary porosity of the dense areas is equal to a cement paste in a concrete with a water/cement-ratio less than 0.35.

Aggregate: A heterogeneous (non-uniform) distribution of the coarse aggregate was found in all the concrete samples. This was shown by a decreasing content of coarse ag-

gregate from the inward surface towards the outward surface of the piles. This was particulary distinct in the concrete of sample T12 (cf. figure 1). On the thin sections, a decreasing content of fine aggregate was observed near the outer surface. The non-uniform distribution of the coarse aggregate, as well as of the fine aggregate, is caused by sedimentation of the aggregate during the casting of the pile elements. These observations show, that the piles were cast with the present outward surface upwards.

Air voids: A weak tendency to higher content of air voids near the outward surface was observed. It is supposed that the increasing air content was caused by rising of air bubbles, during the casting. The content of air voids was everywhere less than 1 % by volume, which is a rather low content, even for a non-aerated concrete. In some parts of the inward surface, irregular (not bubble-shaped) air voids were found. These voids of entrapped air are related to parts of the cement paste, which often have a high content of unhydrated cement clinkers. It is supposed, that the irregular voids were formed in parts of the concrete with low w/c-ratio, resulting in a low slump.

Cracks: A distinction is made between micro cracks with crack width below 0.1 mm and macro cracks with crack width above 0.1 mm. In areas with cement paste of low capillary porosity, as described above, a high content of micro cracks was observed frequently. Apart from this, the content of micro cracks was generally low. Macro cracks with orientation parallel to the exposed surfaces was observed near the outward surface of the supratidal and intertidal zone. The crack width is up to 0.2 mm and the cracks penetrates the concrete to a depth of 70 mm below the outward surface of the intertidal zone. The cracks are related to a general disintegration of the concrete. Crystals of gypsum and ettringite were sometimes observed in the cracks; both indicative of water action. The morphology, the orientation of the cracks and the indications that the cracks sometimes were water-filled show, that the cracking must be due to frost action of the concrete in the intertidal zone of the sheet piling.

Erosion of surface: Disintegration of both the exposed concrete surfaces was extensive in the intertidal zone, where approx. 5-8 mm of the concrete was missing from both the outward and the inward surface of the sheet piling. In the supratidal zone approx. 1 mm of the paste was missing. In the subtidal zone only sporadic erosion of the paste was observed. The examples cited indicates, that the erosion is related to the conditions of exposure - presumably frost action as mentioned in the preceding paragraph.

Carbonation of cement paste: The cement paste of both the inward and the outward surface was carbonated in all samples. The carbonation was most pronounced at the inward surface of the intertidal zone, where the paste was carbonated to a depth of 4-9 mm. In the other tidal zones the carbonation was more pronounced at the inward surface (up to 1-1.5 mm), than at the outward surface (up to 0.4 -1 mm). The age of the concrete

taken into consideration, the carbonation is rather insignificant. This can be explained by the general high humidity of the concrete in the prevailing marine environment.

Indications of leaching: The absence of portlandite (crystalline $Ca(OH)_2$) in cement paste is normally indicative of leaching caused by water penetrating the concrete and thereby dissolving the present portlandite. The occurrence of ettringite in air voids is, in the same way, caused by recrystallization of compounds formerly diluted in the paste. The presence of ettringite in air voids is consequently interpreted as an indication of leaching. Using these indicators, leaching is observed in all zones, but most pronounced in the intertidal zone.

Other transformations: A peculiar blue-colouring of the cement paste was observed in some parts of the concrete. The blue-colouring is related to specific areas just below the inward surface of the sheet piling. In the thin sections it was found, that the blue-colouring was related to areas with a high content of unhydrated cement clinkers, i.e. areas with a low degree of hydration. Moreover the blue-coloured areas generally have a lower capillary porosity, than the remaining part of the cement paste. It was not possible to evaluate, whether the blue-colouring caused the low degree of hydration and the low capillary porosity, or whether the blue-colouring was caused by the low degree of hydration and the low capillary porosity. If the first mentioned is true, the occurrence of areas with low capillary porosity could be explained by the effect of tar applied to the surface of the concrete immediately after moulding. Formerly tar was widely used for sealing of concrete in hydraulic structures.

Encrustations: Both the inwards and outward surfaces of the sheet pilings were plastered with algal mats, carbonate shelled see-living organisms (mostly barnacles), and clay (cf. sketches in appendix). The encrustations of the carbonate shelled organisms are most extensive in the subtidal zone, where almost the whole surface is covered with a 0.1-0.2 mm thick layer of shell-material. These encrustations also appears in the intertidal zone, but not so extensive.

Surface investigated	Outward surface	Inward surface
Cement paste, capillary porosity	equal to w/c < 0.35 in outermost 5-7 mm	equal to w/c < 0.35 in outermost 0.2-1 mm
Aggregate	decreasing content near surface	unchanged
Air voids, content	unchanged	unchanged
Micro cracks <0.1 mm	high content in outermost 5-7 mm	unchanged
Macro cracks ≥0.1 mm	a few parallel with surface	none
Erosion of concrete	1 mm of the cement paste	1 mm of the cement paste
Carbonation of cement paste	0-0.4 mm	0.5-1 mm
Indication of leaching	portlandite absent from paste in outermost 0.1 mm. Ettringite in air-voids	ettringite in air-voids
Other transformations	not observed	blue-colouring of paste in outermost 0.2-0.6 mm
Encrustation	some organic material, sparse	0.2-0.6 mm organic material with detritus

Table 3: Sheet pile #1 - Supratidal zone. Summary of observations in polished and thin sections made from sample A12. For further details - see text.

Surface investigated	Outward surface	Inward surface
Cement paste, capillary porosity	equal to w/c < 0.35 in outermost 0.2-0.3 mm	equal to w/c < 0.35 in outermost 0.5-1 mm
Aggregate	distinct decreasing content near surface	unchanged content near surface
Air voids, content	unchanged	some irregular voids near surface
Micro cracks <0.1 mm	extreme high content in outermost 1 mm of the paste	high content in outermost 2-3 mm of the paste
Macro cracks ≥0.1 mm	Occur parallel to surface to a depth of approx. 70 mm	none
Erosion of concrete	approx. 7-8 mm of the concrete (coarse and fine aggregate + paste)	5-8 mm of the mortar (fine aggregate + paste)
Carbonation of cement paste	0.1-0.4 mm	4-9 mm
Indication of leaching	portlandite depleted from paste in outermost 6-8 mm. Ettringite in air-voids and fine cracks	portlandite depleted from paste in outermost 0.5-1 mm. Ettringite in air-voids.
Other transformations	not observed	blue-colouring of paste in outermost 3-5 mm
Encrustation	some reminiscent from carbonate-shelled organisms. Gypsum and carbonate crystals in cracks	some reminiscent from carbonate-shelled organisms. Gypsum and carbonate crystals in cracks. Some organic material

Table 4: Sheet pile #1 - Intertidal zone. Summary of observations in polished and thin sections made from sample T12. For further details - see text.

Surface investigated	Outward surface	Inward surface
Cement paste, capillary porosity	generally unchanged. In areas depleted from portlandite equal to w/c = 0.7	equal to w/c < 0.35 in outermost 3.5-5 mm
Aggregate	decreasing content near surface	unchanged content near surface
Air voids, content	increasing near surface	some irregular voids near surface
Micro cracks <0.1 mm	unchanged	unchanged
Macro cracks ≥0.1 mm	none	none
Erosion of concrete	sporadic and less than 0.1 mm of the paste	0.1-0.4 mm of paste
Carbonation of cement paste	0.4-1 mm	0.1-1.5 mm
Indication of leaching	in some parts the portlandite is depleted from paste in outermost 0.5-1 mm. Ettringite in air-voids	in some parts the portlandite is depleted from paste in outermost 0.5 mm. Ettringite in air-voids
Other transformations	not observed	distinct blue-colouring of paste in outermost 4-7 mm; weak blue-colouring to approx. 27 mm below surface.
Encrustation	surface covered with reminiscent from carbonate-shelled organisms.	surface covered with reminiscent from carbonate-shelled organisms. Carbonate crystals in air-voids. Some organic material

Table 5: Sheet pile #1 - Subtidal zone. Summary of observations in polished and thin sections made from sample K12. For further details - see text.

3. ESTIMATION OF MIX PROPORTIONS

The content of coarse aggregate (particles larger than 4 mm - gravel), fine aggregate (particles smaller than 4 mm - sand), cement paste and air voids was estimated by point-counting on one thin section and one polished section of sample T12 and T24 respectively.

The water-cement ratio (w/c-ratio) of the concrete was estimated by comparison with concrete standards of known water-cement ratio. The amount of mixing water and cement was calculated from the estimated w/c-ratio on the following assumptions: total hydration of the cement paste, the cement paste was a closed system (i.e. that there was no transport of material in and out of the volume of concrete investigated), and a relative cement density of 3.1.

The composition of the concrete in the two sheet piles appears from the following table 6.

Sheet piling	#1	#2
Sample	T12	T24
Composition of concrete estimated by point-counting		
Coarse aggregate	46 vol%	41 vol%
Fine aggregate	33 vol%	33 vol%
Air voids	<1 vol%	<1 vol%
Cement paste	21 vol%	26 vol%
w/c-ratio estimated from capillary porosity of cement paste		
w/c-ratio	0.55	0.55
Calculated mix proportions (kg/m^3 concrete)		
Coarse aggregate	1202 kg	1066 kg
Fine aggregate	858 kg	859 kg
Cement	235 kg	295 kg
Mixing water	130 kg	162 kg

Table 6: Composition of the concrete estimated by point-counting on two samples. The mix proportions was calculated from the point-counting results assuming the following relative densities: Density of cement - 3.1, density of coarse aggregate - 2.6, density of fine aggregate - 2.6.

Coarse aggregate: The coarse aggregate is dominated by the cretaceous, sedimentary rock type flint, which is widely prevalent in danish gravel deposits. Granite and gneiss is minor. The coarse aggregate is in accordance with see-dredged gravel, as specified in the original mix proportions for the concrete. The distribution of the coarse aggregate is classified as heterogeneous in the concrete represented by sample T12, with a distinct higher content of coarse aggregate in one end of the core (see figure 1). The distribution is less heterogeneous in sample A12 and almost homogeneous in sample K12.

Fine aggregate: The fine aggregate is mainly composed of quartz and feldspar. Chalcedonic flint (in Denmark classified as »dense flint«) and opaline flint (classified as »porous flint«) are minor constituents. The particle shape is classified as rounded. The fine aggregate is homogeneous distributed in the concrete.

Cement paste: The cement used is rather fine-grained, probably of the type Rapid Hardening Portland Cement.

Air-voids: The concrete contains only few voids of entrapped air. The air-voids have the shape of bubbles and are less than 3 mm i cross section.

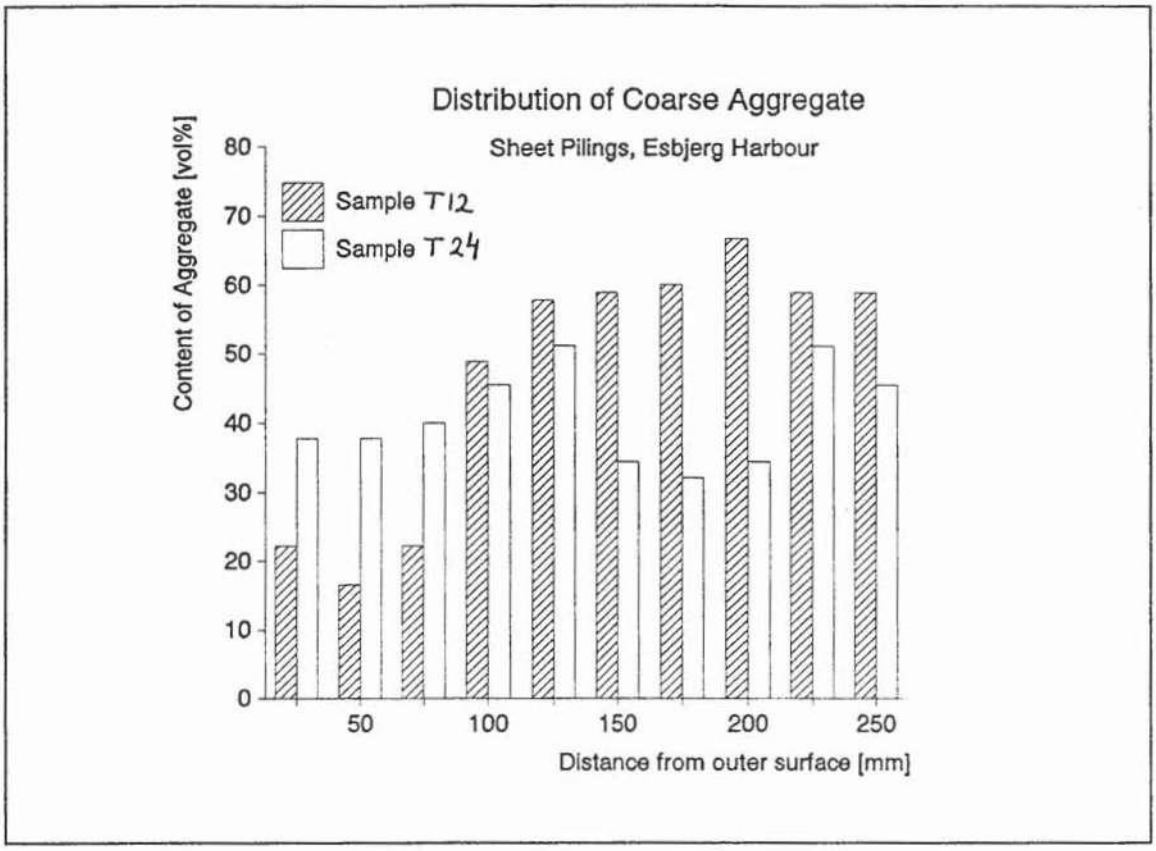

Figure 1: Distribution of coarse aggregate in the sample from sheet pile #1 (Sample T12) and sheet pile #2 (sample T24). The content of aggregate is gradually increasing when mowing from the outward surface towards the inward surface of sheet pile #1. It is caused by sedimentation of the coarse aggregate during casting.

4. CONCLUSIONS

1. The capillary porosity of the cement paste was found equal to a concrete cast with a water/cement-ratio of 0.55. A non-uniform distribution of aggregate and cement paste was observed in both sheet piles indicating, that the piles were cast with the present outward surface upwards. The non-uniform distribution is particulary distinct for sheet pile #2.

2. In the supratidal zone the capillary porosity of the cement paste was reduced to a level corresponding to a concrete cast with a water/cement-ratio of less than 0.35. This effect was most pronounced in the outward surface, where the reduction was found to a depth of 5-7 mm below the surface. In the intertidal zone approx. 5-8 mm of the

surface was missing (eroded away) - only in the outermost 1 mm of the present surface a reduced capillary porosity was observed. In the subtidal zone leaching caused an increase of the capillary porosity in the outermost part of the outward surface, but not at the inward surface.

3. Disintegration of the concrete was observed as proper erosion to a depth of 5-7 mm below the exposed surface in the intertidal zone. Cracking occurred to a depth of 70 mm - but only at the inward surface of the sheet piling. The cracking is found to be caused by frost-action. Erosion and cracking was only observed to a much smaller degree in the supratidal zone and not at all in the subtidal zone.

3. Carbonation of the cement paste was most pronounced at the inward surface of the intertidal zone, where the cement paste was carbonated to a depth of 4-9 mm. In other parts of the sheet piles the carbonation was less than 1.5 mm. It is supposed, that the general high humidity of the concrete in the marine environment caused the rather insignificant degree of carbonation.

4. Both surfaces of the sheet piles were plastered with algal mats and carbonate shelled see-living organisms (mostly barnacles). The encrustations of the carbonate shelled organisms were most extensive in the subtidal zone, where almost the whole surface was covered with shell-material. In the intertidal zone, the surface was covered to a lesser extent.

5. A peculiar blue-colouring of the cement paste was observed in the inward surface of the sheet piling. The blue-colouring was related to areas with a high content of unhydrated cement clinkers, i.e. areas with a low degree of hydration. The blue-coloured areas generally have a lower capillary porosity, than the other parts of the cement paste. The blue-colouring is explained as an effect of tar applied to the surface of the concrete immediately after moulding. Formerly tar was widely used for sealing of concrete in hydraulic structures.

5. REFERENCES

[1] Sandberg, P., 1994: Kloridinitieret armeringskorrosion -Lägesrapport och resultatredovisning för 1992-93. Durability of Marine Concrete Structures.

[2] Hansen, T., S., 1993: Micro- and Macrostructural Analysis of Concrete Cores from Sheet Pilings, Esbjerg Harbour, Test report no. AECprøv93-037.

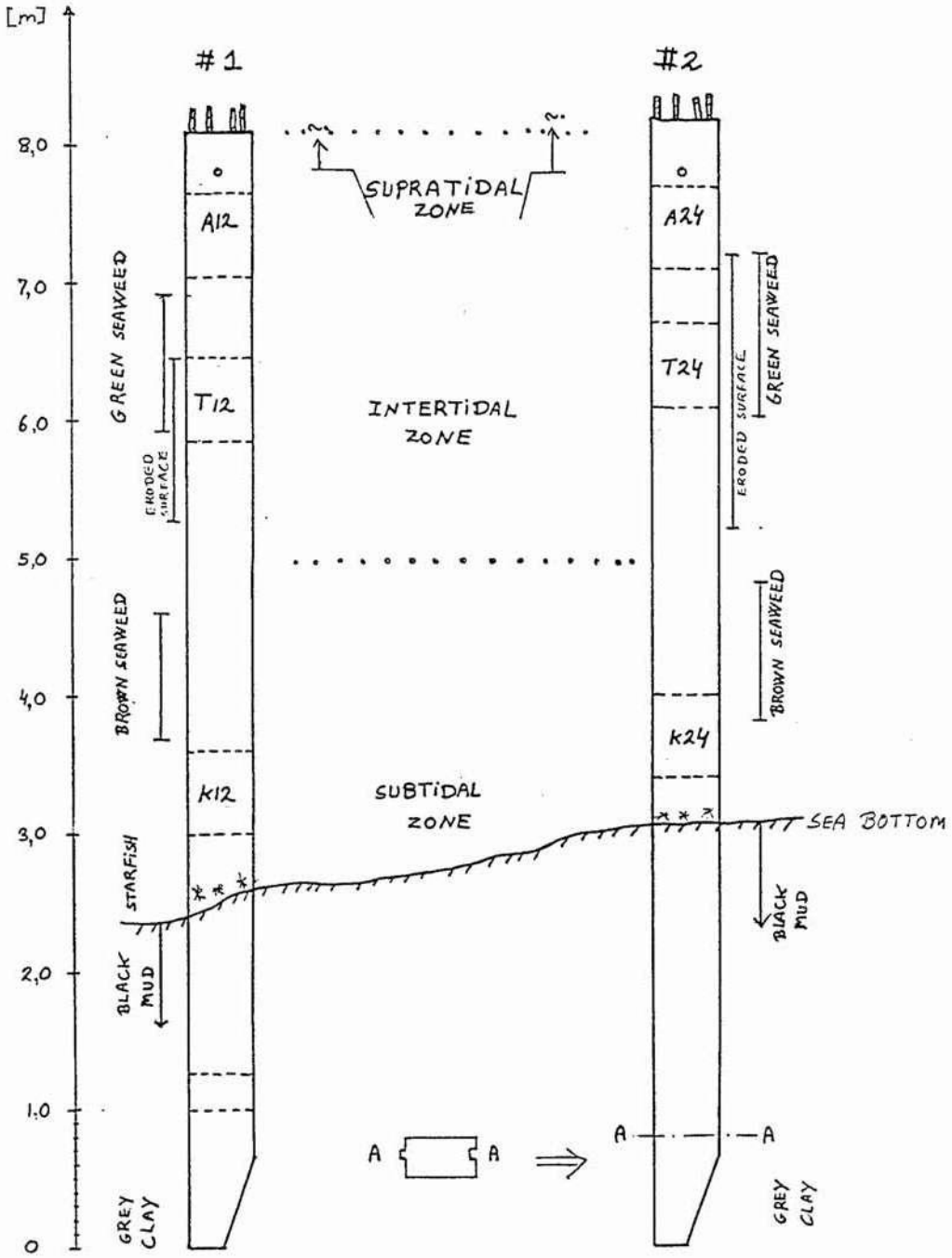

Sketches of the two sheet piles with the location of the samples investigated. The exact placing of the different tidal levels is uncertain.

THEME 2

Chemistry of the pore solution

PORE SOLUTION CHEMISTRY IN CONCRETE

Paul Sandberg
Cementa AB/Byggnadsmateriallära LTH
Forskningsbyn Ideon, 223 70 Lund
fax (+46)-46 211 06 47

1. SIGNIFICANCE

The pore solution chemistry in concrete is important, since it is the wet electrolyte and not the total amount of chloride, which affects the corrosion properties of steel embedded in concrete. Furthermore, a better knowledge on the changes in the pore solution composition, and the chemical potentials triggering these changes, in field exposed concrete over the years, may provide some answers to observed deviations from the simple diffusion equations commonly used in concrete science.

1.1 Free, bound and total chlorides

The total chloride content usually measured in concrete can be divided into free, physically bound and chemically bound chlorides. Only the concentration of free chlorides affect the corrosion properties of steel in concrete. However, the concentration of chlorides in a pore solution of a given concrete is controlled by the ability of the binder to fix chlorides, a property which appears to vary with the pore solution composition as indicated in Fig. 1. The alkalinity and the concentration of sulfate ions have been reported to significantly influence the chloride binding capacity of a given binder /3,4,5/.

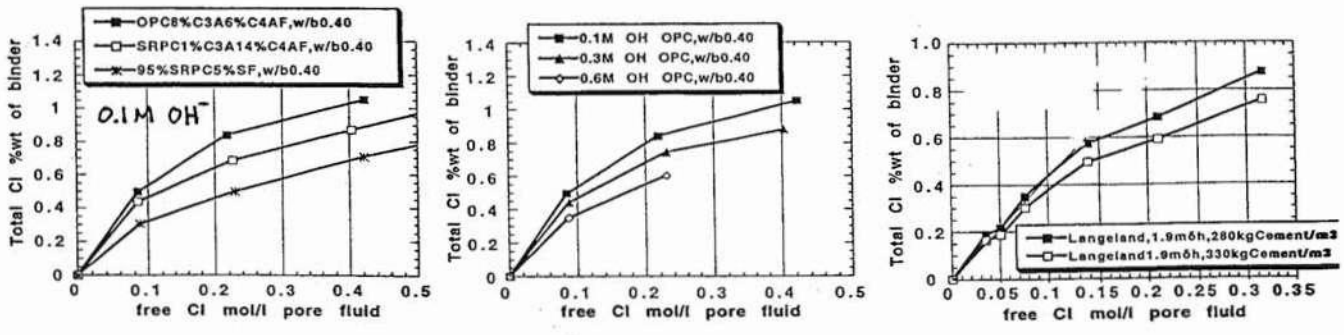

Fig. 1. Examples of chloride binding isotherms. Left: Influence of various binders. Middle: Influence of alkalinity of the pore solution /5,7/. Right: Field estimations of the relationship total chloride - free chloride for a 15 years old marine upper splash zone concrete, calculated from data presented by Sørensen et al /13/.

It is essential to know the chloride binding capacity of a given concrete, in order to translate measured total chloride contents to corresponding concentrations of free chloride ions in the concrete pore solution. The free chloride concentration is related to the total chloride content of a given (hydrated) binder. The relationship is affected by the binder type, degree of hydration, the amount of pore solution as compared to the binder content ("wet porosity"), and the other ions in the pore solution.

1.2 Changes in the field concrete pore solution composition over time

Several researchers, /1,3,6/ among others, have reported a hydroxide permeability of concrete in the same order as chloride permeability. Typical concentration profiles for free chloride and hydroxide ions in field exposed concrete are shown in Fig. 2 /7/. Similar profiles found in a laboratory immersion experiment is shown in Fig. 3 /6/. (The hydroxide ion diffusivity has been reported to be either slightly higher or slightly lower as compared to the chloride ion diffusivity, for a given paste or mortar, depending on experimental conditions /3,6/.)

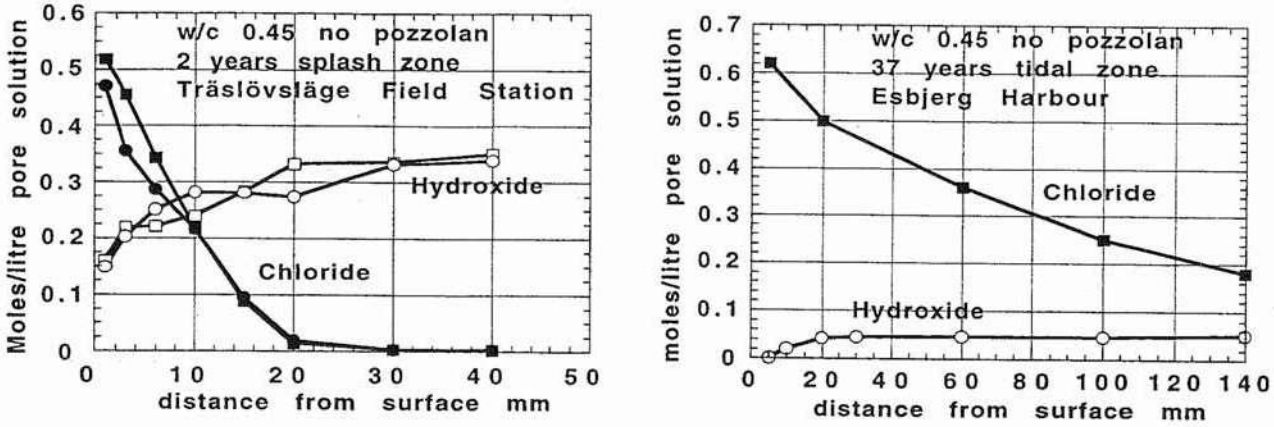

Fig. 2. Left: Hydroxide ions were found to be leached away from a concrete cover as chloride ions penetrate into the concrete (2 years of marine field exposure). Right: Corresponding ion concentrations found in a 37 years old marine concrete (tidal zone). The initial high alkalinity in concrete decreases as the mobile alkali hydroxides are removed /7/.

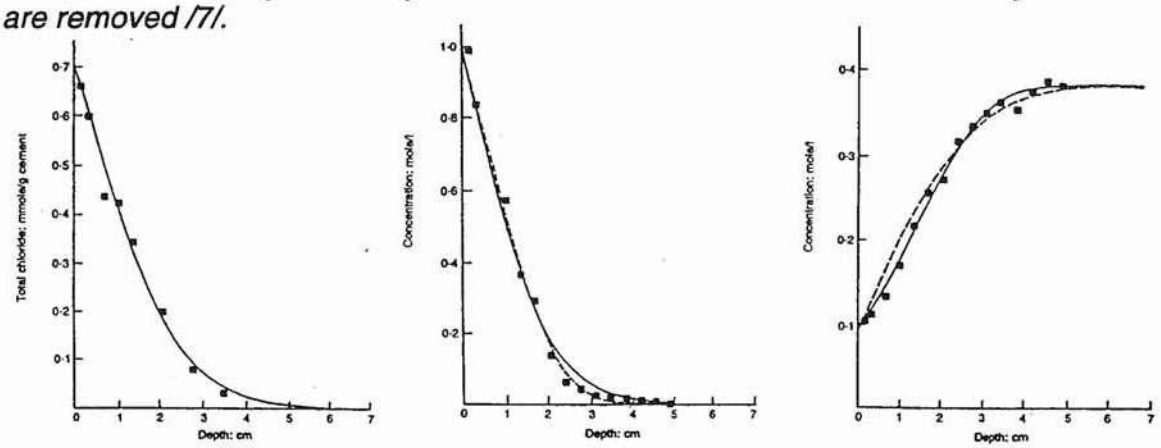

Fig. 3. Concentration profiles of total chlorides (left), dissolved chlorides (centre) and dissolved hydroxides (right), for Portland cement paste of w/c 0.50 immersed for 100 days in a solution of 1.0 M sodium chloride saturated with calcium hydroxide /6/.

1.3 Calcium ion enrichment in concrete pore solution?

The ingress of chlorides into the pore solution in concrete apparently have a significant effect on the chemical equilibrium. Calcium ions in a chloride free pore solution from unleached concrete have a solubility much less than 0.01 M, as the calcium solubility is depressed by the alkali hydroxides in the pore solution /8/.

However, 1-2 orders of magnitude higher free calcium concentrations in chloride contaminated concrete have frequently been measured /3,7/, as illustrated if Fig. 4. Yonezawa attributed the apparent increased calcium solubility to the higher ionic strength in chloride contaminated concrete /3/, but the phenomena has been observed also for chloride contaminated concrete al quite low ionic strengths /3,7,9-12,19/.

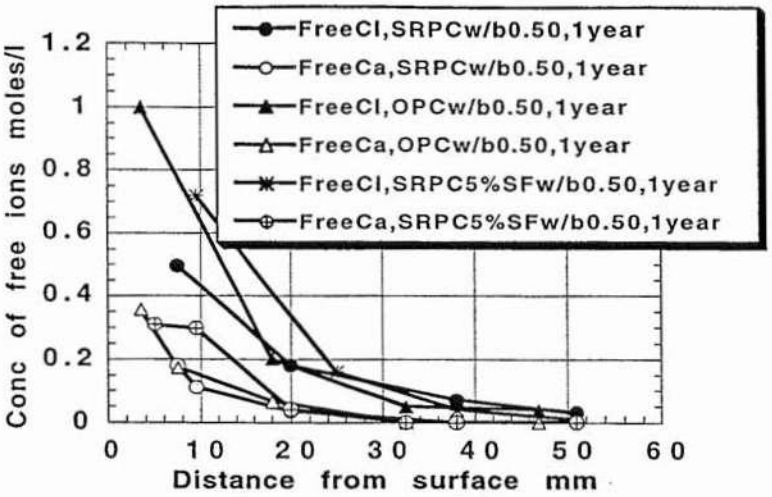

Fig. 4. Concentration profiles of free calcium and chloride ions measured by the pore solution expression method, in submerged marine concrete w/b 0.50, one year exposure /7/.

As reported by Theissing et al /19/, sodium chloride have a much less dramatic effect on the solubility of calcium hydroxide as compared to the concentrations indicated in Fig. 4. Theissing et al proposed the formation of a calcium hydroxide - calcium chloride hydrated complex in the presence of chlorides, thus accounting for some calcium and chloride fixing (which could be altered by the procedure of pore solution expression and analysis).

Moragues et al proposed that calcium and chloride form molecular dissolved species in the pore solution, thus altering the calcium activity in the pore solution. They proposed that the molecular dissolved calcium chloride species may dissociate when analyzed (by titration, etc.), therefore explaining the high apparent concentration of free calcium ions in pore solutions containing chlorides /11-12/.

Chatterji on the other hand proposed that calcium ions co-diffuse (at very high concentrations) with chlorides, but the calcium ion transport would take place in the electrical double layer only /9-10/. However, since the electrolyte in the very thin electrical double layer is impossible to remove by the pore solution expression method, the high calcium concentrations found by this method apparently cannot be explained by the theory proposed by Chatterji (?).

1.4 Chloride ion enrichment in concrete pore solution?

Chloride concentrations in expressed pore fluid from sea water submerged concrete have occasionally been found to be higher as compared to the surrounding sea water /7,22/. The phenomena was illustrated in Fig. 4, for concrete samples w/b 0.50 submerged for one year at the Träslövsläge marine field station at the Swedish west coast. The Träslövsläge sea water normally has a chloride ion concentration of approximately 0.4 M.

The chloride enrichment may be obvious for splash and atmospheric zone concrete, due to salt deposition and drying. However, for submerged concrete diffusion processes are commonly believed to eventually equalise the chloride concentration in the pore solution as compared to the external solution.

Indeed, long term immersion experiments of mortar and concrete submerged in the laboratory or in the field have indicated equalised chloride concentrations in the pore solution, at least if the concrete water to binder ratio is > 0.45 /3/. In Fig. 5, the free chloride profile is shown as measured by the pore solution expression method, for a concrete w/b 0.45, submerged for 20 years at Bergen. The sea water had an approximate chloride concentration of 0.55 M /14/.

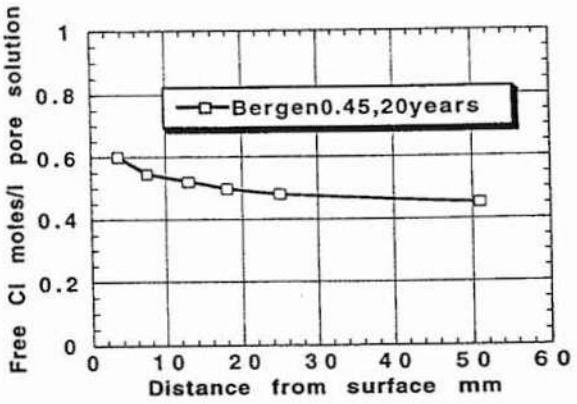

Fig. 5. Pore solution Cl profile for concrete sea water submerged for 20 years /14/.

The hydroxide ion concentration in the 20 years old Bergen concrete was analysed as 0.039M (as was expected).

If it is assumed that the measured free chloride concentrations indicated in Figs. 4-5 are generally correct, they may support the belief that chloride transport in concrete is considerably affected by mechanisms other than diffusion, as described by Fick´s 2 law of diffusion. Mechanisms such as suction + filtering (as proposed by Volkwein /15/), hydroxide leaching, osmotic pressure and other membrane effects may all affect the chloride transport in the concrete pore solution.

Note that the mechanisms proposed by Moragues et al (the formation of molecular dissolved calcium chloride species, affecting the activity of calcium and chlorides) may also explain an apparent free chloride enrichment in the pore solution. However, their theory would not explain why the apparent chloride enrichment is strong at early ages, but diminishing when all concentration gradients are equalised at later ages.

1.5 Critical chloride concentrations for corrosion initiation

Fig. 6 is a schematic presentation of the stability of black steel and the passivating iron oxide film in chloride solution. As indicated to the left, the critical chloride concentration for corrosion initiation varies with the steel potential and the alkalinity of the solution, as expressed by the logarithmic pH scale /1/. The alkalinity level of uncarbonated concrete is also indicated. Some critical chloride concentrations on black steel in mortar or concrete are indicated to the right, as measured by Pettersson /2/. (At a given alkalinity and steel potential, embedded steel in concrete is usually found to be more chloride resistant as compared to naked steel exposed to a similar solution as in the concrete /3/.)

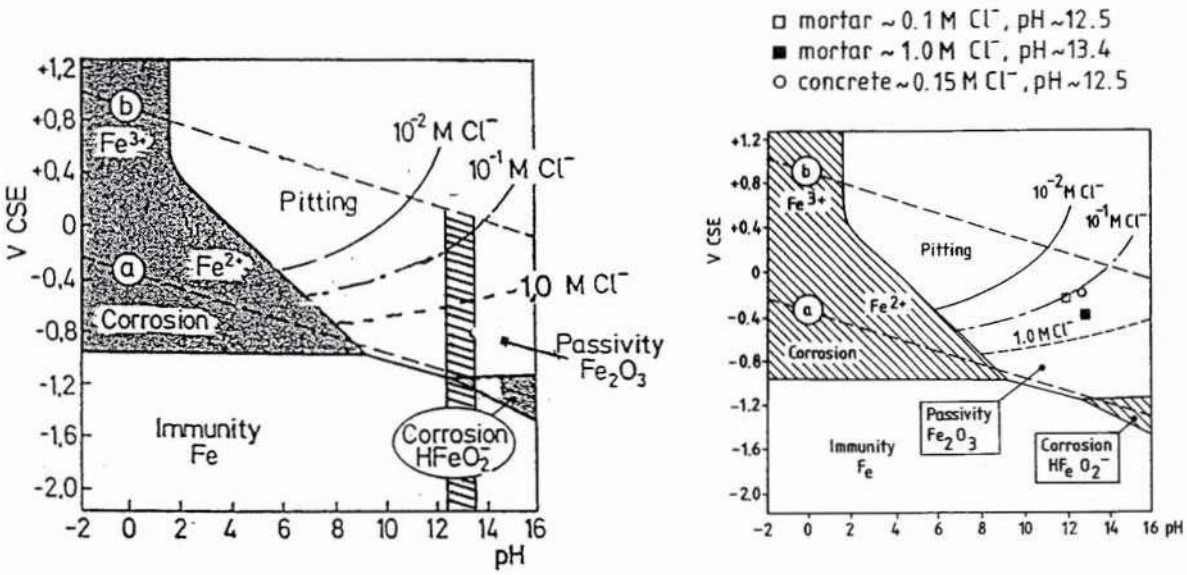

Fig. 6. Left: The stability of black steel and iron oxide in chloride solution. Critical chloride concentrations is indicated as a function of the steel potential and the alkalinity of the solution /1/. Right: Corresponding critical chloride concentrations are indicated as measured for black steel in concrete or mortar by Pettersson /2/.

2. Methods for studying the pore solution chemistry in concrete

2.1 The pore solution expression method

As initially developed by Longuet et al /18/, the pore solution expression method has generally been found to be the most accurate method for studying chlorides and hydroxides in the pore solution of concrete, mortar and paste /16,17,21/. Errors less than 10% have frequently been reported, provided that the amount of expressed solution is not too small, not carbonated and free of colloidal particles.

Several studies (/16,17,21/ among others) have indicated that the varying pressure applied will not significantly alter the composition of the expressed pore fluid. (Pressures applied are apparently too small to significantly alter the solubility of chlorides and hydroxides.)

A typical device for pore solution expression is shown in Fig 7 /16/:

Unfortunately, the pore solution expression method is usually not applicable for semi dry concrete or very dense concrete. At present, no reliable method exists for analysis of the pore solution composition in modern high quality concrete of w/b < 0.40.

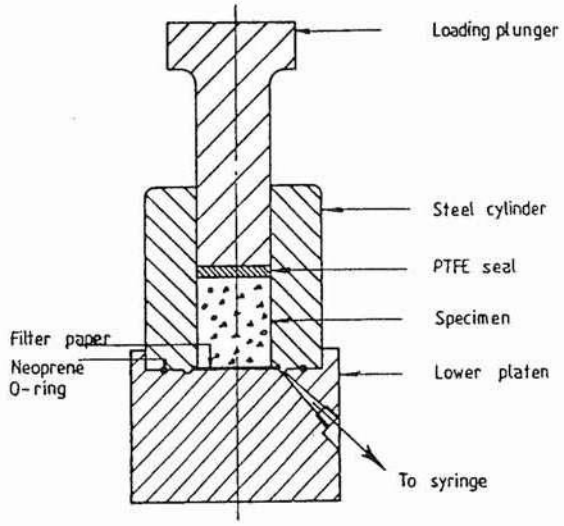

Fig. 7. Illustration of a typical device for pore solution expression /16/.

2.2 Leaching of free ions from the binder matrix.

Several proposed methods are based on leaching of free chloride ions from concrete /16/. Normally the leaching is a very slow process, and therefore the concrete to be analyzed is crushed or pulverised to very small particles. Unfortunately the processes of leaching and drying affects the chloride binding capacity of the binder. Furthermore, the pulverisation of low w/b ratio concrete may release some fresh surfaces of unhydrated cement. All these factors may introduce some error.

However, leaching methods seem to be practical and inexpensive from an engineering point of view. Therefore, in the absence of reliable methods applicable for modern high quality concrete, leaching methods may become more useful in the future. A standard procedure involving crushing of concrete in humid atmosphere, removal of larger aggregates and then immediately followed by leaching, or pore solution expression, of the pore solution, may improve the reliability of methods based on leaching.

2.3 Electro-migration of ions in the pore solution

Electro-migration methods have been proposed by Arup /20/, as a possible tool for i) removal of ions in the pore solution into an inert medium (in which ions from the pore solution may be analyzed), ii) accelerated modification of the pore solution composition in order to simulate long term phenomena such a hydroxide leaching, etc.

3. A DISCUSSION OF THE RESULTS PRESENTED BY LARSSON AND LARSEN

Larsson /23/ and Larsen /24/ both carried out investigations on the composition of the pore solution in paste or mortar being submerged in saline solutions, using the pore solution expression method. Results regarding chloride and hydroxide ion concentrations were presented.

Larsson /23/, studied initially chloride free cement paste discs of w/b 0.40 - 0.75, being stored for 22-31 months in synthetic pore solutions with varying concentrations of chloride and hydroxide. When comparing chloride and hydroxide concentrations in expressed pore solution with the surrounding solution, he noticed a general but not very large enrichment for chlorides, but not for hydroxides, in the expressed pore solution.

The results indicated chloride concentrations some 5 to 36 % higher in extracted pore solution as compared to the surrounding solution. However, only one measurement resulted in a chloride enrichment of more than 20 %. The chloride enrichment in extracted pore fluid was more pronounced at w/b 0.40, and especially so at a lower temperature (+5°C) and when silica fume was incorporated in the binder. But the amount of experimental data was too small and the scatter in the results too high for any conclusions yet to be drawn.

Larsen /24/ studied mortars of w/b 0.60 with and without cast-in chlorides, being stored for 3 months in various salt solutions. Similar to the findings by Larsson, Larsen found a small but in most cases not significant chloride enrichment in the pore solution of originally chloride free samples. Only one measurement resulted in a chloride enrichment of more than 15 %.

Larsens results regarding chloride and hydroxide concentrations in samples with cast-in chlorides show no systematic trend and are somewhat difficult to evaluate. As reported by Yonezawa /3/, the hydroxide concentration is likely to increase initially in samples with cast-in sodium chloride, due to the exchange of chloride ions for hydroxide ions associated with the chloride binding process. The scatter found in some results may indicate that some samples had not yet reached equilibrium. It is interesting, however, that Yonezawa found a similar "inconsistency" for a large number of samples after similar exposure times /3/. For samples with cast-in sodium chloride, it may be possible that the initial chloride binding process (associated with the formation of Friedel´s salt) is unstable and therefore gradually changing.

Larsson, however, found relatively small deviations (Max. 13%) in the hydroxide concentrations when comparing the pore solution to the external solution, for paste submerged for 22-31 months with no cast-in chloride.

Since the enrichment found by Larsson /23/ was stronger for chlorides as compared to hydroxides, and expressed pore solution was analysed simultaneously as the surrounding solution, errors in the analysing procedure are not probable as an explanation for the observations. However, if a molecular dissolved calcium chloride is formed but later dissociated when analyzed, as proposed by Moragues et al, the apparent enrichments in both calcium and chloride would be explained.

4. CONCLUDING REMARKS AND SUGGESTIONS FOR FUTURE RESEARCH

A) The strong pore solution chloride enrichment (sometimes more than 100%) occasionally analysed in submerged field concrete was not found in laboratory immersion of paste or mortar, until equilibrium was reached with the external solution. If the laboratory results are correct, the long term chloride enrichment is in the order of 5-20%, which is within or only slightly above the margin of error normally associated with the pore solution expression method. It may be possible, if the chloride enrichment effect is real at all, that the field observed chloride enrichment is a temporary effect associated with steep gradients of other free ions such as hydroxide and calcium close to the concrete surface. The apparent calcium and chloride enrichment may also be an effect of the formation of molecular dissolved calcium chloride species in the pore solution, as proposed by Moragues et al. The molecular dissolved calcium chlorides would be expressed with the pore solution, and then dissociated when analyzed, thus resulting in the apparent enrichment.

B) The coupled effect of chlorides and other ions entering and leaving the binder phase is not well understood. The pore solution expression method, maybe in combination with electro-migration experiments, may be well suited for such studies.

C) It is most essential to develop accurate methods for studies of the pore solution composition in modern high quality concrete. The pore solution expression method is at present not applicable for such low w/b ratio concrete. In the absence of such an accurate method, it will be difficult to measure critical chloride concentrations for corrosion initiation with any desired accuracy.

5. REFERENCES

/1/ Alekseev, S.N., "Corrosion of Steel Reinforcement", Durability of Reinforced Concrete in Aggressive Media (editor S.K. Mallick), Russian Translation Series 96, A.A. Balkema/Rotterdam/Brookfield, 1993, pp. 164-247, 305-349.

/2/ Pettersson, K.,"Corrosion of Steel in High Performance Concrete", Proceedings 3rd Int. Symp. on Utilization of High Strength Concrete, Lillehammer, Norway 1993.

/3/ Yonezawa, T., Pore Solution Composition and Chloride-Induced Corrosion of Steel in Concrete, British Ph D Thesis, Victoria University of Manchester, Corrosion and Protection Centre, 1988.

/4/ Byfors, K., "Chloride-initiated reinforcement corrosion, Chloride binding", CBI Report 1:90, Swedish Cement and Concrete Research Institute, 1990.

/5/ Sandberg, P., Larsson, J., "Chloride binding in cement pastes in equilibrium with synthetic pore solutions", Proceedings Nordic Seminar on Chloride Initiated Reinforcement Corrosion in Concrete, Gothenburg, Sweden, January 13-14, 1993.

/6/ Sergi, G., Yu, S.W., Page, C.L., "Diffusion of chloride and hydroxyl ions in cementitious materials exposed to a saline environment", Magazine of Concrete Research, 44, No. 158, pp. 63-69, March 1992.

/7/ Sandberg, P., Chloride initiated reinforcement corrosion in concrete, Lund Inst. of Technology, Building Materials, Licentiate thesis 1995-03-01.

/8/ Taylor, H. F. W., Cement Chemistry, Academic Press Ltd., London, pp. 226-230, 1990.
/9/ Chatterji, S. Kawamura, M., "Electrical double layer, ion transport and reactions in hardened cement paste", Cement and Concrete Research, Vol. 22, pp. 774-782, 1992.
/10/ Chatterji, S., "Transportation of ions through cement based materials. Part 3 - Experimental evidence for the basic equations and some important deductions", Cement and Concrete Research, Vol. 27, pp. 1229-1236, 1994.
/11/ Moragues, A., Goni, S., Andrade, C., "Chemical characterization of synthetic concrete pore solutions", Ceramic Transactions, Vol 16, Advances in Cementitious Materials (edited by S. Mindess), pp. 57-65.
/12/ Moragues, A., Macias, A., Andrade, C, Goni, S., "Chemical equilibrium constants of the aqueous cement paste", Materials Engineering, Vol. 1, No. 2, pp. 453-458, 1989.
/13/ Sørensen, B., Maahn, E., "Penetration rate of chloride in marine concrete structures", Nordic Concrete Research, No. 1, Oslo 1982.
/14/ Pettersson, K., Unpublished results on expressed pore solution composition in 20 years submerged concrete at the Laksevåg marine field station, Det Norske Veritas, Bergen, Swedish Cement and Concrete Research Institute, Stockholm, Dec. 1994.
/15/ Volkwein, A., "Convection of chlorides into concrete due to hydration suction and capillary suction", Proceedings 6th Int. Conf. on Durability of Building Materials and Components, Omiya, Japan, pp. 279-288, 26-29 Oct., 1993.
/16/ Arya, C., Newman, J.B., "An assessment of four methods of determining the free chloride content of concrete", Materials and Structures, 23, pp. 319-330, 1990.
/17/ Byfors, K., Hansson, C. M., Tritthart, J., "Pore solution expression as a method to determine the influence of mineral additives on chloride binding", Cement and Concrete Research, Vol. 16, pp. 760-770, 1986.
/18/ Longuet, P., Burglen, L., Zelmer, A., Revue des Materiaux de Construction et de Travaux Publics, No. 676, p. 35, 1973
/19/ Theissing, E.M., Hest-Wardenier, P.V., de Wind, G., "The combining of sodium chloride and calcium chloride by a number of different hardened cement pastes", Cement and Concrete Research, Vol. 8, pp. 683-692, 1978.
/20/ Arup, H., "Liquid/solid phase equilibrium and junction potentials in cement based materials" (in Danish), Force-Institutterne, Denmark 1993.
/21/ Duchesne, J., Bérubé, M.A., "Evaluation of the validity of the pore solution expression method from hardened cement pastes and mortars", Cement and Concrete Research, Vol. 24, pp. 456-462, 1994.
/22/ Nagataki, S., Otsuki, N., Wee, T-H., Nakashita, K., "Condensation of chloride ion in hardened cement matrix materials and on embedded steel", ACI Materials Journal, V. 90, No. 4, July-August 1993.
/23/ Larsson, J., "The enrichment of chlorides in expressed concrete pore solution submerged in saline solution", Proceedings Nordic Seminar on Field Studies of Chloride Initiated Reinforcement Corrosion in Concrete, Lund, Sweden, February 2-3, 1995.
/24/ Larsen, C.K., "The composition of the pore water as a function of the surrounding solution", Proceedings Nordic Seminar on Field Studies of Chloride Initiated Reinforcement Corrosion in Concrete, Lund, Sweden, February 2-3, 1995.

THE ENRICHMENT OF CHLORIDES IN EXPRESSED CONCRETE PORE SOLUTION SUBMERGED IN SALINE SOLUTION.

By Johan Larsson, Avd byggnadsmaterial, LTH box 118, S-221 00 Lund
Euroc Research AB, box 104 S-620 30 Slite

1. INTRODUCTION

This paper present some results from a larger project, aiming at systematic studies and better understanding of the pore solution chemistry in concrete. Some results on chloride binding of various binders submerged in various chloride solution was present in /1/. In order to verify some field observation of chloride enrichment in submerged pore solution, the reported study was carried out on cement past long term exposed under controlled laboratory condition.

The amount of chlorides in extracted cement paste pore fluid and surrounding curing solution were compared. The curing solution used was a pore fluid synthetically prepared with varying chloride and hydroxide content.

Thin discs of hardened cement pastes have been cured in a synthetic pore solution. After 22 to 31 months of storage time, the amount of chloride present in the synthetic pore solution and the pore solution extracted from the sections was determined.

The effect of w/c ratio, temperature, OH^- concentration, and silica fume on the difference between the chloride concentrations was investigated.

Results indicated chloride concentration 5 to 36% higher in the extracted pore solution as compared to the curing solution. The chloride levels in the extracted pore fluid were higher at low temperatures and low chloride levels in the curing solution. A lower w/c ratio also resulted in higher chloride levels in the extracted pore fluid.

2 CHLORIDE CONCENTRATION IN EXPRESSED CONCRETE PORE SOLUTION

In concrete samples submerged in sea water, chloride concentrations in the pore fluid have shown higher levels as compared with the surrounding sea water when the chloride profiles have levelled out. In Fig. 1, the pore solution chloride profile, as measured by pore solution expression method /2/, is shown for Portland cement concrete w/c 0.50. The concrete was submerged for 20 years at the Laksevåg marine field station, Det Norske Veritas, Bergen /3/.

Concrete samples w/b 0.50 submerged for 1 year at the Träslövsläge marine field station, Sweden /4/ show higher chloride levels in the surface layer than the surrounding sea water. See Fig. 1.

Similar findings have occasionally been reported elsewhere /5/. Any process resulting in an enrichment of chloride ions in the concrete pore solution will probably affect the long term chloride

transport rates in concrete. Furthermore, long term enrichment of chloride ions in concrete pore solution may lead to an accumulation of chloride ions at the reinforcement.

This paper will deal with work done with verifying this phenomena and the indications from some variables as to how they affect the higher chloride concentrations.

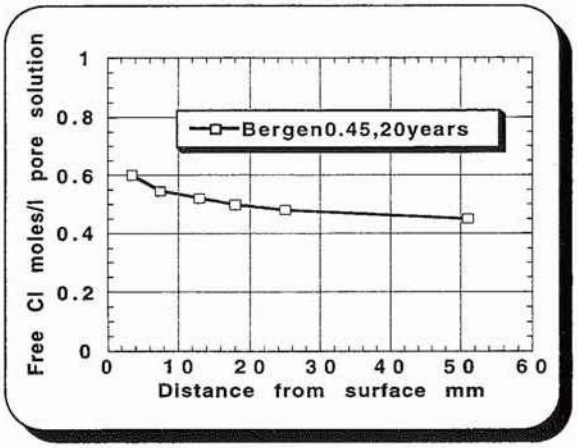

Fig. 1. Pore solution chloride profile, measured by pore solution expression method, in Portland cement concrete w/c 0.50. The concrete was submerged for 20 years at the Laksevåg marine field station, Det Norske Veritas, Bergen /3/.

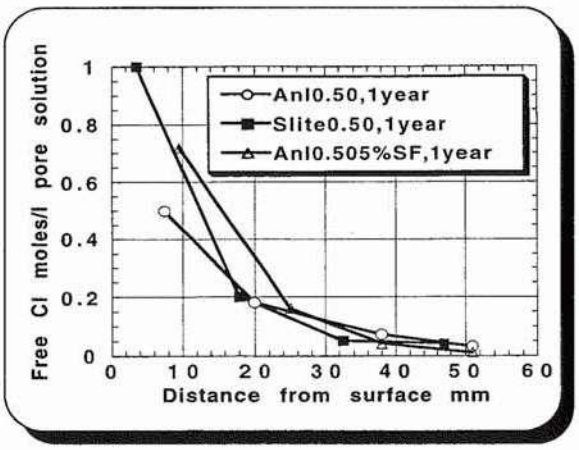

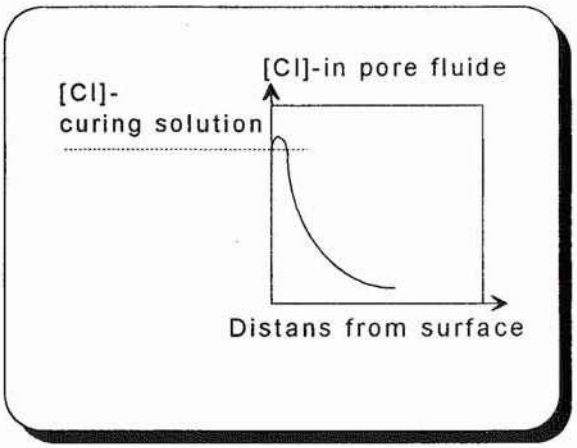

Fig.2. Left: Pore solution chloride solution, measured by pore solution expression method, in various Portland cement concrete w/b 0.50, submerged for 1 year at the Träslövsläge marine field station, Sweden /4/. Right: Principal illustration.

3 METHODOLOGY

Samples of cement paste were made from low alkali sulphate resistant Portland cement. The w/c ratio in the pastes ranged from 0.4 to 0.75. In one paste, 5% silica fume was added. The pastes were membrane cured for 28 days and 3 mm thick discs were prepared. Cement past discs were

placed in synthetic pore fluids with varying OH- and Cl- concentrations at 5° and 20°C for more than 22 months and the pore fluid was extracted.

The pore fluids and the curing solutions were analysed using a potetiometric titration technique with silver nitrate.

4 RESULTS

All extracted pore fluids showed chloride concentrations higher than the surrounding curing solution.

The results indicated chloride concentration 5 to 36% higher in the extracted pore fluid as compared to the curing solution. The chloride levels in the extracted pore fluid were higher at low temperatures and low chloride levels in the curing solution. A lower w/c ratio also resulted in higher chloride levels in the extracted pore fluid.

The results are shown in Table 1.

Table 1. Chloride and hydroxide concentrations in expressed pore solution and in external chloride solution.

Curing solution(1)	**w/c**	**SF** [%]	**T** [°C]	**Cl** curing [mM]	**Cl** pore [mM]	**relative difference** [%]	**Delta** [mM]	**OH** curing [mM]	**OH** pore [mM]
1:1	.40	5	20	96	115	20	19	133	148
1:2	.40	5	20	230	258	12	28	137	133
1:1	.40	0	20	104	115	11	11	139	138
1:2	.40	0	20	229	269	18	40	149	138
1:1	.60	0	20	90	97	8	7	132	138
1:2	.60	0	20	232	248	7	16	136	140
1:1	.75	0	20	96	107	12	11	126	142
1:2	.75	0	20	232	245	6	13	134	150
2:1	.40	0	5	55	75	36	20	329	329
2:2	.40	0	5	101	120	19	19	336	346

(1) 1:1 Original [OH] 1- 150 mM and 2- 300 mM

1:1 Original [Cl] 1- 150 mM and 2- 300 mM

Discussion

The results can only serve as an indication as to what might affect the chloride concentration since the number of samples used in this work are too few. However, the results support earlier indications on the chloride enrichment in concrete pore solution as shown i Figs. 1-2.

One of several mechanisms possible to explain chloride enrichment is reverse osmosis. Assume that the two solutions are in chemical equilibrium and that this equilibrium is affected by a different pressure in the small cement paste pores as compered to the pressure in the external chloride solution, See Fig. 3.

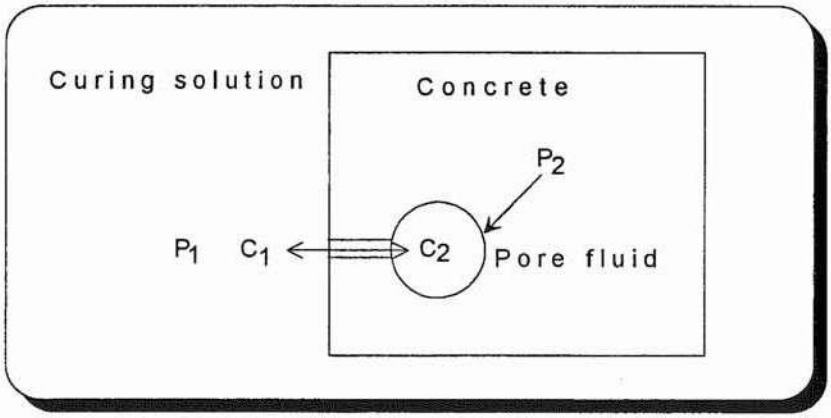

Fig.3. A model for the effect of reverse osmosis on the pore fluid composition at equilibrium $[Cl\text{-}]sl \leftrightarrow [Cl^-]_p$

The pressure on a fluid (p_2) in small spherical pore with a radius r is:

(1) $p_2 = p_1 + \frac{2\gamma}{r}$ where γ is the surface tension and p_1 is the surrounding pressure.

The effect of pressure on the concentration in the pore is:

(2) $c = \frac{\pi}{RT}$ were $\pi = p_2 - p_1$

Which gives the following equation:

(3) $c = \frac{2\gamma}{rRT}$

The equation shows that it is the temperature and pore radius that have an effect on the chloride concentration in the pore fluid

This is a very simplified equation and it does not take into consideration non ideal solutions and other equilibria.

To use the equation to calculate the concentration difference we also need:

* Pore size distribution for the fluid filled pores.

* Surface tension of the fluid in the cement paste.

Several other mechanisms may of course contribute to the observed phenomena of chloride enrichment. An excellent discussion on various mechanisms has been present by Lars Rombén /6/, including several references on the nature of ion transport in cement based materials. Very recently, Chatterji /7/ presented information and a model regarding the nature of ion transport in cement based materials.

6. REFERENCES

/1/ Sandberg, P., Larsson, J., "Chloride binding in cement pastes in equilibrium with synthetic pore solutions", Proceedings Nordic Seminar on Chloride Initiated Reinforcement Corrosion in Concrete, Gothenburg, Sweden, January 13-14, 1993.

/2/ Arya, C., Newman, J:B., "An assessment of four methods of determining the free chloride content of concrete", Materials and Structures, 23, pp. 319-330,1990.

/3/ Pettersson, K., Sandberg, P., Unpublished results on expressed pore solution concentration profile in submerge sea water concrete exposed at the Laksevåg marine field station, Det Norske Veritas, Bergen for 20 years. Swedish Cement and Concrete Institute, Stockholm Dec. 1994.

/4/ Larsson, J., Sandberg, P., Unpublished results on expressed pore solution chloride concentration profile in submerged sea water concrete exposed at Träslövsläge field station for 1 year. Euroc research, Slite, April 1993.

/5/ Sarukawa, Y., Sakai, K., Kubouchi, A.," Japan's 100-Year-Long Otaru Port Breakwater Durability Test", Concrete International, May 1994.

/6/ Rombén, L., "Chloride enrichment in submerged sea water concrete" (In Swedish), Stockholm, Dec, 1994.

/7/ Chatterji, S., "Transportation of ions through cement based materials. Part 3 - Experimental evidence for the basic equations and some important deductions.", Cement and Concrete Research, Vol. 24, No. 7, pp. 1229-1236, 1994.

THE COMPOSITION OF THE PORE WATER AS A FUNCTION OF THE SURROUNDING SOLUTION

Claus K. Larsen, Statens vegvesen, Veglaboratoriet, PB 8142 DEP., N-0033 OSLO, Norway

ABSTRACT

The composition of the pore water of thin slices of mortar, have been compared with the composition of the surrounding salt solution. After curing for three months the mortar (w/c 0.60) slices were submerged in six different salt solutions, made of distilled water and synthetic pore solution. Three months later the pore water was expressed. Analyses of OH^- and Cl^- concentration were taken, both from the salt solution and the pore water. For five of the six solutions, the Cl^- concentration of the pore water was almost identical with the Cl^- concentration of the surrounding solution. The OH^- concentration of the pore water agreed very well with the OH^- concentration of the synthetic pore solution.

Keywords: Mortar, pore water composition, chlorides, hydroxides, equilibrium.

1 INTRODUCTION

It is well agreed, that chloride-induced rebar corrosion is the major concrete durability problem all over the world. The onset of this type of rebar corrosion, is caused by an increased concentration of chlorides, in the pore water solution, above a critical level. Many researchers work hard to establish threshold chloride contents for initiation of chloride-induced corrosion. The threshold values are generally expressed as total amount of chlorides per unit weight of cement.

One obvious difficulty in generalizing the threshold chloride content, based on total content, for initiation of chloride-induced corrosion, is the fact that concrete has a chloride binding capacity. As we know, the chlorides can be bound, both chemically and physically, to the hydrated products in concrete. There is always an equilibrium between the bound and the unbound chlorides, generally known as free chlorides, in the pores that are totally or partly filled with water. The pore water solution is itself in some kind of equilibrium with the surrounding solution. To control the composition of the pore water solution of concrete in an experiment, one usually assumes that the composition of the pore water solution is the same as the surrounding solution. This paper reports experimental work done as an attempt to check this assumption.

2 EXPERIMENTAL

2.1 Materials

The cement used, is a high-strength low-alkali Portland cement, known in Norway as NORCEM HS65. The chemical composition of the cement is shown in Table 1. Sand, basically of granite, diorite and syenite, with fraction 0-4 mm was used as aggregate and chloride-free tab water was used as mix water for both mixes. Chemically purified NaCl was used as chloride source for the mortar made with chlorides in the mix water. Purified laboratory chemicals and distilled water were used in preparation of the salt solutions.

Table 1 Composition (in %) and Blaine finesse (in m^2/kg) of NORCEM HS65

SiO_2	Al_2O_3	Fe_2O_3	CaO	MgO	K_2O	Na_2O Eq	C_2S	C_3S	C_3A	C_4AF	Blaine
22,0	4,1	3,4	64,0	1,4	0,46	0,52	24	52	5,1	10,4	400

2.2 Sample preparation

Both mortars were made with a constant sand : water : cement ratio of 3.17 : 0.60 : 1. One mortar was made with 0.40% chloride by the weight of cement added to the mix water. This mortar is in this paper called E604. The second mortar was made chloride-free, and is coded as E600.

After moulded in steel cylinders, Ø100x200 mm, the mortars were cured for 24 hours at 21°C, then demoulded and sealed in airtight plastic and cured in a fog-room with RH 90-95% and 22-26°C for about three months. The mortar cylinders were then, with as little drying as possible, wet-cut in three mm thin slices. Immediately after cutting, all the samples, consisting of three slices, were submerged in the different salt solutions.

The salt solutions consisted of four synthetic pore water solutions and two distilled water solutions. Table 2 gives the composition of the solutions. After three months all the samples were removed from the solutions, the excess solution wiped off from the surface and without drying sealed in airtight plastic until testing the next day.

Table 2 Composition of the initial salt solutions, in g/l

Solution #	KOH	NaOH	K_2SO_4	$CaCl_2.2H_2O$	NaCl	Cl^-
S1	7,02	11,23	0,58	0,28	0,32	0,33
S2	7,02	11,23	0,58	0,28	2,43	1,61
S3	7,02	11,23	0,58	0,28	15,11	9,30
S4	7,02	11,23	0,58	0,28	30,44	18,60
S5	-	-	-	-	2,64	1,60
S6	-	-	-	-	30,66	18,60

2.3 Test methods

Pore water solution expression
One day after the samples had been removed from the solutions, the pore water solution was expressed using a high-pressure method. A maximum pressure of 300 MPa was applied for 10 minutes for all samples. The pore water solution was collected in a plastic syringe and transferred to a small plastic container, hardly without contact with the air. The container was then immediately sealed with a cap.

Capillary porosity
One slice of each mortar was used to determine the capillary porosity. The procedure is well

known, and includes the volume (V) and the weight of the water-saturated (W_2) the oven-dried (W_1) sample. The capillary porosity (ε_c) is calculated by: $\varepsilon_c = (W_2 - W_1) / V$

Chemical analysis
All chloride concentrations were determined by potentiometric titration using 0,01 N $AgNO_3$ and a chloride-selective electrode. Measurements of the pH, with an accuracy of one hundredth, were done, using a two-electrode setup on the same unit used for potentiometric titration. The concentration of OH^--ions were calculated on the basis of the measured pH. All reported concentrations are an average of two independent analyses.

3 RESULTS AND DISCUSSION

Typical values of capillary porosity, saturated-surface-dry density and the amount of expressed pore water solution as total volume (from each sample) and as percentage of evaporable water, are listed in Table 3.

Table 3 Capillary porosity, density (ssd) and volume of expressed pore water solution

	Cap. porosity %	Density (ssd) kg/dm³	Expr. volume total	Expr. volume % of evap.water
E600	20,79	2,33	1,1-1,4 ml	7-14
E604	21,25	2,29	1,8-2,7 ml	9-17

3.1 Comparison between the [Cl⁻] in the pore water solution and in the salt solution

The chloride concentration of the expressed pore water solution as a function of the chloride concentration in the surrounding solution, for both synthetic pore water solution and distilled water solution, is shown in Figure 1.

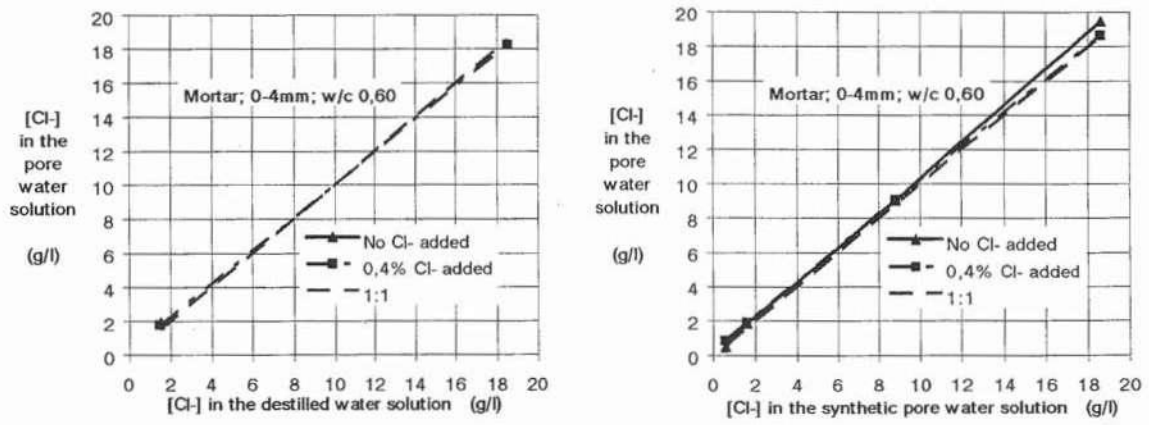

Figure 1 [Cl⁻] of the pore water solution as a function of the surrounding [Cl⁻]

As Figure 1 shows, there is very good agreement between the chloride concentration in the pore water solution and the chloride concentration in the surrounding solution. This yields for both the solutions made of distilled water and of synthetic pore water solution. On the other hand, if the results are to be presented as in Figure 2, as percentages of the chloride concentration in the surrounding solution, the conclusion only yields for the two or perhaps three highest concentrations, S2-S4. The same pattern, though only with two solutions, can be seen for the distilled water solutions, S5-S6. This is shown in Figure 3.

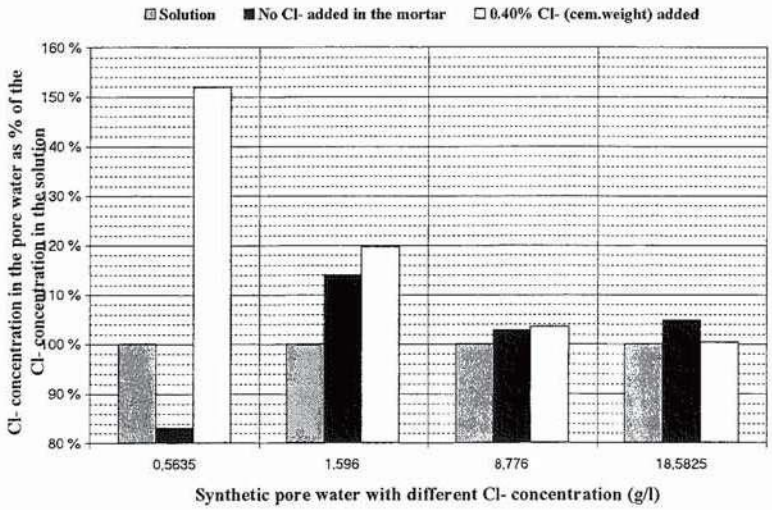

Figure 2 [Cl^-] of the pore water solution as % of the [Cl^-] of the synthetic pore water solution

The initial chloride concentration of the pore water solution of the two mortars, i.e. before they were submerged in the solutions, is shown in Table 4. One possible explanation of the disagreement concerning solution S1, is that the low chloride concentration perhaps yields longer time-to-equilibrium than the higher concentrations. The actual chloride concentration of the pore water solution in the E604 mortar, is *1,5 times higher than the surrounding S1-solution*, and *half the initial* chloride concentration.

Diffusion is of course the chloride transporting process, and the driving force of the diffusion process in the S1-solution are much smaller than the driving force in, at least, solution S3 and S4.

Table 4 The initial [Cl^-] of the pore water solution of the two mortars

E600	E604
< 0,05 g/l	1,60 g/l

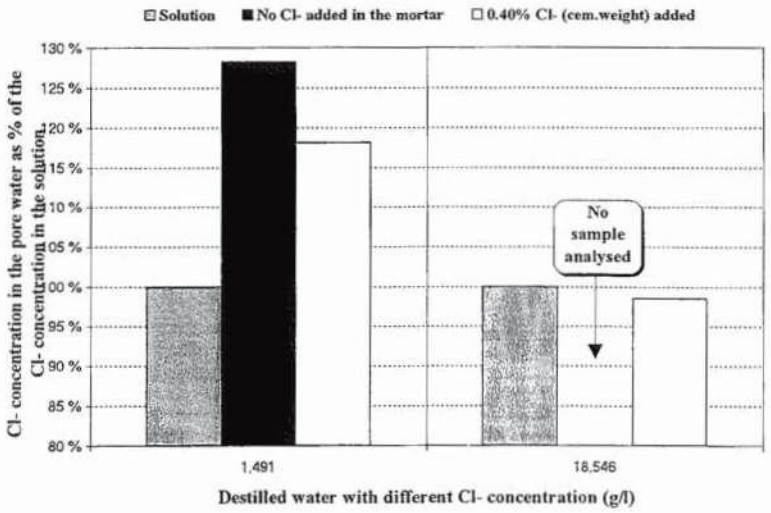

Figure 3 [Cl^-] of the pore water solution as % of the [Cl^-] of the distilled water solution

3.2 Comparison between the [OH^-] in the pore water solution and in the salt solution

The OH^- concentration of the expressed pore water solution as a percentage of the OH^- concentration in the surrounding solution, for synthetic pore water solution and distilled water solution, is shown in Figure 4 and 5. As Figure 4 shows, there is very good agreement between the OH^- concentration in the pore water solution and the OH^- concentration in the surrounding synthetic pore water solution, except E604 in solution S1. This sample has an OH^- concentration of 61% of the OH^- concentration of solution S1.

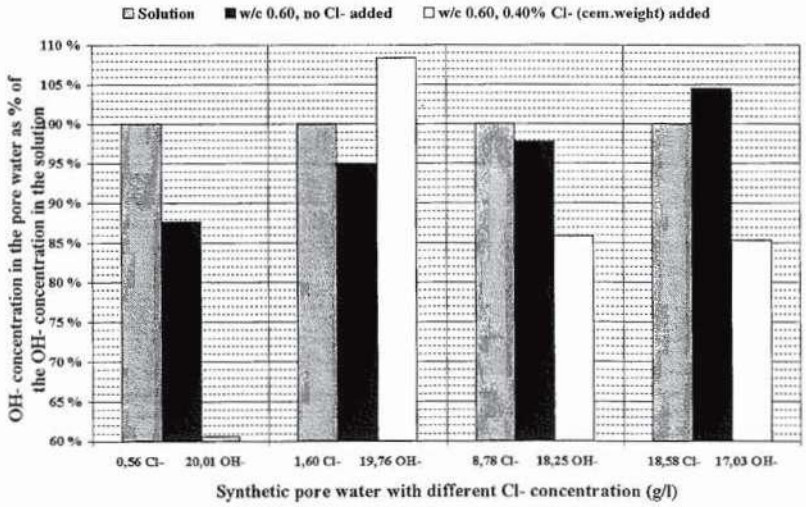

Figure 4 [OH^-] of the pore water solution as % of the [OH^-] of the synthetic pore water solution

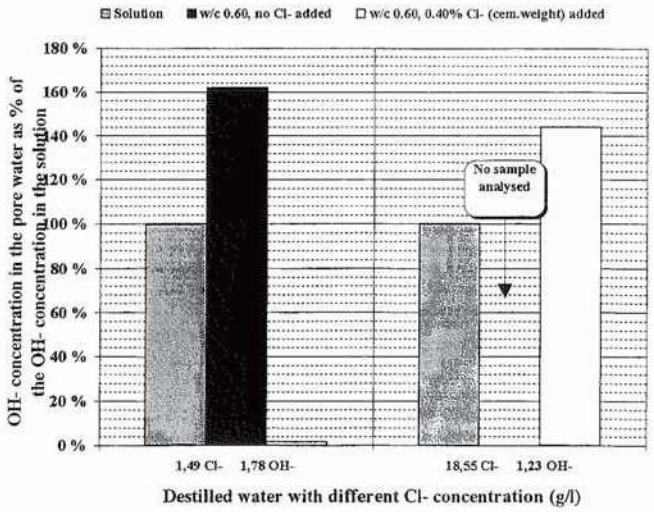

Figure 5 [OH^-] of the pore water solution as % of the [OH^-] of the distilled water solution

As one perhaps should assume, bearing in mind the huge initial difference between the OH^- concentration of the distilled water solutions and the initial pore water solution of the two mortars, the comparison is more difficult for the two distilled water solutions. E604 has an OH^- concentration of only 1% of the OH^- concentration of solution S5 and 145% of solution S6. For the single sample of mix E600, the OH^- concentration is 162% of the OH^- concentration of solution S6.

A calculation of the OH^- concentration based on pH measurements has less accuracy than for example titration. A misreading of pH by two hundredths, will, for all the samples from solution S1-S4, set up an error in the OH^- concentration by about 1 g/l or 5%. Measurement of pH in solutions with low ionic concentration is difficult, and can introduce large errors in the calculation of OH^- concentration.

4 CONCLUSIONS

1. The composition, based on chloride and hydroxide ions, of the pore water solution in two different mortars, is almost identical to the composition of the surrounding synthetic pore water solution.
2. The composition, based on chloride ions, of the pore water solution in two different mortars, is almost identical to the composition of the surrounding distilled water solution.
3. The time-to-equilibrium within the pore water solution, is affected by the concentration of chlorides in the surrounding solution.

5 ACKNOWLEDGEMENT

The present report is part of the "OFU Bridge Repair Project", financed by the Norwegian Public Roads Administration (NPRA), Rescon AS and the Norwegian Industrial and Regional Development Fund (SND). The project is managed by NPRA.

THEME 3

Moisture mechanics and numerical models

UNCERTAINTY OF RH MEASUREMENT RESULTS

Göran Hedenblad
Division of Building Materials
Lund Institute of Technology
Box 118, S-221 00 Lund, Sweden

Introduction

In the measurement of the relative humidity (RH) in a material it is important that every measurement include a correct statement of its uncertainty. If the errors in the calibration process and the measurement process are not known, the total error in the relative humidity can be 5 to 10 % RH. A large error like this is not acceptable in many applications, where one has to know the RH.

In 1994 the United States Department of Commerce, and under them the National Institute of Standards and Technology (NIST) published "Guidelines for Evaluating and Expressing the Uncertainty of NIST Measurements Results /1/. The approach used in /1/ to express the uncertainty of a measurement is also adopted by the International Organisation for Standardization (ISO).

Definitions of the statistical terms used

The following is directly from /1/.

"In general, the result of a measurement is only an approximation or estimate of the value of the specific subject to measurement, that is, the **measurand**, and thus the result is complete only when accompanied by a quantitative statement of its uncertainty."

"The uncertainty of the result of a measurement generally consists of several components which may be grouped into two categories according to the method used to estimate their numerical values:
component Type A: those which are evaluated by statistical methods,
component Type B: those which are evaluated by other means."

"Type A evaluations of uncertainty based on limited data are not necessarily more reliable than soundly based Type B evaluations."

"There is not always a simple correspondence between the classification of

uncertainty components into categories A and B and the commonly used classification of uncertainty components as "random" and "systematic"."

"Random uncertainty: A component of uncertainty arising from a random effect."

"*Systematic uncertainty:* A component of uncertainty arising from a systematic effect."

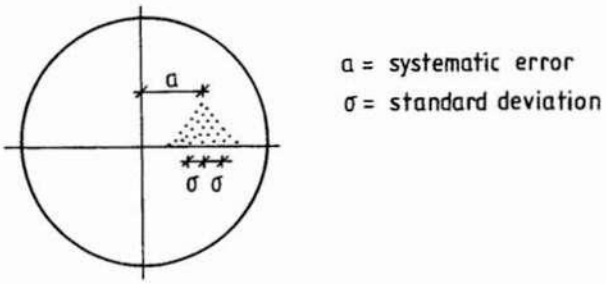

FIG. 1 Hits on a target as a description of systematic and random errors.

"Standard Uncertainty: Represent each component of uncertainty that contributes to the uncertainty of the measurement result by an estimated standard deviation, u_i , termed **standard uncertainty**, equal to the positive square root of the estimated variance u_i^2. "

"Combined Standard Uncertainty: Determine the combined standard uncertainty, u_c , of the measurement result, taken to represent the estimated standard deviation of the result, by combining the individual standard uncertainties u_i (and covariances as appropiate) using the usual "root-sum-of-squares" method, or equivalent established and documented methods."

"It is assumed that a correction (or correction factor) is applied to compensate for each recognized systematic effect that significantly influences the measurement result and that every effort has been made to identify such effects. The relevant uncertainty to associate with each recognized systematic effect is then the standard uncertainty of the applied correction. The correction may be either positive, negative, or zero, and its standard uncertainty may in some cases be obtained from a Type A evaluation while in other cases by a Type B evaluation."

"The uncertainty of a correction applied to a measurement result to

compensate for systematic effect is not the systematic error in the measurement result due to the effect. Rather, it is a measure of the uncertainty of the result due to incomplete knowledge of the required value of the correction."

"Although the combined standard uncertainty, u_c , is used to express the uncertainty of many NIST measurement results, for some commercial, industrial, and regulatory applications of NIST results (e.g. when health and safety are concerned), what is often required is a measure of uncertainty that defines an interval about the measurement result, y, within which the value of the measurand Y is confidently believed to lie. The measure of uncertainty intended to meet this requirement is termed **expanded uncertainty**, suggested symbol U, and is obtained by multiplying u_c by a coverage factor, suggested symbol k."

"Expanded Uncertainty: Determine an **expanded uncertainty** U by $U = k \cdot u_c$. The purpose of U is to provide an interval y-U to y+U about the result y within which the value of Y, the specific quantity subject to measurement and estimated by y, can be asserted to lie with a high level of confidence." In the measurement and calibration of RH the used value of k is 2, see /2/.

Different errors

Lafarie has in /3/ classified the errors that can arise in a measurement of the relative humidity.

Systematic errors:

a) Systematic error of the saturated salt solution, which is used for the calibration of the RH-sensor.
b) Nonlinearity of the RH-instrument.
c) The measurement temperature is different from the calibration temperature.
d) Drift of the RH-instrument, e.g. the reading for a given RH, changes with time.
e) A temperature difference between the RH-sensor and the measured material.
f) The RH measurement is made at a temperature different from the temperature when using the material.

Random errors:

g) Sensor hysteresis, that is different calibration curves at the adsorption and desorption of the RH-sensor.
h) Errors at the calibration of the RH-sensor.
i) Influence of temperature instability during the measurement.

Below follows a short survey of the above mentioned errors.

a) Systematic errors of the salt: The uncertainty figures given in Appendix 1 are the systematic errors of the saturated salt solutions under ideal conditions. The uncertainty figures could be interpreted to mean that the correct RH for a given salt is not known, but lies between the given value ± the systematic error. At the present time, when determining the critical RH for different building materials, this error has not been taken in account. But when using RH measurement in determining the deterioration processes, this error should probably be taken in account.

b) Nonlinearity of the RH-instrument: It is customary that RH-instruments are not linear over the whole range from 0 to 100 % RH. The error differs from instrument to instrument. One example of the nonlinearity of an instrument is shown in FIG. 2.

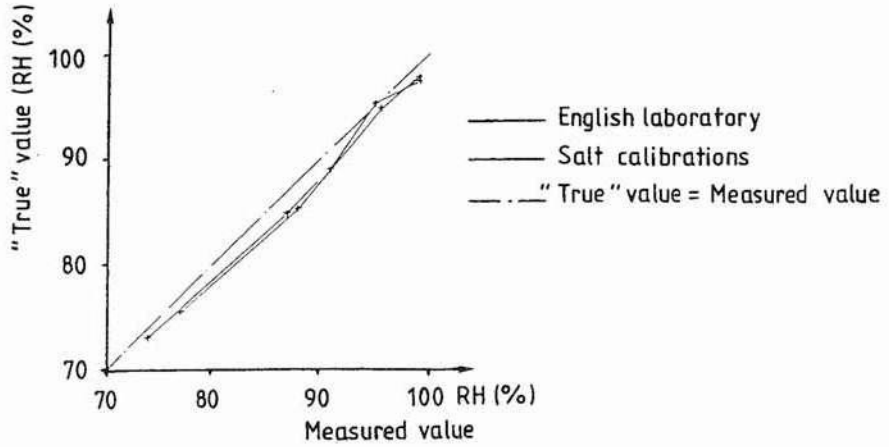

FIG. 2 An example of nonlinearity of an RH-instrument.

The most interesting RH range, when measuring in concrete, is between about 75 to 100 % RH. One way to reduce the linearity error or to totally eliminate it is to make calibrations at several RH-levels within the the actual RH range and after that make a calibration curve, see FIG. 2. In FIG. 2 it is seen that there is a difference between measured and "true" RH.

c) The measurement temperature is different from the calibration temperature: The temperature level at the calibration and measurement affects nearly all

types of RH-instruments. If the instrument does not have a built-in temperature compensator the error can be big (15 - 20 % RH) if the temperature during the measuring differs much from the calibration temperature, see /3/. If the instrument has a temperature compensator, the error is much less, but maybe not always negligible. Lafaire /3/ shows measurements made at NIST in the USA, which show that the error for the tested capacitance RH-instruments was only some percent RH at +40 °C, when the instruments were calibrated at +20 °C.

d) Drift of the RH-instrument: The term "drift" means that the reading of the instrument changes with time (for a given RH). The drift of an instrument changes from time to time. In FIG. 3 two calibrations are shown for the same capacitive RH-instrument. It is about 20 days between the two calibrations. As is seen in FIG. 3 the whole calibration curve is moved in parallel between the two times of calibration.

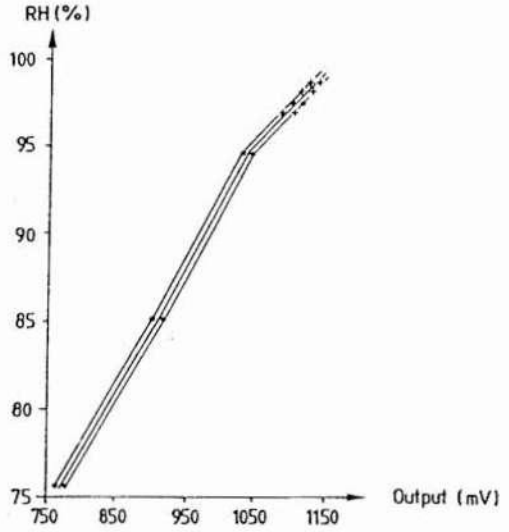

FIG. 3 Calibration curves for a capacitive RH-instrument made with an interval of about 20 days. Hedenblad /4/.

Even the dew point meters that the Division of Building Materials, LTH, uses sometimes have some drift. To assure that there is no drift of the RH-instrument, or that the drift is small, the reading of the instrument should be controlled often and regularly with a saturated salt solution. The solution should have an RH which is in the same range as the estimated RH in the measurement.

e) Temperature difference between the RH-sensor and the measured material: At the measurement of RH one **should** avoid temperature difference between the material and the RH-sensor. In Table I, the systematic error in the RH measurement due to a temperature difference between the material and the

RH-sensor is shown. The RH of the material is 90 % and the temperature is +20 °C .

Table I Error in measured RH due to a difference in temperature between the RH-sensor and the measured material.

Difference in temperature (°C)	Error in RH (% RH)
0.1	0.5
0.2	1.0
0.4	2.0
1.0	5.0

If the temperature of the RH-sensor is higher than the temperature of the measured material, the measured RH is lower than the real RH. The difference in temperature can be caused by the sun which shines or has shone on the material or the RH-instrument. The temperature difference can also be caused by air movements, at the instruments, which have a different temperature than the material. To reduce this kind of error one can place an insulated "box" around the RH-instrument. When measuring through a heat insulation, big errors can also arise if one part of the instrument is at one temperature and another part of the instrument is at another temperature.

f) The RH-measurement is made at a temperature different from the temperature when using the material: Nilsson has shown in /5/ how the temperature level influences RH in concrete at constant moisture content in the material. FIG. 5 is from /5/.

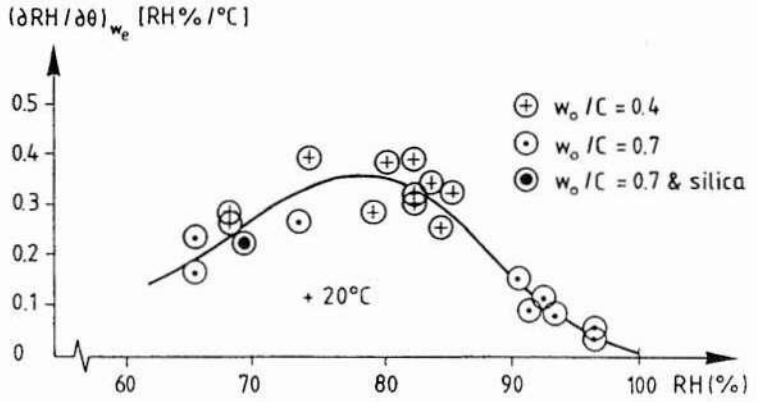

FIG. 5 The measured change in RH due to a change in the temperature of 1 °C as a function of RH at +20 °C. Constant moisture content in the concrete. Nilsson /5/.

If the measurement is made at a temperature which differs markedly from the temperature when using the concrete, there could be errors of several % RH.

Example: If RH in the concrete is measured to be 90 % at +5 °C, the RH is about 92 % when the temperature of the concrete is raised to +20 °C. ((90 + 0.15·15) = 92 % RH). 0.15 is read from FIG. 5 at 90 % RH and 15 is the difference in the temperatures.

If a specimen is taken from a concrete structure and then placed in an impermeable test tube which is transported to a laboratory for determining RH, one gets the RH at the temperature level of the laboratory. This temperature level can be different from the temperature level in situ.

g) Sensor hysteresis: A test which was done at our laboratory of the hysteresis of two capacitive RH-sensors shows that the maximum difference in RH was about 1 % between absorption and desorption. This error is relatively simple to avoid, if the calibrations and measurements are always made from the lowest RH gradually up to the highest RH. The sensor is then, the whole time, on its absorption isotherm. Dew point meters probably have no hysteresis.

h) Errors at the calibration of the RH sensor: According to the American standard ASTM E 104-85, lack of temperature equilibrium (±0.5 °C) during the calibration can increase the systematic error to ±2.5 % RH. According to the same standard the precision of the saturated salt solution is ±0.5 % RH, when the temperature instability of the salt solution is ±0.1 °C. In the standard it is not said if the error is 1, 2 or 3 times the standard deviation, but probably it is 1 standard deviation.

The Division of Building Materials, LTH, has calibrated RH-instruments with a temperature instability of ±0.05 °C, and the measured random error in RH was about ±0.2 % RH (1 standard deviation), see /4/.

According to the committee which worked out the above-mentioned ASTM standard, it was usual that laboratories had a temperature instability which was not better than ±0.5 °C, see /3/. With this temperature instability the uncertainty of RH over the saturated salt solution is not better than ±2.5 % RH.

From the above it is seen that it is extremely important, when calibrating RH-instruments with saturated salt solutions, that this is done at a temperature which is as constant as ever possible.

i) Influence of temperature instability during the measurment: Concrete has a large heat capacity, and the material changes its temperature and moisture content slowly. It is then probable that the results shown in FIG. 5 can be used to take account for temperature changes during the measurement. In /4/ results of measurements of the temperature and RH are shown and the change of RH in the concrete was about ±0.1 % (3 times the standard deviation) when the temperature in the concrete changed ±0.2 °C (3 times the standard deviation).

The expanded uncertainty of an RH-measurement

The systematic errors should be avoided as much as possible, but if it is impossible to do so a correction, if it is known, can be applied to compensate for this error. The uncertainty of a correction is a measure of the uncertainty of the required value of the correction.

The combined standard uncertainty (u_c) represents the estimated standard deviation of the result, by combining the individual standard uncertainties (u_i) with the "root-sum-of-squares" method.

$$u_c = \sqrt{u_{ia}^2 + u_{ib}^2 + + + u_{ii}^2} \qquad (1)$$

The following is directly from /1/.

"For unknown distributions of the uncertainties (type B), the rectangular distribution is a reasonable default model in the absence of any other information. But if it is known that values of the quantity in question near the center of the limits are more likely than values close to the limits, a triangular or a normal distribution may be a better model."

"Rectangular model: Estimate the upper and lower limits a_+ and a_- for the value of the quantity in question such that the probability that the value lies in the interval a_+ to a_- is, for all practical purposes, 100 %. The best estimate of the value of the quantity is then $u_j = a/\sqrt{3}$ where $a = (a_+ + a_-)/2$."

"Triangular model: If the distribution model used to model the quantity is triangular rather than rectangular , then $u_j = a/\sqrt{6}$."

The magnitude of the different standard uncertainties can in some cases be calculated as:

a) Systematic error of the saturated salt solution: At an RH of 94.6 % the uncertainty figure in Appendix 1 is ± 0.7 %. If it is assumed that this is the upper and lower limits of the RH and it is also assumed that the values lie closer to the center than to the limits, the triangular model can be used.
$u_{ja} = 0.7/\sqrt{6} = 0.3$ % RH

b) Nonlinearity of the RH-instrument: Assume that the instrument is calibrated at so many RH-levels that the instrument is linear between the calibration points.
$u_{jb} = 0$
c) The measurement temperature is different from the calibration temperature: Assume that the temperatures are the same.
$u_{jc} = 0$
d) Drift of the RH-instrument: Assume that there is no drift.
$u_{jd} = 0$
e) Temperature difference between the Rh-sensor and the measured material: Assume there is no temperature difference.
$u_{je} = 0$
f) The measurement is made at a temperature different from the temperature when using the materal: Assume that the temperatures are the same.
$u_{jf} = 0$
g) Sensor hysteresis: Assume hysteresis is rectangular distributed with $a = 0.5$
$u_{jg} = 0.5/\sqrt{3} = 0.3$ % RH
h) Errors at the calibration of the RH sensor: Assume in case 1) that the temperature instability is ±0.05 °C and in case 2) ±0.1 °C.
$u_{jh1} = 0.2$ % and $u_{jh2} = 0.5$ % RH
i) Influence of temperature instability during the measurement: Assume that the temperature change in the concrete during the measurement is ±0.5 °C.
$u_{ji} = 0.2$ % RH

The different uncertainties are combined in different ways;

• The best possible combined standard and expanded uncertainty:
$u_{ja} = 0.3\%$, $u_{jh1} = 0.2\%$ and $u_{ji} = 0.2\%$ RH
$u_c = (0.3^2 + 0.2^2 + 0.2^2)^{1/2} = 0.4\%$ RH

$U = 2 \cdot 0.4 = 0.8$ % RH

• A more probable standard and expanded uncertainty:
$u_{ja} = 0.3\%$, $u_{jh2} = 0.5\%$ and $u_{ji} = 0.2\%$ RH
$u_c = (0.3^2 + 0.5^2 + 0.2^2)^{1/2} = 0.6$ % RH

$U = 2 \cdot 0.6 = 1.2$ % RH

• A more probable standard and expanded uncertainty complemented with hysteresis:

$u_{ja} = 0.3\%$, $u_{jg} = 0.3$, $u_{jh2} = 0.5\%$, and $u_{ji} = 0.2\%$ RH

$u_c = (0.3^2 + 0.3^2 + 0.5^2 + 0.2^2)^{½} = 0.7$ % RH

$U = 2 \cdot 0.7 = 1.4$ % RH

The above calculations are examples of the uncertainties which can normally arise in the measurement process. In the individual measurement there can, of course, be variations, e.g. larger hysteresis, larger temperature instability during the calibration and the measurement and so on. Everyone who makes RH measurements has to go through his or her own calibration- and measurement process, and make an analysis of "his" errors and uncertainties.

If the measurements are repeated a number of times (n) then the expanded uncertainty is written as $2 \cdot u_c / \sqrt{n}$. That is, by making repeated measurements the expanded uncertainty can be reduced, see Table II.

Table II The expanded uncertainty (U) of n number of RH measurements, each with the combined standard uncertainty (u_c).

	expanded uncertainty, U, (% RH)			
n	$u_c = 0.4$	$u_c = 0.6$	$u_c = 0.7$	$u_c = 1.0$
1	0.8	1.2	1.4	2
2	0.6	0.8	1.0	1.4
3	0.5	0.7	0.8	1.2
4	0.4	0.6	0.7	1.0
5	0.4	0.5	0.6	0.9
6		0.5	0.6	0.8
7		0.5	0.5	0.8
8		0.4	0.5	0.7
9			0.5	0.7

References

1 Taylor B. N. & Kuyatt C.E. (1994), "Guidelines for Evaluating and Expressing the Uncertainty of NIST Measurement Results". NIST Technical Note 1297, 1994 Edition, U.S. Government Printing Office, Washington, DC, USA.

2 Huang P. H. & Wheatstone J.R. (1994), "New Expressions of Uncertainties for Humidity Calibrations at the National Institute of Standards and Technology". NISTIR 5455, Process Measurements Division, NIST, Gaithersburg, MD 20899, USA.

3 Lafarie J. P. (1988), "Accuracy of Relative Humidity Instruments". Energy Engineering, Vol. 85, nr 2 pp 42-49.

4 Hedenblad G. (1993), "Moisture Permeability of Mature Concrete, Cement Mortar and Cement Paste". Report TVBM-1014, Division of Building Materials, Lund Institute of Technology, Lund, Sweden.

5 Nilsson L-O. (1987), "Temperature Effects in Relative Humidity Measurements on Concrete - Some Preliminary Studies". Fuktgruppen informerar 1987:1, The Moisture Research Group at Lund Institute of Technology, Lund, Sweden.

Appendix 1

Table over RH of saturated salt solutions at different temperatures.

Salt	RH (%)			
	T=+10 °C	T=+15 °C	T=+20 °C	T=+25 °C
LiCl	11.3 ± 0.4	11.3 ± 0.4	11.3 ± 0.3	11.3 ± 0.3
$MgCl_2$	33.5 ± 0.2	33.3 ± 0.2	33.1 ± 0.2	32.8 ± 0.2
$Mg\ (NO_3)_2$	57.4 ± 0.3	55.9 ± 0.3	54.4 ± 0.2	52.9 ± 0.2
NaCl	75.7 ± 0.2	75.6 ± 0.2	75.5 ± 0.1	75.3 ± 0.1
KCl	86.8 ± 0.4	85.9 ± 0.3	85.1 ± 0.3	84.3 ± 0.3
$BaCl_2$	93 ± 2	92 ± 2	91 ± 2	90 ± 2
KNO_3	96.0 ± 1.4	95.4 ± 1.0	94.6 ± 0.7	93.6 ± 0.6
K_2SO_4	98.2 ± 0.8	97.9 ± 0.6	97.6 ± 0.5	97.3 ± 0.5

The values in the above Table are from ASTM E 104-85.

METHODS OF MEASURING MOISTURE PENETRATION INTO CONCRETE SUBMERGED IN SEA WATER

Lars-Olof Nilsson, Building Materials, Chalmers University of Technology,
S-412 96 GÖTEBORG, Sweden

ABSTRACT

The moisture distributions in submerged concrete structures and specimens exposed at a field station were determined in five ways. The relative humidity was measured on samples taken from the site, with cast-in probes and in holes in situ with probes inserted at the occasion of measurement and with probes continuously placed in tubes in the concrete specimens. The degree of capillary saturation was measured on samples taken from the site. The paper describes the methods used for these measurements and gives some examples of results.

Moisture profiles could be measured in situ with what seems to be reliable results only with the PW-probes continuously placed in plastic tubes.

RH-measurements on samples showed remarkable large variations, far from what is normal in other applications. The degree of capillary saturation could be measured more precise. Fairly small samples are needed to improve the resolution in depth.

Keywords: concrete, submerged, moisture, relative humidity, degree of saturation, measurement.

1. INTRODUCTION

The moisture conditions of a concrete structure have a decisive effect on many parts of deterioration processes and consequently have a significant effect on the service-life of a marine structure. For high performance concrete the ingression of chlorides from the sea water will be governed by the penetration of water into the concrete.

These matters are investigated in a joint Swedish/Danish/Norwegian research project called "Durability of Marine Structures" with participation from research groups and researchers in the three countries. In this project the department of building materials at the Chalmers University of Technology is investigating the penetration of chlorides and moisture into concrete structures and specimens. The methods used, and some of the results, from the field exposure site are shown in this paper. The methods where measurements are done on samples were also used on old existing structures. These results are presented elsewhere.

2. EXPOSURE SITE AND SPECIMENS

Concrete specimens were cast in the Building Technology laboratories of the Swedish Testing and Research Institute (SP) in Borås. Specimens 1.0x0.6x0.1m were cast lying down. The penetration depth is referred to as the distance from the bottom surface in the mould. Some of the specimens were containing tubes or cast-in probes for in situ measurements.

After a curing period the specimens were exposed to sea water at the SP field station in Träslövsläge some 100 km south of Göteborg at the west coast of Sweden. The specimens were exposed in such a way that 0.6 m of them was submerged into the sea water at a pontoon floating in the harbour of Träslövsläge. The 0.4 m above sea level are simulating a kind of a splash zone. However, since the pontoon is floating and positioned inside the harbour, the

upper part is not frequently wetted by sea water. Driving rain, however, may hit the surface now and then. The climate is continuously registered by SP. Today (1995) most of the specimens have been exposed for some three years.

The concrete qualities in the specimens are several, from plain OPC concretes with water-cement ratios 0.4-0.7, with and without air entrainment, to high performance concretes with a sulphate resistant low alkali cement sometimes blended with silica fume and fly ash to water-binder ratios down to 0.25.

A specimen, with cast-in tubes for in situ measurement of RH, attached to the pontoon is shown in Fig 1.

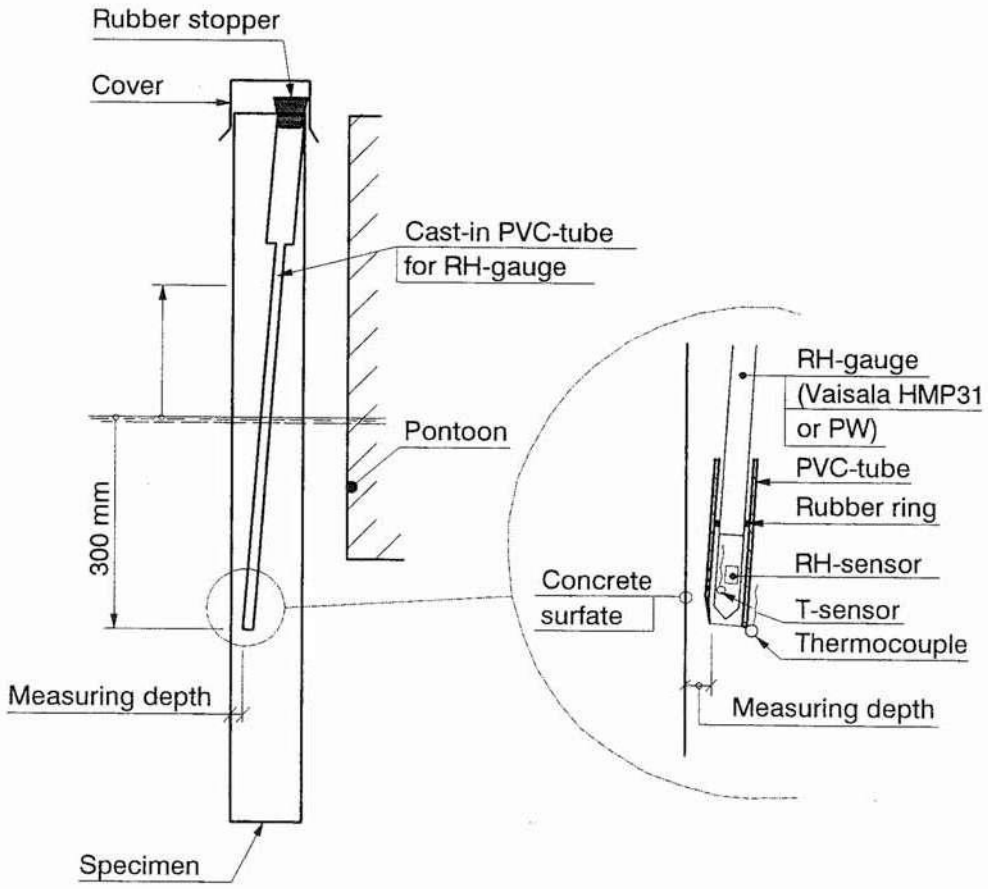

Fig. 1 A concrete slab attached vertically to the pontoon and submerged 0.6 m below the water table. Cast-in tubes for in situ measurement of RH.

3. MEASURING METHODS

Attempts to measure moisture profiles in situ have been done in three different ways. Tubes have been casted in the specimens for later insertion of two kinds of RH-probes; the Vaisala sond and the PW-probe. A new RH-probe, MS102, to be casted in the fresh concrete has also been tested.

At some occasions a vertical slice of the specimens has been cut off. From that slice cores through the 0.1 m thick slice have been drilled out at different levels. From the cores samples have been taken to measure RH and degree of capillary saturation (S_{cap}).

3.1 RH in situ by Vaisala-probes

Vaisala-probes contain a capacitive sensor with a polymeric material as the moisture sensitive element. The changes in RH in the air surrounding the sensor material changes the moisture content of the sensor material. These changes of the moisture content, changes the capacitance of the sensor material, which is measured.

The cast-in plastic tubes for the Vaisala-probe are shown in Fig. 1. The bottom of the tube was sealed against the fresh concrete with a surgical tape that permits moisture to penetrate. A thermocouple was casted in close to the end of the tube to measure the temperature of the concrete. The Vaisala probe includes a temperature sensor. From those two sensors a possible temperature difference between the concrete material and the RH-sensor can be detected.

The top of the plastic tube is sealed with a rubber stopper. The top of the specimen, and the rubber stopper, is covered with a steel plate to protect the tube from sea water and rain.

A measurement is done by removing the rubber stopper, insert a Vaisala RH-probe and wait for equilibrium to be obtained. In the measurements done here some 4-6 hours were used. The reading from the sensor is translated into RH by a calibration curve, individual for each probe.

The results obtained from the measurements by the Vaisala-probes were obviously not correct. The RH:s were very low and had a large, inconsistent variation with depth. The probable explanation is a too short a period to obtain equilibrium between the sensor and the concrete since the concrete surface in "vapour conctact" with the sensor is extremely small and the concrete qualities used are very dense and evaporates moisture to the sensor very slowly.

The results from the Vaisala measurements is not further discussed. A much longer equilibration time is needed.

3.2 RH in situ by PW-probes

PW-probes have a sensor made of a woven synthetic tube containing two wires that act as electrodes. A particular salt solution is impregnated into the woven tube when the sensor is assembled at the start of the measurement. An assembled PW-sensor in a plastic tube with an open bottom is shown in Fig. 2.

Some of the water in the salt solution in the sensor is evaporated and absorbed by the concrete surface at the bottom of the plastic tube. Eventually, usually after a few days, the water content of the sensor is in equilibrium with the RH of this small concrete surface at a defined depth. The conductance between the two electrodes in the sensor is then measured. Since the probe is continuously present in the plastic tube, and close to the concrete surface at the end of the tube, continuous equilibrium between the sensor and the concrete is expected. Consequently the measurement is done within a few minutes.

A reference probe continuously placed above a small container with a saturated salt solution (KCl) giving 85 % RH is also placed in a similar plastic tube in each specimen. The reading

from each sensor is divided by the reading from the reference sensor, which has a temperature very close to the other sensors. The quotient is translated into an RH-value by a calibration curve valid for all PW-sensors. In this way the temperature effects on conductance measurements are heavily reduced.

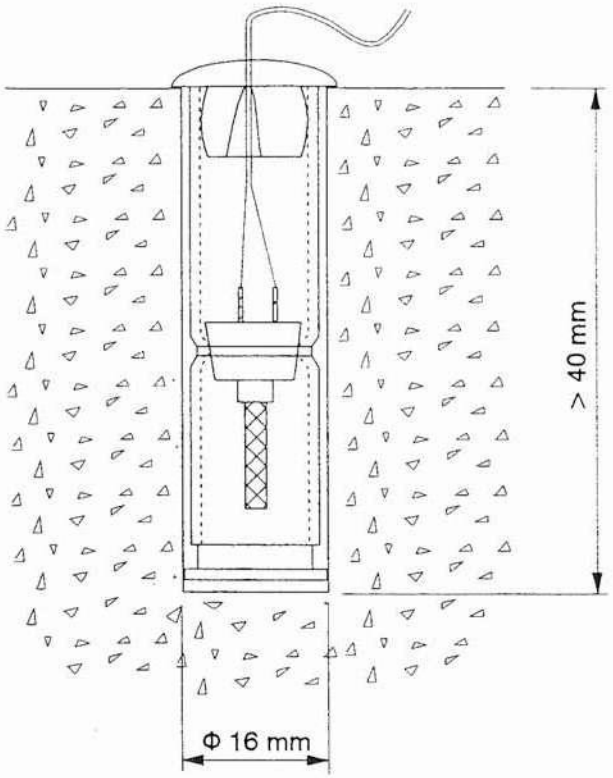

Fig. 2 A PW-sensor inserted into a plastic tube with an open bottom.

The cast-in plastic tubes for the PW-probe are similar to the tubes for the Vaisala-probes, see Fig. 1. The bottom of the tubes ends at four depths from the exposed surface, 20, 30, 40 and 50 mm.

3.3 RH in situ by MS102-probes

A new RH-probe being developed simultaneous to these measurements was tested. The MS102-probe is meant to be cast in fresh concrete, which is a main advantage compared to all the other methods. The probe is shown in Fig. 3.

The sensor in the MS102-probe is a small piece of birch and two electrodes. The sensor is protected by a porous filter. The small piece of wood comes quickly into equilibrium with the moisture in the concrete since the concrete surface in "vapour conctact" with the sensor is fairly large. The resistivity between the electrodes is measured by an ordinary, or sophisticated, wood moisture meter and translated into RH by a calibration curve common for all the sensors.

The first sensors tested, however, did not give reliable results due to a leakage of concrete water into the probes. The results are not further treated here. Later tests in other applications have been successful. The MS102-probes should have a potential for being advantageous also in concrete submerged in sea water since the cast-in procedure is simple.

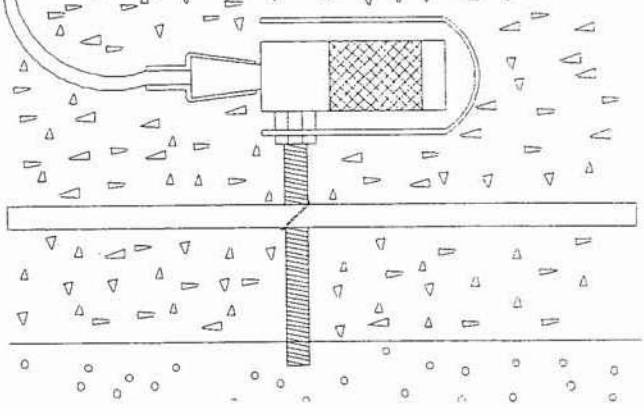

Fig. 3 A MS102-probe casted in concrete at a defined depth ensured by a firm holder.

3.4 RH on samples

Cores taken from the specimen through the whole thickness were sealed and brought to the laboratory. The cores were split lengthwise in four sections. Two of those sections were used for taking samples to measure RH. Samples were taken using hammer and chisel from the inner parts of the sections to avoid parts that could have absorbed drilling water. Each sample was put in a test tube that were sealed by a rubber stopper. Samples were taken from several depths from the exposed surfaces.

The RH of a sample was measured by inserting a Vaisala RH-probe into the test tube and seal the gap between the test tube and the probe with an expandable rubber ring, see Fig. 4.

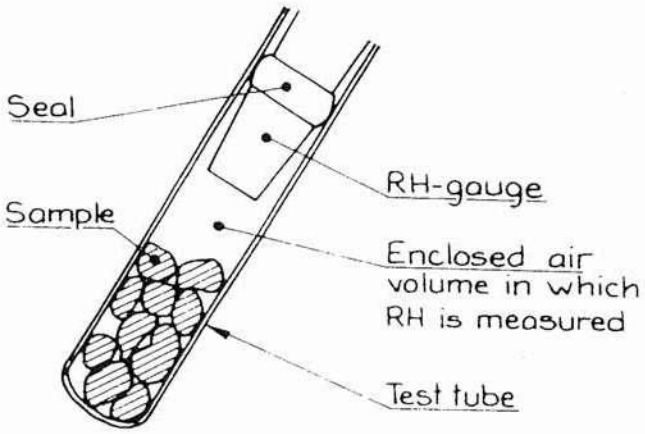

Fig. 4 The method of measuring RH of a sample in a test tube using a Vaisala RH-probe with an expandable rubber ring, Nilsson (1980).

The reading from the sensor is stable after some hours, depending on the concrete quality and a few other parameters. Usually the reading is taken after 8 hours. The reading is translated to RH by a calibration curve that is individual for each RH-probe and taken every other month or so.

3.5 S_{cap} on samples

The two remaining sections of the cores from the specimens were used to take samples for determining the degree of capillary saturation, S_{cap}. The samples were somewhat larger than the samples taken for the RH-measurements, but not too large too obtain a certain resolution with depth.

The original weight m_0 of each sample was carefully determined. One side of the sample were then put in contact with free water and evaporation from the other side was prevented. When the sample was saturated with water the wet weight m_{wet} was determined. The condition of saturation was usually obtained after some days and visible as a darkening of the upper side of the sample. For the samples of high performance concrete a very long time was needed to reach a "constant" weight gain. This procedure needs more investigation for high performance concrete to ensure a saturated condition.

Finally the samples were dried in an oven at +105°C and the dry weight m_{dry} was determined. From those three weights the degree of capillary saturation is calculated as

$$S_{cap} = \frac{m_0 - m_{dry}}{m_{wet} - m_{dry}}$$

The advantage of the degree of capillary saturation is that the possible lack of representativity of a small sample from a concrete containing large aggregate is excluded.

4. RESULTS AND DISCUSSION

Examples of results are shown in Appendix A-C.

4.1 RH in situ

Only the in situ measurements with the PW-probes were succesful. Measurements were done on three slabs. The variations were small between different depths and different exposure times (within a nine month period), only some $\pm$ 2-3 % RH. Since the first measuring depth was 20 mm almost only self-desiccation was visible in the moisture profiles. In slab 3, however, an indication of a penetration depth of 20-25 mm is found, see Appendix A.

4.2 RH on samples

The RH was measured on two core sections and throughout the whole thickness of the slabs. An example is shown in Appendix B. Since no significant difference was visible between the two core sections and the two opposite parts of the slab, all the results are shown as a function of the depth from one of the two exposed surfaces.

The results show a larger variation, ± 5 % RH in the central part of the slab, than usually expected from measurements on samples. A variation larger than ± 1 % RH is normally not satisfactory. Compared to the in situ measurements with the PW-probes, the variation when taking samples is much higher. The explanation for this has not yet been found, but it is obvious that improvement is essential.

In the example in Appendix B a penetration depth of some 20-30 mm can be estimated.

4.3 S_{cap} on samples

The degree of capillary saturation has a somewhat smaller variation, some ± 2-3 %. In some cases the S_{cap} is far from 1.0 also very close to the surface. This is strange and should be further analyzed. The method of removing "loose" water at the surfaces of the samples after saturation must be carefully performed, especially on small samples. This could be one explanation.

5. CONCLUSION

Moisture profiles could be measured in situ with what seems to be reliable results only with the PW-probes continuously placed in plastic tubes. An accuracy better than some ± 2-3 % RH may be obtained.

RH-measurements on samples showed remarkable large variations, far from what is normal in other applications. The degree of capillary saturation could be measured more precise, but since larger samples are needed the resolution in depth in not quite satisfactory. Fairly small samples are needed to improve the resolution in depth.

REFERENCES

Nilsson, L-O & Aavik, J(1993) Moisture measurement in concrete slabs with PW-probes during construction - an evaluation of a new equipment and methodology (in Swedish). Publication P-93:5, Department of building materials, Chalmers University of Technology, Göteborg

Hedenblad, G & Nilsson, L-O (198x) Degree of capillary saturation - A tool for accurate determination of the moisture content in concrete. TVBM-7005, Division of building materials, Lund Institute of Technology, Lund

Nilsson, L-O (1980) Hygroscopic moisture in concrete - drying, measurements and related material properties. TVBM-1003, Division of building materials, Lund Institute of Technology, Lund

Nilsson, L-O, Rodhe, M, Sahlén, S & Roczak, W (1994-95) Moisture distributions in marine concrete structures as a basis for service-life predictions. Parts 1-7. Working reports. Department of building materials, Chalmers University of Technology

Nilsson, L-O (1988) Temperature effects in relative humidity measurements on concrete - some preliminary studies. Proceedings of Symposium and Day of Building Physics in the Nordic Countries, pp. 456-462, Lund University, August 24-27 1987. Swedish Council for Building Research, Document D13:1988, Stockholm

Sahlén, N (1994) Moisture measurement with cast-in probes (in Swedish). Draft report december 1994. Sahléns Fuktkontroll AB, Malmö

APPENDIX A

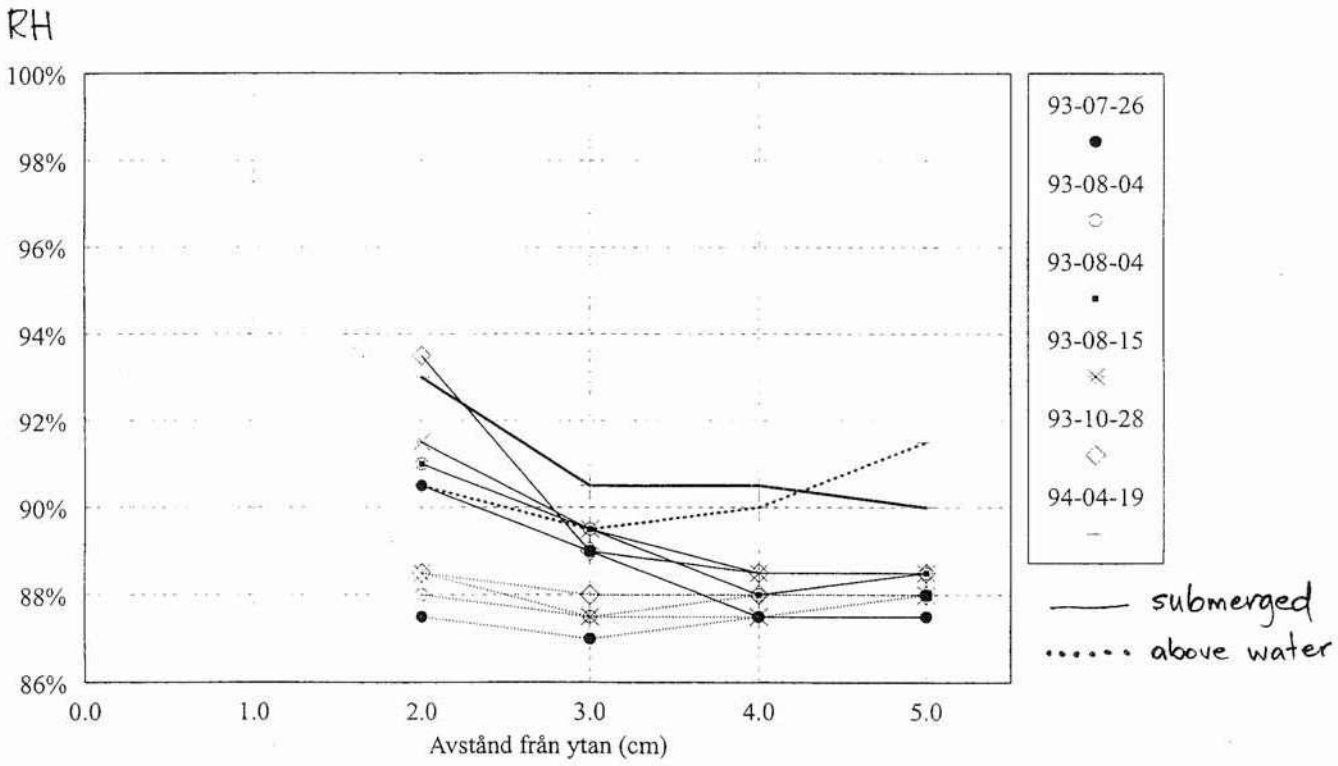

RH measured in situ with PW-probes on slab 3 July/August 1993, October 1993 and April 1994.

APPENDIX B

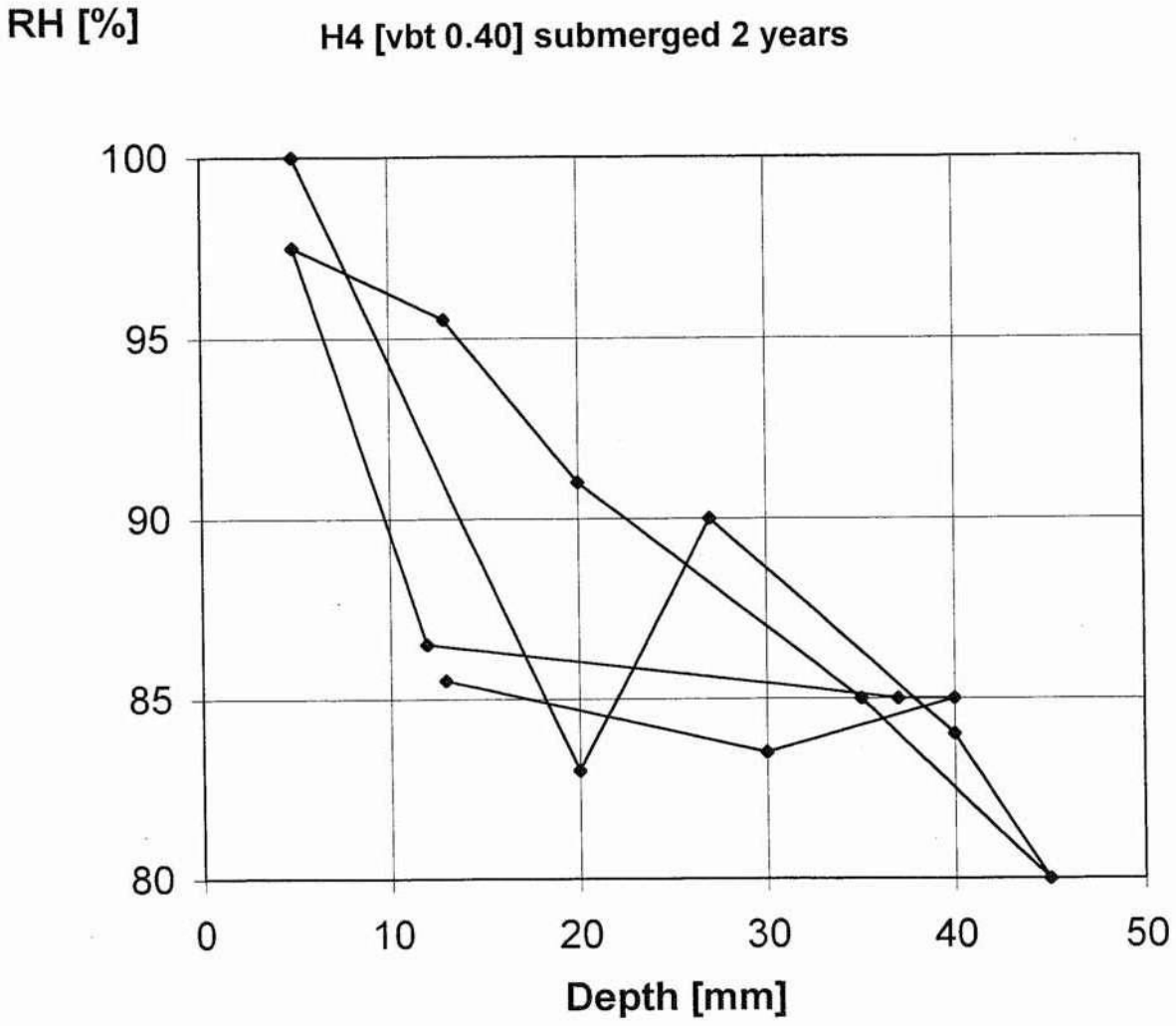

Moisture profiles from samples as RH after two years of exposure in sea water. Slab H4, Degerhamn cement with 5 % silica fume, water-binder ratio 0.40.

APPENDIX C

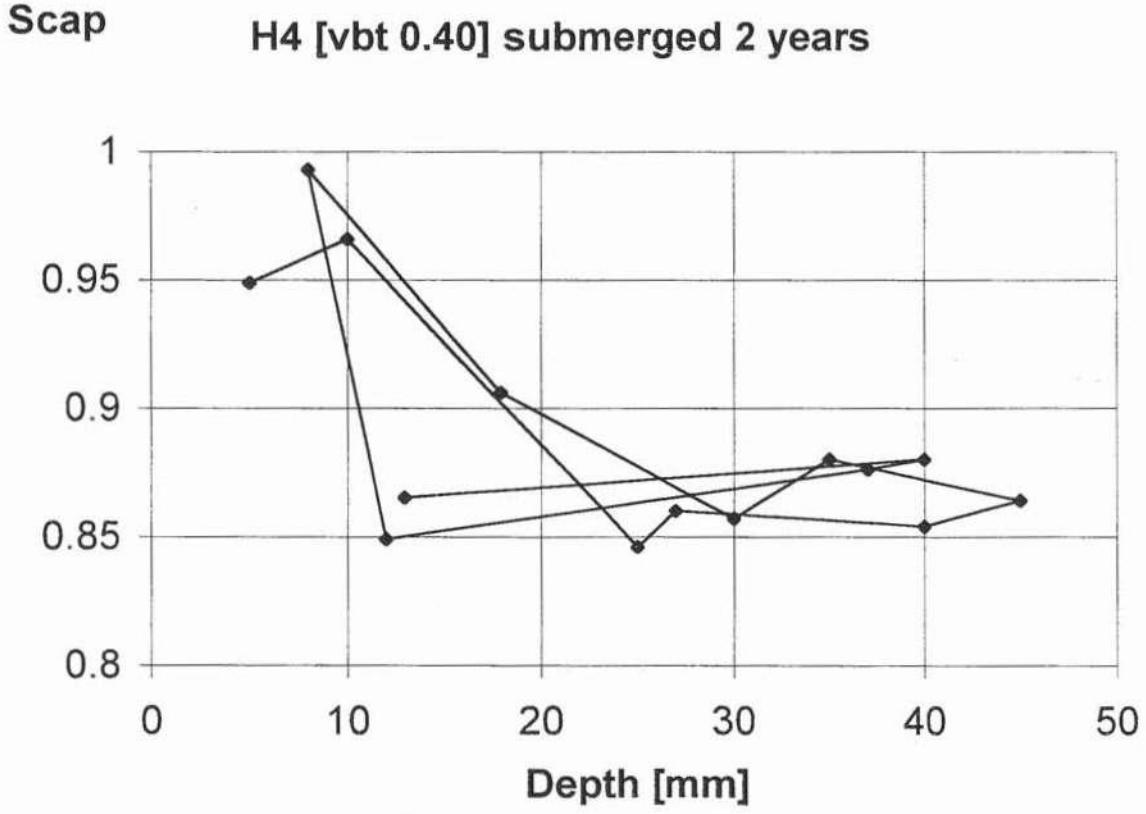

Moisture profiles from samples as S_{cap} after two years of exposure in sea water. Slab H4, Degerhamn cement with 5 % silica fume, water-binder ratio 0.40.

MOISTURE STATE IN A CONCRETE BRIDGE

Erik J Sellevold, NTH, Trondheim

Claus Larsen, Road Research Lab, Oslo

INTRODUCTION

The moisture state of a concrete is of decisive importance for the durability of the concrete in a structure - almost regardless of the mechanism of deterioration the concrete is exposed to. Much laboratory work has been done on the relationship between deterioration and moisture state; however, not much work has been done on the actual moisture state and its variation in concrete structures.

The present paper is a report on work in progress at the Gimsøystraumen bridge near Svolvær, Norway, concerned with determining moisture state and its variation with location in the bridge and season. The moisture state of concrete is defined here by the relative humidity (RH) exerted by the pore water and by the pore water content. The pore water content may be expressed in different ways; the most directly useful one perhaps being the degree of capillary saturation (DS). DS expressed this way is the ratio between the actual pore water content and the maximum pore water content obtained by suction, i e the maximum pore water content should not include filling of the air pores. The RH exerted by the pore water defines the thermodynamic state of the pore water, but not the amount. For many durability related properties the amount of pore water is the most relevant description of the moisture state, f ex frost deterioration, chloride intrusion and rate of corrosion. The relationship between RH and pore water content is given by the sorption isotherms. This is not a unique relationship, but depends on the moisture history of the concrete. Outer boundries for the relationship are given by desorption (upper boundry) and adsorption (lower boundry). Thus, the RH value in field concrete over time does not, by itself, define the moisture state and thereby the potential aggressiveness of a given deteriorating mechanism. A further complication exists in that pore water is not pure water, and the RH it exerts depends not only on physical factores such as internal surface area and pore structure of the concrete, but also on the amount of dissolved ions.

In the present experiments the moisture state is characterized using a variety of methods: 1) RH is continuously monitored in the bridge, 2) Concrete samples are taken from the bridge and RH as well as pore water content and porosity characteristics are determined in the laboratory, and 3) Complete desorption and adsorption isotherms were determined in the laboratory.

2 EXPERIMENTAL

The in situ RH measurement were made using the AHEAD Hygrotemp system with Rotronic F22 sensor. 8 sensor were mounted in the bridge superstructure (box type) from inside the box, positioning the sensor head about 40 mm from the external concrete surface. Datalogging took place every 6 hrs over most of 1994.

Concrete samples were taken from the bridge by cutting 50-60 mm deep tracks about 30 mm apart and chiseling off rectangular pieces. These were immediately wrapped in heavy plastic sheets to prevent moisture loss. It was found that different ratios between the sawn areas and specimen volume did not influence the measured moisture contents; thus it was concluded that the samples did represent the field concrete. In some cases samples were cut in two to obtain two different depths from the surface. When the samples arrived at the laboratory (NBI, Oslo) part of each was crushed and placed in glass tubes for RH-measurements. The remaining larger piece was dried at 105^{0}C, submerged to obtain the suction (or capillary) porosity, and finally pressure saturated with water to obtain the air porosity.

Drilled cores were taken to determine the sorption isotherms on sets of 3 mm thick discs. After water storage the sets were placed in desiccators over saturated salt solutions in the RH-range from 97 to 11% for desorption. The other half of the sets were dried at 50^{0}C and then placed in the same RH environments for adsorption.

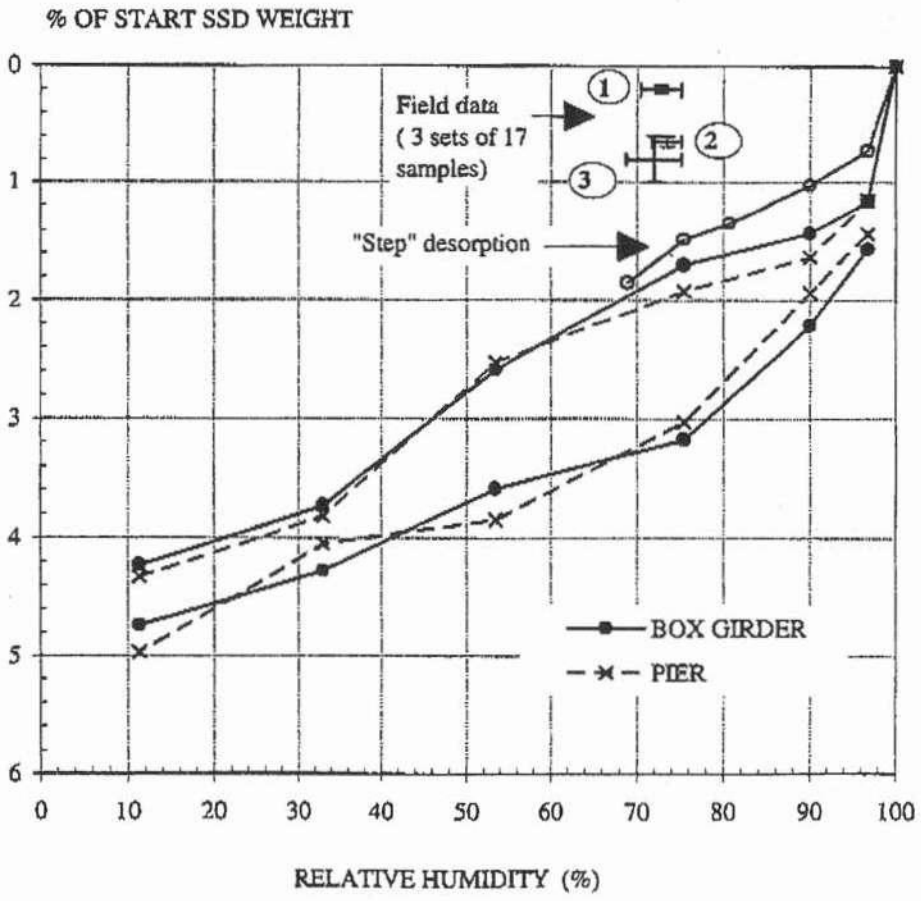

Fig 1 Sorption Isotherms and Field data.
Bars for the field results indicate std dev for each sample set as a whole.

3 RESULTS AND DISCUSSION

Fig 1 shows the desorption and adsorption isotherms for concrete taken from the piers and the superstructure, respectively. The two agree quite well, in spite of the fact that the design specified C35 concrete in the piers and C40 in the superstructure. Core samples from the piers gave compressive strengths in the range 60-70 MPa. The bridge was constructed in 1979-81. The isotherms are plotted relative to the original water stored weights, since final dry weights are not yet available. The curve labelled "STEP" is for a separate set of discs from the superstructure subjected to stepwise desorption. The discrepancy between the desorption curves in the high RH-range is mainly caused by the fact that after 15 days desorption the dry adsorption samples were placed into the same desiccators as the desorption samples. This led to fast desorption and subsequent adsorption for desorption samples placed at 75-90-97% RH. Hence the "STEP" curve is closer to the truth than the two other curves.

Fig 1 also shows the results for 3 sets of field samples taken in June, September and November 1994 from both piers and superstructure. The noteworthy feature of the results is that they fall outside the desorption - adsorption boundries - which in principle is impossible. It should be noted that the results are preliminary in that dry weights for the sorption points have not yet been established - hence there is some uncertainty in the relative ordinate position of field contra sorption samples, and also because the degree of filling of air pores with water in the SSD-state is uncertain. The results are presented here because they illustrate the importance of obtaining actual degree of saturation data in addition to RH values to properly assess the moisture state of field concrete in relationship to durability. The work is continuing, also with respect to the effects of dissolved ions in the pore water on the sorption isotherms.

Another feature to note on the field data is the relatively small deviation within each set, when each is regarded as one set regardless of location and the depth from the surface the samples are taken. The values including std dev for in situ water content (g/g dry) and RH(%), for the three sets are: 0.046 ± 0.003, 0.048 ± 0.005, 0.050 ± 0.005 and 73 ± 2, 74 ± 2, 72 ± 3, respectively. The data indicate a trend to a small increase water content from June to November, but this is not reflected in RH.

RH values from the in situ monitoring also show relatively stable values over time and location; typically around 80% RH in winter to around 75% RH in summer. This is a somewhat higher level than the lab measurements, however, the lab measurements must be considered more reliable considering the many uncertainties involved in field measurements of RH. Recently, one probe over a salt solution has been installed on the bridge to provide "continuous calibration".

4 CONCLUSIONS

The present evidence indicate very high degrees of capillary saturation in the bridge concrete with estimated values of of 91 ± 4, 88 ± 5 and 85 ± 4, respectively for the three sets. The corresponding RH-values are 73 ± 3% for the sets as a whole. Apparantly these results are outside the boundries set by the desorption - adsorption isotherms. It should be emphasized that these are preliminary results from work in progress, and is presented here as a basis for discussion.

5 ACKNOWLEDGEMENT

The present report is part of the "OFU Bridge Repair Project", financed by the Norwegian Public Roads Administration (NPRA), Rescon AS and the Norwegian Industrial and Regional Development Fund (SND). The project is managed by NPRA.

IN-SITU MONITORING OF CONCRETE STRUCTURES

C.F. HENRIKSEN, RH&H CONSULT, COPENHAGEN, DENMARK

1. SYNOPSIS

Evaluation of service life and of the service life of repairs made is normally based on expectations rather than on actual knowledge of a series of control parameters (deterioration rate, initiation time, etc.).

This may lead to wrong evaluations and wrong choice of repair methods.

This situation is, however, a natural consequence of the recent need for exactly this knowledge. A large number of damage cases during the last 5-10 years has created a need for this kind of information, which had not been collected before.

The following section describes the results of observation of a number of different structures so as to provide a more realistic basis for evaluation of conditions of corrosion of steel in concrete in particular, as this is the predominant deterioration mechanism.

Furthermore, the consequences of various repair activities and the future need for further knowledge are described.

2. BACKGROUND

Corrosion is one of the most frequent and serious causes of deterioration of concrete structures. Corrosion is mostly caused either by chloride penetration or by carbonization.

Only the development of the corrosion process will be treated here, the initiation process is treated in other literature.

The primary parameters in the corrosion process of concrete are:

- moisture content
- temperature
- chloride content
- porosity
- anode/cathode relation
- oxygen content at the cathode

The first four parameters can be expressed as a total through the electric resistance of the concrete, which is a control parameter in the corrosion process (the smaller the resistance, the faster the corrosion in most cases). At the same

time these four parameters (the electric resistance) controls the size of the anode/cathode relation (large amounts of reinforcement corresponding to generally occurring structures are assumed, ie the amount of reinforcement is no corrosion-reducing parameter) and the oxygen content at the cathode. But the dependence is difficult to quantify. A high porosity and a high moisture content will give a low resistance and thereby, at first glance, a high corrosion rate. But the corrosion rate will however be low, because the wet concrete will have a high resistance against the diffusion of oxygen necessary for the corrosion.

Because of this uncertainty with regard to the connection between the corrosion-controlling parameters it has been necessary to measure existing structures to gain a better understanding of this connection. In expectation of the controlling role of the resistance of the concrete in the corrosion process, evaluation and observation of reinforced concrete structures in the examples described in the following section have been based on measurement of the electric resistance of the concrete.

3. MEASURING METHOD

Resistance Measuring

The rate of corrosion is primarily controlled by the resistance around the anode. This can be expressed by the following relationship:

$$R = \frac{\rho}{2\,\pi \cdot L}\left(\ln \frac{8L}{D} - 1\right) \text{ where}$$

R is the resistance around the anode

ρ is the specific resistance of the concrete

D is the diameter of the anode

L is the length of the anode

The layout of the electrodes used is based on this relationship. The electrodes and the principle of measuring is shown in figure 1.

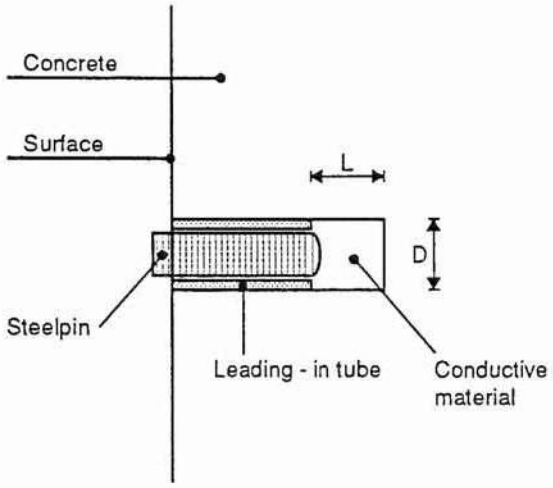

Figure 1
Measuring is either between two elctrodes or between an elctrode and the cast reinforcement. The specific resistance of the concrete is determined on a core sample by the BOX method (measuring the resistance through a core with a well-defined diameter and length).

The specific resistance of the concrete can be determined at different moisture levels by carrying out simultaneous measurements of moisture content and specific resistance on core samples, cf. figure 2.

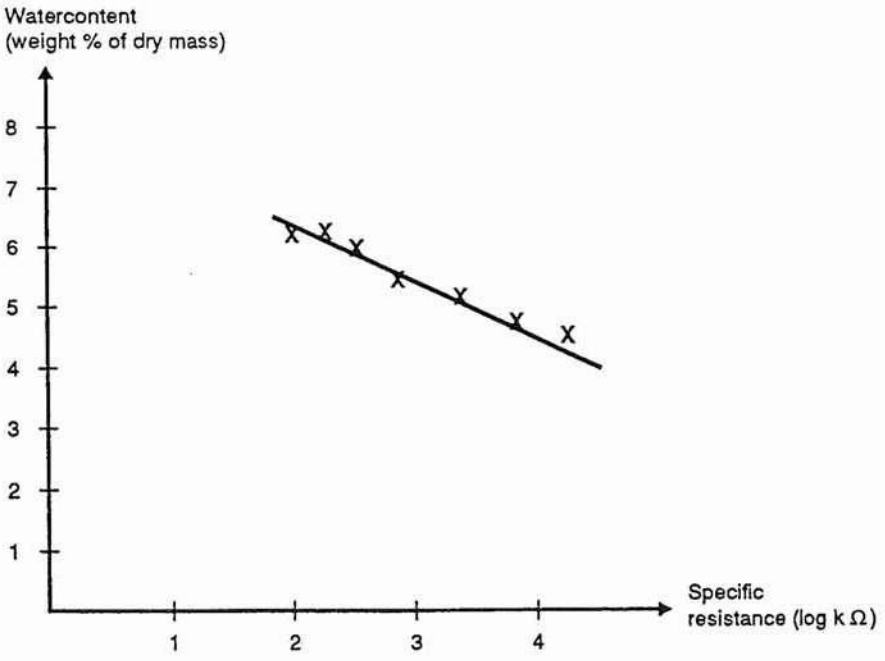

Figure 2
Relationship between water content and specific resistance in concrete cut from a structure. The curve is used to estimate the variation in watercontent based on in-situ measurements of the resistance.

Examples of the dependence of the electric resistance on the moisture content, temperature and porosity are shown in figures 3, 4 and 5 for a certain concrete type (other interrelations will apply for other concrete types).

Figure 6 shows the fundamental dependence of the corrosion flow on the resistance.

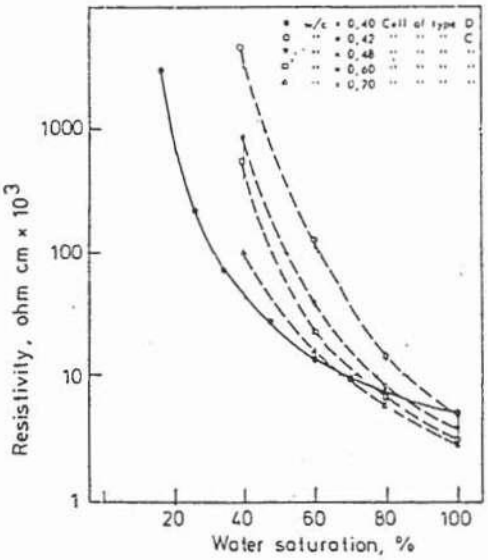

Figure 3
The figure shows the effect of water saturation on the resistivity (specific resistance). From "Corrosion of steel in concrete" by K. Tuutti.

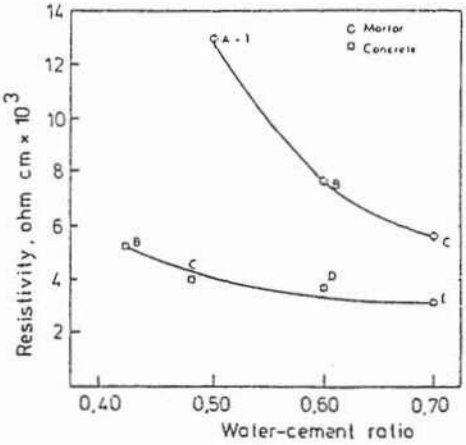

Figure 4
The figure shows the effect of water-cement ratio on the resistivity (specific resistance). From " Corrosion of steel in concrete" by K. Tuutti.

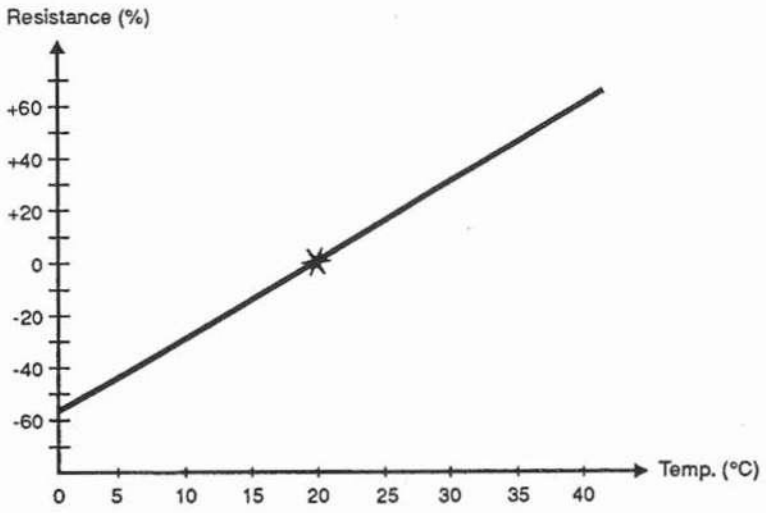

Figure 5
The figure shows a relationship between electrical resistance and temperature.

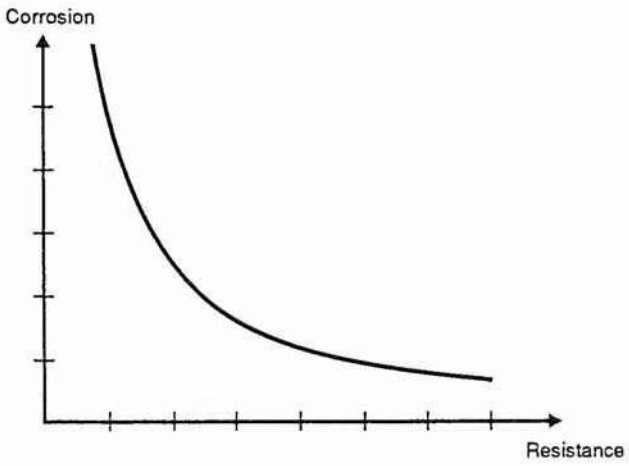

Figure 6
The figure shows the principal relationship between corrosion and resistance.

Potential Measuring

The electrodes used for the resistance measuring have proved sufficiently stable to be used for observation of the corrosion condition.

4. RESULTS OF OBSERVATION

4.1 Moisture Measuring on Bridge Columns

Figure 7 and 8 show the moisture variations on bridge columns over a period of 3 years. Measurements were made at a reinforcement level depth of 40 mm. It appears that:

- the temperature variations are the predominant parameter,
- the moisture variations are rather small,
- the moisture content is much lower at +1 m, where the moisture impact comes only from splashes from traffic or heavy showers, than at ground level, where there is a more constant direct water impact from water from the lanes.

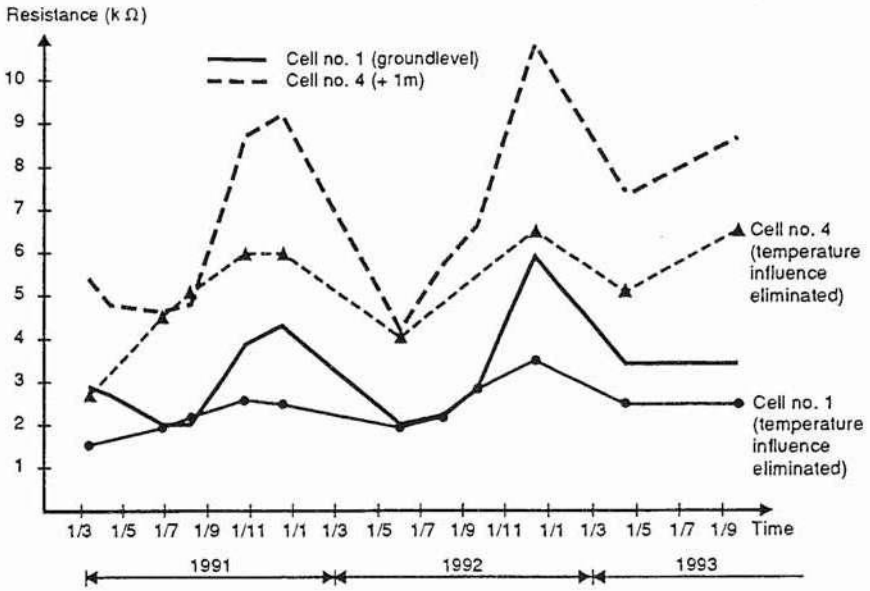

Figure 7
The figure shows the variation of the resistance with time.

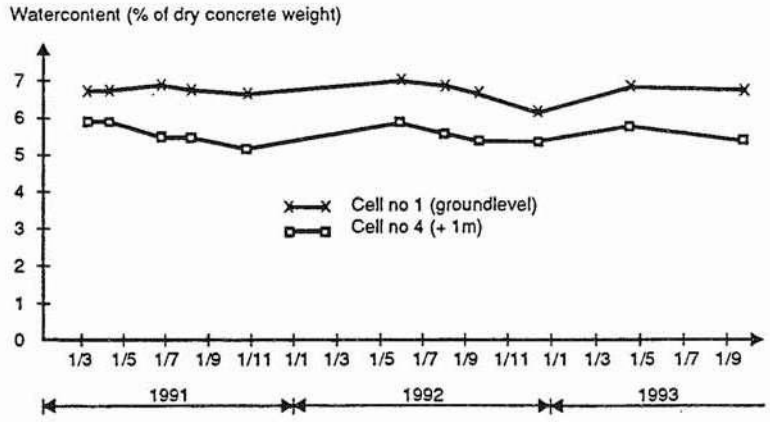

Figure 8
The figure shows the variation in watercontent with time in depth of 40 mm. The watercontent is calculated from the resistancemeasurements, based on the principles described in figure 2. The influence of the temperature is eliminated according to figure 5.

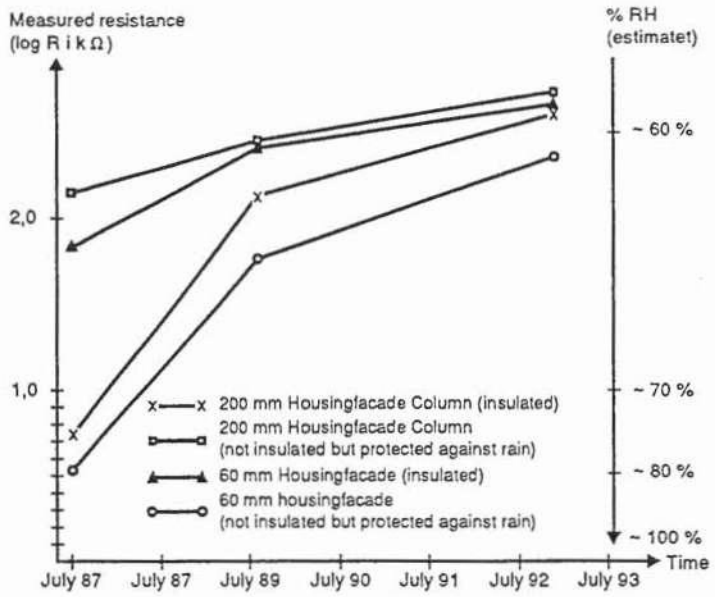

Figure 9
The figure shows the development in resistance with time.

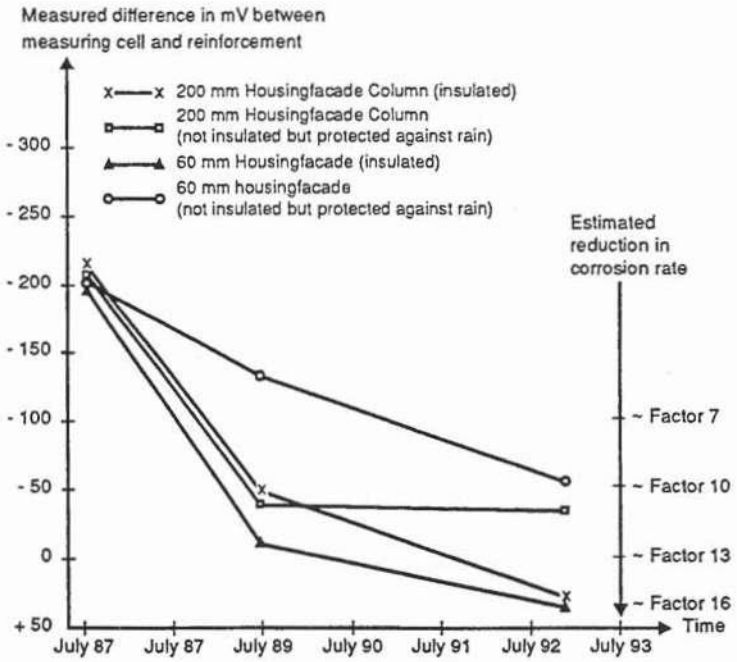

Figure 10
The figure shows the development in potentials with time

4.2 Moisture Measuring on Covered Facade

In figures 9 and 10 the moisture impacts and variations in potentials are measured on a facade, which has been covered as part of a renovation.

It appears that:

- the resistance increases so much that the corrosion stops regardless of whether insulation is used or not.

4.3 Moisture Measuring on Bridge Deck

Figure 11 shows the results of a measurement of the moisture variations on a 1 m thick bridge deck which was repaired because of heavy damage caused by alkali-aggregate reactions and frost. The water content was around 95% of maximum water content at the time of repair. The deck is insulated with a water proof membrane at the top, and the measurering cell is placed around 80 mm above the membrane.

It is seen that the resistance is more or less unchanged over a period of 1½ years, indicating that no drying out has taken place.

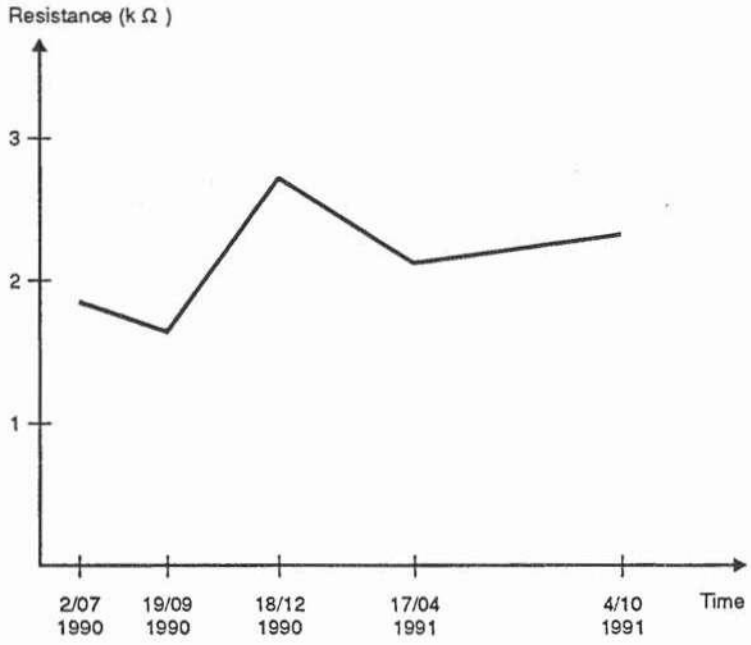

Figure 11
The figure shows the development in resistance in a 1 m thick concrete bridgedeck.

4.4 Moisture Measuring on Surfaced Edge Beam

Figure 12 and 13 show the results of a measurement of the moisture variations on a surfaced edge beam. The edge beam forms part of the large test with surface treatment. The edge beam is treated with different products.

It is seen that:

the resistance variation over the period of 5 years is limited, irrespective of surface treatment or not and the type of product. The moisture level is more or less unchanged over the period, but with a slight tendency of drying of the outermost 40 mm of surfaced elements. The measurement of the profile (fig. 13) is taken in the spring after a longer wet period and the difference probably indicates that a surface treatment decreases the influence of variations in the moisture impact of the surroundings rather than indicates a drying-out effect of a surface treatment.

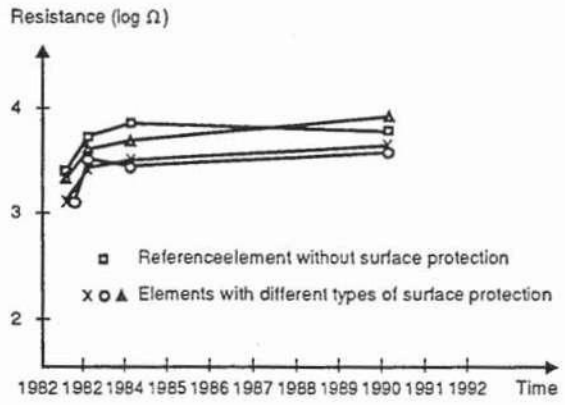

Figure 12
The figure shows the development over years of the restance in concrete in a depth of 40mm. After a change in the beginning of the period (which is due to instability of the electrodes) the resistances show only minor signs of variations in the watercontent in both surfaced on un-surfaced elements. The watercontent in the end of the period was measured to be 80 % of max. watercontent (~ 80 % RH) in the outermost 40 mm. No corrosion activity was detected.

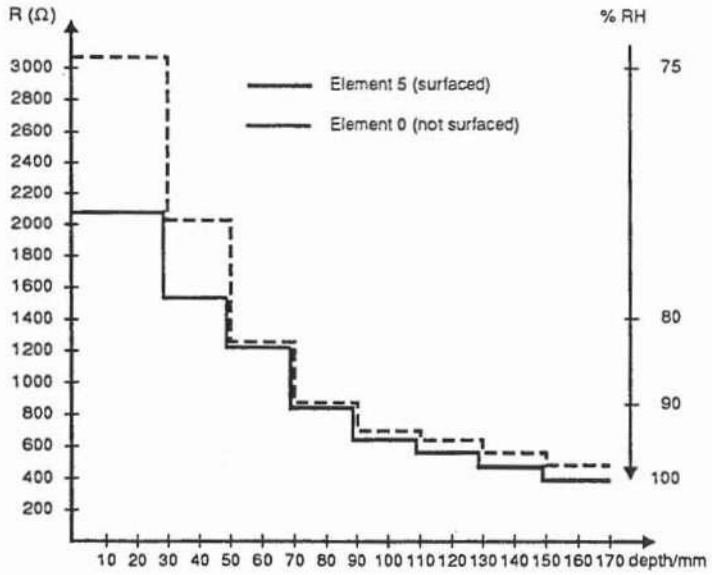

Figure 13
The figure shows the variation of the resistance through the crossection in a surfaced and not surfaced element.

4.5 Moisture Measuring on Surfaced Columns

In connection with a repair of columns, is was chosen not to repair one column, because it did not yet show any signs of corrosion despite of a high chloride content and a nearly saturated concrete.

It was chosen only to apply a surface treatment to see the effect on the development of a corrosionprocess expected to give rise to a need of repair, without surface treatment, within 10 years.

Figures 14 and 15 show the development in water content and potential over a period of 4 years. The water content is calculated based on resistance measurements in accordance with the principles described in figure 2. The influence of temperature is eliminated due to figure 5.

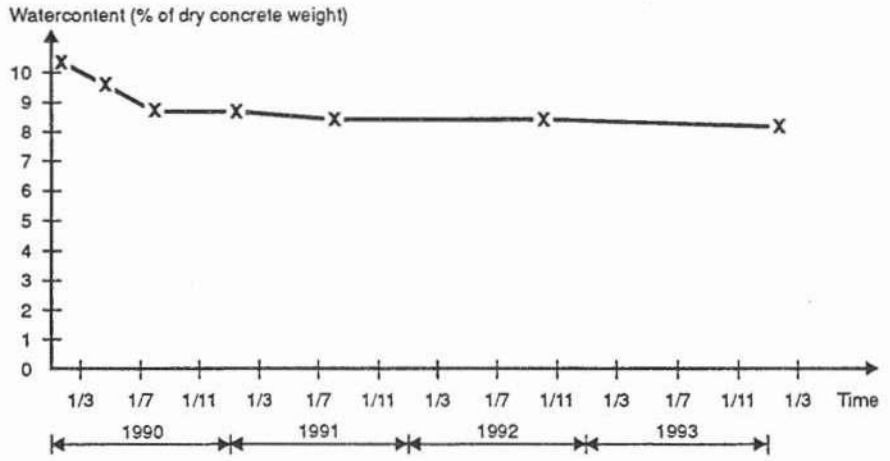

Figure 14
The figure shows the variation of the water content on a column with a surface treatment.

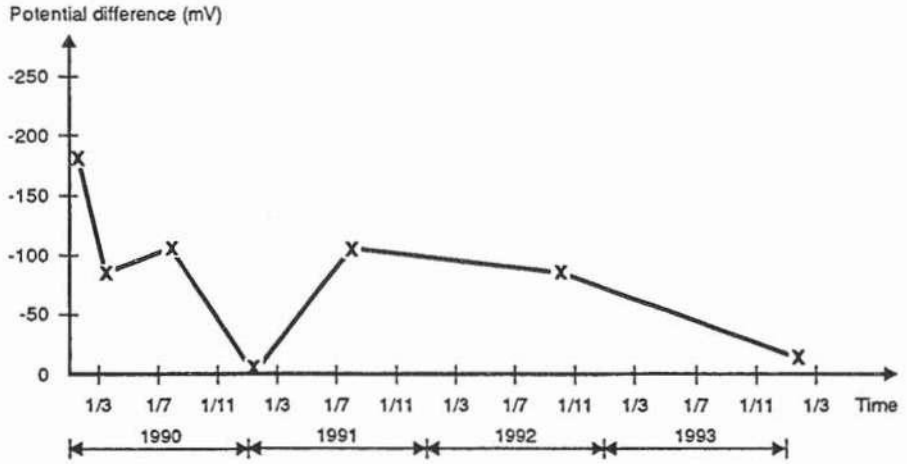

Figure 15
The figure shows the variation in potentialdifference on a column with a surface treatment.

From the figures it appears that the column:

- dries out to approx. 80% of maximum water saturation (~ 90% RH)
- is still in a stable non-corroding condition.

Furthermore the specific resistance is calculated from the measured resistances to be approx 15 $k\Omega \cdot cm$ at the end of the period. A possible corrosion will then still take place at a considerable rate (estimated 0.05 - 0.1 mm/year) with the drying out achieved. This is approximately half of the corrosion rate expected without surface treatment.

5. EVALUATION OF RESULTS OF MEASURING

Based on the observation results achieved the following can be concluded:

- In the Danish climate (average annual temperature and moisture content of 8°C and approx. 80% RF and an annual rainfall of approx. 700 mm) the variations in moisture content at normal reinforcement depth (30-40 mm) on an outdoor structure are limited. The structures adapt to a moisture content which varies only to a limited extent at reinforcement level throughout the service life of the structure. Therefore, the moisture variations in the surrounding environment will have only little influence on the corrosion as long as the concrete is intact. If the concrete cracks due to for example corrosion, the moisture content can vary more. However, there is no indication in the corrosion measure-ments that this should cause an increased corrosion rate. The reason is probably that even if the cracks provide the possibility of larger moisture impact in wet periods they also provide a more efficient drying out in dry periods. Furthermore the cracks cause an increased oxygen supply to the corrosion products which expand and isolate the anode from the cathode to a certain extent and make the anode develop more along the rebar than through its cross-section (ie tends more to increase the corrosion area, than to increase the corrosion rate).

  In the outermost concrete layers the moisture content will vary more. The more porous the concrete is, the deeper the moisture variations in the surroundings can be registered. In the actual cases (water-cement ratio 0.4 to 0.5 and a cover of 40 mm) the variation limit was in front of the reinforcement level i.e. the moisture variation have not influenced an eventually corrosion process.

- On a structure which is not totally saturated, use of surface treatment cannot beforehand be expected to have any effect on the drying out and stopping of for example a corrosion process. Theoretically the concrete can be dried out, but the driving force in the process of drying out will be relatively small and at the same time the cross-sections often to be dried out are very large. Consequently, the theoretical time of drying out will be very long (often > 20-40 years).

- On a totally saturated structure the measurements show that even a limited drying out because of a water-stopping surface treatment can prolong the service life considerably. This is the case for example on structures which are very moisture-loaded locally (eg columns). If the moisture load can be limited in the area with the heaviest moisture load, the effect may be a significant prolongation of the service life even with a minor drying out.

- Use of covering on housing facade elements will usually have a drying and corrosion-stopping effect because of the heat flow through the wall.

- Surface treatment of a chloride-based concrete which has not yet caused corrosion activity will at least double the remaining service life.

- Use of surface treatment to stop corrosion or decrease the corrosion rate cannot in general be recommended or advised against (the positive effect known to prevent from initiation of the corrosion will not be included in this statement). The effect will differ from case to case and has to be decided on the basis of a special investigation. Probably surface treatment will be most efficient when applied to structures which also is exposed to other deterioration mechanisms known to accelerate the corrosion rate (ASR and/or frost). Especially if the structure has allready cracked either due to the deterioration or due to structural or thermal cracking.

6. FINAL REMARKS

The measurements and observations described have not been made as part of a structured investigation project and do not represent an unambiguous truth of the issues mentioned.

The measurements and experience were collected during mutually independent practical assignments and many special inspections. The measurements carried out and the evaluations made on the basis of the measurements are, however, in most cases not surprising compared to either knowledge achieved through laboratory tests or practical experience in general. The measurements confirm to a great extent that theoretical expectations are also in conformity with practice. The practical demonstration of theoretical expectations is very important, because on this basis it will be much easier to carry out correct evaluations when chosing of repair activities.

As mentioned this test is no real documentation, and it is obvious that there is a need for further collection of information. The development has primarily to be based on long-term observation of existing structures, and the measurements described here can be seen as a first phase in this process and as the first information on the size and variation of a series of important parameters in general.

The need to know the parameters determining the deterioration depends on the need to carry out evaluations of service life. The parameters are used for determining, in particular, the deterioration rate.

As far concerns corrosion the measurements indicate that structures are more or less "born" with a corrosion rate (determined by its quality and the surroundings), which can hardly be changed no matter what is done to the structure later, except for preventing the corrosion from starting at all.

This means that except for cathodic protection it will only to a minor extent be possible to stop a corrosion process first started. In the work of optimizing the needed concrete repair it is important to know the corrosion rate. Compared to normal practical needs the estimate of the size of the corrosion rate only has to be a rough one (5-10-15-20 years etc) as deteriorating structures always have to be closely inspected, saying that there is no pratical need for very precise estimates. It makes no sense compared to the uncertainties normally accepted when making service life estimates.

The measurements indicate further - as expected - that the temperature and water content (as a result of both the porosity of the concrete and the water impact from the surroundings) in the concrete are essential parameters and probably the far most important of the parameters to effect corrosion.

Therefore, the additional gathering of information should concentrate specifically on measurement and evaluation of the size and variation of these parameters expressed through the specific resistance which is basically the parameter to control the corrosion rate. Moreover, the observation should aim at division of a geographical area into deterioration zones, depending on type of structure and local meteorological data, helping to set up general, rough estimates of the corrosion rate.

INFLUENCE OF MOISTURE AND CARBONATION ON THE TRANSPORT OF CHLORIDES IN CONCRETE - Some ideas

Göran Hedenblad
Division of Building Materials
Lund Institute of Technology
Box 118, S-221 00 Lund, Sweden

Introduction

Moisture, carbonation and chloride transport in concrete are processess which stongly influence each other. This means that for a correct description of the chloride, moisture and carbonation processes in concrete, which contains all three constitutients, the three processess must be calculated simultaneously. Metha /1/ said "Water is generally involved in every form of deterioration, and in porous solids, permeability of the material to water usually determines the rate of deterioriation. ... However, in practice, deterioration of concrete is seldom due to a single cause. ... In general, the physical and chemical causes of deterioriation are so closely intertwined and mutually reinforcing that even separation of the cause from the effect often becomes impossible."

Moisture transport in mature concrete is relatively well-known, see /2/.
There are also computor programs for moisture transport in different building materials, in one and two dimensions, and there are also some special programs, see /3/ and /4/.
Chloride transport and carbonation can probably be modelled, in principal, in the same way as moisture transport.

The purpose of this paper is only to present some preliminary ideas. The ideas are not thoroughly explicated. Nevertheless, I hope that in the future I will have the opportunity to verify them.

Moisture transport

During the modelling of moisture transport when salts (chlorides) are present the "real" potential is probably the relative humidity (RH), which determines the direction of the moisture flow. The relation between the moisture permeability (δ_v) and the sorption isotherms is shown in FIG. 1.

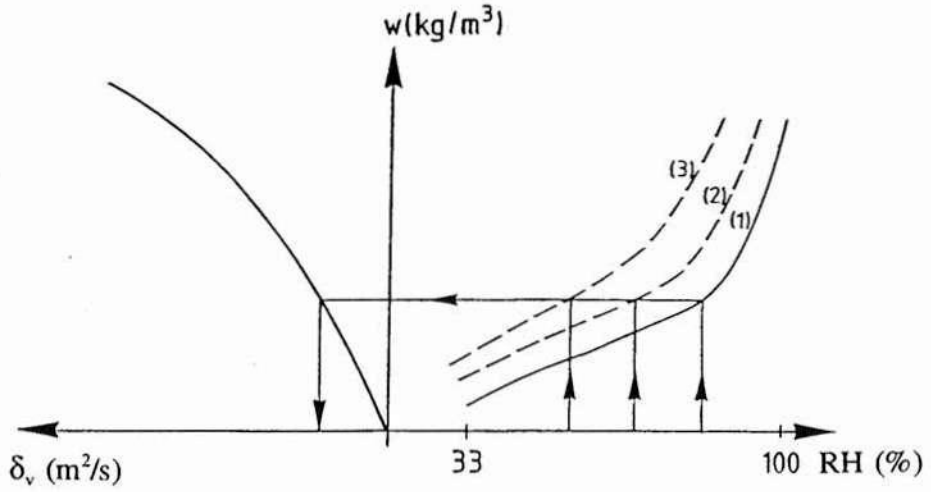

FIG. 1 Relation between the moisture permeability and the sorption isotherms when the materials contain salts, eg. chlorides.

Sorption isotherm (1) is when the material does not contain any salts. Sorption isotherm (2) and (3) are when there are salts in the material. Curve (3) is when there is more salt in the material then in curve (2). This means that when the salt content in the material is changed, the sorption isotherm is changed. In FIG. 1 it is assumed that it is the moisture content in the material and not the change in RH due to salts that affects the moisture permeability.

In FIG. 1 it is also shown that with salt in the pore solution the whole sorption isotherm changes its position with ΔRH_{salt}, where ΔRH_{salt} is the difference in RH at the saturation of the pore system with liquid, and with and without salt.

$$RF_{salt} = RF - \Delta RF_{salt} \tag{1}$$

The influence of salt on the RH at saturation can be calculated with eq.(2)

$$\ln \phi_m = \sum_{i=1}^{n} \nu_i \, m_i^{\alpha} \cdot M_w \cdot \phi_i^{\alpha} \tag{2}$$

ϕ_m = relative humidity at saturation
υ_i = number of ions per salt molecule
m_i^{α} = molality, number of moles of solute per kg solvent
M_w = molecular weight of water = 0.018 kg/mol
ϕ_i^{α} = osmotic coefficient, a function of temperature and molality, see /5/.

The function above does not take into account the pressure in the liquid in the pores or the water vapour pressure in the pores of the material. For materials at atmospheric pressure these two parameters can probably be disregarded, but at "higher" water pressure one should take them into consideration, see /5/.

In addition to chlorides, one sometimes also has to take into account the alkali content (NaOH and KOH) of the cement. The relative humidity in the concrete is also affected by these salts. For concrete made of Slite Standard cement and with low water-cement ratio (w_o/C) there could be a big influence on the RH at saturation. It is probably possible to include the effect of the alkalies in curve (1) in FIG. 1, when calculating the moisture transport in the concrete. For concrete with w_o/C 0.4 and Slite Standard cement the maximal RH due to alkalies is (without chlorides) only about 95 %.

An example of the influence of NaCl on RH at saturation is given in FIG. 2.

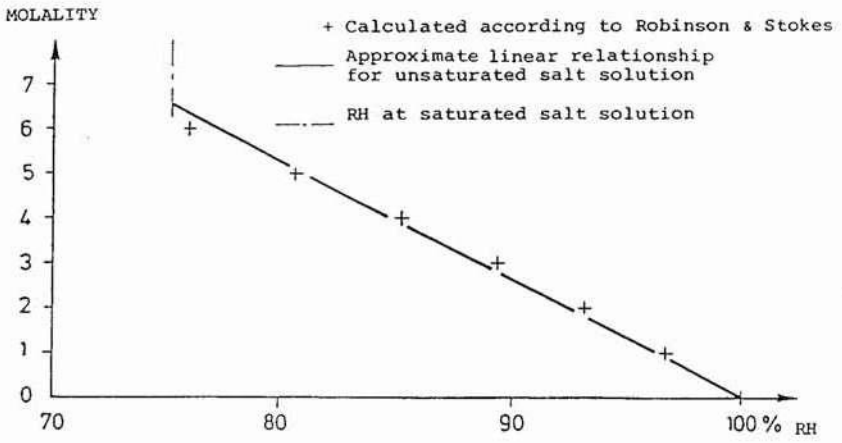

FIG. 2 Effect of the concentration of NaCl in aqueous solution on the saturation-RH. (1mole = 58.5 g NaCl). Hedenblad /5/.

The waters in the oceans have about 35 g NaCl per liter water, which gives a molality of about 0.5, and this molality yields a saturation-RH lower than 100 %, see FIG. 2.

At a combined course of chloride- and moisture transport, the RH in the material is affected both by the content of chlorides and by the moisture content. The relative humidity, on the other hand, affects the moisture transport in a point, i.e. if the moisture transport is to or from that point. For every timestep in the calculations, one must start from the earlier timestep and its concentrations of moisture and chlorides in order to calculate the new concentrations. This means that there is not <u>one</u> single sorption isotherm but an "infinite" number of them, due to the varying content of chlorides. But this is probably relatively easy to model in a "conventional" moisture computor program.

Transport of chlorides

Chloride- and moisture transport in a material have many similarities and can probably be modeled in the same way.

According to data on the "effective chloride diffusivity" received from Sandberg /6/ this coefficient can in principle, at water saturation, be written

$$D_{Cl}^{capillary} = K \cdot (P^{capillary})^2 \qquad (3)$$

K = a constant that depends on the type of cement and so on
$\mathbf{P}^{capillary}$ = the capillary porosity of the hydrated cement

For ordinary OPC concrete **K** is about $2{,}5 \cdot 10^{-10}$ (m^2/s)
Eq. (3) is shown in FIG. 3, with measured results marked with +.
The capillary porosity is calculated with the assumption that the degree of hydration is 0.7.

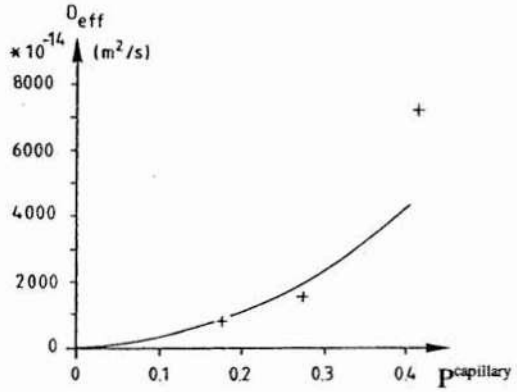

FIG. 3 Effective chloride diffusivity (at water saturation) as a function of the capillary porosity.

The capillary porosity is defined as, (see also /7/)

$$P^{capillary} = (w_0/C - 0{,}39\alpha)/(0{,}32 + w_0/C) \qquad (4)$$

w_0/C = water-cement ratio
α = the degree of hydration

In eq.(4) it is shown that α has a great influence on the capillary porosity, and consequently on the eff. chloride diffusivity. This means that a coefficient w-hich is measured on a relatively young concrete cannot be used to model the chloride transport in the same concrete when the concrete is "old" (mature).

The above relations are valid when the concrete is saturated with water. When the moisture content is lower it is probably true that the transport of chlorides is lower. A reasonable assumption is that the chlorides are transported in the liquid phase in the capillary pores and not in the air phase in those pores. With this assumtion the effective chloride diffusivity then depends on the moisture content in the material, e.g.

$$D_{Cl} = D_{Cl}^{capillary} \cdot (w - w_{45\%})/(w_{capillary} - w_{45\%}) \qquad (5)$$

$\mathbf{D}_{Cl}$ = effective chloride diffusivity (m^2/s)
$\mathbf{w}$ = moisture content by volume (kg/m^3)
$\mathbf{w}_{capillary}$ = moisture content by volume at capillary saturation (kg/m^3)
$\mathbf{w}_{45\%}$ = moisture content by volume at 45 % RH, i.e. when the capillary pores are precisely empty of water (kg/m^3)

In eq. (5) it is seen that if the relative humidity is 45 % or lower there is no transport. According to Sandberg /8/ this is in principle also true; however no experimental data exists.

The effect of the degree of hydration on $\mathbf{D}_{Cl}^{capillary}$

Example 1: Concrete with $\mathbf{w}_0/\mathbf{C}$= 0.5 and α = 0.3 and 1.0.
$\mathbf{P}^{capillary}(0.3) = (0.5\text{-}0.39\cdot0.3)/(0.32+0.5) = 0.467$; $\mathbf{P}^{capillary}(1.0) = 0.134$
$\mathbf{D}_{Cl}^{capillary}(0.3) / \mathbf{D}_{Cl}^{capillary}(1.0) = (0.467/0.134)^2 = 11.6$

If the moisture content after a long time (α=1) should be lower than the moisture content at saturation (for example due to self-dessication) then according to eq.(5) the quotient

$\mathbf{D}_{Cl}^{capillary}(0.3) / \mathbf{D}_{Cl}(1.0)$ can be much larger than 11.6.

Example 2: Concrete with $\mathbf{w}_0/\mathbf{C}$= 0.4 and α = 0.5, 0.9 and 0.95.
$\mathbf{P}^{capillary}(0.5) = 0.285$; $\mathbf{P}^{capillary}(0.9) = 0.068$; $\mathbf{P}^{capillary}(0.95) = 0.041$
$\mathbf{D}_{Cl}^{capillary}(0.5) / \mathbf{D}_{Cl}^{capillary}(0.9) = (0.285/0.068)^2 = 17.6$
$\mathbf{D}_{Cl}^{capillary}(0.5) / \mathbf{D}_{Cl}^{capillary}(0.95) = (0.285/0.041)^2 = 48.3$

In eq.(3) and eq.(5) it is assumed that $\mathbf{D}_{Cl}$ does not depend on the concentration of chlorides in the liquid. But it can turn out, that "big" amounts of bound chlorides or other salts or compounds which are bound to the cement paste can "block" the smallest capillary pores. The consequence of this is lower effective chloride diffusivity than in the above relations.

Marine concrete may be divided into surface concrete and bulk concrete. The surface concrete is affected by sea water, resulting in a densification of the surface concrete due to precipitation of magnesium and calcium salts. Thus, the surface concrete capillary porosity is significantly reduced. The bulk concrete, however, changes very little over time according to experimental data from the new Ölandbridge (no change 6 months - 3.8 years).

Binding of chlorides

The binding of chlorides in concrete probably depends on the specific surface of the hydrated cement and on the concentration of the chlorides in the pore solution. As a simplification we can write

$$Cl_{bound} = K_1 \cdot 0.065 \cdot \alpha \cdot C + K_2 \cdot Cl_{solution} \quad (6)$$

K_1 = a constant that depends on the type of cement and so on. It describes the amount of chlorides which are bound per unit surface of hydrated cement paste independent of the concentration of the chlorides in the pore solution.

$0.065 \cdot \alpha \cdot C$ = the "specific" surface of the cement per m^3 concrete

K_2 = gives the relation between the amount of chlorides, which are bound to the pore structure, when the concentration of the chlorides is changed one unit

The "positive" effect of carbonation (on capillary porosity) is to some extent counteracted by the release of bound chlorides, since carbonated paste binds few or no chlorides. Thus, an increased concentration of free chlorides will result in accelerated Cl-penetration (steep Cl gradient).

Combined effects of moisture and chlorides

One example: During the modelling we can probably assume that the concrete in the inner parts of the construction has a moisture state which is approximatly the same as when the concrete has membrane curing. It is then easy to calculate the moisture content by volume in this part of the concrete.

$$w_{membr.cur} = w_0 / C \cdot C - 0.25 \cdot \alpha \cdot C \quad (7)$$

$w_{membr.cur}$ = the moisture content by volume during membrane curing (kg/m^3)

Hypothetical curves of distribution of the moisture (RH) and the chlorides are shown in FIG. 4 before and after exposure to chlorides for some time. The moisture content is the same in all the sections in both cases.

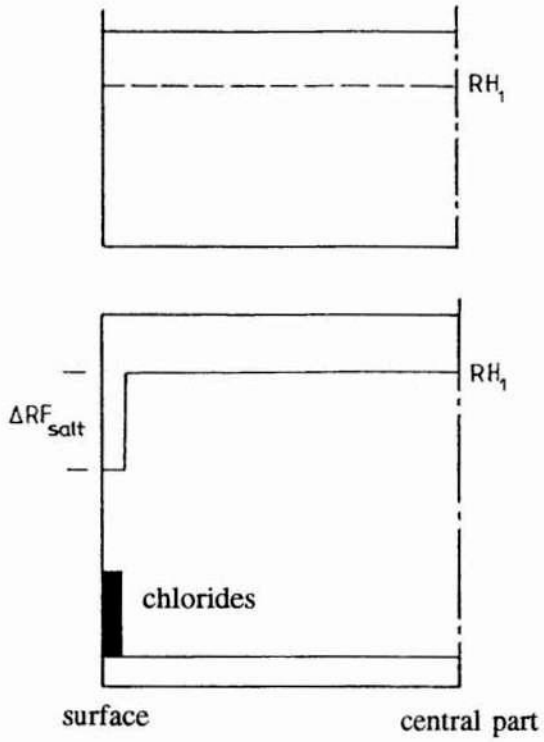

FIG. 4 Hypothetical distribution curves of RH and chlorides in concrete, before and after some hypothetical very rapid chloride penetration. The whole section of the concrete has the same moisture content.

The chloride content in the pore solution lowers RH in the part of the section where there are chlorides. The higher chloride content, the lower RH. The concrete is now sealed, so neither moisture nor chlorides can be transported to or from the section. A redistribution now occurs within the section; moisture is transported to where RH is lowest. This moisture dilutes the chloride concentration in this part of the section. At the same time there is a transport of chlorides towards the central part of the concrete, see FIG. 5 below. The moisture transport continues until RH is the same in the whole section. The

moisture content, however, is not the same, as the sorption isotherms are affected by the concentration of the chlorides in the pore solution. The moisture transport is probably much faster than the chloride transport. This means that when RH is the same in the whole section the chloride profile is not equalized. As the chlorides are leveled out there is a change in RH and consequently a redistribution of the moisture content in the concrete. When the chloride profile is equalized in the whole section, then RH also is equalized, but at a lower value than before the chlorides entered the section. In the above discussion we have not considered the influence of hydration or different moisture isotherms (adsorption and desorption).

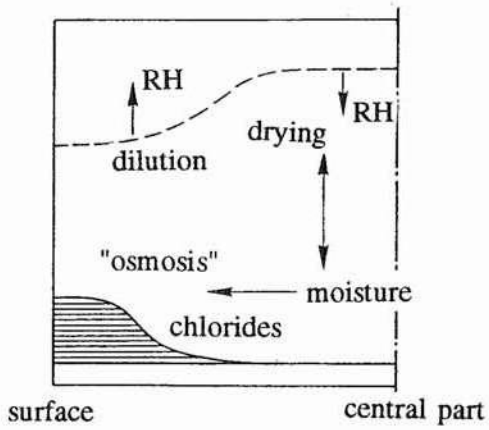

FIG. 5 Chloride- and moisture transport in the concrete in FIG. 4.

If the concrete is saturated with water at the "chloride front" and water is transported from the inner parts of the concrete, this front will be pressed inside or outside due to the "increase of volume" of the chloride water (water is transported faster than chlorides).

Influence of carbonation on the moisture properties

Kropp /9/ has shown that carbonation of cement paste changes the desorption isotherms quite substantially, see FIG. 6.

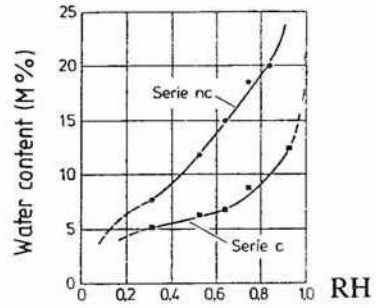

FIG. 6 Desorption isotherms for non-carbonated cement paste (Series nc) and carbonated cement paste (Series c). $w_0/C = 0.5$. Kropp /9/.

The total porosity of the non-carbonated cement paste is 42 %, which gives the moisure content by mass at capillary saturation as 35 %. The total porosity of the carbonated cement paste is 28 %, and an approximative calculation gives the moisture content by mass as 23 %. If we assume that at 45 % RH the small pores (gel pores) are filled with water and bigger pores (capillary pores), which transport water, are starting to fill up at 45 %, we can calculate the ratio between the bigger pores (35-10)/(23-6) = 1.47. This quotient, if it is squared (≈2.2), is in principle a measure of the moisture permeability at saturation /10/.

In FIG. 7 the moisture permeability is shown for cement mortar with w_0/C 0.5, which is non-carbonated (nc) and carbonated (c).

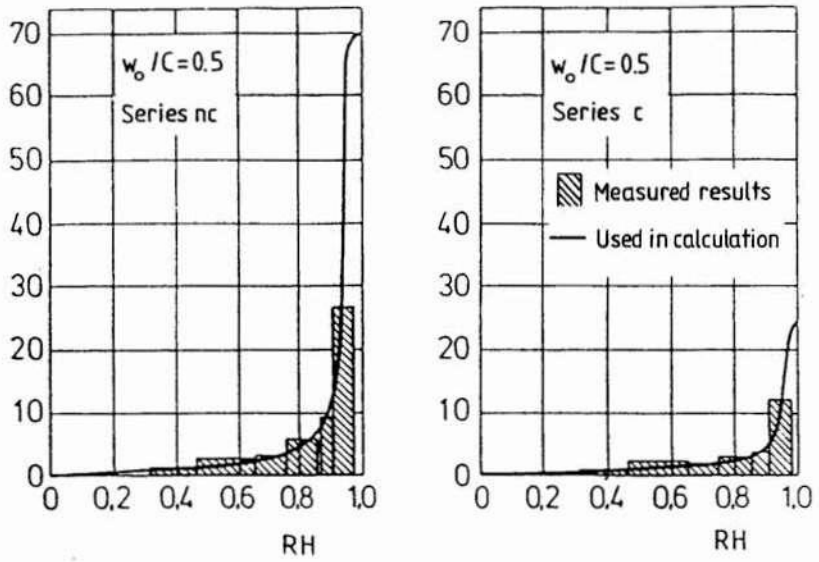

FIG. 7 Moisture permeability for cement mortar with w_0/C 0.5, which is non-carbonated (nc) and carbonated (c). Kropp /9/.

In FIG. 7 it is clearly shown that the carbonation of cement mortar influences the moisture permeability. At high RH a reduction to about 1/3 of the value for non-carbonated cement mortar is achieved.

When comparing the highest measured moisture permeability for non-carbonated and carbonated cement mortar, the quotient between them is (26/12) ≈ 2.2, which is the same as the "theoretical" value on page 8.

Kropp also shows results of the water permeability (K) for non-carbonated and carbonated cement mortar with w_0/C 0.5. $K = 54.4 \cdot 10^{-14}$ (m/s) for non-carbonated cement mortar and $K = 8.6 \cdot 10^{-14}$ (m/s) for carbonated cement mortar. The quotient between the two values is about 6.
The water permeability for cement paste can be described as a function of the

capillary porosity raised to 3.33 (in principle the Kozeny-Carman equation). On page 8 it is shown that the ratio between the capillary porosities for non-carbonated (nc) and carbonated (c) cement paste is about 1.5. This value raised to 3.33 gives about 4. The value 4 is in the same magnitude as the quotient for the measured results (about 6).

In /9/ Kropp has also shown measured drying of two 135 mm thick specimens made of cement mortar. One specimen was non-carbonated and the other specimen was carbonated to a depth of 10 mm from the drying surface. The results are shown in FIG. 8.

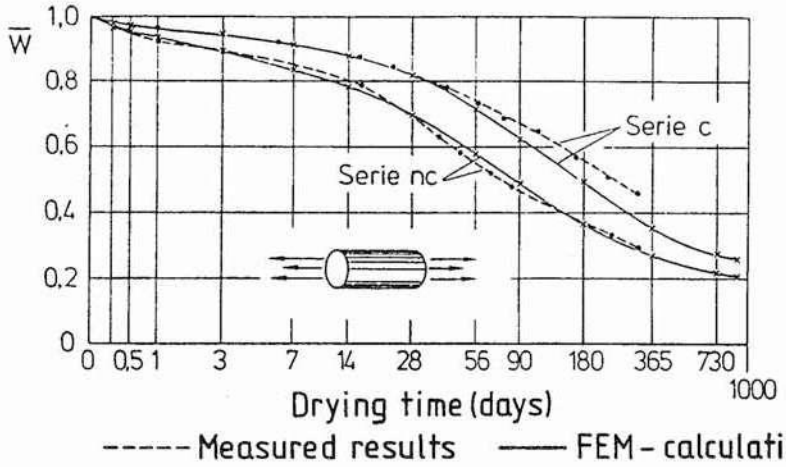

FIG. 8 The drying of specimens of cement mortar with and without a carbonated 10 mm thick zone at the drying surfaces. Kropp /9/.

In FIG. 8 it is clearly shown that the carbonated zone changes the drying time of the cement mortar.

Influence of carbonation on the effective chloride diffusivity

In FIG. 3 it is shown that the effective chloride diffusivity depends approximatly on the capillary porosity raised to two. When the concrete is carbonated the capillary porosity is reduced, see for example FIG.6.

References

1 Metha P.K. (1986), "CONCRETE, Structure, Properties and Materials". Prentice-Hall, Inc., Englewood Cliffs, New Jersey, USA.

2 Hedenblad G. (1993), "Moisture Permeability of Mature Concrete, Cement Mortar and Cement Paste". Report TVBM-1014, Divison of Building Materials, Lund Institute of Technology, Lund, Sweden.

3 Arfvidsson J. (1989), "Computor model for two-dimensional moisture transport, Manual for JAM-2". Lund Institute of Technology, Dept. of Building Technology, Lund, Sweden.

4 Arfvidsson J. & Claesson J (1989), "A PC-based method to calculate moisture transport , heat and mass transfer in building materials and structures", editors Chaddock J.B. & Todorvic B., Hemisphere Publishing Corporation.

5 Hedenblad G. (1988), "Effect of Soluble Salt on the Sorption Isotherm". Report TVBM-3035, Division of Building Materials, Lund Institute of Technology, Lund, Sweden.

6 Sandberg G. (1994), "Kloridinitierad armeringskorrosion"

7 Fagerlund G. (1982), "Concrete Handbook" Chapter 8:2. AB Svensk Byggtjänst, Stockholm, Sweden.

8 Sandberg P. (1994), Private communication

9 Kropp J. "Struktur und Eigenschaften karbonatisierter Betongrandzonen". Bautenshutz · Bausanierung /9.Jahrgang.

10 Hedenblad G. Unpublished Material

NUMERICAL SIMULATIONS OF CHLORIDE PENETRATION

Björn Johannesson 10 Jan 95
Building Materials, Lund Institute of Technology
John Ericssons väg 1, Box 118, S-221 00 LUND
Telephone: +46 46 104052, 107000
E-mail: Bjorn.Johannesson@byggtek.lth.se

ABSTRACT

The differential equations describing ion penetration into concrete has been dealt with. These equations have been solved with the finite element method. Calculations demonstrate the importance of determining the binding rate $\overline{Q}$ [ions / (s m^3)] for chloride ions. The binding rate $\overline{Q}$ depends on the concentration in the pore solution, moreover it probably exists a maximum value for the amount of physically bounded chloride ions. This value must be determined after a long exposure time. Furthermore, the binding rate strongly effects the rate of flow of chloride ions since the physical binding removes ions from the diffusion process. To achieve an appropriate physical explanation for the chloride penetration into concrete which allows us to extrapolate the behaviour in time eventually leads us to the two parameters, binding rate $\overline{Q}$ and the 'true' diffusion coefficient $D\,[m^2/s]$. The method of solving the differential equations describing ion diffusion allows us to have the material parameters $\overline{Q}$ and D depending upon relative humidity, rate of hydration, depth etc.

1 INTRODUCTION

In the numerical simulation of chloride penetration into concrete by computational analysis, proper modelling of the material properties is a key issue. A careful theoretic analysis contributes to methods of measuring chloride penetration, and it informs us of which conclusions that could be made from measurements. The simulation presented in this report has been performed using a finite element code combined with personal programming for material modelling. The influence of several parameters should be considered in order to describe the penetration of chloride ions into concrete, for example.

1.) Diffusion coefficient
2.) Binding rate
3.) Temperature
4.) Moisture content

The parameters of greatest interest in this report are 1 and 2. The aim of the project is to create a theoretic model that makes it possible to evaluate existing data, moreover suggestions to complementary measurements have been proposed. All of the used equations in the theoretic model have been carefully derived. The theory of the finite element method will not be described here, but it can be studied elsewhere, e.g. Ottosen and Peterson 1992 [6] and Zienkiewicz and Taylor, vol. 1 1989 [10] and vol. 2 1991 [11].

2 DIRECT FORMULATION OF TIME DEPENDENT PHYSICAL PROBLEMS SUCH AS CHLORIDE DIFFUSION

2.1 The 'quasi -harmonic' equation with time differentials.

In many physical problems the quasi -harmonic equation takes up a form in which time derivatives of the unknown function Φ occur [11]. In the general three -dimensional case typically we might have

$$\frac{\partial}{\partial x}\left(k\frac{\partial \phi}{\partial x}\right)+\frac{\partial}{\partial y}\left(k\frac{\partial \phi}{\partial y}\right)+\frac{\partial}{\partial z}\left(k\frac{\partial \phi}{\partial z}\right)+\left(\overline{Q}-\mu\frac{\partial \phi}{\partial t}-\rho\frac{\partial^2 \phi}{\partial t^2}\right)=0 \qquad (2.1)$$

Equation 2.1 with $\rho = 0$ is the standard transient heat conduction equation [1], the same equation holds for diffusion of ions. In the above, quite generally, all the parameters may be prescribed as functions of time, or in non -linear cases of Φ, as well as of the space coordinates $\mathbf{x}$, $\mathbf{x}=[x\ y\ z]$, i.e.

$$k = k(\mathbf{x},\phi,t) \qquad \overline{Q} = \overline{Q}(\mathbf{x},\phi,t) \qquad \text{etc.} \qquad (2.2)$$

In diffusion problems, k is identified as the diffusion constant, in the isotropic case. $\overline{Q}$ is the ion supply constant, or source term. In the standard transient heat conduction equation, k stands for the heat conductivity [W/m K] and the constant μ stands for heat capacity [J/kg K]. However, determination of μ is in general difficult as the knowledge of the viscous matrix μ is lacking for many different kinds of diffusion processes such as diffusion of chloride ions. It is often assumed, therefore, that the viscous matrix μ is a linear combination of the diffusion constant [11], i.e.

$$\mu = \alpha k \qquad (2.3)$$

Here α is determined experimentally. The constant α is a combined property of the viscosity for the transported medium and the degree of dense of the material in which the ions are transported in, i.e. the diffusion constant k. The constant α is often referred to as the diffusion coefficient D_α in problems dealing with chloride penetration. D_α is not to be mistaken for the diffusion constant, k.

$$\alpha = \frac{\mu}{k} = D_\alpha \qquad (2.4)$$

The property of the ion supply, $\overline{Q}$, is a most useful material parameter, because the amount and rate of physically, immobilised, chloride ions could be described. It will be shown later that $\overline{Q}$ (the rate of the flow of free ions from pore solution to concrete structure) influences the amount of penetrated ions strongly.

3 DERIVATION OF DIFFUSION TRANSPORT EQUATION IN ONE -DIMENSION.

Let us now establish the differential equation which controls the ion flow in a material [6]. For this purpose, consider an infinitely small part dx of the material, as shown in figure 3.1.

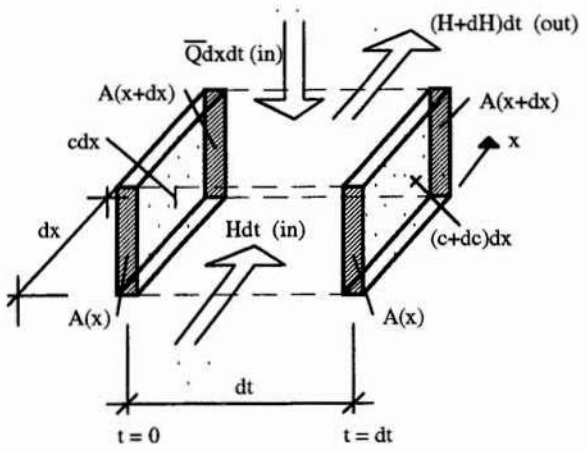

H =The amount of ions flowing in per unit time [ions /(m^2 s)]

$\overline{Q}$ =The amount of ions flowing in. $-\overline{Q}$ is the amount of ions which are being immobilised per unit time [ions /(m^3 s)]

c = The concentration of ions [ions / m^3]

x = The space coordinate [m]

t = time [s]

Figure 3.1 Infinitely small part of the material under an infinitely short time

In this figure, H denotes the ion inflow per unit time at position x and H + dH denotes the ion outflow per unit time at position x + dx. Both H and H + dH are considered positive when directed along the x -axis. We also have an ion supply per unit time given by $\overline{Q}$dx. $\overline{Q}$ is considered positive when ions enter the diffusion process.

Let us first establish a balance or conservation equation. We can express the fact that the total ion inflow per unit time equals the total ion outflow per unit time. With references to figure 3.1, we have

$$Hdt - (H + dH)dt + \overline{Q}dxdt = (c + dc)dx - cdx \tag{3.1}$$

i.e.

$$\overline{Q} = \frac{dH}{dx} + \frac{dc}{dt} \tag{3.2}$$

We next invoke a constitutive, i.e. a relation which describes how ions flow within the material. With c being the concentration and D_{cl} the diffusion coefficient for chloride ions in the material. Fick's law of diffusion from 1855, then states that the flux q is given by

$$q = -D_{cl}\frac{dc}{dx} \tag{3.3}$$

where q is now the number of ions passing through a unit area per unit time, i.e. q has the dimension [ions/m^2 s]. The diffusion coefficient D_{cl} then takes the dimension [m^2/s].

By definition, H can be described with the flux q(x) and the cross section area A(x). In figure 3.1 has H already been treated as a flux of ions, i.e. the cross section area A(x) is equal to A = 1 in a one -dimensional problem. We have

$$q(x) = H(x) \tag{3.4}$$

Insertion of the constitutive relation (3.3) into (3.2) yields (with help from (3.4)) the following differential equation.

$$\overline{Q} = -D_{\alpha} \frac{d^2c}{dx^2} + \frac{dc}{dt} \tag{3.5}$$

i.e.

$$\frac{dc}{dt} = D_{\alpha} \frac{d^2c}{dx^2} + \overline{Q} \; ; \qquad 0 \le x \le L \tag{3.6}$$

The one -dimensional ion diffusion equation established, applies for a region where the equation holds, i.e. in this case noted with $0 \le x \le L$. We now observe that equation 3.6 is the same equation as (2.1) with $\rho = 0$.

In order to solve this differential equation, we require boundary conditions at the ends of the interval $0 \le x \le L$. As we have a second -order differential equation we must require two boundary conditions. At the ends we may assume either that the concentration c is given or that the flux q is given. If, for example, the concentration at the surface of the concrete is known, this would be one boundary condition. Far enough from the surface we know that the flux q is zero, this would be our second boundary condition, i.e.

$$\begin{aligned} c(x = o) &= g \\ q(x = L) &= -\left(D_{\alpha} \frac{dc}{dx} \right)_{x=L} = h \end{aligned} \tag{3.7}$$

where h and g are known quantities.

The so -called strong formulation of our problem is then given by the differential equation (3.6) together with the boundary conditions (3.7). These types of equations can be solved with, for example, the finite element method. This method requires discretization of the space elements, as well as for the time elements. The calculations of chloride penetration in the next chapter has been carried out with the finite element method.

4 INTERPLAY BETWEEN THE DIFFUSION AND THE BINDING RATE

Measurements have indicated that the concentration of ions in the concrete is considerably higher than the outer concentration. This means that chloride ions in the pore solution must be removed to a state where the ions no longer influence the diffusion process. Ions which are removed from the pore solution will be absorbed in the concrete structure. Measurements carried out in Lund on the surface concentration on concrete specimens exposed to chloride ions indicates that the amount of immobilised chloride ions is about six times higher than the amount of ions in the pore solution, after three months exposure time [3]. In this study it has been assumed that the concentration in the pore solution, near the surface, is equal to the concentration in the solution that the specimen has been exposed to.

The pure diffusion of ions must be influenced by the fact that ions are removed from the pore solution. This is taken care of by the term $\overline{Q}$ in equation (3.6). According to figure 3.1, the term $\overline{Q}$ is negative in the case of removed ions. We might as well state that $\overline{Q}_{\alpha} = -\overline{Q}$, and call the term $\overline{Q}_{\alpha}$ the binding rate [ions/m^3 s].

Furthermore there must exist a relation between the binding rate $\overline{Q}_{\alpha}$ and the concentration c in the pore solution, figure 4.1. This relation could be investigated by measuring concentrations of ions at the exposed surface of the concrete at different times. This test should also be done with different concentrations in the saline water which the specimens are exposed to. These types of tests could also result in that we are able to measure the diffusion coefficient D_{α}, since we consider the binding rate $\overline{Q}_{\alpha}$ at the same time. There are good possibilities that the most important material parameters, which needs to be known to make extrapolation in time, could be measured simply by studying the surface concentrations for different times and different outer concentrations.

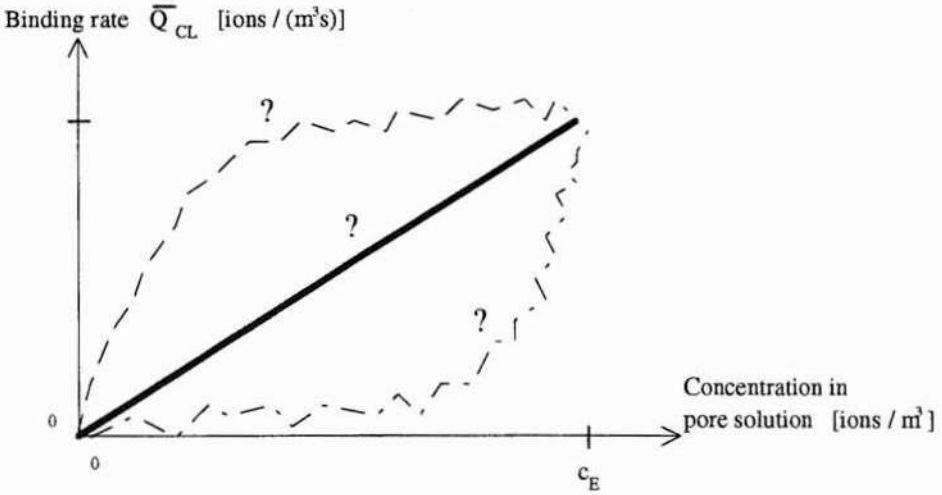

Figure 4.1 Relation between the binding rate and the concentration in the pore solution. c_E *is the concentration when the outer surrounding concentration and the pore solution concentration are equal.*

To illustrate the importance to deal with the immobilised chloride ions in a proper way, some calculations have been done. In figure 4.2 are some chloride profiles for different times shown. This calculation have been carried out without considering that ions immobilise into the concrete structure.

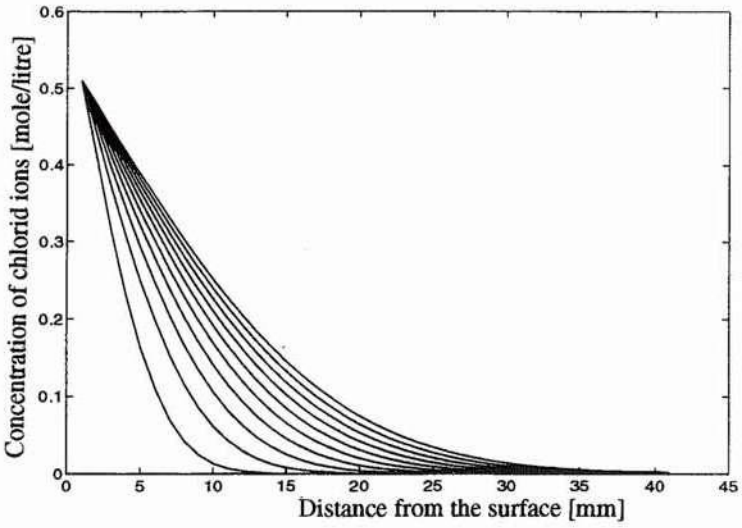

Figure 4.2 Calculation with D_{cl} = 4e-12 [m^2/s]. The outer concentration is 0.52 [mole/litre], which correspond with normal sea water. All ions are considered as free. The first curve shows the profile after 25 days, the time interval then increases with 25 days up to 250 days (from left to right).

We now make another calculation (see figure 4.4) with the same value of the diffusion coefficient, D_{cl} = 4e-12 [m^2/s]. But at the same time we consider that ions are immobilised at a rate of $\overline{Q}_{cl}$ = 2.35e-8 [mole/litre s], when the pore solution concentration is equal to c_E, according to figure 4.1. Further the binding rate must depend on the actual concentration in the pore solution. In the next example it is assumed that this dependent is linear down to zero as shown in the middle curve in figure 4.1. This kind of assumption is also illustrated in figure 4.3.

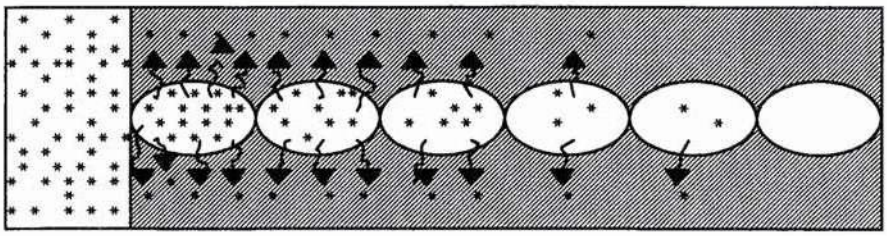

Figure 4.3 Relation between the binding rate (illustrated with arrows) and the concentration in the pore solution. The concentration c_E is the outer concentration (at left in the figure). It should be observed that the removed ions influence the driving force, the potential.

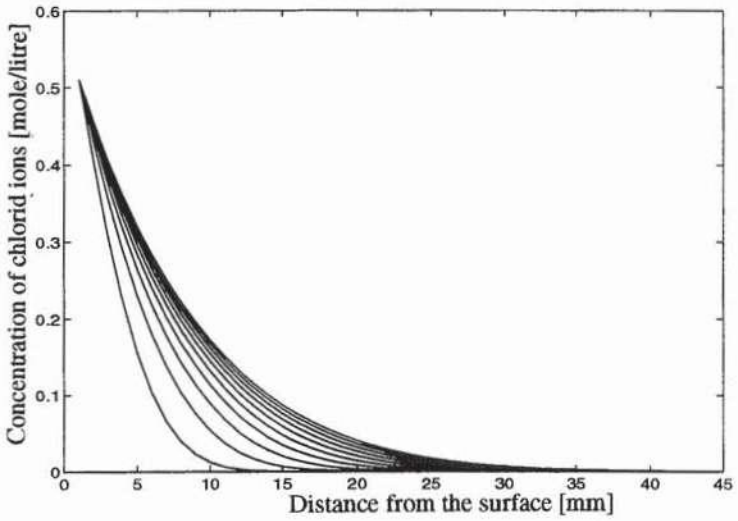

Figure 4.4 Calculation of the free chloride ions with D_{cl} *= 4e-12 [m²/s]. The outer concentration is 0.52 [mole/litre], which correspond with normal sea water. Simultaneous with the diffusion process there is an outflow of ions, ions are being immobilised, to a rate of* $\overline{Q}_{cl}$ *= 2.35e-8 [mole/litre s], when the concentration in the pore solution is equal to* c_E*. The outflow of free ions to immobilised ions is assumed to be proportional to the actual concentration according to the middle curve in figure 4.1. The first curve shows the profile after 25 days, the time interval then increases with 25 days up to 250 days (from left to right).*

In the next calculation the sum of the free and immobilised ions has been studied, see figure 4.5.

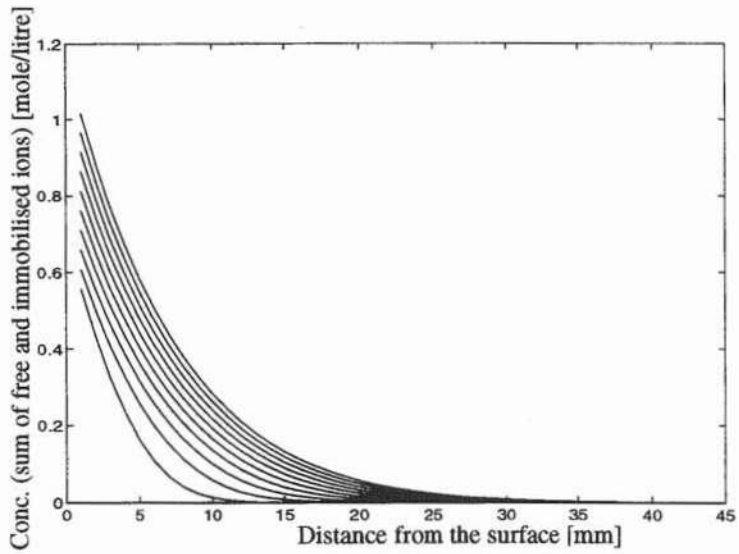

Figure 4.5 Calculation of the sum of free chloride ions and immobilised ions. The input data is the same as in the previous example, see figure 4.4, the difference is that in this calculation the amount of ions flowing out has been recorded. It should be noted that the concentrations of ions in the concrete structure increases to a higher value than the outer concentration, (0.52 [mole/litre]). . The first curve shows the profile after 25 days, the time interval then increases with 25 days up to 250 days (from left to right).

It is experimentally proved that the chloride penetration behaves in a similar manner as shown in figure 4.4 [8],[3], i.e. the surface concentration increases to a certain limit that is higher than the outer concentration.

Since only the free chloride ions contribute to making further movements of ions to lower concentrations, there are no similarities between the curves shown in figure 4.2 and 4.4. This is an important statement, if this phenomena is not taken in account there could not be any realistic extrapolations of chloride profiles in time. By measuring the bonding rate $\overline{Q}_{\alpha}$, curves like the ones shown in figure 4.5 could be calculated. These types of curve are actually the chloride profiles that could be measured in the lab.

When chloride profiles are measured it is almost impossible to separate the free and immobilised ions [7], the results from measurements gives the sum of free and immobilised ions, as shown in figure 4.5. It is no use to make a curve fitting on these profiles to get a diffusion coefficient which correspond with the data. The reason to this is simple, the appearance of the chloride profile is strongly influenced of the immobilised ions, and these ions do not move as the free ions do. There are also difficulties involved with calculating the amount of free chloride ions along a chloride profile curve that contains the sum of free and immobilised ions. The reason for this is that the binding rate $\overline{Q}_{\alpha}$ is history dependent, i.e. the binding rate depends on the actual concentration in the pore solution. It should be observed that it is impossible to model chloride penetration by changing only the diffusion coefficient (often referred as D_{EFF}) as the outflow of ions from the pore solution influence the driving force, the potential, which controls the diffusion process.

All the problems to evaluate the measured chloride profiles, discussed above, would be solved if we were able to measure the binding rate $\overline{Q}_{\alpha}$:s relation to the pore solution and the 'true' diffusion coefficient D_{α}. These properties could probably be found by studying the surface concentration with different outer concentrations, as discussed before.

At last it should be mentioned that there must exist a maximum value of immobilised ions. When this value is reached, free ions will pass through the concrete without being immobilised. To illustrate this phenomena the next calculation has been carried out with the assumption that the concrete structure is able to immobilise ions to a maximum level of 0.25 [mole / litre] :

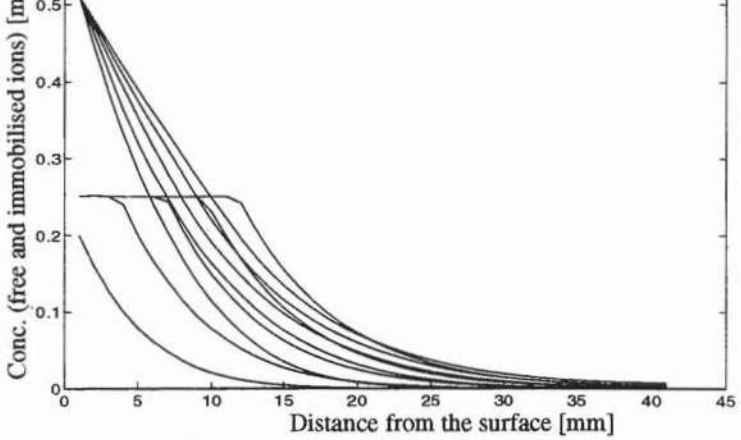

Figure 4.6 Calculation of the free chloride ions (upper curves) and immobilised ions (lower curves). Computation of the free chloride ions with D_{Cl} *= 4e-12 [m²/s]. The outer concentration is 0.52 [mole/litre], which correspond with normal sea water. Simultaneous with the diffusion process there is an outflow of ions, ions are being immobilised, to a rate of* $\overline{Q}_{Cl}$ *= 2.35e-8 [mole/litre s], when the concentration in the pore solution is equal to* c_E*. Moreover the concrete structure is able to immobilise ions to a maximum level of 0.25 [mole / litre] . The outflow of free ions to immobilised ions is assumed to be proportional to the actual concentration according to the middle curve in figure 4.1. The first curve shows the profile after 100 days, the time interval then increases with 100 days up to 500 days (from left to right).*

Performed tests indicate that the amount of ions in pore solution is at least six times smaller than the amount of ions which are immobilised [3], after three months exposure time. This means that the previous example should have been more realistic if it was calculated with a maximum value of immobilised ions of 2.5 [mole/litre] (ten times larger than the maximum concentration used in the example shown in figure 4.6).

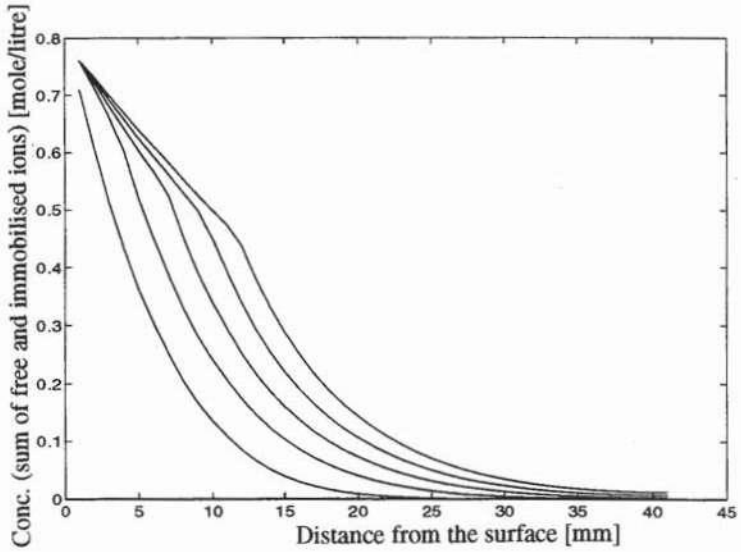

Figure 4.7 Calculation of the sum of free chloride ions and immobilised ions. The input data is the same as in the previous example, see figure 4.6.

5 REFERENCES

[1] Crank, J. 1986. *The mathematics of diffusion, second edition*, Clarendon press, Oxford.

[2] Fagerlund, G. 1990. *Betongkonstruktioners beständighet, en översikt.* Cementa.

[3] Janz, M. and Johannesson, B. 1993. *En studie av kloridinträngning i betong, med försök till livslängdsberäkning.* Rapport TVBM-5026. Avdelningen för Byggnadsmaterial, Lunds Tekniska Högskola.

[4] Johannesson, B. 1994. *Numerisk simulering av kloridinträngning i betong, del 1.* Rapport TVBM-9021. Avdelningen för Byggnadsmaterial, Lunds Tekniska Högskola.

[5] Johannesson, B. 1994. *Numerisk simulering av kloridinträngning i betong, del 2.* Rapport TVBM-9022. Avdelningen för Byggnadsmarerial, Lunds Tekniska Högskola.

[6] Ottosen, P. and Peterson, H. 1992. *Introduction to the finite element method.* Prentice Hall, London.

[7] Peterson, O. 1993. *Provning av kloridanalys på betong.* Rapport TVBM 7045 Avdelningen för Byggnadsmaterial, Lunds Tekniska Högskola.

[8] Sandberg, P and Larsson, J. 1993. *Chloride binding in cement pastes in equilibrium with synthetic pore solutions, second draft.* Euroc Research Ideon Lund.

[9] Tuutti, K. 1982. *Corrosion of steel in concrete.* CBI research Fo 4:82. Stockholm.

[10] Zienkiewicz, O. C. and Taylor, R. L. 1989. *The finite element method, fourth edition, vol. 1.* McGraw-Hill, London.

[11] Zienkiewicz, O. C. and Taylor, R. L. 1991. *The finite element method, fourth edition, vol. 2.* McGraw-Hill, London.

[12] Information from reports produced in association with *'Nordiskt miniseminarium, kloridinträngning i betongkonstruktioner'*. 1993. Byggnadsmaterial, Chalmers Tekniska Högskola, Göteborg.

THEME 4

Electrochemistry

THE CHLORIDE THRESHOLD OF STEEL IN CONCRETE - IS IT A FUNCTION OF POTENTIAL ?

Hans Arup - Hans Arup Consult
Dyreborgskovvej 16
DK-5600 Faaborg

ABSTRACT

The meaning of the expression "chloride threshold" is discussed, and it is argued, that it must depend on a number of factors, including the potential of the embedded steel. In a recently started research project it is attempted to determine chloride thresholds as a function of the applied potential. A special test unit for use in this work is described.

1. Introduction

The "chloride threshold" for steel in concrete is the maximum amount of chloride, which can be tolerated in concrete, if corrosion of the embedded steel shall be prevented. This is not a very precice definition; both the pH of the concrete porewater, the permeability of the concrete and the potential of the steel - and maybe other factors - are important and will be discussed later.

It is generally agreed, that thresholds determined in solutions are not valid for steel in concrete, and the same applies to thresholds determined in concrete with mixed-in chlorides. It is necessary to have specimens with chloride diffusing in from the surface, wait for corrosion to initiate and then determine the chloride content at the level of the steel surface either by analysis of a thin layer of concrete near the steel surface or by calculation based on diffusion data.

Normally the primary analytical data obtained in such tests are in units of chloride by weight of total (dry) mass of sample. This is useful for life time predictions based on chloride profiles measured in the field, which makes use of the same units. But the pH is also important and is seldom measured in the same sample. The pH is initially determined by W/C-ratio and the binder components and in service it will be affected by leaching water or carbonation (which also affect chloride binding), and they normally act differently in laboratory samples compared to structures exposed in natural environments.

More consistent results might be expected, if it were possible to express experimental data in term of pore water chemistry (pH and chloride concentration). Pore water expression or leaching of samples can be attempted, or calculations can be made. Pore water analysis would then suffice for the prediction of thresholds in e.g. concretes with puzzolanic additions, which influence the pH of porewater. But comparable data are difficult - and expensive - to obtain from samples taken in the field.

It is also known - or at least strongly suspected - that the threshold is also a function of the

potential of the embedded steel. Or vice versa, that there exists a critical potential - a pitting potential - which is a function of the chloride level. The rest of the paper will discuss this and other factors.

2. The potential as a factor in threshold determinations.

H. Arup was perhaps the first to present results from longterm potentiostatic tests on steel in concrete (1), but this was in chloride-free concrete, and the design of the test electrodes was not very fortunate.

C. Hansson and B. Sørensen (2) determined chloride thresholds for steel held at one constantly held potential in cement mortar test samples exposed to chloride. The potential was chosen to represent the highest potential likely to be met in field exposure, but tests were not done at a range of potentials. A similar form of exposure had earlier been used in Austria. Later B. Sørensen with other co-authors (3) has used a range of potentiodynamic, slow potential stepping and potentiostatic techniques to characterise stainless steels and a black steel reference sample in concrete with chloride either mixed in or entering by diffusion.

The use of impressed potentials, which are below or close to the highest potential likely to be met in practice, i.e. below the oxygen equilibrium potential, will not change the chemical environment around the embedded steel. Some accelerated tests use much higher potentials or impressed currents, which will acidify the surrounding concrete and inevitably induce corrosion.

The potential of steel in a real concrete structure is a function of oxygen availability, and steel in permanently wet concrete or in concrete under water has much lower potential than has steel in concrete exposed in the atmosphere. This probably explains why steel in marine concrete structures seldom corrodes under water; corrosion always start above water, where more oxygen is available.

The spreading use of preventive cathodic protection, e.g. of motorway bridges in Italy, is based on the assumption, that the chloride threshold is raised by a lowering of potential. The applied potentials used presently could probably be lowered, if data on the dependency were available, and this might reduce the cost of this new technique.

3. Other factors.

Before largescale chloride initiated corrosion takes place, micropits will repeatedly initiate and die within a small fraction of a second. This can be detected by oscillations of the electrochemical potential. The newly formed pit can only survive, if a very high anodic current density can be maintained, so the low pH in the middle of the pit can be maintained and not be neutralised by diffusion of OH^--ions from the surrounding concrete. The current must come from the neighbouring area of the steel, acting as a cathode. But the I*R drop in the concrete, the polarisation of the cathode and the slow diffusion of oxygen will all work together and more often than not prevent the necessary rise in current, and the pit will die. Eventually a stable pit will form, and the lowering of potential around it can no longer prevent the growth of the pit, which now has a stable low pH, high chloride centre, but the initiation of new pits near it will be effectively prevented for a long time.

This model explains why other factors, such as the electrical conductivity and the diffusivity of the concrete, must be important. The two factors mentioned are closely related in water saturated concrete, but in partially dry concrete these factors change in different ways, and so will the pore water composition. The most important factor in drying concrete is perhaps the drastic increase in oxygen availability. The understanding of pitting models, diffusion, porewater changes and thresholds in semidry concrete is far from being complete !

The model also suggests, that the total size or surface of the steel sample must have an influence. A very small sample will not provide enough cathode surface to keep a small pit alive. It has been suggested in one paper, that steel fibres seem to tolerate more chloride than the solid reinforcement, and this is also to be expected. No systematic investigation of this factor seems to have been made, but it would be nice to know, if there is a limit to the size of small test samples to be used in concrete, e.g. in corrosion monitoring equipment.

It could be argued, that potentiostatic testing at different potentials will eliminate or minimise the hampering effect of limited cathode size, polarisation, oxygen availability and I*R drops. This is why a multipotential, potentiostatic technique has been developed for measuring the potential dependence of the chloride threshold. This will be described later.

But there are still factors, we do not know enough about, if a potentiostatic test is applied. Will the "quality" of the passive film be affected by the impressed potential ? and will the quality of the film be the same, if a given potental is the result of a natural oxygen level instead of being an impressed potential, maybe in an oxygenfree concrete ? This will be a very difficult question to answer by way of experiment.

A final difficulty in all work on corrosion of steel in concrete is the large spread in experimental results. This is the experience of anybody who has dared to use multiple samples. Mainly this reflects the heterogeneity of the material, we are working with - concrete - and this is of course even more pronounced in real structures, but to some degree it is also a characteristic of pitting potential studies in pure electrolyte systems.

4. Determination of chloride thresholds as a function of potential

Early in 1993 the Swedish CEMENTA-EUROC decided to sponsor a Swedish/Danish research programme aimed at determining chloride thresholds as a function of potential, and a new test unit was designed, which made use of many years of experience at the former Danish Corrosion Centre and the AEC laboratory. The new test unit (Fig.1) has the following characteristics:

1. A large number of test electrodes - normally twenty - are used in each experiment in order to enable statistical analysis of results and reduce scatter.

2. The test electrodes are U-shaped, or rather they have their coated ends bending away from the chloride front. This will minimise the occurrence of corrosion pits being initiated at the edge of a coating or at a crevice, if a fixture is used to hold the electrode. The test electrode is therefore shaped very much like a stirrup, normally the part of the reinforcing, which corrodes first.

3. The test electrodes are prepositioned in a mortar slab with very precise dimensions. The mortar slab also contains prepositioned counter electrodes and a reference

electrode to be used in potentiostatically controlled tests. The geometry of the arrangement should minimise errors due to IxR drops. This design allows electrochemical monitoring or control from the moment of casting and it will also allow electrochemical control of specimens, which are not immersed in an electrolyte, e.g. in atmospheric or spray chamber exposure.

4. The precise geometry of the whole precast unit, which also contains precisely positioned inserts for later mounting of the test unit, means that the the exact position of each test electrode and its cover can be verified at any time. There is great freedom in the way in which the test concrete or mortar can be cast, trowelled or even sprayed over the test electrodes. Casting can be done in horizontal or vertical position, with or without formwork, and any form of posttreatment can be applied. If wanted, the whole test unit - or a modified form of it - could be installed in a real structure during construction.

The use of this test unit for the determination of chloride thresholds as a function of potential is described in detail in a specification called APM 303 by the AEC laboratory.

The principle for the test is the following:

The test concrete is cast over the test electrodes with a welldefined cover, usually obtained by diamond cutting. Two specimens are unconnected (freely corroding) the others are potentiostatically held two and two at 9 different potentials, normally over a range of 500 mV. The initiation of pitting is measured by the sudden increase of current flowing to the specimen, which is then isolated from the potentiostat.

Two or three times during the chloride exposure chloride profiles are determined by grinding. It can be done on the test block itself, but in these tests the cut-off part of the block represents an identical sample, which is used instead. Interpolation between chloride profiles - or calculation from the derived diffusion parameters - allows the determination of chloride content at the depth of cover at the time of corrosion initiation for each specimen.

References

1) Potentiostatic corrosion tests of steel in concrete for prolonged periods in field and laboratory. By Hans Arup, NACE CORROSION/79, Atlanta 1979.

2) The Threshold Value of Chloride Concentration in Concrete for the Initiation of Reinforcement Corosion, by C.M. Hansson and B. Sørensen, Proc. ASTM Symposium on "Porosity and Permeability of Concrete", 1988.

3) The Corrosion Properties of Stainless Steel Reinforcement, by B. Sørensen, Per B. Jensen and E. Maahn, in "Corrosion of Reinforcement in Concrete" Ed. Page, Treadaway and Bamforth, publ. by SCI.

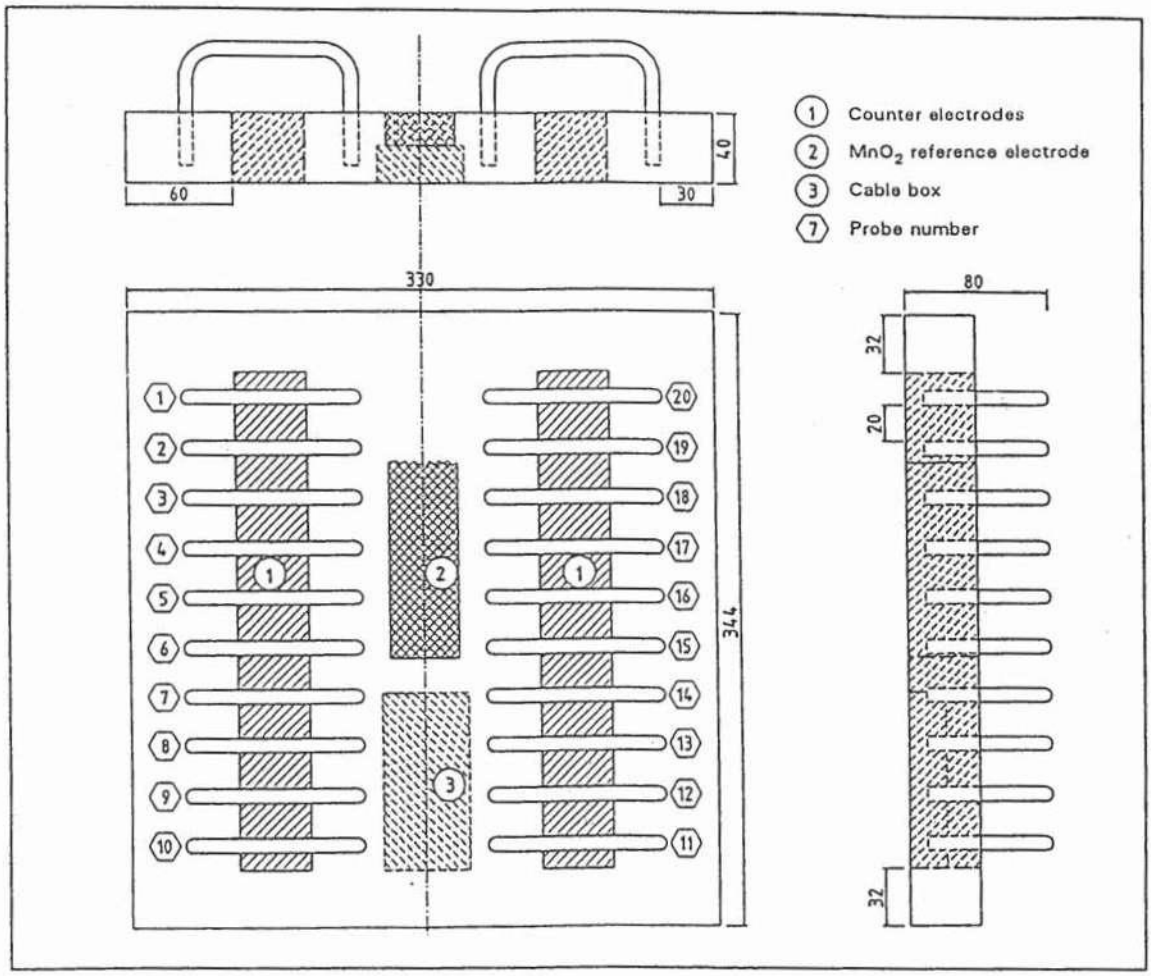

Figure 1. Drawing of test unit with 20 electrodes.

CHLORIDE THRESHOLD VALUE AND THE CORROSION RATE IN REINFORCED CONCRETE

K. Pettersson Cement och Betong Insitutet 100 44 STOCKHOLM, Sweden

ABSTRACT

Corrosion of steel in concrete occurs whenever the external influences change the composition of the pore solution to an aggressive condition. Chloride ions and carbonation of the concrete can destroy the passivity which results in corrosion of the steel.
This paper presents an investigation which shows that the critical chloride content, necessary to initiate corrosion, is influenced by the relative humidity, the water/binder ratio and additives such as micro silica. The water binder ratio is the factor that have the greatest influence on the critical chloride concentration. The corrosion rate is also strongly influenced by this factor.
The critical chloride concentration and the corrosion rate were measured indirectly and directly using polarization resistance technique.

Keywords: corrosion, chloride, corrosion rate, threshold value, silica, relative humidity, water binder ratio.

INTRODUCTION

The chloride threshold value in concrete can be defined as the highest chloride content that does not cause any risk of corrosion on the reinforcement. The chloride will get in contact with the concrete through sea water or deicing salt. The chloride content is almost always defined as the total chloride content compared to the cement content, % Cl^- per cement because it´s an easy way to analyse the amount of chlorides. We know that it´s the free chloride content in the pore solution that is the most interesting for corrosion on the reinforcement.
Different cement types have different content of alkali ions, and these ions are important for the chloride threshold value. When the critical chloride value to onset corrosion, has been reached, the corrosion will start and continue with variating rate. The identification of the corrosion start and the corrosion rate were measured with the polarization resistance technique.

In this investigation the chlorides have penetrated the concrete by diffusion or convection.
The threshold values are presented as free chloride ions in the pore solution, mg Cl^-/l
and as the $\frac{[Cl^-]}{[OH^-]}$ ratio.

Threshold value of chloride

The chloride threshold value is not a fixed value. It should rather be grouped in intervals than be given in specific values. Figure 1, Brown/1980/ shows where the acceptable chloride content is presented for uncarbonated concrete in marine condition. The chloride threshold value is one of the most important factors for the lifetime of a concrete structure. Hausman /1967/ indicated critical chloride concentrations which initiate the corrosion process for steel in basic solutions. According to Hausmann, this threshold value is a function of the hydroxyl concentration:

$\frac{[Cl^-]}{[OH^-]} \leq 0{,}61$, the Cl- and OH^- are the concentration in mole per litre, M. This relation should give values on the safe side for mortar and concrete since the embedded steel is surrounded by a pore system that makes it more difficult for aggressive ions to reach the corrosion area.

Chloride concentration %Cl per cement weight	Possibility for corrosion
< 0.4	negligible
0.4-1.0	possible
1.0-2.0	probable
> 2.0	certain
Values usually agreed concerning the critical chloride content in not carbonated concrete around plain carbon steel. This table shows that the critical content in concrete has no constant v It depend on other parameters than only the concrete mass.	

Figure. 1 Accepted chloride concentration in uncarbonated concrete before corrosion starts

Corrosion rate

The most important factors to influence the corrosion rate are the resistivity and the oxygen content in the mortar and concrete specimens. The resistivity and the oxygen will control the cathodic process in a corrosion area. This process controls the corrosion rate. If chloride gets in mortar and concrete the resistivity will decrease and the corrosion rate will increase. If the relative humidity is more than 98% the corrosion rate will decrease because of the limiting oxygen content, Tuutti/1982/.

EXPERIMENTAL WORK

Mortar and concrete have been tested for two types of normal standard Portland cement, Degerhamn and Slite. Degerhamn is a low alkali cement and Slite is a high alkali cement.

Mortar specimens

Test specimens for chloride threshold value and corrosion rate measurement were, 100x70x25 mm3 . Three electrodes with a cover of 5 mm were cast in each specimen. A typical mortar specimens is shown in Figure 2. The middle electrode is a graphite electrode and the other one are steel electrodes. The diameter of the electrodes are 5mm.

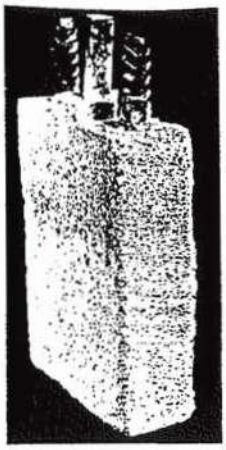

Figure 2. Mortar specimens

The w/b was varied from 0,30 to 0,75. Silica is given the efficiency factor =1. The following different curing condition were applied:

- in 80% relative humidity, 20°C.

- in 60% relative humidity, 20°C.

- in 50% relative humidity, 20°C.

- outside, not sheltered from rain.

The corrosion rate as a function of the chloride content was measured on the mortar specimens with w/b 0.50. In these specimens the chloride was admixed with 1.0, 3.0 and 5.0% Cl^- per cement weight. Sodium chloride was used. The specimens without added chloride were sprayed with saturated sodium chloride every second week until the corrosion started. In some of the specimens, 5 or 10% of the cement content was replaced with silica fume.

Concrete specimens

In the concrete slabs the threshold value was measured indirectely through the corrosion rate.
The dimension of the concrete slabs were 300x100x300 mm^3. The placing of the three electrodes was the same as for the mortar specimens. After curing, the concrete slabs were soaked for 14 days in 3% sodium chloride solutions followed by drying in 40% relative humidity air for 14 days. The slabs were exposed to this same cycle until the corrosion started.

TESTING

The linear polarisation technique was used for corrosion measurements on all the specimens. When the corrosion was initiated, the concrete near the steel was removed and analysed for chloride content with a solid state chloride electrodes. The hydroxyl content was also analysed by titration with acid solution. In the concrete slabs the chloride - respectively hydroxyl ions were leached out from 3 gram of the concrete with destillated water. In the mortar specimens the poresolution from mortar near the steel (5mm) were squeezed out. The ions were analysed as free ions in mg/1.

Polarisation resistance measurements

In 1957, Stern and Geary published their first paper on the well known relationship between a small step of potential, ΔE, applied at the corrosion potential, and the electrode response, I, which they defined as the polarisation curve for a few millivolts around the corrosion potential follow a linear relationship. The slope of this relationship is called polarisation resistance, Rp.
In a simplifide expression the I_{corr} can be shown as

$I_{corr} = B/Rp$ *where:*

$\mathbf{I_{corr}}$ is the corrosion intesity $\mu A/cm^2$

B represents a value that varies from 13 to 52 mV in the majority of metal/medium systems

Rp is the polarization resistance, kohm, Andrade et al /1986/

In order to assess the accuracy of this technique, the I_{corr} versus time curves are integrated and the 'total corrosion current' obtained is introduced into Faraday's Law to calculate the steel weight loss per square centimetre.

$$\int_0^t I_{corr}\,dt = I_{corr\,T} = \text{total current involved in the corrosion process}$$

$$g/cm^2 = \frac{I_{corrT} \cdot t \cdot Wm/V}{F} \quad \text{(Faraday's Law)} \qquad (5)$$

where

Wm = molecular weight
t = time
V = valency
F = 96500 coulombs

The technique is very fast and has the very important advantage of being non destructive.

RESULTS

A summary of the test results are shown in Figures 3-8. Typical results of the influence of the w/b on the chloride threshold values are shown in Figures 3, 4 and 5. All the mortar specimens are stored in 80% relative humidity at 20°C. The concrete slabs were stored as was explained in 3.2.
In Figures 3 and 4 the chloride threshold values are presented as mg free chlorides per litre pore solution.

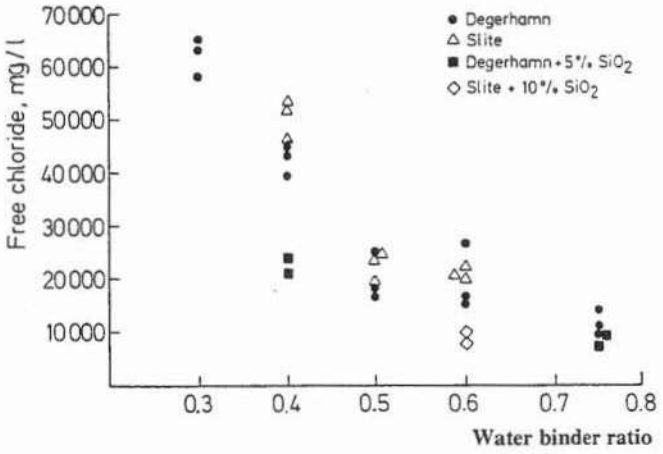

Figure 3. Chloride threshold value for mortar specimens versus the water binder ratio.

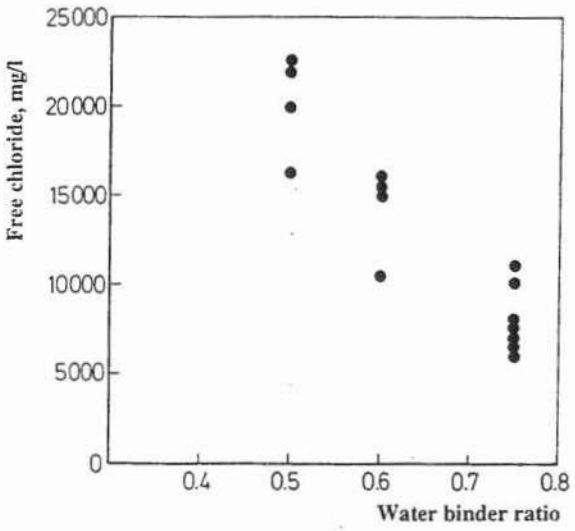

Figure 4. Chloride threshold value for concrete slabs versus the water binder ratio.

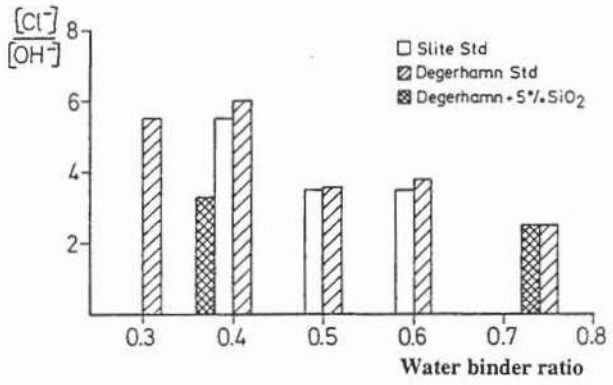

Figure 5. Chloride threshold value for mortar specimens versus the water binder ratio.

In Figure 5 the chloride threshold value are presented as the $\frac{[Cl^-]}{[OH^-]}$ ratio. The concentration is molar, M.

In Figure 6 the chloride threshold values are presented for mortar specimens with w/b 0.50 cured in different relative humudity.

Figure 7 shows the effect of the relative humidity, caused by different curing, on the corrosion rate and chloride content. The specimens were mortar with w/b 0.50.

The corrosion rate on the rebars in silica mortar is shown in Figure 8.
5 or 10% of the cement content was replaced with silica fume.

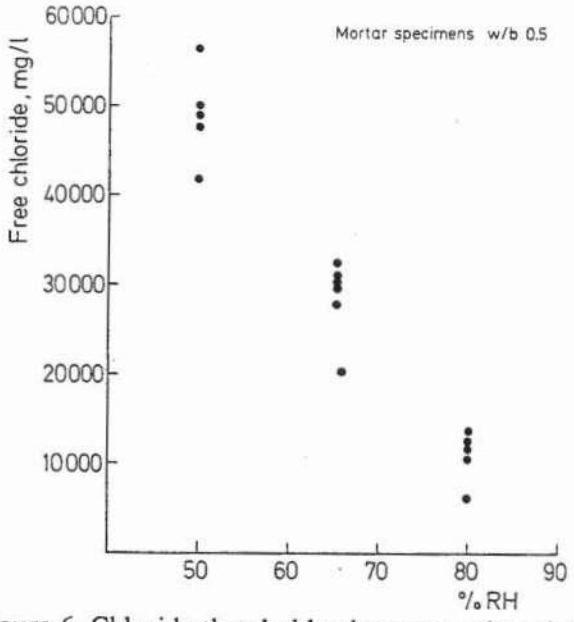

Figure 6. Chloride threshold value versus the relative humidity.

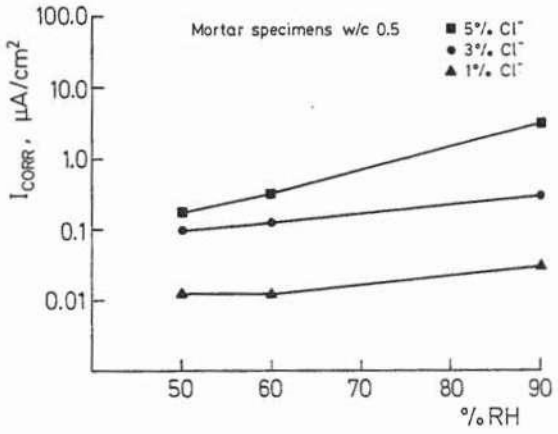

Figure 7. Corrosion rate for mortar with admixed chloride versus the relative humidity.

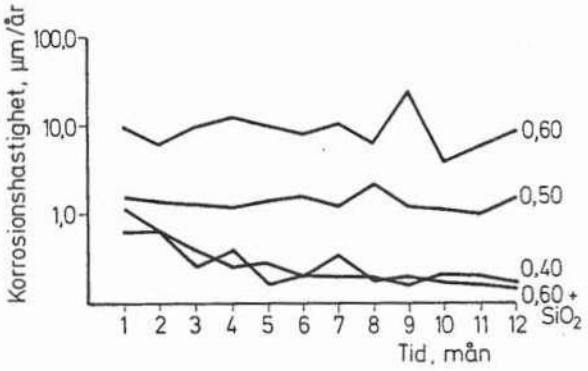

Figure 8. Corrosion rate for mortar specimens with and without micro silica.

DISCUSSION

Chloride threshold value as a function of w/b in mortar and concrete

As shown in Figures 3 and 4, the free chloride content to onset corrosion, is dependent on the w/b.
The lower the w/b the higher is the chloride content that can be tolerated before corrosion starts, Pettersson/1992/. Figure 4 shows the critical chloride content for concrete slabs. Compared to the mortar specimens, Figure 3, these chloride contents are lower. An explanation for this could be the more inhomogenous structure in the concrete. The consequence of this will be more anodic and cathodic and cathodic areas on the rebar, Tuutti/1993/. This will cause potential differences which will lead to corrosion. The mortar specimens will bring more cement paste around the rebar than the concrete does.

Chloride threshold value as a function of admixed silica

The chloride content, to onset corrosion for mortar specimens with silica, Figure 3, is less than for mortar without silica. An explanation for this could be the lower hydroxyl content in the silica specimens. Silica will consume the hydroxyl ions and the pH in the pore solution will be reduced. The lower the hydroxyl concentration is the lower chloride can be accepted.
Hanson and SØrensen/1988/ and Janz and Johannesson/1993/ shows that the initiation time for chlorides in mortar and concrete, will increase of a factor of 2-3, when silica is added.

Chloride threshold value as a function of the hydroxyl content

The chloride threshold value has been defined as the $\frac{[Cl^-]}{[OH^-]}$ ratio in some papers.

In this investigation the $[Cl^-]$ and $[OH^-]$ have been determined by analyzing 5mm thick concrete or mortar samples nearest the steel.

This investigation showed that the $\frac{[Cl^-]}{[OH^-]}$ ratio for mortar specimens was between

2,5 to 6. This is about 10 times higher than the results form Hausman/1967/. His reults were carried out from saturated calciumhydroxide solution where the oxygen content was limited. Small defects on the rebar will be very sensitive areas when the rebar is in a solution. This because the ions are more mobile in the solution and therefore it is easier to reach the defect area on the rebar, Tuutti/1993/. In the mortar specimen the passive film around the rebar will be much stronger than in a solution. An defect on the rebar will be of less importance in this case than in the solution case. It is also more difficult for the aggressive ions to reach the defect area in the mortar specimens, because of the material structure.

Chloride threshold value as a function of the relative humidity

The chloride threshold value decreased with increasing relative humidity, Figure 6. This was probably because the amount of the electrolyte in the mortar was increased with higher relative humidity. With low electolyte content it is difficult for the corrosion to start, in this case a high chloride content is needed to onset corrosion.

The corrosion rate as a function of the relative humidity and the chloride content.

Corrosion rate of the rebar in mortar increased with increasing relative humidity (within tested interval) and increasing chloride content, Figure 7.
The most important factors for ongoing corrosion is the resistivity(electolyte) and the oxygen content in the mortar. In this case the oxygen content is constant in the tested environment. The resistivity in the mortars will vary because of the chloride content and the relative humidity. The chloride ions can bind water and therefore the resistivity will decrease and the corrosion will increase. Figure 7 shows that corrosion on the rebar in mortar can proceed when the relative humidity is as low as 65% and the chloride content is 3% Cl^- per cement. This is a high chloride content for concrete structures in the field. In this investigation mortar specimens were tested and they tolerate such high chloride content.

Corrosion rate as a function of the admixed silica fume.

The mortar specimens, containing silica fume, give a lower corrosion rate than the specimens without silica fume. This is probably due to the higher resistivity in the silica specimens, Gjörv/1993/. The silica content will also give a more dense structure which will make it more difficult for the oxygen to penetrate. The oxygen and the resistivity controls the corrosion rate Wranglén/1967/. Figure 8 shows mortar specimens w/b 0.30 with 5 and 10% silica fume. The corrosion rate, after the corrosion had been initiated, is shown. Corrosion rates lower than 0,2μA/cm^2 can be defined as no corrosion rates.

CONCLUSIONS

The test results of this investigation showed that:

1. The chloride threshold value appeared to be between 65 and 10 g chloride per litre pore solution in **mortar** specimens with w/b between 0.30 and 0.75

2. The chloride threshold value appeared to be between 25 and 5 g chloride per litre pore solution, in **concrete** slabs with w/b between 0.50 and 0.75.

3. The chloride threshold value will increase when the relative humidity decrease. This will be significant for both mortar and concrete specimens.

4. Admixed silica in the mortar specimens leads to a reduction of the chloride threshold value. The corrosion rate will decrease when micro silica is added. The diffusion rate for chlorides in concrete will also decrease. We could say that the net effect of the micro silica on corrosion caused by chlorides, is therefore, positive.

5. The corrosion rate increases with increasing relative humidity.

6. Increasing chloride content leads to higher corrosion rate.

REFERENCES

Andrade, C.Castelo, V. Alonso, C and González, J: The determination of the corrosion rate of steel embedded in concrete by the polarization resistance and AC impedance methods. ASTM-STP 906, 1986, pp43-62.

Arup, H: bestemmelse af tröskelvärde for forskellige betonkvaliteter. Seminarium Marina betongkonstruktioners livslängd. 1993, Stockholm, Cementa AB.

Brown , R.D et al: Marine dutability survey of the Tongue Sand Tower, Concrete-in the Oceans Technical Report. P4 Final Report. Cement och Concrete Association. 1980, London.

Gjörv, O: Oral information, Division of Building material. University of Trondheim the Norwegian Institute of Technology, 1993.

Hausman, D. A: Steel corrosion in concrete. Materials protection, Nov, pp 19-23. 1967.

Janz, M and Johannesson, B. A study of chloride penetration in concrete with an attempt ro estimate the liftetime. Division of Building Materials University of Lund.(TVBM-5026), 1993.

Pettersson, K: Corrosion threshold value and corrosion rate in reinforced concrete. Swedish Cement och Concrete Resarch Institute. CBI report 2:92, Stockholm.

Stern, M and Geary, AL: A theoretical Analysis of the shape of Polarization Curves. Journal of Electrochemical Society, 1957, vol 4, p. 56.

Sörensen, B and Hanson, C: The threshold concentration of chloride in concrete for initiation of reinforcement corrosion. ASTM Sumposium in Baltimore, June 29, 1988.

Tuutti, K: Oral information, 1993.

Tuutti, K: Corrosion of steel in concrete. Swedish Cement and Concrete Instiute, CBI, research Fo 4:82, Stockholm.

Wranglén, G: Metallers korrosion och ytskydd. Almqvist & Wiksell AB, Stockholm, 1967.

PROBLEMS WITH ELECTROCHEMICAL METHODS FOR THE STUDY OF CORROSION OF STEEL EMBEDDED IN CONCRETE

Ketil Videm. Centre for Materials Research, University of Oslo, PO. Box 1033, 0315 Oslo, Norway.

Roar Myrdal, Rescon A/S, Vallsetvegen 6, 2120 Sagstua; Norway.

ABSTRACT.

A brief review of methods for estimation of the severity of corrosion of steel embedded in concrete is given. Then are experiments with the objective of obtaining reliable data for the polarisation resistance described and the problems of estimating the severity of corrosion discussed. The effort includes studies in the laboratory and at a concrete bridge.

KEYWORDS: Corrosion measurements, concrete, steel, polarisation resistance.

INTRODUCTION.

It is more complicated to investigate the corrosion of steel in concrete by electrochemical techniques than for metals exposed to liquids. In liquids one can usually arrange an electrode system with a good geometry. The reliability of the electrochemical measurements can be evaluated with samples that can be retrieved for inspection and weight loss determination. In concrete one is more dependent upon theoretical considerations for the interpretation of the measurements. However, the theoretical base for the interpretation of the electrochemical measurements in concrete is weaker than for exposures in aqueous solutions due to lack of homogeneity and because the environment in contact with the steel is not well known and varies from region to region.

This paper gives first a brief introduction to the various methods used to evaluate the severity of the corrosion of the reinforcement. Then experiments in the laboratory as well as in the field are described focused on obtaining more reliable estimates of the severity of corrosion.

SURVEY OF METHODS TO EVALUATE THE SEVERITY OF CORROSION.

Electrical resistance probes.

Electrical resistance probes are not electrochemical, but rely on changes of the electrical resistance of a thin strip of metal that gets thinner with on-going corrosion. As the metal gets thinner, the electrical resistance increases. Complete systems are commercially

available including probes, cables, electronics and readout systems. CorrOcean AS, Trondheim, Norway, belong to the market leaders and deliver tailor made systems of own, patented designs. Electrical resistance probes function in concrete.

Linear polarisation resistance (LPR).

The working principle and recommendations for use are outlined in ASTM guide on making "Polarisation Resistance measurements" [1]. The measurements provide instantaneous corrosion rates and are based on sound electrochemical foundations when used in liquids. The probe consists of a metal piece with a known area on which it is impressed a potential change and the current measured (or current impressed and potential change measured). The plot is linear for small changes, explaining the name "linear polarisation resistance" LPR. Potential change divided with current change is resistance. The corrosion rate, expressed as the corrosion current, is obtained by dividing an "LPR-constant" (0.026V often used) with the polarisation resistance. Probes cast into the concrete when the structure is built, are often used. Different probe designs are on the marked for application in concrete. With sensors with different concrete overlays, on can follow the increase in corrosion rate due to chloride ingress - first at the outer elements and with time for those further into the concrete. At Gimsøystraumen bridge in Northern Norway another solution has been applied, the steel reinforcement has been cut to have access to steel bars with a known length that are not in electrical contact with the main reinforcement.

LPR with guard electrodes.

The objective of instruments with guard electrodes is to carry out LPR- measurements on the main reinforcement without having access to a known and well-defined steel area. The working principle of the guard electrode is shown in Figure 1. The current is impressed by two electrodes. The outer electrode, called the guard electrode is not directly involved in the LPR-measurements, but used to direct the current perpendicular to the steel from the central counter electrode. Provided that the current flows as shown on the figure, and that the diameter of the steel bar is known, the area of the steel getting current from the central electrode is known. The corrosion rate can then be estimated from the relationship between the potential and current, as described for linear polarisation. The commercial instruments are aimed at overcoming also the problem of not having a reference electrode close to the steel. This is handled by measuring the resistance between the concrete surface and the steel with AC. The DC polarisation measurements then contain an ohmic resistant drop of the potential in the concrete, that can be calculated and corrected for.

AC electrochemical impedance spectroscopy (EIS).

EIS provided more information than just the corrosion rate. The commercial systems available are mainly used in the laboratories, but start to become more widely applied in

industries which have corrosion experts in the staff who can be involved in the interpretation of the data. EIS is based on the use of AC-signals with a wide range of frequencies from 0.001 to 5000 Hertz. The measurements provide the impedance and the phase angle as a function of frequency. Such measurements have generated much insight in the fundamentals of corrosion. The great advantage concerning use in concrete is the methods capability to give accurate data about corrosion of metals in an environment with low electrical conductivity. Information about the corrosion rate, the resistance drop in the concrete and about the role of oxygen diffusion on the corrosion is obtained. Although a single measurement is time consuming (a single cycle of 0.001 Hertz obviously takes 1000 s), the equipment bulky and the interpretations difficult, the ability to handle the low electrical conductivity of concrete has led to use in the field. Sagues gives interesting examples [2].

Electrochemical noise.

This method differs from the other in that respect that it is not necessary to impress current at the metal. The corrosion potential of a passive metal exhibits small and slow changes, typical in the sub-mV range in time spans of minutes. Localised corrosion usually takes place with multiple breakdowns of protective films. A film rupture, e.g. caused by chloride for passive steel, will give an instantaneous decrease of the corrosion potential. The simplest way to arrange the measurements are to use two electrodes and monitor their potential difference. If both electrodes suffer localised corrosion, the potential peaks will seldom occur simultaneously for both metals, so irregular signals occur. By an analysis of the magnitude and the shape of the potential peaks, one can work out estimates for the corrosion rate. The technique is at a relatively early stage of development and a reliable base for relating noise signals to corrosion rate is hardly available.

Measurements of Macro-cell currents.

The current flow between anodic and cathodic regions of the reinforcement can occasionally provide useful information about the corrosion activity. The concept is used in laboratory tests and in industrial applications. This technique can be used in the field if different parts of the reinforcement can be broken so they no longer are in metallic contact. No sophisticated instrumentation is required. The currents are then measured with a zero-resistance ammeter or with a low resistance shunt. The main disadvantage is that in the case both steel regions corrode fast, the current resulting from the imbalance can be small.

Potential mapping.

When the steel is passive, a corrosion potential of about 0 to -300 mV versus the copper/copper sulphate electrode is typical [2, 4, 5]. As the corrosion potential of the steel reinforcement usually is reduced when the steel is corroding rapidly, the open circuit potential of the steel can be considered as a rough indication of the state of corrosion for

the system. Low potentials and large differences from spot to spot indicate corrosion problems. The method is described in an ASTM-standard [5]. Manual mapping of the corrosion potential with a reference electrode at the external concrete surface is extensively used to survey corrosion of the steel reinforcement. However, the correlation between corrosion rate and potential is not universal. A wide range of corrosion rates may occur in a narrow potential range. Low corrosion potentials may occur not only as a result of high corrosion rates, but also because of low oxygen levels and high pH (that tend to give low corrosion rates). The distribution of potentials at the external concrete surface is not the same as for the concrete in intimate contact with the steel. The potential distribution becomes broader at the surface, than what it would be with electrodes close to the steel bar. Another possible cause of divergence is the presence of junction potentials.

LABORATORY EXPERIMENTS.

Experiments carried out.

Carbon steel specimens were exposed in three different ways:

in KOH solutions with different concentrations of NaCl
in sand soaked with KOH solutions with different concentrations of NaCl
in small concrete slabs

The experimental techniques are described in a resent report [4]. The polarisation experiments were carried out galvanostatically with monitoring of potential as a function of time. A computer program calculated the interfacial capacitance of the electrode and the polarisation resistance from the curves.

Passivity and localised corrosion in solutions.

Steel was found to be passive in the potential range -1.0 to 0.5 V (SCE) in nitrogen flushed 0.3 and 0.6 M KOH. The passive current was independent of the potential in this range. The passive current decreased with time and was about $2*10^{-7}$ A cm^{-2} after 3 days exposure at -0.2 V (SCE). After some hours under aerated conditions the potential was in the region -0.3 to -0.2 V (SCE), i.e. in the passive region. In solutions with 0.3M KOH and above 0.01M NaCl low corrosion potentials (-0.57 to -0.35 V (SCE)) indicated localised attack.

Polarisation behaviour.

The potential as a function of time for steel subjected to galvanostatic polarisation was investigated under a variety of conditions. The shape of the cathodic polarisation curves was sometimes in agreement with charging curves for an RC-parallel circuit. However, anodic polarisation curves approached a linear increase with time after a certain period, as seen in Figure 2 for times above 1500s. Studies of the interfacial capacitance showed that

the deviations from an RC-model were caused by growth of the passive film induced by anodic polarisation.

Figure 3 shows charging curves for steel embedded in concrete and in one case without addition of chloride to the cement and in another with chloride addition of 2% of the cement weight. It is seen that much higher current densities had to be applied to obtain the same potential change with chloride addition, and that the time constant in the potential-time plots was much smaller.

Table 1 shows corrosion current obtained with a commercial instrument with a guard electrode on slabs with different chloride additions compared with results from the galvanostatic method.

FIELD MEASUREMENTS.

Polarisation resistance of reinforcement bars of a known area.

The measurements were carried out at a large bridge at the coast in Northern Norway. Steel with a known surface area was obtained by cutting the reinforcement bars to break the electrical contact with the main reinforcement. Electrical connections were made and the grooves filled with epoxy. Stainless steel counter electrodes and reference electrodes were installed in drilled holes and mounted with a slightly expanding mortar. This was done about year before the measurements described in this report were carried out. In the present measurements the 8 cm long bars were subjected to current steps with a battery operated galvanostat and the potential difference between the bars and permanently reference electrodes measured in the same way as for the laboratory specimens.

Figure 4 and 5 show examples of polarisation curves obtained respectively at a site where the steel was passive and a site with a moderate corrosion rate. The figures also show the computed potential as a function of time based on a RC-circuitry with the component values given in Table 2. It is seen that the analogue circuit with the values indicated, fitted nicely with the observed behaviour. Measurements with different direction of the current and different current densities polarisation also resulted in the same resistance and capacitance values. The much lower value of the electrolyte resistance at the site with the highest corrosion rate indicate a more moist concrete and/or a higher chloride content.

DISCUSSION.

It is difficult to obtain data for making Tafel diagrams for iron even in aqueous solutions at high pH due to changes of the electrodes caused by the polarisation. The studies of capacitance showed that the thickness of the corrosion film increased under anodic polarisation. Earlier studies [6] indicated that oxide reduction occurred under cathodic polarisation. With lack of Tafel curves it is difficult to have a qualified opinion about the value of the "constant" used to convert polarisation resistance to corrosion rate. 0.026V is

used in this work. More problematic is the fact that the attack is non-uniform so the benefit of a correct "LPR-constant" is limited. Thus one is faced with the use of non-quantitative "rules of thumb". A concrete resistivity less than 20 kOhm*cm is suggested to indicate possible corrosion problems. However, problems caused by macro galvanic corrosion exists that reduce the reliability of polarisation resistance for predicting the severity of corrosion of the steel reinforcement in concrete.

The polarisation induced changes of the electrodes consume current and disturb the measurements of polarisation resistance. The procedure used in this work, to determine the resistance and capacitance that correspond to the first part of charging curves under galvanostatic polarisation is likely the method being the least disturbed by the phenomena described. It is interesting that changes of the corrosion film interfered less for the measurements at the bridge than in the laboratory. The 13 years exposure of the reinforcement in the bridge has possibly created more stable oxide films than those in the short time laboratory exposures.

It is difficult to install an electrode system with a good cell geometry in concrete. The main problem with a poor cell geometry is undesired resistance. For case B in Table 2 the polarisation resistance was determined to 25 kohm cm^2 and the resistance drop between the permanently installed reference electrode and the steel bar corresponded to 60 kohm cm^2 . The LPR value obtained by a potentiostatic technique (without compensation for the resistance drop) would be the sum of the resistance and would be misleading. Compensation of the resistance drop under potentiostatic conditions requires sophisticated studies to determine the settings. Therefore, the determination of charging curves combined with computerised analysis used in this investigation, appears to be better for this reason alone. Use of AC-impedance spectroscopy, as advocated by Sagues [2], is very informative, but time consuming and requires expensive equipment.

The charging of the large interfacial capacitance creates large problems for the use of potentiodynamic sweeps. With a capacitance of 1000 μFcm^{-2} , a potentiodynamic sweep with a rate of 0.5 mV/s gives capacitive charging current of $0.5 * 10^{-6}$ Acm^{-2}. However, the Faraday current was often found to be less than 10^{-7} Acm^{-2} at a potential 10 mV from the corrosion potential and will be overshadowed by the charging current in this case. A scan rate below about 0.03 mV/s should be used under these conditions. But this makes the measurements too slow for field use. Even with moderate corrosion, the current used for charging of the interfacial capacitor will disturb with potentiodynamic scans with usual rates. Potentiostatic exposures are better. From the present experience, the galvanostatic technique appears to be the first choice.

As the capacitance of the iron electrode in alkaline solutions is only little affected by the corrosion potential, and as this capacitance determines the potential change rate in the first moments after a current pulse is applied, it is difficult to use short time polarisation data for corrosion rate estimates.

electrode instrument used in this investigation had a maximum polarisation time of 100s. It is not known whether this explains the disagreements shown in Table 1.

CONCLUSIONS.

Anodic polarisation caused growth of the corrosion film and also cathodic polarisation affected the electrodes. These effects make it difficult to obtain good polarisation data for steel in alkaline solutions and in concrete.

Potentiodynamic scans are hardly suited for determination of the polarisation resistance of steel in concrete. The high interfacial capacitance often leads to a capacitive charging current that overshadow the galvanic current. For passive steel a scan rate as low as 0.03 mV/s is desirable, making the measurements very time consuming. A better technique is to use potentiostatic measurements, about 5 mV from the corrosion potential.

Permanently installed reference electrodes, aimed at being close to the steel surface, picked up an ohmic resistance drop in the concrete that seriously disturbed LPR measurements obtained under potentiostatic conditions without correction of this resistance drop. This problem occurred only when the corrosion rate was relatively high.

Computer modelling of the potential as a function of time determined under galvanostatic polarisation was found to be a satisfactory method for obtaining the polarisation resistance of steel with a known surface area. This applied with and without chloride present for steel in KOH solutions, in sand saturated with KOH solutions, for steel in laboratory concrete slabs and reinforcement bars in a 13 year old bridge.

The measurements with a galvanostat and measurement of the potential as a function of time, combined with a computer aided determination of the component values of analogue RC-circuitry also gave values for the interfacial capacitance and the potential drop in the concrete between the steel electrode and the reference electrode. As this method is little disturbed both by the ohmic resistance drop in the concrete and by polarisation induced changes of the steel surface, this method has definite advantages provided that the measuring period has sufficient duration.

ACKNOWLEDGEMENT.

Some of the work presented in this report is a part of the "OFU Bridge Repair Project", funded by the Norwegian Road Administration (NPRA), Rescon AS and the Regional Development Fund (SND). The authors wish to thank these institutions.

REFERENCES.

1 ASTM Standard G59 (1993) Standard Practice for Conducting Potentiodynamic Polarization Resistance Measurements.

2. A. A. Sagues: Corrosion Measurement Techniques for Steel in Concrete. NACE, Houston, TX, USA, CORROSION/93 Report 353.

3 B. Bazzoni and Luciano Lazzarri: Interpretation of Potential Mapping on Bridge Decks for Reinforcement Corrosion Prediction. NACE, Houston, TX, USA, CORROSION/94 Report 281.

4 K. Videm, J. Lehrmann and R. Myrdal: Evaluation of the Corrosion of Steel Reinforcement in Concrete by Electrochemical Methods. Int. Conf. Corrosion in Natural and Industrial Environments - Problems and Solutions. Grado, Italy, May 1995

5. ASTM C876-91 Standard Test Method for Half-Cell Potentials of Uncoated Reinforcing Steel in Concrete.

6 C. Simon and T. Hurlen: Acta Chemica Scandinavia 43 (1989) 851-854

Table 1. Corrosion currents of steel embedded in concrete slabs with different chloride contents. 18 months curing time. Measurements with galvanostatic technique and with commercial instrument with guard electrode.

		Galvanostat		Guard electrode instr.
Cl^- %	Potential V (SCE)	LPR KOhm*cm^2	Corr. current μAcm^{-2}	Corr. current μAcm^{-2}
0	-0.063	1500	0.017	0.031
0	-0.073	1900	0.014	
1	-0.358	13.6	1.9	0.81
1	-0.354	15.0	1.7	0.084
1	-0.306	24.0	1.1	0.27
2	-0.388	0.28	93	1.1

Table 2. Corrosion potential, interfacial capacitance, polarisation resistance and electrolyte resistance measured at cut reinforcement bars.

Site	A	B
Potential (V manganese dioxide)	-0.153	-.375
Capacitance (μFcm^{-2})	700	1000
LPR (kOhm cm^2)	2000	25
Resistance between reference and working electrode (kOhm cm^2)	120	60

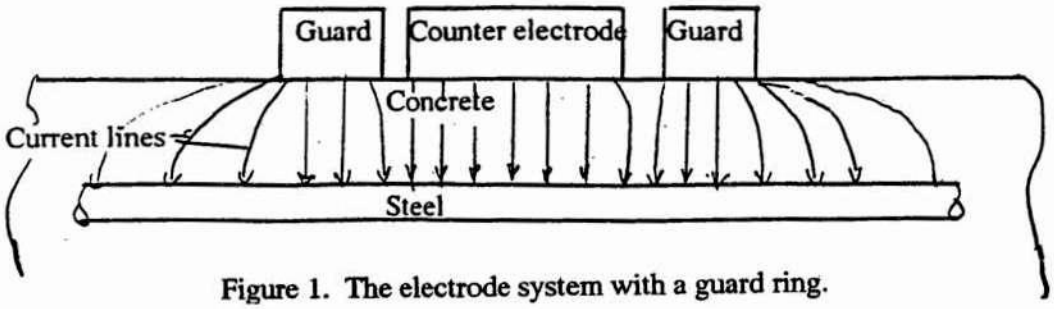

Figure 1. The electrode system with a guard ring.

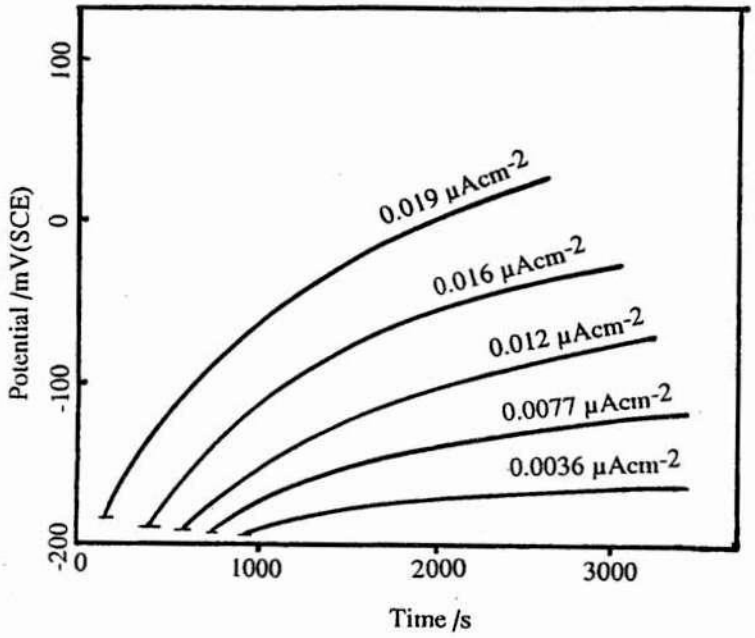

Figure 2. Potential as a function of time for steel in 0.3M KOH. Anodic current densities are indicated on the figure.

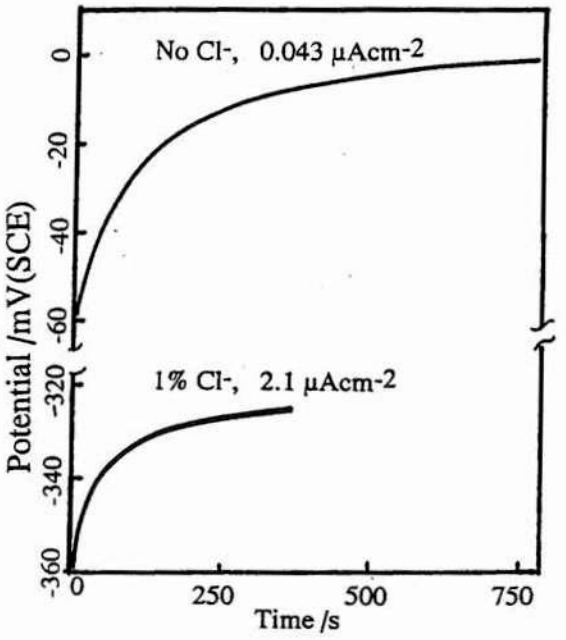

Figure 3. Potential as a function of time for steel in concrete with 1% chloride of the cement weight and in concrete without chloride addition. Anodic polarisation.

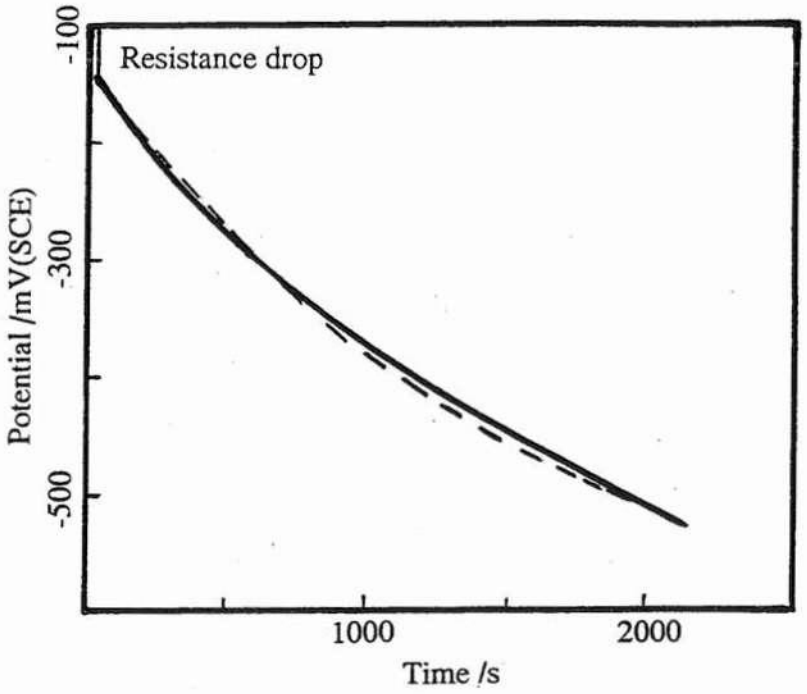

Figure 4. Potential as a function of time for a cut reinforcement bar in concrete bridge. Cathodic polarisation with 0.025 μAcm^{-2}. A site with a very low corrosion rate.
Full drawn line:
Broken line: Calculated curve based on the component values given in Table 2.

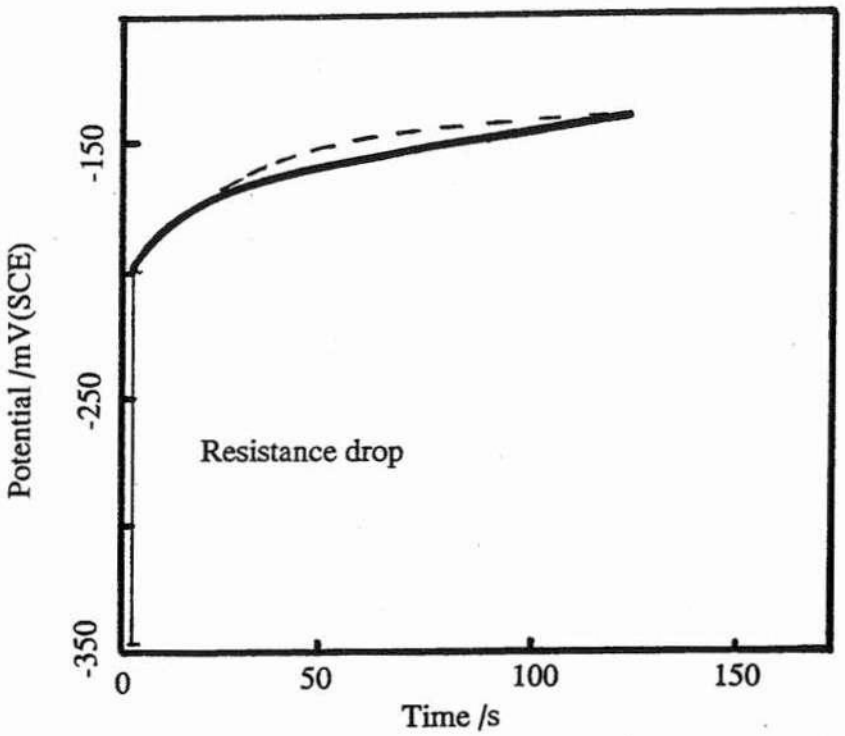

Figure 5. Potential as a function of time for a cut reinforcement bar in concrete bridge. Anodic polarisation with 2.5 μAcm^{-2}.
Full drawn line: Measured.
Broken line: Calculated curve based on the component values given in Table 2.

IN SITU MONITORING OF REINFORCEMENT CORROSION BY MEANS OF ELECTROCHEMICAL METHODS

Oskar Klinghoffer, FORCE Institute
Park Alle 345, DK-2605 Broendby, Denmark

ABSTRACT

The well-known and usually adapted potential mapping technique, measuring half-cell potential on concrete surface leads to some misinterpretation especially in structures placed in wet and anaerobic environment.

In order to avoid these problems additional polarization technique has been introduced.

The method, called *galvanostatic pulse technique*, is now succesfully applied on site.

Measurements have been performed on different structures and its elements, such as supporting beam, bridge pillars and concrete decks.

The results of these measurements are presented in the paper and show that it is also possible to detect the corrosion state when the half-cell potential are difficult to interpret.

1. INTRODUCTION

Steel reinforcement embedded in concrete will not normally corrode due to the formation of a protective iron oxide film which passivates the steel in the strongly alcaline conditions of the concrete pore fluid. This passivity can be destroyed by chlorides penetrating through the concrete and due to carbonation. Corrosion is then initiated. Steel corrosion is an electrochemical process involving establishment of corroding and passive sites on the metal surface. Fig. 1 illustrates a mechanism of such corrosion process, in which both anode and cathode reactions are taking place.

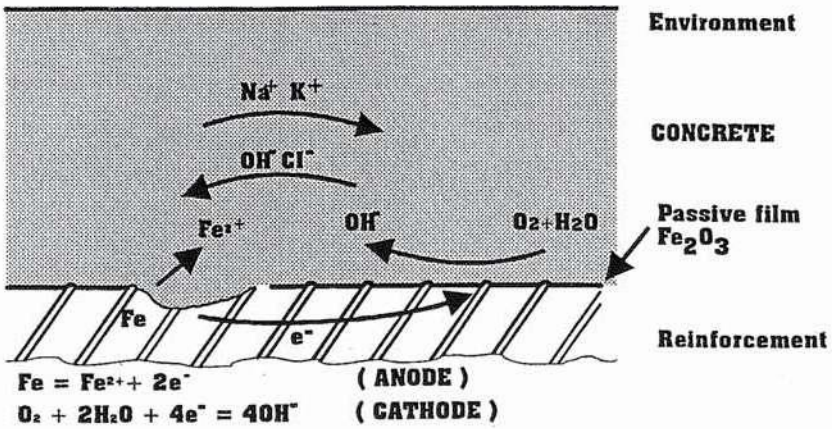

Fig. 1 Mechanism of reinforcement corrosion.

The anode reactions are:

$$Fe = Fe^{++} + 2\,e^{-} \quad \text{(metal dissolution, active corrosion)}$$
$$3Fe + 4\,H_2O = Fe_3O_4 + 8\,H^{+} + 8\,e^{-} \quad \text{(formation of passive layer)}$$

The released electrons travel through the steel to the local cathode on which they are used in the oxygen reduction reaction,

$$O_2 + 2H_2O + 4e^{-} = 4OH^{-}$$

These reactions leads to the development of regions of differing electrochemical potentials and resulting in current flow within the concrete. Measuring the potentials and the magnitude of corrosion currents may, in principle, enable the detection of existing corrosion sites and the present rate of corrosion to be assessed. As long as the ambient conditions do not change, predictions of future corrosion failure can be made. In practice, concrete has cracks, flaws and aggregate particles, which affect diffusion flow characteristics, and it is not in uniform contact with reinforcement. Therefore measurements of electrical characteristics can only provide a general guide to corrosion condition.

On the other hand these measurements are based on the non-destructive methods and, therefore, offer a wide range of possibilities for obtaining information about what is happening below the surface of hardened concrete on site. Assessment of the risk and extent of corrosion of embedded steel forms a current major area of concern, and is particulary important in relation to maintenance an repair programs.

In this paper two of these methods will be described and discussed regarding both advantages and problems occurring during measurements and interpretation of results. The well known half-cell potential mapping will be compared with the galvanostatic pulse method.

2. HALF-CELL POTENTIAL MAPPING.

This method was first developed in the late 1950's (1) and has since been extensively used, particulary in the USA, for the assessment of concrete bridges. It was adopted in 1977 as an ASTM method C876 (2). The method has also found wide use in Europe, among other countries also in Denmark since beginning of 1980 (3). The method measures the electrochemical potential of reinforcement against a reference electrode placed on the concrete surface. The basic set up of this method is shown in fig. 2. Prior to testing, electrical continuity of reinforcement is checked by applying a potential difference across rebar at different sections

of the structure. Normally a measured resistance of less than 1 ohm is used to indicate continuous electrical connection of reinforcement.

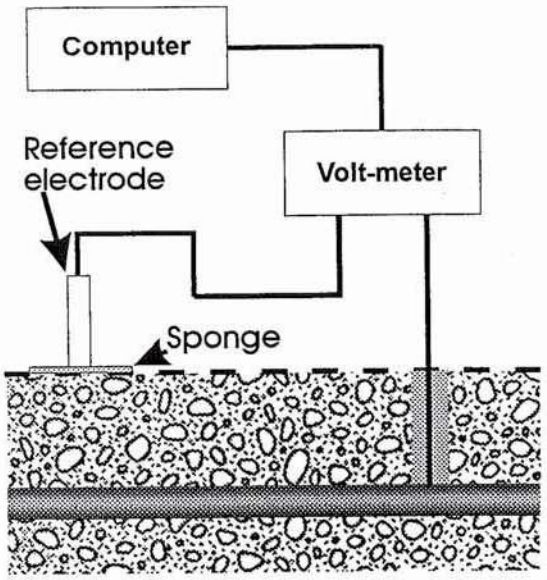

Fig. 2 Set-up of half-cell potential measurements.

In order to ensure a good contact with the reference electrode the concrete surface requires prewetting. A number of reference electrodes may be used , including copper/copper sulphate (CSE), silver/silver chloride or calomel (SCE). Potentials are measured with a high impedance voltmeter (>10 Mega ohm) to ensure low current conditions during testing. The evaluation of the results is normally performed by means of a personal computer. ASTM C876-87 provides a classification for assessing the results of the half-cell potential mapping.

There is a special difficulty in interpreting the results which lie between -200 and -350 mV vs CSE. Comparing neighbouring surface potentials, i.e. potentials gradients, is a more appropriate procedure (4). Measurements are then presented in the form of equipotential contour maps from which areas of suspected corrosion are identified.

The measured electrochemical potentials are affected by a number of factors and these should be considered in interpreting the results. One of the most important factors is the quality of the cover concrete, particulary its moisture condition and contamination by carbonation and/or chlorides. Also oxygen access strongly determines the potential values of passive steel in concrete. Low oxygen content results in decrease of the potential. In wet concrete, due to low oxygen admission, conditions may prevail resulting in a shift of the potential to comparably low values. Consequently passive steel may show low potentials similar to those of corroding steel. This leads to the risk that passive areas under low aeration conditions will be classified as corroding areas. A further limitation of this method is that the results only give an indication of whether corrosion is thermodynamically possible and no information relating to corrosion kinetics can be obtained.

It resulted in the need to supplement or replace this method with another in which these difficulties could be overcome. The galvanostatic pulse technique is a good choice in order to eliminate these problems.

3. GALVANOSTATIC PULSE METHOD

Galvanostatic pulse method is a rapid non-destructive polarization technique. The method set-up is shown in fig. 3. A short-time anodic current pulse is impressed galvanostatically from a counter electrode placed on concrete surface together with an reference electrode of the same type as previously described for potential mapping measurements. The small anodic current results in change of reinforcement potential which is recorded by means of datalogger. Reinforcement is polarized in anodic direction compared to its free corrosion potential.

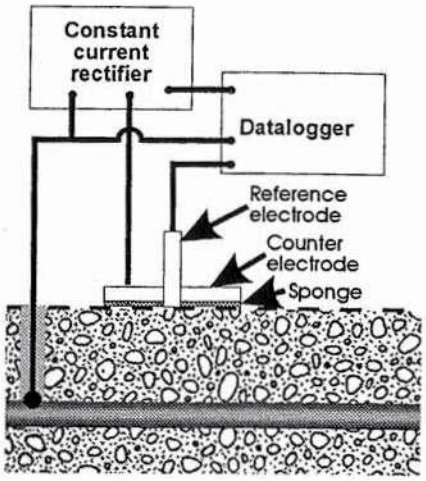

Fig. 3 Set-up of galvanostatic pulse measurements

The extend of this polarization depends on the corrosion state. The reinforcement is easy to polarize in the passive state, which is illustrated by the big difference between the free corrosion potential and the polarized potential. This difference is much lower for a rebar which is corroding. The galvanostatic pulse method yields much better information on the corrosion behaviour. The superiority of this method has been confirmed in the recently published works (5,6), which emphasize its applicability to wet concrete, where the problems with interpretation of low potentials registered by potential mapping technique occur.

Together with the more reliable qualitative information concerning classification of passive and corroding areas this technique gives also possibility for quantitative evaluation, namely calculation of the corrosion current (7). Under assumption that the area of the polarized reinforcement is known this corrosion current can be converted to the corrosion rate.

When the potentials are recorded on the concrete surface the measurements include the ohmic voltage drop which must be eliminated in order to obtain a true polarization value.

Schematic theoretical galvanostatic pulse results are shown on Fig. 4. When the constant current I_{app} is applied to the system, the polarized potential of reinforcement V_t, at given time t can be expressed as (7):

$$V_t = I_{app}[R_p[1 - \exp(-t/R_pC_{dl})] + R_{ohm}] \qquad [1]$$

where:

R_p = polarization resistance in ohm
C_{dl} = double layer capacitance in mikroFarad
R_{ohm}= ohmic resistance in ohm

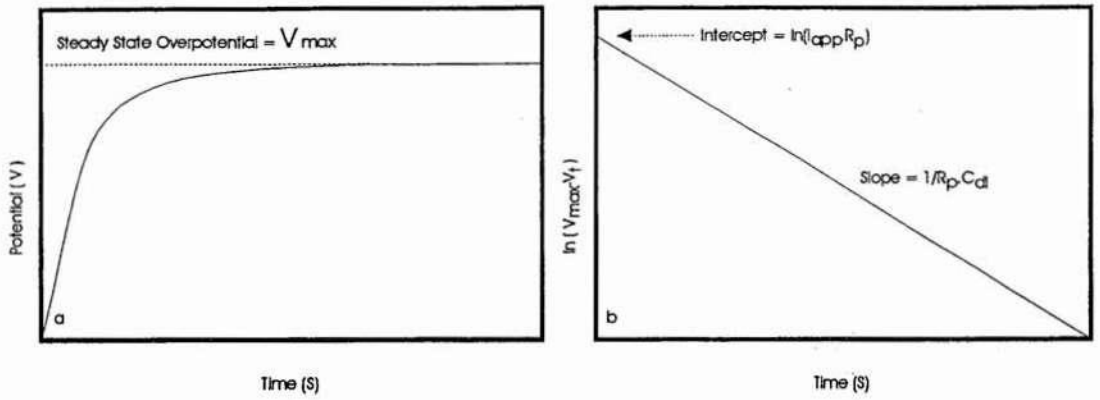

Fig. 4 Schematic illustration of galvanostatic pulse results

In order to obtain values of R_p and C_{dl} separate from the ohmic resistance R_{ohm} this equation can be transferred to linear form

$$\ln (V_{max}-V_t) = \ln (I_{app}R_p) - t/R_pC_{dl}) \qquad [2]$$

where V_{max} is the final steady state potential value.

Extrapolation of this straight line to t = 0, using least squares linear regression analysis, yields an intercept corresponding to $\ln(I_{app}R_p)$ with a slope of $1/R_pC_{dl}$. The remaining overpotential corresponds to $I_{app}R_{ohm}$ which is the ohmic voltage drop. After the polarization resistance R_p is determined by means of this analysis the corrosion current I_{corr} can be calculated from Stern-Geary formula (8):

$$I_{corr} = B/R_p \qquad [3]$$

where B is an empirical constant determined to be 25 mV for actively corroding steel and 50 mV for passive steel.

4. MEASUREMENTS ON SITE

These measurements were performed on the structures placed in wet and anaerobic environments. According to the reason mentioned in section 2 in such structures the half-cell potential measurements could lead to the misinterpretation of the corrosion state.

By means of a setup shown on Fig. 3 both half-cell potential and galvanostatic pulse measurements were conducted.

A constant anodic current pulse in the range of 80 μA to 100 μA was applied to the reinforcement from a stainless steel counter electrode. The current source was connected to the datalogger which also controlled its operation.

Potential measurements were performed by means of silver/silver chloride reference electrode and registered in the datalogger together with the potential changes due to the applied pulse.

In the beginning the potential changes were registered with 27 msec interval (approx. 50 records), followed up by 125 msec between the remaining measuring points.

All data were collected in the datalogger and then evaluated by means of a special developed software in personal computer.

In the following measurements performed on three different structures are reported.

4.1. Measurements on the supporting beam of the seawater laboratory

Fig. 5 shows the results of measurements performed on the 24 years old supporting beam located at the coast. The polarization transient, which is the difference between the half cell potential and the final steady state potential V_{max} from galvanostatic pulse is registered at different locations at the beam and then plotted as a function of the distance coordinate. The varying polarization transients are registered at different beam locations. These differences are biggest in the end and lowest in the middle of the beam.

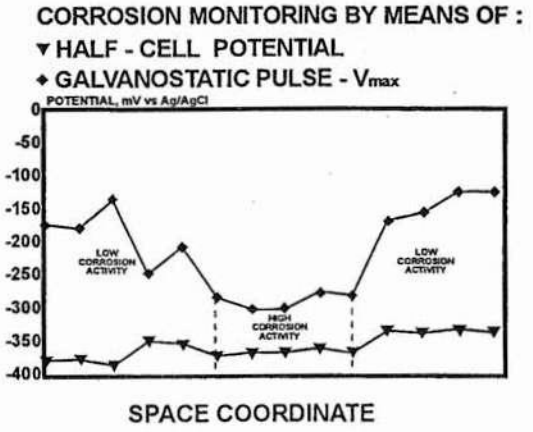

Fig. 5. Results of corrosion monitoring by means of half-cell potential and galvanostatic pulse measurements on the supporting beam.

According to the theory described in section 3, it means that the corrosion activity should be lower in the ends than in the middle part of the beam.

These results were confirmed by visual inspection carried out at selected locations at the beam. After removal of the concrete it was demonstrated that the corrosion attack on reinforcement in the middle section was much heavier then in the ends. Looking on results of half-cell potential only it was not possible to distinguish these differences in corrosion activity.

In order to achieve a better quantification of the corrosion activity the effective polarization resistance was calculated from pulse measurements based on relationship [1] and [2] in section 3 and assuming constant polarized area. The results of this calculations are collected in table 1. With one exception the calculated polarization resistance is lowest at locations in the middle of the beam and highest in the ends. These results have a significant importance for evaluation of corrosion activity at different location of the beam.

It is not possible to calculate the corrosion rate from polarization resistance values, because the polarized reinforcement area is not being exactly defined. Variation in concrete resistivity and varying rebar density at different measurement locations may influence the results (9). In order to obtain the true polarization resistance, which can be converted to the corrosion rate, it is necessary to assure an uniform distribution of the electrical current on the defined area of reinforcement.

Distance (cm)	Halfcell potential (mV)	Galvanostatic pulse		
		V_{max} (mV)	V_{max}-(I_{app}-R_{ohm}) (mV)	R_p eff (ohm)
0	-380	-172	14	303
40	-377	-178	5	65
80	-385	-134	20	1946
120	-350	-255	2	1851
160	-352	-207	5	1946
200	-371	-281	9	68
240	-367	-299	3	32
280	-366	-300	4	105
320	-359	-272	4	95
360	-366	-279	5	72
400	-332	-166	4	165
440	-337	-153	15	173
480	-330	-123	17	342
520	-334	-120	13	238

All potential values are in mV vs Ag/AgCl.

Table 1. Calculation of effective polarization resistance from galvanostatic pulse measurements performed on supporting beam

4.2. Measurements on concrete deck at power station

Another possibility for comparison of results from half-cell potential measurements and galvanostatic pulse is shown on fig. 6. These measurements are performed on concrete deck at the local power station. This concrete deck is placed 20 cm over sea level. The upper part of the fig. (6a) shows potential gradients obtained from half-cell potential mapping.

It is noticed that only few potential gradients are registered, furthermore in the region, where it is difficult to interpret the results. This picture changes when we look at the lower part of the fig. (6b), which represents the results from galvanostatic pulse measurements. These results are plotted as a polarized potentials (the steady state overpotential V_{max} with the potential drop subtracted, $I_{app}R_{ohm}$), at different neighbouring locations. Now it is possible to find much more detailed picture of the corrosion state than by means of half-cell potential mapping. Especially the area between 0 and 180 cm (x coordinate) is divided in five different regions compared to only two gradients obtained by the potential mapping technique. Galvanostatic pulse technique provides us, therefore, with more reliable results than it is possible by means of half-cell potential mapping in order to distinguish different corrosion activity.

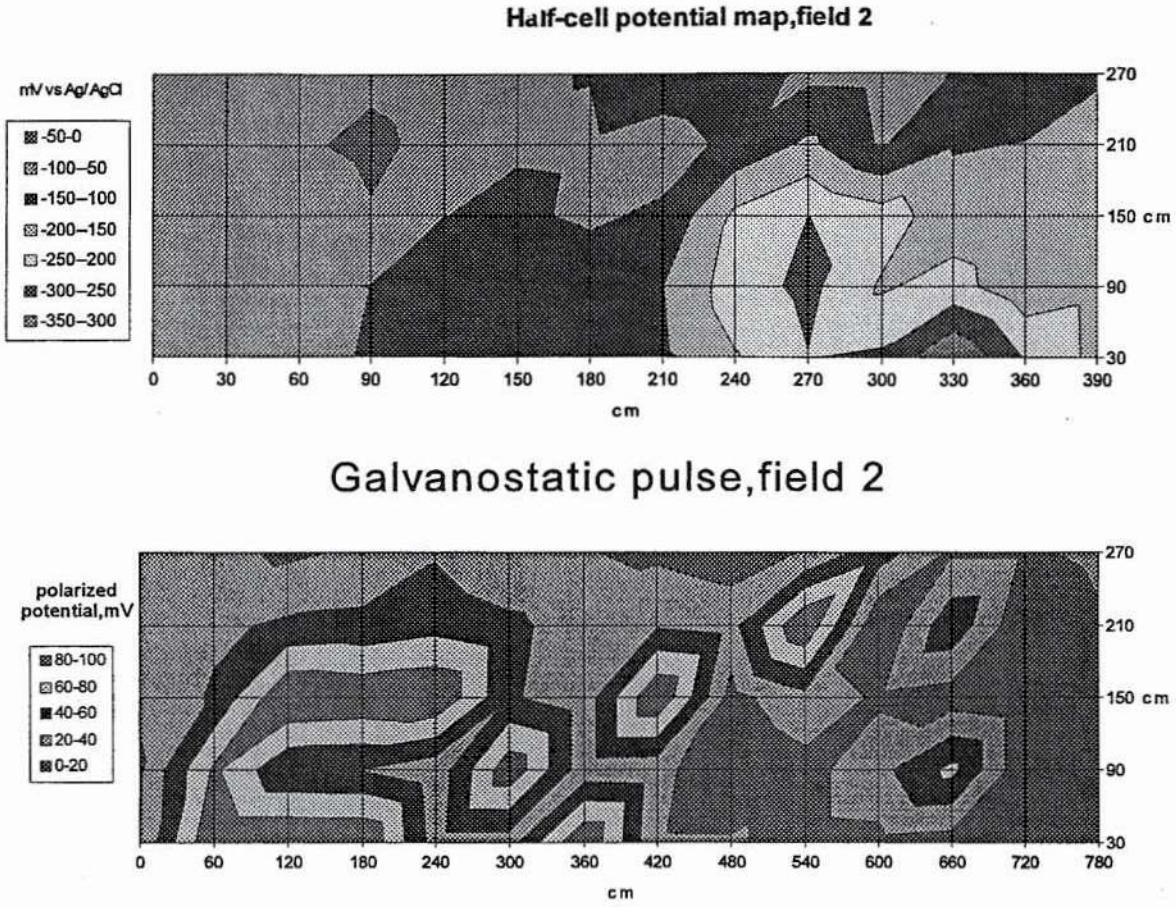

Fig. 6 Corrosion monitoring by means of :
6a - half-cell potential measurements - 6b - galvanostatic pulse measurements.

4.3. Measurements on a bridge pillar

These measurements have been performed on the pillar of a highway bridge. Measurements cover two opposite sides of the pillar regarding orientation to the road (one towards and second against the road). In both cases measurements are carried out on 3 meter of the pillar width and 1 meter of the pillar height.

Before the galvanostatic pulse is applied the free corrosion potentials are registrered at each measuring point. Thereafter the reinforcement is polarized galvanostatically and both the ohmic resistance R_{ohm} and the effective polarization resistance R_p are determined.

The ohmic resistance is calculated as a difference between the free corrosion potential and the first value of the polarized potential divided by the applied current. These ohmic resistance values are then plotted against the determined effective polarization resistance (Fig.7).

The trend line can be drawn if, as reported by Elsener (6), a linear relationship resistance exists. In praxis due to differences in homogeneity and humidity within the concrete only a qualitative relation between these two parameters shall be expected.

Therefore, it is important not only to determine the ohmic resistance but also to analyse the linear part of the galvanostatic pulse curve from which the polarization resistance is calculated.

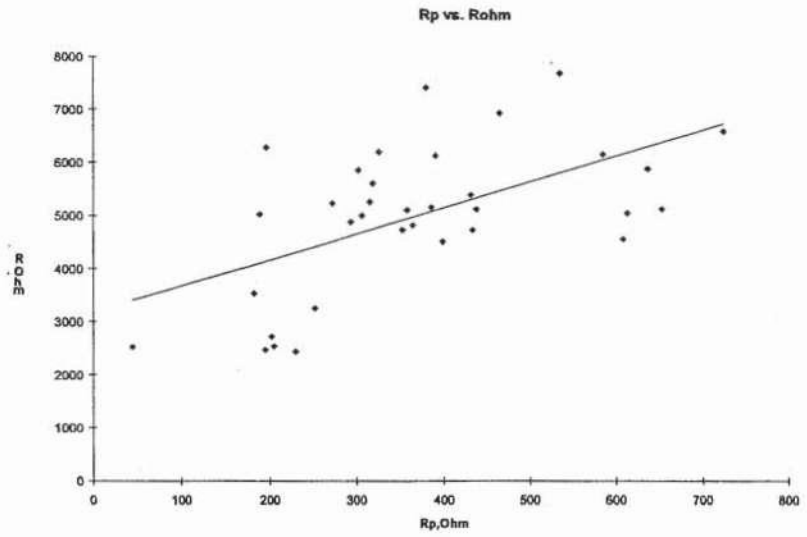

Fig. 7. Ohmic resistance plotted as a function of the effective polarization resistance

Fig. 8 shows the variation of half-cell potential, ohmic resistance and polarization resistance through the pillar width at height of 0,75 meter above the ground level These measurements are performed on the pillar side towards the road.

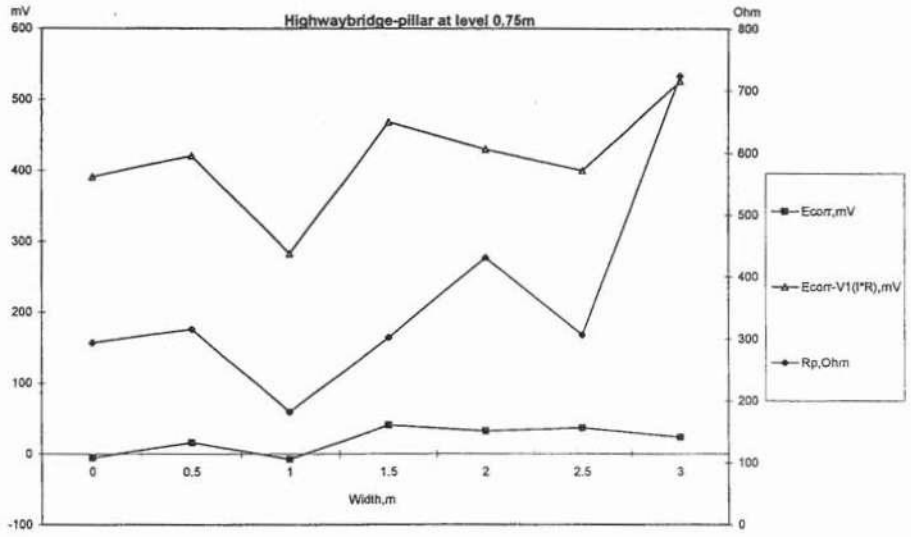

Fig. 8. Half-cell potential, ohmic resistance and polarization resistance determined at 0,75 meter of pillar height.

The values of the registered free corrosion potentials (half-cell poetntials) are almost uniform in the whole measurements area.

Looking at the determined ohmic resistance R_{ohm} and the effective polarisation resistance R_p it is possible to identify the location at 1 meter of pillar width as the point of the enhanced corrosion risk. Also the location at 2,5 meter of pillar width shall be concerned in this respect. Therefore, contrary to the half cell potential measurements, it is also possible to perform a semi-quantitative evaluation of the corrosion state knowing both ohmic and polarization resistance derived from the galvanostatic pulse measurements.

5. CONCLUSIONS

- The potential mapping technique is not sufficient for detection of the local corrosion problems occurring in structures placed in wet and anaerobic environment.
- In such cases the galvanostatic pulse method is a valuable alternative, which provides much better possibility for classification of different corroding areas.
- The pulse technique is a non-destructive and quick method, which allows rapid monitoring of reinforcement corrosion, because within a few seconds the free corrosion potential, the ohmic resistance and the polarization resistance are determined.
- By means of this polarization technique the effective polarization resistance can be calculated. In order to obtain the true polarization resistance, which can be used for calculation of corrosion rate it is necessary to know exact area of the polarized reinforcement.

ACKNOWLEDGEMENT
The author would like to express his thanks to T.Frølund, B.Kofoed and H.Clausen (all FORCE Institute), who performed the measurements on site and to E.Rislund, also FORCE Institute, who contributed with valuable comments during preparation of this paper.

REFERENCES

(1) Stratfull,R.F.: "The Corrosion of Steel in a Reinforced Concrete Bridge". Corrosion, Vol. 13, pp 173-179.

(2) American Society of Testing and Materials. Standard Test Method for Half-Cell Potentials of uncoated Reinforcing Steel in Concrete. ASTM C876-87.

(3) Arup,H.: "Potential Mapping of Reinforced Concrete Structures". The Danish Corrosion Centre Report, January 1984.

(4) Hansson,C.M.:"Comments on Electrochemical Measurements of Corrosion of Steel in Concrete". Cement and Concrete Research, Vol.14,1984, pp 574-584.

(5) Mietz,J., Isecke,B.: "Electrochemical Potential Mapping on Reinforced Concrete Structures using Anodic Pulse Technique". Proceedings of Conference "Non-Destructive Testing in Civil Engineering". Liverpool 1993, pp 567-577.

(6) Elsener,B., Wojtas,H., Bohni,H.: "Gavanostatic Pulse Masurements - Rapid on Site Corrosion Monitoring". Proceeding of International Conference held at the University of Sheffield,24-28 July 1994.

(7) Newton,C.J., Sykes,J.M.: "A Galvanic Pulse Technique for Investigation of Steel Corrosion in Concrete"; Corrosion Science,Vol.28,1988, pp 1051-1073.

(8) Stern,M., Geary,A.L.: "Electrochemical Polarization, I. A Theoretical Analysis of Shape of Polarization Curves". Journal of the Electrochemical Society, Vol. 104, 1957., pp 56-63.

(9) Feliu,S., Gonzales,J.A., Andrade,C., Feliu,V.: "On Site Determination of the Polarization Resistance in a Reinforced concrete Beam", Corrosion Engineering, Vol. 44, 1988, pp 761-765.

January 1995

FACTORS AFFECTING THE ELECTROCHEMICAL POTENTIAL OF REFERENCE ELECTRODES EMBEDDED IN CONCRETE

Roar Myrdal, Rescon A/S, Vallsetvegen 6, N-2120 Sagstua, Norway.

Ketil Videm, Centre for Materials Research, University of Oslo, P.O. Box 1033, N-0315 Oslo, Norway.

ABSTRACT

The potentials of embeddable reference electrodes for concrete have been measured in synthetic pore water solutions and in a concrete slab. Manganese dioxide, graphite and lead electrode potentials are sensitive to changes in pH. Graphite and lead electrodes respond to changes in oxygen partial pressure. The electrochemical reactions involved are briefly discussed, and comments on potential stability and use in concrete are given.
Keywords: Reference electrode, electrochemical potential, manganese dioxide, graphite, lead, concrete, rebar corrosion.

INTRODUCTION

A technique commonly used in corrosion supervision of steel reinforced concrete structures is the so called "surface potential mapping", summarized by ASTM C876-91 "Standard Test Method for Half-Cell Potentials of Uncoated Reinforcing Steel in Concrete" [1]. The technique consists of manual mapping of the corrosion potential using a reference electrode that is placed consecutively at evenly spaced spots along the concrete surface. Low potentials and large differences from spot to spot indicate corrosion problems. However, difficulties connected to the accessability to parts of the structure (e.g. large bridges) and the concrete surface conditions (e.g. coatings) make it desirable to find other solutions.

Another technique, less common, is to monitor the potential of the reinforcement with permanently installed reference electrodes. Embeddable reference electrodes are either cast in place during construction, or installed in drilled holes in hardened concrete using a suitable mortar. This technique will overcome the difficulties mentioned above. In addition it provides the possibility of continuous monitoring. This procedure also has the advantage that the tip of the reference electrode can be closer to the steel surface and hence reduces the disturbance by resistance drops in the concrete.

In order to achieve reliable corrosion potential data from measurements with reference electrodes, the potential of the reference electrode must be stable and unaffected by the chemical constituents in the environment in which it is placed. However, several types of embeddable reference electrodes commonly used in concrete, do not satisfy these requirements. Therefore, a change in voltage observed between the steel reinforcement and the reference electrodes cannot always be attributed to a change in the state of rebar corrosion alone. The observed voltage change may partly be due to the reference electrode itself, i.e. the reference electrode respons to some changes in the chemical environment.

In order to study the electrchemical potential of the reference electrode itself another reference electrode has to be used. Since absolute electrode potentials not exist, a relative potential scale

has been worked out. By convention, the standard hydrogen electrode (SHE) defines the zero point on this scale. All other electrodes, also reference electrodes, have potentials that are related to this standard.

An ideal reference electrode should possess the following properties [2]:

1. Have a stable potential.
2. Meet the demands of charge transfer imposed by the measuring instrument without changing its potential (be nonpolarizable).
3. Return to its fixed reference potential after accidental polarization.
4. Obey the Nernst equation for some species in solution.

Examples of reference electrodes which possess all of the above properties for use in aqueous solutions are the saturated calomel electrode (SCE) and the silver-silver chloride electrode (Ag/AgCl). These electrodes are normally designed for laboratory use and do not possess the ruggedness that is required for embedding in conctrete. However, Ag/AgCl electrodes specially designed for concrete are available and used [3]. Although not ideal reference electrodes, graphite [4-6] and lead [6] are examples of embeddable electrodes used in concrete. Reference electrodes commonly used in concrete are manganese dioxide electrodes [7]. All electrode potentials will hereafter be measured and discussed with respect to SCE. The potential of SCE is +0,242 V vs SHE at 25°C.

This paper describes laboratory experiments with manganese dioxide, graphite and lead reference electrodes. Short-term potential stability and electrode responses to the chemical composition of the environment, mainly pH and oxygen partial pressure, will be treated. The electrochemical reactions involved will be discussed. Also some comments on the problems connected with the calibration of embedded reference electrodes in concrete will be given.

LABORATORY EXPERIMENTS

Electrode materials

The following materials have been investigated:

- Commercial manganese dioxide electrodes for concrete (MnO_2)
- Commercial graphite electrodes for concrete (C)
- Lead (Pb), with the same purity as used in commercial electrodes

The commercial electrodes were used as received. Lead electrodes were made from a lead rod that was cut in pieces (diameter 8 mm and length 20 mm) and connected to standard insulated copper leads by soldering. The connection point was encapsuled in epoxy.

Synthetic pore solutions

The electrodes were exposed in saturated calcium hydroxide or potassium hydroxide solutions. Variations in dissolved oxygen were obtained by bubbling gas through the solution. The gas was either oxygen, air without CO_2 or 99,999% nitrogen. A saturated calomel electrode (SCE) was used to measure the electrode potential. The reference electrode (SCE) was separated from the test solution with a gel filled capillary, and the potentials were recorded with a pH meter,

i.e. a high impedance voltmeter. The experiments were carried out at room temperature.

Concrete slab

Graphite and lead electrodes were cast into a concrete slab with dimensions 8 cm x 15 cm x 31 cm. The concrete mix is given in Table 1. The fresh mix contained about 7 vol-% air. The concrete thickness at the active part of the electrodes was about 3 cm. The potentials of the embedded electrodes were measured by placing the calomel electrode with a small moist sponge (tap water) at the concrete surface. Measurements were taken after allowing the system to stabilize for about 15 minutes. When the slab was submerged in water, the measurements were carried out according to the same procedure as in synthetic pore solutions.

Table 1
Concrete mix (kg/cm^3)

Water	Cement (OCP)	w/c-ratio	Aggregate (0-8 mm)	Plasticizer (lignosulp.)
200	330	0,6	1785	2,5

RESULTS

Table 2 shows the electrode potentials as a function of time for manganese dioxide electrodes, graphite and lead in saturated calcium hydroxide solutions open to air and without stirring. Large amounts of calcium hydroxide was added to ensure a saturated solution, and pH was checked regularly using a pH meter. Throughout the entire period pH was found to be 12,45 ±0,05.

Table 2
Electrode potentials in saturated $Ca(OH)_2$. Room temperature.

Electrode material	Electrode potential vs SCE (mV)				
	10 min	1 h	24 h	100 h	>100 h
MnO_2	+94	+100	+111	+117	---
C	-108	-104	-84	-82	-81 (430 h)
Pb	---	-748	-747	-741	-730 (1500 h)

It is seen that the electrode potentials increased with time during the experiment. The potential values presented for manganese dioxide electrodes and graphite represent the average value of two and six electrodes respectively. Average calibrated values received from the suppliers (calibrated in saturated $Ca(OH)_2$ at room temperature) were +142 mV for manganese dioxide and -97 mV for graphite. The potential difference between the two manganese dioxide electrodes examined was 8-10 mV throughout the exposure period. According to the suppliers information the difference should have been 2 mV (+141 mV and +143 mV respectively). The difference between highest and lowest potential recorded for the six graphite electrodes was

19 mV after 1 hour exposure, but only 2 mV after prolonged exposure (430 h). Acoording to the suppliers own calibration the potential difference was 13 mV. Lead stabilized at about -730 mV(SCE) after prolonged exposure in saturated calcium hydroxide.

Figure 1 shows the potential responses of reference electrodes to changes in pH. The electrodes were kept overnight in $KOH/Ca(OH)_2$ solutions open to air before the potentials were recorded. After the recording pH was checked. The observed potential changes per pH-unit, i.e. the dE/dpH slopes, are given in Table 3.

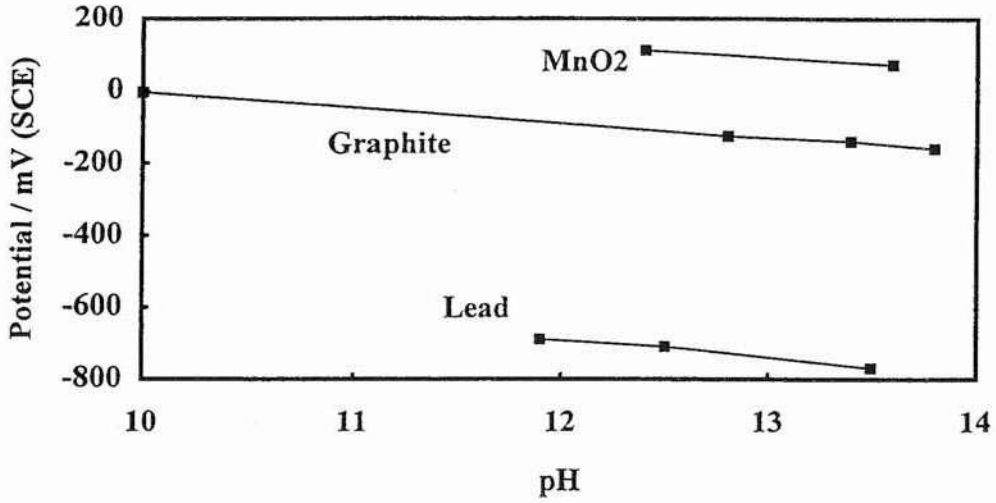

Figure 1. Potentials of manganese dioxide, graphite and lead as a function of pH in $KOH/Ca(OH)_2$ solutions. Room temperature.

Table 3
Observed dE/dpH slopes.

Electrode material	dE/dpH (mV)
MnO_2	-30
C	-40
Pb	-55

The potentials of graphite and lead electrodes as a function of oxygen partial pressure in 0,03M KOH (pH=12,5) are shown in Figure 2. Platinum, an electrocatalyst for oxygen reduction is included for comparison. Manganese dioxide was not included in this experiment because this electrode does not respond to changes in oxygen level. The electrodes were kept overnight in a solution with constant oxygen partial pressure before the potentials were recorded. The oxygen sensivity, i.e. the dE/dp_{O2} slope, was greater for graphite than lead.

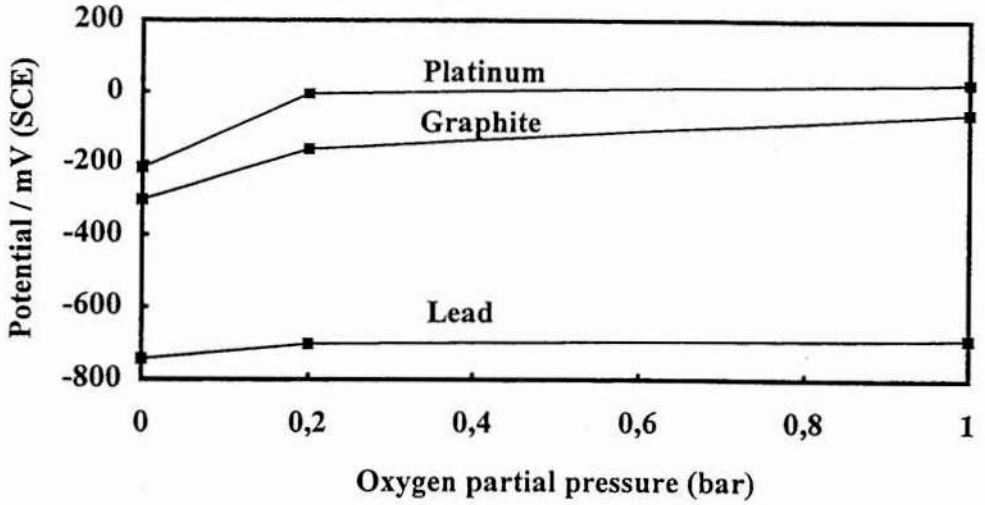

Figure 2. Electrode potentials of platinum, graphite and lead as a function of oxygen partial pressure in 0,03M KOH (pH=12,5). Room temperature.

Figures 3 and 4 show respectively the potential as a function of time for graphite and lead electrodes embedded in concrete. In the first period the concrete slab was stored in air. In the period between day 60 and 74 the slab was completely submerged in tap water and then taken back to air. It is seen that the period in water had an effect on the embedded electrode potentials. When the slab was restored in air the electrodes did not return to their original potential values, but stabilized at 20-30 mV above the "pre-submersion" values.

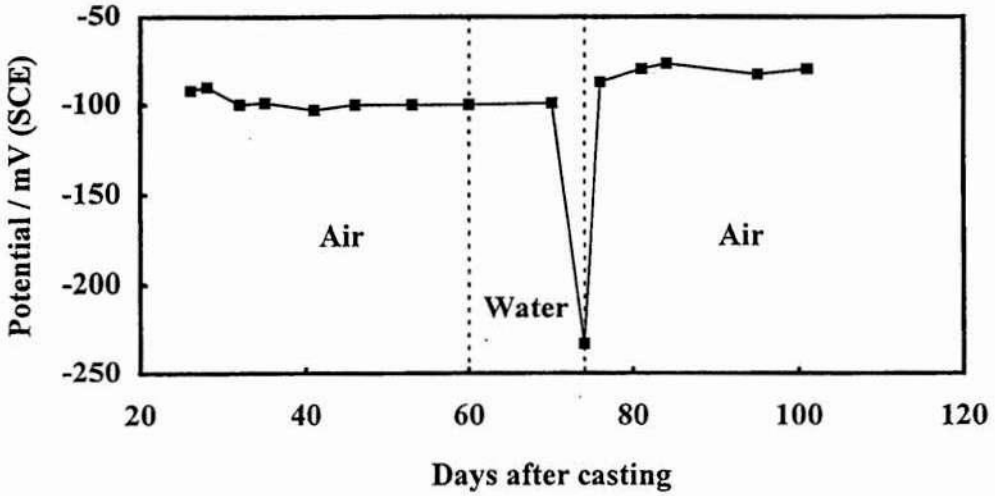

Figure 3. The electrode potential of graphite cast in concrete as a function of time. The slab was submerged in tap water between day 60 and 74. Average of three electrodes. Room temperature.

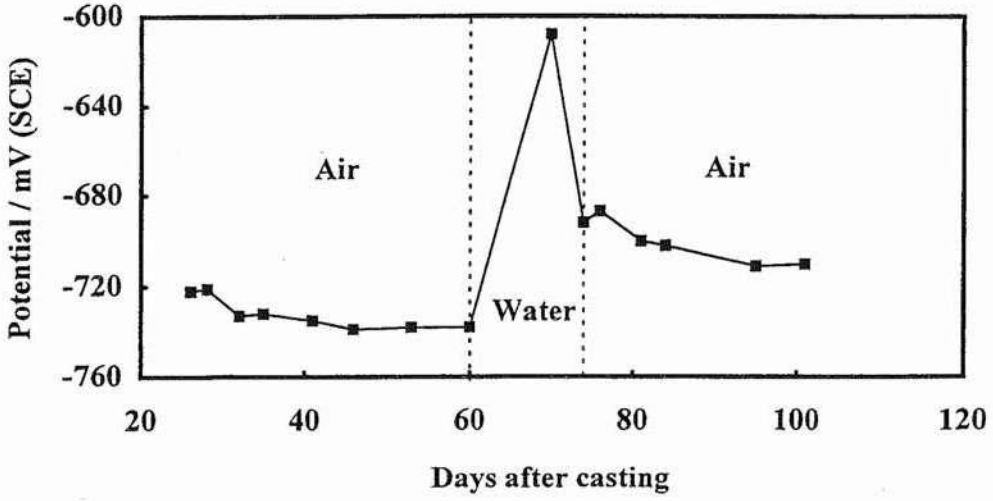

Figure 4. The electrode potential of lead cast in concrete slab as a function of time. The slab was submerged in tap water between day 60 and 74. Average of three electrodes. Room temperature.

As shown in Figures 5 and 6, the divergence between individual embedded electrodes was very different for graphite and lead in the submerged period. The divergence between three lead electrodes was below 10 mV. In the "air period" the divergence was even smaller. When submerged in water the three graphite electrodes showed a divergence up to 300 mV. However, in the air period, the divergence for graphite resembled that of lead. The potential difference between embedded graphite and lead stabilized at 630-640 mV when the concrete slab was stored in air.

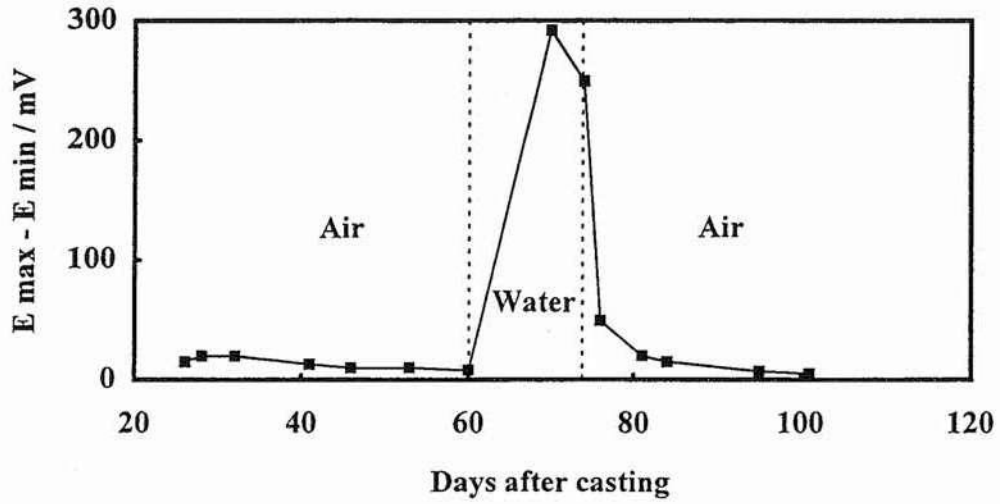

Figure 5. The divergence in graphite electrode potentials given in Figure 3.

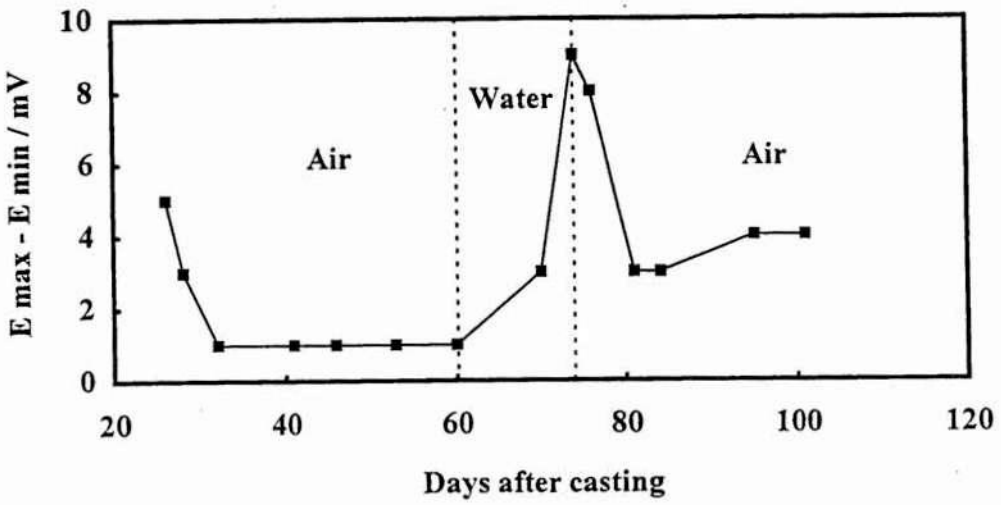

Figure 6. The divergence in lead electrode potentials given in Figure 4.

DISCUSSION

Manganese dioxide

The commercial manganese dioxide electrode [7] is a so called double junction electrode containing an inner alkaline electrolyte. The pH of this electrolyte corresponds to that of pore water in normal concrete. A pourous cement based plug makes the diffusion barrier between the electrode (half-cell) and the environment in which it is placed. The electrode is claimed to have a potential determined by the MnO_2/Mn_2O_3 equilibrium [7]. In alkaline solutions this equilibrium is given by the following ideal half-cell reaction:

$$2MnO_{2(s)} + H_2O + 2e^- = Mn_2O_{3(s)} + 2OH^- \qquad (1)$$

where (s) denotes solid state. Based on standard Gibbs free energies of formation [8], the calculated value of the standard potential (E_o) for this reaction is +0,98 V (SHE) or +0,74 V(SCE) at 25°C. Using the Nernst equation one finds that E=-37 mV(SCE) at pH=13 and that the dE/dpH slope is -59 mV. This is not in harmony with the results obtained in this study (see Tables 2 and 3), which indicates a non-reversible behaviour in the thermodynamic sense. Also the suppliers general specification and laboratory tests reported [7] reveal a mismatch of more than 100 mV (up to 150 mV) between the theoretical and the measured potential values. However, the dE/dpH slope found in this study (approximately -30 mV), which is in accordance with the slope reported by Arup [7], should not be related to the electrode reaction alone. Diffusion potentials may also contribute as emphasized by Arup [7]. Nevertheless, the large difference between the calculated and measured potential values cannot be entirely due to diffusion potentials alone. The fact that manganese oxides exist in several modifications, i.e. different crystal structures - often nonstoichiometric, make their electrochemistry complex. The type of manganese dioxide used in the reference electrode is probably of the same type as used in battery technology [7], i.e. γ-MnO_2 [9]. However, stable standard potentials with γ-MnO_2 is difficult to measure because of its ability to form solid solutions with lower

manganese oxides over a wide range of compositions [9]. Furthermore, the manganese(III) oxide involved in reaction (1) may be α-MnO(OH) rather than Mn_2O_3 [9]. Taking this into account, and allowing the activity coefficients of the oxides to be different from unity in the solid solution, the standard potential of the γ-MnO_2/α-MnO(OH) electrode should be more positive than the calculated value above [9], thus approaching the values obtained from measurements. However, even if such electrochemical "possibilities" may explain the potential behaviour of the manganese dioxide reference electrode, it is difficult to place it among the ideal ones mentioned above.

Graphite

According to the suppliers certificates for the graphite reference electrodes used in this study the average potential value should be -97 mV(SCE) in saturated calcium hydroxide. Our laboratory tests showed that the electrode potential increased with time and matched the suppliers data after 4 hours exposure. Prolonged exposure resulted in a mismatch of about 15 mV.

The graphite electrodes responded to shanges in pH and oxygen level in the solution. This was expected since carbon materials, like platinum (see Figure 2), act as electrocatalysts for oxygen reduction. The oxygen reaction is considered to proceed by either a direct 4-electron pathway or a 2-electron pathway (peroxide pathway), or a combination of the two [10]. However, the oxygen reaction is known to be highly irreversible. It is very difficult to obtain theoretical potential values on most materials and in real solutions. Theoretically, the potental in a pH=13 solution open to air should be +0,21 V(SCE) at 25°C. This is almost 300 mV higher than measured. Furthermore, the theoretical dE/dpH and dE/dlogp_{O2} slopes are -59 mV and +15 mV respectively. Such slopes were not found in the experiments which indicates a non-reversible behaviour in the thermodynamic sense. Consequently, the graphite electrode does not possess the important property required for an ideal reference electrodes. However, the electrocatalytic nature of carbon materials implies that graphite of different origins, or some sort of graphite surface modifications, may exhibit different potential responses.

Graphite embedded in the concrete slab stabilized at about -100 mV(SCE) prior to the submergence in water and about -80 mV(SCE) when the slab was restored in air (see Figure 3). The latter value corresponds to the potential obtained after prolonged exposure in saturated calcium hydroxide. Taking into account the observed dE/dpH slope in KOH solutions (about 40 mV) the 20 mV increase in electrode potential corresponds to an apparent reduction in pH in the concrete pore solution from roughly 13,0 to 12,5. Is it really possible that this water treatment resulted in some sort of permanent change in the concrete pore water composition 3 cm inside the slab? One factor that supports such possibility is the high air content in the fresh concrete mix (about 7 vol-%) which may lead to high permeability. Another factor is that the 18 liters of tap water used for submergence showed pH=10.9 when the slab was taken out. Taking into account the carbonation of this water during the entire period (14 days), the high pH indicates a significant loss of alkaline species from the concrete. Therefore, one cannot ignore the possibility that the 20 mV increase in embedded graphite electrode potentials might be attributed to a decrease in pH inside the slab. However, diffusion potentials may also contribute. Further investigations are needed to clarify this.

Lead

During the experiments we observed that small lead samples simply disappeared in KOH

solutions due to self corrosion. Thus the lead electrode potential is in fact the corrosion potential of this metal. The corrosion potential is a mixed potential related to the coupling of anodic and cathodic prosesses at the interface between the metal surface and the solution. The experiments also showed that the potential of lead is affected by changes in pH and oxygen concentration in the solution. The total corrosion reaction probably consists of dissolution of lead, i.e. oxidation to Pb^{2+} (anode) and reduction of oxygen to OH^- (cathode). This is certainly not an ideal reference electrode, in fact it is not an electrochemical half-cell or an electrode at all in the strict electrochemical sense, but a corrosion cell. However, the lead potential is surprisingly stable in alkaline solutions. In our experiments the potential stabilized at about -730 mV(SCE) in saturated calcium hydoxide at room temperature.

Lead embedded in the concrete slab stabilized at about -740 mV(SCE) and -710 mV(SCE) in air before and after water submergence respectively. The dE/dpH slope observed in KOH solutions was approximately 55 mV. Also this indicates that the water submerged period reduced the pH by about half a unit (from roughly 13,0 to 12,5 - see discussion above). During the submersion in water the potential was up to -610 mV(SCE), indicating a still lower pH in this period. This value is in good aggreement with data reported by Vennesland [11] for lead in concrete submerged in water. One supplier of electrodes states that the nominal potential value for lead in concrete i -660 mV(SCE) without stating whether the concrete is in air or water. Pediferri et al [6] report potentials for lead in concrete slabs about -700±40 mV(SCE) in 1000 day tests.

CONCLUSIONS

The potential of manganese dioxide electrodes, graphite and lead is influenced by pH, lead being most affected.

The potential of graphite and lead electrodes is sensitive to the oxygen level, graphite being the most sensitive.

The electrochemical reactions leading to the observed potential of the manganese dioxide electrode is rather complex. It is difficult to identify thermodynamic reversible reactions for this electrode.

The graphite electrode acts as an electrocatalyst for oxygen reduction. It is non-reversible in a thermodynamic sense.

The lead electrode corrodes in concrete pore water. Its potential (mixed potential) is determined by both anodic and cathodic reactions.

Due to lack of short-term potential stability and/or lack of well-defined Nernstian behaviour, none of the electrodes examined falls into the category of ideal reference electrodes.

ACKNOWLEDGEMENT

The present report is part of the "OFU Bridge Repair Project", financed by the Norwegian Public Roads Administration (NPRA), Rescon AS and the Norwegian Industrial and Regional Development Fund (SND). The project is managed by NPRA.

REFERENCES

1. ASTM C 876-91, American Society for Testing and Materials, 1991, p. 437-442.

2. R. D. Caton, Jr., "Reference Electrodes", Journal of Chemical Education, vol 50, no 12, 1973, p. A571-A578.

3. F. J. Ansuini and J. R. Dimond, "Long-Term Stability Testing of Reference Electrodes for Reinforced Concrete", Corrosion/94, paper no 295, NACE, Houston, TX, USA, 1994.

4. A. A. Sohangpurwala, W. T. Scannell and A. LaConti, "Improvement of Graphite Reference Cell for Reinforced Concrete", Corrosion/94, paper no 307, NACE, Houston, TX, USA, 1994.

5. D. G. Manning, "Cathodic Protection of Concrete Highway Bridges" in "Corrosion of Reinforcement in Concrete", ed. C. L. Page, K. W. J. Treadaway and P. B. Bamforth, Elsevier Applied Science, New York, 1990, p. 486-497.

6. P. Pedeferri, G. Mussinelli and M. Tettamanti, "Experiences in Anode Materials and Monitoring Systems for Cathodic Protection of Steel in Concrete", see Reference 5, p. 498-506.

7. H. Arup and B. Sørensen, "A New Embeddable Reference Electrode for Use in Concrete, Corrosion/92, paper no 208, NACE, Houston, TX, USA, 1992.

8. "Handbook of Chemistry and Physics", 64th edition, CRC Press, Florida, 1983-84.

9. C. C. Liang, "Manganese", Encyclopedia of Electrochemistry of the Elements, ed. A. J. Bard, vol 1, chapter 6, Marcel Dekker Inc., New York, 1973, p. 349-398.

10. E. Yeager, "Electrocatalysts for O_2 Reduction", Electrochimica Acta, vol 29, no 11, 1984, p. 1527-1537.

11. Ø. Vennesland, "Reference Electrodes for Monitoring the Corrosion of Steel Embedded in Concrete", Third International Conference on the Durability of Building Materials and Components, Espo, Finland, Aug. 1984, p. 239-249.

CORROSION MONITORING OF CONCRETE PILLARS IN MARINE ENVIRONMENT

Øystein Vennesland, Norwegian Institute of Technology, Per Austnes, Møre and Romsdal Road Office and Olav Ødegård, Ødegård and Lund A/S

ABSTRACT

A trial repair project is described where various corrosion parameters are monitored. The aim of the project is to study any changes in the corrosion activity of steel in concrete pillars which are coated with a dense epoxy coating. Measurements from surface coated pillars are compared to corresponding measurements from untreated reference.
Keywords: Concrete pillars, Steel corrosion, Monitoring, Coating.

1. INTRODUCTION

This work presents some results from a trial repair at Stokksund bridge, a coastal bridge in the county of Møre and Romsdal.

The aim of the work is to monitor the corrosion activity in concrete piles where a dense epoxy coating is applied at the concrete surface.

By reducing the oxygen transport to the reinforcement the cathodic activity might be reduced to such a degree that the corrosion activity is considerably less than in untreated references.

Theoretically a dense membrane might function in two different ways:

* By acting as a diffusion barrier for oxygen
  The oxygen transport is directly affected

* By acting as a diffusion barrier for water
  The oxygen transport is affected by increased water content in the concrete and thereby reduced oxygen transport

In the monitoring plan of this project great emphasize has been made at making it possible to record parameters which both directly and indirectly affect the oxygen transport in the concrete.

Three columns of the bridge are included in the program, one reference, one which is coated from the top structure and down to the foundation and one which is coated from the top structure, beyond the foundation and below lower water level.

2. CONDITION CONTROL

A very thorough condition control has been made before installation of the measuring probes. The following are very carefully monitored and recorded:

- Accurate locations of reinforcement
- Steel potentials
- Cover thicknesses
- Chloride profiles

In addition test for evaluating the concrete quality has been made.

3. PARAMETERS

The following parameters shall at intervals be studied in the future:

- **Corrosion activity for the reinforcement**
  By measuring the potential Vs embedded reference electrodes.

- **Corrosion rate for the reinforcement**
  By measuring the polarization resistance using embedded reference electrodes and stainless steel counter electrodes.

- **Oxygen content**
  By measuring the potential difference between one reference electrode affected by the oxygen content and one reference electrode unaffected by the oxygen content. Changes in oxygen content will be reflected in changes in potential between the electrodes.

- **Oxygen transport**
  By polarizing an embedded stainless steel electrode with a defined surface area to a potential where oxygen reduction is the only cathodic reaction. At limiting current density the current is a direct measure of the transport of oxygen to the electrode.

- **Resistivity**
  By AC measurements between two embedded stainless steel electrodes.

- **Temperature**
  By thermoelement measurements.

It is very important that the connecting leads are not acting as "channels" for diffusion of oxygen. Special care have therefore been made in the connections between leads and the installed electrodes.

4. INSTALLATION AND MEASUREMENTS

All necessary monitoring equipment have been installed in bands of about 10 cm with a distance of 1 meter between each band in order to monitor the effect of increasing height from sea level.

The installation was made just before application of the coating.

One reference measurement has been made. Further measurements will be made at regular intervals.

5. RESULTS

5.1 Resistivity

The results are shown in Table 1.

Table 1. Resistivity measurements 1994-05-10 at Stokksund bridge (ohms)

Level above water	Pillar no		
	5	6	7
5			3067
4		2404	2521
3	1905	2681	2484
2	1592	4953	2815
1	4865	5662	2263

5.2 Potential measurements

The results are shown in Tables 2 - 4.

Table 2. Potential measurements 1994-05-10 at Stokksund bridge between reference electrodes ERE10 and Dur (mV)

Level above water (meters)	Pillar no		
	5	6	7
5			-119
4		-211	-227
3	-149	-229	-210
2	-174	-225	-241
1	-179	-209	-206

Table 3. Potential measurements 1994-05-10 at Stokksund bridge between reference electrode ERE10 and the reinforcement (mV)

Level above water (meters)	Pillar no		
	5	6	7
5			-204
4		-95	-146
3	-163	-112	-111
2	-161	-142	-128
1	-190	-137	- 98

5.3 Oxygen transport

The results are shown in Table 5.

Table 5. Oxygen reduction current measurements 1994-05-10 at Stokksund bridge (μA)

Level above water (meters)	Pillar no		
	5	6	7
5			0,85
4		1,54	1,53
3	2,56	1,31	0,96
2	2,22	0,95	2,08
1	1,28	0,50	0,83

6. EVALUATION

It is too early to have any opinion on the effect of the surface coating on the columns. All recordings are sensible, however, indicating that instrumentation and monitoring system are functioning as planned.

Electrical Resistivity of Concrete

Sammendrag

In 1993, the Norwegian Public Roads Administration together with the Nordland County Road Administration started a rehabilitation project at the Gimsøystraumen Bridge in Nordland County, Norway.

This project had a dual purpose. One was to build up national competence in Norway on coastal concrete bridge status, by focusing on one particular bridge, Gimsøystraumen. Methods to determine the degree of passivity and corrosion state of the reinforcement were to be systematically tried out, as well as different types of sensor systems installed to provide continuous data on state changes over time. The other purpose was to test out different preventive measures and to undertake a complete rehabilitation of the bridge.

The present report is part of the status assessment work. It concerns the use of concrete resistance data as a means to monitor moisture content changes in the concrete cover over the reinforcement over time. The project included literature studies and laboratory experiments on the materials and environmental factors influencing the electrical resistance of concrete, and was carried out at the Norwegian Road Research Laboratory, Oslo.

The work was carried out by William Elkey MSc under the supervision of Prof. Erik J. Sellevold, Dr. Elisabeth Schjølberg and Dr. Håvard Østlie. Mr. Elkey was associated with the Road Research Laboratory (Feb. - Nov. 1994) on an internship sponsored by the Valle Foundation, University of Washington, Wa., USA. Facilities and practical support for the project was provided by the Road Research Laboratory, Oslo, and the Gimsøystraumen Project.

Emneord: *Concrete, electrical resistance, moisture content, chloride content, temperature.*

Seksjon: *45 - Concrete*
Saksbehandler: *William Elkey and Erik J. Sellevold*
Dato: *January 1995*

Content

Summary

The purpose of the present work was to explore the use of electrical resistance measurements in field concrete as a means of monitoring changes in the moisture content of the concrete over time. Presently the only practical means of monitoring state of field concrete is to measure relative humidity (RH) over time. The RH defines the thermodynamic state of the pore water, but not the amount, which probably is more important than RH for several durability properties. Hence our interest in resistance measurements.

The work is presented in two parts: A literature review and the results of an experimental program carried out in the laboratory.

The literature review covers existing knowledge of the effects of experimental factors such as method of contact between electrode and concrete, applied voltage and frequency. The importance of concrete mix proportions and choice of mix components (cement, silica fume, curing temperature etc.) are covered, as is the more scarce information on the important environmentally determined parametres - the moisture content, the pore water composition in the concrete and the concrete temperature.

The experimental program focuses on the three factors believed to be most important in interpreting continuous resistance measurements in field concrete: Moisture content (expressed as DS = degree of saturation), chloride concentration in the pore water and concrete temperature.

The results demonstrated the extreme importance of the contact between the electrode and the concrete - particularly when measurements are carried out at less than saturated moisture contents.

Over the whole degree of saturation range tested the DS-value has the greatest effect on the electrical resistance which increases several orders of magnitude from wet to dry state. However, for Norwegian coastal bridges the practical DS range is about 70 to 100 %, and in this range the resistance of concrete changes roughly as follows:

- 3 % per °C temperature change
- 3 % per % change in degree of saturation
- 50 % due replacement of pore water by 3 % or 6 % NaCl solution.

Clearly more experimental work must be carried out to better resolve the influence of chlorides. From the results as a whole it is quite clear that even a rough monitoring of changes in moisture content in field concrete by means of resistance measurements requires accurate simultaneous temperature measurements. Any change in the chemical composition of the pore water is likely to effect the resistance values significantly.

1 Introduction

The moisture condition and its variation in a concrete structure are probably the most important factors for the durability of the structure, regardless of the deteriorating mechanism. The rates and consequences of reinforcement corrosion, freeze/thaw attack, alkali-aggregate reactions, etc. all depend strongly on the moisture condition of the concrete. Consequently, it is of obvious importance to obtain reliable information on the moisture state in concrete structures. Such information is, however, scarce in literature. One reason is the practical difficulties in obtaining reliable information. The most obvious method is to remove concrete from the structure in a non-disrupting manner, seal the pieces and then make measurements in the laboratory. This is certainly the most accurate method, but is laborious and somewhat destructive; hence very few systematic investigations have been reported.

The most practical method would be to install a monitoring system allowing periodic readings to be taken automatically. Recently several types of relative humidity (RH) probes have become available on the market, opening the possibility of continuous recording of RH-values at selected positions. In our opinion it has not yet been shown that such probes are reliable over time in natural exposure conditions. For laboratory work the probes can give reliable results only when the temperature is controlled and frequent calibrations are performed. However, RH-data alone only defines the thermodynamic state of the pore water, and not directly the amount of the pore water (or degree of saturation). For many deterioration mechanisms, notably freeze/thaw attack and probably the rate of corrosion, the degree of saturation is the relevant parameter. The relationship between RH and the amount of pore water (sorption isotherm) for concrete show a large hysteresis; i.e., the difference between the water contents at a given RH can be quite large and depends on whether a given RH-value is achieved by adsorption or desorption. In addition, the RH-value exerted by the pore water is influenced by the concentration and types of dissolved ions. Consequently, even reliable RH-records would give incomplete information about the moisture state in a concrete structure.

Electrical resistivity measurement is an alternative, potentially useful method to monitor the moisture state of in-situ concrete, aside from the intrinsic value of such data for the corrosion process [1]. Electrical resistivity in concrete is expected primarily to be a function of the degree of water saturation of a given concrete (rather than the RH). However, resistivity also depends on temperature and pore water composition. The present work includes a review of existing literature on resistance measurements in concrete as well as the results of well-controlled laboratory experiments. The primary purpose was to evaluate the use of resistance measurements as a means of monitoring the moisture state in concrete.

The study presented is in two parts: first, a review of previous studies and second, a laboratory investigation. The review will examine the trends observed among many studies, to identify similarities as well as discrepancies. In addition, it will focus on the methods used in their determination of the electrical resistance or resistivity of concrete, in an attempt to understand how results can be influenced by, for example, electrode type, method of contact, the voltage and (in the case of alternating current) frequency of the measuring instrument, and the specimen dimensions. The laboratory investigation focuses on three important parameters that affect the electrical resistivity of a given concrete: moisture condition, temperature, and chloride concentration in the pore water.

2 Literature review

Durability and Electrical Resistance

Pore water is an electrolytic solution containing, mostly K^+, Na^+, Ca^{++}, SO^- and OH^- [2]. Additional ions (such as chlorides) can also be present due to infiltration from other sources (such as seawater), increasing the concentration of ions in the pore water and, presumably, reducing the electrolytic resistance. The other major factors for concrete resistivity are the pore structure and degree of saturation. The resistivity is the combined result of many factors, and is therefore sometimes used as an indicator of the ability of a given concrete to protect the steel from corrosion. The first studies of electrical resistivity in concrete came about when the industry needed to develop a highly resistive concrete for railroad ties, as electrical signals were being sent through the rails [3, 4], but recently corrosion detection and prevention have been the main focuses of these studies. It has been shown that the resistivity of the concrete is a controlling factor in the rate of corrosion [5, 6].

The level of resistivity needed to prevent corrosion has been examined in various studies, with varying results. Most studies confirm that a resistance of 5,000 Ohm-cm or lower will very likely result in corrosion occurring [7], but the level of resistivity necessary to protect from corrosion is less defined. Several studies have stated that resistance greater than 10,000 Ohm-cm, although one study suggested 60,000 Ohm-cm is necessary for adequate protection [8]. Burke [9] discovered two specimens for which severe corrosion occurred at resistivities of 48 000 and 73,000 Ohm-cm, which clouds the range even further. Figure 1 shows the relationship between corrosion current (I_{coir}) and electrical resistance [1].

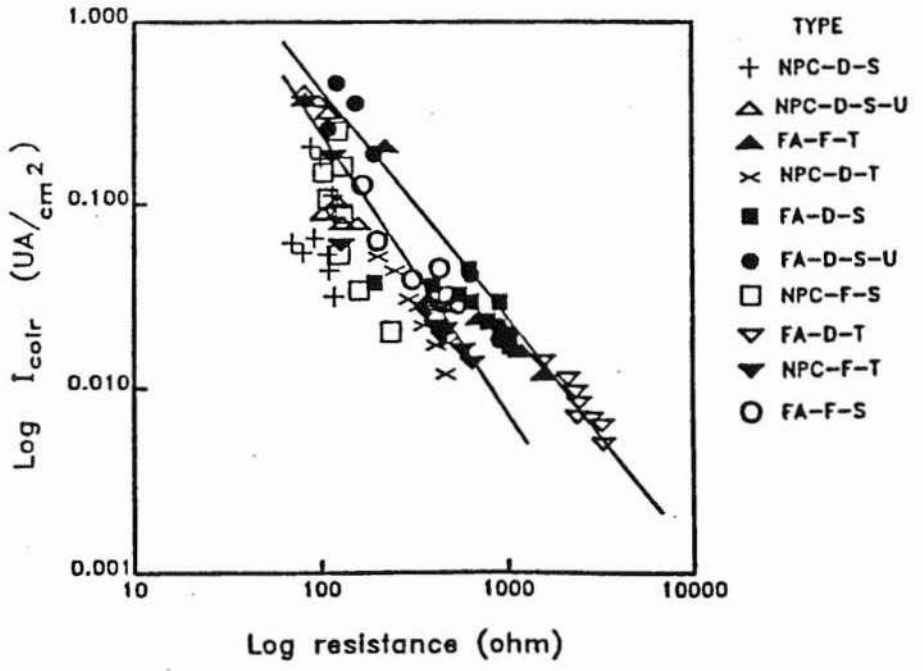

Figure 1. Influence of Electrical Resistance on Corrosion Current, after Cabrera et al. [1].

It is shown in this figure, although it is obscured by the many different mix types used, that a linear relationship exists between the electrical resistivity of the concrete and the corrosion current, indicating that the rate of corrosion in high resistivity concrete should be lower than that of lower resistivity, given the same exposure.

Factors Influencing Electrical Resistance in Concrete

In saturated concrete electrical current is passed predominantly by the movement of ions in the pore water [10]. From this it can be inferred that, for saturated concrete, two fundamental factors deciding concrete resistivity are the pore structure characteristics (total porosity, pore size distribution and degree of continuity) and the total ionic concentration of the pore water. How these parameters can be altered and, in turn, alter the electrical properties of concrete has been compiled from various studies.

Effect of Paste Volume

The influence of paste volume on concrete resistivity is shown in figure 2 [11]. It shows that, for a constant water/cement ratio, increasing the paste volume decreases the resistivity at a rate of approximately 1 % per 1 % paste. Changing the water cement ratio, while altering the particular resistivity level for each concrete, does not alter either the direction or magnitude of this trend. The increase of paste content creates more channels for electrolytic liquid (pore water). Therefore this trend is consistent with a simple composite model for concrete, with the paste as the "conducting" component.

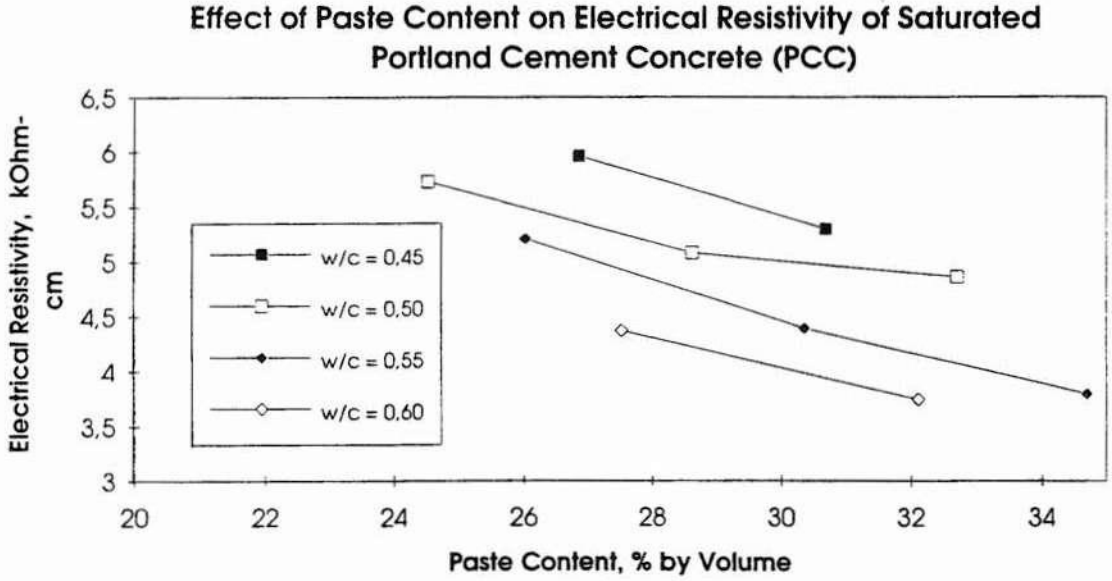

Figure 2. Influence of Paste Content on Electrical Resistivity of Saturated PCC, after Hughes et al. [11].

Effect of Cement Type

Intrinsically, the type of cement used in a particular mix has an impact both on the pore structure characteristics and the pore water chemistry. Figure 3 [12] shows the relationship between cement type and resistivity for concrete made with four portland cement types: two ordinary portland cements (OPC1, OPC2), a modified portland cement containing 20 % fly ash (MP) and a high strength portland cement (HS).

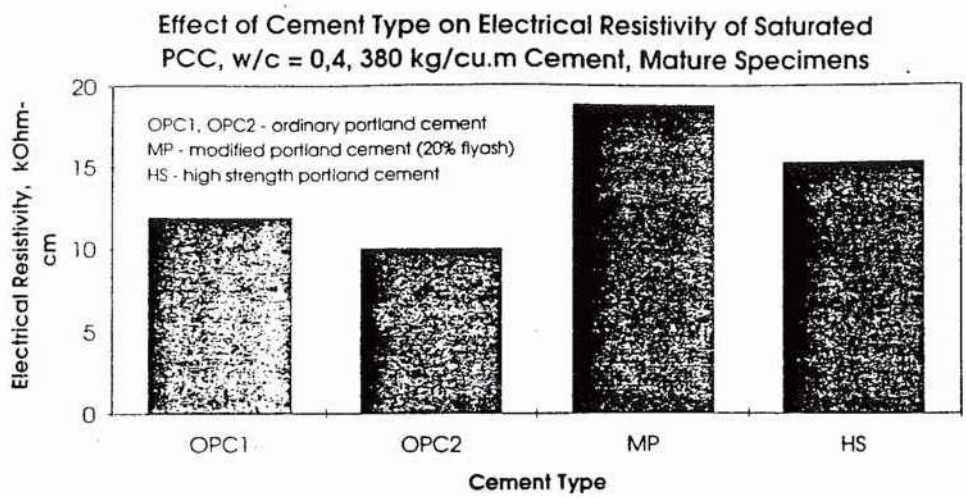

Figure 3. Influence of Cement Type on Electrical Resistivity of Saturated PCC, after Vennesland et al. [12]

This figure shows that even for two types of ordinary portland cement there is a noticeable difference in resistivity between the concretes made with ordinary portland cement from different manufacturers. MP and HS concretes, however, both showed a substantial increase in electrical resistivity when compared to OPC. Other studies have shown much larger differences in resistance. For example, Hammond [3] showed that a high alumina cement had a mature resistivity of 10 times that of OPC with the same water/cement ratio and curing.

Effect of Water/Cement Ratio

The water/cement ratio in concrete is a major factor in determining the pore structure of hardened concrete. It is known from other studies that as the water/cement ratio increases, the pore structure becomes coarser and more continuous. From this it can be inferred that an increase in the w/c-ratio will cause a decrease in the electrical resistivity. Figure 4, which compiles the data from three independent studies [9, 11, 13], shows a linear trend with a rate of change of approximately -0.22 kOhm-cm/0.01 w/c ratio.

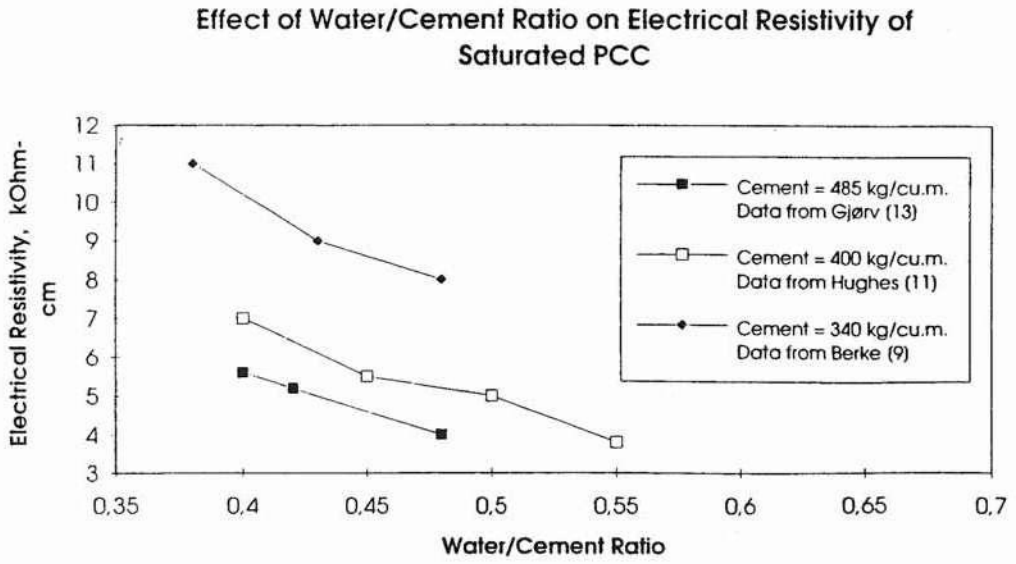

Figure 4. Influence of Water/Cement Ratio on Electrical Resistivity of Saturated PCC [9, 11, 13].

Figure 4 shows that the dependance of this trend on other concrete parameters (i.e., curing, cement type, silica fume content) is most likely not substantial given the limited information on the particular mix designs and curing procedures for these studies. In addition, the increase in paste content, while decreasing the resistivity, does not alter these trends.

Effect of Curing Temperature

In 1993, Hauck [14] performed chloride migration studies to examine the effect of curing temperature and silica fume content. During this process a record of the electrical resistivity, both before and after chloride migration (steady state chloride transport in a 12 V field), was kept. Figure 5 shows how curing temperature effects the electrical resistivity of PCC (measured before the migration test) for varying silica fume contents.

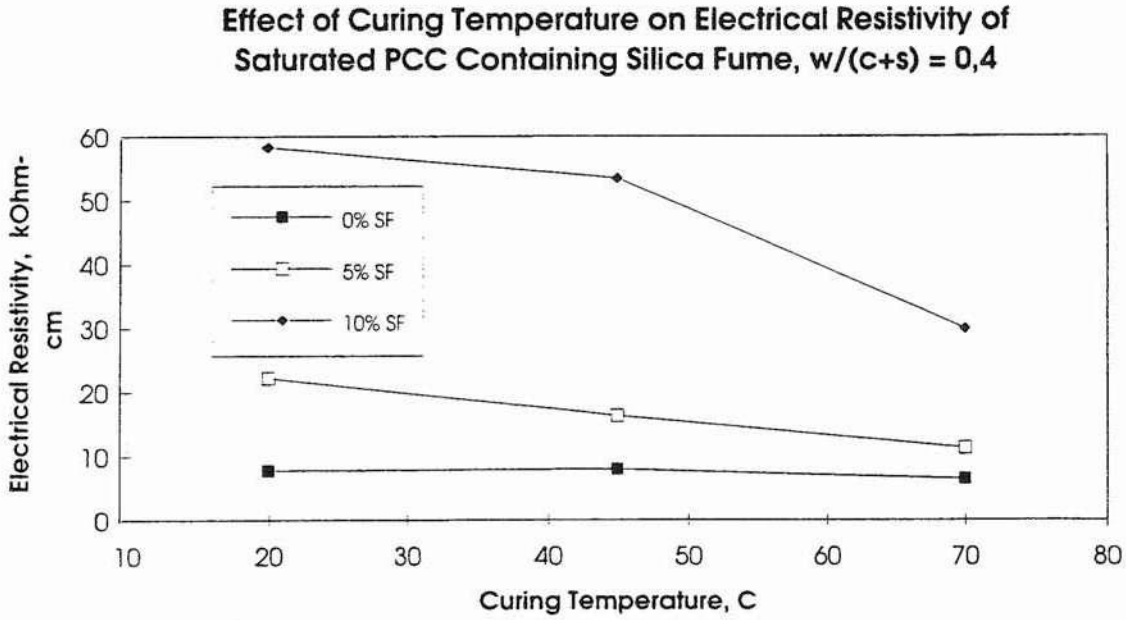

Figure 5. Influence of Curing Temperature on Electrical Resistivity of Saturated PCC, after Hauck [14].

Figure 5 shows that as the curing temperature increases the electrical resistivity decreases, and that this trend becomes much more noticeable as silica fume is added. This may indicate that the concrete has a different ionic concentration in the pore water, but more likely shows that the pore structure itself becomes coarser and more continuous due to the increased curing temperature, as has already been shown by low temperature calorimetry.

Effect of Silica Fume

It is well understood that when silica fume (or fly ash) is added to a concrete mix it results in a much finer pore structure [9] as well as lower ionic concentration in the pore water [15]. Both factors are expected to increase the resistivity. Figure 6 illustrates the relationship between silica fume content and electrical resistivity, as collected from two independent investigations [9, 14].

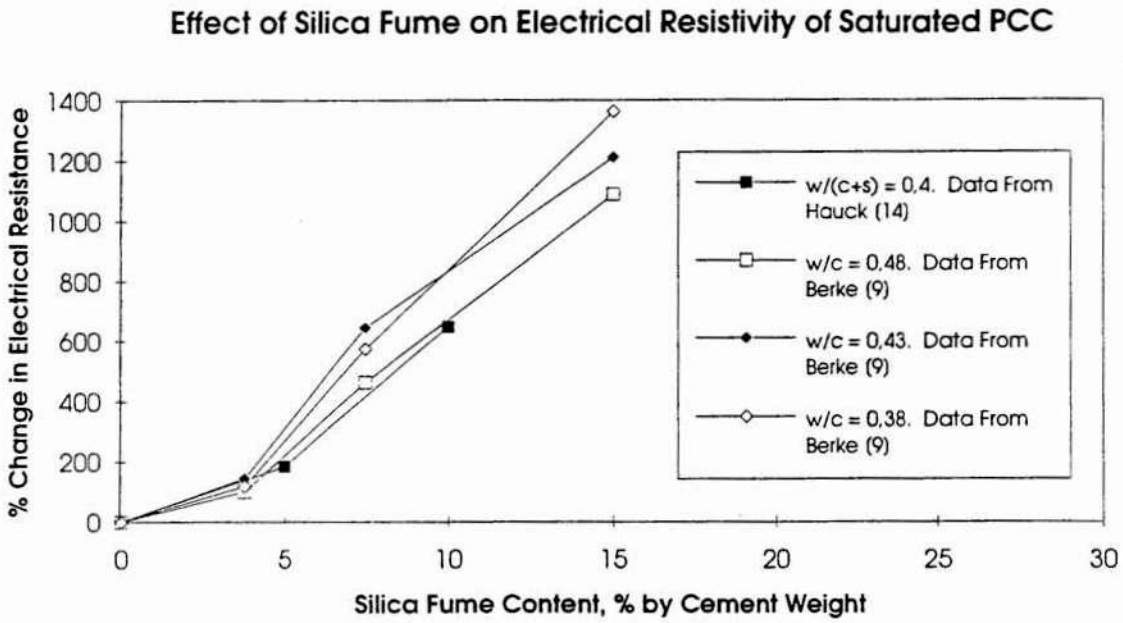

Figure 6. Influence of Silica Fume on Electrical Resistivity of Saturated PCC [9, 14].

Figure 6 shows that the electrical resistivity, as expected, increases substantially with increasing silica fume content. The differences in resistivity among mixes of various w/c-ratios, in addition, appear to become more defined at higher concentrations of silica fume. In an extreme case, Hansson [10] showed that dense mortar containing silica fume (w/c = 0.15) had a mature resistivity of 200 kOhm-cm.

Effect of Temperature

Like all materials, concrete's electrical properties are affected by temperature. This phenomenon is also complicated by the change in the pore water chemistry that occurs along with change in temperature. At higher temperatures, more ions will dissolve into the pore water, and then precipitate out as the water cools. Woefl and Lauer [2] performed independent studies on the effect of temperature as well, superimposing their results with those of Monfore [9] and Spencer [16]. All three sets of data indicated a sensitivity of about 3 % per degree C (with reference to 21 °C), with resistance increasing with decreasing temperature. Figure 7 shows a composite plot of data collected by Woefl and Lauer and data from Monfore superimposed on a curve developed by Spencer, showing the multiplying factor needed to change a resistance taken at other temperatures to that measured at 21 °C. The conformity of these independent studies suggests that this temperature phenomenon is independent of other concrete aspects, such as porosity, cement content, etc. It would be useful to compare the temperature effects on concrete resistivity to the temperature effects on a solution with the same ionic composition as pore water in the concrete.

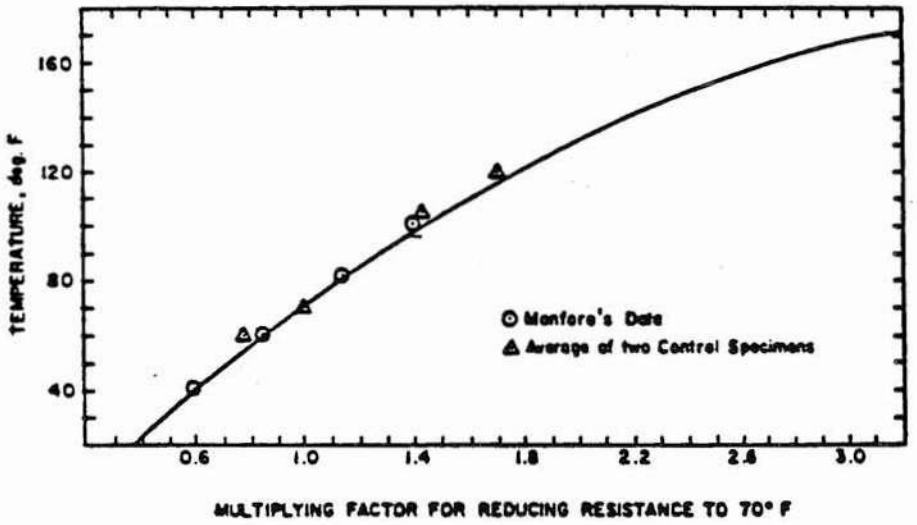

Figure 7. Temperature Reduction Curve, after Woefl and Lauer [2].

The fundamental variation of phenomena such as resistivity to temperature can be expressed by the Hinrichson-Rasch Law:

$$R_2 = R_1 \cdot e^{A(1/T2-1/T1)} \qquad \text{(Eq. 1)}$$

where

R_1 is the resistivity at temperature T1
R_2 is the resistivity at temperature T2
T1, T2 are temperatures (Kelvin)
A is the activation energy (Kelvin).

Figure 8 shows a typical plot of electrical resistivity versus the inverse of the absolute temperature based on data from Monfore and Hope [4, 8] for both concrete and paste specimens of different w/c ratios.

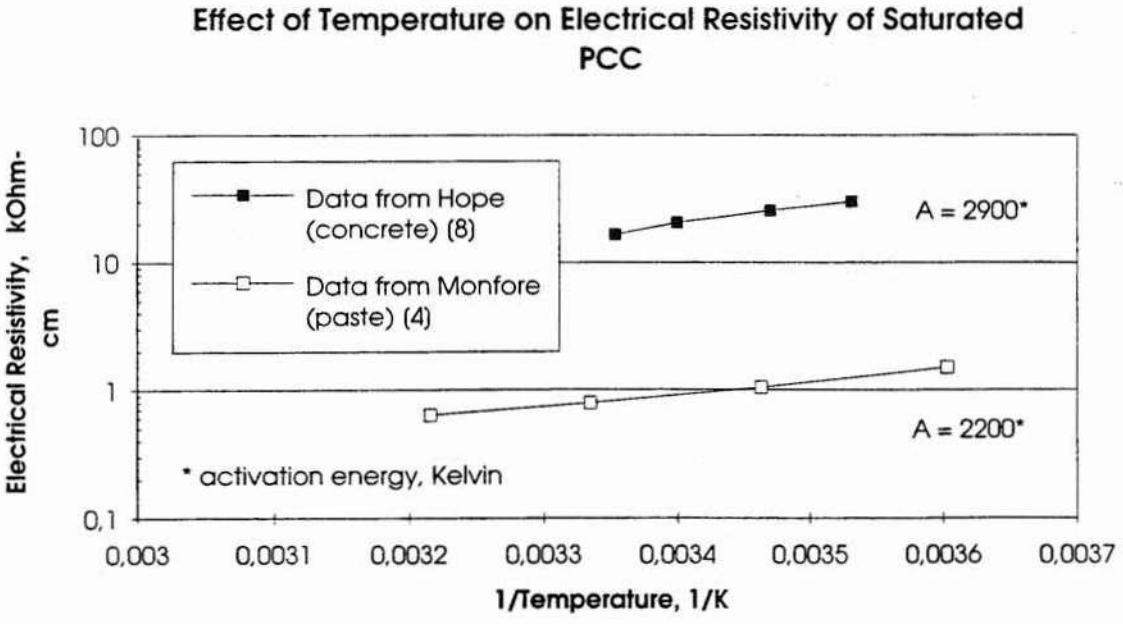

Figure 8. Influence of Temperature on Electrical Resistivity of Saturated PCC [4, 8].

Figure 8 shows that the relationship between resistivity and temperature is consistent with equation 1. Activation energies for the concrete and the paste were 2900 and 2200, respectively. Other sources have calculated values for A from 2000 to 5000, which represents approximately 3% to 5% per °C at 21 °C. The most commonly observed is around 3000 [8]. Other studies have shown that this sensitivity can vary depending on the moisture condition [17], but further studies should be performed to examine this effect.

Effect of Chlorides

As chloride intrusion is a chief cause of corrosion of the reinforcing steel, the influence of chlorides on the electrical resistivity of concrete has been of interest in previous studies, particularly involving the addition of chlorides to the mixing water. It is expected that the additional ions introduced into the pore water will cause a decrease in electrical resistance, but as it is not understood how these ions will interact with those already present in the pore water, the amount of change in electrical properties is unknown.

Figure 9 shows the relationship between percent of calcium chloride (CaCl) added to the mixing water and the percent change in electrical resistivity of a mature (more than 3 months cured) concrete. This figure includes data from two studies [4, 13] and shows that the electrical resistivity drops quickly at low concentrations, but the marginal change after 2 % CaCl addition is not as extreme, appearing to stabilize at approximately 50-60 % of its original resistance. This suggests that after a certain level of chlorides is attained in the pore water additional chlorides do not substantially increase the total ionic concentration. However, it is also known that the concrete pore structure is altered when CaCl is added to a mix. Furthermore, such studies should also distinguish between chlorides in the concrete and those intruded after hardening.

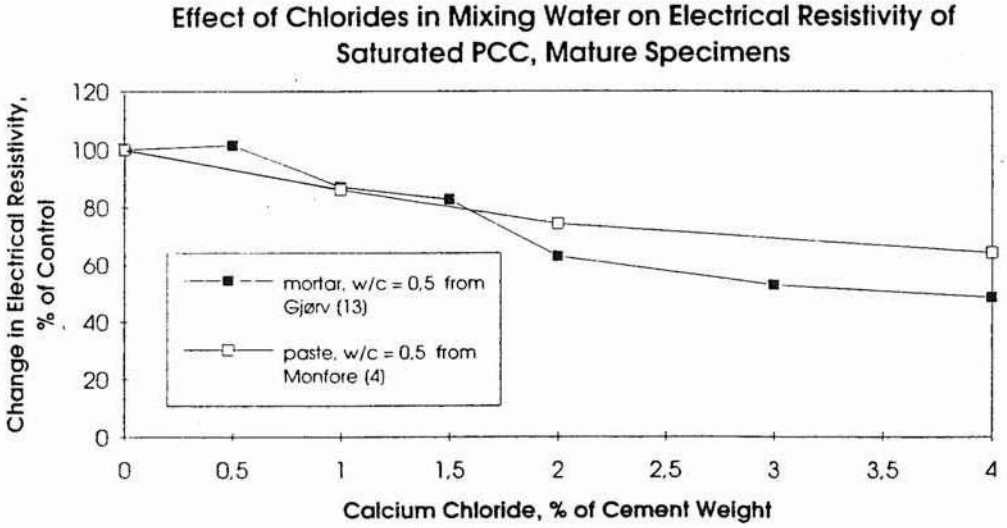

Figure 9. Influence of Chlorides in Mixing Water on Electrical Resistivity of Saturated PCC [4, 13].

The study by Hauck [14] showed a substantial decrease in resistance after the 12 Volt migration test was completed, as compared to before (particularly for concrete with silica fume). This is presumable a result of altered pore water composition since chloride ions are supplied to the pore water. Such experiments thus offer the opportunity to separate the chemical from the physical (pore structure) effect on concrete resistance.

Effect of Moisture Content

Moisture content is a major factor deciding the electrical resistivity of concrete. As the pore water acts as an electrolyte with lower resistivity than that of the solid matrix, the moisture content is inherently a major factor affecting the concrete's electrical properties. As has been shown, a normal (OPC) saturated concrete has a resistivity between 1000-10 000 Ohm-cm, depending on mix parameters, while dry concrete reaches 10^8-10^9, showing the importance of pore water on resistance [7]. Figures 10 [2] and 11 [13] show the effect of degree of saturation on electrical resistance.

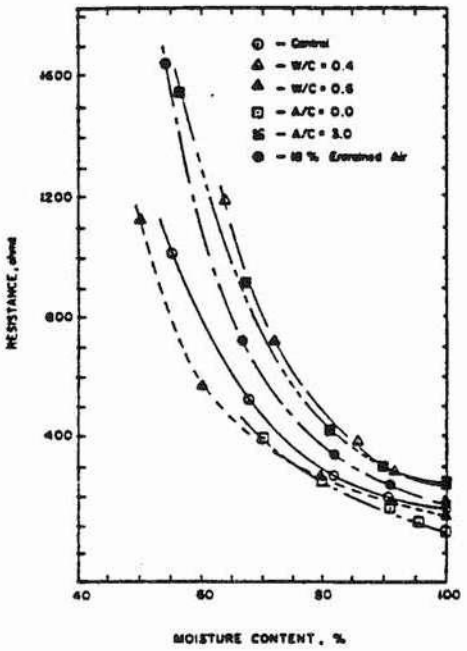

Figure 10. Influence of Moisture Content on Electrical Resistance of PCC, after Woefl and Lauer [2].

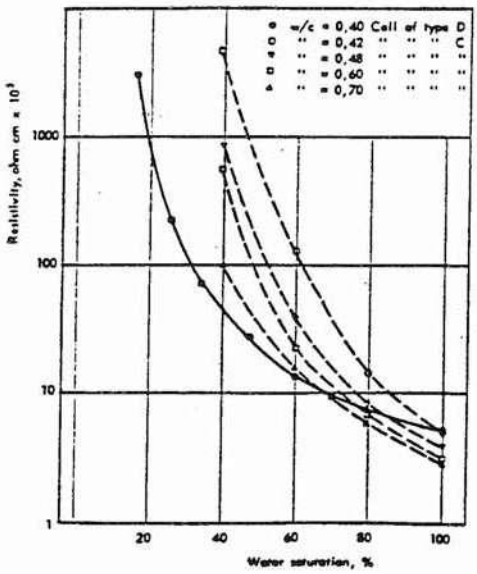

Figure 11. Influence of Moisture Content on Electrical Resistivity of PCC, after Gjørv et al. [13].

Both figures also show that decreasing w/c ratio increases the rate of change of resistance. It is also shown that the critical range, where the increase in resistance becomes more rapid, occurs at a high moisture content, 60 % to 80 % degree of saturation. This suggests the range where the pore water begins to lose continuity, decreasing the number of available electrical channels substantially.

Review of Testing Methods

Of the testing procedures for electrical resistance reviewed for this study, the aspects that varied most frequently and which may have significant contributions to the results were: voltage type and/or frequency, specimen size and shape, electrode type, and the method of attaining proper contact. A summary of these parameters is shown in table 1.

Table 1. Summary of Test Methods.

Study	Voltage type (Frequency)	Specimen Description	Electrode Type	Method of Contact
Monfore, 1968 [4]	DC (4 - 10 V) AC (2 - 8 V) (0.1 - 10 kHz)	cubes (1"and 4")	brass plates (external)	stiff graphite gel
Hammond & Robson, 1955 [3]	DC (55-3 kV) AC (0.002 - 25 kHz)	cubes (4") prisms (4 x 4 x 1")	brass plates (external)	stiff graphite gel
Hughes, 1985 [11]	DC (4 - 8 V) AC (10 V) (1kHz)	cubes (150 mm)	brass plates (external)	fluid cement paste (w/c = 0.5)
Woefl, 1979 [2]	AC (6 V) (60 Hz)	prisms (1 x 2 x 6")	slim rods (mat. N/A)	cast in
Hauck, 1993 [14]	AC	cylinders (100 mm dia. x 51 mm)	iron mesh (external)	electrolytic solution
Hope, 1985 [8]	AC (1kHz)	prisms (25 x 25 x 100 mm)	brass or steel rods	cast in
Bracs, 1970 [18]	Not Available	cubes (6")	steel wire	cast in
Cabrera, 1994 [1]	AC (10 V) (1 kHz)	cubes (100 mm)	brass plates (external)	fluid cement paste
Schiessl, 1993 [19]	AC (120 Hz)	Not Available	Multi-Ring Electrode	cast in
Hansson, 1983 [10]	DC (3 - 9 V)	prisms (90 x 70 x 50 mm)	perforated steel plates (30 x 30 mm)	cast in
Bhargava, 1978 [20]	AC (0.5 - 1.5 V) (0.1 - 50 kHz)	prisms (40 x 40 x 160 mm)	hardened cement paste w/ Pt black	cast in

Voltage and Frequency

Measurements of the electrical resistivity of concrete have been performed using both direct and alternating current at various frequencies. As concrete pore water is an electrolyte, the application of direct current causes a polarization potential, or back electromotive force (EMF), which alters the resistance readings [4]. A direct current also causes a net transport of ions in the electrolyte, thereby altering the electrolytic composition. The true resistance can then be calculated by using Ohm's Law.

$$R = \frac{Ea - Ep}{I} \qquad \text{(Eq. 2)}$$

where

R is the electrolytic resistance (Ohms)
Ea is the applied potential (Volts)
Ep is the polarization potential/back EMF (Volts)
I is the electrical current (Amperes).

This method, while accurate, has been criticized as the resistance cannot be measured directly, but instead must be calculated using other electrical data. As shown in Table 1, alternating current (AC) has been the more frequently used type for the measurement of electrolytic resistance due to the elimination of the polarization effect [3]. The range of frequencies used has been from 2 Hz in an early experiment by Hammond and Robson up to 50 000 Hz used by Bhargava. Voltage levels have ranged from 0.5 to 3000 Volts.

Recently impedance has been suggested as a more reliable measurement than resistance based on the voltmeter-ammeter (V-A) method, but some studies show that the difference is nominal for frequencies below 25 000 Hz [20]. Impedance is inversely related to both capacitance and resistance. As the frequency decreases, however, the capacitance of the concrete becomes much greater. Therefore, resistance has a greater influence on the impedance, and, as a result, impedance values are usually nearly identical to the resistance values measured.

It has been suggested that frequencies that are not multiples of 100 Hz are best for these measurements, as most interference from other sources would occur on these century points. A frequency of 108 Hz, consequently, has been suggested for the Multi-Ring Electrode [19]. In 1978 Bhargava examined the resistance of concrete at different voltages and frequencies, the results of which are shown in figure 12 [20].

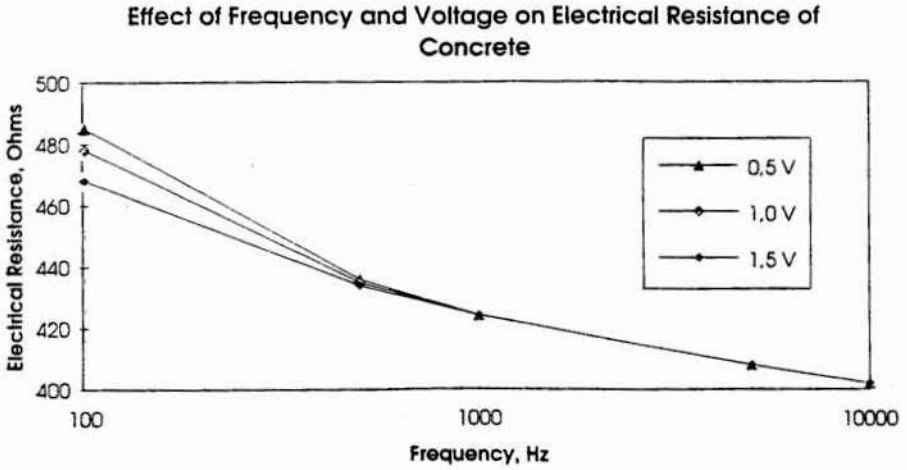

Figure 12. Influence of Frequency and Voltage on Electrical Resistance of PCC, after Bhargava [20].

It is noticed in figure 12 that, after 1000 Hz frequency, the difference between the resistance measured at various voltages disappears and as a result he recommends, for the V-A method, a frequency of at least 1kHz should be used. Other studies, however, have not seen the same drop in the measured resistance with increased frequency. Calleja [21] showed in his study that the decrease in resistance from 40 to 20 000 Hz was only 10 %, about half the magnitude of change shown in figure 12 for a much larger range of frequencies.

Specimen Size and Shape

Specimen size varied considerably in many previous experiments, depending on the parameters to be studied. Specimen sizes ranged from over 3000 cm^3 of concrete [11] to less than 100 cm^3 [6], with the smaller specimens generally being necessary for quick moisture conditioning while larger specimens were used for better representation of the concrete mass, for the study of age and mix design effects. Most of the studies used concrete prisms or cubes that, for the case of external electrodes, gave two even surfaces to apply the electrodes.

Electrode Type

Table 1 shows that brass was the most common choice of electrode material for the studies reviewed. All other types of electrodes were also either metal or metallic coated (i.e., platinum black coating on hardened cement paste). For external-type electrodes plates, grids or meshes were used most commonly, while internal electrodes were normally wires or thin rods. Typically the internal electrodes were deformed by notching or knurling to insure a good bond with the cement paste. Other than the inherent difficulty in calculating resistivity from data collected using internal point or line electrodes, none of the studies showed any noticeably different trends that were considered the result of the electrode type. Internal electrodes have the advantage of being cast in place, which allows for quicker resistivity measurements as well as a constant contact zone.

Method of Intimate Contact

Intimate contact, an expression used frequently in many of the studies reviewed, refers to the achievement of the best possible electrical contact between the concrete and the electrodes, or more accurately, the pore water system and the electrodes. Intimate contact allows for the actual resistance of the specimen to not be altered by additional resistance between the electrodes and the concrete. In general, at saturated conditions intimate contact with external electrodes is much easier to attain than at drier conditions as the water is removed from the contact zone first. One study [13] used five types of electrical cells, a group of three that used solutions of $Ca(OH)_2$ and steel plate electrodes and a group of two that used brass mesh electrodes. This latter group is of higher interest since it uses similar electrodes but two methods to attain intimate contact. The first method (cell type C) involved simply placing the brass mesh electrodes on opposite ends of a specimen, while the second method (cell type D) involved casting the brass meshes into the concrete specimens. A diagram of both methods of contact is shown in figure 13.

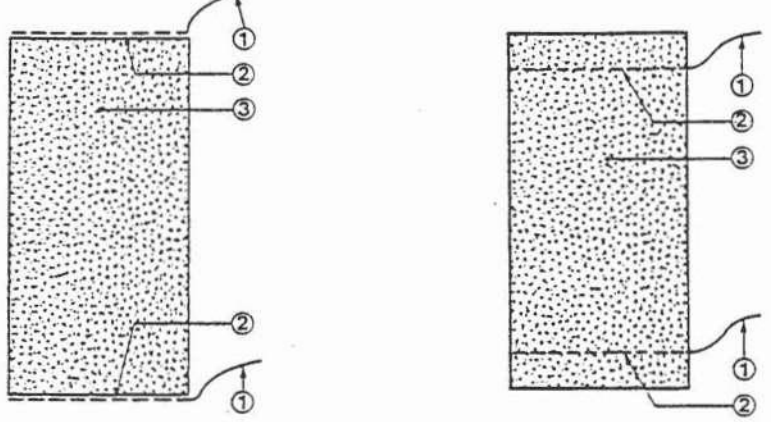

Figure 13. Diagram of Test Specimens Using Different Methods of Contact, after Gjørv [13].

A comparison of the results of these two methods of contact is shown in figure 11 [13]. The divergence of the resistance values below saturated conditions of the two similarly designed mixes shows that cell type D is creating a higher degree of contact once the moisture has been removed, and furthermore that the degree of intimate contact is of decisive importance for resistance values in concrete tested at less than full saturation.

3 Experiments

Specimen Description

It was decided for quick moisture conditioning and resistance stabilization to use a mature concrete with a water/cement ratio of 0.6 although a 0.4 mix was also available. The 0.6 concrete allowed for quicker equilibration at a given moisture level due to the coarser pore structure. The 0.4 concrete was used for a companion study of temperature sensitivity in the saturated state. The cement used for both mixes was a standard P30 cement (16 %, 59 %, 7.5 % and 10.4 % for C_2S, C_3S, C_3A and C_4AF respectively). The pertinent information of the two mix designs is shown in table 2.

Table 2. Mix Design Information.

w/c	Cement (kg/m^3)	Silica Fume (% of cement)	Curing Type & Period	90 Day Str. (MPa)
0.6	350	0	Wet 8 mo.	48.8
0.4	390	4.9	Wet 4 mo.	71.4

Examination of the types of cells used previously suggested that, again for quick stabilization, specimens with a large surface area to volume ratio were necessary. All of the specimens for each water/cement ratio were cut from the same 5 cm thick slab. The specimens were approximately 10 cm x 5 cm x 2 cm. Precise measurements have been obtained to calculate specific resistance.

Fifteen specimens were prepared with 0.6 concrete, three parallels for each of five studies: temperature sensitivity at saturated condition, different degrees of saturation using stepwise desorption, and stepwise absorption from a 50 °C dry state using pure water as well as 3 and 6 % NaCl solutions. In addition, four saturated specimens of 0.4 concrete were prepared for a parallel temperature sensitivity study at saturated conditions. Complete mix design information is shown in Appendix A.

Measurement Type and Voltage

For this study a voltage of 0.9 volts and frequencies of 1 kHz and 120 Hz were used for resistance measurements. Upon comparison of data from both frequencies, it was discovered that the resistance measurements, although nearly identical at saturated conditions, deviated at lower moisture conditions, as is shown in figures 14 and 15, the latter of which shows that the ratio between the two measurements also changed with changing moisture content. Because of this phenomenon and the other evidence suggesting that 1 kHz and higher frequencies have greater stability, the remainder of the results will be expressed in terms of 1 kHz frequency and 0.9 Volt potential.

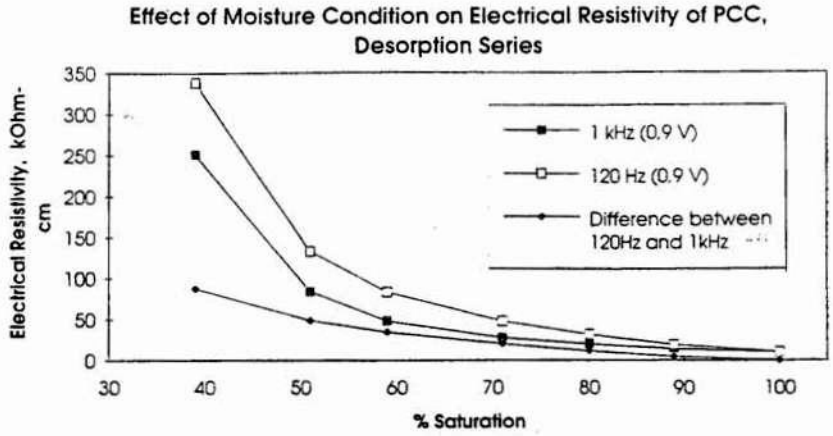

Figure 14. Influence of Measuring Frequency on Electrical Resistivity of PCC at Various Moisture Conditions.

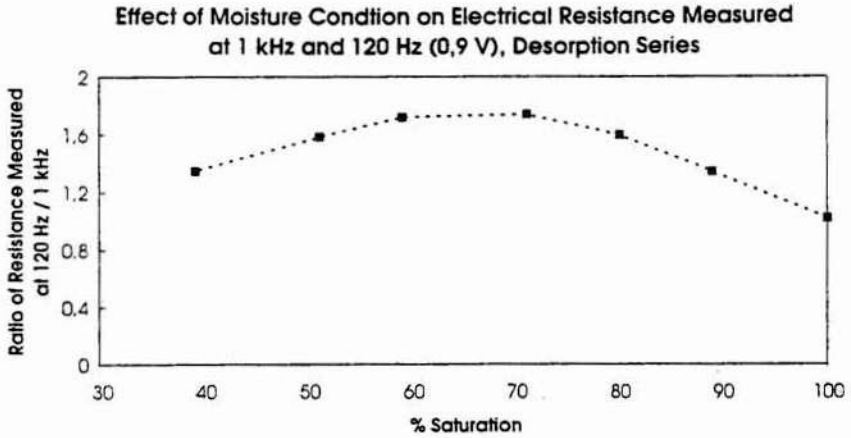

Figure 15. Influence of Measuring Frequency on Electrical Resistanse Measured at 1 kHz and 120 Hz (0.9 V).

Intimate Contact

As mentioned previously, various methods to attain intimate contact between the electrodes and concrete were used in other studies, from liquid cement paste to salt water. Since the specimens that were prepared for this study were to be tested at various moisture conditions, these water-based methods of contact were not usable and a method of dry contact needed to be found. The extreme importance of contact on the resistance results has been demonstrated in figure 11 [13]. Several types of metallic meshes, wools and foils were attempted, but it was learned that the amount of force that held the electrodes in place affected the resistance measured, with resistance decreasing with increasing force. In addition, once the outer film of water was lost on saturated specimens, resistance increased significantly with the loss of contact points. The method of brass meshes cast into the specimens allows for good contact, but as the specimens to be used for this study were already cast this was impractical.

The next attempted method of intimate contact was graphite paint of the type used in cathodic protection of concrete. There are several advantages to this method of contact: it is permanently fixed to the face of the concrete (allowing for quick measurement), the contact area is constant, and the moisture condition in the concrete can be controlled easily after the paint is cured. There is some increase in weight of the specimens due to the paint and leads; this was noted for each specimen and weights were adjusted.

The most important aspects of determining the acceptability of this method of contact were its reproducibility (consistency of results between identical specimens) and accuracy when compared to other accepted methods. Six saturated 100 mm cubes were prepared to study this aspect, as this size cube is generally accepted to be a large enough quantity of concrete to represent a mix; variation in results due to heterogeneity of the concrete should be small. Three of the cubes were 0.6 w/c concrete, while the other three were 0.4 w/c concrete. Two cubes from each set were prepared with the graphite paint electrodes, with two opposite sides painted on each cube and leads attached. The final cube from each set was tested with liquid electrodes, which simply involved saturating an absorbent pad with water from the same water bath that the specimens were stored. The resistances were checked in this saturated surface dry condition, and then were allowed to air-dry for 72 hours, after which the resistances were retested. Results from this study are shown in figure 16.

It is shown in figure 16 that resistance measurements taken using the graphite paint electrodes are not only reproducible, but compare favorably with the water electrode, suggesting that this is an acceptable method of contact. In fact, the graphite paint showed the least amount of change from the wet to the drier state. This is most likely due to the uneven drying due to the highly impermeable graphite paint. The contact with the moisture on these faces was not lost. Since there is no substantial divergence, unlike that shown previously in figure 11, this electrode type was considered adequate for the intended purpose. Thus, the specimens for use in the full studies were prepared with this electrode type, with the sides measuring 100 mm x 20 mm painted. A diagram of a typical test cell is shown in figure 17.

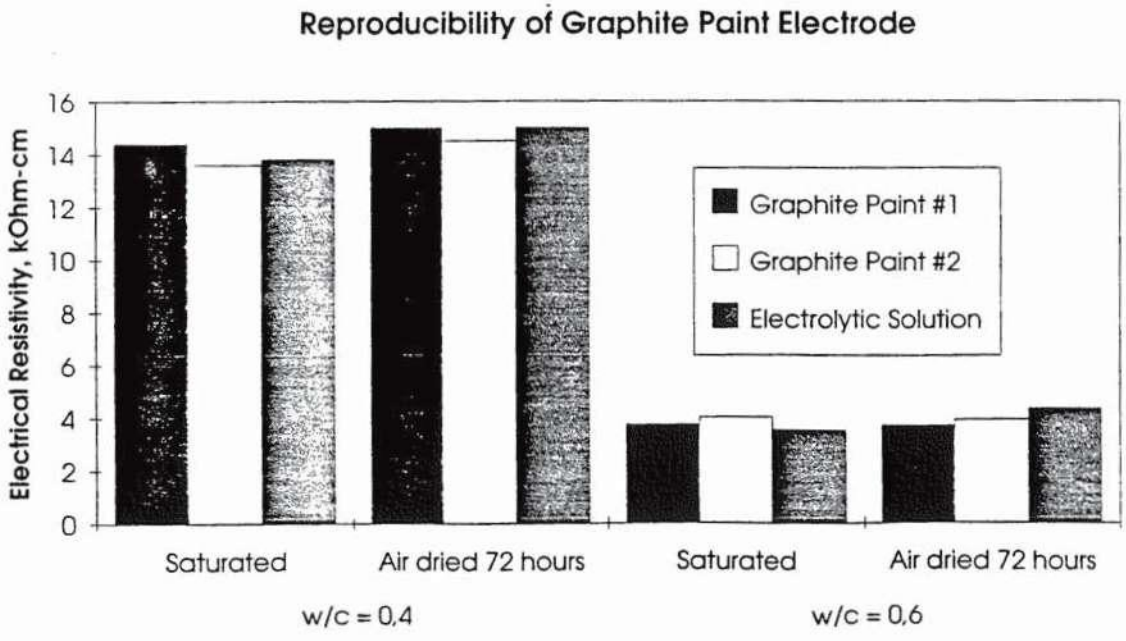

Figure 16. Reproducibility of the Graphite Paint Electrode.

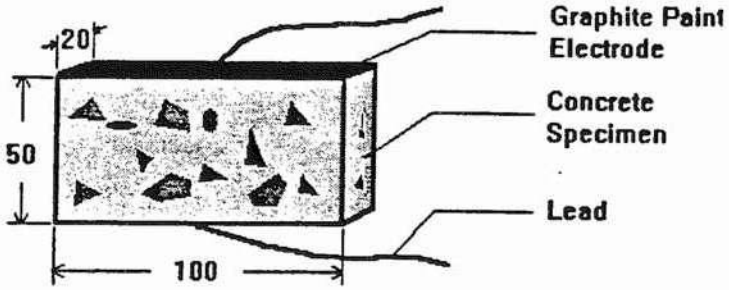

Figure 17. Diagram of Typical Concrete Specimen Used for Electrical Resistance Studies (Dimensions in mm).

Resistivity Calculation

To determine resistivity from electrical resistance, precise measurements of the sample needed to be obtained. Three measurements were taken in each dimension for a representative average. The calculation of resistivity is:

$$R = \rho \cdot A_{ave}/L_{ave} \qquad \text{(Eq. 3)}$$

where

R is the resistivity (kOhm-cm)
ρ is the resistance (kOhm)
L_{ave} is the average distance between electrodes (cm)
A_{ave} is the average cross section perpendicular to the electrodes (cm).

L_{ave} was used for easy calculation. The distance between electrodes varied little so that the difference between L_{ave} and the true effective path length was about 1 %. The true effective path length was found by simulating a concrete specimen as several parallel circuits with resistances reflecting the range of values measured for the distance between the electrodes.

Moisture Conditioning

There were two separate series studied in this experiment, the desorption and absorption series. Specimens were conditioned by either stepwise drying from a saturated state or stepwise rewetting from a 50 °C dry state to attempt to define the outer edges of the hysteresis curve. An estimate for the moisture content of the specimens was obtained by drying three dummy specimens at 105 °C for twenty-four hours. This gave moisture contents of 5.7 %, 5.7 % and 5.8 % by weight of dry concrete. Thus, for preliminary

calculation of moisture conditions, all specimens were assumed to have a saturated moisture content of 5.7 %. After completion of the experimental procedure, the specimens were dried at 105 °C for twenty-four hours to obtain the true saturated moisture content of each specimen, and moisture conditions were adjusted accordingly.

For desorption, the chosen method of drying depended on the degree of saturation needed. Drying from saturated conditions to 90 % and then to 80 % was accomplished by placing the samples in open air until the proper weight was achieved (0-3 days). To dry to lower moisture states, however, it was required to place the specimens in a 50 °C oven until the desired weight was achieved. It was felt that this temperature was low enough to prevent any pronounced drying cracks.

For absorption, the specimens were first dried at 50 °C to constant weight (approximately 14 days), and then conditioned by placing the specimens in a bath of either 0 %, 3 %, or 6 % NaCl until the next desired weight increase was reached. After the proper weights were attained, both absorption and desorption specimens were sealed in plastic and placed in a temperature controlled room for equilibration.

4 Results

Results are shown in figures 18 through 26. Figures 19 through 26 depict average values for both the equilibrium resistivity and, where applicable, the moisture condition of three specimens. As moisture conditions were not precisely calculated until after the testing procedure had been completed, estimates were occasionally different than actual saturation percentages and it was necessary to average the moisture condition along with the resistivity values. In addition, the temperature that the resistance measurements were taken varied from 15 to 18 °C, so all these measurements have since been normalized to 16 °C using the simultaneously collected temperature sensitivity data.

Except for the final resaturation stage of testing, specimens were considered at equilibrium when there was no change in electrical resistance between consecutive days or if any slight increase could be attributed to a change in the measured room temperature. Due to time constraints, for the final stage the resaturated specimens were removed before equilibrium was achieved, but all resistance values were believed to be less than 5 % from their final equilibrium values.

Figure 18 shows how the coefficient of variation (CV) among the parallel specimens changed with the moisture conditioning. Generally, the highest CV's occurred at very low percent saturation (under 40 %), indicating that the greatest differences occurred between specimens when the pore water system becomes discontinuous. Above 40 % saturation, however, it is shown that nearly all parallel studies had CV's of under 20 %. Thus, given the large amount of data, results will be presented without 95 % confidence ranges to clarify observed trends.

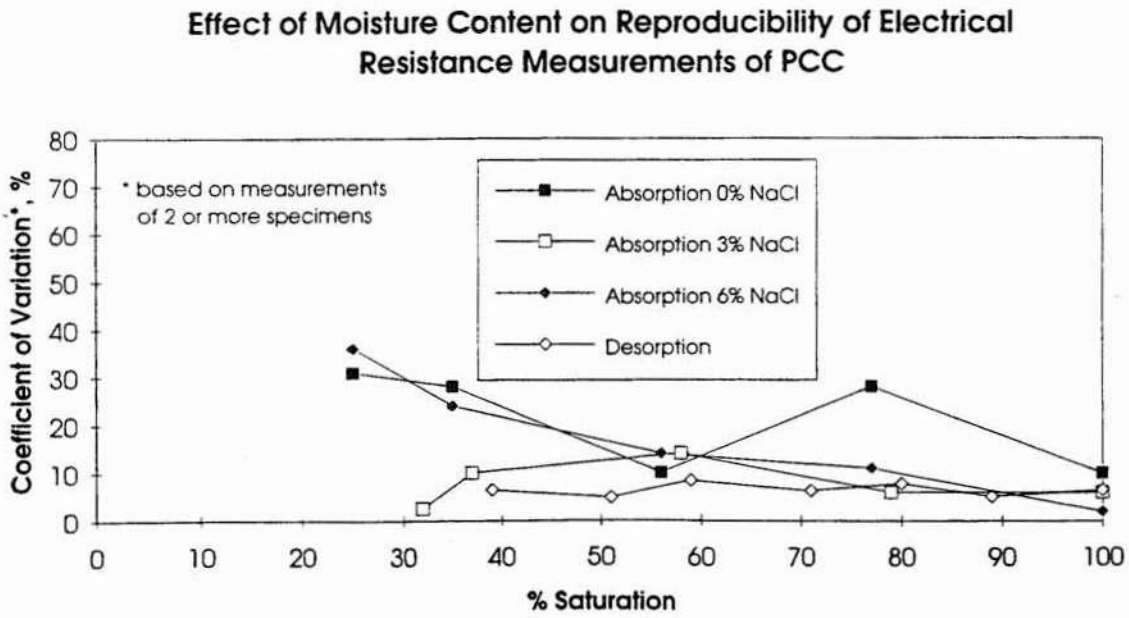

Figure 18. Influence of Moisture Condition on Reproducibility of Electrical Resistance Measurements of PCC.

Complete results for each specimen, including temperature sensitivity analysis, can be found in Appendix B.

5 Discussion of results

Effect of Moisture Content

The electrical resistivity of concrete increases with decreasing moisture content. Figures 19 and 20 show that the effect of moisture content on electrical resistivity is large, with resistance increasing by orders of magnitude at low moisture contents. Figure 20 is plotted against a linear (rather than logarithmic) Y-axis to show that all the mixes showed a sharp change in the rate of resistance increase or decrease between 40-60 % saturation. This suggests the range where the pore water in the concrete begins to gain or lose continuity, resulting in more substantial change in the number of electrical flowpaths.

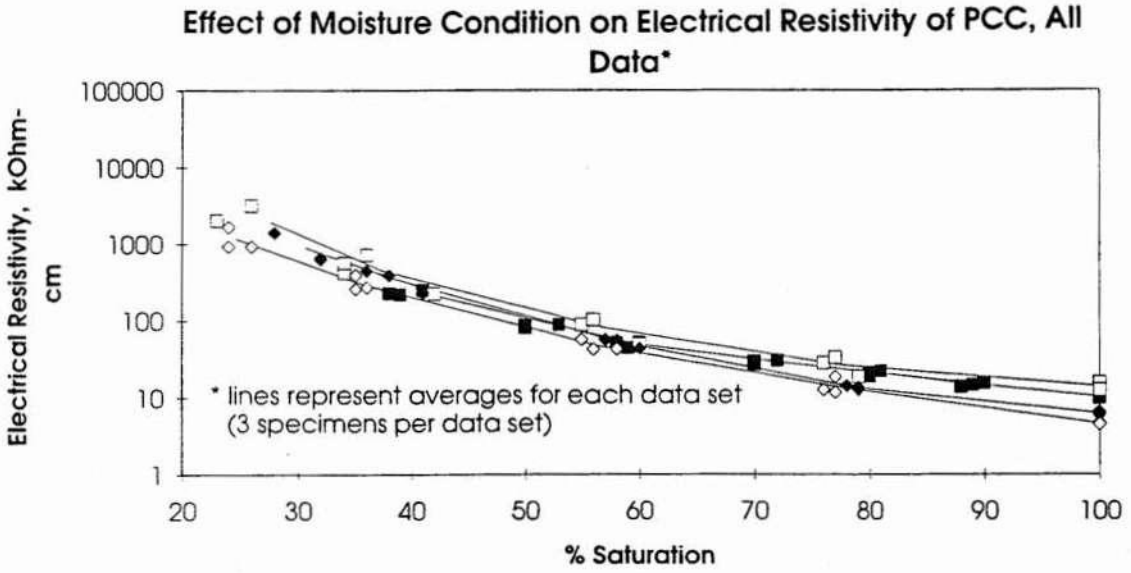

Figure 19. Influence of Moisture Condition on Electrical Resistivity of PCC.

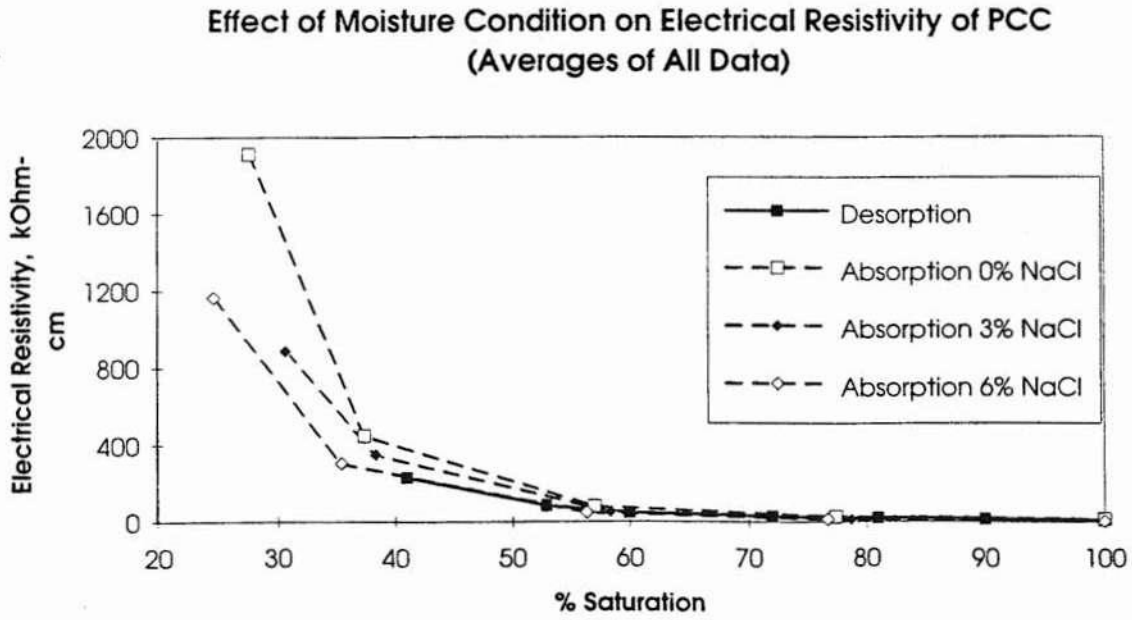

Figure 20. Influence of moisture Condition on Electrical Resistivity of PCC.

Figure 21 shows the effect of drying and rewetting on the saturated resistance levels. The comparison in this figure shows that, upon rewetting, resistances are higher than before conditioning. Generally it has been shown that, upon drying and rewetting concrete specimens, most parameters that indicate the relative continuity/discontinuity of the pore system (i.e., permeability, ice formation, chloride transport) suggest a more continuous pore system, so the electrical resistivity was also expected to decrease after this process. However, the resistance increased both for the desorption specimens and the specimens that absorbed pure water. We note that, as it was required to leave the specimens in a water (or salt) bath for a two week period, it is possible that ions were leached from the pore water system, increasing the measured resistance. Otherwise we have no explanation for this surprising result.

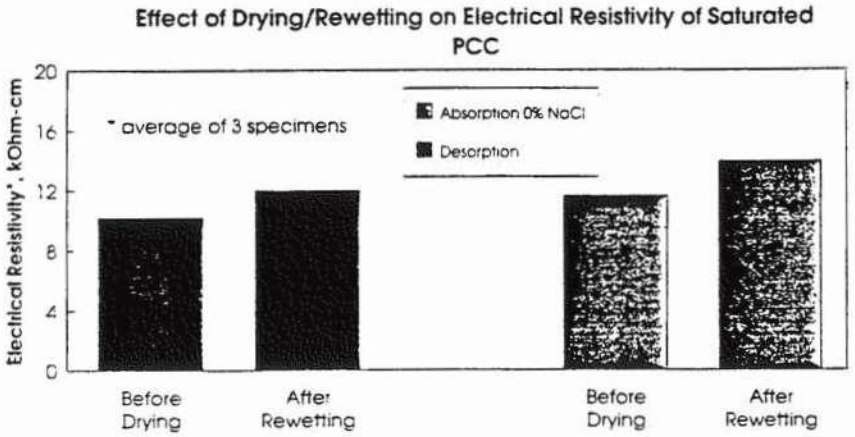

Figure 21. Influence of Drying/Rewetting on Electrical Resistivity of Saturated PCC.

Effect of Temperature

Figure 22 shows a comparison of two concretes, 0.4 and 0.6 water-cement ratio, tested at various temperatures in saturated conditions. It shows that the effect of temperature (at levels above freezing) is near constant between these two mixes, with activation energy (A) values of approximately 2300 and 2450 for 0.6 and 0.4, respectively, both of which correspond with approximately 3 % change per degree C at 21 °C. The data, plotted against the graph by Woefl and Lauer in figure 23, also agrees with the three previous studies suggesting that, at saturated conditions, the pore water's temperature sensitivity is independent of mix design.

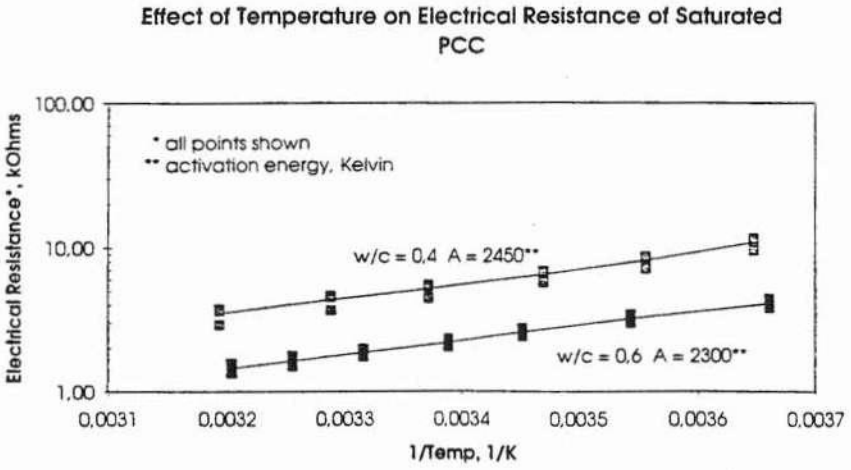

Figure 22. Influence of Temperature on Electrical Resistance of Saturated PCC.

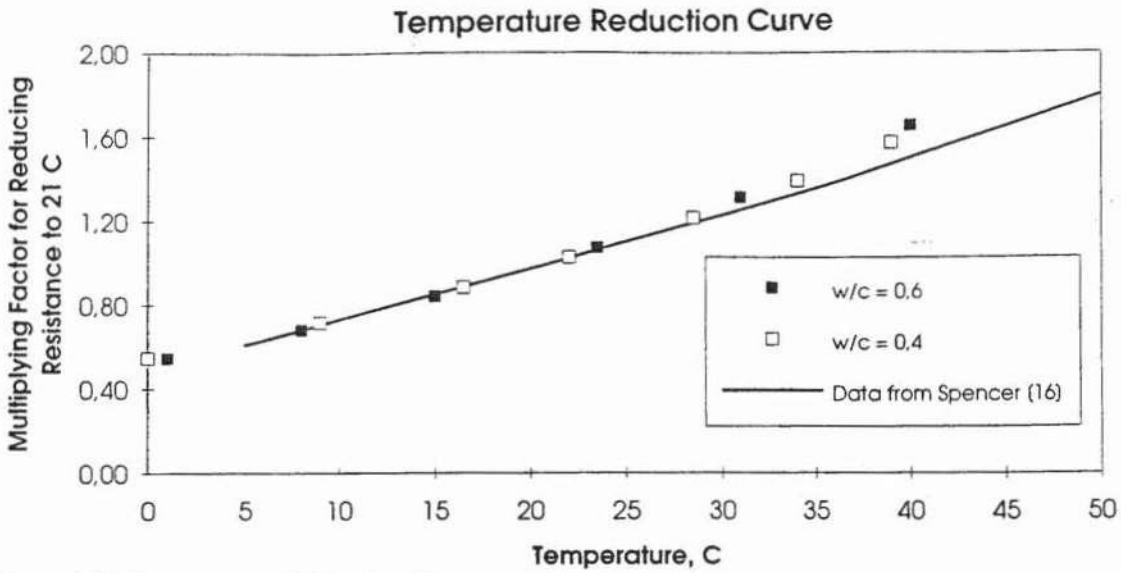

Figure 23. Temperature Reduction Curve.

Measurements of resistance at several different temperatures at each moisture condition were also made, as indicated earlier, and values for the activation energy were calculated. These values are shown in figure 24, with higher A values indicating increased sensitivity to temperature. This figure suggests that the sensitivity to temperature is related to the degree of saturation, with decreasing degrees of saturation resulting in increased sensitivity to temperature. Under 30 % saturation, for example, the activation energy calculated corresponds to a sensitivity of about 5 % per degree C at 21 °C, whereas above 70 % the sensitivity is about 3 % per degree C. This creates a second order problem when both moisture content and temperature are varying, as moisture content affects the temperature sensitivity as well as the electrical resistivity of concrete.

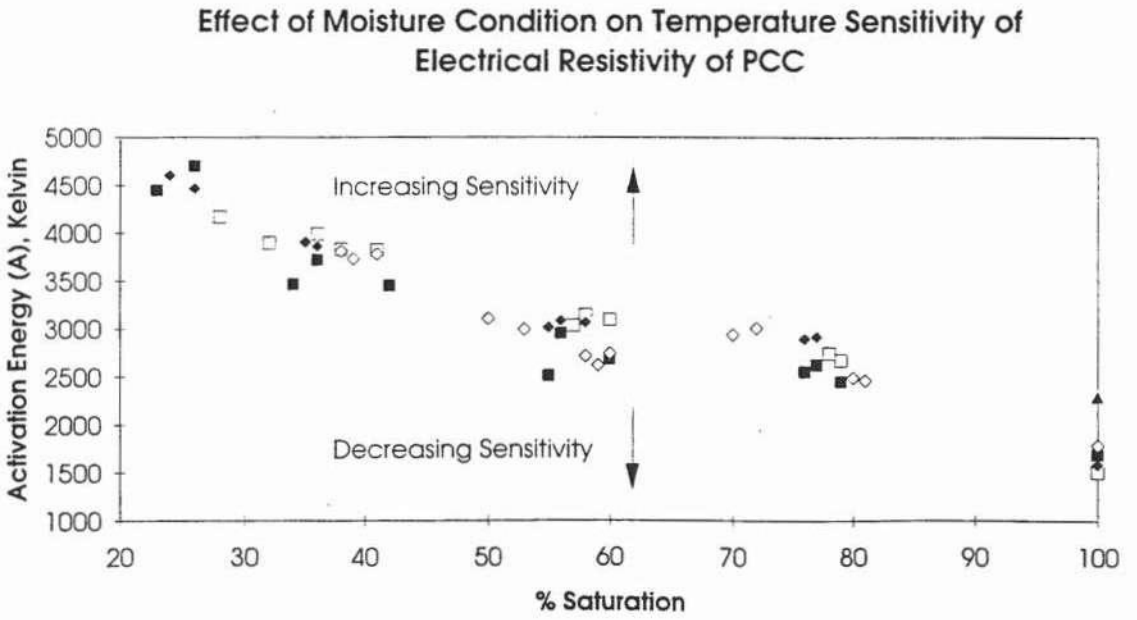

Figure 24. Influence of Moisture Condition on Temperature Sensitivity of Electrical Resistivity of PCC.

The activation energies calculated from the desorption and absorption series at fully resaturated conditions show a sensitivity that is lower than the trend lines would indicate. This is possibly due to a laboratory error (i.e., the resistances were recorded before thermal equilibrium was reached). Also shown in figure 24 is the A value for the 0.6 w/c saturated specimens used for the initial temperature study (see figure 22) which, at a value of 2300, falls in the anticipated range.

Effect of Chlorides

The stabilization of the concrete resistance after suction of a given amount of liquid is shown in figure 25. It should be noted that, for all of the specimens (desorption or absorption), stabilization always involved an increase in resistance over time, with an average time to stabilization at 15 °C of about two weeks. This is most likely not due to loss of moisture to the air, as initial and final weights (after equilibration) were usually identical. For pure water the equilibration process was relatively rapid. However, increasing levels of NaCl in the liquid slowed the process of stabilization. This suggests at least two possible mechanisms are involved in the stabilization process: first, redistribution of the liquid from the surface throughout the pore system and, second, dissolution of ions crystallized in the pores and chemical binding of the chloride ions. The latter process appears to slow the total equilibration process.

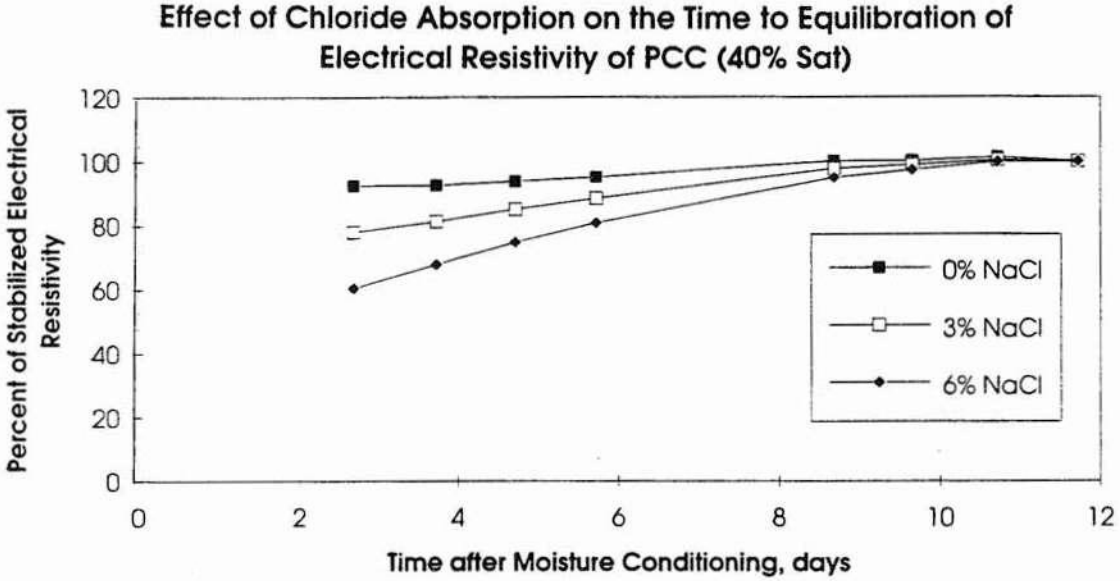

Figure 25. Influence of Chloride Absorption on Equilibration Time of Electrical Resistivity of PCC.

The increase in resistance during the equilibration period appears logical when considering the process involved. When water is either added or removed from the concrete pore system, the previous equilibrium condition is changed to two relatively "wet" and "dry" zones, with the wet zone being near the surface for the absorption series and near the core for the desorption series. At that time the wet zone conducts most of the electrical current through its relatively continuous pore water system. Migration of the pore water to the dry zone during equilibration results in a loss of continuity in the wet zone. It is believed, although the total moisture content has remained unchanged, the smaller, continuous wet zone in concrete conducts better than the full concrete body with moisture equally distributed. A similar gradual increase in resistance was noticed when the concrete specimens were returned to fully saturated conditions, which does not

agree with this theory. As noted earlier, it is possible that ions were leached from the pore water system during the lengthy resaturation process, which could explain this gradual increase.

Figure 26 shows that the effect of chlorides becomes more pronounced when compared to pure water as the degree of saturation increases. This is most likely due to the increased amount of salt water relative to the unaltered pore water that remained in the pore system after 50 °C drying. This figure also shows that, for a given moisture condition, the chloride concentration has little effect on the resistivity. This is a surprising result with the implication that the final ionic concentration of the pore water solution is the same for both initial chloride concentrations. This trend is similar to that seen by Gjørv and Monfore for chlorides added to the mixwater (see figure 9), where above a certain concentration of chlorides added the decrease in electrical resistance was small.

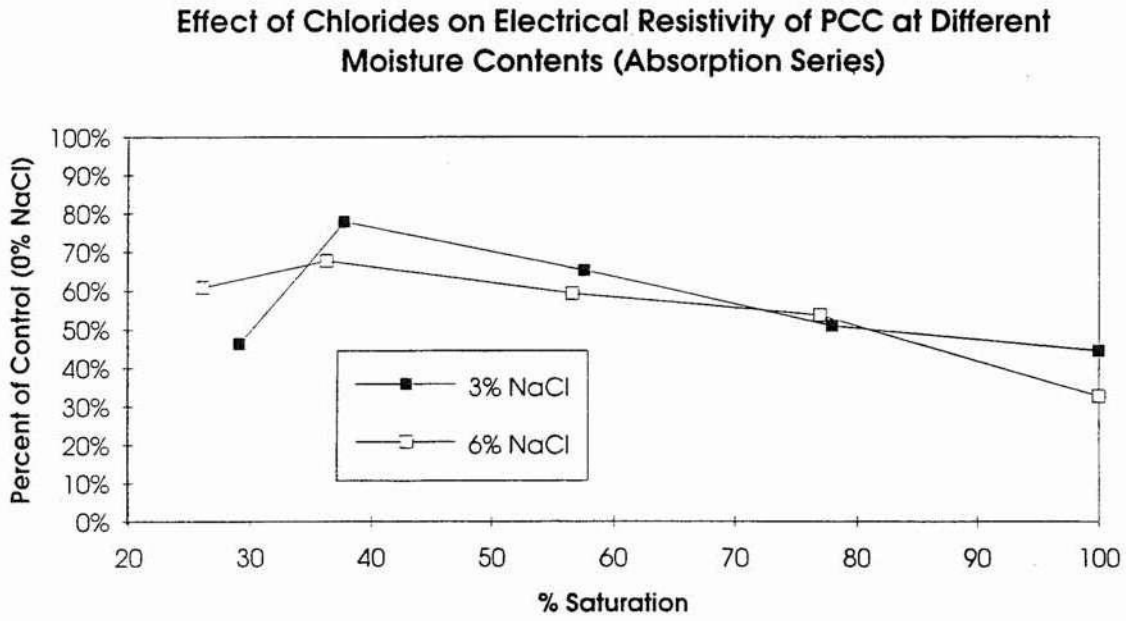

Figure 26. Influence of Chlorides on Electrical Resistivity of PCC.

6 Conclusions

From this investigation of electrical resistance in concrete, the following conclusions can be drawn:

1) Moisture content greatly affects the electrical resistance in concrete. For high moisture contents the rate of change is constant or only slightly increasing, but in the range of 60 to 40 % (presumably where continuity of the pore liquid begins to disappear) the rate of resistance increase rises sharply. From 40 % to 100 % degree of saturation, the range of concrete resistivity for a 0.6 water/cement ratio and no additional chlorides is approximately 250 kOhm-cm to 10 kOhm-cm.

2) Temperature affects the electrical resistivity in concrete. At saturated conditions a rate of 3 % change per °C (at 21 °C) was found, with resistance decreasing with increasing temperature. At lower degrees of saturation, however, this sensitivity increased, with a value of approximately 5 % per °C at 25 % saturation.

3) The addition of chlorides into the pore water system decreased the resistance substantially, with the effect increasing at higher levels of saturation. At saturated conditions, electrical resistivity for concrete with pore water containing 6 % NaCl was less than 40 % than that of concrete with no additional chlorides. The difference between 3 % and 6 % NaCl pore water was surprisingly low, however. No apparently significant difference was noticeable between the two chloride concentrations.

The influence of frequency varied. A previous study examined (see figure 12) showed a resistance at 1 kHz of only 85-90 % of that observed at 100 Hz. This study also showed a similar level of sensitivity at saturated conditions, but that changed as the concrete was dried (see figure 15). At 60-70 % saturation the resistance measured at 1 kHz to be approximately 60 % of that observed at 120 Hz, while at 40 % saturation it was nearly 80 % again. We note that, except for the temperature study at saturated conditions, all of the presented results are for concrete with w/c = 0.6, and the conclusions are therefore limited.

7 Practical consequences

The purpose of this study was to evaluate the applicability of electrical resistance measurements on in-situ concrete to monitor changes in moisture content. Other than the differences which come from mix design differences (i.e., w/c-ratio, silica fume, curing temperature), this study focused mostly on environmental factors: temperature, chloride concentration, and moisture content. Now quantified, the influence of each of these parameters on field concrete needs to be discussed.

The small amount of Norwegian field data on concrete moisture contents suggest that the degree of saturation (DS) at least 20 mm from an exposed vertical surface is unlikely to be less than 70 %. Thus, the range from 70 to 100 % saturation is of particular interest. Figure 27 shows a "blowup" of the resistance-degree of saturation curve (figures 19 and 20) in this range. Above about DS = 70 % the rate of change is close to linear for the four data sets with a slope of about 3 % change in resistance per 1 % degree of saturation. Below this range the slope increases sharply.

In the same DS range of 70 to 100 % the temperature sensitivity has been shown earlier to be about 3 % change in resistance per °C. Consequently a very accurate temperature record is required at the same location where the resistance is measured, if a resistance change is to be interpreted in terms of moisture change.

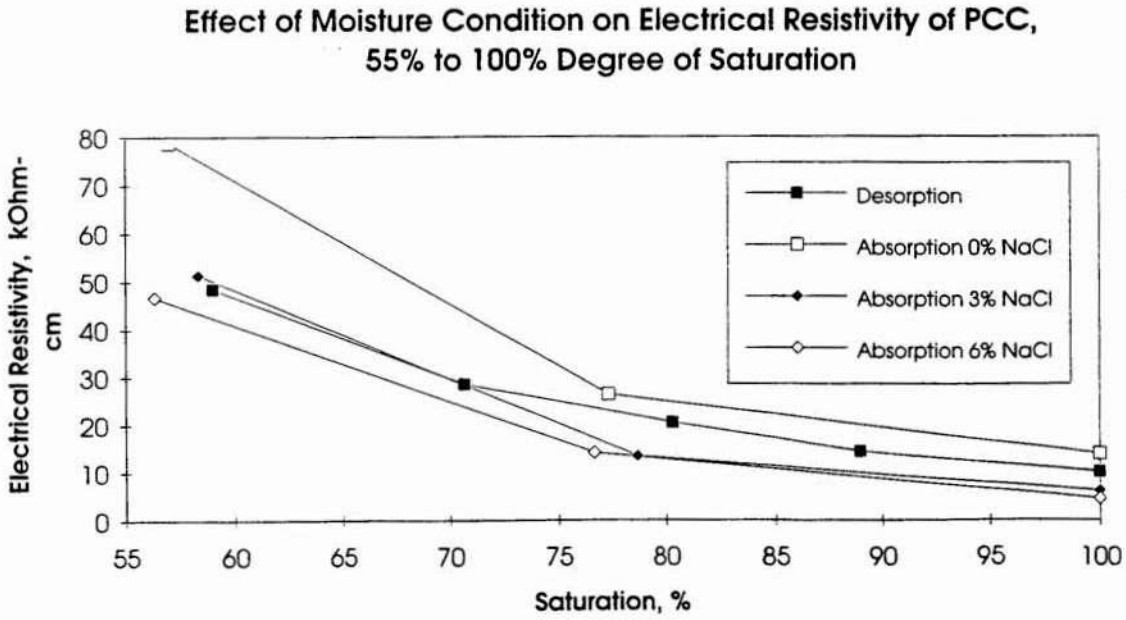

Figure 27. Influence of Moisture Condition on Electrical Resistivity of PCC for High Moisture Conditions.

The influence of chlorides is, as already presented, quite large, but by no means linear. A 3 % (or 6 %) NaCl solution in the pores cuts the resistance by a factor of about 2. More work is definitely needed on the effects of chlorides. However, chlorides normally penetrate slowly into the concrete. Thus, over a shorter term, the chloride concentration a bit inside an exposed surface probably can be assumed constant. Then, according to figure 27, the slope of resistance vs. degree of saturation may possibly be assumed to hold regardless of chloride content. Interpretation of resistance changes in terms of changed degree of saturation of course still presupposes very accurate temperature data.

In summary:

Exposed coastal concrete structures in Norway appear to have quite high moisture contents: in the range of 70 to 100 % degree of saturation.

In this DS range the resistance of the concrete changes roughly as follows:

- 3 % per °C temperature change
- 3 % per % change in degree of saturation
- 50 % due to the ingress of chlorides.

This is a slow process and the chloride content may possibly be assumed to be constant over short periods.

Even a rough monitoring of changes in moisture content in field concrete by means of resistance measurements require accurate simultaneous temperature monitoring.

8 Recommendations

The following recommendations for the measurement of electrical resistivity in concrete are offered:

1) For measurement of electrical resistivity, alternating current at a frequency of at least 1000 Hz is recommended to minimize differences in resistance measurements due to voltage level. Further study should be performed to explain the changing difference between electrical resistivity readings at 1 kHz and 120 Hz with changing degree of saturation.

2) For measurement of electrical resistivity with the emphasis on determining moisture content, simultaneous temperature measurements must be carried out to eliminate the creation of a second order problem, as moisture content not only affects the resistivity but also the temperature sensitivity of the resistivity.

3) Further work should be performed to explain the increase in electrical resistance after drying and resaturation, which is in contradiction to other concrete measurements (i.e., permeability, chloride transport), as well as to explain the gradual increase in resistivity with time after water absorption.

9 References

1. Cabrera, J. G. and Ghoddoussi, P., *The Influence of Fly Ash on the Resistivity and Rate of Corrosion of Reinforced Concrete*, Conference on Concrete Durability: Papers, Nice, France, 1994, pp. 229-244.

2. Woelfl, G. A. and Lauer, K., *The Electrical Resistivity of Concrete with Emphasis on the Use of Electrical Resistance for Measuring Moisture Content*, Cement, Concrete, and Aggregates, CCAGDP, Vol. 1, No. 2, 1979, pp. 64-67.

3. Hammond E. and Robson T. D., *Comparison of Electrical Properties of Various Cements and Concretes*, The Engineer, Jan. 21, 1955, pp 78-80.

4. Monfore, G. E. *The Electrical Resistivity of Concrete*, Journal of the PCA Research and Development laboratories, May 1968, pp. 35-48.

5. Cavalier, P. G. and Vassie, P. R., *Investigation and repair of reinforcement corrosion in a bridge deck*, Proceedings, Institution of Civil Engineers, Part I, Vol 70, Aug. 1981, pp. 461-480.

6. Alonso, C., Andrade, C. and Gonzalez, J. A., *Relation Between Resistivity and Corrosion Rate of Reinforcements in Carbonated mortar made with Several Cement Types*, Cement and Concrete Research, Vol. 15, No. 5, 1988, pp. 667-698.

7. Neville, A. M., Properties of Concrete -- Third Edition, Longman Scientific & Technical, 1981.

8. Hope, B. B., Ip, A. K. and Manning D. G., *Corrosion and Electrical Impedence in Concrete*, Cement and Concrete Research, Vol. 15, No. 3, 1985, pp. 525-534.

9. Burke, N. S., Dallaire, M. P. and Hicks, M. C., *Plastic, Mechanical, Corrosion, and Chemical Resistance Properties of Silica Fume (Microsilica) Concretes*, Proceedings, 4th Annual Conference on Fly Ash, Silica Fume, Slag and Natural Pozzolans in Concrete, Istanbul, Turkey, May 1992, pp. 1125-1149.

10. Hansson, I. L. H. and Hansson, C. M., *Electrical Resistivity Measurements of Portland Cement Based Materials*, Cement and Concrete Research, Vol. 13, 1983, pp. 675-683.

11. Hughes, B. P., Soleit, A. K. O. and Brierley, R. W., *New Technique for Determining the Electrical Resistivity of Concrete*, Magazine of Concrete Research, Vol. 37, No. 133, 1985 pp. 243-248.

12. Havdahl, J. and Vennesland, Ø., *Utvikling av Kloridbestandig Betong*, SINTEF Rapport nr 70032/5, Trondheim, Norway, Aug. 1994.

13. Gjørv, O. E., Vennesland, Ø., and El-Busaidy, A. H. S., *Electrical Resistivity of Concrete in the Oceans*, 9th Annual Offshore Technology Conference: Papers, Houston, TX, May 1977.

14. Hauck, C. J., *The Effect of Curing Temperature and Silica Fume on Chloride migration and Pore Structure of High Strength Concrete*, Doctoral Dissertation, Norges Tekniske Høgskole (NTH), University of Trondheim, Norway, 1993.

15. Page, C. L. and Vennesland, Ø. *Pore Solution Composition and Chloride Binding Capacity of Silica-Fume Cement Pastes*, Materials and Structures, Vol. 16, No. 91, 1983, pp. 19-25.

16. Spencer, R. W., *Measurement of the Moisture Content of Concrete*, Journal of the American Concrete Institute, Vol. 9, no. 1, Sept. - Oct. 1937, pp. 45-61.

17. Millard, S. G., *Effects of Temperature and Moisture upon Concrete Permeability and Resistivity Measurements*, Workshop on In-Situ Measurement of Concrete Permeability, University of Loughborough, Dec. 12, 1989, p. 9.

18. Bracs, G., Balint, E. and Orchard, D. F., *Use of Electrical Resistance Probes in Tracing Moisture Permeation Through Concrete*, Journal of the American Concrete Institute, Vol. 67, Aug. 1970, pp. 642-646.

19. Schiessl, P., Breit, W. and Raupach, M., *Investigation into the Effect of Coatings on Water Distribution in Concrete Using Multi-Ring-Electrodes*, Proceedings, ACI Convention, Minneapolis, MN, Nov. 1993.

20. Bhargava, J. and Rhenstrom, Å, *Electrochemical Aspects of Electrical Resistance Gauges for Concrete*, Swedish Council for Building Research, Doc. D11: 1978, 1978.

21. Calleja, J. Journal of the American Concrete Institute, Vol. 25, 249, 1953.

ELECTROCHEMICAL MEASUREMENTS IN A SIMULATED CORROSION CELL ON EPOXY COATED STEEL REINFORCEMENT - A LONG TERM FIELD TEST IN CONCRETE

Bror Sederholm, Swedish Corrosion Institute, Roslagsvägen 101, hus 25, 104 05 Stockholm

ABSTRACT

During the latter part of the 1980s fusion-bounded epoxy was introduced in Scandinavia, for corrosion protection of steel reinforcement. Epoxy coated reinforcements are being used particularly in new structures and in the repair of large concrete constructions exposed to aggressive environments, e.g. de-icing salt or sea water.

During the handling of the reinforcement bars it is however inevitable that the epoxy coating is mechanically damaged locally, where the steel will be exposed to the corrosive concrete environment.

At the Swedish Corrosion Institute it is investigated whether such damage has any significant effect on the protective efficiency of the epoxy coating. One part of the investigation aims to determine whether a corrosion cell may form on coated steel reinforcements, where the steel surface beneath the epoxy coating could act as an efficient cathode and the small uncoated steel surface in the coating damage could act as an anode. To determine the corrosion current (the corrosion rate) and the current direction in such a cell the measurement has to be carried out in a simulated corrosion cell where the anode and cathode surfaces are physically separated from each other.

This paper describes in detail the experimental technique and the results obtained during three years of outdoor exposure. During an initial period no corrosion current could be measured in the corrosion cell, probably due to the passive state of the uncoated steel surface. After approx. 2 years a small corrosion current from the free steel surface was recorded. This current is still increasing with time.

Keywords: Long term outdoor exposure, electrochemical measurements, epoxy coated steel reinforcement, corrosion, concrete.

1. INTRODUCTION

The initial stage of the project involved an extensive literature investigation and collection of experience primarily concerning epoxy-coated reinforcement rods (1). The literature investigation showed among other things that the protective efficiency of the epoxy coatings under the severe Scandinavian climatic conditions had not been completely clarified. Some questions asked were:

- Does the epoxy-coated reinforcement surface act as a large efficient cathode surface towards the small anode surface if the coating is damaged so that the steel is exposed locally?

- If this is the case, may the corrosion current (rate of corrosion) become so large that the corrosion becomes severe enough to reduce the mechanical strength of the rods. Can the corrosion products become so voluminous that the concrete eventually cracks?

- Does the corrosion continue beneath the coating so that it separates from the steel surface, and can the adhesion between reinforcement rod and concrete be reduced by that?

- How important is the size of the coating damage; what is the maximum acceptable size of damage?

Experimental outdoor investigations were started with the aim of finding answers to these questions.

2. EXPERIMENTAL TECHNIQUES

2.1 Test materials

All investigations have been carried out on epoxy-coated reinforcement rods (cam rods) manufactured at Fundia Norsk Jernverk A/S in Mo in Rana, Norway. During the manufacture, the rods are coated with epoxy powder from 3M in USA. It is applied by electrostatic spraying (1). Since the rods are blasted and heated in advance, the epoxy powder is sprayed and melted onto the rods and forms a continuous protective coating. Rods with a diameter of 12 mm were cut to lengths of 0,5 m. TAB 1 shows the chemical composition of the steel of the epoxy-coated test rods.

Before the test rods were cast in concrete, the epoxy coating on each individual test rod was characterized with respect to the occurrence of pores (both open and closed pores) and layer thickness. The number of closed pores in the epoxy layer was determined in a small sample from each test rod by examining a cross section of the coating in a metal microscope. The number and distribution of pores in the examined coating surface were determined in an image analyser. The porosity was classed according to a grading system proposed by Fundia Norsk Jernverk A/S, FIG 1.

Penetrating pores were measured by Fundia Norsk Jernverk AS with a high-voltage pore finder. No penetrating pores were detected.

The thickness of the epoxy layer was determined for each test rod by measuring on at least 10 points with a film thickness gauge, Elcometer 300. A small sample was also taken from each test rod for a examination of the cross section surface of the epoxy layer by a metal microscope.

All test rods in the investigation were cast into slabs of chloride-containing concrete with dimensions 0.42 x 0.42 x 0.05 m. The concrete contained 2 per cent by weight of Cl^-/dry cement weight and had a water/cement ratio (the ratio of the proportion of water to the proportion of cement in the concrete) of 0.7. The covering layer of the concrete (distance between test rod and concrete surface) was 1 cm thick. The composition of the concrete blocks is given in TAB 2.

2.2 Test procedure

In order to determine whether a corrosion cell may develop on the coated steel, it was decided to monitor the corrosion current. In such a cell the steel surface beneath the epoxy coating could act as an efficient cathode and the small uncoated steel surface in the coating damage as an anode. To be able to measure the corrosion current (the corrosion rate) and the direction of the current (determination of the anodic and cathodic sites) in such a cell the measurement has to be carried out in a simulated corrosion cell where the anode and cathode surfaces are physically separated from each other. A steel rod with an undamaged epoxy coating and a small uncoated steel specimen were cast into chloride-containing concrete slabs. The coated rod (the simulated cathode) and the small steel specimen (the simulated anode) were connected by a test cable via a zero-resistance ammeter. The ammeter was connected to a data logger that continuously records the corrosion current and the direction of the current, FIG 1.

Three such tests were arranged with uncoated steel speciemen areas of 10, 20, and 60 mm^2 respectively. Into each test slabs further three coated test rods were also cast, each of which had a coating damage of the same size as the surface area of the external uncoated steel specimen, FIG 2.

3. RESULTS AND DISCUSSION

The results in FIG 3 of the determinations of epoxy layer thickness with a film thickness gauge, and by metallographic investigation in a microscope, show that the average coating thickness on all the test rods is between 150 and 300 µm, FIG 3.

According to the ASTM standard A775/A775M-88a "Standard Specification for Epoxy-Coated Reinforcing Steel Bars", it is evident that the best properties, considering both bending resistance and corrosion protection, are obtained when the thickness of the epoxy coating is between 130 and 300 µm.

As shown by the investigation with the pore finder, no penetrating pores could be found. Concerning the pores enclosed in the epoxy layer, it is shown in FIG 4 that a small number occurs in all the test rods investigated. These pores in usually occur close to the steel surface.

The results of the continuous current measurements in the thre concrete slabs are shown in FIG 5. Positive current means that the uncoated steel specimen is acting as an anode and the coated steel rebar is acting as a cathode in the corrosion cell. Negative current means that the steel specimen acts as a cathode and that the coated rebar acts as an anode. FIG 5, show that the uncoated steel specimens can act both as anode and cathode surface. The corrosion current from all the uncoated steel specimens to the steel under the epoxy layer is negative in the beginning of the exposure, i.e. the bare steel area acts as cathode. FIG 5 shows that the uncoated steel specimens can act both as anode and cathode surface. The corrosion current in the beginning of the exposure, i.e. the bare steel area acts as cathode.

The reason why the current direction was negative in the beginning of the exposure is probably that the uncoated steel surface was in a passive state. The electrode potential of the this surface was thus more positive than the electrode potential of the steel covered by the epoxy coating. To get a corrosion current directed from the uncoated steel to the epoxy-coated steel surface, the passivity of the uncoated steel specimen must be broken down. The electrode

potential of the uncoated steel then becomes more negative than that of the steel surface under the epoxy coating. That is what has happened after approx. 850 days of exposure in the lower diagramme (size of damage, 60 mm^2) in FIG 5.

After 300 days of exposure the current became very small and sometimes negative for all uncoated steel specimens. This probably means that all the uncoated steel surfaces were still in passive state.

To be able to quantify and with greater certainty estimate the influence of the size of the damage on the corrosion protection ability of the epoxy layer a considerably longer exposure time is required. In order to determine more exactly the corrosion current between uncoated steel and the epoxy-coated steel surface, the test arrangement has been modified slightly after appprox. 300 days of exposure by suspending the concrete slabs in the air in order to avoid completely the possibility that "creep currents" from the ground might distort the measured values.

After approx. 600 days of exposure one concrete slab was split open and the uncoated steel specimen surface (size 20 mm^2) was visually inspected.. From this inspection, it was evident that the uncoated steel surface was still uncorroded. This agrees quite well with the continuous measurements of the corrosion current.

In order to activate the uncoated steel surface, the concrete slabs have been sprayed once per week with chloride-containing water after approx. 600 days of exposure.

After approx. 850 days of exposure, the corrosion current from the uncoated steel specimen (60 mm^2 size) started to increase. The corrosion current from the small steel specimen (10 mm^2 size) was still very small, and after three years of exposure still remains very small.

After three years exposure the two remaning concrete slabs (steel surface 60 mm^2 och 10 mm^2) were broken up and the uncoated steel specimens were visually inspected. From the visual inspection, it was evident that the large (60 mm^2) uncoated steel surface was attacked by shallow pitting corrosion after three years of exposure. The small (10 mm^2) uncoated steel surface was uncorroded and showed no pitting which means that this surface was still in a passive state, TAB 3. These observations agree very well with the continuous measurements of the corrosion current.

4. CONCLUSIONS

From the investigations, the following conclusions can so far be drawn:

- The measurements of the epoxy coating thickness before exposure, by two different methods, showed that the average coating thickness on all test rods is between 150 and 300 µm.

- The investigation by the high-voltage pore finder showed that there were no penetrating pores in the epoxy coating on any of the test rods.

- The microscopic investigaton of cross sections of the epoxy layer from all test rods, showed that the coatings have a small number of enclosed pores.

- The continuous electrochemical current recordings and a visual inspection show also that the uncoated steel surface was still in a passive state after approx. 600 days of outdoor exposure .

- After approx. 850 days of outdoor exposure, the corrosion current from the 60 mm^2 uncoated steel specimen started to increase. The corrosion current from the small 10 mm^2 steel specimen was still very small.

- After three years of outdoor exposure the corrosion current from the uncoated (60 mm^2) steel specimen was still quite high. The current from the 10 mm^2 specimen remained very small.

- From the visual inspection after three years of outdoor exposure it was evident that the 60 mm^2 uncoated steel specimen was attacked by pitting corrosion. The 10 mm^2 steel specimen was uncorroded which means that the this steel surface was still in a passive state. This agrees very well with the continuous measurements of the corrosion current between the uncoated steel specimen and steel surface covered by epoxy layer.

- The results from three years of continuous electrochemical recording of the corrosion current between uncoated steel and coated steel, show that the uncoated steel can act both as anode and cathode surface towards the coated steel.

- The agreement between the continuous corrosion current measurements and the visual observations show that this experimental setup is suitable for investigation of corrosion cells on steel rebars in concrete

5. REFERENCES

1. Sederholm, B & Pettersson K: Epoxy coatings as corrosion protection of reinforced steel in concrete constructions. KI Report 1989:5, the Swedish Corrosion Institute 1989. (in Swedish)

2. Sederholm, B: Field test of corrosion protection properties of epoxy coating on reinforcement steel in chloride-containing concrete. KI Report 1994:1, the Swedish Corrosion Institute 1994. (in Swedish)

TABLE 1. Chemical composition of the steel in the epoxy-coated test rods (2) (per cent by weight).

C	Si	Mn	P	S	N	Cr	Cu	Mo
0,17	0,26	0,74	0,02	0,04	0,01	0,09	0,32	0,02

TABLE 2. Total weight of components used for each concrete slab (2).

Cement, Slite Std	2,6 kg
Aggregate size 0-8 mm 8-16 mm	 9,2 kg 8,0 kg
Water	1,82 kg
NaCl, purum	0,086 kg

TABLE 3. Results of the metallographic investigation by microscope of pickled corroded steel surfaces, after the outdoor exposure in concrete

Size of damage (mm^2)	Exposure time (year)	Number of pits	Max. pit depth (µm)
10	3	0	0
20	1½	0	0
60	3	8	65

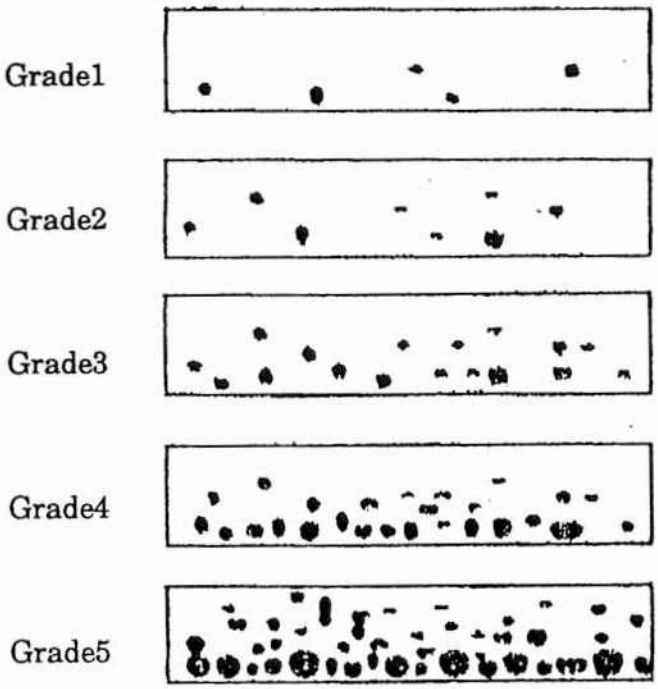

FIGURE 1. Rating by number of closed pores in cross sections of the epoxy layers. Grades 1-3 are acceptable. Grades 4-5 are not acceptable (2).

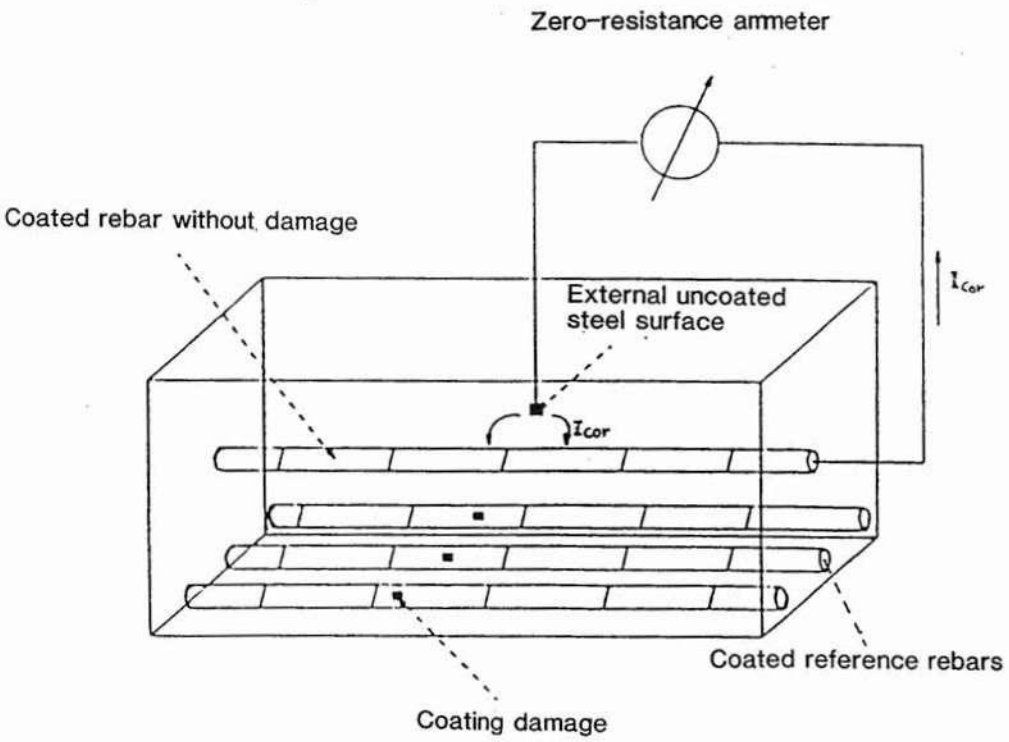

FIGURE 2. Schematic description of test arrangement (2).

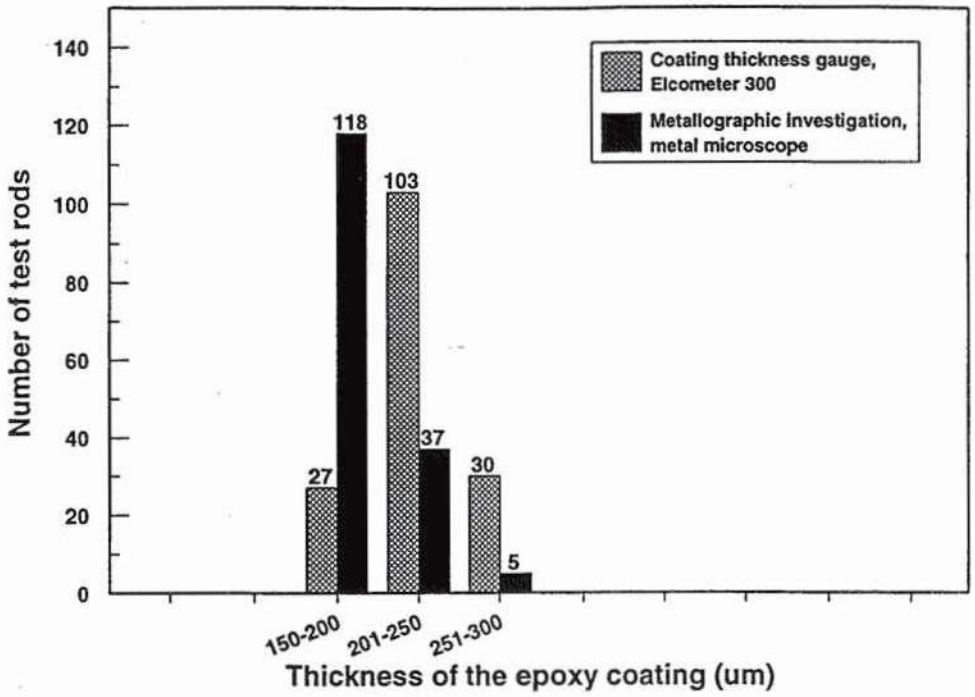

FIGURE 3. The average epoxy layer thickness of the test rods determined by two methods: (a) by taking a small sample from each test rod and examining the cross section of the epoxy layer in a metal microscope at high magnification (b) by using a coating thickness gauge directly on the surface of the test rods (2).

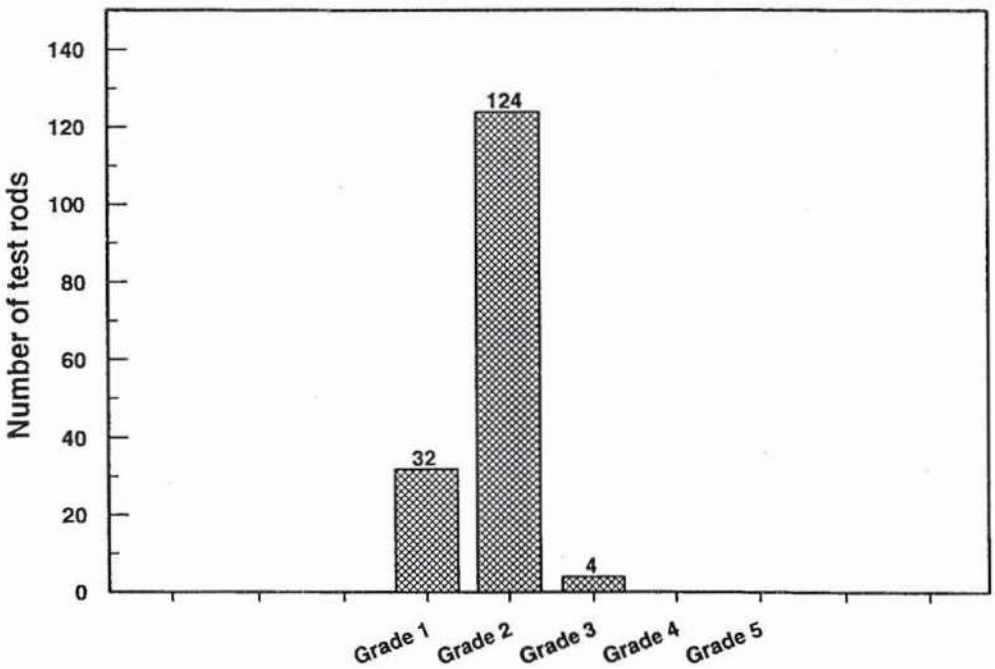

FIGURE 4. Results of the metallographic investigation of the proportion of closed pores in the epoxy layer of each test rod (2).

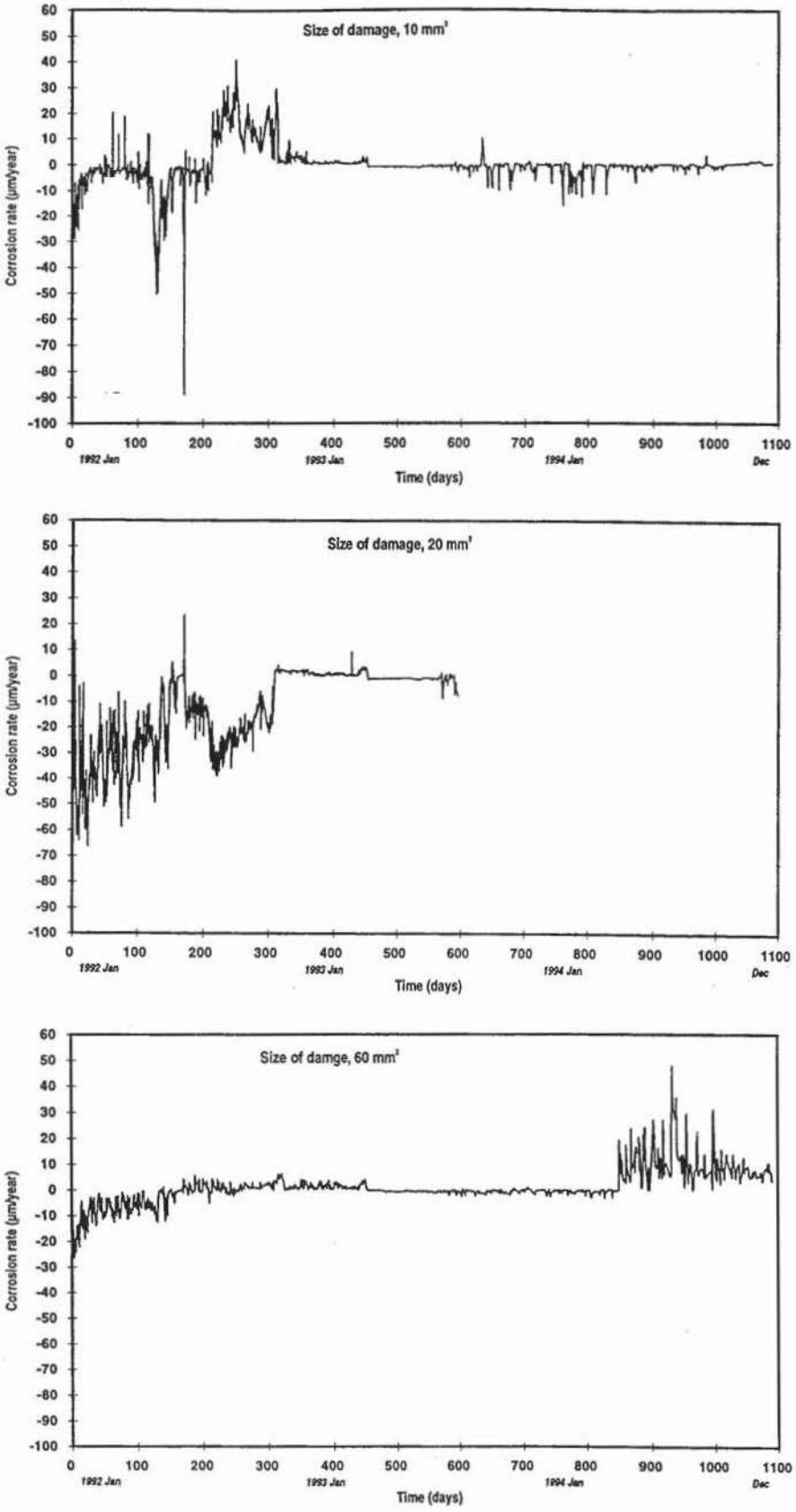

FIGURE 5. Corrosion currents recorded with a zero-resistance ammeter between bare steel surfaces (10, 20 and 60 mm^2) and undamaged epoxy-coated reinforcement rod as a function of time. A positive corrosion current shows that the bare steel acts as an anode and the coated steel surface as a cathode.

THEME 5

Laboratory test methods

AN ELECTROCHEMICAL METHOD FOR ACCELERATED TESTING OF CHLORIDE DIFFUSIVITY IN CONCRETE

Tiewei Zhang and Odd E. Gjørv
Division of Building Materials
The Norwegian Institute of Technology - NTH
N-7034 Trondheim - NTH, Norway

ABSTRACT

In the present paper an electrochemical method for accelerated testing of chloride diffusivity in concrete is presented. The method is based on a theoretical relationship between chloride diffusivity and observed steady-state rate of chloride migration through the concrete. The concentration of the chloride source solution has a significant influence on the rate of chloride migration and, therefore, a correction factor for ionic interaction in the relationship is introduced. It is shown that the relationship can be used for calculation of chloride diffusivity under various testing conditions. Some experimental results are also presented.

INTRODUCTION

Over recent years an increasing amount of premature steel corrosion in concrete structures exposed to chloride containing environments has created an increasing problem. This is partly due to an increasing use of deicing salts and partly due to an increasing amount of concrete construction in marine environment[1]. For several reasons concrete codes and job specifications have been insufficient and unsatisfactory in preventing corrosion of the reinforcing steel. There is a great need, therefore, to develop better test methods and more relevant quality parameters and criteria for evaluation of the resistance of concrete against chloride penetration. This is important in order to provide a better basis both for job specification and control of in situ quality[2].

Depending on environmental conditions, chloride ions may penetrate concrete through various mechanisms such as diffusion, permeation and capillary suction. In general, capillary suction may dominate the penetration through a surface layer of the concrete which is very porous and only partly water saturated. However, if the porosity is very low or the concrete is very wet, a diffusion mechanism may dominate the penetration of chloride ions.

The conventional testing of chloride diffusivity of concrete is based on immersion of concrete specimens in various types of salt solution. After a certain time of exposure, the penetration is measured in the form of a chloride profile, from which the chloride diffusivity is calculated on the basis of Fick's second law for semie-finite diffusion. One of the shortcomings of this type of testing is the long time of testing normally involved. In order to use chloride diffusivity as a more general parameter for evaluation of concrete quality, it has been an increasing interest to apply various types of accelerated test methods. One approach is to increase the concentration of the chloride source

solution[3], but in that case the diffusion behavior may not follow Fick's law due to the effect of ionic interaction[4]. Another approach is to apply an external electrical field for accelerating the chloride penetration. This is an approach which has been more widely adopted.

In the USA, the application of an external electrical field was introduced in the "Rapid Chloride Permeability Test" (AASHTOT277-83) already in the early 1980's[5,6]. However, since this method is based only on the measurement of the total electrical charge passed through the concrete over a short period of time, it does not give any specific information about the resistance of the concrete against chloride penetration. In Norway, therefore, a similar method was introduced, where the so-called "Chloride Permeability" was based on the observed rate of chloride migration through the concrete[7]. Since the beginning of the 1980's, this method has been widely used in Norway for general quality evaluation of concrete durability[8-13]. However, this "Chloride Permeability" is also an empirical quality parameter which is strongly dependent on the particular testing conditions used. Thus, the observed rate of chloride penetration both depends on the level of applied voltage and the concentration of the chloride source solution. Conventional diffusion testing has shown that the presence of other types of ions in the system also affect the rate of chloride intrusion[14-18]. Thus, a change in type of cation from sodium to calcium in the chloride source solution may increase the rate of chloride penetration substantially as demonstrated in Fig. 1.

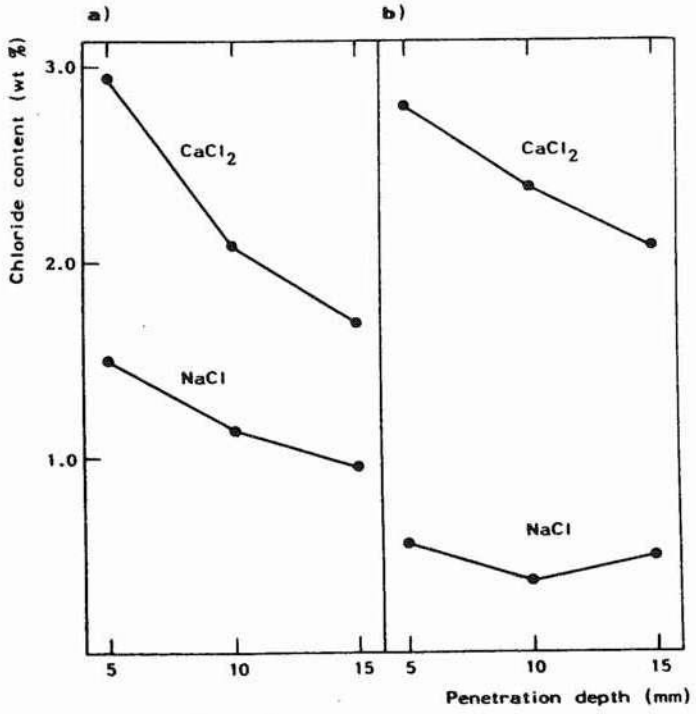

Figur 1. **Rate of chloride diffusion into cement paste from two different types of salt solution with the same chloride concentration: a) 2 days of hydration and b) 40 days of hydration before exposure[15].**

It is a great need, therefore, both to provide more basic information about the mechanisms which control the chloride penetration and to develop test methods which can provide more basic quality parameters for characterizing the resistance of concrete against chloride penetration under various conditions.

In Sweden, an accelerated, non-steady state migration method for determination of chloride diffusivity has been introduced[19]. After exposure to the electrical field, the diffusivity is calculated on the basis of the observed depth or profile of chloride penetration in the concrete specimen. A more general analysis of testing of chloride diffusivity in concrete based on migration measurements has recently been carried out by Andrade[20]. A similar study was also carried out by the present authors, from which an accelerated, steady-state migration method for determination of chloride diffusivity was developed. This method is described in the following.

THEORETICAL BACKGROUND

Diffusion

Diffusion is the result of a random motion of molecules and ions, where the flux caused by the diffusion is proportional to the concentration gradient of the diffusion species as expressed by Fick's first law:

$$J = -D \frac{dc}{dx} \quad (matter \cdot cm^{-2} \cdot s^{-1}) \tag{1}$$

where J = flux of the diffusing species ($matter \cdot cm^{-2} \cdot s^{-1}$)
D = diffusion coefficient of the diffusing species ($cm^2 \cdot s^{-1}$)
dc/dx = concentration gradient of the diffusing species ($mol \cdot cm^{-4}$)

Eq. (1) is valid only for a steady-state diffusion, while for a non-steady state process, Fick's second law is applies:

$$\frac{\partial c}{\partial t} = D \frac{\partial^2 c}{\partial x^2} \tag{2}$$

The special solution to Eq. (2) which can be obtained by establishing certain boundary conditions[21,22], is commonly used for calculation of chloride diffusivity in the conventional diffusivity testing[12, 23-27].

It is important to note, however, that Fick's laws for diffusion are only a good approximation for the diffusion in a non-interacting system. For ionic solutions, even at very low concentrations, an ion-ion interaction exists which reduces the chemical potential

and thus the driving force for the diffusing species[4]. Hence, the diffusion coefficient becomes concentration dependent. Under the action of an external electrical field, the migration behavior is also affected by the ionic clouds surrounding the diffusing ions. Therefore, proper attention to the effect of ionic interaction is important also in migration testing. A more thorough discussion of this topic has been the subject for a separate paper[28].

Migration

When the randomly drifting ions are driven by an external electrical field, the ions will move toward the oppositely charged electrodes causing a flow of current or migration. The electrical driving force acting on an ion is equal to the charge of the ion times the field at the point where the ion is located[29-31]:

$$F_d = z_i\, e_0\, E\, \frac{1}{300} \quad (dynes \cdot ion^{-1}) \tag{3}$$

where F_d = driving force (dynes)
z_i = valence of ion
e_o = charge of proton (or electron) (4.8×10^{-10} e.s.u.)
E = electrical field (volt$\cdot$cm^{-1})

When the electrical field is large enough to overcome the resistance of the medium to the motion of the ions, the steady-state drift velocity of the ions (v_d) is proportional to the driving force (F_d). Hence, the drift flux of the ions is proportional to the applied electrical field (E):

$$Flux \propto F_d \propto v_d \propto E \tag{4}$$

This is the fundamental basis for describing the macroscopic behavior of the migration process.

The drift velocity of an ionic species when subjected to a driving force depends on its mobility, which is defined as the drift velocity of the ion under a unit driving force:

$$u_{abs} = \frac{v_d}{F_d} \quad (cm \cdot dyne^{-1} \cdot s^{-1}) \tag{5}$$

where u_{abs} = absolute mobility (cm$\cdot$s$^{-1}\cdot$dyne^{-1})
v_d = drift velocity (cm$\cdot$s^{-1})
F_d = driving force (dynes)

The driving force expressed in Eq. (5) can either be a chemical driving force due to a concentration gradient or an electrical force caused by an external electrical field[34]. Therefore, if there is a concentration gradient in addition to the electrical field, the motion of the ions is caused by the combined effect of the electrical field and the chemical driving force.

Relationship between diffusion and migration

Although diffusion and migration have different mechanisms, an intrinsic relationship between them exists, which is expressed by the Einstein equation[29-33]:

$$D = u_{abs}\, kT \quad (cm^2 \cdot s^{-1}) \tag{6}$$

where
- D = diffusion coefficient of the ionic species ($cm^2 \cdot s^{-1}$)
- u_{abs} = absolute mobility of the ions in the same medium ($cm \cdot s^{-1} \cdot dyne^{-1}$)
- k = Boltzman constant (1.38×10^{-16} ergs$\cdot K^{-1}$)
- T = absolute temperature (K)

Since both the diffusion coefficient and the mobility reflect the easiness with which the ions move in the medium, the proportionality between them is clear. When chemical and electrical driving forces coexist, the flux of the ionic drift can be expressed as:

$$J = \frac{D}{RT} czFE - D\frac{dc}{dx} \quad (mol \cdot cm^{-2} \cdot s^{-1}) \tag{7}$$

where R and F are the gas constant and Faraday constant, respectively. This equation is normally referred to as the Nernst-Plank equation[29-33], in which the first and second term represent the contribution of migration and diffusion, respectively. Before a calculation of the diffusion coefficient based on this equation can be obtained, a set of simplified boundary conditions and assumptions have to be made.

PRINCIPLE OF TESTING

The migration process

Concrete is a porous material with both a micro and macro level interconnected pore system, which provides the channels for fluid flow and ion transport[34]. For the present test method, a moisture saturated pore system is assumed.

In principle, the experimental setup is schematically shown in Fig. 2, where Cell (1) contains the chloride source solution and Cell (2) the chloride collecting solution. Normally, Cell (1) contains a NaCl solution, while Cell (2) is filled with a NaOH solution of the same molar concentration as that of the chloride source solution. Two mesh electrodes are placed, one on each side of the concrete specimen in such a way that the

electrical field primarily is applied across the test specimen. This is the same experimental setup as that used for determination of chloride permeability[5-11].

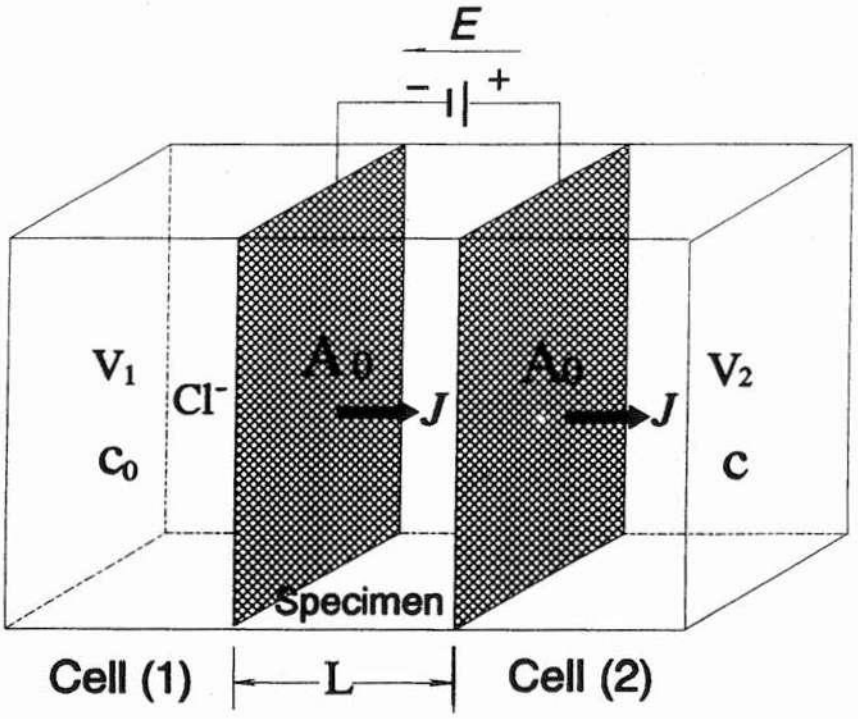

Figur 2. Prinsiple of testing.

In a well cured concrete on a portland cement basis, the pore solution inside the specimen mainly contains hydroxyl ions in addition to sulphate ions and trace amounts of sodium an potassium ions[35-37]. When the electrical field is applied, all the ions in the system start to move under the action of the electrical driving force (F_1) (Fig. 3). For some of the ions the movement will also be due to a chemical driving force (F_2) caused by initial concentration gradients. However, all the ions but the chlorides will finally cease to move due to the formation of an equilibrium distribution in the system. Therefore, when a steady-state migration is reached, most of the ions which pre-existed in the concrete specimen have been driven out in such a way that mostly Cl^- and Na^+ ions are dominant in the specimen. There may still exist a small amount of Ca^{+2} and OH^- ions in the concrete due to a continued dissolution of calcium hydroxide crystals in the cement paste. During the time of testing the chloride penetrating profile moves forward by the electrical driving force, while the concentration gradient decreases until a steady-state migration is reached. Then, the chloride flux and the concentration increase in the chloride collecting cell become constant. At this stage, a constant drift velocity of the chloride ions inside the specimen ("equivalent drift velocity") can be assumed and its value determined. The influence of the chloride concentration gradient inside the specimen during the steady-state migration will not be noticeable because the external electrical field is high enough to overwhelm the chemical driving force. For a voltage of 6 to 12 V the ratio of electrical driving force to chemical driving force (F_1/F_2)

is in the order of several hundreds[28].

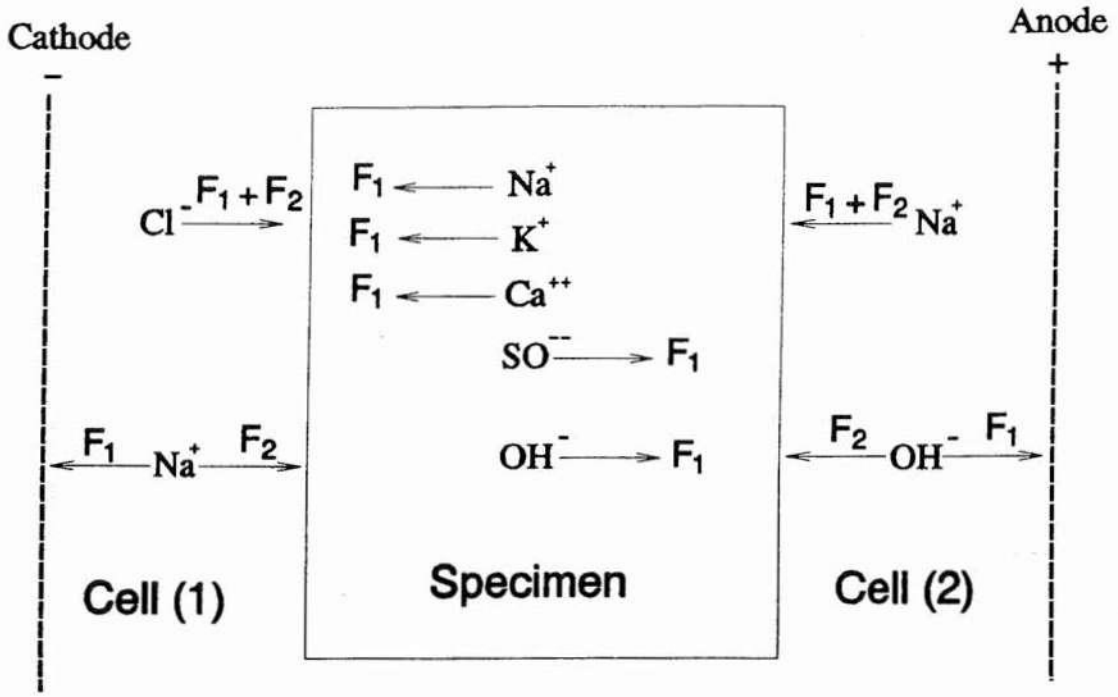

Figur 3. Principle of ion movements caused by electrical driving force (F_1) and chemical driving force (F_2).

Calculation of diffusivity

According to the theoretical relationship between diffusion and migration expressed by the Einstein equation, the diffusion coefficient can be obtained by measuring the actual mobility of the chloride ions in the concrete specimen during the steady-state migration.

As a first approximation, the chloride source solution is assumed to be infinitively diluted so that the migration behavior of the chlorides through the concrete can be assumed to follow the Einstein equation (Eq. 6). Then, similarly to Eq. (5), the actual mobility (u_{act}) of the chloride ions can be defined as:

$$u_{act} = \frac{v_{eq}}{F_d} \tag{8}$$

where v_{eq} is the mean equivalent drift velocity of the chloride ions through the concrete

during the steady-state migration, and F_d is the electrical driving force given by Eq. (3).

By replacing the "absolute mobility" (u_{abs}) with the "actual mobility" (u_{act}), Eq. (6) becomes:

$$D = u_{act}\, kT \tag{9}$$

By combining Eq. (3), (8) and (9), the following expression is obtained:

$$D = 300\, \frac{kT}{ze_o\, E}\, v_{eq} \tag{10}$$

During the steady-state migration the total amount of chloride ions passing through the cross section (A_o) in Fig. 2 during a period of time (t), is

$$Q = J \cdot t \qquad (\text{mol}\cdot\text{cm}^{-2}) \tag{11}$$

where J is the flux of chloride ions. A differentiation of Eq. (11) gives:

$$dQ = J \cdot dt = \frac{V_2}{A_0}\, dc \qquad (\text{mol}\cdot\text{cm}^{-2}) \tag{12}$$

where V_2 is the volume of Cell (2) and dc is the incremental increase of chloride concentration in Cell (2). In the following, V_2 is replaced by V. Then, the flux of chlorides out of the specimen (J_{out}) can be expressed as:

$$J_{out} = \frac{V}{A_o}\, \frac{dc}{dt} \qquad (mol\cdot cm^{-2}\cdot s^{-1}) \tag{13}$$

The flux entering the specimen (J_{in}) can be expressed as:

$$J_{in} = v_{eq} c_0 \tag{14}$$

During the steady-state period, the following equilibrium exists:

$$J_{in} = J_{out} \tag{15}$$

By working out Eq. (13) through Eq. (15), the following equation is obtained:

$$v_{eq} = \frac{J}{c_0} = \frac{V}{c_0 A_0}\frac{dc}{dt} \quad (cm \cdot s^{-1}) \tag{16}$$

By combining Eq. (10) and (16) the diffusion coefficient (D) can be expressed as:

$$D = 300\frac{kT}{ze_o E}\frac{V}{c_o A_o}\frac{dc}{dt} \quad (cm^2 \cdot s^{-1}) \tag{17}$$

which gives the theoretical relationship between the diffusion coefficient and the steady-state migration rate of chlorides (dc/dt).

Since a constant DC power is applied during testing, the electrical field will be a constant given by:

$$E = \frac{\Delta\psi}{\Delta x} = \frac{\Delta\psi}{L} \quad (V \cdot cm^{-1}) \tag{18}$$

where $\Delta\Psi$ is the applied electrical potential, and L is the distance between the two electrodes which can be put equal to the specimen thickness.

Eq. (17) then finally becomes:

$$D = \frac{300kT}{ze_o\Delta\psi}\frac{LV}{c_0 A_o}\frac{dc}{dt} \quad (cm^2 \cdot s^{-1}) \tag{19}$$

From this equation it can be seen that the increasing rate of chloride concentration in the chloride collecting cell (dc/dt) is the only variable in the determination of the diffusion coefficient (D). It should be noted, however, that this expression is based on both certain assumptions and testing conditions which need special attention.

Assumptions and testing conditions

During testing the following factors may affect the observed test results:

(1) Interaction between ions in the migration system.

(2) Evolution of hydrogen gas at the cathode and oxygen at the anode due to

electrochemical reactions between the electrodes and water.

(3) Evolution of chloride gas at the anode if the applied voltage is too high and the electrical resistivity of the concrete is too low.

(4) Evolution of heat and creation of a temperature increase.

(5) A concentration gradient inside the concrete specimen.

Even though all of the above factors will influence the test results to some extent, most of them can be controlled in such a way that the testing can be satisfactory carried out. A concentration gradient inside the concrete specimen will create an additional driving force, but as already discussed, this effect will be negligible. Formation of gas at the electrodes can be controlled by keeping the current low enough, or the voltage low enough in relation to the electrical resistance of the concrete specimen. A moderate voltage will also give a moderate evolution of heat and rise of temperature. In most cases a voltage of 12 V is acceptable, but it may be higher depending on the electrical resistivity of the concrete. If the temperature should increase during testing, Eq. (19) also accounts for this effect to some extent.

Another possible factor which may affect the test results is a reduced chloride concentration (c_o) in the chloride source solution during testing. In order to avoid this effect, the volume of Cell (1) in Fig. 2 must be big enough or the time of testing short enough to maintain an approximately constant c_o.

A chemical binding and a physical adsorption of chlorides inside the concrete specimen may also reduce or block the flow channels through the concrete. Under the influence of a strong electrical field, however, it is assumed that this effect is negligible.

From a more thorough analysis of ionic interaction, it is clear that this effect can not be neglected[4,28]. Eq. (19) is based on the assumption of an infinite dilute chloride source solution. The higher the chloride concentration (c_o), the more retarded is the observed drift velocity of the chlorides (v_{eq}) compared to that from an infinite dilution. Hence, a correction factor for ionic interaction in the calculation of the diffusivity has to be introduced[28].

$$\beta_o = \frac{v_o}{v} \tag{20}$$

where: β_o = correction factor for ionic interaction
v_o = drift velocity of chloride ions from an infinite dilute solution without ionic interaction
v = drift velocity of chloride ions from a concentrated solution

The correction factor β_o depends on both type and concentration of chloride solution as well as temperature during testing but is independent of applied electrical field.

By introducing the correction factor β_o in Eq. (19), the following equation for calculation of the diffusivity is obtained:

$$D = \beta_o \frac{300kT}{ze_o\Delta\psi} \frac{LV}{c_o A_o} \frac{dc}{dt} \tag{21}$$

For convenience, all universal constants in the above equation can be combined into an overall correction factor β and all experimental parameters into another factor α, where:

$$\beta = \beta_o \frac{300k}{ze_o} \tag{22}$$

and

$$\alpha = \frac{T}{\Delta\psi} \frac{LV}{c_o A_o} \tag{23}$$

Thus, the following expression for calculation of the chloride diffusion coefficient (D) becomes:

$$D = \beta \cdot \alpha \frac{dc}{dt} \tag{24}$$

Some values of β and β_o for a NaCl solution of various concentrations are shown in Table 1. For an increasing chloride concentration from 0.1 to 0.5 M NaCl, it can be seen from this table that β_o increases from 1.22 to 1.70. Often, a 3% NaCl solution is used, which roughly corresponds to a 0.5 M concentration. If higher chloride concentrations are used, the theoretical basis for making a correction is no longer valid[28].

From Table 1 it can further be seen that an increasing temperature from 20 to 25°C during testing only has a minor effect.

Table 1. Correction factors for ionic interaction[28].

c_o (NaCl) $mol \cdot l^{-1}$	$\beta^0 = \nu^0/\nu$					
	20°C	21°C	22°C	23°C	24°C	25°C
0.1	1.22	1.23	1.23	1.24	1.24	1.25
0.2	1.35	2.36	1.37	1.37	1.38	1.39
0.3	1.47	1.48	1.49	1.50	1.51	1.53
0.4	1.58	1.59	1.61	1.63	1.64	1.66
0.5	1.70	1.71	1.74	1.76	1.78	1.80
c_o (NaCl) $mol \cdot l^{-1}$	$\beta = \beta_o \cdot 300k \cdot z^{-1} \cdot e_o^{-1} (x10^{-4})$					
	20°C	21°C	22°C	23°C	24°C	25°C
0.1	1.06	1.06	1.06	1.07	1.07	1.08
0.2	1.16	1.17	1.18	1.19	1.19	1.20
0.3	1.26	1.27	1.29	1.29	1.30	1.32
0.4	1.36	1.37	1.39	1.40	1.42	1.43
0.5	1.46	1.48	1.50	1.52	1.53	1.55

EXPERIMENTAL

Experimental details

As part of a more comprehensive ongoing research program on chloride penetration into concrete, a few preliminary experimental test results on the effect of voltage level as a test parameter are presented.

For the present experiments the same experimental setup and roughly the same procedure as that for determination of chloride permeability was used[7-11]. This is also the same experimental setup as that used in the AASHTO T 277-83 method[6].

Based on an ordinary portland cement, one type of concrete and one type of mortar with the same water-cement ratio were tested, the mix proportions of which are shown in Table 2. Test cylinders of ϕ100 x 200 mm were prepared and cured in water for two months. Each cylinder was first surface dried, and then embedded in epoxy and cut into three 50 mm thick slices from top (T) middle (M) and bottom (B) of the test cylinders, respectively. Before testing, all specimens were subjected to vacuum saturation.

Table 2. Concrete mixtures.

Mix	Specimen no.	w/c	Mix proportions (kg/m^3)				Air content %	Compressive strength (MPa)
			Cement	Water	Aggregate			
					0-8 mm	8-16mm		
Concrete	A2	0.5	330	165	756	1310	1.2	59.5
Mortar	D7	0.5	330	165	1894	-	3.9	38.0

Using the same test specimens, three different runs of experiment were carried out with the voltage successively increasing from 6, 9 to 12 V. Before each change of voltage, both the chloride source solution and the solution in the chloride collecting cell were renewed. A chloride source solution of 0.3 M NaCl was used.

The increasing chloride concentration in the chloride collecting cell was monitored periodically by use of a spectrophotometric method[38]. A typical plot of observed chloride penetration is shown in Fig. 4.

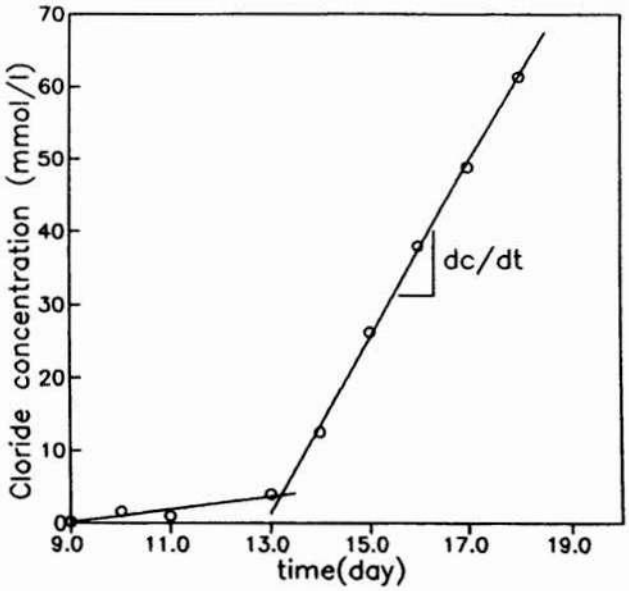

Figur 4. A typical plot of observed chloride penetration.

Test results and discussion

All individual test results are shown in Table 3, from which it can be seen that in spite of a constant water-cement ratio, the mortar showed a higher resistance to chloride penetration than the concrete. This is in accordance with previous experience[39,40]. For the mortar, the diffusion coefficient varied from 11.9 to 19.4 $x10^{-9}$, while for the concrete it varied from 28.6 to 36.5 $x10^{-9}$ $cm^2 \cdot s^{-1}$. The scatter of test results mostly reflects inhomogeneities in the concrete specimens, but it is partly also due to a certain scatter in the measurements of chloride concentration.

The test results clearly demonstrate, however, that chloride diffusivity can be used as a general quality parameter for evaluation of the resistance of concrete against chloride intrusion.

Table 3. Diffusion coefficients ($cm^2 \cdot s^{-1}$) $\times 10^{-9}$.

Specimen no.	Voltage (V)			Statistical parameters		
	6	9	12	$\Sigma x/n$	σ_{n-1}	Std. dev.(%)
A2-3 T	33.4	32.0	29.7	31.7	1.9	6.0
M	35.5	38.0	39.3	37.6	1.9	6.0
B	40.1	39.5	33.7	37.8	3.5	9.3
Average	**36.3**	**36.5**	**34.2**	**35.7**	**2.4**	**7.1**
A2-4 T	30.0	28.9	33.2	30.7	2.2	7.2
M	29.2	37.5	31.5	32.7	4.3	13.1
B	26.6	31.1	30.5	29.4	2.4	8.2
Average	**28.6**	**32.5**	**31.7**	**30.9**	**3.0**	**9.5**
D7-4 T	22.1	23.5	18.1	21.2	2.8	13.2
M	18.6	18.0	16.6	17.7	1.0	5.6
B	17.6	17.7	14.8	16.7	1.6	9.6
Average	**19.4**	**19.7**	**16.5**	**18.5**	**1.8**	**9.5**
D7-5 T	12.3	11.8	11.7	11.9	0.3	2.5
M	12.0	11.6	12.0	11.9	0.2	1.7
B	13.4	13.0	11.9	12.8	0.8	6.3
Average	**12.6**	**12.1**	**11.9**	**12.2**	**0.4**	**3.5**

The experimental results also show that for the level of concrete quality tested, an increasing voltage from 6 to 12 V did not affect the observed chloride diffusivity. In order to reduce the time of testing, the voltage should be as high as possible provided that no evolution of gas at the electrodes develops. Based on the present test results it appears that a voltage of at least 12 V can be used for the testing of a moderate concrete quality.

CONCLUSIONS

Based on the theoretical analysis and the experimental results presented in the present paper, the following conclusions can be drawn.

(1) The electrochemical test method presented can be used for a rapid determination of chloride diffusivity in concrete.

(2) The concentration of the chloride source solution has a significant influence on the rate of chloride migration due to ionic interaction. Hence, for a more general determination of chloride diffusivity, the introduction of a correction for ionic interaction is necessary.

(3) Eq. (21) can be generally used for calculation of chloride diffusivity with a satisfactory accuracy for practical purposes. This diffusion coefficient is independent of both testing potential and chloride source solution.

(4) The chloride diffusivity as determined by the present test method, can be used as a general quality parameter for evaluation of the resistance of concrete against chloride intrusion. Such a quality parameter can be used both for job specification and control of in situ quality, and hence provide a better basis for assuring proper durability.

REFERENCES

(1) Gjørv, O.E., "Steel Corrosion in Concrete Structures Exposed to Norwegian Marine Environment", P.K. Mehta Symposium on Durability of Concrete, Nice, France, May 23, 1994, Proceedings (in print).

(2) Gjørv, O.E., "Important Test Methods for Durability of Reinforced Concrete", M. Malhotra Symposium on Concrete in the 21st Century, San Fransisco, USA, March 21-22, 1994, Proceedings (in print).

(3) Sørensen, H. and Fredriksen, J.M., "Testing and Modelling of Chloride Penetration into Concrete", Nordic Concrete Research, Research Projects 1990, Oslo, 1990, pp. 354-356.

(4) Zhang T. and Gjørv, O.E.," A Fundamental Study of Chloride Diffusion into Cementitious Materials", Journal of Physical Chemistry (paper submitted).

(5) Whiting, D., "Rapid Determination of the Chloride Permeability of Concrete", Report No. FHWA/RD-81/119, Portland Cement Association, NTIS DB No. 82140724, Aug. 1981.

(6) AASHTO Designation T 277-83, "Standard Method of Test for Resistance of Concrete to Chloride Ion Penetration", American Association of State Highway and Transportation Officials, Washington D.C., 1983.

(7) Nordtest Method, NT BUILD 355, ISSN 0283-7153, 1989.

(8) Detwiler, R.J., Kjellsen, K.O. and Gjørv, O.E., "Resistance to Chloride Intrusion of Concrete Cured at Different Temperatures", ACI Materials Journal, Vol. 88, No. 1, 1991.

(9) Zhang, M.-H. and Gjørv, O.E., "Permeability of High-Strength Lightweight Concrete", ACI Materials Journal, Vol. 88, No. 5, 1991, pp. 463-469.

(10) Sandvik, M. and Gjørv, O.E., "High Curing Temperatures in Lightweight High-Strength Concrete", Concrete International, Vol. 14, No. 12, 1992, pp. 40-42.

(11) Gjørv, O.E. and Martinsen, J., "Effect of Elevated Curing Temperature on High-Strength Lightweight Concrete", 3th. International Symposium on Utilization of High-Strength Concrete, Lillehammer, Norway, June 1993, Proceedings, pp. 706-712.

(12) Gjørv, O.E., Tan, K. and Zhang, M.-H., "Diffusivity of Chlorides from Seawater into High-Strength Lightweight Concrete", ACI Materials Journal (in print).

(13) Gjørv, O.E., Tan, K. and Monteiro, P.J.M., "Effect of Elevated Curing Temperature on the Chloride Permeability of High-Strength Lightweight Concrete", Cement, Concrete and Aggregate (in print).

(14) Ushiyama, H. and Goto, S., "Diffusion of Various Ions in Hardened Portland Cement Pastes", 6th. International Congress on the Chemistry of Cement, Moscow, Vol. II, 1974, pp. 331-337

(15) Gjørv, O.E. and Vennesland, Ø. "Evaluation and Control of Steel Corrosion in Offshore Concrete Structures", Katharine and Bryant Mather International Conference on Concrete Durability, Proceedings, J.M. Scanlon (Ed.), ACI SP-100, Vol. 2, 1987, pp. 1575-1602.

(16) Gjørv, O.E. and Vennesland, Ø., "Diffusion of Chloride Ions from Seawater into Concrete", Cement and Concrete Research, Vol. 9, 1979, pp. 229-238.

(17) Feldman, R.F., "Pore Structure, Permeability and Diffusivity as Related to Durability", 8th. International Congress on the Chemistry of Cement, Brazil, Vol. 1, 1986, pp. 336-356.

(18) Ushiyama, H., Iwakakura, H. and Fukunaga, T., "Diffusion of Sulphate in Hardened Portland Cement", Cement Association of Japan, Review of 30th General Meeting, 1976, pp. 47-49.

(19) Tang, L. and Nilsson, L.-O., "Rapid Determination of the Chloride Diffusivity in Concrete by Applying an Electrical field", ACI Materials Journal, Vol. 89, No. 1, 1992, pp. 49-53.

(20) Andrade, C., "Calculation of Chloride Diffusion Coefficients in Concrete from Ionic Migration Measurements", Cement and Concrete Research, Vol. 23 1993, pp. 724-742.

(21) Crank, J., "The Mathematics of Diffusion", 2nd edition, Oxford, 1979.

(22) Brophy, J.H., Rose, R.M. and Wulff, J. "The Structure and Properties of Materials", Vol. II, Thermodynamics of Structure, John Wiley & Sons, New York, 1964.

(23) Midgley, H.G. and Illston, J.M., "The Penetration of Chlorides into Hardened Cement Pastes", Cement and Concrete Research, Vol. 14, 1984, pp. 546-558.

(24) Gautefall, O. and Havdahl, J., "Effect of Condensed Silica Fume on the Mechanism of Chloride Diffusion into Hardened Cement Paste", Fly Ash, Silica Fume, Slag and Natural Pozzolans in Concrete, Proceedings, Third International Conference, Trondheim, Norway, ACI SP-114, 1989, pp. 849-860.

(25) Collepardi, M., Marcialis, A. and Yurriziani, R., " The Kinetics of Penetration of Chloride Ions into the Concrete", Il Cemento, Vol. 4, 1970, pp. 157-164.

(26) NAGANO, H. and NAITO, T., "Application of Diffusion Theory to Chloride Penetration", Transactions of the Japan Concrete Institute, Vol. 7, 1985, pp. 157-165

(27) West, R.E. and Hime, W.G., "Chloride Profiles in Salty Concrete", Materials Performance, July, 1985, pp. 29-35

(28) Zhang, T. and Gjørv, O.E., "Effect of Ionic Interaction in Migration Testing of Chloride Diffusivity in Concrete", Cement and Concrete Research (paper submitted).

(29). Atkins, P.W. "Physical Chemistry", Oxford University, 1978.

(30) Bockris, J.O.M. and Reddy, A.K.N. "Modern Electrochemistry", Plenum Press, New York, 1974.

(31) Newman, J.S., "Electrochemical System", Prentice Hall, Englewood Cliffs, New Jersey, 1991.

(32) Bard, A.J. and Faulkner, L.R., "Electrochemical Methods - Fundamentals and Applications", John Wiley & Sons, 1980.

(33) Southampton Electrochemistry Group - Instrumental Methods in Electrochemistry, Southhampton, 1990.

(34) van Brakel, J. and Heertjes, P.M., "Analysis of Diffusion in Microporous Media in Term of a Porosity, a Tortuosity and Constructivity Factor", International Journal of Heat and Mass Transfer, Vol. 17, 1974, pp. 1093-1103.

(35) Nixon, P. and Page, C., "Pore Solution Chemistry and Alkali Aggregate Reaction", Concrete Durability, Katharine and Bryant Mather International Conference on Concrete Durability, Proceedings, J. M. Scanlon (Ed) ACI SP-100, Vol. 2, 1987, pp. 1833-1862.

(36) Diamond, S., "Pore Solutions and Alkali-Aggregate Attack", Proceedings of the Symposium on Alkali-Aggregate Reaction, Reykjavik, Aug., 1975, Icelandic Building Research Institute, pp. 165-182.

(37) Diamond, S., "Long-Term Status of the Saturation of Pore Solutions in Hardened Cements with Respect to Calcium Hydroxide", Cement and Concrete Research, Vol. 5, 1975, pp. 607-616.

(38) Vogel's Textbook of Quantitative Inorganic Analysis, 4th. Edition, Longman, 1978, pp. 754-755.

(39) Gjørv, O.E. and Vennesland, Ø., "Electrical Resistivity of Concrete in the Oceans", 9th. Annual Offshore Technology Conference, Proceedings, Houston, Texas, 1976, Paper No. 17, 12 p.

(40) Gjørv, O.E., Vennesland, Ø. and El-Busaidy, A.H.S., "Diffusion of Dissolved Oxygen through Concrete", Materials Performance, Vol. 25, No. 12, 1986, pp. 39-44.

MEASUREMENT OF CHLORIDE CONTENT IN CONCRETE. A NORWEGIAN INTERLABORATORY TEST COMPARISON

Kåre Reknes, Norwegian Building Research Institute, Box 134 Blindern, N-0314 Oslo, Norway

ABSTRACT

An interlaboratory test comparison was carried out with the Norwegian Building Research Institute as co-ordinator and with the Directorate of Public Roads as initiator. 36 laboratories participated in the interlaboratory test comparison. The following test methods were used: RCT, Quantab, Volhard, potentiometric titration, potentiometric measurement with ion selective electrode, spectrophotometric measurement.

The measured chloride content varied very much between the laboratories, due to lack of verification of the results of the measurements. The main factor concerning the accuracy of the results was the experience of the operator. A method for the verification of the results of chloride measurements is proposed.

Keywords: chloride content, interlaboratory test comparison, chloride analysis, repeatability, reproducibility, precision

1. INTRODUCTION

Each year the Directorate of Public Roads is inspecting many of the concrete bridges in Norway. During these inspections measurements of the chloride content of the concrete are done to map the posibility of corrosion of the steel reinforcement. The depth of penetration is dependent on factors such as concrete permeability, humudity and chloride exposure. Therefore, in addition to the usual measurements of chlorides, there is often a wish to map the amount of penetration of chlorides into the concrete through the measurement of concentration gradients or profiles. This makes great demands not only to the chemical analysis, but also to the sampling technique. The measurements have to be carried out with a high precision, repeatability and reproducibility also for low concentration of chlorid.

On a number of occasions it has been reported measurements of chloride content showing considerable variations between different techniques as well as between laboratories. Variations of up to 100 % are not uncommon. Techniques where variations have been observed cover all the more frequently used test such as titrations (Vollhard, potentiometric), Quantab test, rapid chloride test (RCT) and analysis with chloride selective electrodes.

In 1992 the Norwegian Building Research Institute co-ordinatet a Nordtest round robin test with the participation of five Nordic laboratories /1/. The aim was to do a systematic investigation of the variations in measured chloride concentrations using laboratory made reference concrete samples with known chloride content. A poor reproducibility was observed. On this background, the Directorate of Public Roads initiated a interlaboratory test comparison with 36 laboratories participating and with the Norwegian Building Research Institute as co-ordinator /2/. The aim was to:

- establish an overview of the used analysis techniques
- investigate the repeatability and reproducibility of the used analysis techniques
- design an extraction and analysis procedure for each used analysis technique

Definitions:

precision: The closeness of agreement between mutually independent test results obtained under stipulated conditions. (Precision depends only on the distribution of random errors and does not relate to the true value, conventional true value or specified value. Repeatability and reproducibility are concepts of precision.)

repeatability: The closeness of agreement between mutually independent test results obtained under repeatability conditions.

repeatability conditions: Conditions where mutually independent test results are obtained with the same method on identical test material in the same laboratory by the same operator using the same equipment within short intervals of time.

reproducibility: The closeness of agreement between test results obtained under reproducibility conditions.

reproducibility conditions: Conditions where test results are obtained with the same method on identical test material in different laboratories with different operators using different equipment.

2. INTERLABORATORY TEST COMPARISON

2.1 Preparation of test samples

The concrete used, was designed on the basis of a typical mix proportion for bridge concrete from the Directorate of Public Roads. The concrete mix proportions are shown i table 2.1. The chloride was added as NaCl dissolved in a part of the mixing water.

Table 2.1
Mix proportions

Mix No.	1	2	3	4
Chloride content in % of cement weight	0.10 %	0.25 %	0.40 %	1.00 %
	kg/m^3	kg/m^3	kg/m^3	kg/m^3
Cement	400	400	400	400
Silica	12	12	12	12
W/(c+2s)-ratio	0.37	0.37	0.37	0.37
Aggregate:				
0-8 mm	1181	1181	1181	1181
8-11 mm	664	664	664	664
Admixture:				
SP	3.00	3.00	3.00	3.00
P	4.00	4.00	4.00	4.00
Air	0.80	0.80	0.80	0.80

The concrete was mixed as 10 l batches, and casted in 100 mm x 100 mm x 100 mm cubes. After curing for 28 days at +20 °C and 99 % relativ humidity, the cubes were grounded to dust with a particel size smaler then 150 µm. The concrete dust was packed in 28 ml containers.

2.2 Documentation of test samples

Before packing of the concrete dust, the chloride content of 10 samples of each conctere mix were analysed. The mean value of these analysis are shown in table 2.2 and the results are plotted in fig. 2.2a. To control the results of the chloride analysis, control samples of reference dust /3/ were analysed. The results are plotted in fig. 2.2b.

Table 2.2
Chloride content of the concrete dust

Mix No.	Mean value of chloride content % by weight of concrete	Standard deviation
1	0.0225	$0.7 \cdot 10^{-3}$
2	0.0474	$0.5 \cdot 10^{-3}$
3	0.0731	$1.8 \cdot 10^{-3}$
4	0.1681	$2.2 \cdot 10^{-3}$

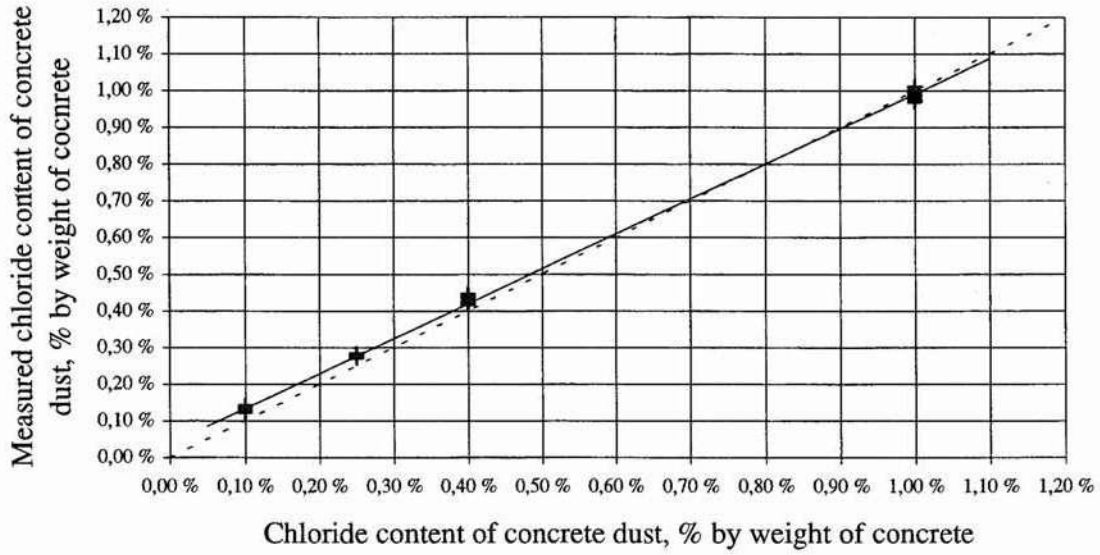

Fig 2.2a
Measured chloride content of the concrete dust. The coeffisient of regression is 0.9991.

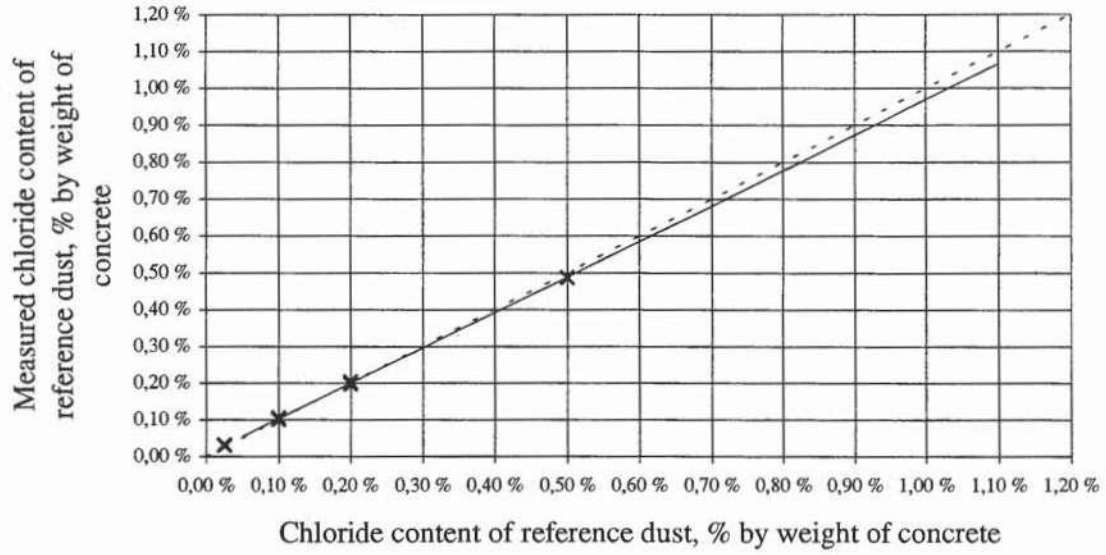

Fig 2.2b
Measured chloride content of the reference dust. The coeffisient of regression is 0.9998.

3. RESULTS

36 laboratories participated in the interlaboratory test comparison. Each laboratory recieved one set of test samples consisting of one sample of mix No. 1, 2 and 4, and two samples of mix No. 3. The chloride contents of the test samples were unknown to the laboratories. Each laboratorie analysed the chloride content of the test samples using the standrad analysis technique of the laboratorie. The results of the analysis were reported to the Norwegian Building Research Institute.

The mean values and standard deviations of the analysis results are shown in table 3a. The data of the regresion analysis of the results of analysis are shown in table 3b.

Table 3a
Mean value and standard deviation of analysis results

		Mix No. 1		2		3[1]		4	
		Chloride content, % by weigth of concrete 0.0225		0.0474		0.0731		0.1681	
Analysis technique	Number of analysis for each chloride concen-tration	Mean value % by weight of concret	Standard deviation	Mean value % by weight of concret	Standard deviation	Mean value % by weight of concret	Standard deviation	Mean value % by weight of concret	Standard deviation
RCT	43	0.0165	$3.9 \cdot 10^{-3}$	0.0361	$6.4 \cdot 10^{-3}$	0.0546	$11.6 \cdot 10^{-3}$	0.1416	$25.1 \cdot 10^{-3}$
Quantab	19	0.0243	$11.1 \cdot 10^{-3}$	0.0501	$7.8 \cdot 10^{-3}$	0.0745	$13.7 \cdot 10^{-3}$	0.1622	$14.2 \cdot 10^{-3}$
Volhard	11	0.0162	$9.6 \cdot 10^{-3}$	0.0394	$14.8 \cdot 10^{-3}$	0.0669	$6.5 \cdot 10^{-3}$	0.1572	$21.3 \cdot 10^{-3}$
Potentimetric titration	9	0.0221	$0.9 \cdot 10^{-3}$	0.0485	$1.7 \cdot 10^{-3}$	0.0742	$2.4 \cdot 10^{-3}$	0.1809	$10.6 \cdot 10^{-3}$
Potentimetric measurement with ion selectiv electrode	3	0.0204	$9.9 \cdot 10^{-3}$	0.0505	$15.6 \cdot 10^{-3}$	0.0841	$27.3 \cdot 10^{-3}$	0.1730	$47.5 \cdot 10^{-3}$
Spectrophometric measurement	1	0.0280	-	0.0540	-	0.0785	-	0.1860	-

Table 3b
Regression data from the results of analysis

Analysis technique	Number of laboratories	Coefficient of regression R^2	Regression line $y = a + b \cdot x$	
			a	b
RCT	17	0.8988	-0.0057	0.8640
Quantab	11	0.9335	0.0048	0.9403
Volhard	4	0.9308	-0.0052	0.9697
Potentimetric titration	3	0.9910	-0.0040	1.0934
Potentimetric measurement with ion selectiv electrode	2	0.7512	0.0051	1.0158
Spectrophometric measurement	1	0.9983	0.0012	1.0903

3.1 RCT - Rapid Chloride Test

The scatter of the analysis results is high. The mean value of the measured chloride concentration is lower then the actual concentration for all chloride contents. 50 % of the participating laboratories achieved a satisfactory repeatability, and the repeatability increased with increasing chloride content. The very low reproducibility caused the great scatter of the analysis results as shown in fig. 3.1a and 3.1b.

[1]Double test set, i.e. number of analysis x2.

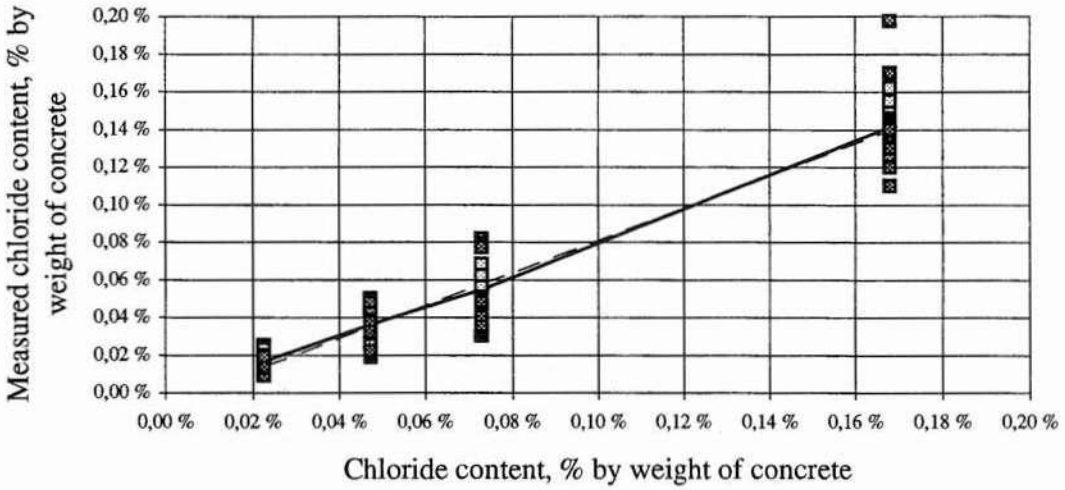

Fig. 3.1a
RCT: Measured chloride content in % by weight of concrete.

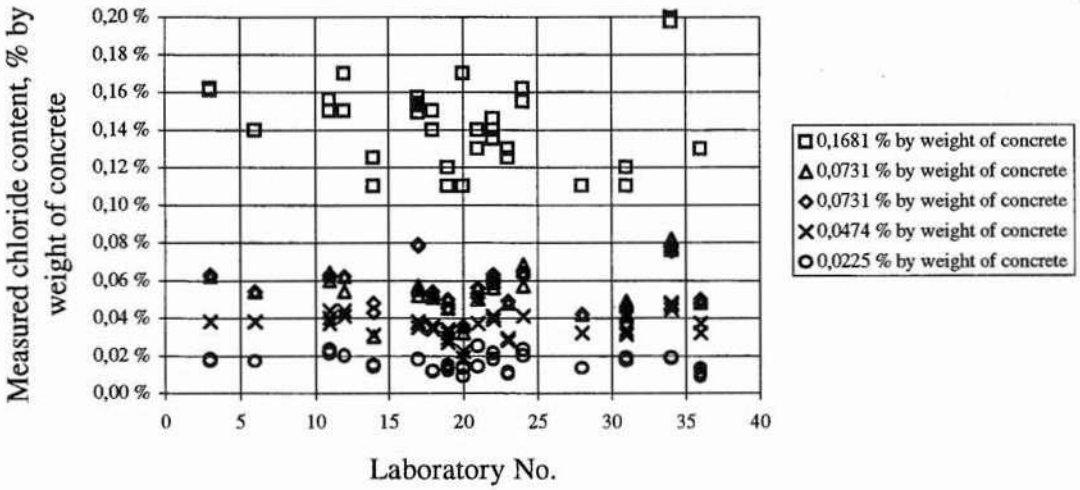

Fig. 3.1b
RCT: Measured chloride content plottet for each participating laboratory.

3.2 Quantab

The scatter of the analysis results is high. The mean value of the measured chloride concentration is close to the actual concentration for all chloride contents. 50 % of the participating laboratories achieved a satisfactory repeatability, and the repeatability increased with increasing chloride content. The very low reproducibility caused the great scatter of the analysis results as shown in fig. 3.2a and 3.2b.

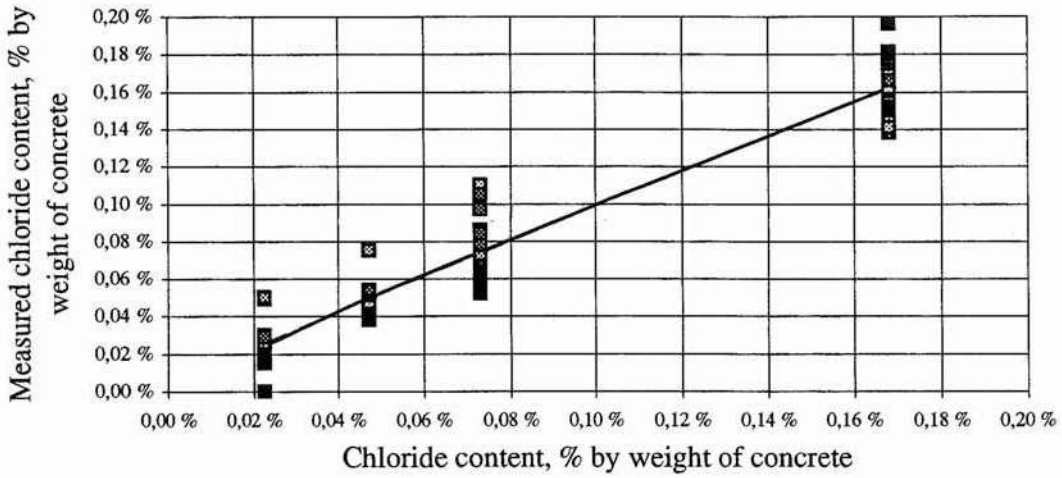

Fig. 3.2a
Quantab: Measured chloride content in % by weight of concrete.

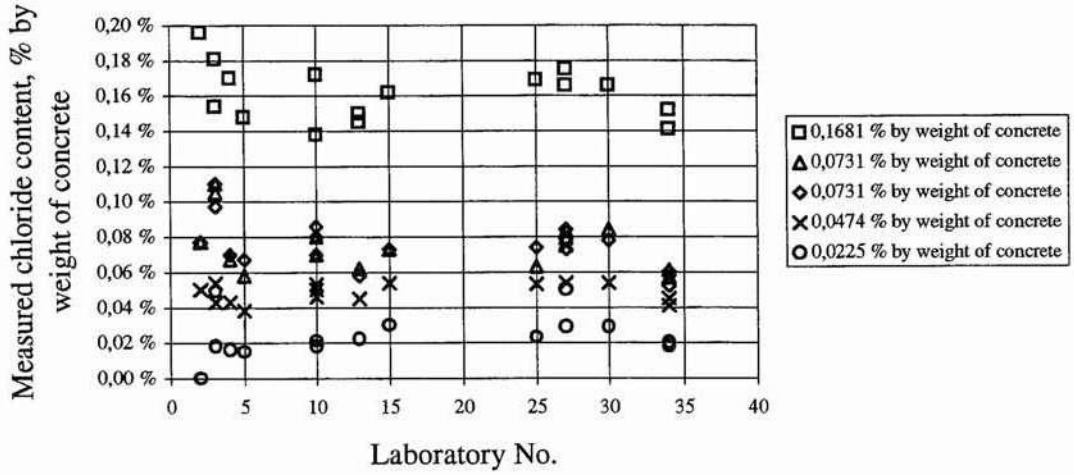

Fig. 3.2b
Quantab: Measured chloride content plottet for each participating laboratory.

3.3 Volhard

The mean value of the measured chloride concentration is, for all chloride contents, lower then the actual concentration. Three out of four laboratories achieved a satisfactory repeatability, and the repeatability increased with increasing chloride content. The reduced reproducibility caused the scatter of the analysis results as shown in fig. 3.3a and 3.3b.

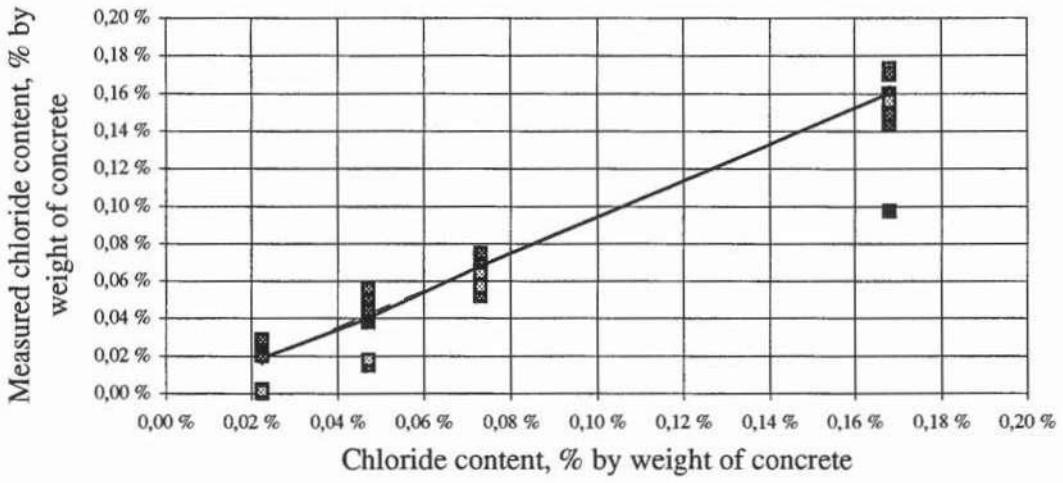

Fig. 3.3a
Volhard: Measured chloride content in % by weight of concrete.

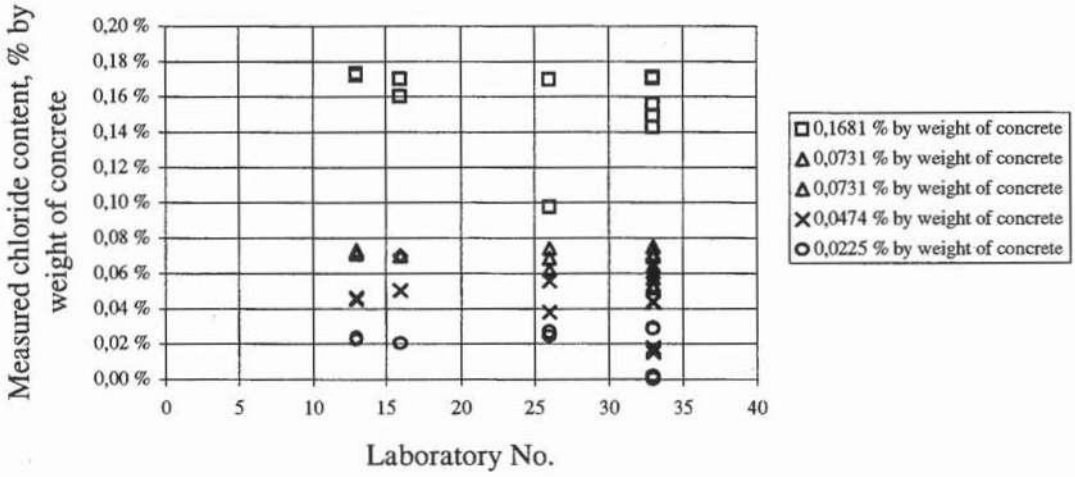

Fig. 3.3b
Volhard: Measured chloride content plottet for each participating laboratory.

3.4 Potentiometric titration

The mean value of the measured chloride concentration is, for all chloride contents, close to the actual concentration. The laboratories achieved a satisfactory repeatability, and the repeatability increased with increasing chloride content. The reduced reproducibility at the highest chloride content caused the scatter of the analysis results as shown in fig. 3.4a and 3.4b.

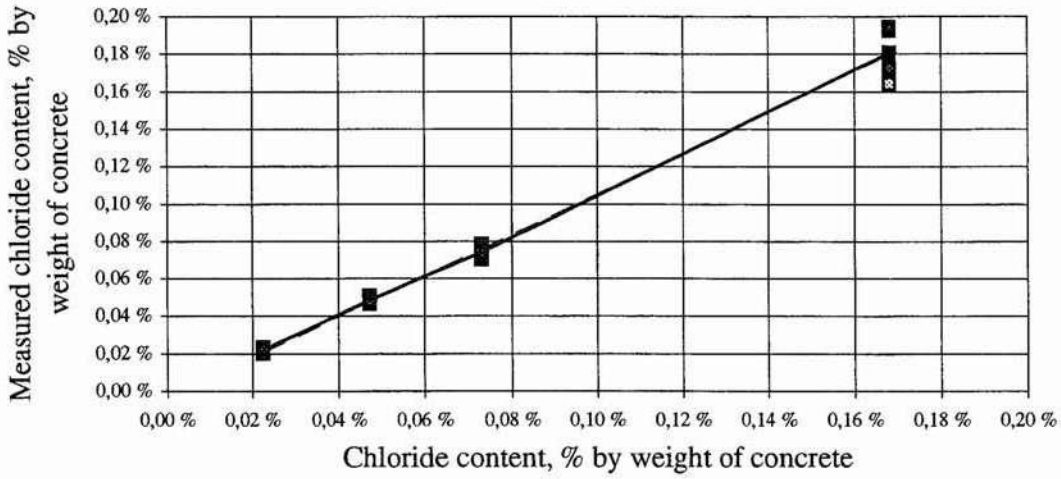

Fig. 3.4a
Potentiometric titration: Measured chloride content in % by weight of concrete.

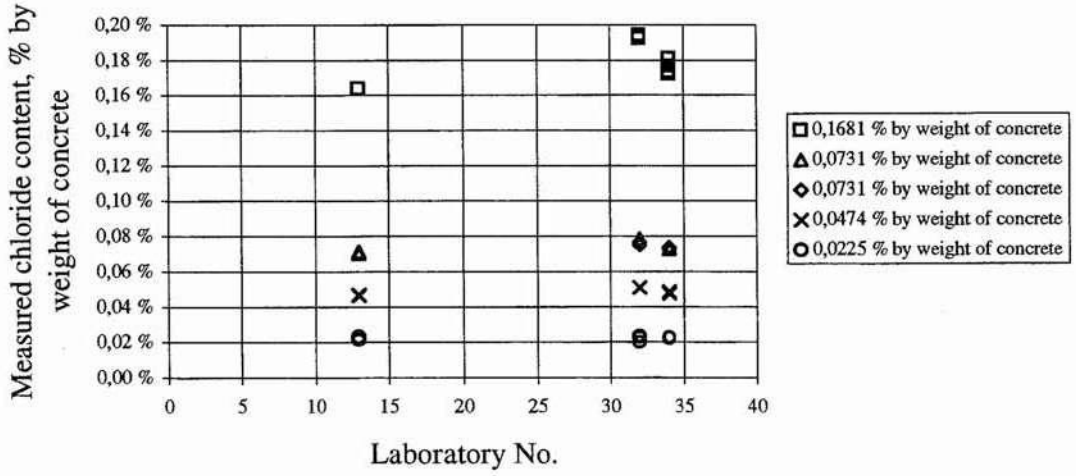

Fig. 3.4b
Potentiometric titration: Measured chloride content plottet for each participating laboratory.

3.5 Potentiometric measurement with ion selective electrode

The reproducibility was very low. It was not possible to find the cause of the low reproducibility, and to draw a conclusion from the reported chloride concentration.

3.6 Spectrophotometric measurement

Only one laboratory participated, and consequently a conclusion can not be drawn.

4. CONCLUSIONS

The precision and the reproducibility of each analysis technique is limited, and to achieve a satisfactory repeatability and reproducibility, the following has to be take care of:

- the operator has to have fixed and written work specifications for the actual analysis technique
- the operator has to be experienced with the actual analysis technique
- the equipment has to be calibrated and maintained

The analysis has to be carried out with a great accurasy.

The measured chloride content varied very much between the laboratories. The repeatability is satisfactory for about 50 % of the analysis, and the over all reproducibility is to small.

The participating laboratories did not verify the results of their analysis.

The results of analysis have to be verified and documentet. The verification is easy done by including controle samples as blind samples[2] of reference dust in the series of samples to be analysed. This would have the effect of assisting the operator to detect errors in procedure and faulty apparatus, as well as being of great help to operators that are unfamiliar with chloride analysis.

The main factor concerning the accuracy of the results is the experience of the operator, the more experienced the operator is, the more accurate are the analysis carried out. The documentation of the analysis through a journal, is the best way of collecting experience.

5. REFERENCES

/1/ H. Chr. Gran, Measurement of chlorides in concrete. An evaluation of three different analysis techniques, NBI-prosjektrapport nr. 110, Oslo 1992
(NODRTEST Technical Report 188)

/2/ K. Reknes, Måling av kloridinnhold i betong. Felt- og laboratoriemålinger. Ringforsøk, NBI-prosjektrapport nr. 149, Oslo 1994

/3/ A. M. Waters and A. T. Blake, Certificates of test. Chloride conctent of reference dust. 14 different certificates, Taylor Woodrow Research Laboratories, Taywood Engineering Ltd., 1991

[2]The term blind sample has unfortunately recived two different interpretations in recent years. Originally and retained in this article, the term was restricted to a sample of known concentration that was submitted as a run-of-the-mill unkown, with analyst unaware that there was anything special about the sample. Only the laboratory supervisor or quality assurance officer knew that it was a check sample.

THEME 6

Future demands and possibilities

CORRODSION RESEARCH TODAY AND TOMORROW

Kyösti Tuutti, Division of Building Materials, Lund Institute of Technology, Box 118, S–221 00 Lund, Sweden.

ABSTRACT

This report deals with the author's view of present corrosion research within the field of concrete. The introduction contains a general presentation of the parameters that are usually used for simple estimations of the service life of structures. In studying the articles that were submitted to this seminar, the subjects selected agree relatively well with the pattern that may be seen at international congresses. Since the discovery of the potential dangers of chloride penetration, this has been the most discussed subject in the past 20 years. New knowledge is starting to make its appearance in various subjects, such as electrochemistry, moisture mechanics, statistics, etc. which are being successively coupled to the durability problem caused by chloride ions. The proposed co–ordination of result reporting in some form of common data bank should be a means of minimizing the risks of future work duplication and as a stimulus to research to employ different scientific disciplines.

Keywords: corrosion, model, visions, data bank

1 SIMPLIFIED MODEL FOR THE CORROSION PROCESS

It is well known and accepted that the course of corrosion of steel in concrete must be divided into two phases,
the initiation phase, in which it is necessary to clarify the processes that take place during the time required to initiate the corrosion process, and
the propagation phase, in which it is necessary to clarify the processes that take place when corrosion has been initiated.

Initiation is achieved almost completely either by neutralization of the concrete around the reinforcement, so–called carbonation,
or by an excessive chloride concentration around the reinforcement. The rate of corrosion after initiation is determined by the electrochemical conditions in and around the corrosion area.

1.1 Chloride initiation

Chloride initiation normally implies that chloride ions penetrate into the concrete from the external surroundings, resulting in successive raising of the chloride concentration at the surface of the cast–in steel. At a certain concentration, which is dependent on the electrochemical conditions and the chemical environment adjacent to the steel, the corrosion process will be activated. This process is one of diffusion, but is not of the

stationary type with constant conditions. The following parameters must be taken into account in the calculation:

- the concrete impermeability as regards chlorides
- the concrete's ability to bond chlorides
- the threshold value for activating the corrosion process in different environments
- the surrounding's chloride concentration, seasonal variations

The initiation time in this case coincides with the time it takes for the chloride concentration to reach the threshold value at the surface of the steel, i.e. the cover is of significance.

There are several methods that are reported in literature on the subject of the way in which mathematical methods can be used to calculate or estimate the penetration of chloride ions into different concretes. But there are at present no safe threshold values that have been verified in practical situations. This method may be used for an approximate calculation of the initiation time if data from experience is available for the corresponding environment.

1.2 Propagation stage

The electro–chemical conditions control the rate of corrosion after initiation. Factors that are of great importance are:

- electrolyte quantity
- concrete resistivity
- electrolyte composition
- temperature

The first three factors are usually replaced by the concrete's moisture content, which affects both the cathode's access to oxygen and the electrical conditions that control the corrosion process.

There exists today practical experience in various countries on corrosion rates for cast–in steel in different environments. Basically, these may be divided into four groups:

- no corrosion or insignificant corrosion, which implies that the corrosion period is longer than the normally prescribed service life. This environment exists and can be exemplified by the Scandinavian indoor climate, structures that are always completely submerged in sea water without water pressure gradients.
- low rate of corrosion as a result of limiting any factor that controls corrosion, which may be an extremely impermeable concrete, intermittent moistening separated by long dry periods, etc.
- normal rate of corrosion after carbonation initiation in an outdoor environment.

- normal rate of corrosion after chloride initiation in an outdoor environment.

Due to differences in temperature and the external climatic differences in the wet and dry periods the values differ in different parts of Europe. These values from experience may be used to specify a rate of corrosion. Different concrete compositions affect the primary factors so much that it is necessary to differentiate between different compositions.

New electrochemical methods of measurement have been developed that provide an indication of the relevant rate of corrosion in a sample. Such methods of measurement can be used to advantage for determining the rate of corrosion in structures or samples. But the measurement values usually indicate a higher rate than the mean rate of corrosion acting over a long period of time, which results in a conservative assessment.

The corrosion process results in there gradually building up visible damage that is felt by the general public to be problematic. With the appearance of such damage the corrosion phase is completed and the end of the service life has thereby been reached. A reliable value that is easy to apply to the time this occurs for normal concretes can be specified by a mean corrosion depth of 0.1 mm.

2 REFLECTIONS ON STUDIES REPORTED IN THE LITERATURE

The model described above is accepted but sometimes used in too rough a way. In comparative studies of the durability qualities of different grades of concrete, it is still assumed that a product which, after exposure for a certain time has permitted the least chloride penetration will have the longest service life. The researcher assumes in such a case that the tolerance level for chlorides is of the same order of magnitude for all products, which is not the case. In principle, all specified parameters must be treated, even in a very rough servicelife estimate, for the results to be credible. Further, some form of reference should be done to reality if the study is made in a laboratory with small test specimens and idealized exposures.

Reported results are very often specified with rough dimensions. The researcher is satisfied to test large pieces of concrete taken from one or a few deep locations in the structure. The chloride concentration is specified in per cent by weight of the total weight of concrete. Unfortunately, this type of rough measurement provides so little information that it cannot be used as reference material by other researchers. Modern methods are based on analysis of complete chloride profiles, millimetre by millimetre into the structure being studied. In such a complete analysis it is possible to see local variations at, for example, the steel surface or in parts of the covering layer, so that the transport mechanisms can be discussed in a completely different way. In addition to chloride profiles, these variations must be related to the material or amount of mortar, suitably via the measured calcium oxide content.

The electrochemical conditions in concrete structures are decided by the binder used as well as by the moisture conditions round the structure. The question to which an

answer is still being sought is whether or not a concrete can be made so impermeable that even if the corrosion process is initiated, the rate of corrosion will be limited by the material's resistivity in a decisive way. Such resistivity measurements have been made for almost 20 years, but the results are only presented as a function of the concrete type. Why has nobody endeavoured to relate this type of measurement to an estimate of the duration of the corrosion period under different environmental conditions?

As regards moisture conditions, both the threshold levels and the rate of corrosion after initiation are probably affected in a decisive way by the climate closest to the steel surface. Moisture mechanics is a well studied subject and there exist today instruments to calculate moisture conditions around reinforcement steel, even if the climate varies at the outside of the concrete surface. In simultaneous measurement of corrosion conditions and relative humidity interesting information has been obtained that increases understanding of the mechanisms acting in this type of decomposition. It is with pleasure that it is possible to note that contributions about moisture mechanics around reinforcement have become increasingly common in various corrosion seminars and congresses.

Finally, a trend is starting to emerge towards more detailed investigations of the corrosion complex. A structure as simple as a bridge pier in sea water can be divided into a number of micro environments according to their position relative to sea level. By means of this type of accurate analysis of relevant conditions at different times, it will probably be possible to find new explanations for the way in which the surrounding environment affects the reinforcement. Statistical methods can be used to advantage on as inhomogeneous a material as concrete. We have mostly assumed that there are no variations that exert a primary influence on the various component parameters that we present in reports and talks. As simple a circumstance as the fact that most structures contain cracks, from the invisible micro cracks to large ones that are accepted by concrete standards, are not dealt with as a result of the complexity. It is probable that an even more detailed division of the micro environment in concrete cover is required before it will be possible to make more correct predictions about the service life of a structure.

3 FUTURE VISIONS

A key factor for good future development in all fields of research is co-operation between different researchers and disciplines. Limited facilities will be available for research in the field of construction, which also increases the demand for co-operation, not only nationally but also internationally. A prerequisite is that research results produced be published in a way that is easily accessible for colleagues. Data banks for PC processing and which could be exchanged should therefore be built up. In other words it is only necessary to reach a general agreement on the data to be stored in our future investigations in some simple system that can be handled by the EXCEL programming language.

In the field of electro-chemical research there remains a great deal to be studied. This applies, above all, to the way of optimizing concrete in relation to steel grades. Steel

has often been regarded as a constant, which cannot be considered satisfactory. It is true that there are some pioneering reports on the subject, but more results are required. Above all, it is necessary to provide an anchoring of the results of the way stainless steels act in practice, where the micro environment varies more than in the laboratory.

New instruments are being produced continually and discoveries made in other areas that are not directly connected to the field of corrosion. Adjacent fields, such as electrochemistry, have already been firmly tied to concrete research, but successful researchers will look for new knowledge in areas that we do not employ today. Statistical processing of corrosion data and concrete properties is one such area of the future.

Finally, testing stations will be built up in fields in which concrete samples will be exposed to the natural effects of the environment, without acceleration. Accurate methods of analysis will successively expose the acting mechanisms, not only their function but quantitative data will constitute basic information for relevant exact servicelife predictions. Even today it is possible to see large structures being provided with test specimens that can be dissected at different times in the future. This will be more the rule than the exception in the future.

Life time modelling - requirements and possibilities.

Birgit Sørensen, COWIconsult, 15 Parallelvej, DK-2800 Lyngby, Denmark.

ABSTRACT

Life time modelling of reinforced concrete structures exposed to ingress of chloride is very complex due to the large amount of parameters, which influences the life time, and the limited possibilities to verify these parameter values on real structures. However, from a practical point of view, even a rough model will give valuable information, although such models will tend to predict lifetimes much on the safe side.

For existing structures, the need of life time models and verification of models by assessment are highly dependent on whether the structure is expected to be maintained by preventive maintenance or by repairs. Modelling, assessment and maintenance strategies should therefore as far as possible be planned as an integrated unit from an early stage of a structures life.

Keywords: Life time modelling, corrosion parameters, ingress of chloride, assessment, maintenance.

1. INTRODUCTION

Life time modelling is for the time being an art of fashion in the concrete world. The conception is often used in connection with prediction of the residual service life of exciting concrete structures as well as in connection with the theoretical modelling of the expected lifetime of a concrete structure in the design phase.

Life time modelling is a subject of interest to design engineers, supervision engineers and scientists. Although these groups of people to some extent works with the same mathematical models as a basis, their aims and need of detailing are quit different and so are their time limits.

The scientist has time to refine his model, to include all possible parameters and to verify their relative importance by test in the laboratory and on site. On the other hand, the supervision engineer has to make decisions based on few observations, he will anyhow have

to include safety margins in his evaluations, but first of all: he has to make his decision here and now, which of course limits his possibilities to improve his basis for decision making.

This paper only deals with life time modelling in cases where the lifetime is limited by the ingress of chloride ions and subsequent reinforcement corrosion. Other mechanisms of deterioration may of course be relevant as the most important or as contributing factors.

2. NEED OF MODELS

The overall model for the life of a chloride exposed concrete structure, as illustrated by fig. 1 has been recognized for many years. This model distinguish between the **initiation period**, where chloride ions penetrate the concrete cover, **corrosion initiation**, where the critical chloride concentration is reached at the level of the reinforcement and corrosion is initiated and the **propagation period**, where corrosion and accompanying deterioration of the structure takes place.

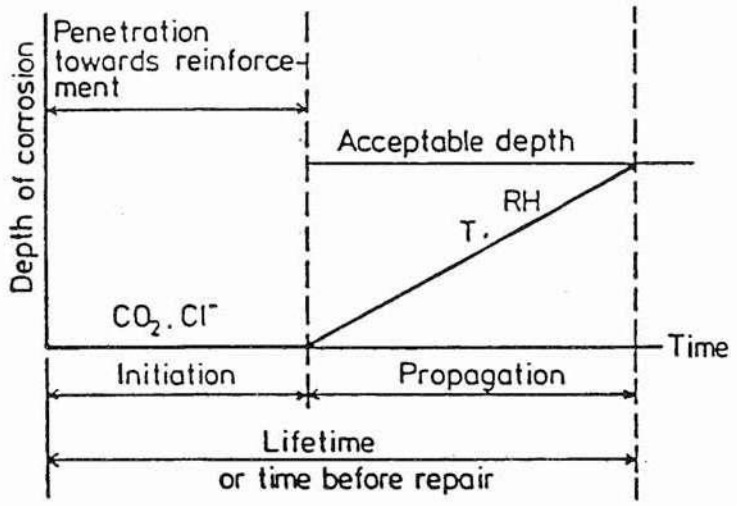

Fig. 1 Schematic sketch of steel corrosion sequence in concrete. Tuutti:CBI Fo 4:77.

In principle, a life time model might consider the hole lifetime of the structure, that is the time from construction and until the structure no more fulfil its design requirements. However, frequently models are applied, which only consider the period of time until repair is needed or even only until corrosion initiation takes place.

The time scale for a model depends on which of the following situations that is considered:

1. Life time design of a structure yet in the design phase,

   In this case, the time scale is often set by the owner of the structure, who would typically specify 100 - 120 year without major repairs. It is then the designers job to select structural design, concrete cover, concrete type, need of supplementary protective measures etc. to fit this requirement. A typical and safe design basis in this situation would be to use the time to corrosion initiation as the design parameter.

2. Estimation of the time to action for an exciting structure, where preventive maintenance is considered,

   In this case the time scale will be limited to the time to corrosion initiation. However, if for instance measures to prevent or reduce further ingress of chloride, such as for instance coating of the concrete surface, are considered, it need to be applied at a much earlier time limit. This limit is the "point of no return", where even a reduction in ingress of chloride and/or re-distribution of the chloride, which is already present in the concrete cover will lead to initiation of corrosion at a later stage. To avoid unnecessary or too early application of preventive measures, this approach requires detailed and accurate models in combination with frequent verification of the relation between model and practice.

3. Estimation of the time to action for an exciting structure where maintenance by repair is considered.

   In this case the time scale lies beyond corrosion initiation. It is of less importance to be able to predict the time to corrosion initiation, as long as it is possible to establish the time when corrosion initiation takes place, to follow the progress of the deterioration and to establish the maximum degree of deterioration, which is allowed from a structural (safety) point of view. In this case structural calculations and assessment are the important input to the decision making, but modelling of the propagation phase might be useful.

These three situations are illustrated in fig. 2.

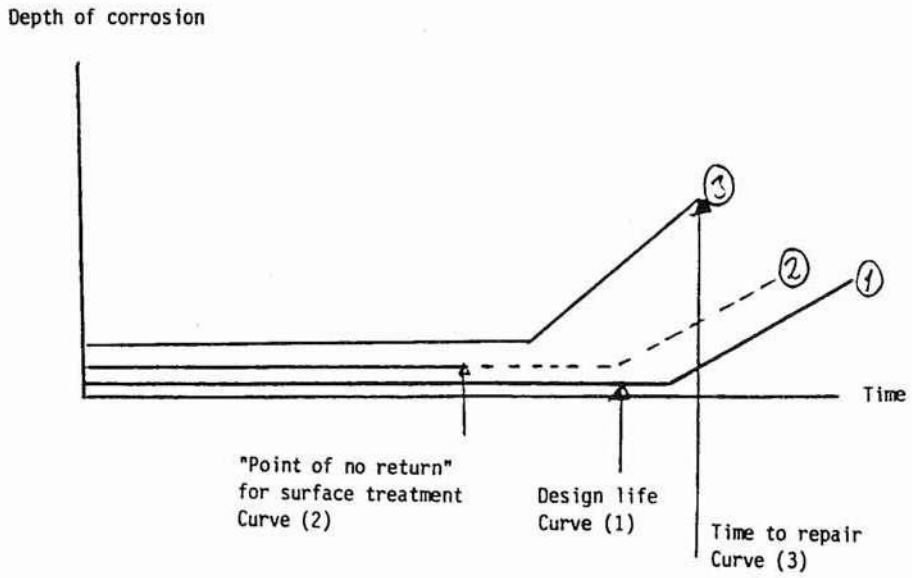

Fig. 2 Time scales for modelling.

3. MECHANISMS

Modelling of the initiation of corrosion is based on an estimate of the rate of ingress of chloride and of the critical chloride concentration.

For a long period of time it has normally been assumed that chloride ions will penetrate the concrete partially together with the water which is sucked into the surface layer of the concrete (capillary suction) or pressed into the concrete (permeation) and partially by diffusion, where chloride ions moves into the concrete due to the concentration gradient between the outer, chloride rich surface layer, and the interior, chloride free part of the concrete. Electromigration due to potential differences is also sometimes mentioned as a mechanism of chloride transport.

In practice, further simplifications has normally been assumed in connection with modelling: The effect of the capillary action is in a relatively dense and uncracked concrete expected to be confined to a relatively thin surface layer. This effect is therefore often ignored. Furthermore, the ingress of chloride is often modeled by the error function solution to Fick's second law for semi infinite diffusion, assuming constant diffusion parameters (surface concentration and diffusion coefficient), formula 1.

$$\frac{C_s - C_x}{C_s - C_0} = \mathrm{erf}\left(\frac{X}{2\sqrt{Dt}}\right) \quad [1]$$

Finally, critical chloride concentrations in the area of 0.05% - 0.1% chloride by weight of concrete is often assumed. These values are based on experience from assessments of old concrete structures, and consequently related to the type of structures, which are in fact deteriorating, and the cement types and mix design, which were used more than twenty years ago.

The above simplified approach has recently been exposed to severe criticism on the following basis:

- The effect of capillary action will have a significant effect on the transport process and the level of chloride if [1] the concrete is of a poor quality, with an open capillary pore system and/or surface connected cracks or [2] the concrete structure is relatively young, meaning that the chloride front is relatively close to the front of ingress caused by capillary suction.

- The diffusion parameters cannon be considered constant. The surface concentration is not necessarily constant in time, but might tend to increase during the first years or more after exposure. Furthermore, the diffusion coefficient is not necessarily constant in time, but tends to decrease.

- Chloride binding is extensive and non-linear. If this is not taken into consideration major errors might be made if a chloride profile is extrapolated in order to estimate the time to corrosion initiation.

- The critical chloride concentration is highly dependant on parameters such as chloride binding, the electrochemical potential of the reinforcement and the pH of the pore water. As the critical chloride concentration is of crucial important to the time to corrosion initiation significant errors might be introduced if standard values (such as 0.05 - 0.1%) are used to estimate the time to corrosion.

- The diffusion coefficient is not solely a material parameter, but will also be influenced by the environment, for instance: D will be dependant of the chloride concentration and the concentration of other ions in the media which is in contact with the concrete.

- The ingress of chloride will only take place to a fixed depth, determined by the connectivity of the pores in the surface layer, and then stop or be reduced to an insignificant level. (percolation theory).

With regard to the mechanism of propagation (deterioration), this is well understood: The volume of corrosion products is larger than the volume of the equivalent amount of metallic

iron. This means that a pressure will built up in the concrete cover, which eventually spalls off. However up till now only few attempts have been made to model this phase, and none of them convincingly.

4. NEED OF KNOWLEDGE

As demonstrated above there are serious deficits in our understanding and quantification of the parameters which influences the ingress of chloride and the time to corrosion initiation.

The parameters, which need to be analyzed to provide full understanding, relates to:

Chloride binding:

- effect of the chemical composition of the cement (or binder)
- effect of the fineness of the cement (or binder)
- kinetics of chemical and physical binding (rate of binding and reversibility)
- effect of other ions

All this as a function of chloride concentration

Effective transport mechanisms as a function of:

- Concrete quality (including also defects etc.)
- exposure conditions

How does effective transport parameters on a given structure depend on variations in:

- allowable variations in concrete composition or properties of raw material
- casting and hardening conditions (leading for instance to bleeding or cracking)
- exposure condition (as for instance humidity or variations in humidity of the concrete or the salinity of the environment)

The limited knowledge we have today with regard to ingress of chloride in existing structures indicate, that it might be very difficult to find even approximative algorithms which takes all these parameters in consideration, and which are generally applicable. Even very simple correlations such as for instance the effect of the height above the water table on the estimated diffusion parameters cannot be generalised from structure to structure.

One reason for the lack of consistency in field observations might be that different transport routes are domination in different concretes. These different routes may be capillary pores, gel pores, cracks or contact zones between aggregate and paste.

With regard to the propagation phase, this is today often "modeled" by assuming that the time from corrosion initiation and to repair is needed is say 10 to 15 years. Again, this is based on experience from old structures and cannot be generalized to the present day concrete, especially not the types with low w/c and pozzolanic additives, which will strongly increase the resistivity of the concrete, perhaps with a factor of 5 - 10 compared to old concrete types. How this will limit the corrosion rate is a question of crucial importance. If the corrosion rate is strongly limited, it might be of less importance to take measures as for instance the use of coated reinforcement, to avoid corrosion initiation or to extent the initiation period.

5. DIFFERENT APPROACHES TO MODELLING

Due to the very limited systematism in observations on different structures it is likely that the use of a model, which takes all or the majority of the above parameters under consideration, will require extensive assessment and measurements. Whereas the very simplified model based on the error function solution to Fick's second law with fixed parameters only require the measurement of the total chloride content as a function of depth below the concrete surface, an extended model might require measurements of free and bound chloride, humidity, electrochemical potential measurements, evaluation of the critical chloride concentration in the specific concrete at different electrochemical potentials of the reinforcement etc. This approach might therefore lead to exorbitant expenses to assessment.

On the other hand, use of models with few and fixed parameters will typically - but not necessarily - lead to conservative life time estimates. This happens because all parameters, typically will be estimated conservatively. In this case preventive measures might be applied long before needed, which will lead to unnecessary expenses.

In stead of using conservative parameter estimates, another possibility is to use a statistical (probabilistic) approach, where where the uncertain parameters are modelled by random variables in stead of using fixed parameter estimates. An example: The critical chloride concentration lies between 0.05% and 0.1%, it is most likely 0.075% and the coefficient of variation is estimated to say 10%. An conservative estimate would be to use the value 0.05%.

The probabilistic approach can as a second benefit be used to provide sensitivity study of the different parameters. From such an analysis it will be known which parameters should

be determined with great accuracy to reduce the uncertainty on the best estimate of a limit state (as for instance the time to corrosion initiation), and which parameters that are more inferior. Sensitivity analysis may of course also be carried out if a fixed parameter, conservative estimate is used.

Using this probabilistic approach the model can be updated after repeating measurements on the same structure, adjusting the model and reducing the uncertainties The need of further assessment may consequently be reduced in time. Fig. 3 demonstrates the principle difference in the type of results which is a result of the statistical analysis, compared to the analysis with the conservatively estimated fixed parameters.

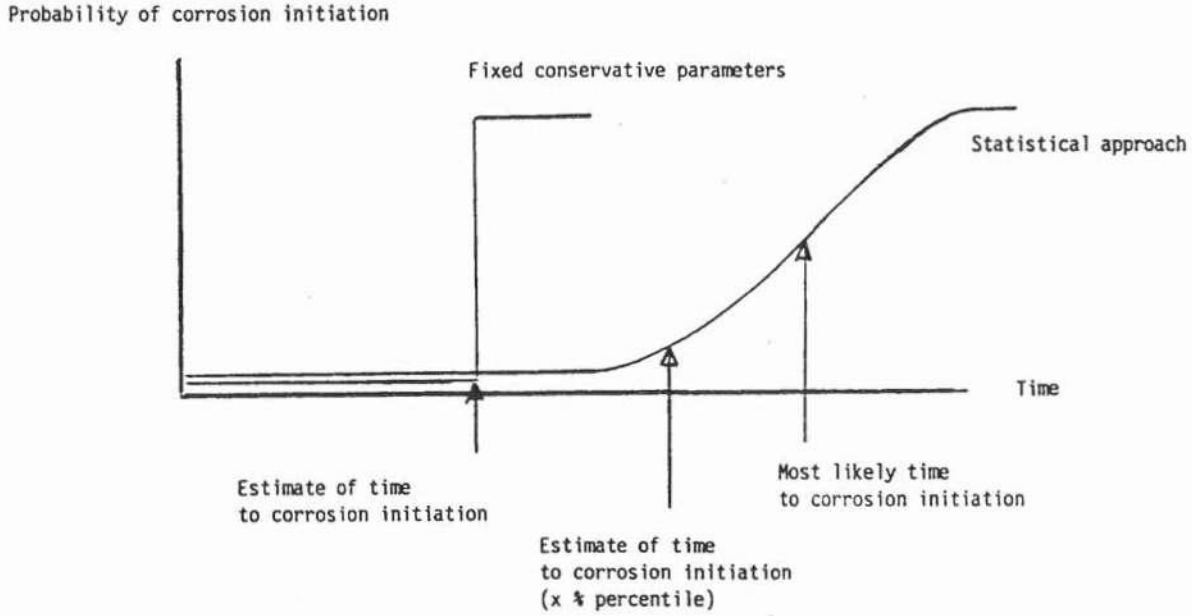

Fig. 3 Example: Estimate of time to corrosion initiation by a fixed parameter and a statistical approach.

At this stage, no overall and verified model taking all parameters in consideration is available, and it is easy to point out the weaknesses in the more simplified models, which is used extensively. This has had the consequence that some engineers and researchers have taken the position to abandon the used of models for life time prediction until further knowledge has been gained. From a practical engineers point of view this is a step in the wrong direction, because it leaves us with nothing except "engineering judgement". Even the simplest model gives some limits, inside which the right answer shall be found.

The largest uncertainty is related to life time design of new structures. Practical experience from existing structures in only applicable with a high degree of uncertainty, and the extrapolation from short term laboratory testing of trial castings might lead to a significant

conservatism in the life time estimate, leading to unnecessary expenses due to for instance the use of very dense concrete types or supplementary preventive measures. Models which relates short term laboratory measurements to long term behaviour of real structures are under development, but it will take a long span of years to prove their practical relevance.

The uncertainty is significantly smaller if the models are used for estimation of the time to corrosion initiation on existing structures, where the predictions of the model can be calibrated by results of tests and inspections.

SYSTEMATIC COLLECTION OF FIELD DATA FOR SERVICE LIFE PREDICTION OF CONCRETE STRUCTURES

Paul Sandberg
Cementa AB/Byggnadsmateriallära LTH
Forskningsbyn Ideon, 223 70 Lund
fax (+46)-46 211 06 47

Abstract

A systematic approach for collection of field data for service life prediction of concrete structures is proposed. Some general guidelines for such an approach are presented. In addition, some procedures for collection of relevant field data are listed. Most procedures have been tested in the field and evaluated during the last years in Scandinavia.

This proposal may serve as an introduction to future discussions concerning field monitoring of concrete structures.

Introduction

Several long-term field studies of concrete have revealed the need for a systematic approach for collecting field data for service life prediction of concrete structures /1-5/. These field studies among others indicated that field testing of concrete will generate a wide spread of data for a given concrete mix, depending on curing conditions, exposure length and micro climate.

Several critical evaluations of laboratory testing have revealed the shortcomings of most laboratory tests at use today, /6,10/ among others. Today the correlation between performance in most laboratory durability testing and the corresponding field performance of concrete structures are unknown, if existing at all. However, the establishment of a common approach for field monitoring of concrete would eventually make it possible to correlate the performance of concrete in certain laboratory testing to the actual field behaviour, for a given type of structure in a given environment. A common approach for field monitoring of concrete would also help to create a database of experience for future planning and design of concrete structures. A general systematic methodology for service life predictions of building materials and components by CIB/RILEM /29/ and ASTM /30/ may be used as a base for this work.

A systematic approach for collecting field data for service life prediction has been discussed and tested in the last years within the project "Durability of Marine Concrete Structures" in Sweden and Denmark /6/. This paper briefly summarise two proposals /7,8/ within this project.

Control slabs for systematic inspection of concrete structures

The collection of relevant data for service life prediction of concrete structures today requires destructive testing methods. It is therefore suggested that control slabs are specified and cast parallel to the actual structure, as illustrated in Fig. 1. The control slabs should be cast at the same time as the original structure. The control slabs must be large enough and cast similar to the original, in order to reflect the micro structure of the original structure.

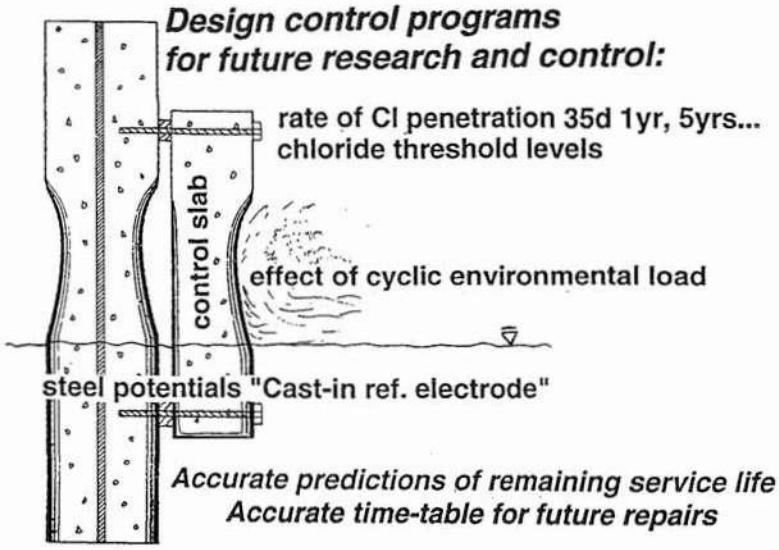

Fig. 1. Control slabs placed parallel to concrete structures, for field monitoring of concrete.

The total economy of a structure (including inspection, repair etc.) will benefit from the parallel design and casting of control slabs at the construction site.

Already existing structures will face extra costs for the casting of control slabs. Furthermore, it will be more or less difficult to obtain the very same concrete as used for the origin structure. In addition, the exposure history for such "secondary" control slabs will become different from that of the original structure.

Location of control slabs and sampling sites

The location of control slabs and sampling sites are of primary concern, since the micro-climate may vary extensively within quite small distances. The investigation of a 37 years old concrete harbour in Esbjerg, Denmark, revealed dramatic differences in field chloride penetration at various heights from the mean water table, as illustrated in Fig. 2 /9/. Similar variations can also be found when comparing various quarters, wind directions etc.

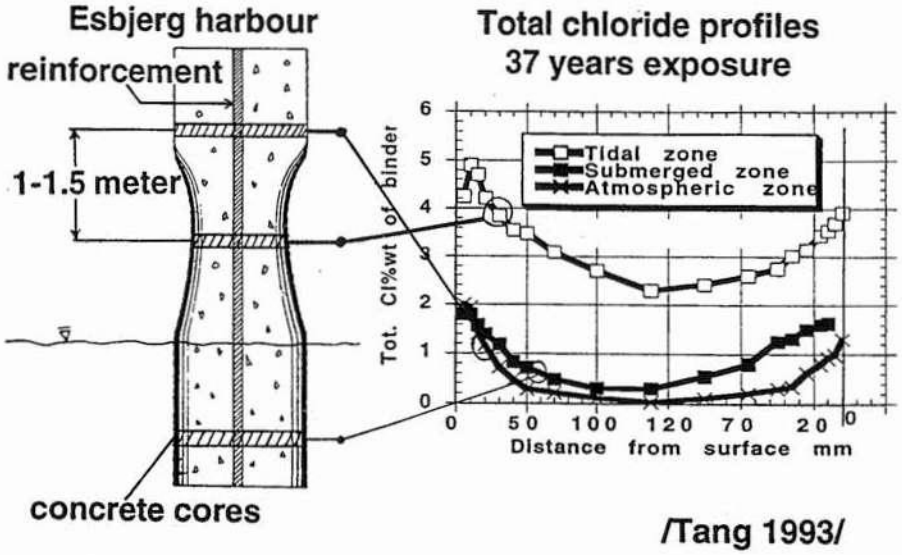

Fig 2. Field chloride penetration in 37 years old high performance concrete at various levels from the mean water table /9/.

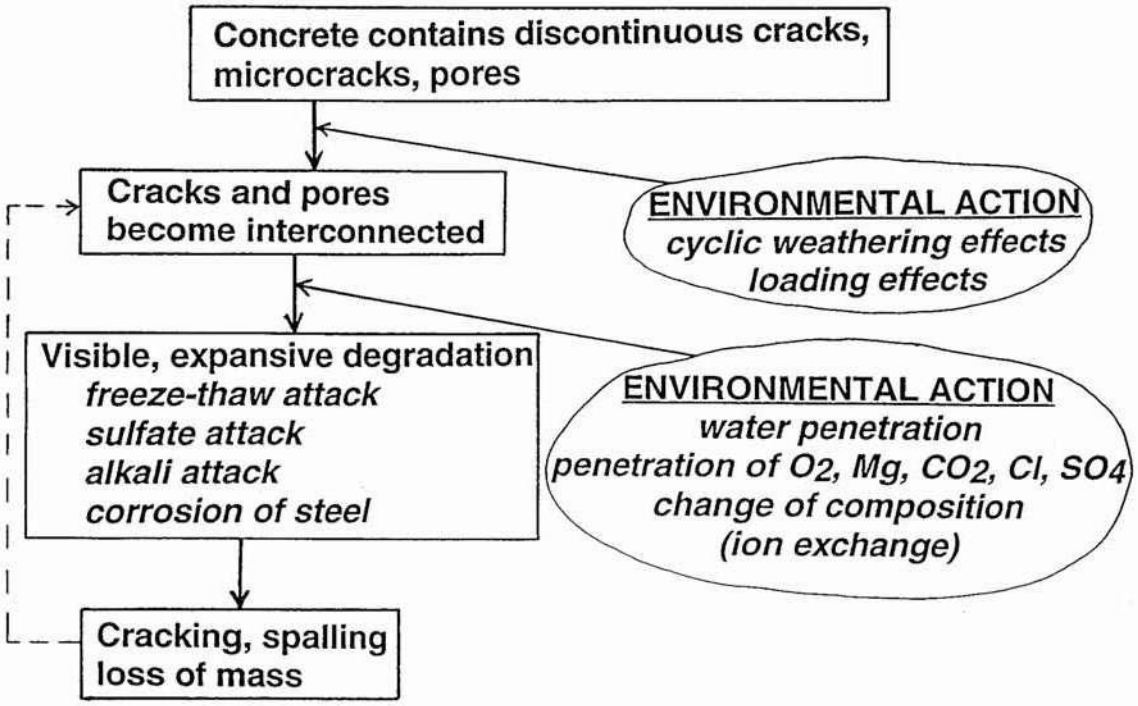

Fig. 3. A schematic sketch of the gradual degradation of concrete in the field, after /10,11/.

Planning for inspection

Several durability-related concrete parameters changes with time, such as the moisture state and the coefficient of chloride transport in concrete. The breakdown of concrete in the field gradually continues from the beginning of field exposure to the end of the service life, as illustrated in Fig. 3 (sketch after Mehta /10/ and discussed by Moskvin et. al. /11/).

The net rate of concrete breakdown is non-linear over time. During the first years of exposure, the permeability of a good quality marine concrete cover decreases over time, due to continued hydration, densification of the concrete surface, etc. /6/. However, after some 10-20 years of service, freeze-thaw attack etc. may become a dominant degradation mechanisms, now increasing the permeability over time.

Such a scenario was probably true for the 37 years old high performance concrete (>90 MPa) at Esbjerg, since it had degraded significantly only in a specific tidal zone /9/. In Fig. 4, various scenarios for the net rate of concrete breakdown is illustrated by the coefficient of chloride transport ("effective diffusivity") over time.

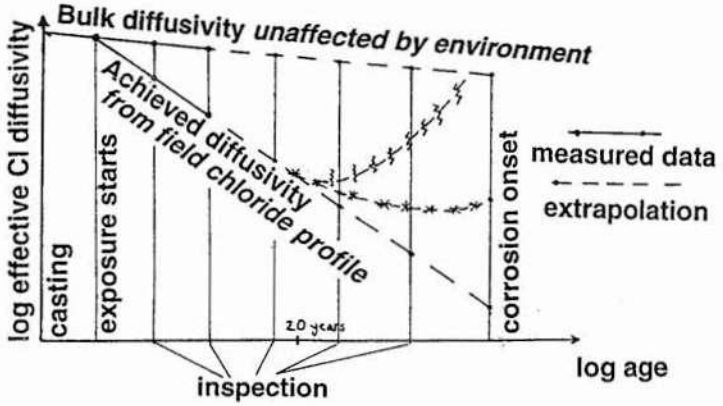

Scenarios

1 – – – – – *No change degradation path*

2 ✳ ✳ ✳ ✳ ✳ *Some changes degradation path*

3 ⊣ ⊣ ⊣ ⊣ ⊣ *Servere cracking, spalling (Esbjerg)*

Fig. 4. Various scenarios for the chloride transport coefficient "effective diffusivity" over time in field exposed concrete. Scenario 1) -A linear relation over time. 2) - Some degradation mechanisms become more important after 20-30 years of service, due to a coarser porosity, inter-connection of cracks and accumulation of freezable water. 3) - Servere freeze-thaw attack is accompanied with sulfate attack, salt accumulation and alkali-silica reaction etc.

Due to changes in concrete properties over time, recurrent inspection must be planned at various ages. Since most properties are believed to roughly follow a square root dependency, the inspection frequency may be higher at early ages.

Swedish results from recurrent inspections of concrete field exposed for 0-4 years, indicate that the following scheme could be useful for planning. The field data obtained from 0-5 years of exposure is intended for planning of future inspections and service life prediction. Present models for service life prediction may of course later on become adjusted for the knowledge achieved from future inspections.

Inspection number	time of exposure (years)	
1	0	(inspection at the day of field exposure)
2	1	
3	2	
4	5	
5	10	
6	20	
7	35	
8	50	
9	70	
10	100	

A standard methodology for field inspection

Non-accelerated field testing of concrete is very costly and time consuming. It is therefore necessary to establish standard procedures for collecting and reporting of field data. The more field data which can be made available for various concrete qualities and binders, for various structures, climates, micro climates, ages etc., the more accurate service life predictions can be made. A big problem today among concrete engineers is a lack of confidence in handling and using durability data from "foreign sources".

Classification into exposure zones

All structures must be divided into various exposure zones, depending on the environmental loads on both macro-climatic and micro-climatic level. Here only marine concrete and concrete exposed for deicing salts are briefly discussed.

Exposure zones in marine environments

The following exposure zones are suggested when applicable:

Atmospheric zone not sheltered from rain

No regular splashing from waves. However, the salt spraying by wind may be significant. Significant temperature cycles, wetting and drying, freezing and thawing may occur.

Atmospheric zone sheltered from rain

As above, but the effect of stronger drying may cause significant capillary chloride transport. Carbonation may be important.

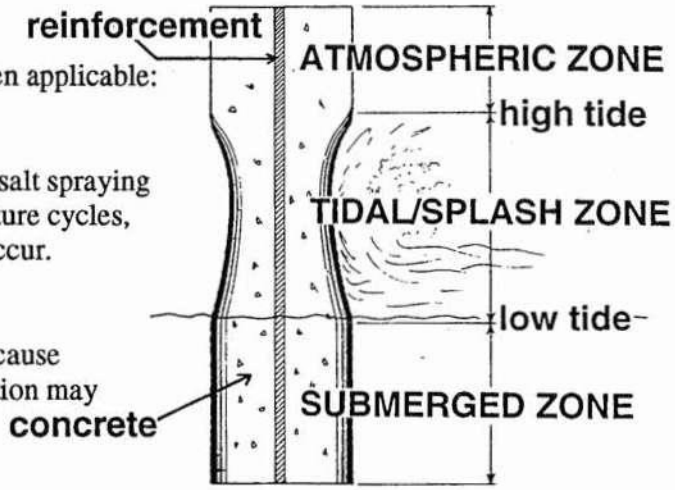

Fig. 5. Exposure zones in marine environment

Splash zone not sheltered from rain

Regular splashing from waves. Significant temperature cycles, wetting and drying, freezing and thawing, erosion may occur.

Splash zone sheltered from rain

As above, but the effect of stronger drying may cause significant capillary chloride transport. Carbonation may be important. Occasionally very high salt levels and scaling has been observed in this climate, due to continuous capillary suction and evaporation of water at the concrete surface.

Tidal zone

Tidal cycles cause temperature cycles, wetting and drying, freezing and thawing. Long term field studies indicated the tidal zone as the most servere exposure zone, since tidal water causes 2 cycles of freezing and thawing every day /11/.

Submerged zone

The environmental load is relatively constant. This zone is an important reference zone when evaluating chloride ingress etc. in zones above the water table. Swedish field studies indicated that for good quality concrete with no or little damage, the chloride penetration is most rapid in the submerged zone (due to continuous chloride exposure). However, the reverse appears to be true once significant deterioration take place in the splash zone /6/.

Deep submerged zone

This zone is only applicable for deep water structures and has not been studied in this work.

Zones of primary interest

The splash and tidal zones are by far the most servere exposure zones in a marine environment. However, it is strongly recommended also to monitor the submerged and atmospheric zones, since these less servere zones will submit reference data of importance when evaluating the degradation path in more damaged concrete.

Exposure zones in deicing salt environments

The classification above seems useful also when considering deicing salts:

Atmospheric zone not sheltered from rain

Some salt spraying and significant temperature cycles, wetting and drying, freezing and thawing may occur.

Atmospheric zone sheltered from rain

As above, but the effect of stronger drying may cause significant capillary chloride transport. Carbonation may be important.

Splash zone not sheltered from rain

Regular splashing by deicing salts. Significant temperature cycles, wetting and drying, freezing and thawing may occur.

Splash zone sheltered from rain

As above, but the effect of stronger drying may cause significant capillary chloride transport. Carbonation may be important. Occasionally very high salt levels and scaling has been observed in this climate, due to continuous capillary suction and evaporation of water at the concrete surface.

Concrete parameters of interest

Field chloride profiles are of primary concern when evaluating resistance to chloride penetration. A field chloride profile reflects the net result of all kinds of environmental action and the materials properties from the beginning of exposure to the time of measurement. However, field chloride profiles alone may not be sufficient for service life prediction. A laboratory measurement of the bulk diffusivity in unexposed bulk concrete will give useful indications on the "intrisinic" permeability of the concrete itself. Since most degradation mechanisms are governed by moisture transport, registration of moisture state and transport data is also of primary concern for improving service life prediction.

Studies of pore solution chemistry is important when evaluating chloride threshold levels for activation of reinforcement corrosion. Pore solution chemistry may also give important information for better understanding of transport mechanisms and degradation processes. Unfortunately no accurate method exists for such measurements in high quality concrete of low water/binder ratios. However, several indirect methods may reveal useful information.

Optical microscopy will supply very useful general information about micro structural degradation such as cracking, leaching, densification, carbonation, expansive reactions etc. In addition, thermogravimetric studies may supply useful quantitative data to support observations in the microscopy.

Measurements of corrosion potentials and -rates are useful for evaluating if the reinforcement is actively corroding or not. Information about chloride threshold levels can be obtained if such measurements are combined with chloride profiles and pore solution studies.

In Table 1 a more detailed list of suggested measurements are given. The recommended numbers of cylinders are minimum requirements for a reasonable accuracy in one exposure zone, based on experience from Swedish field studies.

Drilled concrete cylinders of minimum diameter 100 mm should if possible be drilled deep enough to involve >50 mm bulk concrete unexposed to chlorides.

Table 1. List of relevant studies for service life prediction of concrete structures exposed to sea water or deicing salts

pos	study	method /reference/	No of cylinders	ranking
1)	total chloride profile	profile grinding 7-9 depths /12/	4	v.good
2)	total binder profile	same powder fractions as pos 1) /9/	0	v.good
3)	water soluble Cl, OH, Ca, SO4, Na, K	same powder fractions as pos 1) /13,16/	0	research/ reason-able f.Cl
4)	Bulk chloride diffusivity	unexposed bulk concrete, several lab. methods apply: immersion test, diffusion cell/14/, electrical field /15/	unexposed part of cyl above	v.good
5)	water soluble Cl, OH, Ca, SO4, Na, K	pore pressing if possible w/b >0.45 /16/	2	good if w/b>0.45
6)	moisture profiles, RH and degree of capillary saturation	cylinders divided in 10-15 mm slices without using water /17-19/	2	good
7)	coefficient of moisture transport at steady state conditions	cylinders cut in slices thicker than maximum aggregate size /20/	2	good
8)	TG profile of hydrates & carbonates	powder/concrete from pos 2) or 6) /28/	0	good
9)	RH continuously in situ	Cast in tubes for replacement of RH-sensors /21/	no cylinders	good/ research
10)	Optical microscopy	cracking, leaching, carbonation, ASR, porosity /22/	2	v.good
11)	corrosion rate, potentials, resistivity, threshold levels for corrosion initiation	several methods apply: polarisation resistance, potential mapping, anodic pulse etc. /23,24/. Cast in reference electrodes recommended	no cylinders	good/ research
12)	continuous logging of corrosion data in situ	cast in reference electrode and corrosion cells, optional with controlled potentials /23,25/	no cylinders	research
13)	resistance to salt scaling	lab. testing of field concrete /26/	3	v.good
14)	compressive strength	lab. testing of field concrete, cover and bulk /27/	3	v.good

This program may be carried out more or less extensively, depending on desired accuracy in service life prediction, research needs, environmental conditions etc.

The column "ranking" indicates the efficiency of each method as judged by the author.

Note that several studies are sensitive to the moisture state, such as studies of moisture profiles, pore solution chemistry and corrosion studies. These measurements should be carried out immediately after sampling.

Discussion

The goal of this paper is to initiate a constructive discussion on the principles for monitoring field data for service life prediction of concrete structures. Some principles and methods used in Scandinavia are listed. This paper may serve as an introduction to future discussions concerning field monitoring of concrete structures. Certainly several improvements can be identified by a careful examination and discussion of the proposed principles and methods.

Several methods are currently under development, such as methods for studying chloride threshold levels for the initiation of active corrosion and methods for accurate monitoring of pore solution chemistry in dense concrete.

References

/1/ Tuutti, K., "Korrosion på armering" (in Swedish), Marina betongkonstruktioners livslängd - Seminars in Sweden and Denmark, Dansk Betoninstitut/Aalborg Portland /Cementa 1993.

/2/ Concrete in the Oceans technical report No. 24 "Effectiveness of Concrete to protect Steel Reinforcement from Corrosion in Marine Structures", OTH 87 247, London 1988.

/3/ Maage, M., Helland, S., Carlsen, J. E., "Chloride penetration in high performance concrete exposed to marine environment", 3rd int. symp. on Utilization of High Strength Concrete, Lillehammer, Norway 1993.

/4/ Vejdirektoratet Broområdet "Kloridbetinget Korrosion - Undersögelse af kloridbelastning og korrosion på brosöjler" (in Danish), Köpenhamn 1991.

/5/ Vegdirektoratet Bruavdelning/Norges Byggforskningsinstitutt "Kloridbestandighet for kystbruer av betong" (in Norwegian), Oslo 1993.

/6/ Sandberg, P.,"Kloridinitierad armeringskorrosion - Lägesrapport och resultatredovisning för 1992-93" (in Swedish), Durability of Marine Concrete Structures, Lund 1994.

/7/ Poulsen, E. "Estimering af levetid for armerede betonkonstruktioner i marint miljö ved planlagt inspektion" (in Danish), Durability of Marine Concrete Structures, AEC laboratory, Vedbaek 1993.

/8/ Sandberg, P. " Förslag till metodik tillståndsbedömning broar i fält" (in Swedish), Durability of Marine Concrete Structures, Lund 1993.

/9/ Tang, L., "Chloride Penetration into a 37-year-old concrete structure in Esbjerg Harbour", Durability of Marine Concrete Structures, Chalmers, Göteborg 1993

/10/ Mehta, P.K., "Concrete Technology at the Crossroads - Problems and Opportunities", Concrete Technology: Past, Present and Future, San Francisco March 1994

/11/ Moskvin, V., Ivanov, F., Alekseyev, S., Guzeyev, E., "Concrete and Reinforced Concrete Deterioration and Protection", Mir Publishers, Moscow 1983.

/12/ Sörensen, H., Frederiksen, J.M., "Testing and modelling of chloride penetration into concrete", Nordic Concrete Research, Seminar Trondheim 1990, pp. 354-356.

/13/ Pettersson, K., Woltze K., Sandberg, P. "Mätning av fria klorider i betong, jämförelse porpressning - lakning av frässpån" (in Swedish), Durability of Maring Concrete Structures, Lund 1994.

/14/ Tang, L., Nilsson. L.-O., "Methods of determining chloride ion diffusion into hardened cement paste, mortar and concrete", RILEM TC 116-PCD, Gothenburg 1990.

/15/ Tang, L., Nilsson, L-O., "Rapid Determination of the Chloride Diffusivity in Concrete by Applying an Electrical Field", ACI Materials Journal, V.89, No1, Jan/Feb 1992, pp 49-53.

/16/ Arya, C., Newman, J. B., "An assessment of four methods of determining the free chloride content of concrete", Materials and Structures, Vol. 23, 1990, pp 319-330.

/17/ Aavik, J., Sahlén, S., Norling-Mjörnell, K., personal communications on methodologies for measurements of RH and degree of capillary saturation on concrete in the field, Lund and Chalmers Institutes of Technology 1992-94.
/18/ Fagerlund, G., "Betongens fuktmekanik" (in Swedish), Betonghandboken Material, Svensk Byggtjänst, 1982.
/19/ Nilsson, L.-O., "Beräkningar av fuktprofiler och fuktvariationer i en brokonstruktion" (in Swedish), Marina betongkonstruktioners livslängd - Seminars in Sweden and Denmark, Dansk Betoninstitut/Aalborg Portland /Cementa 1993.
/20/ Hedenblad, G: "Moisture permeability of mature concrete, cement, mortar and cement paste", TVBM-1014, Lund Institute of Technology, 1993.
/21/ Nilsson, L.-O., Aavik, J., "Fuktmätning i betongbjälklag med PW-givare under byggtiden" (in Swedish), P-93:5, Chalmers, Gothenburg 1993.
/22/ Hansen, T., S., "Micro- and Macrostructural Analysis of Concrete" using Thin Section and Polished Section Microscopy, APM201-202, AEC, Vedbaek, 1993.
/23/ Schiessl, P. "Corrosion of Steel in Concrete", London/New York: Chapman and Hall, Nov 1988, RILEM-report TC 60-CSC.
/24/ Pettersson, K. "Corrosion threshold value and corrosion rate in reinforced concrete", Swedish Cement and Concrete Research Institute, CBI report 2:92, Stockholm 1992.
/25/ Arup, H., "Bestemmelse af chloridtaerskelvaerdi" (in Danish), Marina betongkonstruktioners livslängd - Seminars in Sweden and Denmark, Dansk Betoninstitut/Aalborg Portland /Cementa 1993.
/26/ SS 13 72 44, "Betongprovning - Hårdnad betong - Frostresistens" (Swedish standard for testing of freeze-thaw resistance of concrete in saline environment.), Byggstandardiseringen, Stockholm 1988.
/27/ SS 13 72 10, "Betongprovning - Hårdnad betong - Tryckhållfasthet utborrade cylindrar" (Swedish standard for testing of compression strength in concrete.), Byggstandardiseringen, Stockholm 1988.
/28/ Atlassi, H. Unpublished results from TG-studies on field exposed concrete, Durability of Marine Concrete Structures, Chalmers 1994.
/29/ Masters, L., W., Brandt, E., "Prediction of service life of building materials and components", CIB W80/RILEM 71-PSL Final Report, 1987.
/30/ ASTM E632, "Standard Practise for Developing Accelerated Tests to Aid Prediction of the Service Life of Building Components and Materials, 1988.

CHARACTERISATION OF VARYING MICRO-ENVIRONMENTAL ZONES ON CONCRETE STRUCTURES

Paul Sandberg
Building Materials
Lund Institute of Technology
S-221 00 Lund, Sweden

ABSTRACT

Recent field studies of concrete structures in saline environment have indicated large differences in chloride penetration at various locations on single parts of the structures. Such large differences in chloride penetration was in some cases found even though the concrete quality was found to be quite uniform in the structural parts studied. Thus it has been suggested that the local micro-environment is of major importance concerning chloride penetration into field concrete structures.

Similar findings have been reported concerning atmospheric corrosion on the exterior of ancient buildings. The time of wetness and the chloride absorption has been identified as two main parameters influencing the aggressiveness of the micro-environment. The same parameters have been suggested to control the amount and rate of chloride transport into a given concrete quality exposed in the splash- and atmospheric zones.

Today sensors are available for collection of micro-environmental data in terms of time of wetness and chloride absorption. In this paper such a sensor system is discussed for the use on concrete structures in saline environments. More detailed information on variations in the micro-environment at concrete structures would be very useful both for future design and predictions on future repair zones.

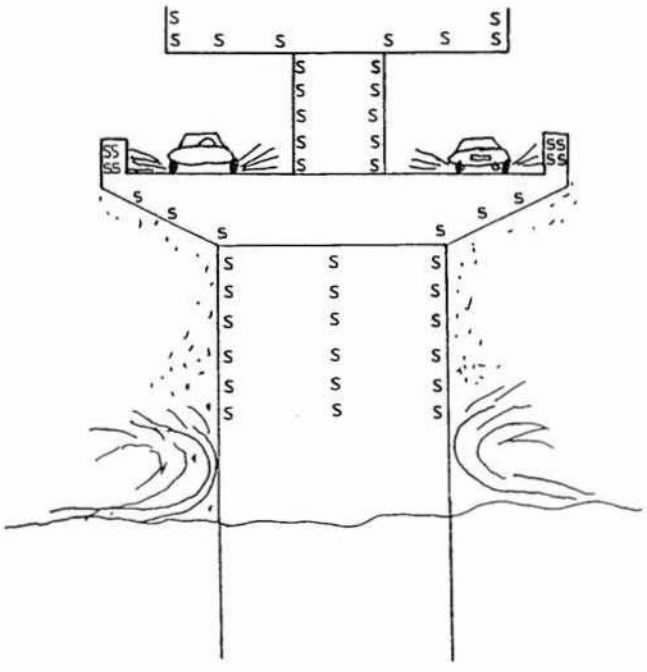

Fig. 1. Mounting of micro-environmental sensors "S" for registration of time of wetness and chloride absorption at various levels and directions on concrete structures in saline environment.

1. INTRODUCTION

In recent years the relative importance of the micro environmental load on chloride penetration into concrete has became evident from several studies of field exposed concrete. Fig. 2 illustrates the micro environmental influence on chloride profiles after 4 years of field exposure, at various sampling positions at the same side of a single marine concrete column at the New Öland bridge, Sweden. The concrete used was a uniform, high quality air entrained concrete with water to binder ratio < 0.40. /1,2/.

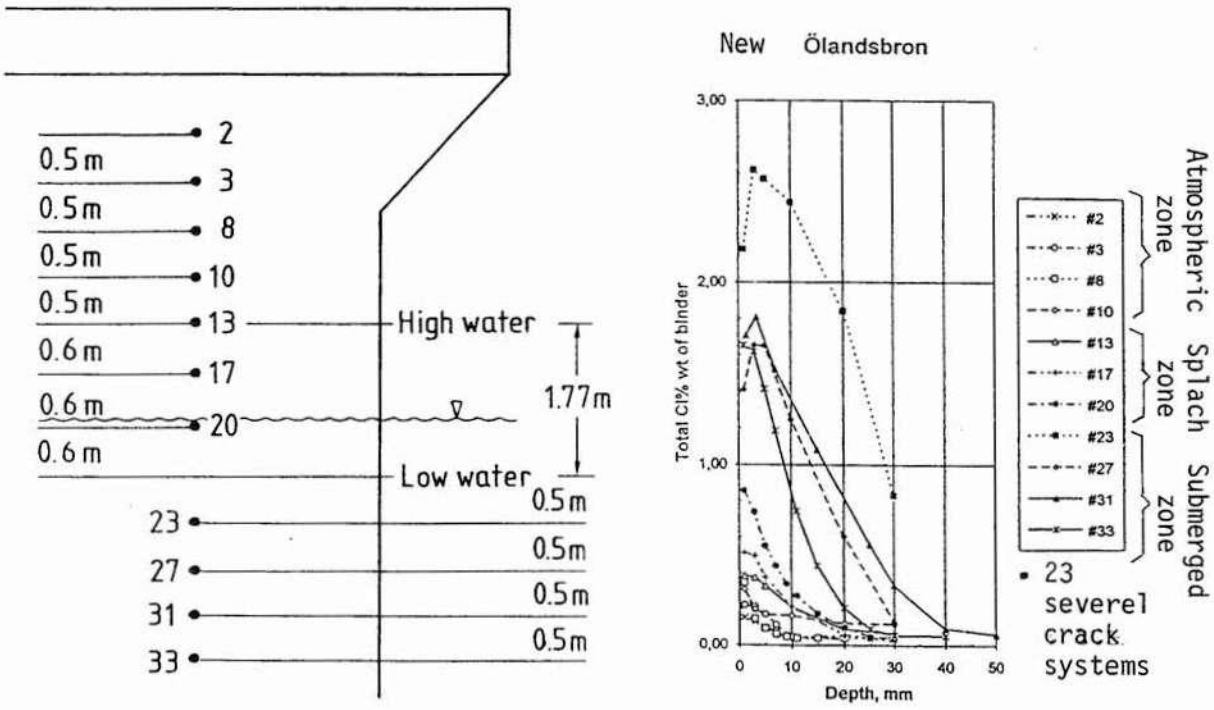

Fig. 2. The effect of micro environment on chloride penetration in high performance concrete at various heights from the mean water level. Chloride profiles were analyzed on concrete cores drilled after 4 years of exposure /1,2/.

A recent field study of 8 concrete bridges exposed 2 - 40 years in marine environment in Norway indicated large variations in chloride penetration at various positions on single bridges. The variations in "effective chloride diffusivity" (calculated using Fick´s second law of diffusion on measured chloride profiles) were larger at various positions on a given bridge than when comparing bridges at various locations at the Norwegian coastline /3,4/.

Similar findings have been reported from large field investigations on 20 concrete bridges exposed for chlorides from deicing salts and/or the sea, by the Danish Road Directorate /5,6/, and from field studies of concrete platforms /7/.

In Fig. 3 some most aggressive exposure zones are indicated for concrete exposed to chlorides from the sea or from deicing salts.

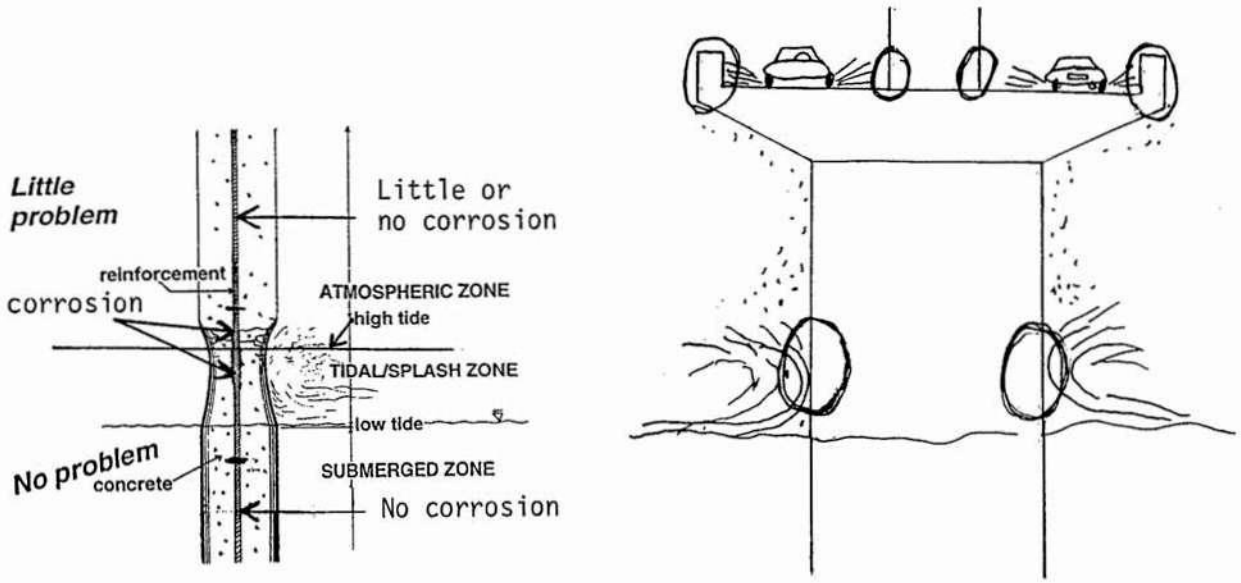

Fig. 3. Some identified critical exposure zones regarding chloride induced reinforcement corrosion.

Similar findings have been reported concerning atmospheric corrosion on the exterior of ancient churches, monuments, etc. /8/. The time of wetness and the chloride absorption has been identified as two main parameters influencing the aggressiveness of the micro-environment. The same parameters have been suggested to control the amount and rate of chloride transport into a given concrete quality exposed in the splash- and atmospheric zones.

Today sensors are available for collection of micro-environmental data in terms of time of wetness and chloride absorption.

2. REGISTRATION OF TIME OF WETNESS

In the EUREKA project EU 614 EUROCARE WETCORR, a system originally developed by the Norwegian Institute for Air Research has been implemented for monitoring of the real time of wetness in the micro climate of various structures /8/. The WETCORR system is described more in detail in Appendix.

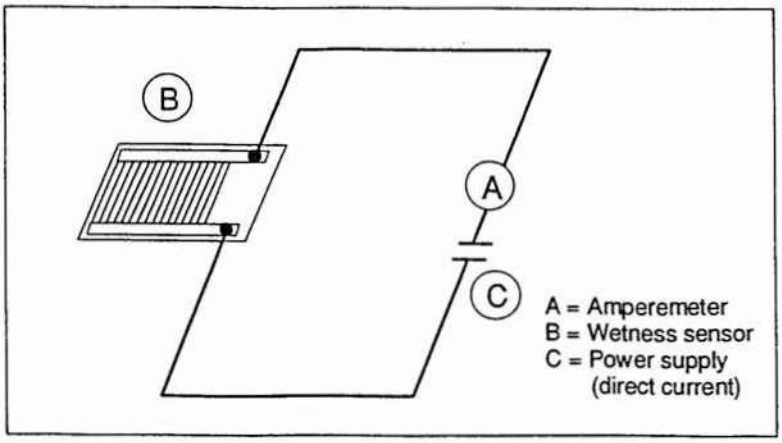

Fig. 4. A schematic illustration of the WETCORR measuring circuit /8/.

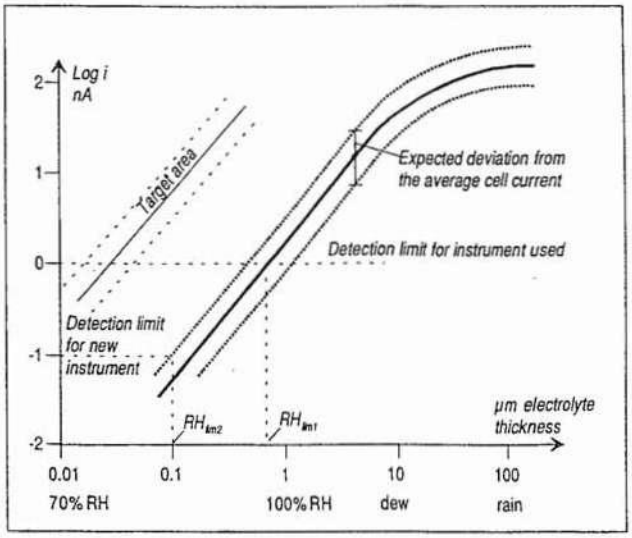

Fig. 5. Calculated current output for different moisture states as controlled by the electrolyte thickness on sensors. As indicated, sensors available today act as dry-wet sensors. Free water is needed to get sufficient response from the sensor /8/.

The WETCORR system includes a number of corrosion cells, Fig. 4. The corrosion current in each cell depends on its moisture state, Fig. 5. Thus, the corrosion cells are used as moisture sensors. The sensors are connected to a data logger system for continuous registration of the moisture state at each sensor, Fig. 6.

No information yet exists on the use of the WETCOOR type of moisture sensors for monitoring of the moisture state when cast into a concrete structure. However it has been successfully used when mounted on the surface of several buildings, such as the Royal Palace in Stockholm and Nidaros Cathedral in Trondheim. Therefore, the WETCORR system would probably also become useful for the monitoring of the local moisture state in various micro climates found on concrete exposed to deicing salts or marine salts. However, regular cleaning of sensors would probably be necessary in zones of frequent chloride absorption, due to the hygroscopic effects of deposited salts.

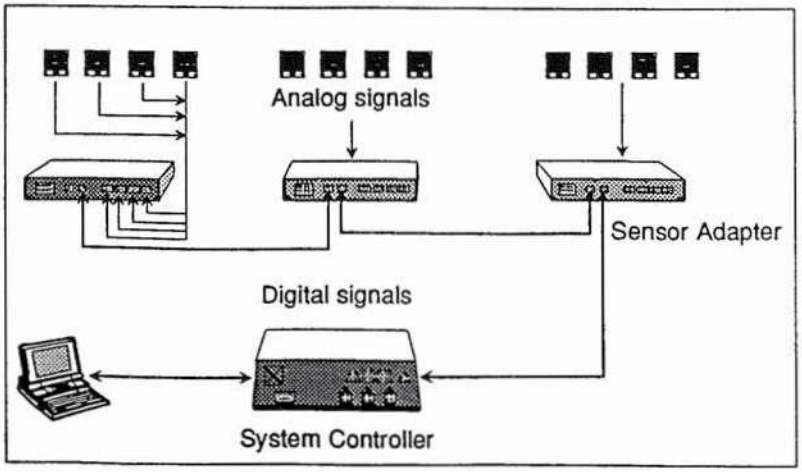

Fig. 6. Data logger system for continuous registration of the moisture state at each sensor /8/.

3. REGISTRATION OF SURFACE CHLORIDE ABSORPTION

A system for monitoring the chloride absorption parallel to the time of wetness is suggested, since chloride absorption on semi-dry concrete may vary significantly from one micro climate to another. A simple chloride absorption monitoring system is outlined in Fig. 7, based on a number of standard size discs made of concrete or mortar, using a standardised mix design.

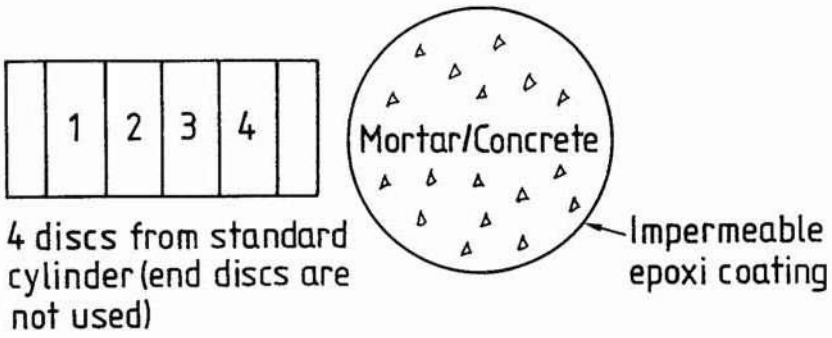

Fig. 7. Chloride absorption standard discs made of concrete or mortar using a standardised mix design.

The factors controlling the amount of salts deposited on the surface of a given concrete or mortar quality is not yet fully understood /9/. The amount of chlorides bound on a concrete surface is known to vary significantly due to variations in cement content, open porosity, alkalinity, carbonation, etc. One important factor is probably the moisture state, since it controls the rate of carbonation of the surface. (A carbonated binder looses most of the uncarbonated chloride binding capacity.)

4. DISCUSSION

The use of moisture sensors mounted in various micro climates on a concrete structure will provide important information on the local moisture variations affecting the concrete. Such information is very useful for the prediction of the moisture state inside the concrete, a property which is important for chloride transport rates and corrosion properties of the reinforcement (such as steel potentials, critical chloride concentrations for corrosion initiation, etc.).

A combination of moisture sensors and chloride absorption standard discs will provide important information on the relationship moisture state - chloride absorption. Such data is useful for the prediction of future chloride transport rates.

It may be possible to obtain relationships chloride disc absorptio - in situ chloride profiles measured in the parent structure. Since the chloride disc absorption would be likely to vary with the season, a minimum exposure time of a year would probably be required to obtain such relationships.

Furthermore, The chloride absorption standard discs will indicate the relative aggressiveness of various micro climates. This information may be useful both for identifying potential repair zones for a given structure, and for the design of future structures exposed to similar micro environments.

If desired, chloride absorption discs of any mix design may of course be placed in addition to the standard chloride absorption discs. It would for instance be suitable to mount chloride absorption discs made of identical concrete as the parent structure of interest. However, "identical concrete" discs must probably be drilled from field concrete manufactured at conditions relevant to the parent structure.

The production cost for standard chloride absorption discs would probably be quite low due to the simple design. On the other hand, discs are consumed when analyzed. Therefore, it is probably wise to place a number of discs in each micro climate.

The WETCORR system is more costly to acquire and to maintain, especially if periodic cleaning of sensors are necessary. The sole use of chloride absorption discs is probably much cheaper than the combined system, but the important information regarding varying moisture states is then not available.

5. REFERENCES

/1/ Sandberg, P., Tang, L., "A field study of the penetration of chlorides and other ions into a high quality concrete marine bridge column", Proceedings 3rd CANMET/ACI Int. Conf. on Durability of Concrete, Nice, May 22-28, 1994, pp. 557-571.

/2/ Tang, L., "Chloride profiles from New Ölandsbron after 4 years of exposure", Technical note, Durability of Marine Concrete Structures, Chalmers University of Technology, 1993-06-28.

/3/ Norwegian Road Directorate/Norwegian Building Research Institute, "Chloride durability of concrete coastal bridges" (in Norwegian), Oslo, 1993.

/4/ Sand, B.T., "The Effect of the Environmental Load on Chloride Penetration - a discussion", Proceedings Nordic Seminar on Chloride Initiated Reinforcement Corrosion in Concrete, Gothenburg, Sweden, January 13-14, 1993.

/5/ Danish Road Directorate, "Chloride initiated corrosion - field investigations of chloride load and corrosion on bridge columns" (in Danish), Copenhagen, 1991.

/6/ Henriksen, C.F., Stoltzner, E., "Chloride Corrosion", Proceedings Nordic Seminar on Chloride Initiated Reinforcement Corrosion in Concrete, Gothenburg, Sweden, January 13-14, 1993.

/7/ Sandvik, M., Wick, S., "Chloride Penetration into Concrete Platforms in the North Sea", Proceedings Nordic Seminar on Chloride Initiated Reinforcement Corrosion in Concrete, Gothenburg, Sweden, January 13-14, 1993.

/8/ EUREKA project EU 615 EUROCARE WETCORR, "Report from the NBS-MK seminar at ABB Conference Centre", Billingstad, Nov. 24, 1993.

/9/ Frederiksen, J.M., "Chloride binding in concrete surfaces", Proceedings Nordic Seminar on Chloride Initiated Reinforcement Corrosion in Concrete, Gothenburg, Sweden, January 13-14, 1993.

APPENDIX

REPRINT FROM

/8/ EUREKA project EU 615 EUROCARE WETCORR, "Report from the NBS-MK seminar at ABB Conference Centre", Billingstad, Nov. 24, 1993.

4. The WETCORR instrument – Concept and characteristics

4.1. Scientific background – critical humidity for deterioration

Material deterioration is caused by chemical reactions where moisture very often plays an important role. The chemical reactions will accelerate with increasing humidity, and for most materials a critical humidity (CH) level can be defined where above the deterioration will be substantial. Generally, the time when the material is exposed to conditions above this critical level is defined as "the time of critical humidity" (TOCH).

The understanding of the processes is best known for metals, but the humidity impact is also observed for materials like wood, stone, rendering and concrete.

For metals the corrosion is caused by electrochemical reactions on the surface and the formation of an electrolyte is essential. The formation of the electrolyte depends on humidity and the pollutants available, as illustrated in Figure 1 for carbon steel. In extreme clean laboratory conditions, 100% relative humidity (RH) and dew are needed to start the corrosion. In practice the electrolyte will be formed at lower RH due to pollutants. In areas where gas pollutants like SO_2 are present, a critical humidity level of 80% for corrosion is observed, and in areas with sea-salt aerosols the critical humidity level will be even lower. From these relationships the well-known term Time of Wetness (TOW) has been generated as the time when humidity is above a critical level where metal corrosion is substantial.

From empiric observations, the term TOW for metals is defined as the time when the relative humidity is greater than 80% at temperature above 0°C. This definition is used in ISO standard 9223 "Corrosion of metals and alloys - corrosivity of atmosphere - classification".

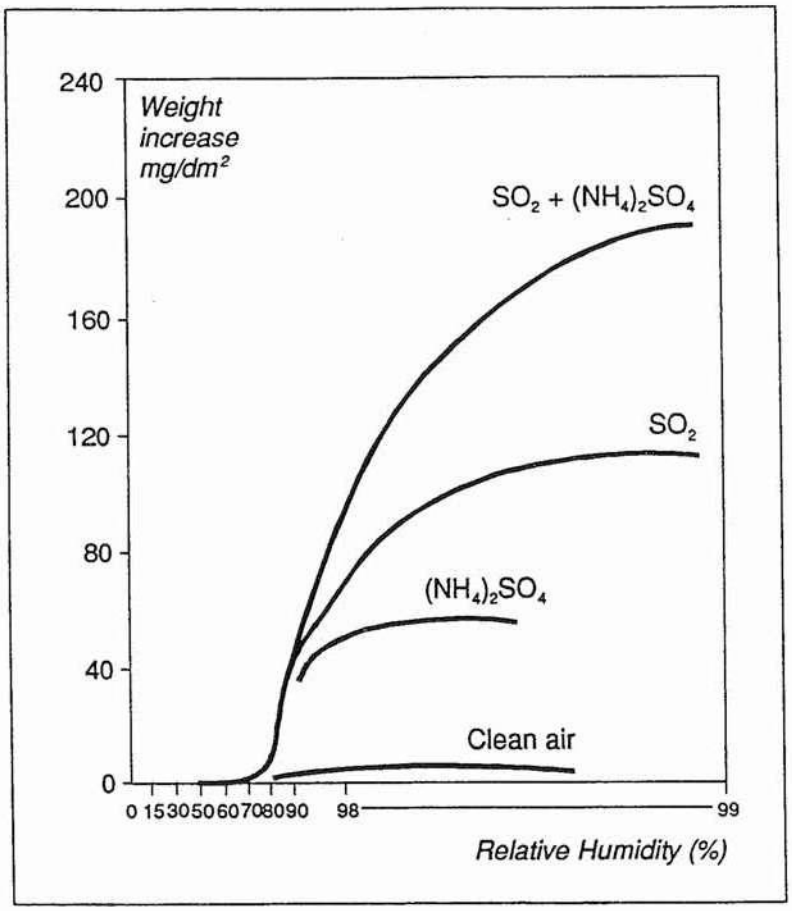

Figure 1: Corrosion attack on carbon steel at increasing relative humidity, based on work by W.H. Vernon (Bardal, 1985).

In the actual micro environment for constructions deviations from this simple correlation will occur. The critical humidity level is dependent on the materials and the pollutants present. For steel corrosion is proved to take place even at temperatures down to -4°C. Consequently there is a great need for developing monitoring methods for mapping the critical humidity conditions and the time above these levels (TOCH) in the micro environment for the various constructions and materials in use.

4.2. The critical humidity level measurements

The WETCORR instrument is designed for recording of the humidity and temperature condition in the micro environment of constructions.

The measuring principle makes use of the electrochemical nature of the corrosion processes by measuring the current flow in an electrochemical cell as a function of the humidity film on the electrode surface. The principle was proposed by Professor Thomashov as early as in 1950ies and has later been adapted and modified by other groups such as The National Research Council of Canada, The Swedish Corrosion Institute, The Norwegian Institute for Air Research, and The

Swedish Institute for Building Research (see the reference list). In Figure 2 the simple measuring circuit used is illustrated. The wetness sensor is connected to a constant voltage power supply (P) and the current flow through the system is measured with a zero-resistant amperemeter.

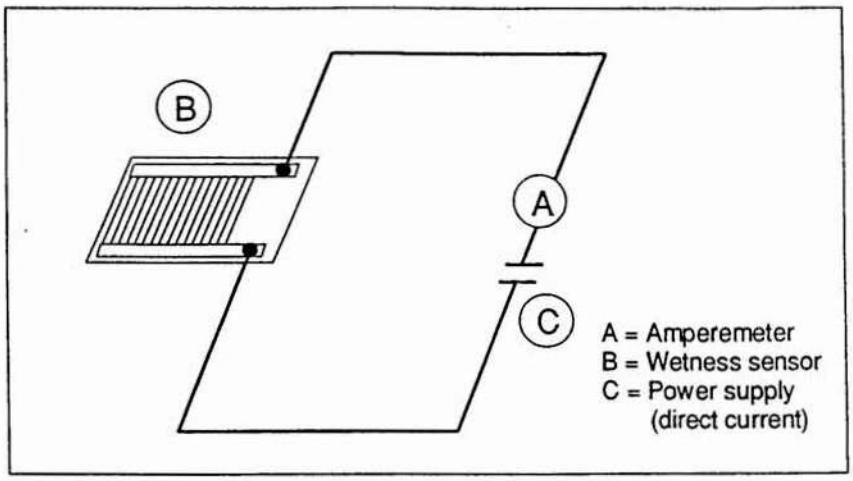

Figure 2: A schematic layout of the measuring circuit.

Based on the electrochemical reactions which take place on the surface of the cell, the theoretical correlation between the current flow and the electrolyte thickness can be calculated. A theoretical study in the 1980ies showed that an electrochemical cell will have a log-log relationship between the current flow and the electrolyte thickness up to a thickness of approximately 10 µm and little increase at even thicker layers. The basic results of the theoretical studies in the 1980ies are expressed in Figure 3 for *one selected* cell geometry. Parameters which will effect the current output are the design of the cell, the conductivity of the electrolyte and the material used in the cell.

In the instrument development phase the sensor used consists of a small gold cell for wetness measurements and a temperature sensor for recording the surface temperature.

To ensure that the temperature sensor follows the surface temperature, the cell backing is made of aluminium oxide with good thermal conductivity.

The gold wetness sensor is made of two gold electrodes arranged in a finger pattern. A fixed voltage usually selected in the range between 100 mV and 200 mV is applied and the current flow is measured. To prevent polarization of the electrodes the direction of the voltage is changed every 30 sec.

The current output for the gold sensors used in the development phase, is shown in Figure 3. The detection limit for the instrument was 1 nanoampere (nA) and this limit corresponds to a relative humidity in the air close to 100% RH, marked in the figure as RH_{lim1}. When standard deviations in the current output from the

different sensors are accounted for, the sensors used in the development phase will act as *a wet-dry sensor* where dew or rain is needed to get sufficient response from the sensor.

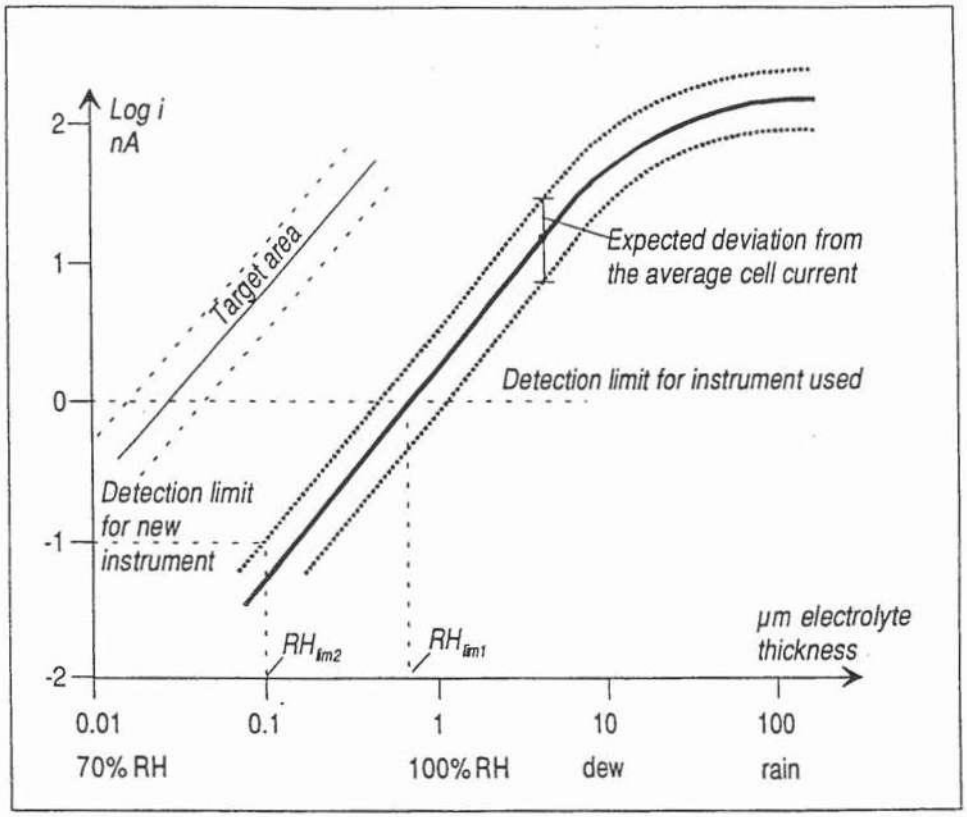

Figure 3: Calculated current output for different electrolyte thickness on Au wetness sensor and the target area for a new generation of sensors.

Two measures are undertaken to increase the sensibility and thereby enabling determination of critical humidity in a broader relative humidity regime.

Firstly, the instrument detection limit is lowered to 0.1 nA (see Figure 3). This is now electronically feasible, and the new adapters for sale will be delivered with these characteristics. Corresponding limiting relative humidity is RH_{lim2} and close to 80%.

Secondly, emphasis is now on developing more sensitive sensors. The system will be delivered with the Au sensors, but we aim at delivering various types of well characterized humidity sensors. Promising results with Cu sensors, painted sensors and other types have already been obtained.

In outdoor application pollutants will be attached to the sensor and the current response will increase due to increased conductivity, and because the pollutants normally are hygroscopic and therefore absorb and build up the electrolyte thickness needed at lower relative humidity.

The surface condition of the sensor will therefore change with time in the same way as the condition of the construction surface itself. A freely exposed sensor in fairly clean areas will keep a current response similar to the curve in Figure 3 for a long time, while in more polluted areas and in sheltered positions the current output will increase.

4.3. The WETCORR instrument

The principle for the WETCORR instrument is shown in Figure 4.

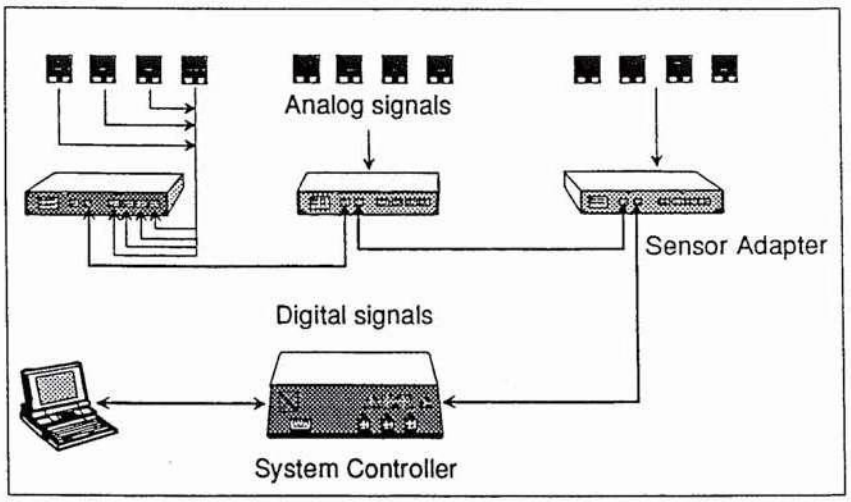

Figure 4: The principle for the WETCORR instrument.

The instrument consists of the following modules

1 System Controller (SC)
1-16 Sensor Adapters (SA)
1-64 Sensors

The technical specification is given in the attached technical data sheets.

The System Controller is the control unit for communication with the Sensor Adapters, and is also the unit for the external communication with a PC directly or through a modem. The SC is also the power source for the sensors and SA, and sampling unit for all measuring data.

The Sensor Adapter is the control and recording unit for four sensors. The data are recorded as average values over one minute. The SA will convert all data recorded to digital signals before transferring the data to the System Controller. This is done to reduce the influence of stray currents and radio signals on the measured data. Therefore the sensor cables are kept short, 2 metres, while the cables for the digital signals can be long, up to 250 metres in two directions. The Sensor Adapter can be placed outdoors in rain and wind.

The parameter set-up for one adapter is valid for all the sensors connected to this adapter, while each adapter in a system can be configured individually. The parameters are cell voltage and sampling period.

4.4. Presentation of results

The instrument is delivered with one software programme for communication, parameter setting and recording of data. The amount of data has always been a problem in this type of measurements, and great emphasis is put on solving this problem through user-friendly database design and management, and data presentation tools.

The instrument will therefore be supplied with Windows based software package for presentation of the data, using Microsoft Access version 1.1 and Visual Basic Pro 3.0. Presentations within geographical information systems (GIS) will also be available shortly.

The following presentation forms will be available:

- Plots of currents versus time and temperatures versus time
- Total current output from the cells in the period
- % time with current above the selected critical humidity levels (TOCH)
- % time with the temperature above or below selected temperatures
- Frequencies for TOCH and temperature above selected values
- Min., Max. and Mean values for current and temperature
- Min., Max. and Mean values for the time with TOCH.

4.5. Interpretation of data for the wet/dry Au sensor

The interpretation of the current reading *will depend on the pollution level* in the micro environment where the sensor is applied.

4.5.1. Sensors freely exposed

The current is expected to change about two decades from complete dry to soaking wet. In polluted area and in the coastal zone the *wet* current may be substantial, but in background areas less than 100 nA. For calculation of the time of critical humidity (TOCH), in this case real time of wetness, a corresponding current threshold must be selected. The threshold value must be selected below the normal variation of the current observed during rain periods. As a code of practice for the gold sensors, the following equation can be used to define the threshold current for the critical humidity level (i_{thres})

$$\log i_{thres} = \log i_{min.} + \frac{\log i_{max.} - \log i_{min.}}{2} = \frac{\log i_{max.} + \log i_{min.}}{2}$$

An illustration of the way to calculate the threshold current is given in Figure 5A.

Interpretation of the threshold value will depend on the environmental condition and the material in use.

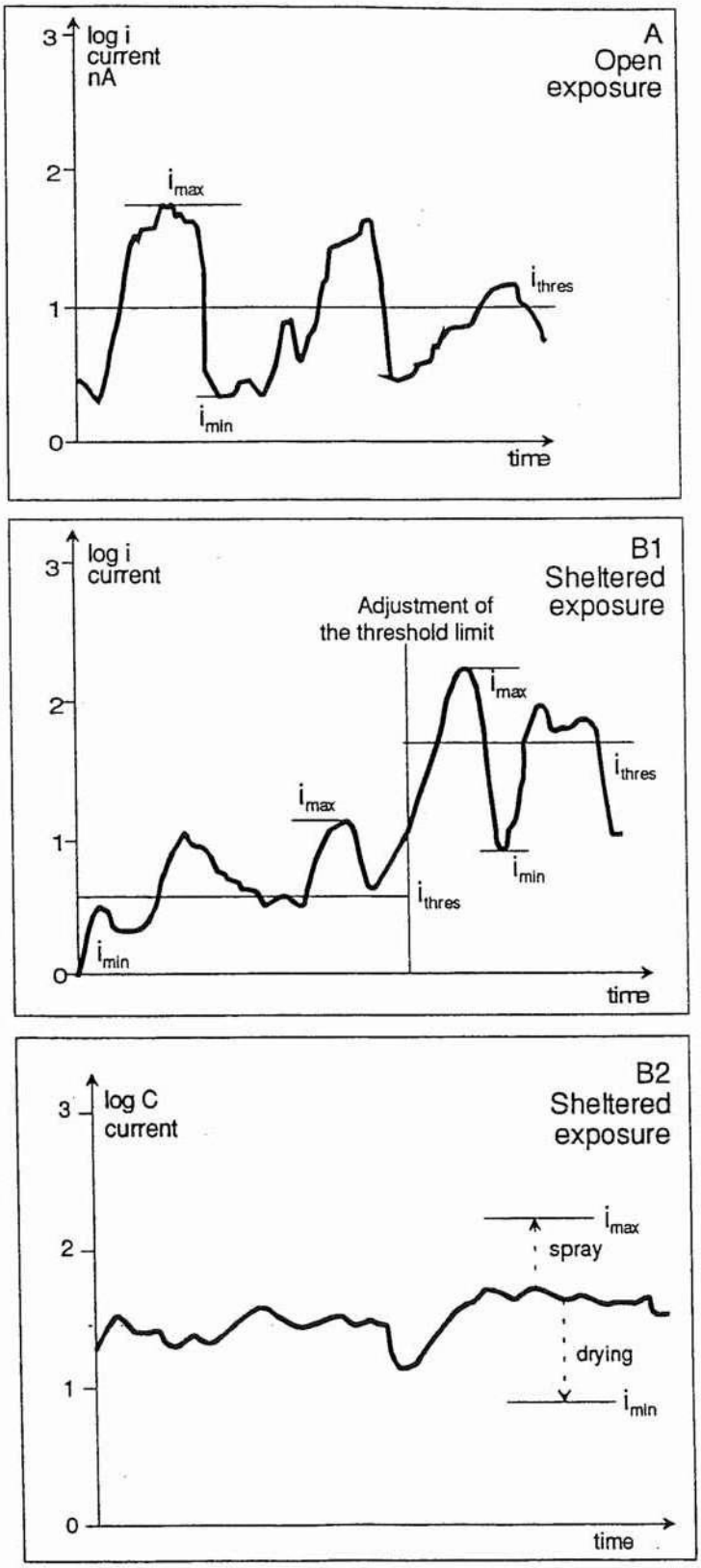

Figure 5: Illustration of the way to calculate the threshold sensor current in open position A and sheltered position B1 and B2.

4.5.2. Sensors in sheltered position

The current observed on a sheltered sensor will change with time. In the beginning when the sensor is clean very little happens. With time the response of the sensor will increase. The baseline will reach values above 1 nA and the time with moisture on the sensor will increase due to pollution deposits (see Figures 5B1 and 5B2). In the end the current levels can be higher than on freely exposed sensors and the TOCH will also exceed the results of the freely exposed sensor. In areas with high amount of hygroscopic salts and high humidity, as in coastal areas, the sensor will hardly ever be dry, except for sensors which can be heated by the sun radiation.

If the sensors have current fluctuation of the same magnitude as for freely exposed sensors, the same method for calculation of TOCH can be used for shorter periods. Adjustments of the threshold level must be carried out with the time because of the change of the baseline (see Figure 5B1).

For sensors with more or less the same current the whole time, the wet and dry current of the sensor must be defined. The dry current can be defined by drying the surface artificially with an IR-lamp. If the current seems to be low, the wet current can be established by light spraying of water on the surface (Figure 5B2).

4.6. Service life of a sensor

The wetness and temperature sensors are quite durable and may have long lasting lifetime. The experience with the temperature sensor is that mechanical breakdown of the connecting legs is the most dominating failure. The output signal will then be constant -38.4°C. With badly insulated legs leakage current between the legs will break the legs after a short time.

Mechanical damage of the gold wetness sensor can make a short circuit of the cell and create a very large current through the electric circuit. The pollutant layers formed on the sensor may cause the same reaction. Under open exposure this may happen by soot or salt particles bridging the electrodes. Cleaning of the sensor may help. However, in environments with soot and salt particles reduced service life for sensors can be expected. The situation in sheltered position has many of the same aspects as the bridge in open positions. However, if the exposure situation for the sensor and the material is the same, the goal of the project is decisive for whether the sensor signal still has relevance or if the sensor needs to be replaced.

4.7. Application of the WETCORR instrument in environmental studies

Through the last year's testing of the WETCORR instrument, several interesting applications have been accomplished. The applications can be divided in the following groups:

- mapping of the wetness impact on different sides and parts of buildings (Royal Palace – Stockholm, Nidaros Cathedral – Trondheim)
- wetness studies on panels and artificial facade details
- wetness studies on building parts (windows).

Earlier, interesting tests have been carried out with painted sensors and with sensors applied inside materials like chipboard.

For further information, see the Appendices.

4.8. The attachment of the sensors to different surfaces

The attachment of the sensor to the selected surfaces by double sticking thin tape is easy on a smooth, clean surface like a facade sheet. Problems may occur on these surfaces if they are dirty, and cleaning may be necessary.

On rough facades, such as old stone wall, double sticking tape directly applied will not work and we need to use thicker glue with curing time. One way to solve the problem is to apply small metal sheets like aluminium on the stone by use of silicone glue and let it cure before the sensor is applied on metal sheet by use of the double sticking tape.

5. Calibration test

At the previous WETCORR seminar in Stockholm 28 April 1993, it was decided to make a standardized calibration test for the use of the WETCORR instrument. The main purpose for the calibration test was to define the spread in the temperature and the time of wetness results for sensors which was exposed under the same condition. The calibration test had the following steps:

1. 8 cells were attached to the same material and mounted to a rack facing south at a 45° angle. The exposure period should be about 2 months.

2. The same 8 cells should be exposed in a climate chamber for one week at different relative humidities. At the end an artificial rain shower was introduced.

Step 1 of the test was carried out at the Norwegian Institute for Building Research (NBI), Trondheim, SBI and NILU. Similar tests had earlier been carried out at SIB and KI. Step 2 of the test was carried out at SBI and NILU.

The main conclusions from the results listed in Appendix B were:

- The cell current response was comparable and the current pattern was identical. The spread was within a range of 10-30%. At some test sites the sensor response was at two different levels even if the current pattern was comparable.
- The spread in the temperature sensors used was higher than expected, and not sufficiently accurate for the use planned.
- Out of 40 adapters tested one sensor had a poor connection.
- For some of the adapters an intermittent failure without data recorded were observed.
- In the climate chamber the gold sensors had no response before the rain was introduced.

The following suggestions for improvements and better use of the sensors were made:

The temperature sensor:

- One point calibration of the temperature sensor is insufficient and two point calibration or the use of better quality sensors could improve the accuracy needed.

The current sensor:

- The spread in the results is acceptable since the current pattern is identical. However, if the threshold current takes into account that the levels for two sensors could be different, the spread could be reduced (see 4.5.1).
- The current output from the gold cells was low and efforts to increase the output and the sensitivity at lower relative humidities should be carried out.